

**GOCE DELCEV UNIVERSITY, SHTIP, NORTH MACEDONIA  
FACULTY OF ELECTRICAL ENGINEERING**

# **ETIMA 2021**

**FIRST INTERNATIONAL CONFERENCE**

**19-21 OCTOBER, 2021**



**TECHNICAL SCIENCES APPLIED IN ECONOMY,  
EDUCATION AND INDUSTRY**



---

УНИВЕРЗИТЕТ „ГОЦЕ ДЕЛЧЕВ” - ШТИП  
ЕЛЕКТРОТЕХНИЧКИ ФАКУЛТЕТ

UNIVERSITY „GOCE DELCHEV” - SHTIP  
FACULTY OF ELECTRICAL ENGINEERING

ПРВА МЕЃУНАРОДНА КОНФЕРЕНЦИЈА  
FIRST INTERNATIONAL CONFERENCE

**ЕТИМА / ETIMA 2021**

ЗБОРНИК НА ТРУДОВИ  
CONFERENCE PROCEEDINGS

19-21 Октомври 2021 | 19-21 October 2021

**Главен и одговорен уредник / Editor in Chief**

Проф.д-р Сашо Гелев

Prof.d-r Saso Gelev

**Јазично уредување / Language Editor**

Весна Ристова (Македонски) / Vesna Ristova (Macedonian)

**Техничко уредување / Technical Editing**

Доц.д-р Далибор Серафимовски / d-r Dalibor Serafimovski

**Издавач / Publisher**

Универзитет „Гоце Делчев“ - Штип / University Goce Delchev - Stip

Електротехнички факултет / Faculty of Electrical Engineering

**Адреса на организационен комитет / Adress of the organizational committee**

Универзитет „Гоце Делчев“ – Штип / University Goce Delchev - Stip

Електротехнички факултет / Faculty of Electrical Engineering

Адреса: ул. „Крсте Мисирков“ бр. 10-А / Address: Krste Misirkov, 10 - A

Пош. фах 201, Штип - 2000, С.Македонија / PO BOX 201, Stip 2000, North Macedonia

**E-mail:** [conf.etf@ugd.edu.mk](mailto:conf.etf@ugd.edu.mk)

CIP - Каталогизација во публикација

Национална и универзитетска библиотека "Св. Климент Охридски", Скопје

62-049.8(062)

004-049.8(062)

МЕЃУНАРОДНА конференција ЕТИМА (1 ; 2021)

Зборник на трудови [Електронски извор] / Прва меѓународна

конференција ЕТИМА 2021, 19-21 Октомври 2021 = Conference proceedings /

First international conferece ЕТИМА 2021, 19-21 October 2021 ; [главен и

одговорен уредник Сашо Гелев]. - Штип: Универзитет "Гоце Делчев",

Електротехнички факултет = Shtip: University "Goce Delchev", Faculty of  
Electrical Engineering, 2021

Начин на пристапување (URL): <https://js.ugd.edu.mk/index.php/etima>. -

Текст во PDF формат, содржи 358 стр.илустр. - Наслов преземен од

екранот. - Опис на изворот на ден 15.10.2021. - Трудови на мак. и англ.

јазик. - Библиографија кон трудовите

ISBN 978-608-244-823-7

1. Напор. ств. насл.

а) Електротехника -- Примена -- Собири б) Машинство -- Примена -- Собири

в) Автоматика -- Примена -- Собири г) Информатика -- Примена -- Собири

COBISS.MK-ID 55209989



Прва меѓународна конференција ЕТИМА  
19-21 Октомври 2021  
First International Conference ETIMA  
19-21 October 2021

**ОРГАНИЗАЦИОНЕН ОДБОР  
ORGANIZING COMMITTEE**

**Василија Шарац / Vasilija Sarac**

Електротехнички факултет,  
Универзитет „Гоце Делчев” - Штип, Северна Македонија  
Faculty of Electrical Engineering,  
Goce Delchev University - Stip, North Macedonia

**Сашо Гелев / Saso Gelev**

Електротехнички факултет,  
Универзитет „Гоце Делчев” - Штип, Северна Македонија  
Faculty of Electrical Engineering,  
Goce Delchev University - Stip, North Macedonia

**Тодор Чекеровски / Todor Cekerovski**

Електротехнички факултет,  
Универзитет „Гоце Делчев” - Штип, Северна Македонија  
Faculty of Electrical Engineering,  
Goce Delchev University - Stip, North Macedonia

**Далибор Серафимовски / Dalibor Serafimovski**

Електротехнички факултет,  
Универзитет „Гоце Делчев” - Штип, Северна Македонија  
Faculty of Electrical Engineering,  
Goce Delchev University - Stip, North Macedonia

**Маја Кукушева Панева / Maja Kukuseva Paneva**

Електротехнички факултет,  
Универзитет „Гоце Делчев” - Штип, Северна Македонија  
Faculty of Electrical Engineering,  
Goce Delchev University - Stip, North Macedonia

**Билјана Читкушева Димитровска / Biljana Citkuseva Dimitrovska**

Електротехнички факултет,  
Универзитет „Гоце Делчев” - Штип, Северна Македонија  
Faculty of Electrical Engineering,  
Goce Delchev University - Stip, North Macedonia

**Весна Конзулова / Vesna Konzulova**

Електротехнички факултет,  
Универзитет „Гоце Делчев” - Штип, Северна Македонија  
Faculty of Electrical Engineering,  
Goce Delchev University - Stip, North Macedonia





Прва меѓународна конференција ЕТИМА  
19-21 Октомври 2021  
First International Conference ETIMA  
19-21 October 2021

**ПРОГРАМСКИ И НАУЧЕН ОДБОР  
SCIENTIFIC COMMITTEE**

**Со Ногучи / So Noguchi**

Висока школа за информатички науки и технологии  
Универзитет Хокаидо, Јапонија  
Graduate School of Information Science and Technology  
Hokkaido University, Japan

**Диониз Гашпаровски / Dionýz Gašparovský**

Факултет за електротехника и информатички технологии,  
Словачки Технички Универзитет во Братислава, Словачка  
Faculty of Electrical Engineering and Information Technology  
Slovak Technical University in Bratislava, Slovakia

**Антон Белан / Anton Belán**

Факултет за електротехника и информатички технологии  
Словачки Технички Универзитет во Братислава, Словачка  
Faculty of Electrical Engineering and Information Technology  
Slovak Technical University in Bratislava, Slovakia

**Георги Иванов Георгиев / Georgi Ivanov Georgiev,**

Технички Универзитет во Габрово, Бугарија  
Technical University in Gabrovo, Bulgaria

**Ивелина Стефанова Балабанова / Ivelina Stefanova Balabanova,**

Технички Универзитет во Габрово, Бугарија  
Technical University in Gabrovo, Bulgaria

**Бојан Димитров Карапенов / Boyan Dimitrov Karapenev**

Технички Универзитет во Габрово, Бугарија  
Technical University in Gabrovo, Bulgaria

**Сашо Гелев / Saso Gelev**

Електротехнички факултет,  
Универзитет „Гоце Делчев“ - Штип, Северна Македонија  
Faculty of Electrical Engineering,  
Goce Delchev University - Stip, North Macedonia

**Влатко Чингоски / Vlatko Cingoski**  
Електротехнички факултет,  
Универзитет „Гоце Делчев” - Штип, Северна Македонија  
Faculty of Electrical Engineering,  
Goce Delchev University - Stip, North Macedonia

**Божо Крстајиќ / Bozo Krstajic**  
Електротехнички факултет  
Универзитет во Црна Гора, Црна Гора  
Faculty of Electrical Engineering,  
University in Montenegro, Montenegro

**Милован Радуловиќ / Milovan Radulovic**  
Електротехнички факултет  
Универзитет во Црна Гора, Црна Гора  
Faculty of Electrical Engineering,  
University in Montenegro, Montenegro

**Гоце Стефанов / Goce Stefanov**  
Електротехнички факултет,  
Универзитет „Гоце Делчев” - Штип, Северна Македонија  
Faculty of Electrical Engineering,  
Goce Delchev University - Stip, North Macedonia

**Мирјана Периќ / Mirjana Peric**  
Електронски факултет  
Универзитет во Ниш, Србија  
Faculty of Electronic Engineerig,  
University of Nis, Serbia

**Ана Вучковиќ / Ana Vuckovic**  
Електронски факултет  
Универзитет во Ниш, Србија  
Faculty of Electronic Engineerig,  
University of Nis, Serbia

**Тодор Чекеровски / Todor Cekеровски**  
Електротехнички факултет,  
Универзитет „Гоце Делчев” - Штип, Северна Македонија  
Faculty of Electrical Engineering,  
Goce Delchev University - Stip, North Macedonia

**Далибор Серафимовски / Dalibor Serafimovski**  
Електротехнички факултет,  
Универзитет „Гоце Делчев” - Штип, Северна Македонија  
Faculty of Electrical Engineering,  
Goce Delchev University - Stip, North Macedonia

**Мирослава Фаркаш Смиткова / Miroslava Farkas Smitková**

Факултет за електротехника и информации технологии  
Словачки Технички Универзитет во Братислава, Словачка  
Faculty of Electrical Engineering and Information Technology  
Slovak Technical University in Bratislava, Slovakia

**Петер Јанига / Peter Janiga**

Факултет за електротехника и информации технологии  
Словачки Технички Универзитет во Братислава, Словачка  
Faculty of Electrical Engineering and Information Technology  
Slovak Technical University in Bratislava, Slovakia

**Јана Радичова / Jana Raditschová,**

Факултет за електротехника и информации технологии  
Словачки Технички Универзитет во Братислава, Словачка  
Faculty of Electrical Engineering and Information Technology  
Slovak Technical University in Bratislava, Slovakia

**Драган Миновски / Dragan Minovski**

Електротехнички факултет,  
Универзитет „Гоце Делчев” - Штип, Северна Македонија  
Faculty of Electrical Engineering,  
Goce Delchev University - Stip, North Macedonia

**Василија Шарац / Vasilija Sarac**

Електротехнички факултет,  
Универзитет „Гоце Делчев” - Штип, Северна Македонија  
Faculty of Electrical Engineering,  
Goce Delchev University - Stip, North Macedonia

**Александар Туцаров / Aleksandar Tudzarov**

Електротехнички факултет,  
Универзитет „Гоце Делчев” - Штип, Северна Македонија  
Faculty of Electrical Engineering,  
Goce Delchev University - Stip, North Macedonia

**Владимир Талевски / Vladimir Talevski**

Електротехнички факултет,  
Универзитет „Гоце Делчев” - Штип, Северна Македонија  
Faculty of Electrical Engineering,  
Goce Delchev University - Stip, North Macedonia



## Прва меѓународна конференција ЕТИМА First International Conference ETIMA

---

### **PREFACE**

The Faculty of Electrical Engineering at University Goce Delcev (UGD), has organized the International Conference ***Electrical Engineering, Informatics, Machinery and Automation - Technical Sciences applied in Economy, Education and Industry-ETIMA***.

ETIMA has a goal to gather the scientists, professors, experts and professionals from the field of technical sciences in one place as a forum for exchange of ideas, to strengthen the multidisciplinary research and cooperation and to promote the achievements of technology and its impact on every aspect of living. We hope that this conference will continue to be a venue for presenting the latest research results and developments on the field of technology.

Conference ETIMA was held as online conference where contributed more than sixty colleagues, from six different countries with forty papers.

We would like to express our gratitude to all the colleagues, who contributed to the success of ETIMA'21 by presenting the results of their current research activities and by launching the new ideas through many fruitful discussions.

We invite you and your colleagues also to attend ETIMA Conference in the future. One should believe that next time we will have opportunity to meet each other and exchange ideas, scientific knowledge and useful information in direct contact, as well as to enjoy the social events together.

*The Organizing Committee of the Conference*

### **ПРЕДГОВОР**

Меѓународната конференција ***Електротехника, Технологија, Информатика, Машинство и Автоматика-технички науки во служба на економија, образование и индустрија-ЕТИМА*** е организирана од страна на Електротехничкиот факултет при Универзитетот Гоце Делчев.

ЕТИМА има за цел да ги собере на едно место научниците, професорите, експертите и професионалците од полето на техничките науки и да представува форум за размена на идеи, да го зајканува мултидисциплинарното истражување и соработка и да ги промовира технолошките достигнувања и нивното влијание врз секој аспект од живеењето. Се надеваме дека оваа конференција ќе продолжи да биде настан на кој ќе се презентираат најновите резултати од истражувањата и развојот на полето на технологијата.

Конференцијата ЕТИМА се одржа online и на неа дадоа свој допринос повеќе од шеесет автори од шест различни земји со четириесет труда.

Сакаме да ја искажеме нашата благодарност до сите колеги кои допринесоа за успехот на ЕТИМА'21 со презентирање на резултати од нивните тековни истражувања и со лансирање на нови идеи преку многу плодни дискусии.

Ве покануваме Вие и Вашите колеги да земете учество на ЕТИМА и во иднина. Веруваме дека следниот пат ќе имаме можност да се сретнеме, да размениме идеи, знаење и корисни информации во директен контакт, но исто така да уживаме заедно и во друштвените настани.

*Организационен одбор на конференцијата*



## Содержина / Table of Contents

ASSESSING DIGITAL SKILLS AND COMPETENCIES OF PUBLIC ADMINISTRATION AND DEFINING THEIR PROFICIENCY LEVEL .....	12
PWM OPERATION OF SYNCHRONOUS PERMANENT MAGNET MOTOR .....	21
SPEED REGULATION OF INDUCTION MOTOR WITH PWM INVERTER .....	30
WI-FI SMART POWER METER .....	42
RF SENSOR SMART NETWORK.....	50
FREQUENCY SINUS SOURCE.....	62
MEASUREMENT ON COMPENSATION CAPACITANCE IN INDUCTIVE NETWORK BY MICROCONTROLLER .....	70
ИЗРАБОТКА НА ВЕШТ НАОД И МИСЛЕЊЕ ОД ОБЛАСТА НА ЕЛЕКТРОТЕХНИЧКИТЕ НАУКИ .....	79
SIMULATION OF AN INDUSTRIAL ROBOT WITH THE HELP OF THE MATLAB SOFTWARE PACKAGE.....	86
BATTERY ENERGY STORAGE SYSTEMS AND TECHNOLOGIES:A REVIEW ..	95
POWER-TO-X TECHNOLOGIES.....	105
NEW INNOVATIVE TOURISM PRODUCT FOR REANIMATING RURAL AREAS .....	115
PROPOSED MODEL FOR BETTER ENGLISH LANGUAGE ACQUISITION, BASED ON WEARABLE DEVICES.....	123
OPEN SOURCE LEARNING PLATFORM – MOODLE .....	132
СПОРЕДБЕНА ТЕХНО-ЕКОНОМСКА АНАЛИЗА ПОМЕЃУ ТЕРМИЧКИ ИЗОЛИРАН И ТЕРМИЧКИ НЕИЗОЛИРАН СТАНБЕН ОБЈЕКТ .....	139
COMPARISON OF PERT AND MONTE CARLO SIMULATION .....	149
E-LEARNING – CYBER SECURITY CHALLENGES AND PROTECTION MECHANISMS .....	156
SECURITY AND PRIVACY WITH E-LEARNING SOFTWARE .....	164
ROOTKITS – CYBER SECURITY CHALLENGES AND MECHANISMS FOR PROTECTION .....	174
TOOLS AND TECHNIQUES FOR MITIGATION AND PROTECTION AGAINST SQL INJECTION ATTACKS .....	182
INFLUENCE OF ROTATION ANGLE OF LUMINAIRES WITH ASYMMETRICAL LUMINOUS INTENSITY DISTRIBUTION CURVE ON CALCULATED PHOTOMETRIC PARAMETERS.....	189
PHOTOMETRIC PARAMETERS OF LED LUMINAIRES WITH SWITCHABLE CORRELATED COLOUR TEMPERATURE .....	197
ENERGY-EFFICIENT STREET LIGHTING SYSTEM OF THE CITY OF SHIP USING SOLAR ENERGY AND LED TECHNOLOGY .....	204
NANOTECHNOLOGY–BASED BIOSENSORS IN DRUG DELIVERY SYSTEMS: A REVIEW .....	212

<b>IOT SYSTEM FOR SHORT-CIRCUIT DETECTION OF DC MOTOR AT EKG-15 EXCAVATOR .....</b>	<b>222</b>
<b>DESIGN OF A PHOTOVOLTAIC POWER PLANT .....</b>	<b>231</b>
<b>DEVELOPMENT OF COMPUTER SOFTWARE FOR CREATING CHOREOGRAPHY .....</b>	<b>241</b>
<b>AUTOMATED SYSTEM FOR SMART METER TESTING.....</b>	<b>249</b>
<b>INFLUENCE DIMING OF LED LAMPS TO ELECTRICAL PARAMETERS .....</b>	<b>255</b>
<b>INRUSH CURRENT OF LAMP .....</b>	<b>261</b>
<b>COMPLEX EVALUATION MODEL OF A SMALL-SCALE PHOTOVOLTAIC INSTALLATION PROFITABILITY .....</b>	<b>269</b>
<b>IMPACT OF FAULTS IN TRANSMISSION AND DISTRIBUTION NETWORK ON VOLTAGE SAGS .....</b>	<b>278</b>
<b>ON APPLICABILITY OF BLACK-SCHOLES MODEL TO MSE .....</b>	<b>290</b>
<b>ACOUSTIC SIGNAL DENOISING BASED ON ROBUST PRINCIPAL COMPONENT ANALYSIS .....</b>	<b>300</b>
<b>INVESTIGATION OF EFFICIENCY ASPECTS IN 3×3 PHOTOVOLTAIC PLANT USING MODEL OF SHADING .....</b>	<b>309</b>
<b>PROGRESS OF NO-INSULATION HTS MAGNET DEVELOPMENT TOWARDS ULTRA-HIGH MAGNETIC FIELD GENERATION.....</b>	<b>319</b>
<b>GRID-CONNECTED HYBRID PV SYSTEM WITH BATTERY STORAGE.....</b>	<b>326</b>
<b>INVESTIGATION ON STABILITY OF PANCAKE COILS WOUND WITH BUNDLED MULTIPLE REBCO CONDUCTORS .....</b>	<b>336</b>
<b>ON-LINE МУЛТИМЕДИСКИ ОБРАЗОВНИ КАРТИЧКИ .....</b>	<b>343</b>
<b>АЛГОРИТАМОТ „ВЕШТАЧКА КОЛОНИЈА НА ПЧЕЛИ“ .....</b>	<b>352</b>





## ASSESSING DIGITAL SKILLS AND COMPETENCIES OF PUBLIC ADMINISTRATION AND DEFINING THEIR PROFICIENCY LEVEL INVITED LECTURE

**Bekim Fetaji<sup>1</sup>**

<sup>1</sup>Mother Teresa University, Informatics, North Macedonia, (Bekim.fetaji@unt.edu.mk)

### Abstract

*The focus of the research study is on analyses, assessment and evaluation of the digital skills and competencies of administration and defines their proficiency levels in order to offer a solution for a better development in administrative work. Every individual is meant to have a certain level of proficiency in digital skills. However, the current education system has fallen short of providing our future generations with the basic understanding of what it takes to succeed in a digital environment. The goal of this paper is to assess the digital skills and competencies of administration and define their proficiency levels. Depending on their findings, the study suggest recommendation and ways by which universities can improve on their curriculum so that students are better equipped when they enter the workforce. Digital competency is a term used to describe the skills and knowledge required to be digitally literate. Given the widespread use of digital technologies across the administration, competencies are needed to properly drive the digital change. Technologies are increasingly complex, diverse and with a fast-paced evolution that requires governments to increase efforts to keep the skill sets of public officers updated, but also to anticipate the needs associated with emerging change. This assessment in the form of strategic digital skills from an educational viewpoint is an essential measurement of the required skills of the future workforce.*

**Key words** Digital Skills, Assessment, Public administration proficiency, digital competences

### 1. Introduction

The internet and other digital technologies have changed our lives dramatically. Nowadays, we feel like we can't escape the digital world and its influence on our daily life. Digital literacy is a part of our everyday life. It helps us communicate with others, find information, solve problems and much more.

Digital literacy is not just about knowing how to use computers or smartphones - it includes many different skills such as using social media networks or using mobile payment apps, knowing how to create content online, understanding cybercrime and safety issues etc.

Peter Drucker is famously quoted as saying, "You can't manage what you can't measure." Drucker's axiom according to [1] embodies the recent spike in efforts to define, measure and assess digital skills — steps essential toward building and managing a digitally skilled workforce.

The main skills that all adults should have so that we can safely and effectively take part in digital life.

Digital literacy is a set of skills and competencies which enable people to use digital technology in ways that create value for themselves and others. The following will assess the digital skills and competencies of administration and define their proficiency levels. Digital literacy can be assessed to determine the proficiency levels of an individual. The assessment



should measure the digital literacy skills and competencies, identify gaps in knowledge and recommend ways to fill them.

The assessment should be conducted by professionals who are knowledgeable in the field of digital media communication, learning design, educational assessment or instructional design.

Digital skills and proficiency, which are fundamental for human development [2], have been a matter of intense debate for decades. The proficiency levels of the digital skills depend on how well it applies to an individual’s work.

Any knowledge worker in today’s world needs to have a basic proficiency in digital skills as discussed by [3]. And this is not just true for administration but also for college graduates but also for high school graduates. Digital skills and proficiency, which are fundamental for human development, have been a matter of intense debate for decades. The proficiency levels of the digital skills depend on how well it applies to an individual’s work. Any knowledge worker in today’s world needs to have a basic proficiency in digital skills. And this is not just true for college graduates but also for high school graduates. Digital skills and competencies are essential for today's workforce in order to meet the needs of an ever-changing digital environment.

Digital literacy is a vital skill for all professionals, but it is especially important for administration professionals because their jobs focus on day-to-day operations within a business. This means that they need to be able to read and understand instructions, instructions, and manuals written in digital formats. They also need to know how to use different software programs and applications that are prevalent in the workplace.

An assessment of digital skills should take into account five different levels: foundation, intermediate, advanced, specialized, and professional. It should also include a variety of tasks relevant to the individual’s job responsibilities such as using email, using social media platforms like Facebook or Twitter, or creating documents with different word processing. There are many different ways to assess the digital skills of an administration. However, it is difficult to define their proficiency level based on these assessments.

2. Literature review

Digitalization has been identified as the most significant technological trend according to [6] that is changing, society, education and business [4]. Nowadays, firms are constantly under pressure to use digital technologies and to adapt their business models to this new reality [5].

On June7th, 2021, a search was conducted using Google Scholar citation database of peer-reviewed literature. The initial search criterion was based on the word “digitalization in administration “in the article titles. The initial search revealed 56,700 documents, which included journal articles in the English language to enable interpretation. Table1presents an overview of the review process.

Table 1 . Literature Review

Google Scholar database		Documents
Search term “Digitalizationin administration”	All fields	56627
	Title-Abstract-Keywords	43954
	Article title	7441
Language	English	2218
Source type	Journal	1572
Document type	Article	1442

Self-assessment surveys can easily be added to existing surveys or other large-scale sampling measures. The ITU and Eurostat (Eurostat) are examples of organizations incorporating self-report surveys as part of their larger data collection process. The total number of specific skills questions is fewer than other methods because the survey covers other topics as well. In the ITU ICT Household Survey Questionnaire, question HH15 raised 9 ICT skills, mainly computer-based skills, covering basic and intermediate skills, and a computer programming question [7]. The rest of the survey covers other problems of access and use of ICT. Eurostat has developed a digital skills indicator based on in DigComp [8]. A person reports if they have performed various activities in the four competency areas: information skills, communication skills, problem-solving skills, and software skills. A person's score is "no ability", "low", "basic" or "higher than basic" [9]. The use of the Eurostat digital skills measurement standard has items restricted to European countries.

Other evaluations are implemented as independent investigations. Digital Skills to Tangible Outcomes (DiSTO) was originally built and verified in the UK and in the Netherlands [10]. Recently, through association, these surveys have been used as part of specific research projects in Australia, Chile, Brazil, Uruguay, and the United States (London School of Economics and School of Political Science, date unknown). DiSTO uses the Likert scale, which covers mobile and online skills. Another survey developed as part of the research project is the ICT Skills Index (ISI). This online survey using the Likert scale asked 4,444 advanced ICT skills in young people aged 16-35 in small island developing States [10].

..

### 3. Devising Public Administration Profficiency Levels

Based on a comparison framework for curriculum and competencies conducted by [6] and the number of categories covered in total by these frameworks and curriculums, it can be concluded that the following four categories cover the most relevant skills and competencies required to make use digital technologies adequately.

**Communication and collaboration.** In terms of communication, it includes exchanging information with the other users on digital platforms using various strategies to collaborate, share, and communicate.

**Digital content creation.** The category of creation includes engaging in digital spaces to design, create, and revise online content.

**Privacy and Security.** Include the key functions comprised of maintenance of practices to secure digital identity, recognize threats, and understand the broader safety implications of working in a digital environment.

**Information and data literacy Skills.** The category of information skills includes the required skills to apply, evaluate, and manage information across digital and physical environments.

**Problem solving** - To identify needs and problems, and to resolve conceptual problems and problem situations in digital environments

Table 2. **Digital Skills Profficiency Levels**

Levels	Levels expressed in number	Complexity of Tasks	Aythonomy	Cognitive Domain
Foundation	1	Simple	With guidance	Remembering
	2	Simple	Guidance and help	Remembering
Intermediate	3	Well defined	Certain Autonomy	Understanding

	4	Well defined	Autonomy on their own	Understanding
Advanced	5	Different tasks	Independent	Applying
	6	Most appropriate	Independent and guide others	Applying
Specialized	7	Resolve complex tasks limited solutions	Integrate contributions	Evaluating
	8	Resolve complex tasks interacting	Integrated solutions	Evaluating
Professional	9	Resolve complex tasks with no delays	Propose new solutions	Creating
	10	Resolve complex tasks multitasking	New creative solutions and ideas	Creating

The assessment will be conducted through a survey at the link (<https://forms.gle/XpzhfEZqJmZaNx6a6>).

The following questions have been set: 1) What type of computing device do you use at work? 2) How often do you use your device? 3) How would you grade your level (1-10) of digital skills? 4) Do you know how to solve problems when using computers or mobile devices? 5) Grade your ability to identify spam, phishing, malware, viruses? 6) Can you troubleshoot your device such as printer, keyboard, mouse, etc.? 7) How would you grade your skills for creating content for a report, essay? 8) Can you evaluate and analyze properly content? 9) Grade your ability to use social media accounts for communication and collaboration? 10) Can you recognize threats in internet?

An example of a lower-level digital skill would be, "Albert can identify how and where to organize and keep track of job ads in a job app on his laptop in order to retrieve them when he needs them." At level 5, an employment example of proficiency would be one’s ability to "use a specialized app (e.g. Photoshop, IBM SPSS), to provide instructions to develop a report to introduce a new procedure, and to resolve issues such as printer would not print and to fix problems with installing the drivers."

#### 4. Outcomes from the pre-research study

A pre-research study was conducted through a survey with 34 administrators in University, whereby the survey was used as an instrument to analyze their skills in the usage of digital platforms, word processing, publishing, communication and collaboration, social media platforms and features.

Within the survey, students were asked to provide the following information:

- The forms of media that administration post on social media platforms. (text, image, etc.)
- The safety level applied to their social media engagement. (private, public, etc.)

According to Figure 1, most of the participants with 66% responded that they use text and image combined while posting, followed by 34% that preferred only images, and 14% use mostly video and audio.

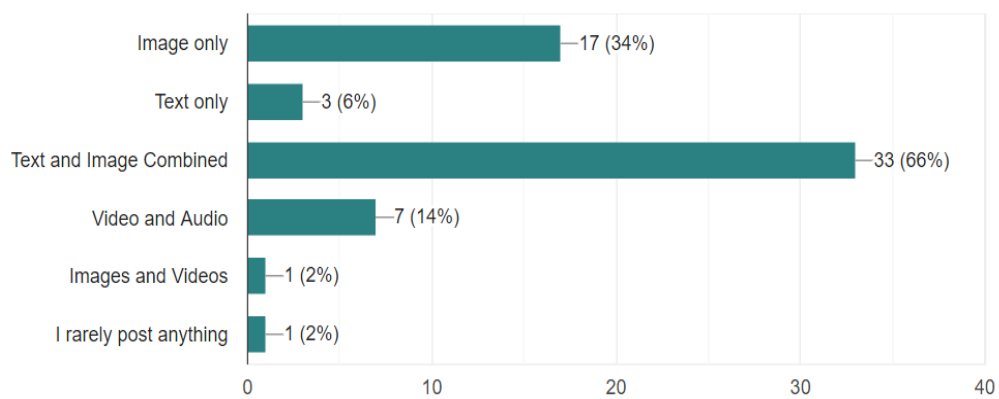


**Fig. 1.** What do you usually use while posting?

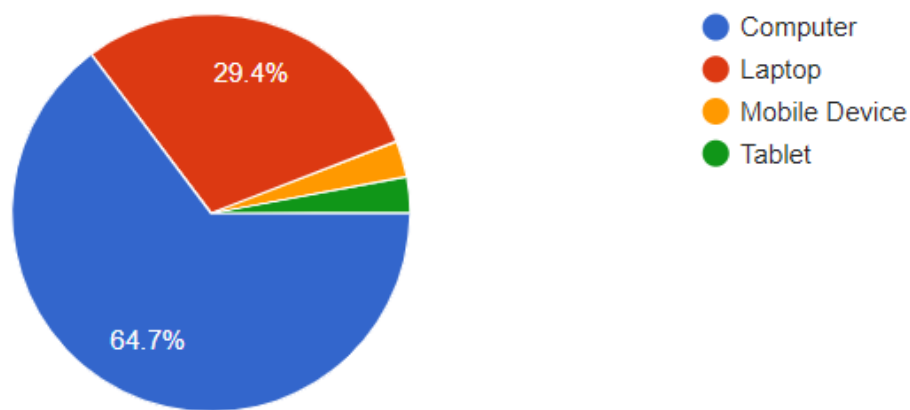


**Fig.2.** What type of computing device do you use at work?

From the feedback can be concluded that most of the participants with 64.7% responded that they use mainly computers, followed by 29.4% that use laptops and 1% using mobile device and tablet.

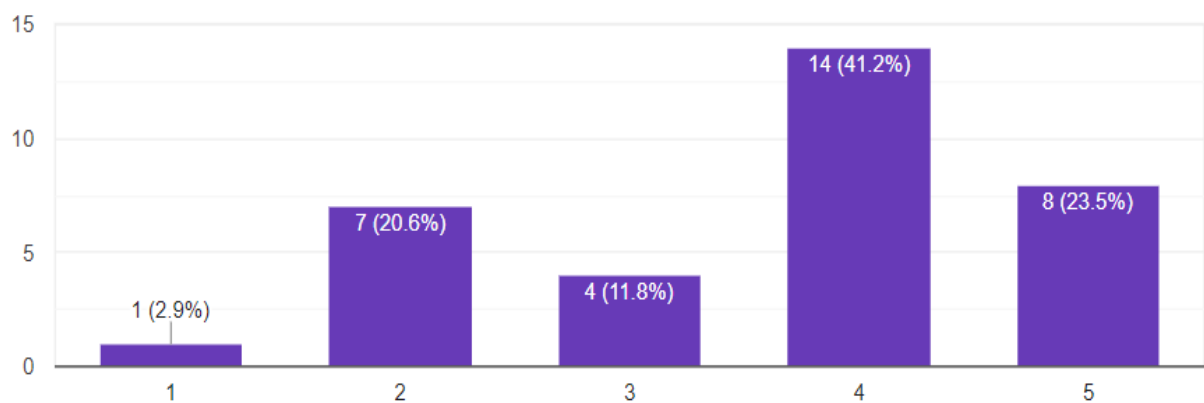


**Fig.3.** How often do you use computing device do you use at work?



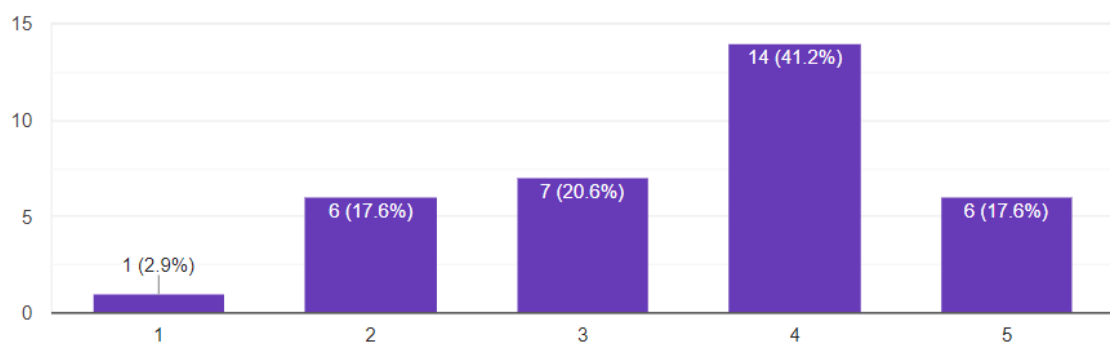


**Fig.4.** Do you know how to solve problems when using computers or mobile devices?

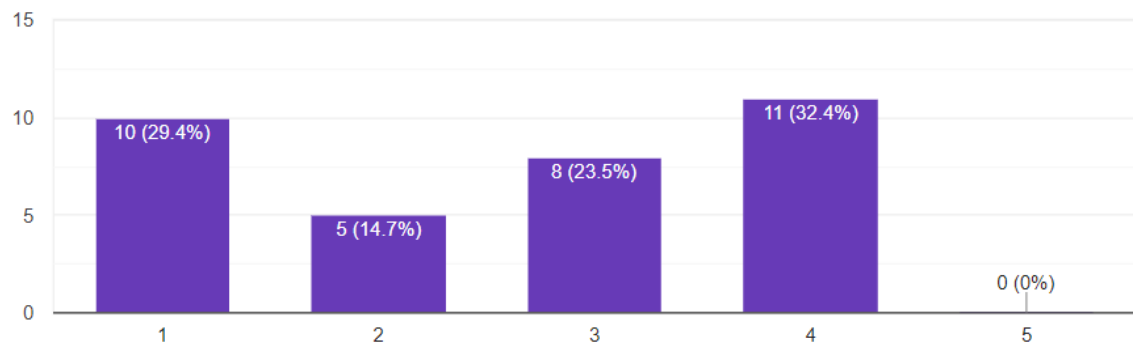


**Fig.5.** Grade your ability to identify spam, phishing, malware, viruses?

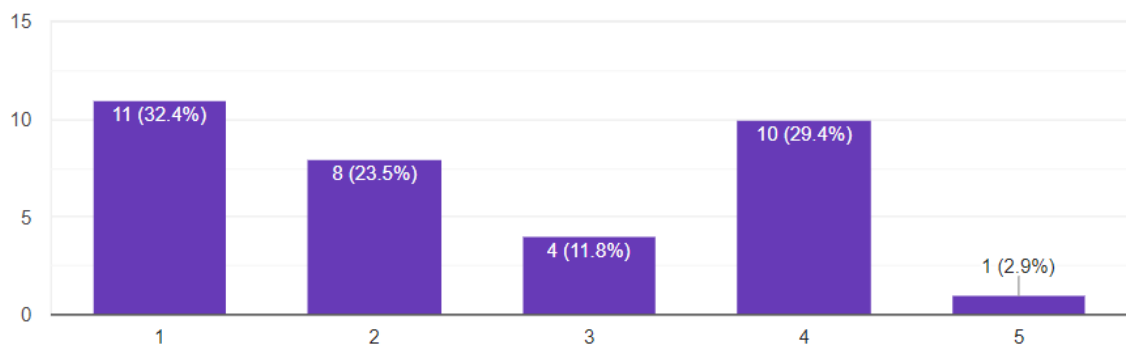


**Fig.6.** Can you troubleshoot your device such as printer, keyboard, mouse, etc.?

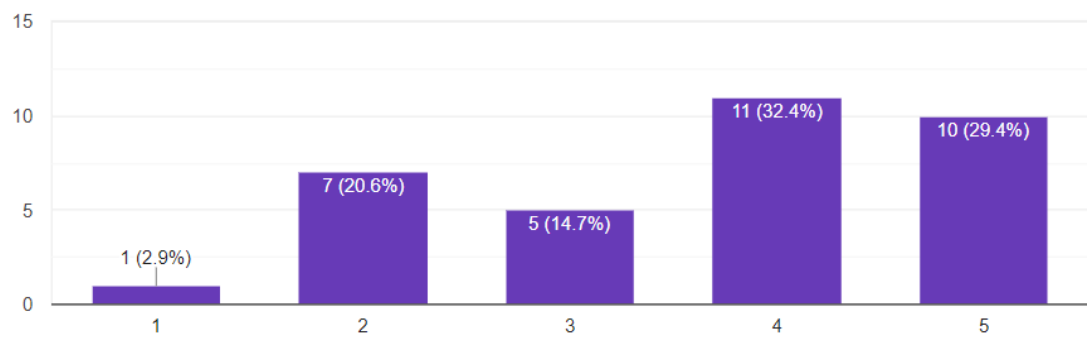


**Fig.7.** How would you grade your skills for creating content?

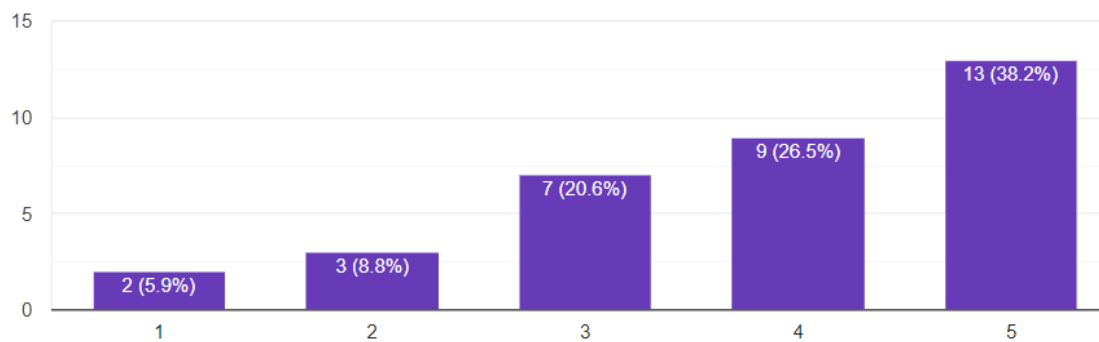


**Fig.8.** Can you evaluate and analyse properly content?

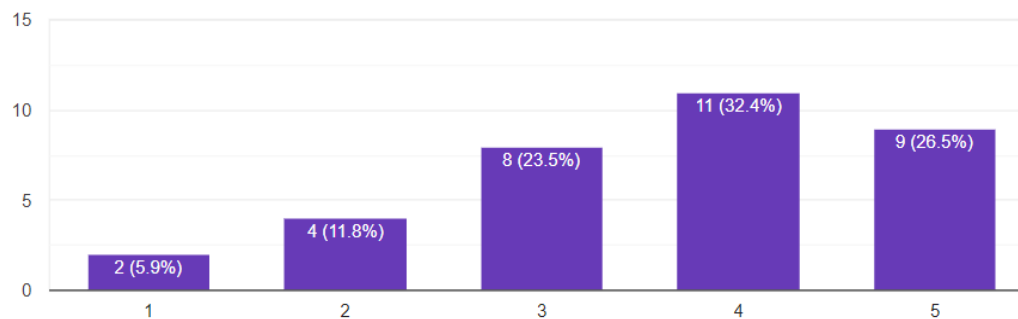


**Fig.9.** Grade your ability to use social media accounts for communication and collaboration?

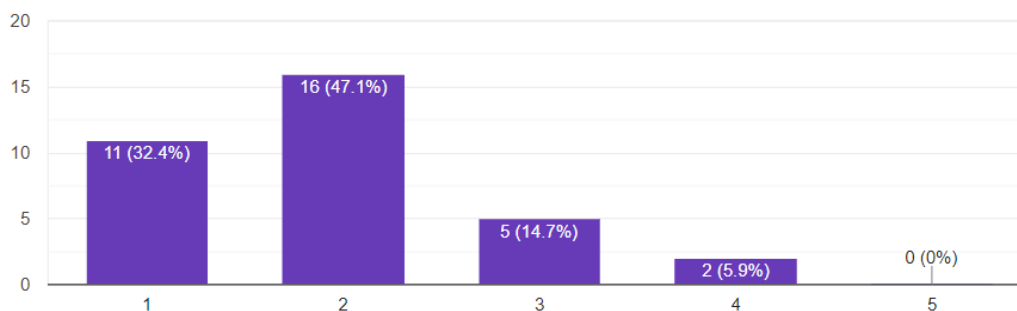


**Fig.10.** Can you recognize threats in internet?

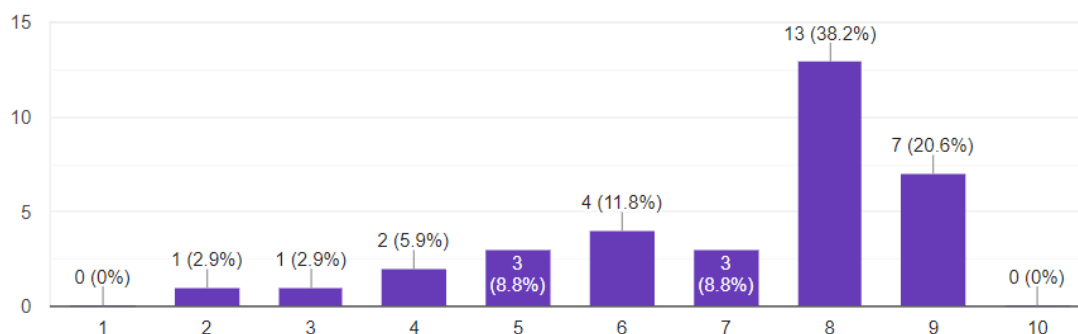


**Fig.11.** How would you grade your level (1-10) of digital skills?

## 5. Results and Discussion

Analyses were further carried out through IBM SPSS Statistics. Descriptive statistics and correlations between variables were firstly calculated. Table 1 shows descriptive statistics, Cronbach's alpha ( $\alpha$ ) and the matrix of correlations of Skills and Competences, which were used to carry out multiple regression analyses. Two multiple regressions were performed on

the digital skills considered as independent variables and subsequently as dependent variables, Time to Finish the Task (TFT), Correctness Level (CL), Number of Errors (NE), Self-Esteem (SE) and Satisfaction (S).

**Table 1.** Multiple regression, Digital Skills and Competences

	Skills			Competences		
	<i>B</i>	SE	β	<i>B</i>	SE	β
<b>Information and data literacy</b>	16.563	4.721		7.635	3.238	
<b>Communication and collaboration</b>	0.153	0.042	0.201**	0.061	0.051	0.131
<b>Privacy and Security</b>	0.217	0.557	0.162	0.003	0.071	0.021
<b>Digital content creation</b>	0.069	0.065	0.024	0.015	0.015	0.036
<b>Problem solving</b>	0.346	0.186	0.115	0.155	0.174	0.128
<b>Time to Finish the Task (TFT)</b>	0.159	0.052	0.203**	0.067	0.052	0.134
<b>Correctness Level (CL)</b>	0.047	0.246	0.032	0.061	0.120	0.075
<b>Number of Errors (NE)</b>	0.046	0.035	0.084	0.045	0.035	0.073
<b>Self-Esteem (SE)</b>	0.304	0.237	0.162	0.007	0.074	0.023
<b>Satisfaction (S).</b>	0.243	0.309	0.063	0.152	0.133	0.143
	<i>R</i> <sup>2</sup> = 0.29			<i>R</i> <sup>2</sup> = 0.139		
	<i>F</i> = 7.13, <i>p</i> < 0.001			<i>F</i> = 3.54, <i>p</i> < 0.01		

\**p* < 0.10, \*\**p* < 0.05, \*\*\**p* < 0.01.

### 6. Conclusion and Future Work

The impact on Digital Skills and Competencies has been analyzed, and insights and results have been provided. Our method shows that finding out whether different ways of participating in these asesement can lead to the realization of Competencies is novel. For this reason, we consider digital skills as a relevant factor. The results show that when young workers have the necessary skills, they tend to establish and maintain strategic relationships to provide critical information and improve their workstatus. This means that young people should know how to identify the correct information to connect with their inner circle to actively plan an activity and to consciously participate in a group to achieve a specific goal. The aim is for them to

know whom to add as friends to their contacts based on the information shared by these people so that when they know how to work together through specialized apps, they get social capital. Having strategic skills can also improve the self-esteem, life satisfaction, and SW of young graduates. This means that when administrator workers acquire the strategic skills necessary to use to achieve specific goals, they feel better because they have a more positive image of themselves. The security that strategic digital skills provide can also encourage them to feel more satisfied with their lives. When young people have these digital skills, it has also been observed that psychosocial variables increase, this variable considers indicators such as social support, perception of support, feelings, business, and community awareness.

## References

1. Kemp, S (2021). Digital 2021: Global Digital Overview. Datareportal.com, published 15 March 2020, <https://datareportal.com/reports/digital-2021-global-overview-report>
2. Commission, E. (2017). New report shows digital skills are required in all types of jobs, <https://ec.europa.eu/digital-single-market/en/news/new-report-shows-digital-skills-are-required-all-types-jobs>
3. Jashari, X., Fetaji, B., Nussbaumer, A., & Gütl, C. (2020, February). Assessing Digital Skills and Competencies for Different Groups and Devising a Conceptual Model to Support Teaching and Training. In International Conference on Remote Engineering and Virtual Instrumentation (pp. 982-995). Springer, Cham.
4. Ahmad, M., Murray, J.: Understanding the connect between digitalisation, sustainability and performance of an organisation. *IJBEX* 17(1), 83–96 (2019)
5. Wedlake, S., Keyes, D., & Lothian, K. (2019). Digital Skill Sets for Diverse Users: A Comparison Framework for Curriculum and Competencies. Available at SSRN 3427252.
7. EC (2014). Measuring Digital Skills across the EU: EU wide indicators of Digital Competence. <https://ec.europa.eu/digitalagenda/en/news/measuring-digital-skills-across-eu-eu-wide-indicators-digital-competence>
8. Eurostat. (n.d.-a). Individuals who have basic or above basic overall digital skills by sex (tepsr\_sp410). Retrieved 25 May, 2021, from [https://ec.europa.eu/eurostat/cache/metadata/en/tepsr\\_sp410\\_esmsip2.htm](https://ec.europa.eu/eurostat/cache/metadata/en/tepsr_sp410_esmsip2.htm)
9. Van Deursen, A.J.A.M., Helsper, E.J. & Eynon, R. (2014). Measuring Digital Skills. From Digital Skills to Tangible Outcomes project report. Available at: [www.oii.ox.ac.uk/research/projects/?id=112](http://www.oii.ox.ac.uk/research/projects/?id=112)
10. Redeker, D. & Sturm, I. (2019). ICT skills in small island developing states: ICT capacity building, economic opportunities and brain drain. *ITU Digital Insights*, 73–84





## PWM OPERATION OF SYNCHRONOUS PERMANENT MAGNET MOTOR

*Vasilija Sarac*<sup>1</sup>

<sup>1</sup>Faculty of Electrical Engineering, University Goce Delcev, email: [vasilija.sarac@ugd.edu.mk](mailto:vasilija.sarac@ugd.edu.mk)

### Abstract

*The paper presents a simulation circuit in Simulink of 2.2. kW synchronous permanent magnet motor, supplied by pulse width inverter (PWM inverter) with two closed control loops per rotor angle and motor current. The various motor operating regimes are simulated at and above the rated speed and with different step loads. The obtained results present the motor normal operation with rated speed and load as well as its operation above the rated speed where the effect of the field weakening can be observed. At higher speeds, the torque is considerably reduced and in the case of rated load at higher speeds, the motor cannot maintain the synchronism. Besides motor speed, motor current, torque, and output voltage from the inverter can be analyzed, from the simulation results. The analysed control scheme is useful for the analysis of motor operation at various speeds.*

### Keywords

*Synchronous permanent magnet motor, PWM inverter, field –weakening*

### Introduction

Synchronous permanent magnet motors (SPMM) have gained popularity due to their outstanding performances such as high efficiency and power factor considerable higher than at their main competitor-three phase squirrel cage asynchronous motor. Their main drawback is the inability to direct start with the power supply from the mains. The development of power electronics has promoted this type of motor as the main competitor of the asynchronous motor, especially at high-speed applications.

The permanent magnet synchronous motor is started with the aid of inverter which also regulates the motor speed in wide operating range. In range above the rated speed (base speed) motor enters the field weakening region where the voltage is limited by the available voltage from the inverter. In the same time the induced voltage is proportional to rotor speed while motor torque is proportional to motor current and flux. At low speed, the rated stator current and the rated excitation flux are used to obtain the rated torque. The voltage and the output power, both, rise linearly with the speed. This operating range is referred to as constant-torque or constant-flux region. Above rated speed, the voltage is kept constant and the flux is decreased (weakened). The torque is inversely proportional to the speed increase. As the power is constant beyond the rated speed, this is called constant-power region or field weakening region.

Over the last two decades various control techniques of the inverters have been developed. In [7] a novel field-weakening algorithm which is robust to flux linkage uncertainty is introduced. Field weakening problem is formulated as an optimization problem which is solved online using projected fast gradient method. Based on current research into the mathematical model of the permanent magnet synchronous motor (PMSM) and the feedback linearization theory, a control strategy established upon feedback linearization is proposed in [8]. Compared with three-phase motors, multi-phase motor speed control systems have many advantages, which

make them to have good prospects in many fields, such as the control system of electric vehicle power equipment. In these control systems, it is necessary for the motor to have a wider speed range [9]. Comparison of the operation in field-weakening region of various types of the synchronous motors has been described in [5]. Other authors focus on optimization of the motor itself in terms of improving the efficiency, dynamic characteristics and reducing the cogging torque [1], [2].

The paper presents simulation circuit in Simulink of 2.2. kW synchronous permanent magnet motor, supplied by pulse width inverter (PWM inverter) with two closed control loops per rotor angle and motor current. The various motor operating regimes are simulated at and above rated speed and with different step loads. The obtained results present the motor normal operation with rated speed and load as well as the operation above the rated speed where the effect of the field weakening can be observed. At higher speed the torque is considerably reduced and in case of rated load at higher speeds, the motor cannot maintain the synchronism. Besides motor speed, motor current, torque and output voltage from the inverter can be analysed, from the simulation results. The analysed control scheme is useful for analysis of motor operation at various speeds. The model is universal and can be used for arbitrary synchronous permanent magnet motor by inputting the adequate motor parameters. Further research should be focused on improving the distortion of the motor current from the harmonics, present due to the PWM inverter.

## 2. Methodology and simulation circuit

The synchronous motors have been known for high efficiency and power factor which are their main advantages over asynchronous motors. Their main drawback, besides the price, is the inability of self-starting i.e. they require the inverter circuit for starting and operation. A permanent magnet synchronous motor requires a control system, for example, a variable frequency drive.

There are many control techniques implemented in control systems. The choice of the optimal control method mainly depends on the task that is put in front of the electric drive. The main methods for controlling a permanent magnet synchronous motor are shown in the Table 1 [3].

**Table 1 Control strategies of SPMM**

Control				Advantages	Disadvantages
nSinusoidal	Scalar			Simple control scheme	Control is not optimal, nor suitable for tasks with the variable load. Loss of control is possible
	Vector	Field oriented control	With position sensor	Smooth and precise setting of the rotor position and motor rotation speed, large control range	Requires rotor position sensor and powerful microcontroller inside the control system
			Without position sensor	No rotor position control is required. Smooth and precise setting of the rotor position and motor rotation speed. Large control range, but less than with the position sensor	Sensorless field oriented control over full speed range is possible only for PMSM with a salient rotor, a powerful system is required
		Direct torque control		A simple control circuit, good dynamic performance, wide control range, no rotor position sensor is required	High torque and current ripple

Trapezoidal	Open-loop		Simple control scheme	Control is not optimal, nor suitable for tasks where there is a variable load, loss of control is possible
	Closed-loop	With position sensor (Hall sensors)	Simple control scheme	Hall sensor required. There are torque ripples. It is intended for the control of PMSM with trapezoidal back EMF. When controlling PMSM with sinusoidal back EMF, the average torque is lower by 5 %.
		Without sensor	A more powerful control system required	

Source: <https://en.engineering-solutions.ru/motorcontrol/pmsm>

In this paper a 2.2 kW motor with sinusoidal back EMF is analyzed in Simulink with the aid of simulation circuit presented in Fig. 1.

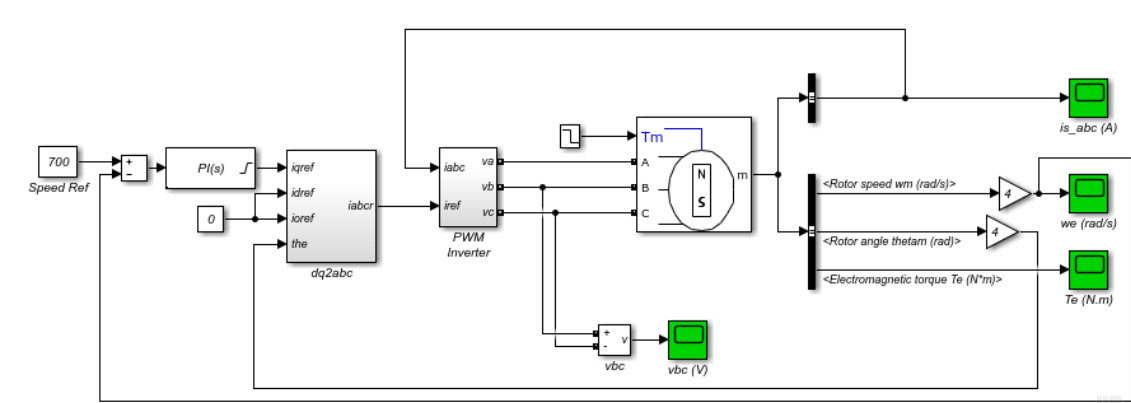
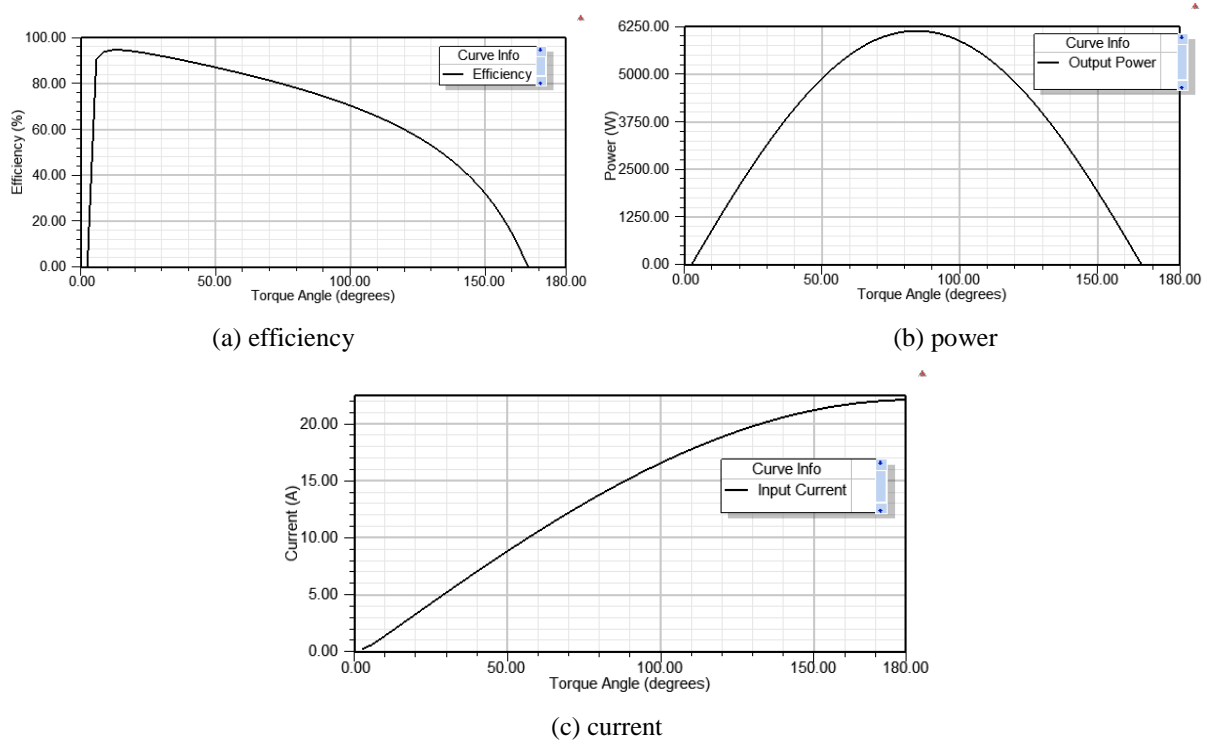


Fig. 1. Synchronous permanent magnet motor fed by the inverter

The motor data are presented in Table 2. They are based on analytical calculations of the motor. Besides motor data also the steady-state characteristics of efficiency, current and output power are presented in Figure. 2. The data presented in Table 2 and Fig. 2 can serve for the verification of the obtained results by the simulation circuit in Simulink.

Table 2 Data of PMSM

Parameter	Value
rated power (W)	2,200
rated current (A)	3.56
rated speed (rpm)	1,500
efficiency (%)	93.7
power factor (/)	0.99
torque angle (°)	18.5
no-load current (A)	0.3



**Fig. 2. Steady-state characteristics of efficiency, power, and current**

The simulation circuit has two control loops. The inner loop regulates the motor's stator currents. The outer loop controls the motor's speed. The reference speed is set at the input of the PWM inverter. The motor model has a round type of rotor with sinusoidal back EMF. The EMF and the flux density of the motor are presented in Fig.3. The load is applied to the motor and in this model the step load is used. As an output from the simulation circuit the motor speed, current and torque are obtained. By setting the values of reference speed and of the step load various operating regimes can be simulated i.e. with rated speed and above the rated speed combined with various step loads.

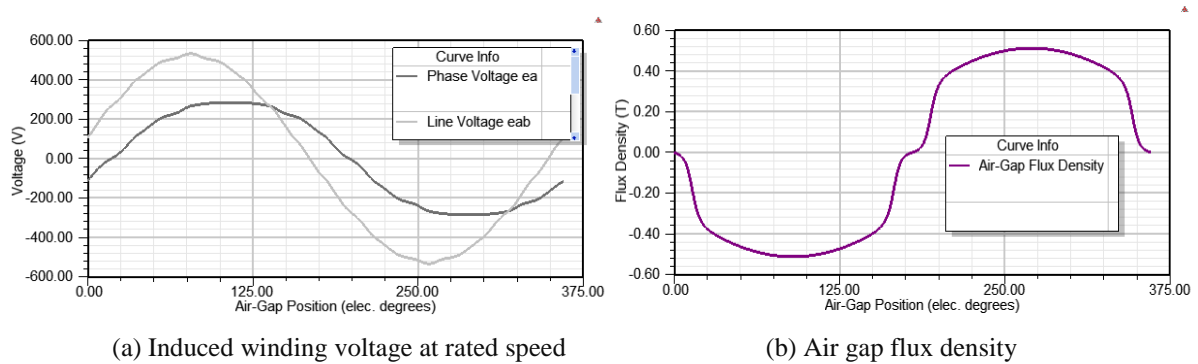


**Fig. 3. Back EMF and air gap flux density of analyzed motor**

### 3. Results and discussion

#### 3.1 Operation with a rated speed

Firstly, the simulation model is set for operating with the rated speed (i.e. 1,500 rpm or 157 rad/s). The motor operates with step load, i.e. 0.35 seconds after the acceleration has finished the step load of 14 Nm is coupled to the motor shaft. The presented Simulink model in Fig.1 is universal and can be easily adapted to any synchronous motor with round type rotor by inputting parameters of the stator winding (resistance and inductance) as well as a number of pair of poles and moment of inertia. The obtained results of motor speed, torque, and current

at step load of 14 Nm is presented in Fig. 4. As expected, the motor accelerates and reaches the synchronous speed of 157 rad/s at 0.15 seconds. After 0.35 seconds the step load of 14 Nm is applied to the motor shaft. The motor continues to operate with synchronous speed without losing the synchronism. The motor torque after the acceleration drops down to the no-load torque and quickly increases again to the rated torque of 14 Nm when the step load is coupled to the motor shaft. Similar behavior can be observed in the transient characteristic of motor current, the current decreases to the no-load current (0.26 A for the analyzed motor) and later quickly rise again to the rated current (app. 3.5 A rms value) when the rated load is applied to the motor shaft. Obtained results of current from simulation model correspond to the presented data in Table 1.

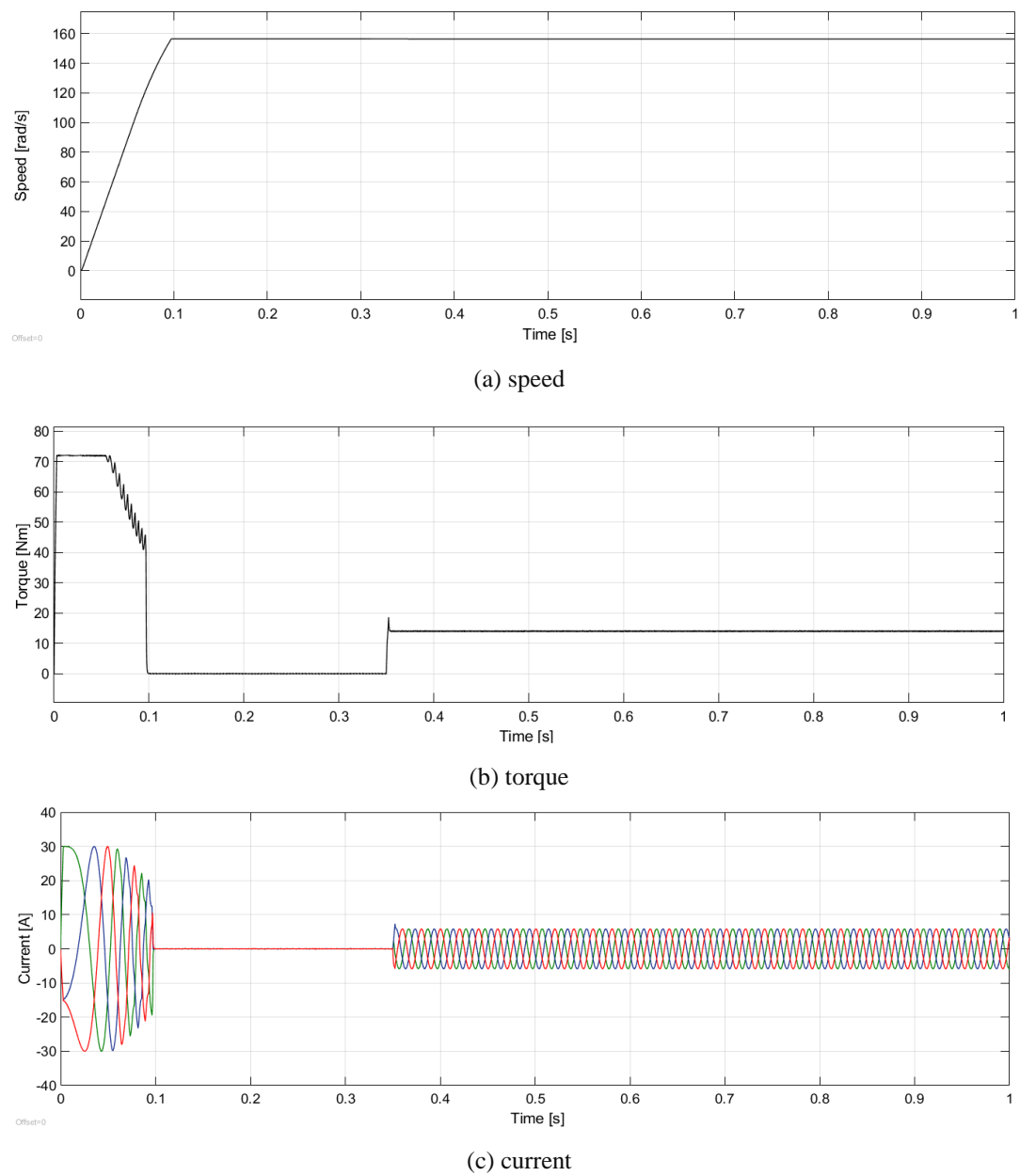


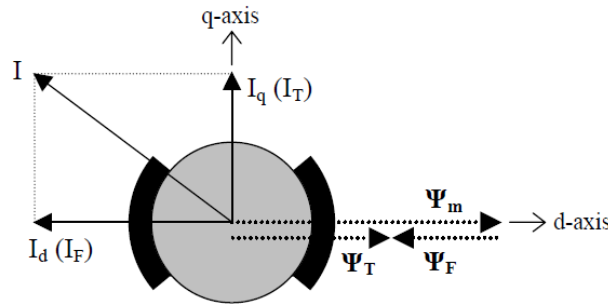
**Fig. 4. Transient characteristics at rated speed and with a step load of 14 Nm**

### 3.2 Operation above rated speed

Permanent magnet synchronous motors have a single stator winding which generates a current phasor  $I$ . This current phasor can be split into the two components along the d- and q-axis,  $I_d$  and  $I_q$  [4].

$$I = \sqrt{I_d^2 + I_q^2} \quad (1)$$

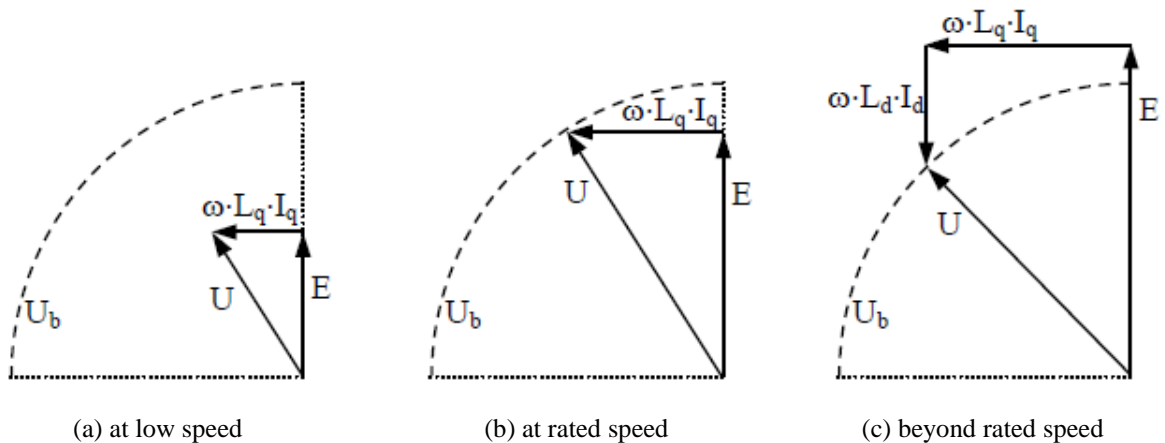
However, in permanent magnet machines, the flux is produced by permanent magnets, thus the magnetic field (excitation) or magnetic flux cannot be controlled by varying the field current. The permanent magnets are considered as “fixed excitation flux” sources  $\Psi_m$ . Therefore, control of the excitation field (flux control or field-weakening) is achieved by introducing an opposing field  $\Psi_F$  against the fixed excitation from the permanent magnets. It is achieved by injecting a negative d-current  $I_d$  (or field current  $I_F$ ), as shown in Fig. 5 [4].



**Fig. 5. Transient characteristics at rated speed and with step load [4]**

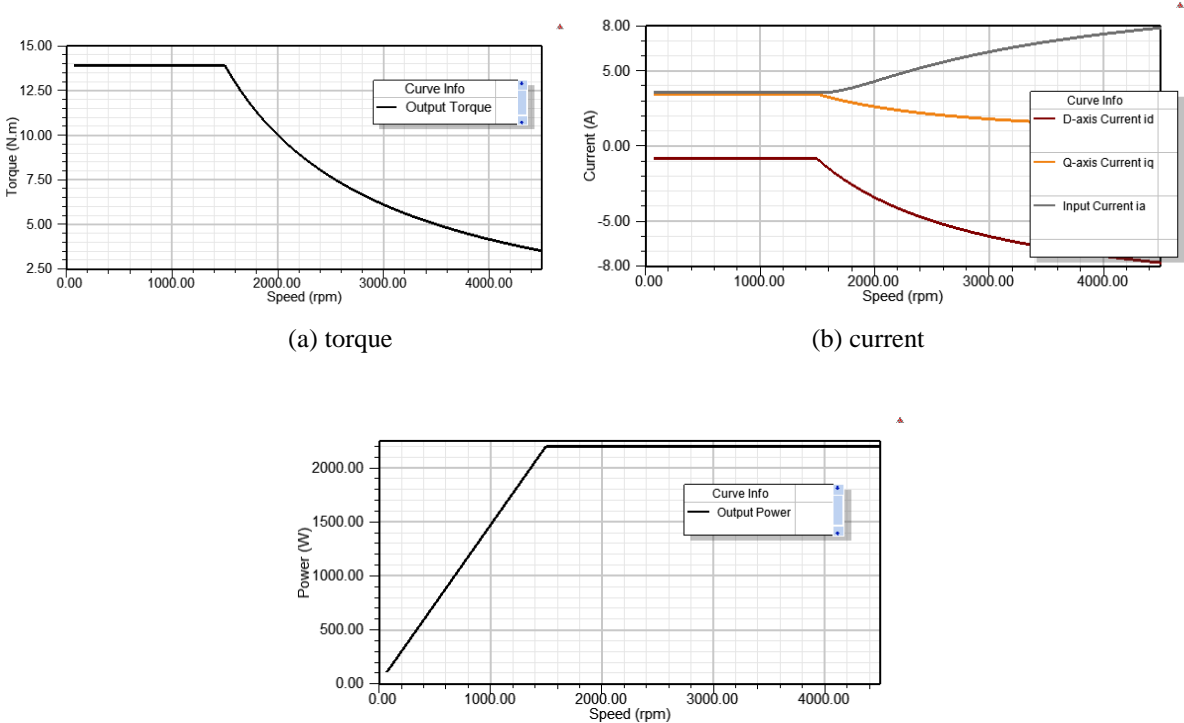
Figure 6 (a) shows the voltage phasor diagram when the motor is running at a low speed well below the rated speed. When the motor is operated at rated conditions, as shown in Figure 6 (b), it can be noted that the voltage vector is on the voltage limit contour (maximum voltage  $U_b$ ). It is virtually impossible to increase the speed by keeping a current  $I$  along the q-axis once the induced voltage  $E$  equals the rated voltage.

To increase the speed beyond this limit, the current phasor should be rotated towards the negative d-axis (introduction of a negative d-axis current  $I_d$ ). Figure 6 (c) shows that the voltage vector  $U$  is kept within the voltage limit [4].



**Fig. 6. Voltage phasor diagram of PMSM [4]**

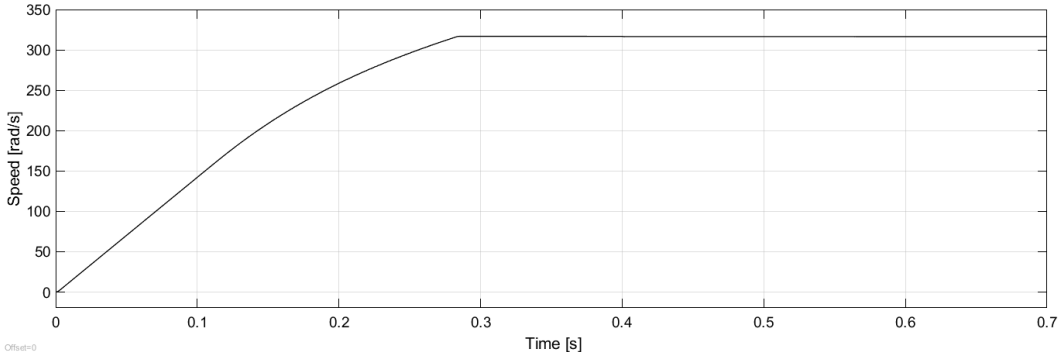
For the analyzed motor beyond the rated speeds of 1,500 rpm or 157 rad/s, the effect of field weakening is present, and the torque decreases as the motor speed increases to maintain the constant power. The effect of the field weakening for the analyzed motor is shown in Fig.7. It is based on the analytical calculation of the motor in the program Ansys and predicts the motor behavior and operation above the rated speed in terms of the steady-state characteristics.



**Fig. 7. Characteristics of torque, speed, and power of the analyzed motor in field weakening operation**

In the Simulink circuit, the motor speed is set to 314 rad/s. The step load of 7 Nm is coupled to the motor shaft 0.3 seconds after the start of the motor. The obtained characteristics of torque, speed, and current are presented in Fig. 8. The motor can maintain synchronism with a load of 7 Nm at 314 rad/s speed or 3,000 rpm. According to Fig. 7 (a), the torque reduction in the field weakening region at 3,000 rpm is at 6 Nm. The obtained result of torque from simulation differs slightly from the analytical result of 6 Nm. This is due to the simulation circuit in which the obtained torque is electromagnetic torque, slightly bigger than motor output torque presented in Fig. 7 (a). The result of current obtained from Simulink is within the expected value of 7 A rms value. A similar result is obtained for Fig. 7 (b) where at 3,000 rpm the motor current is 7 A. Obtained results from Simulink are in good agreement with the results from the analytical calculation of the motor (steady-state characteristics).

Finally, the step load of 8 Nm is applied to the motor shaft and the obtained results are presented in Fig. 9. As can be seen from Fig. 9 because of flux weakening, the motor cannot operate under this load, i.e. the motor losses the synchronism (Fig. 9).





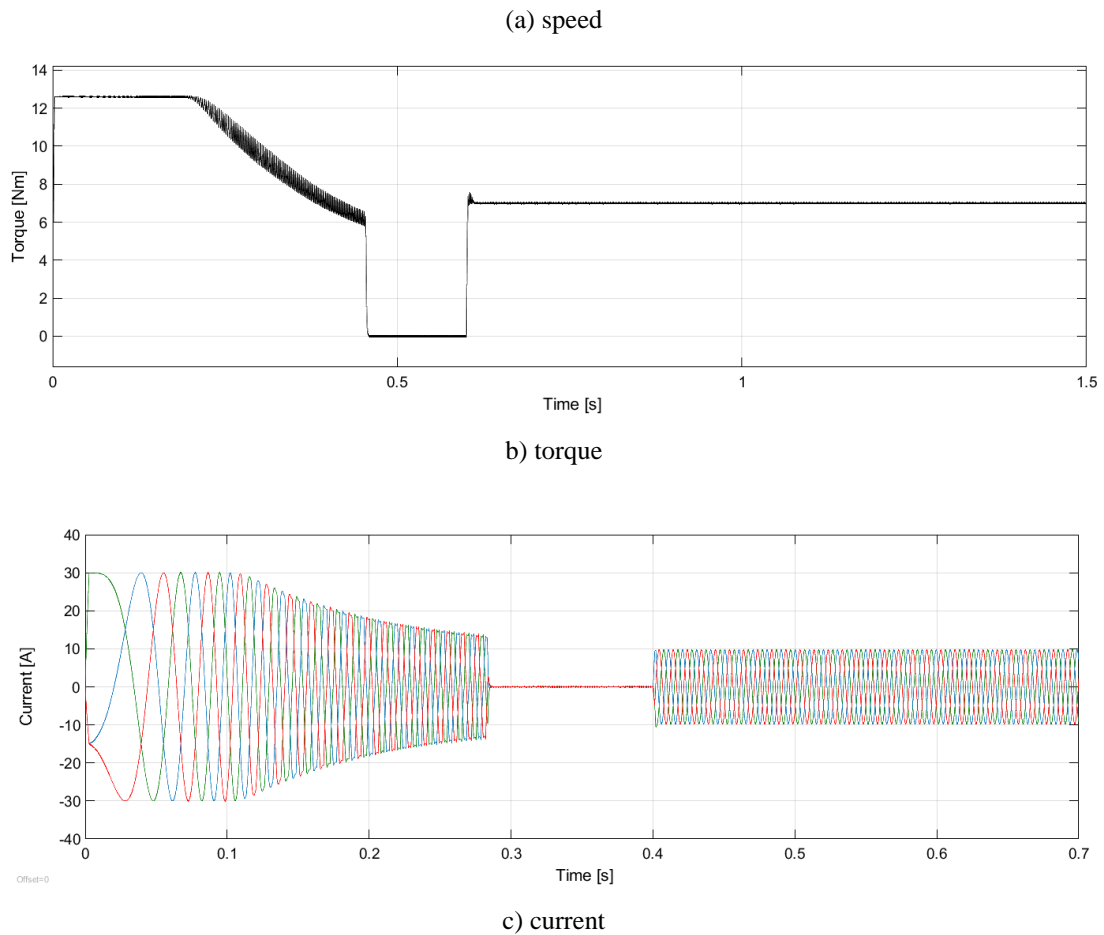


**Fig. 8. Transient characteristics beyond the rated speed and with a step load of 7 Nm**

The stator currents are quite "noisy," which is expected when using PWM inverters. The noise introduced by the PWM inverter is also observed in the waveform of torque. However, the motor's inertia prevents this noise from appearing in the motor's speed waveform [5].

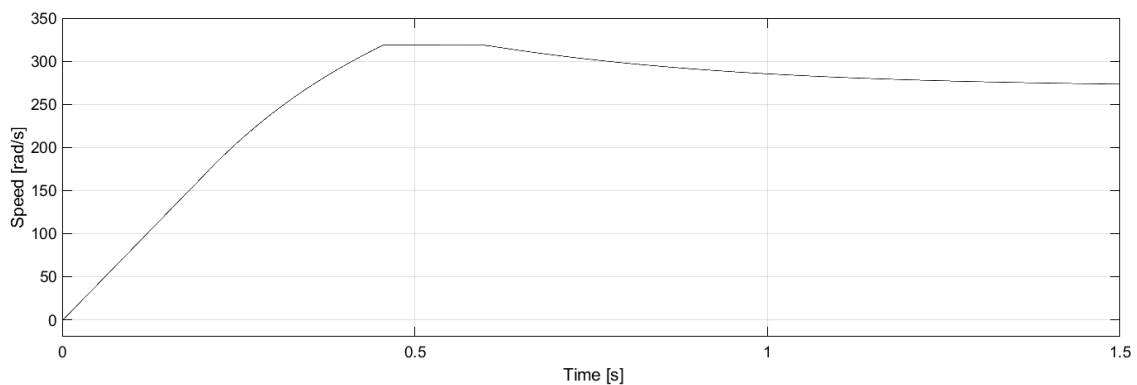


**Fig. 9. Loss of synchronism at 8 Nm due to field-weakening**

## Conclusions

The synchronous permanent magnet motor with embedded or surface-mounted magnet always operates together with the inverter, used for motor starting but also motor operation with variable speed. Up to the rated speed, the motor operation is determined by the rated parameters of the motor. Beyond the rated speed, the effect of field weakening decreases the motor torque and the motor enters the so-called region of operation with constant power. As the speed increases, to maintain constant power, the motor torque decreases.

The paper also illustrates the operation of synchronous motor with inverter at rated speed and above it. Above the rated speed, motor enters the field weakening region which can be observed from the reduced capability of the motor to operate under various loads. The obtained transient characteristics of speed torque and current determine the motor dynamic behavior at two different speeds and with various step loads applied to the motor shaft. The obtained transient characteristics (i.e. values of current, speed and torque) are compared with motor data from the analytical calculation (steady-state characteristics) and this comparison shows reasonable agreement between both methods. The used simulation circuit from Simulink is universal and can be easily adapted to any synchronous motor by entering the adequate motor parameters. It is a useful tool in analysis of motor dynamics.

Further research should be focused on improvement of harmonic content and elimination of harmonics present in motor current due to the power supply from the inverter. Often, they are the source of additional losses and overheating of the motor which makes the operation of the synchronous motor with the inverter more complex and increases the operational costs.

## References

- [1] Baek, Soo-Whang / Lee, Sang Wook: “Design Optimization and Experimental Verification of Permanent Magnet Synchronous Motor Used in Electric Compressors in Electric Vehicles”, *Applied Sciences*, 10 (3235), 2020, pp. 1-16.
- [2] He, Ren/ Han, Qingzhen: “Dynamics and Stability of Permanent-Magnet Synchronous Motor”, *Mathematical Problems in Engineering*, Volume 2017, 2017, pp. 1-8.
- [3] Levkin Dimitry: “Permanent Magnet Synchronous Motor”, *Engineering Solutions*, 2021, available at: <https://en.engineering-solutions.ru/motorcontrol/pmsm>
- [4] Meier, Stephan: “Theoretical design of surface-mounted permanent magnet motors with field weakening capability”, *Master Thesis*, Stockholm, 2002.
- [5] Mathworks, Matlab 2018b
- [6] Soong, Wen L. / Ertugrul, Nesimi: “Field-Weakening Performance of Interior Permanent-Magnet Motors”, *IEEE Transactions on Industry Applications*, 38 (5), 2002, pp. 1251-1258.
- [7] Jerčić, Tino, et al: “Constrained field-oriented control of permanent synchronous machine with field-weakening utilizing a reference governor”, *Automatika*, 58(3), 2017, pp. 439-449.
- [8] Zhou, Kai et al “Field Weakening Operation Control Strategies of PMSM Based on Feedback Linearization” *Energies*, 12 (4526), 2019, pp 1-18.
- [9] Zhu, Jianguang / Chu, Xu: “Research on Control Methods of Six-phase Permanent Magnet Synchronous Motor”, *IOP Conf. Series: Materials Science and Engineering*, 790, 2020, pp 1-7.



## SPEED REGULATION OF INDUCTION MOTOR WITH PWM INVERTER

*Vasilija Sarac, Goce Stefanov, Dragan Minovski*

<sup>1</sup>Faculty of Electrical Engineering, University Goce Delcev, email: [vasilija.sarac@ugd.edu.mk](mailto:vasilija.sarac@ugd.edu.mk); [goce.stefanov@ugd.edu.mk](mailto:goce.stefanov@ugd.edu.mk); [dragan.minovski@ugd.edu.mk](mailto:dragan.minovski@ugd.edu.mk)

### Abstract

*This paper presents the speed regulation of a 2.2 kW asynchronous squirrel-cage motor, a product of company Rade Koncar, with the aid of a voltage inverter controlled by the pulse-width modulation principle. The simulation circuit is developed in software Powersim. The exact motor data are input in the simulation model and the operation of the motor is simulated for various operating frequencies of the inverter. As an output, the transient characteristics of speed, current, and torque are obtained at various operating speeds i.e. below and above the rated speed of the motor. The effect of the field weakening is observed at higher operating speeds. Obtained results of speed, torque, and currents are compared with the motor data obtained from the analytical model of the motor and data of the manufacturers of variable speed drives, for operating regimes different than the rated. The simulation can serve as an example that proves the theoretical principles of pulse-wide modulation where the desired motor speed is easily obtained with the variation of frequency of modulating signal of the inverter.*

### Keywords

*Asynchronous squirrel cage motor, PWM inverter, field –weakening, transient characteristics*

### Introduction

The development of power electronic and static converters has reshaped the drive technology and has opened a wide field of application for variable speed drives. This is especially important for the asynchronous squirrel cage motors as they have been considered the prime moving force of the industry mainly because they are robust, inexpensive, almost maintenance-free, but with limited capabilities for speed regulation. The voltage inverters and various techniques for speed regulation have made the asynchronous motors an attractive choice in many applications where variable speed of the drive is required.

There are two different inverter control types: scalar (open loop) and vector (open or closed-loop). The scalar control is based on the original concept of a frequency inverter: a signal of a certain voltage/frequency ratio is imposed onto the motor terminals and this ratio is kept constant throughout a frequency range, to keep the magnetizing flux of the motor unchanged. It is applied when there is no need for fast responses to torque and speed commands and is particularly interesting when there are multiple motors connected to a single drive [10]. The control is open-loop and the speed precision obtained is a function of the motor slip, which depends on the load, since the frequency is imposed on the stator windings. To improve the performance of the motor at low speeds, some drives make use of special functions such as slip compensation (attenuation of the speed variation as a function of the load) and torque boost (an increase of the V/f ratio to compensate for the voltage drop due to the stator resistance) so that

the torque capacity of the motor is maintained. This is the most used control type owing to its simplicity and to the fact that most applications do not require high precision or fast responses of the speed control. The vector control enables fast responses and a high level of precision on the motor speed and torque control. The motor current is decoupled into two vectors, one to produce the magnetizing flux and the other to produce torque, each of them regulated separately. It can be open-loop (sensorless) or closed-loop (feedback) [10].

Traditional inverters can be replaced by pulse width modulation (PWM) control Z-source inverter (ZSI) which offers buck-boost operation capability by utilizing shoot-through state and provides less EMI noise [8]. The operation of voltage source inverters can be analyzed for different conduction modes of the switches [1]. Other researchers focused on the simulation of minor deteriorations in the operating conditions of a standard motor controlled from a voltage source drive and whether the worsening condition can be detected at an early stage in the case of the V/f and sensorless vector operating mode of the inverter [3]. Interesting findings regarding transient characteristics of motor speed, current, and torque with various modulation indexes can be found in [5]. Transient characteristics of the induction motor fed by voltage inverter can be simulated in various software and one such example in Matlab/Simulink is analyzed in [4]. Comparison between transient characteristics of the induction motor, fed by the mains and by the voltage inverter, is presented in [2].

This paper presents the transient characteristics of a 2.2 kW three-phase induction squirrel cage motor simulated in V/f control mode in an open control system in Powersim software. The transient characteristics were obtained for various speeds, below, at, and above the rated speed. As the constant V/f ratio was kept, above the rated speed, the effect of the field-weakening can be observed. In addition, the harmonic content of the output voltage of the inverter was analyzed. Finally, the advantages and drawbacks of the operation of the asynchronous motor with a voltage inverter are outlined. The presented simulation circuit is useful for analyzing the operation of asynchronous motors at various operating speeds and estimation of the dynamic behavior of the motor.

## 2. Methodology and simulation circuit

The static converters have been proven to be the most successful and most economical way to control the speed of the asynchronous motors turning the asynchronous motor into the full controllable motor concerning the speed of rotation, i.e. the speed varies linearly with the supply frequency. The torque developed by the asynchronous motor follows the equation below [10]:

$$T = k_1 \phi_m I_2 \quad (1)$$

By neglecting the voltage drop caused by the stator impedance, the magnetizing flux can be found from:

$$\phi_m = k_2 \frac{V_1}{f_1} \quad (2)$$

Where:

$T$  is the torque available on the motor shaft (Nm)

$\phi_m$  is the magnetizing flux (Wb)

$I_2$  is the rotor current (A) which depends on the load

$V_1$  is the stator voltage (V)

$k_1$  and  $k_2$  are the constants and they depend on the material and machine design

$f_1$  is the frequency of the power supply

Considering a constant torque load and by varying proportionally amplitude and frequency of the supplying voltage resulting in constant flux and consequently constant torque, the motor

current remains unchanged. Therefore, the motor provides continuous adjustments of speed and torque concerning the mechanical load. The ratio  $V_1/f_1$  is kept constant up to the motor base (rated) frequency. From this frequency upwards the voltage is kept constant at its base (rated) value, while the frequency applied on the stator windings keeps growing, as shown in Fig. 1 (a).

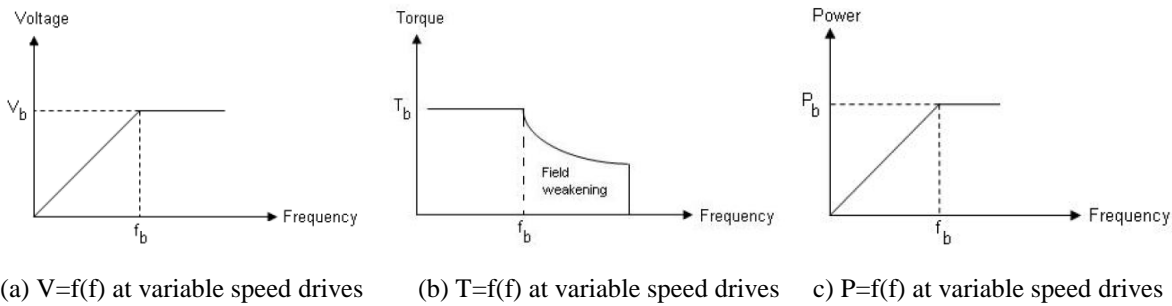


**Fig. 1. Flux, torque, and output power at variable speed drives [10]**

Thereby the region above the base frequency is referred to as field weakening, in which the flux decreases because of frequency increase, causing the motor torque to decrease gradually. The typical torque versus speed curve of an inverter fed motor is presented in Fig. 1 (b). It comes out that torque is kept constant up to the base frequency and beyond this point, it falls (weakening field). Since the power output is proportional to the torque times speed, it grows linearly up to the base frequency and from that point upwards it is kept constant. This is summarized in Fig. 1 (c).

The presented theoretical principles of speed regulation are applied in the simulation circuit of three-phase squirrel cage motor fed by the voltage inverter with rated data, presented in Table 1. The corresponding simulation circuit is presented in Fig. 2.

Table 1 Rated data of the analyzed motor

Parameter	Value
rated power (W)	2200
rated current (A)	5.2
rated speed (rpm)	1355
efficiency (%)	79.4
power factor (/)	0.8
rated torque (Nm)	15.5
locked-rotor torque (Nm)	35.2
locked rotor phase current (A)	21.4

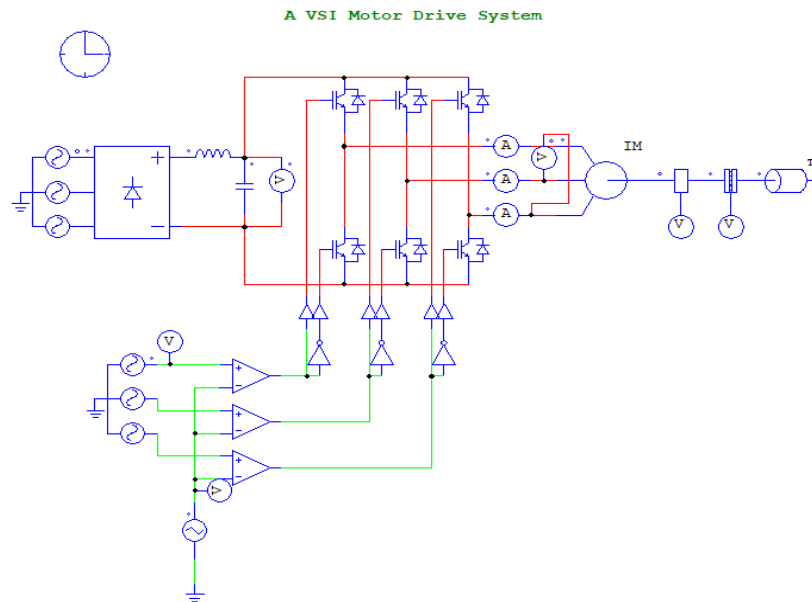
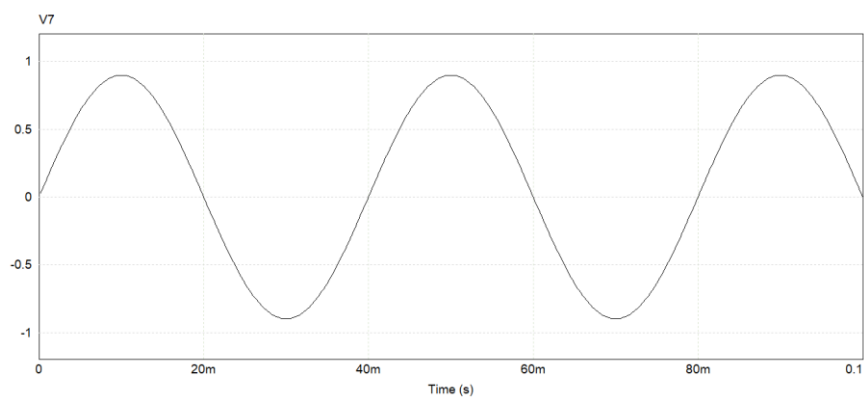
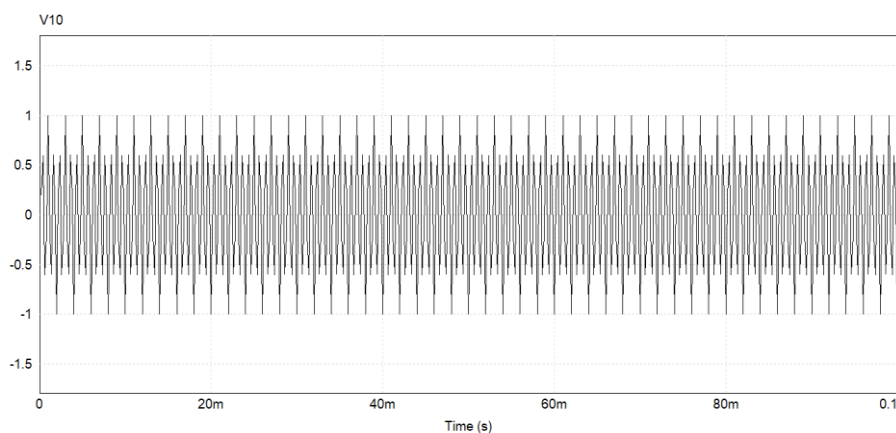


**Fig. 2. Flux, torque, and output power at variable speed drives [6]**

The speed regulation is achieved by the PWM principle of control of conduction period of transistors, determined by the cross-section point of the carrier signal (usually signal in form of a triangle) and modulating sinusoidal signal. By varying the frequency of the modulating signal the various operating speeds of the motor are obtained. Both signals are presented in Fig. 3.



a) modulating signal



b) carrier signal

**Fig. 3. Signals from the control circuit**

The supply voltage from the network is fed to the diode bridge and afterward, the DC link voltage is fed into the inverter. The voltage measured at the DC link is presented in Fig. 4. According to [10], the DC link voltage should be  $1.41V_{in}$  or for an input voltage of 380 V the presented DC link voltage in Fig. 4 satisfies the expected value.

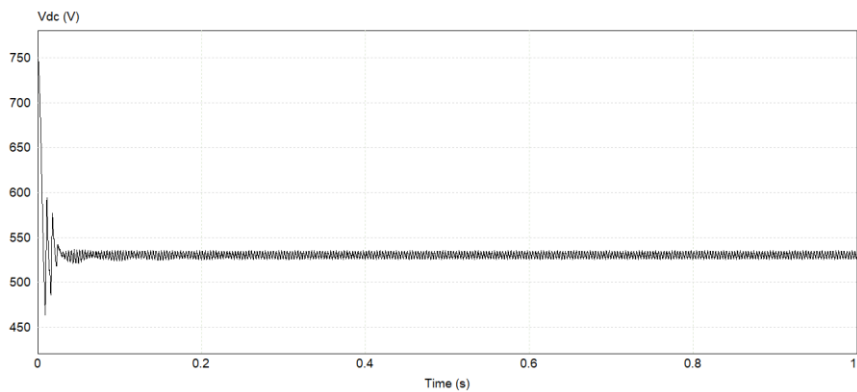
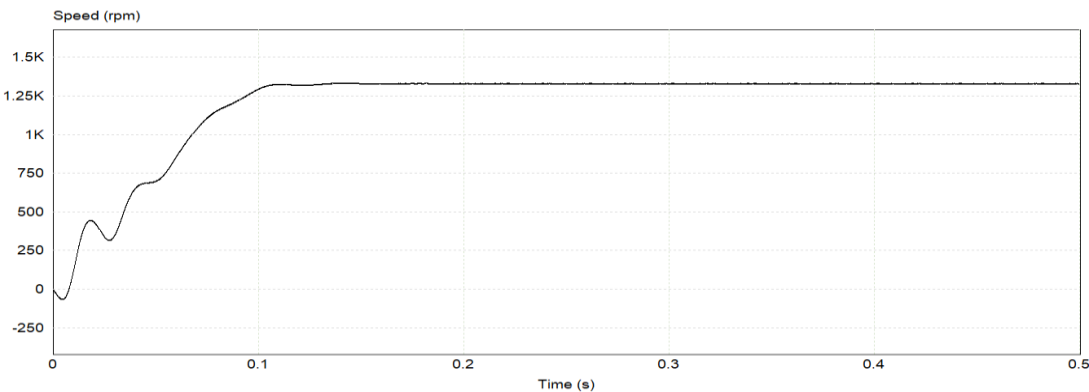


Fig. 4. DC link voltage

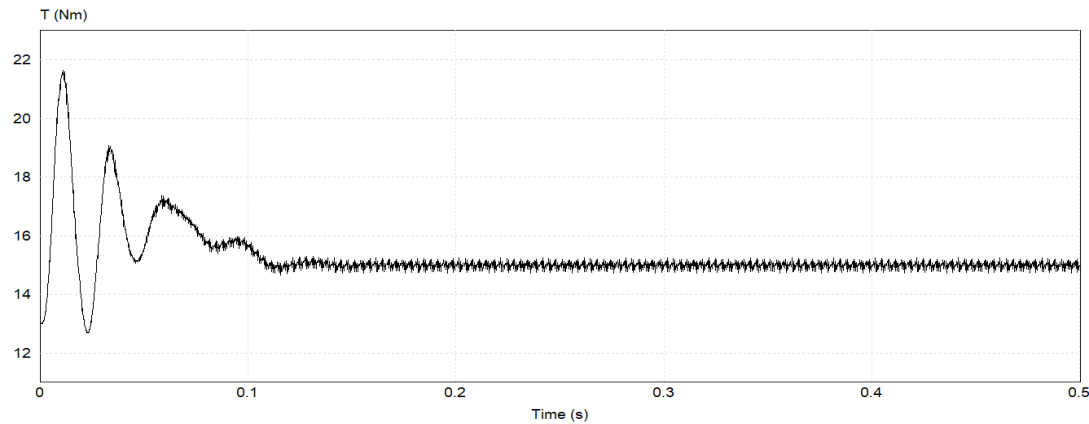
The output voltage from the inverter will be presented in the next section together with its harmonic analysis. Additionally, the speed, current, and motor torque, below, at and over the rated speed will be presented as well.

3. Results and discussion

The motor is constructed for operation with a rated load of 15.5 Nm and a rated speed of 1,355 rpm. Therefore the frequency of the modulating signal is set to the rated frequency of 50 Hz and the motor is loaded with 15 Nm. From the data, presented in Table 1, it can be observed that the motor starting torque is sufficiently large to allow acceleration of the motor with the rated load. The obtained results of the motor speed, torque, and current are presented in Fig. 5.



(a) speed





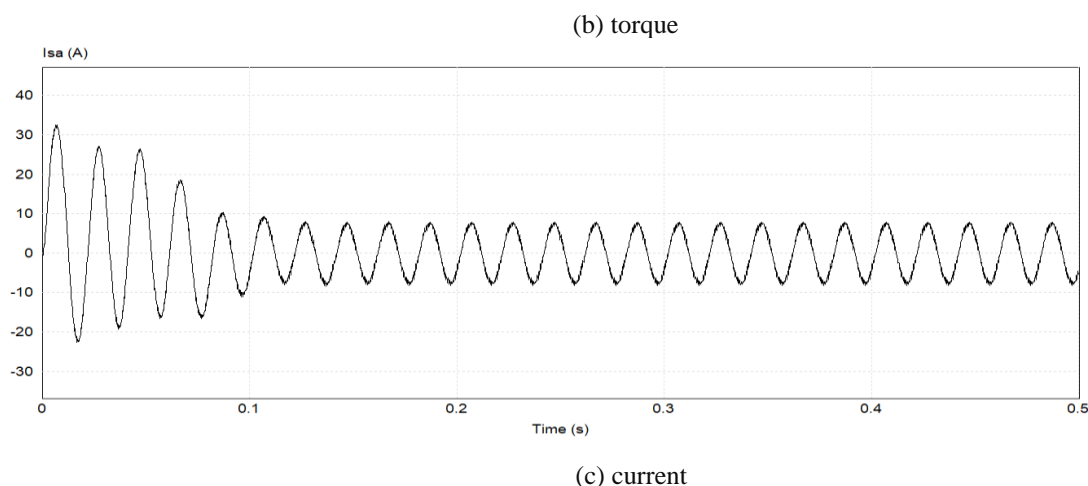
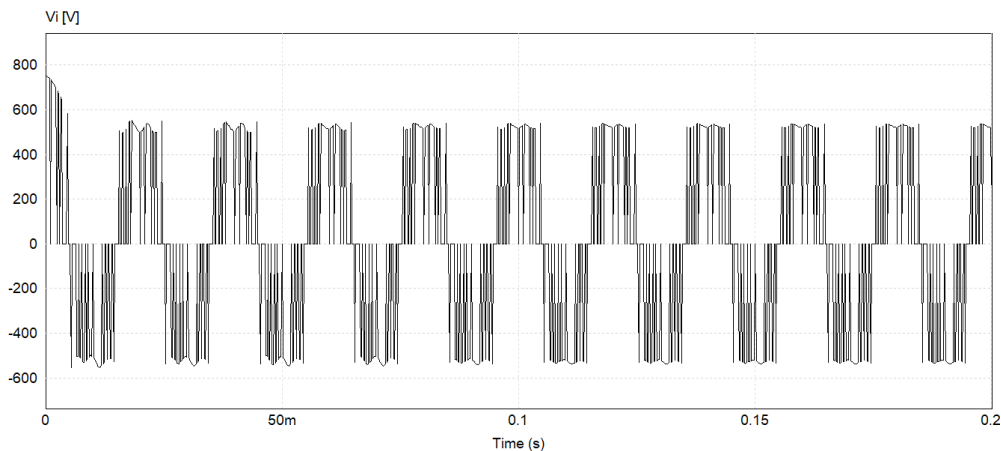
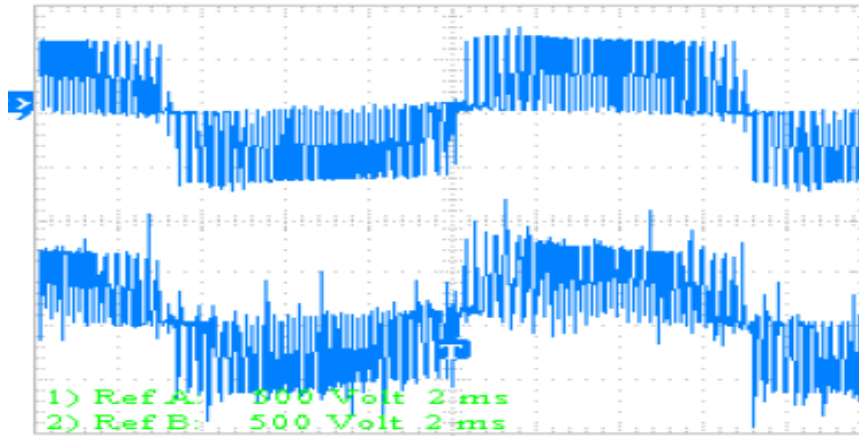


**Fig. 5. Motor characteristics at rated speed (supply with 50 Hz)**

From the results presented in Fig. 5 it can be observed that after the acceleration with a rated load of 15 Nm, the motor reaches the speed of 1,310 rpm which is in good agreement with the rated speed of the motor from analytical calculations of 1,355 rpm. After the transients have been suppressed and the motor has accelerated the output torque reaches 15 Nm, the result which can be expected considering that the motor is loaded with a 15 Nm load. As for the current, at motor starting it reaches the value of 25 A, still corresponding to the calculated starting current of 21 A. After the steady-state operation is achieved the motor current has a RMS value of 6 A and it corresponds to the calculated value in Table 1 of 5.2 A. The inverter output voltage is presented in Fig. 6 (a). Additionally, typical waveforms from measurements of the voltage at the output of the PWM inverter and on the input of the motor are presented in Fig. 6 (b) [10].



**(a) voltage of the inverter output (simulation)**



b) Voltage on the inverter output and motor input [10]

**Fig. 6. Motor characteristics at rated speed**

The harmonic content of the voltage on the output of the inverter is presented in Fig. 7.

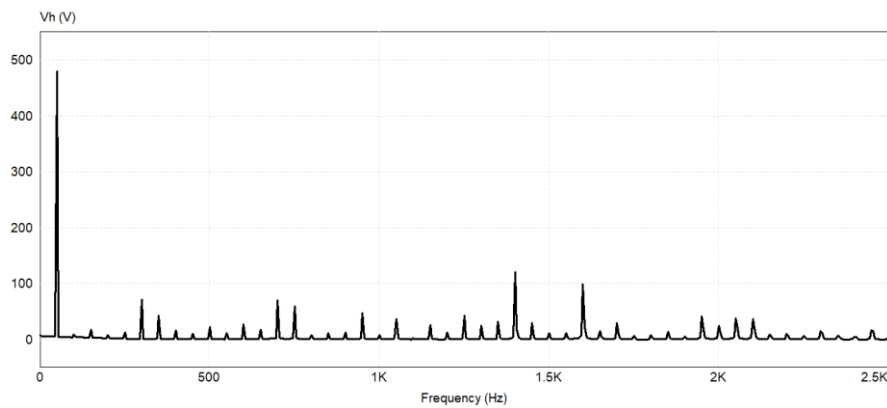


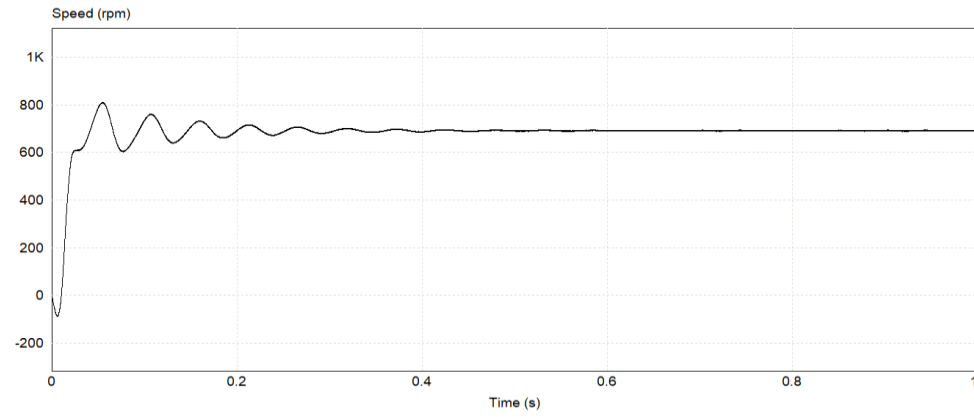
**Fig. 7. Harmonics at the output voltage of PWM inverter**

Increased harmonic content in the output voltage from the inverter increases the motor losses, heating, vibrations, and motor noise. Furthermore, other effects may appear when induction motors are fed by inverters. Insulation system dielectric stresses and shaft voltages allied with potentially damaging bearing currents are well-known side effects [10]. There are several measures that can be overtaken to improve the level of the high order harmonics. Some of them are installation of output passive filters, usage of multi-level inverters, pulse-width modulation quality improvement, and increase of the switching frequency.

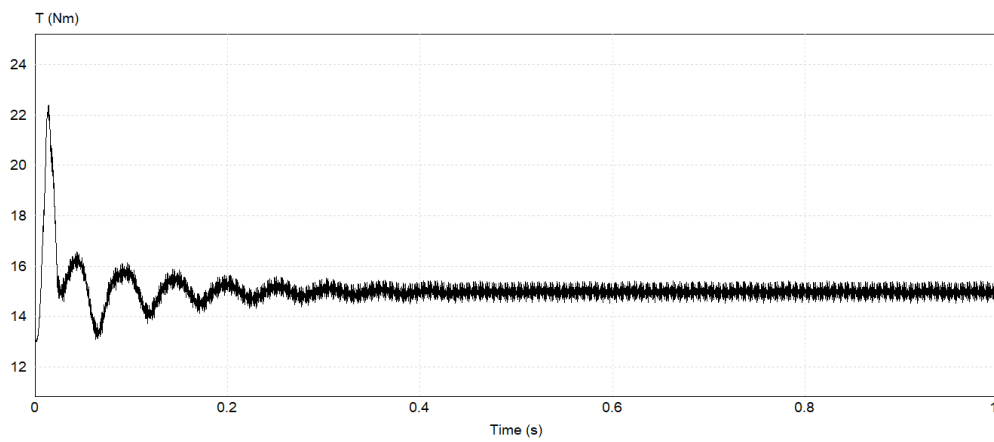
A fundamental function of a variable speed drive is to adjust the speed of an electric motor. The basic command frequency for variable speed drives is normally from 0 Hz to 50 Hz, but mostly with the capability to be adjusted up to 400 Hz. If the base frequency of a motor is 50 Hz, then the final speed will be 8 times the base frequency of the motor with the command frequency set at 400 Hz. Due to their design, it is not normal for standard induction motors to operate at these high frequencies. In practice, a command frequency set point of between 25 Hz and 75 Hz is acceptable without compromising performance or introducing any mechanical damage to the motor. At low-frequency set points, care must be taken that there is enough cooling for the motor produced by the mechanical fan [7].

The next step in the analysis of motor operation with the voltage inverter is to decrease the speed below the rated speed. For that purpose, the frequency of the modulating signal was decreased to 25 Hz also the amplitude of the modulating signal to keep the flux constant and

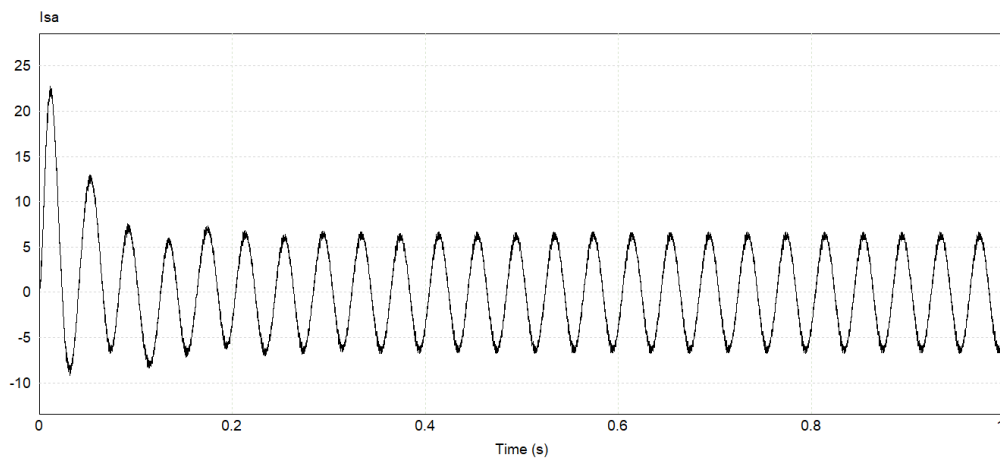
to operate the motor at low speed with the rated load of 15 Nm. The obtained characteristics of speed, current, and torque below the rated speed are presented in Fig. 8.



(a) speed



(b) torque



(c) current

**Fig. 8. Motor characteristics below rated speed (supply with 25 Hz)**

Following the basic equation which determines the motor synchronous speed

$$n = \frac{60 \cdot f}{p} \quad (3)$$

with the supply of 25 Hz, a speed below 750 rpm is expected. The characteristic of speed presented in Fig. 8 (a) reaches the speed of below 750 rpm after the acceleration has finished. The motor is loaded with 15 Nm. As the ratio between voltage and flux is kept constant, there is no limitation for the motor not to be loaded with the rated load. The characteristic of motor output torque presented in Fig. 7 (b) reaches the steady-state value of 15 Nm after the acceleration of the motor has finished. At motor operation below the rated speed, the motor current is decreased. One example of how the current varies with speed and torque is presented in Fig. 9 and can be found in [9]. All quantities are normalized so that the rated or base value is 1.0. In this case, the analyzed motor current is decreased to 4 A or compared to the data presented in Fig. 9 expected current, in this case, is 3.5 A taking into consideration that for the full load and speed reduction of 50% a reduction of current of 58%, from the rated current of 6 A, can be expected (Fig. 9). Obtained result of the simulated current agrees well with the expected value of the current.

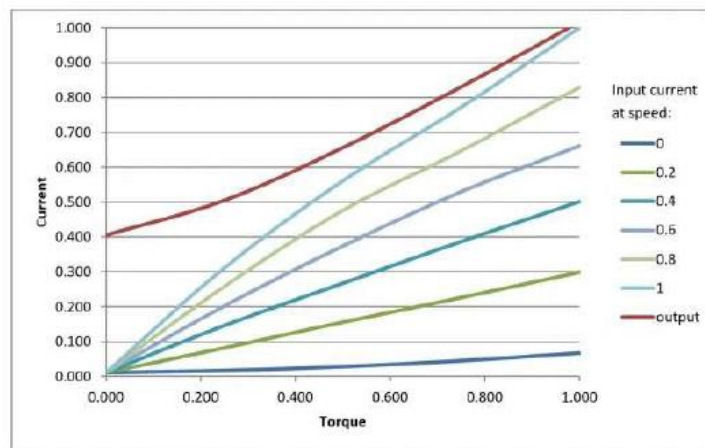


**Fig. 9. Variation of the drive input current with torque and speed [9]**

The operation of the motor above the rated frequency is analyzed as well. Therefore, the frequency of the modulating signal is set to 75 Hz. The amplitude of the voltage of the modulating signal remains unchanged. According to Eqs. (1) and (2), the motor enters the field-weakening region. i.e. the reduction of the load torque which can be sustained by the motor, when it operates with a constant V/f ratio or constant flux. One example what are the ranges of reduction of the motor torque can be found in [10]. They are presented in Fig. 10.

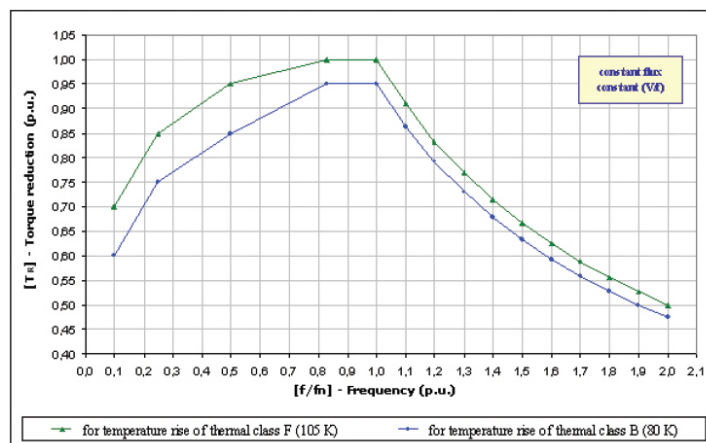
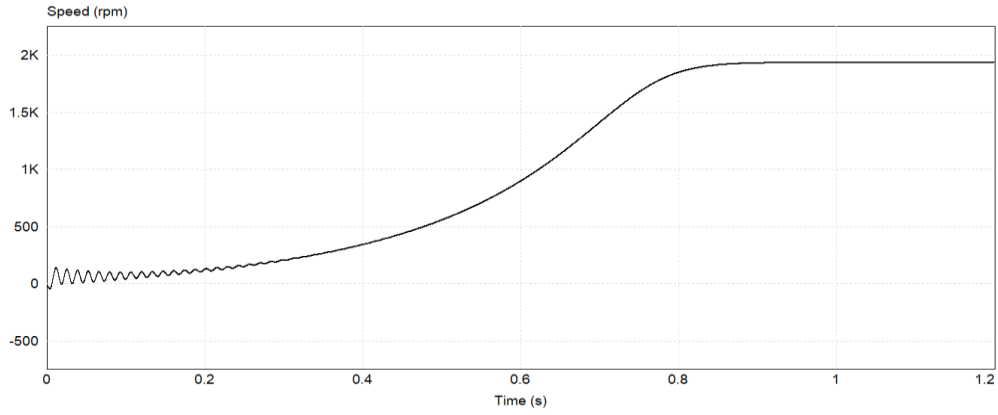
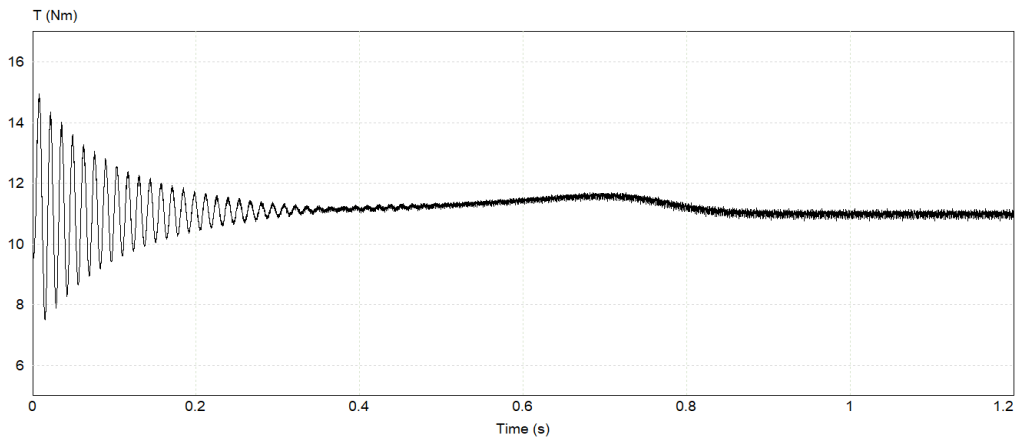


**Fig. 10. Torque reduction for constant flux operation [10]**

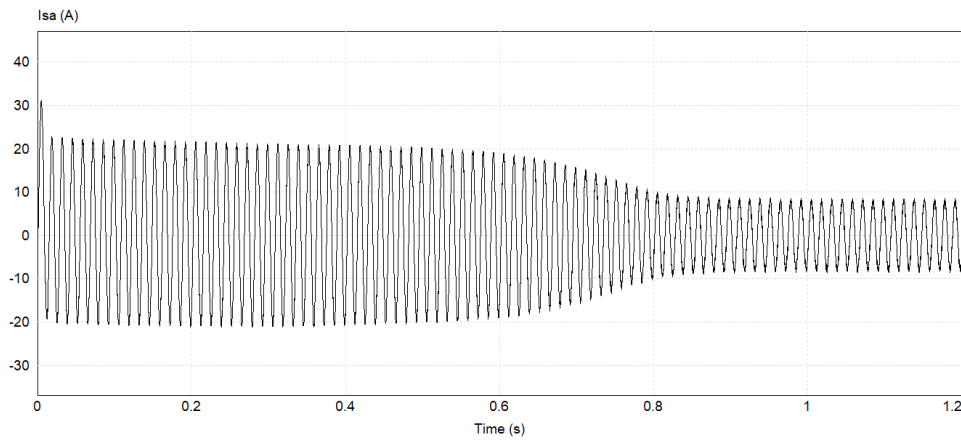
Fig. 11 presents the transient characteristics of speed, torque, and current for motor operation above the rated speed.



(a) speed



(b) torque



(b) current

**Fig. 11. Motor characteristics above rated speed (supply with 75 Hz)**

According to Eq. (3) expected motor speed is 2,000 rpm for a 75 Hz power supply. The obtained value of motor speed in Fig. 11 (a) is a little below the 2,000 rpm and corresponds to the expected theoretical value. According to Fig. 11 at 1.5 times the rated frequency, a torque reduction of 67% is expected, or for rated torque of 15 Nm, the torque reduction is 10 Nm. The obtained result of the simulation in Fig. 11 (b) presents the torque reduction from 15 Nm to 11 Nm, that agrees well with the expectations. As the motor operates at flux weakening region, the acceleration time of the motor is increased. By reducing the load, the acceleration time is decreased. The motor current after the acceleration time is finished, is reduced up to the rated

current, as the motor operates with constant power and constant voltage in flux weakening region.

The application of voltage source inverters in variable speed drives has many advantages and drawbacks. For the completeness of the analyses, we will name some of them. The main advantages are speed control, smooth controllable starting and stopping, energy saving through current limiting feature of the inverters, flexibility to set up and configure a variable speed drive for various applications, e.g. constant torque, variable torque, hoisting, and many others. One of the drawbacks is audible noise from the motor due to the various switching frequencies. To overcome this problem switching frequency can be increased but this also increases the harmonic content in the supply voltage, losses, and worsens the overall efficiency of the system. Another issue is Radio Frequency Interference (RF interference) generated by variable speed drives that can be very problematic, introducing faults on other equipment close to the installed unit. Apart from these, the harmonic content of the supply voltage from the inverter is responsible for poor power factor, excessive heating of neutral conductors (single-phase loads only), excessive heating of induction motors, and high acoustic noise from transformers, bus bars, switchgear, etc., abnormal heating of transformers and associated equipment, damage to power factor correction capacitors. Yet, the variable speed drives are an irreplaceable part of every industry, and their importance and development will continue in the years to come.

## Conclusions

Variable speed drives are the prime moving force of many industries. The three-phase asynchronous squirrel-cage motor, despite all its drawbacks, still dominates in many industries, due to its robustness, simplicity, and low operational costs. The paper analyzes the operation of three-phase squirrel cage motor at various operating speeds, i.e. at, below, and above the rated speed.

The main goal of the paper is to illustrate the theoretical principles of operation of the asynchronous motor with the voltage inverter at a constant  $V/f$  ratio, supported by the corresponding analysis from the simulation. The simulation circuit from the software Powersim allows obtaining the transient characteristic of motor speed, torque, and current along with various operating voltages such as the voltage of the output of the inverter. The accuracy of obtained transient characteristics at rated speed is verified by comparing them with rated data of the motor obtained by analytical formulas. The accuracy of the obtained results at speeds below and above the rated speed is compared with available data from the motor producers who present the motor operating characteristics at frequencies different from the rated one. At lower speed, the motor can sustain the rated load as a constant  $V/f$  ratio is maintained. The motor operates within a constant torque region as described in section 2 of the paper. Above the rated speed, the motor enters the field-weakening region as the  $V/f$  ratio cannot be maintained constant i.e. the voltage is kept unchanged, but the frequency is increased. Motor enters the constant power region, where the capability of the motor to sustain the rated load is reduced. The presented simulation circuit is very useful in the analysis of variable speed drives with asynchronous motors, especially in cases where no experimental equipment is available. The theoretical principles of voltage-fed asynchronous motor can be analyzed and illustrated comprehensively. The simulation circuit allows analysis of various measuring quantities such as voltage or current at different points of the circuit. Furthermore, the Fast Fourier Transformation (FFT) can be performed on measured voltages allowing estimation of the power quality of the supplied voltage.

Further research should be focused on improving the harmonic content of the inverter voltage thus improving the overall operating characteristics of the drive system in terms of reduced losses and improved efficiency.

## References

- [1] Annapurna, G: "Analysis of Induction Motor speed control fed from three phase inverter", International Journal of Engineering Development and Research, 8 (1), 2020, pp.1-6.
- [2] Kumar Dinesh: "Performance Analysis of Three-Phase Induction Motor with AC Direct and VFD", IOP Conference Series: Materials Science and Engineering, 331 012025, 2018, pp. 1-10.
- [3] Lane, M et al: "Investigation of reductions in motor efficiency and power factor caused by stator faults when operated from an inverter drive under open loop and sensorless vector modes", Systems Science & Control Engineering, 5 (1), 2017, pp. 361-379.
- [4] NaliniDevi, M/ Sudharan, S: "Open Loop Volts/Hertz Speed Control of Induction Motor with Voltage Fed Inverter", "International Research Journal of Engineering and Technology", 7(6), 2020, pp. 4497-4502.
- [5] Pande, Saurabh/ Singh, Saket: "Operation of Induction Motor with Different Modulation Index", International Research Journal of Engineering and Technology, 4(4), 2107, pp. 2002-2006.
- [6] Power System: Powesim, v.12.01.
- [7] R G van der Merwe / Hoogendoorn, C: "VSD advantages, disadvantages, selection criteria and installation tip", Energize, 2005, pp. 44-54.
- [8] Sharma, Mahima / Lalwani, Mahendra: "Performance Evaluation of Three-Phase Induction Motor Drive Fed from Z-Source Inverter", International Journal of Applied Engineering Research, 13 (8), 2018, pp. 6098-6109.
- [9] Technical: "Current, power and torque in variable speed drives", 2017, available at: <https://www.theautomationengineer.com/technical/current-power-torque-variable-speed-drives/>.
- [10] WEG "Induction motors fed by PWM frequency inverters", Technical guide, 2009.





## WI-FI SMART POWER METER

*Goce Stefanov<sup>1</sup>, Vlatko Cingoski<sup>2</sup>*

<sup>1</sup>Faculty of Electrical Engineering University Goce Delcev Stip R.Macedonia, goce.stefanov@ugd.edu.mk

<sup>2</sup>Faculty of Electrical Engineering University Goce Delcev Stip R.Macedonia, vlatko.cingoski@ugd.edu.mk

### Abstract

*In the paper are presents the results of a practically realized on process Smart Power meter. The application is intended for data collection for the voltage, the current in processing plants. By processing them, data on power, energy, frequency and power factor are obtained. These quantities are visualized on an LCD display, stored in an excel log file, and are distributed on the Internet via a WI-FI interface. The solution was realized with the smart power module PEZ004 and Node MCU ESP 8266.*

### Key words

*Power meter, WI-FI, Data Log.*

### 1. Introduction

The data for energy consumption in industrial process plants are essential for the efficient operation of the work process. On the basis of the data on the consumed energy, on the one hand the production process can be planned, and on the other hand it is possible to take measures to improve the efficiency and reduce the energy consumption [1], [2].

Built-in devices for measuring energy and power depend on the degree of development of the measurement technique at the moment of realization of the industrial process. Thanks to the development of the electronics, today's energy and power measurement systems enable the measurement values of process quantities to be visualized on display, sent remotely and stored in a file compatible for future user processing [3], [4]. In the Fig. 1 is shown block diagram on one smart power system for energy and power measurements.

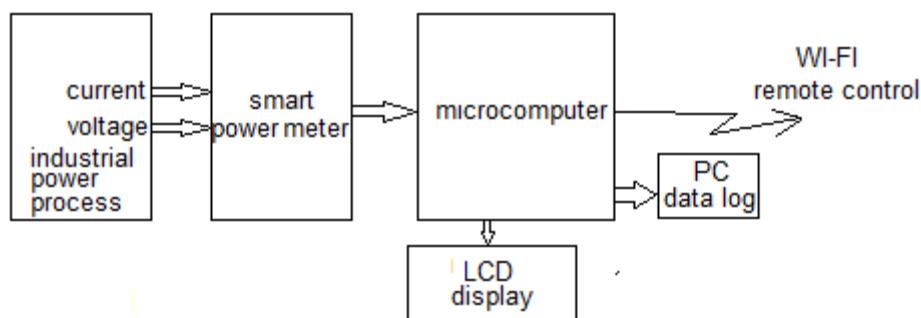


Fig. 1. Block diagram on one smart power system for energy and power measurements.

From Fig. 1 can be see that smart power system is based on microcomputer. It collects data on the quantities of current and voltage in industrial power process and calculated data for energy and power. The microcomputer sends this data to the Internet with a Wi-Fi modem [4]. The microcomputer with the UART port it is connected to a personal computer to which it sends the data to the Intra network. This hardware architecture provides on the one hand the data adequate for energy consumption in the industrial power process to be collected and visualized

on LCD displays and on a personal computer, and on the other hand the possibility for distribution of data in the Internet network is created.

## 2. Design on Wi-Fi smart power meter

In this part an WI-FI smart power meter is designed. The designed solution will collect data for the current from current transformer and the voltage on which is connected device in industrial power process. In the Fig. 2 is shown block diagram of the specific solution of WI-FI smart power meter.

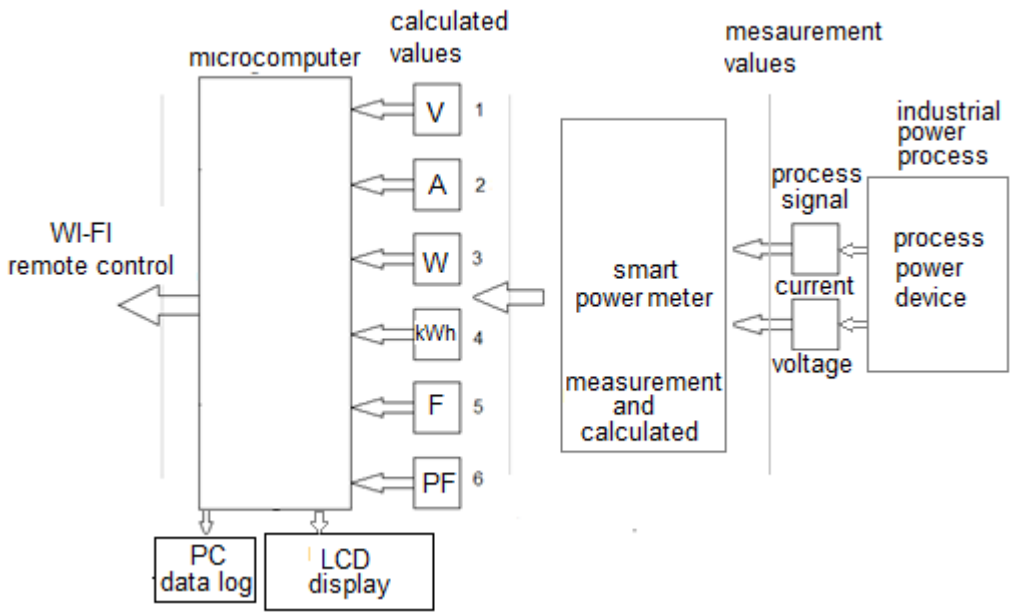


Fig. 2. Block diagram of the specific solution of WI-FI smart power meter.

The main part of this WI-FI smart power meter is the microcomputer. In the solution is selected the NodeMCU ESP8266 [5], [6]. Smart power meter takes data on the current and the voltage from the power device. The current data is taken with a current transformer. The voltage data is obtained from the voltage of the device terminals. Based on the current and voltage, the power meter calculates power, energy, frequency and power factor and sends it to the microcomputer together with the current and voltage data. In the fig. 2 calculated values are marked as: 1 is the data for voltage marked as V, 2 is the data for current marked as A, 3 is the data for power marked as W, 4 is the data for energy marked as kWh, 5 is the data for frequency marked as F and 6 is the data for power factor marked as PF. The power meter is connected to the microcomputer with the serial port. The microcomputer sends data on the current values of the quantities, on a personal computer, compatible in an excel file and also sends these quantities to the Internet via a WI-FI connection. In the Fig. 3 is shown the connection diagram of the realized solution.

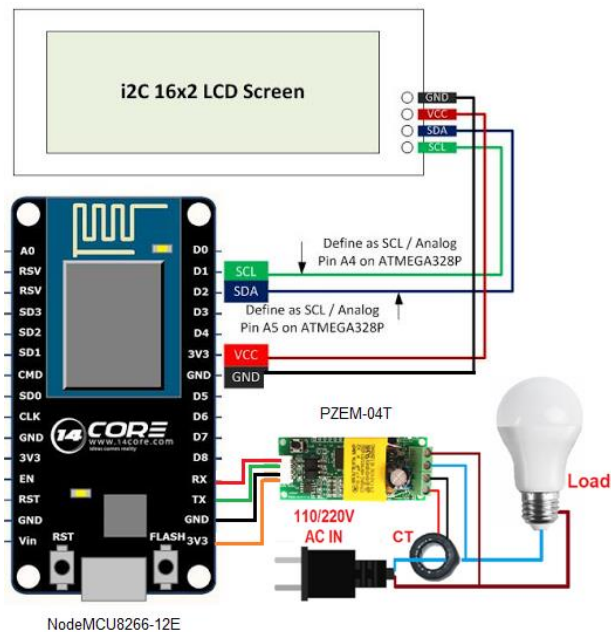


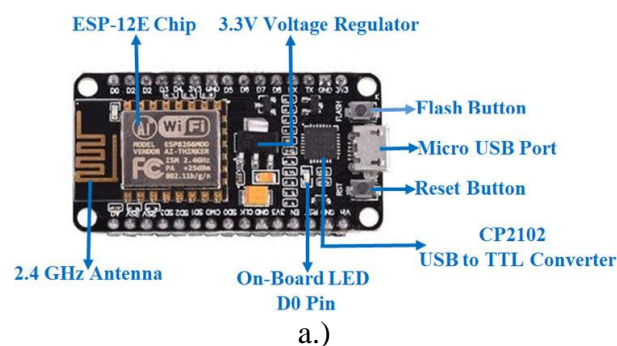
Fig. 3. Connection diagram of the realized solution.

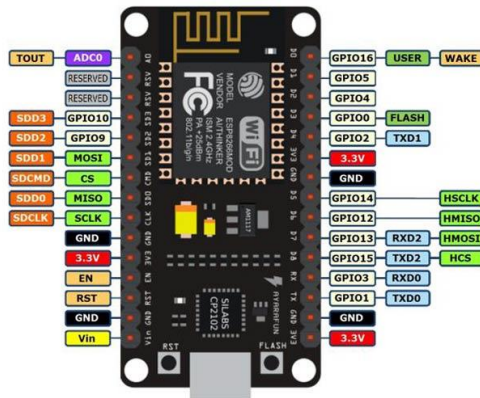
Figure 3 shows that the solution was realized using Node8266MCU and a power meter PZEM 004T.

## 2.1 Features of the used hardware

### a.) Microcomputer NodeMCU ESP8266

The NodeMCU ESP8266 development board comes with the ESP-12E module containing ESP8266 chip having Tensilica Xtensa 32-bit LX106 RISC microprocessor. This microprocessor supports RTOS and operates at 80MHz to 160 MHz adjustable clock frequency. NodeMCU has 128 KB RAM and 4MB of Flash memory to store data and programs. Its high processing power with in-built Wi-Fi / Bluetooth and Deep Sleep Operating features make it ideal for IoT projects. NodeMCU can be powered using Micro USB jack and VIN pin (External Supply Pin). It supports UART, SPI, and I2C interface. In the Fig. 4 is shown NodeMCU ESP8266 and his pinout.





b.)

Fig. 4. a.) NodeMCU ESP8266 and b.) his pinout

NodeMCU is an open-source based firmware and development board specially targeted for IoT based Applications. It includes firmware that runs on the ESP8266 Wi-Fi SoC from Espressif Systems, and hardware which is based on the ESP-12 module.

NodeMCU ESP8266 Specifications & Features

- Microcontroller: Tensilica 32-bit RISC CPU Xtensa LX106
- Operating Voltage: 3.3V
- Input Voltage: 7-12V
- Digital I/O Pins (DIO): 16
- Analog Input Pins (ADC): 1
- UARTs: 1
- SPIs: 1
- I2Cs: 1
- Flash Memory: 4 MB
- SRAM: 64 KB
- Clock Speed: 80 MHz
- USB-TTL based on CP2102 is included onboard, Enabling Plug n Play
- PCB Antenna
- Small Sized module to fit smartly inside your IoT projects

The NodeMCU ESP8266 board can be easily programmed with Arduino IDE since it is easy to use.

In Table 1 is given pinout at this microcomputer.

Table 1: NodeMCU Development Board Pinout Configuration

Pin Category	Name	Description
Power	Micro-USB, 3.3V, GND, Vin	<p><b>Micro-USB:</b> NodeMCU can be powered through the USB port</p> <p><b>3.3V:</b> Regulated 3.3V can be supplied to this pin to power the board</p> <p><b>GND:</b> Ground pins</p> <p><b>Vin:</b> External Power Supply</p>
Control Pins	EN, RST	The pin and the button resets the microcontroller
Analog Pin	A0	Used to measure analog voltage in the range of 0-3.3V

GPIO Pins	GPIO1 to GPIO16	NodeMCU has 16 general purpose input-output pins on its board
SPI Pins	SD1, CMD, SD0, CLK	NodeMCU has four pins available for SPI communication.
UART Pins	TXD0, RXD0, TXD2, RXD2	NodeMCU has two UART interfaces, UART0 (RXD0 & TXD0) and UART1 (RXD1 & TXD1). UART1 is used to upload the firmware/program.
I2C Pins		NodeMCU has I2C functionality support but due to the internal functionality of these pins, you have to find which pin is I2C.

**b.)Power meter PZEM-004T**

The power meter is mainly used for measuring AC voltage, current, active power, frequency, power factor and active energy, the module is without display function, the data is read through the TTL interface. PZEM-004T-10A built-in shunt have measuring range 10A, and PZEM-004T-100Awith external transformer have measuring range 100A, [7] . In the fig. 5a is shown the board on PZEM-004T power meter, and Fig. 5b is shown block diagram on this module.

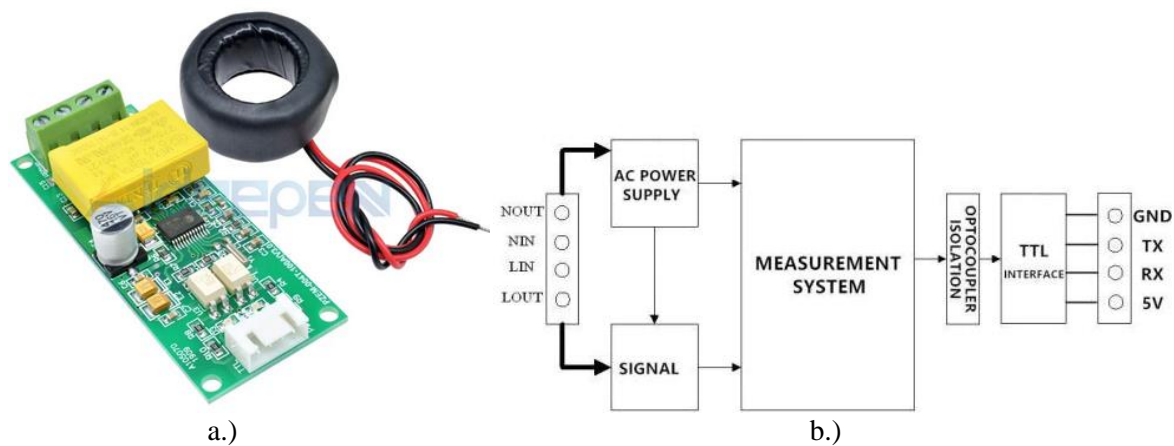


Fig. 5. a.) The board on PZEM-004T power meter, and b.) block diagram on this module.

The current signal is connected to power meter on the terminals NIN and NOUT, and the voltage is connected on the terminals LIN and LOUT. The power meter is supply with 5 VDC voltage. The terminals TX and RX are for serial communication.

**Function description**

Voltage measuring range is 80~260V.

Current measuring range is 0~10A(PZEM-004T-10A); 0~100A(PZEM-004T-100A)

Active power measuring range is 0~2.3kW(PZEM-004T-10A); 0~23kW(PZEM-004T-100A)

Starting measure power is 0.4W. Resolution is 0.1W.

Display format: < 1000W, it display one decimal, such as: 999.9W. ≥1000W, it display only integer, such as: 1000W. Power factor measuring range is 0.00~1.00 , resolution is 0.01.

Frequency measuring range is 45Hz~65Hz, resolution is 0.1Hz.

Active energy measuring range is 0~9999.99kWh, resolution is 1Wh.

Display format: < 10kWh, the display unit is Wh(1kWh=1000Wh), such as: 9999Wh

≥10kWh, the display unit is kWh, such as: 9999.99kWh

Over power alarm

Active power threshold can be set, when the measured active power exceeds the threshold, it

can alarm. Communication interface is RS485 interface.

### **Communication protocol**

Physical layer use UART to RS485 communication interface. Baud rate is 9600, 8 data bits, 1 stop bit, no parity. The application layer use the Modbus-RTU protocol to communicate. At present, it only supports function codes such as 0x03 (Read Holding Register), 0x04 (Read Input Register), 0x06 (Write Single Register), 0x41 (Calibration), 0x42 (Reset energy).etc. 0x41 function code is only for internal use (address can be only 0xF8), used for factory calibration and return to factory maintenance occasions, after the function code to increase 16-bit password, the default password is 0x3721.

The address range of the slave is 0x01 ~ 0xF7. The address 0x00 is used as the broadcast address, the slave does not need to reply the master. The address 0xF8 is used as the general address, this address can be only used in single-slave environment and can be used for calibration etc.operation.

The command format of the master reads the measurement result is(total of 8 bytes): Slave Address + 0x04 + Register Address High Byte + Register Address Low Byte + Number of Registers High Byte + Number of Registers Low Byte + CRC Check High Byte + CRC Check Low Byte.

The command format of the reply from the slave is divided into two kinds: Correct Reply: Slave Address + 0x04 + Number of Bytes + Register 1 Data High Byte + Register 1 Data Low Byte + ... + CRC Check High Byte + CRC Check Low Byte Error Reply: Slave address + 0x84 + Abnormal code + CRC check high byte + CRC check low byte.

### **3. Experimental results**

The design of an WI-FI smart power meter are consists of hardware design and software design.

#### ***Hardware design***

According to the description of the characteristics of the hardware components given above and the main purpose of the paper, in the Fig. 3 is shows the electrical circuit of the WI-FI smart power meter. The circuit consists of NodeMCU8266-12E, PZEM-004T power meter and LCD display. The operation of the circuit is described in point 2.

#### ***Software design***

The software is written in micro C. NodeMCU ESP8266 software is compatible with the Arduino IDE platform. The software ensures that the microcomputer receives the signals from the power meter and, after processing, displays the current values on the voltage, current, power, energy, frequency and power factor on LCD display, sends them as a data log file for building a database compatible with an excel file, and distributes them to the WI-FI Internet network.

According to the above, the software consists of several steps.

*Defining on variables and libraries:*

```
#include <PZEM004Tv30.h>
#include<stdlib.h>
/* ESP & Blynk */
#include <ESP8266WiFi.h>
#include <BlynkSimpleEsp8266.h>
#include <SimpleTimer.h>
#define BLYNK_PRINT Serial // Comment this out to disable prints and save space
#include <LiquidCrystal.h>
#include <Wire.h>
#include <LiquidCrystal_I2C.h>
```

*Setting for WI-FI connection:*



```
char auth[] = "-DcVhdifI2ct0VC7JpbM4QoWSXEaGthM"; //obtained from APP Store
/* WiFi credentials */
char ssid[] = "my_network"; //defining on WI-FI network
char pass[] = "Elsa1101"; //defining on passport on WI-FI network
```

```
Building a data log file:
Serial.print(value()); // Read value from sensor and send its value to Excel
Serial.print(","); // Move to next column
```

```
Sending data to GI-FI:
Blynk.virtualRead(V3, variable);
```

```
Reading data on display:
lcd.print("name:");
lcd.print(variable);
lcd.print("unit");
```

In the Fig. 6a is shown the experimental prototype on the WI-FI smart power meter, and the Fig. 6b is shown the complete process WI-FI smart power meter. In the Fig. 7a is shown excel data log file.

For remote transmission and display of current values of measurement data in the WI-FI network is built SCADA based on APP Store platform. In the Fig. 7b is shows the screen of an Android mobile device on which are showing the current values of the measurement data.

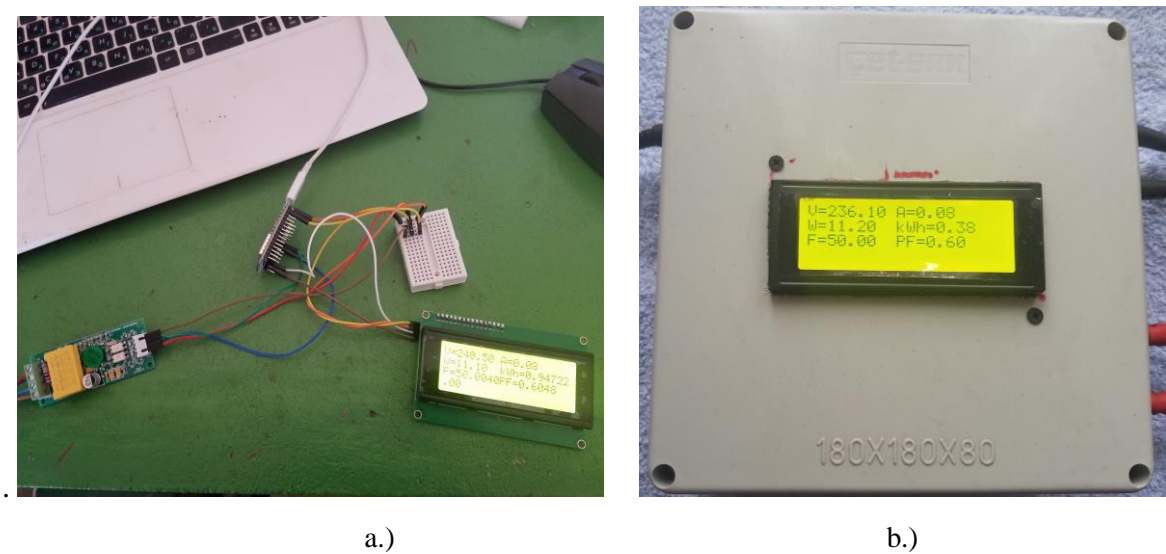


Fig. 6. Experimental results: a.) prototype on the WI-FI smart power meter and b.) the complete process WI-FI smart power meter.

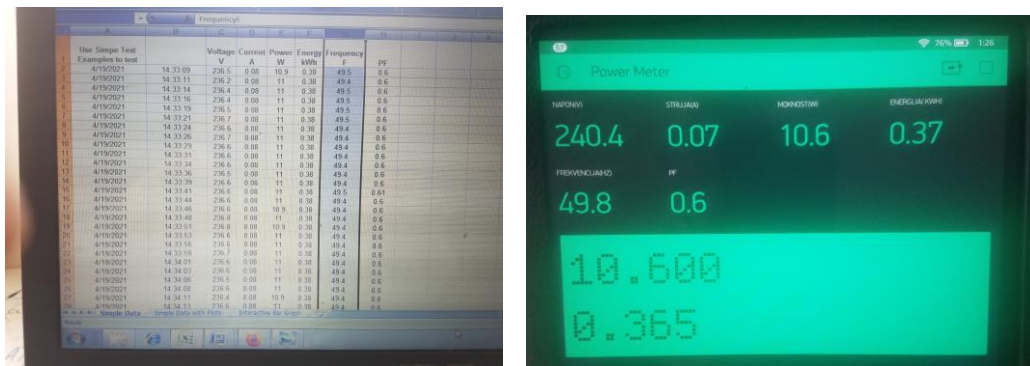


Fig. 7. a.) Excel data log file, b.) screen of an Android mobile device on which are showing the current values of the measurement data.



## Conclusions

In the paper with theoretical analysis is designed and practically realized WI-FI smart power meter. The power meter allows data on power, energy, frequency and power factor to be obtained only by measuring the voltage and current of a process device. Then these data are processed, visualized on an LCD screen, sent as a data log in an excel file and distributed remotely via a WI-FI connection. The solution also provides the ability to remote control on the process quantities.

## References

- [1] S. Bennett, S. Linkens, Computer Control of Industrial Processes, D.A. (Eds.), IEEE, 1982.
- [2] Ching-Lai Hor and Peter A. Crossley, Knowledge Extraction from Intelligent Electronic Devices, Lecture Notes in Computer Science pp. 82-111, January 2005.
- [3] Teen-Hang Meen, Wenbing Zhao and Cheng-Fu Yang Special Issue on Intelligent Electronic Devices Reprinted from: Electronics 2020, 9, 645.
- [4] By M.A. Matin and M.M. Islam, Wireless Sensor Network, <https://www.intechopen.com/books/wireless-sensor-networks-technology-and-protocols/overview-of-wireless-sensor-network> September 6th 2012, DOI: 10.5772/49376.
- [5] Manoj R. Thakur , NodeMCU ESP8266 Communication Methods and Protocols : Programming with Arduino IDE, 2018.
- [6] ESP8266: Programming NodeMCU Using Arduino IDE - GetStarted With ESP8266, <https://stoveraci.firebaseio.com/aa009/esp8266-programming-nodemcu-using-arduino-ide-get-started-with-esp8266-by-upskill-learning-1534822666.pdf>.
- [7] PZEM004T V3.0 User Manual, <https://innovators-guru.com/wp-content/uploads/2019/06/PZEM-004T-V3.0-Datasheet-User-Manual.pdf>



## RF SENSOR SMART NETWORK

*Goce Stefanov<sup>1</sup>, Maja Kukuseva Paneva<sup>2</sup>*

<sup>1</sup>Faculty of Electrical Engineering University GoceDelcevStip R.N. Macedonia, goce.stefanov@ugd.edu.mk

<sup>2</sup>Faculty of Electrical Engineering University Goce Delcev Stip R. N. Macedonia, maja.kukuseva@ugd.edu.mk

### Abstract

*In the paper are presents the results of a practically realized process RF sensor network. The application is intended for data collection in remote processing plants and their transmission to the main central control panel. The solution is based on the RF interface module NRF24L01 and microcontroller. Two such modules communicate in the RF connection, as transmitter and receiver. On the receiving side, the received process data is displayed on an LCD display and stored in an excel log file.*

### Key words

*NRF24L01module, Microcontroller, RF sensor network.*

### 1. Introduction

In industrial processes, usually there is a need for data transmission in remote areas that are not covered by internet network, [1], [2], [3]. In such cases, a convenient solution is radio transmission and use of interfaces, sensors and controllers that support radio frequency transmission[4].

There are various wireless communication technologies used in building IoT applications and RF (Radio Frequency) is one of them. Usually such radio communications are two-way. In the Fig 1 is shown block diagram of one RF sensors network.

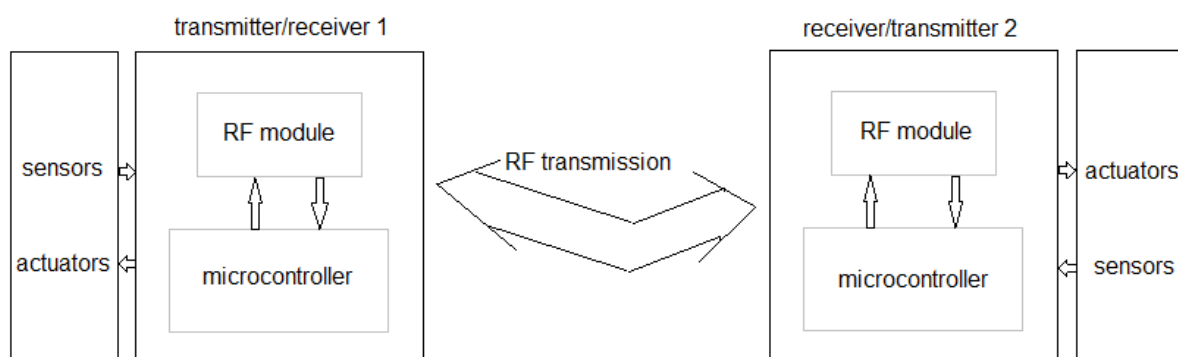


**Fig.1.** Block diagram of RF sensors network.

Transmitter/receiver 1 and receiver/transmitter 2 on both sides are consist of sensors network and actuators, RF module and microcontroller.

The main goal in this paper is the design of the RF sensor network. For the realization of the goal, the RF module NRF24L01 [5] and a microcontroller Atmega 328P are used on an Arduino uno board platform, [6].

## 2. Design on RF sensor network based on NRF24L01 and microcontroller

The designed sensor network in this paper has the task to measure temperature and humidity at the measuring point and send measured values via RF transmission to the receiving point where these values are displayed on LCD screen and stored on PC in a data log file compatible with Microsoft Excel. In the Fig. 2 is shown block diagram of designed RF sensor network[5].

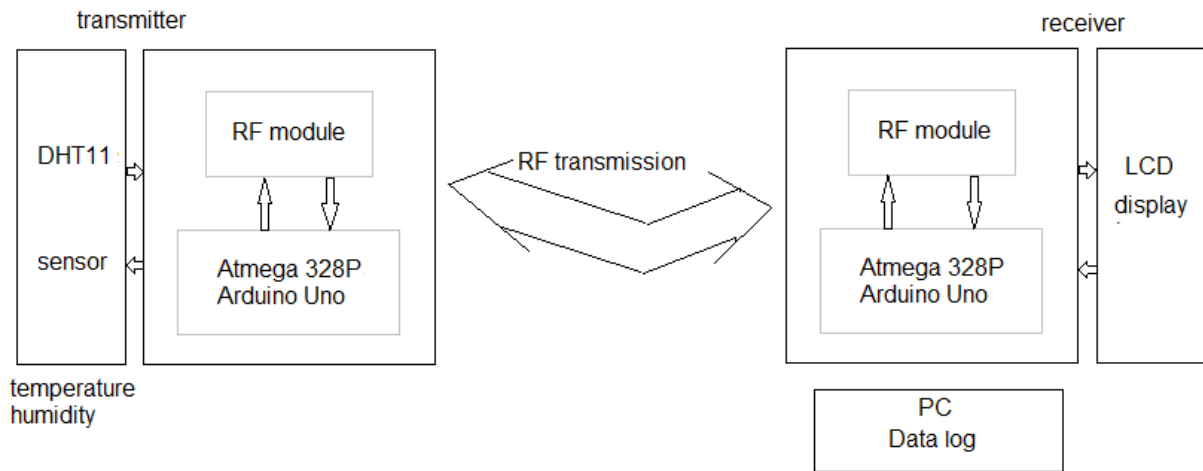


**Fig. 2.** Block diagram of designed RF sensor network.

The sensor network designed in this paper consists of a transmitter and a receiver. The transmitter consists of a temperature sensor with component DHT11, NRF24L01 module and microcontroller Atmega 328P on Arduino uno board. The receiver consists of NRF24L01 module, Atmega 328P microcontroller on Arduino uno board and LCD display.

Guided by the main goal of the paper, design of RF sensor network, in the next section are given the theoretical foundations of the components used.

### 2.1 Features of the used hardware

#### a.) *NRF24L01 module*

NRF24L01 is a single-chip radio transceiver module that operates on 2.4 - 2.5 GHz (ISM band)[5]. This transceiver module consists of a fully integrated frequency synthesizer, a power amplifier, a crystal oscillator, a demodulator, a modulator, and Enhanced ShockBurst protocol engine. Output power, frequency channels, and protocol setup are easily programmable through an SPI interface. Built-in Power Down and Standby modes make power saving easily realizable. In the Fig. 3 is shown electronic board on NRF24L01 module and its pinout.

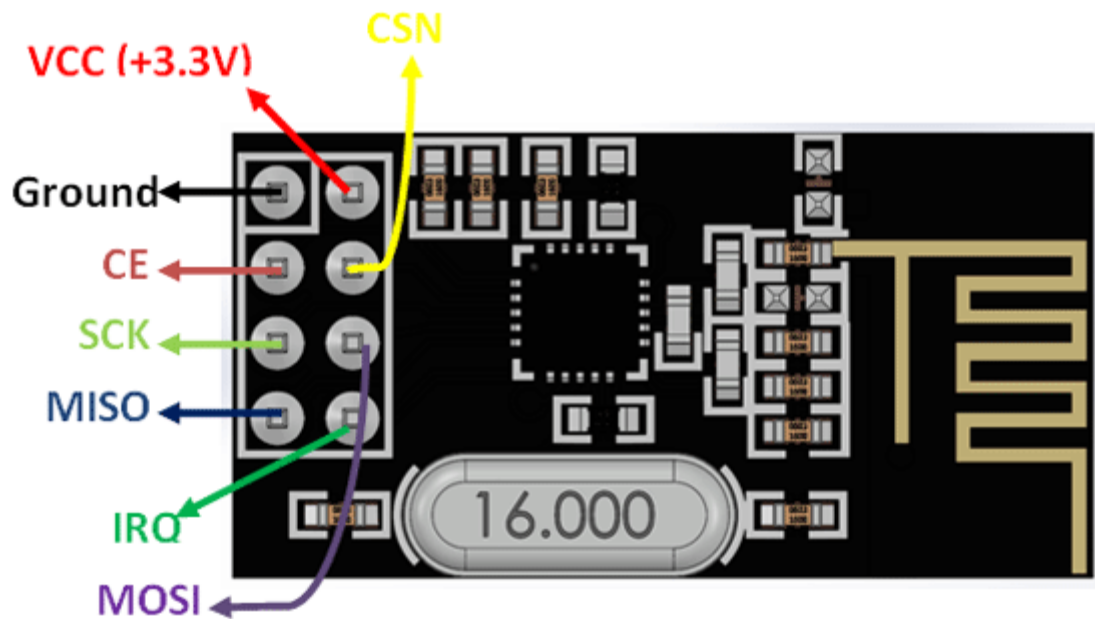


**Fig.3.** Electronic board on NRF24L01 module and his pinout.

In the Fig. 4 is shown block diagram of electronic components of NRF24L01 module.

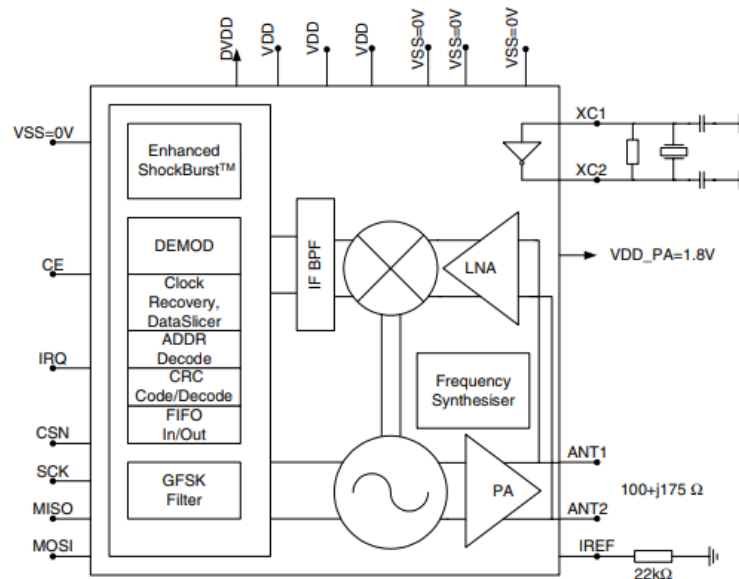


**Fig. 4.** Block diagram on the electronic components at NRF24L01 module.

In the Table 1 are given pinout configuration on NRF24L01 module.

**Table 1: Pinout configuration on NRF24L01 module**

Pin Number	Pin Name	Abbreviation	Function
1	Ground	Ground	Connected to the Ground of the system

2	Vcc	Power	Powers the module using 3.3V
3	CE	Chip Enable	Used to enable SPI communication
4	CSN	Ship Select Not	This pin has to be kept high always, else it will disable the SPI
5	SCK	Serial Clock	Provides the clock pulse using which the SPI communication works
6	MOSI	Master Out Slave In	Connected to MOSI pin of MCU, for the module to receive data from the MCU
7	MISO	Master In Slave Out	Connected to MISO pin of MCU, for the module to send data from the MCU
8	IRQ	Interrupt	It is an active low pin and is used only if interrupt is required

#### NRF24L01 Features:

- 2.4GHz RF transceiver Module
- Operating Voltage: 3.3V
- Nominal current: 50mA
- Range : 50 – 100 m
- Operating current: 250mA (maximum)
- Communication Protocol: SPI
- Baud Rate: 250 kbps - 2 Mbps.
- Channel Range: 125
- Maximum Pipelines/node : 6
- Low cost wireless solution

The NRF24L01 is a wireless transceiver module, meaning each module can both send as well as receive data. The operating frequency is 2.4 GHz, which falls under the ISM band and hence it is legal to use in almost in all countries for engineering applications. When the modules operate efficiently can cover a distance of 100 meters (200 feet) which makes it a great choice for all wireless remote controlled projects.

The module operates at 3.3V hence can be easily used with 3.2V systems or 5V systems. Each module has an address range of 125 and each module can communicate with 6 other modules hence it is possible to have multiple wireless units communicating with each other in a particular area. Hence mesh networks or other types of networks are possible using this module. Therefore, this module is an ideal choice for practical applications.

The NRF24L01 module works by means of SPI communications. These modules can either be used with 3.3V microcontroller or a 5V microcontroller with SPI port. The complete details of usage of this module through SPI is given in the data sheet below. The circuit diagram in the Fig. 5 showshow the module should be interfaced with the microcontroller.

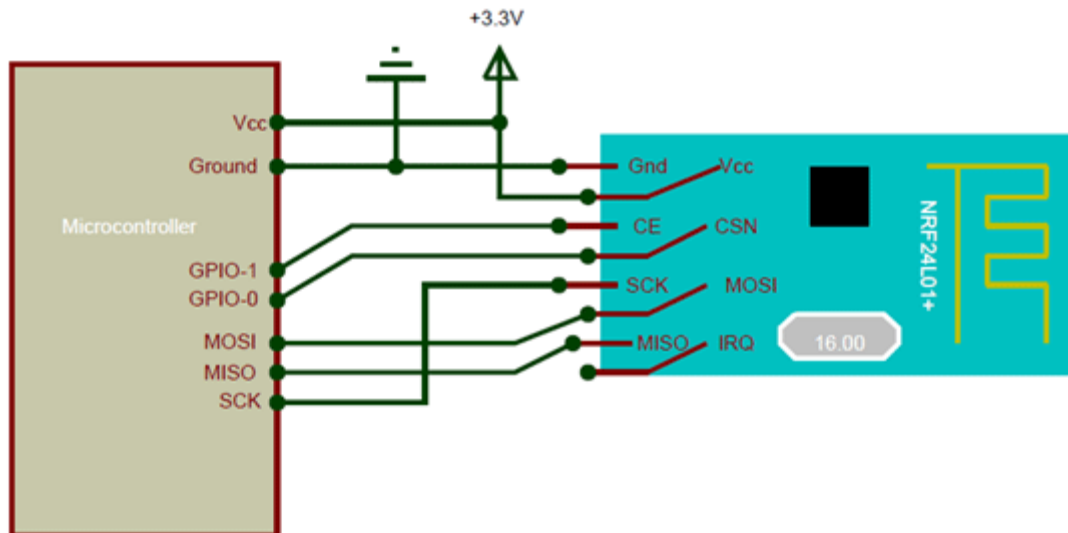


**Fig. 5.** NRF24L01 module interfaced with a microcontroller.

On Fig.5 is shown the usage of 3.3V microcontroller, but it is applied same for a 5V MCU. The SPI Pins (MISO<MOSI and SCK) are connected to the SPI pins of the Microcontroller and the signal pins (CE and CSN) are connected to the GPIO pins of the MCU.

There are ready made available libraries, like R24 Library, for interfacing this module with Arduino. With help of these libraries NRF24L01 can be easily interfaced with Arduino with few lines of code. If using some other microcontroller, the datasheet has to be read in order to understand how to establish SPI communication.

The NRF24L01 module is a bit tricky to use especially since there are many cloned versions in the market. In case of troubleshoot, 10 $\mu$ F and 0.1 $\mu$ F capacitors should be added in parallel to source Vcc and Ground pins. Also, the 3.3V supply should be clean and does not have any noise coupled in it.

### ***b.) Microcomputer Atmega 328P***

The Arduino Uno is an open-source microcontroller board based on the Microchip ATmega328P microcontroller and developed by Arduino.cc. The board is equipped with sets of digital and analog input/output (I/O) pins that may be interfaced to various expansion boards (shields) and other circuits. The board has 14 digital I/O pins (six capable of PWM output), 6 analog I/O pins, and is programmable with the Arduino IDE (Integrated Development Environment), via a type B USB cable. It can be powered by the USB cable or by an external 9-volt battery, though it accepts voltages between 7 and 20 volts. The word "uno" means "one" in Italian and was chosen to mark the initial release of Arduino Software. The Uno board is the first in a series of USB-based Arduino boards; it and version 1.0 of the Arduino IDE were the reference versions of Arduino, which have now evolved to newer releases. The ATmega328P on the board comes preprogrammed with a bootloader that allows uploading new code to it without the use of an external hardware programmer[6]. In the Fig. 6a is shown electronic board on Arduino Uno with build Atmega 328P microcontroller, and in Fig. 6b is shown its pinout.



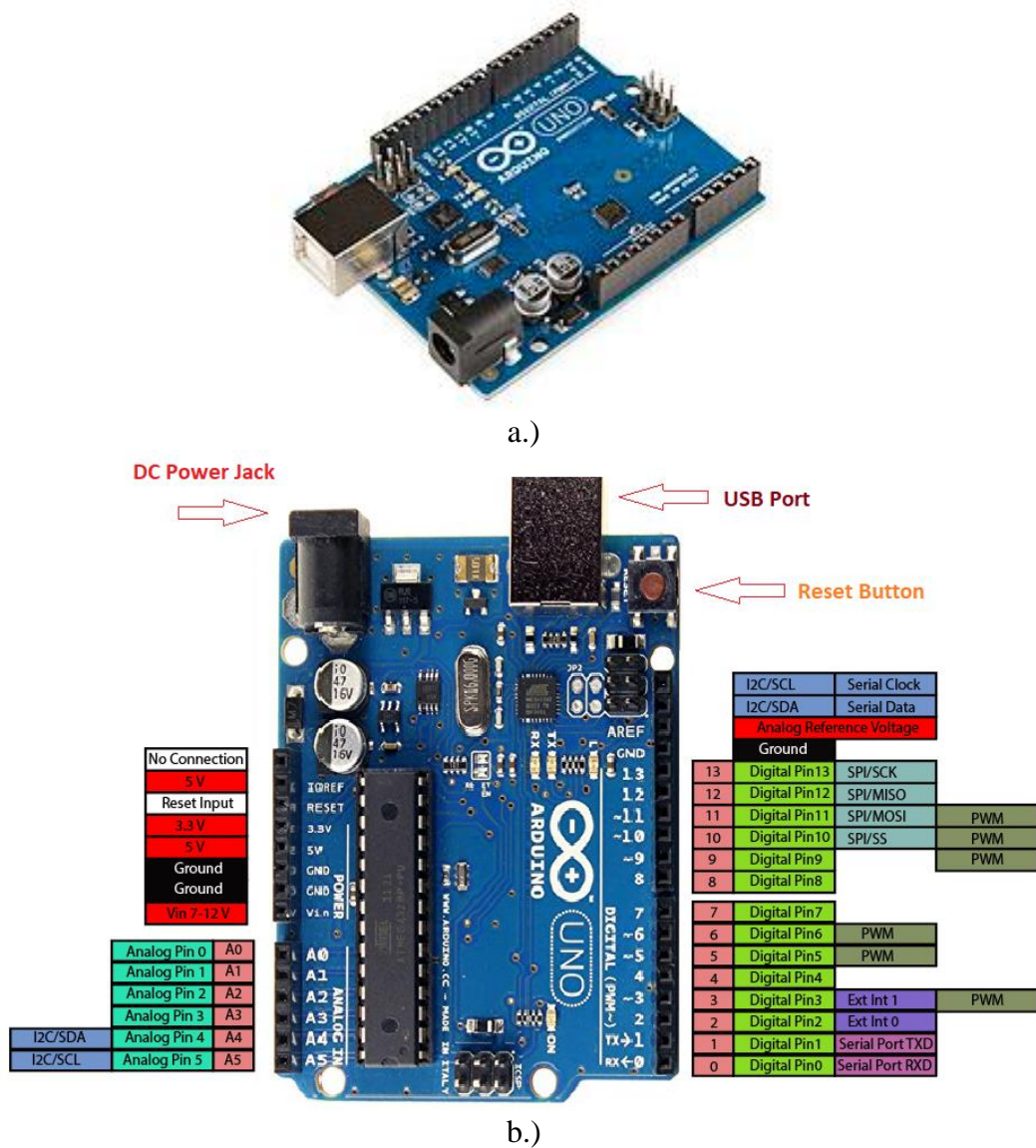


Fig.6.a.) Arduino Uno and b.) pinout

### c.) DHT11 temperature and humidity sensor

The DHT11 is a commonly used temperature and humidity sensors. The sensor comes with a dedicated NTC to measure temperature and an 8-bit microcontroller to output the values of temperature and humidity as serial data. The connection diagram for this sensor is shown in the Fig. 7.

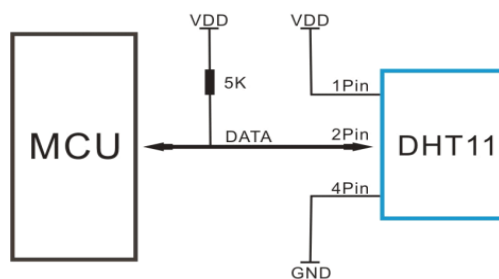
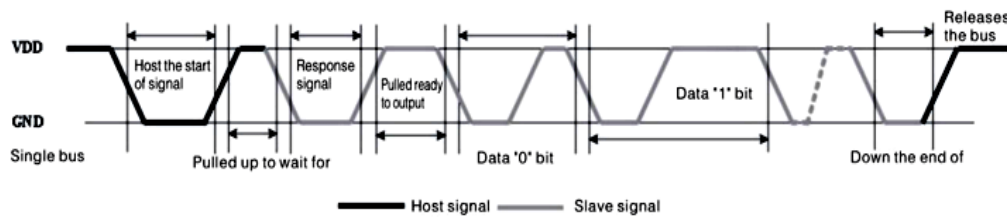


Fig. 7. Connection diagram for DHT11 sensor.



The sensor is also factory calibrated and hence easy to interface with other microcontrollers. The sensor can measure temperature in range from 0°C to 50°C and humidity from 20% to 90% with an accuracy of  $\pm 1^\circ\text{C}$  and  $\pm 1\%$ . The DHT11 sensor is factory calibrated and outputs serial data and hence it is highly easy to set it up. From Fig.7 can be seen that the data pin is connected to an I/O pin of the MCU and a 5K pull-up resistor is used. This data pin outputs the value of both temperature and humidity as serial data. For interface of DHT11 with Arduino there are ready-made libraries for quick start. If it is needed to interface it with some other MCU then the datasheet given below will come in handy. The output given by the data pin is sent in the order of 8 bit humidity integer data + 8bit the Humidity decimal data + 8 bit temperature integer data + 8 bit fractional temperature data + 8 bit parity bit. To request the DHT11 module to send these data the I/O pin has to be momentarily made low and then held high as shown in the timing diagram in Fig.8.



**Fig. 8.**Timing diagram for DHT11 sensor

The duration of each host signal is explained in the DHT11 datasheet, with neat steps and illustrative timing diagrams. This sensor can be used for temperature and humidity measurement, local weather station, automatic climate control, environment monitoring. In Fig.9 is shown DHT11 sensor in real size with its pinout.

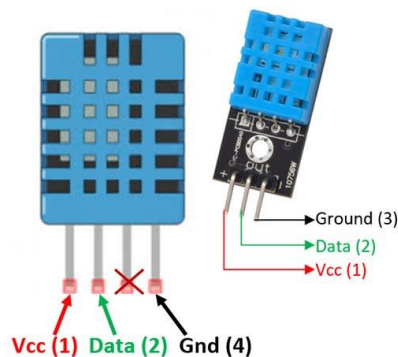


**Fig. 9.** DHT11 sensor in real size with his pinout.

#### DHT11 Specifications:

- Operating Voltage: 3.5V to 5.5V
- Operating current: 0.3mA (measuring) 60uA (standby)
- Output: Serial data
- Temperature Range: 0°C to 50°C

- Humidity Range: 20% to 90%
- Resolution: Temperature and Humidity both are 16-bit
- Accuracy:  $\pm 1^{\circ}\text{C}$  and  $\pm 1\%$

The DHT11 sensor can either be purchased as a sensor or as a module. Either way, the performance of the sensor is same. The sensor comes as a 4-pin package out of which only three pins are used whereas the module comes with three pins as shown above. The only difference between the sensor and module is that the module will have a filtering capacitor and pull-up resistor inbuilt, and for the sensor, are externally used if required.

#### d.) *LCD display*

LCD 16x2 display is used for visualization on date values on the voltage and the current. LCD is connection with expander circuit by parallel data port. In Figure 10 is shown LCD 16x2 display.

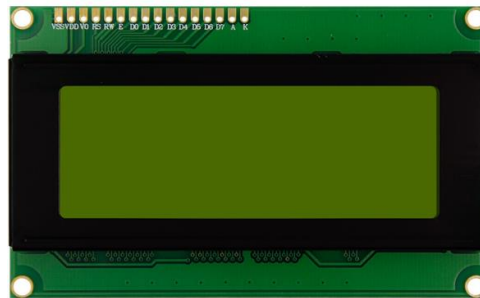


**Fig. 10.** LCD 20x4 display.

### 3. Experimental results

#### a.) *RF Transmitter side*

In Fig. 11 is shown the connection of the components of RF transmitter side. The transmitter side consists of an Arduino UNO, NRF24L01 module and DHT11 sensor. Interfacing of the Arduino UNO with NRF24L01 and DHT11 is shown below. Arduino continuously gets data from the DHT11 sensor and sends it to the NRF24L01 Transmitter. Then the RF transmitter transmits the data into the environment.

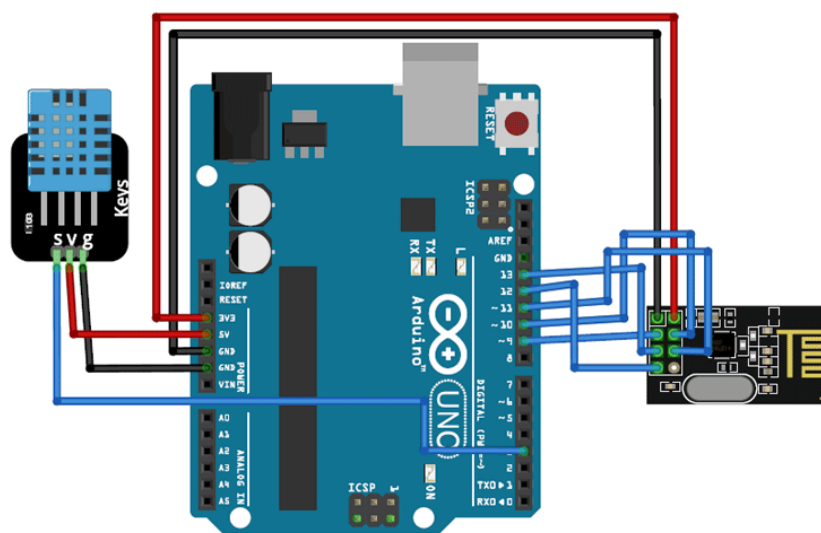


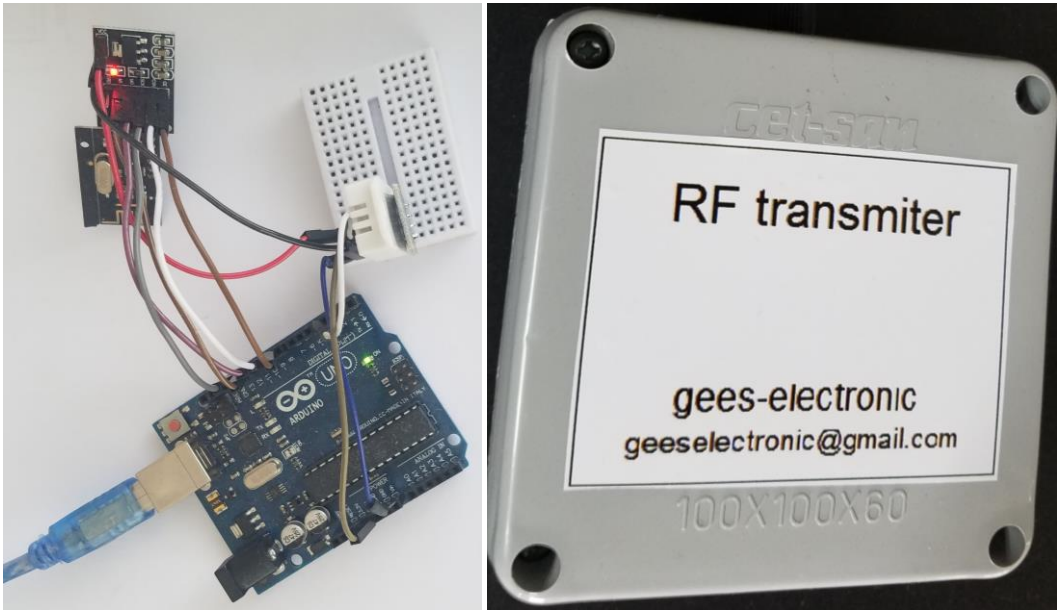
**Fig.11.** The connection of the components of RF transmitter side

In the Table 2 are given pinouts connection on NRF24L01 module, DHT11 and Arduino uno on transmitter side.

**Table 2:** Pinouts connection on NRF24L01 module, DHT 11 and Arduino uno on transmitter side

NRF24L01	Arduino Uno
VCC	3.3V
GND	GND
CE	Pin 9
CSN	Pin10
SCK	Pin 13
MOSI	11
MISO	12
DHT11	Arduino Uno
VCC	5V
GND	GND
DATA	3

In Fig. 12a is shown the practically realized prototype of the RF transmitter, andFig. 12b shows the finished RF transmitter device.



a.) b.)  
**Fig. 12.** RF transmitter device: a.) practically realized prototype of the RF transmitter and b.) finished RF transmitter device.

**b.) RF receiver side**

In Fig. 13 is shown the connection of the components on receiver side. The receiver side consists of an Arduino UNO, NRF24L01 module, and 16x2 LCD display. At the receiver side, NRF module receives the data from the transmitter and sends it to Arduino. Interfacing of the Arduino with NRF24L01 and LCD display is shown below.

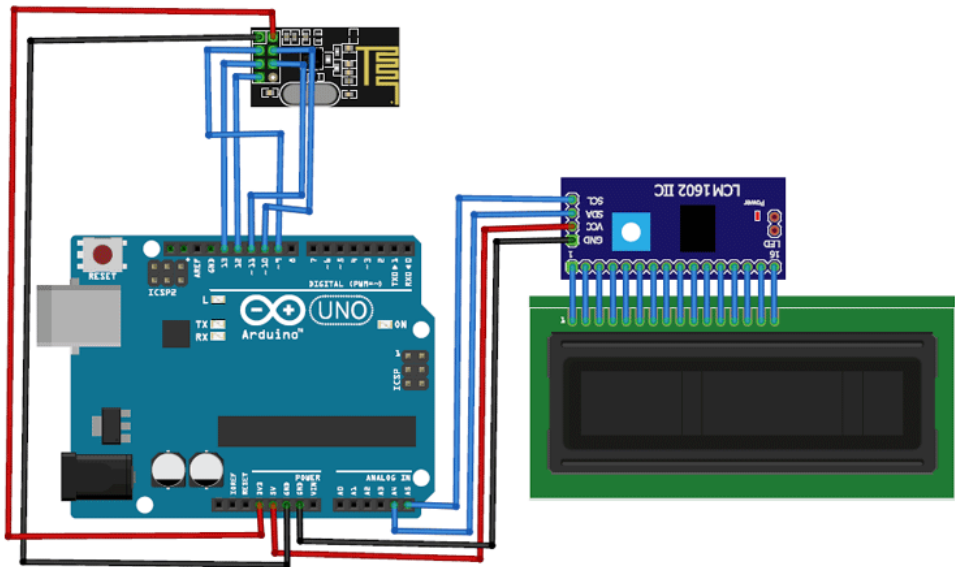


**Fig. 13.** The connection of the components of RF receiver side.

**Table 3:** Pinouts connection on NRF24L01 module, LCD display and Arduino uno on receiver side

NRF24L01	Arduino Uno
VCC	3.3V
GND	GND
CE	Pin 9
CSN	Pin10
SCK	Pin 13
MOSI	11
MISO	12
LCD With I2C Module	Arduino Uno
VCC	5V
GND	GND
SCL	A5
SDA	A4

In Fig. 14a is shown the practically realized prototype of the RF receiver, and inFig. 14b is shown the finished RF receiver device.

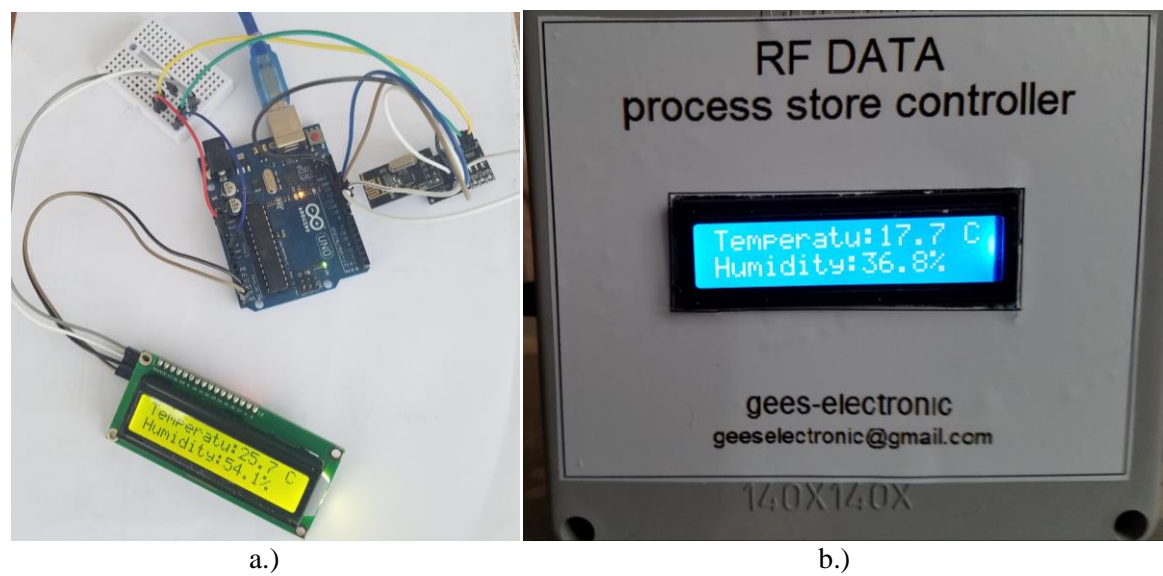


**Fig. 14.** RF receiver device: a.) practically realized prototype of the RF receiver and b.) finished RF receiver device.

In Fig. 15 is shown data for the temperature and the humidity measured by the DHT11 sensor, sent by the RF transmitter and received from the RF receiver in a data log file compatible with Microsoft Excel.

	A	B	C	D	E
1	Date	Time	Temperature°C	Humidity(%)	
2	6/11/2021	11:41:32	26.5	56.9	
3	6/11/2021	11:42:27	26.5	56.8	
4	6/11/2021	11:42:47	26.7	56.6	
5	6/11/2021	11:42:52	26.7	56.6	
6	6/11/2021	11:42:58	26.7	56.6	
7	6/11/2021	11:43:03	26.7	57.1	
8	6/11/2021	11:43:08	26.7	57.5	
9	6/11/2021	11:43:13	26.7	57.1	
10	6/11/2021	11:43:18	26.8	56.5	
11	6/11/2021	11:43:23	26.8	56.3	
12	6/11/2021	11:43:28	26.8	56.1	
13	6/11/2021	11:43:33	26.8	56.2	
14	6/11/2021	11:43:38	26.8	56	
15	6/11/2021	11:43:43	26.8	56.1	
16	6/11/2021	11:43:48	26.8	56.2	
17	6/11/2021	11:43:53	26.8	56.2	
18	6/11/2021	11:43:58	26.8	56	
19	6/11/2021	11:44:03	26.8	55.9	
20	6/11/2021	11:44:08	26.9	55.8	
21	6/11/2021	11:44:13	26.8	55.7	
22	6/11/2021	11:44:18	26.8	55.7	

Simple Data
Simple Data with Plots
Interactive Bar Graph

**Fig.15.** Temperature and the humidity data measured by the DHT11 sensor, sent by the RF transmitter, received from the RF receiver in a data log file

## Conclusions

In this paper with theoretical analysis is designed and practically realized process RF sensor smart network. Sensor network measurement and collection data for temperature and humidity in measurement point at one remote processing plants and transmission to the main central control panel. The data is displayed on the LCD display and stored in an excel log file. The solution also provides the ability for upgrade to remote transfer on the data over the internet.

## References

- [1] S. Bennett, S. Linkens, Computer Control of Industrial Processes, D.A. (Eds.), IEEE, 1982.
- [2] Ching-Lai Hor and Peter A. Crossley, Knowledge Extraction from Intelligent Electronic Devices, Lecture Notes in Computer Science pp. 82-111, January 2005.
- [3] Teen-Hang Meen, Wenbing Zhao and Cheng-Fu Yang Special Issue on Intelligent Electronic Devices Reprinted from: Electronics 2020, 9, 645.
- [4] S. Bennett, S. Linkens, Computer Control of Industrial Processes, D.A. (Eds.), IEEE, 1982.
- [5] Single chip 2.4 GHz Transceiver NRF24L01, Nordic Semiconductor ASA - Vestre Rosten 81, N-7075 Tiller, Norway
- [6] ATmega 328P 8-bit AVR Microcontroller with 32K Bytes In-System, [https://ww1.microchip.com/downloads/en/DeviceDoc/Atmel-7810-Automotive-Microcontrollers-ATmega328P\\_Datasheet.pdf](https://ww1.microchip.com/downloads/en/DeviceDoc/Atmel-7810-Automotive-Microcontrollers-ATmega328P_Datasheet.pdf)



## FREQUENCY SINUS SOURCE

*Goce Stefanov<sup>1</sup>, Vasilija Sarac<sup>2</sup>*

<sup>1</sup>Faculty of Electrical Engineering University Goce Delcev Stip R.Macedonia, goce.stefanov@ugd.edu.mk

<sup>2</sup>Faculty of Electrical Engineering University Goce Delcev Stip R.Macedonia, vasilija.sarac@ugd.edu.mk

### Abstract

*In the paper are presented the results of a practically realized on variable frequency sinus source. This source generated sinusoidal voltage with amplitude from 0 to 220 V and frequency from 0 to 100 Hz. The solution is based on EG8010 integrated circuit and driver circuit IR2010s. Control electronics operate IGBT transistors in the topology of full bridge. The operation of the circuit is verified with oscillograms and data obtained from measurements of the practically realized prototype.*

### Key words

*PWM signal, frequency, sinus.*

### 1. Introduction

The electronics converters used to control in power actuators (motors, heating devices) at the output generate voltage and current with a square waveform or waveform which in the first approximation is a modified sine wave. Therefore, there is a harmonic distortion of the output voltages and currents at these power sources. This causes a reduction in the power factor and the efficiency of the source [1]. One of the main tasks of electronics that deals with this issue is the design of electronic components and devices that will provide a sine wave form of the output voltage and current of the power source.

On the other hand electronic devices that control converters that drive induction motors, need to provide a variable frequency waveform. This is in line with the requirement for the induction motors to run at a constant torque, ie the operation of the motor at a constant torque requires the V/f ratio to be constant.

A sinusoidal wave source is also required and for laboratory research.

Development of the electronic components and devices for power source is based on the development of microelectronics circuits [2]. There are mainly two directions of development of integrated circuits that are used in the power electronics. On one side are microcomputers [3], [4], [5], and on the other side are typical integrated circuits designed for special purposes [6], [7]. Microcomputers are intelligent electronic component which have a number of advantages over discrete electronic components. Their main advantage is the packing density of the chip itself. It is the result of the development of microelectronics and enables over one million discrete electronic elements to be embedded on a surface of 1 cm<sup>2</sup>. Their second advantage, which distinguishes them from discrete electronic components, is their application flexibility [3], [4], [5]. The latter implies the ability to run different applications with the same network hardware, and with software changes. But on the other hand, the design of electronic circuits with a microcomputer requires knowledge of appropriate software and in the development of the product converter it is necessary to include more specialists who know the hardware, software and related knowledge to the topologists of the converters.



Unlike from design of the converters based of microcomputer, design based of special circuit requires reduced knowledge of hardware, software, and only a good knowledge of converter topology is enough to make a successful converter product [6], [7]. Clearly, which approach will are choose in the design of the converter depends on its nominal power. But for small and medium power up to 5kW, it can be said that the design of a converter with special circuits is more economically justified.

Therefore in this paper we want to verify the possibility of using an sinus source based on special circuit that, in variable frequency and amplitude conditions, gives optimal results comparable to a normal inverter system, with the difference that this system uses a low-cost microcontroller. Indeed, the purpose is to evaluate the degree of precision that can be achieved by using this integrated solution. Frequent sine source is based on SPWM technique and SPWM signal.

Guided by the main goal of the paper, implementation of the special integrated circuit in generating SPWM (sine pulse wave modulation) signals and realization of the converter with power driver, here will be explained the functioning of these three interconnected parts, ie. SPWM, integrated circuit and power driver.

In the Fig. 1 is shown a block diagram on 1-phase motor which is controlled by special integral circuit.

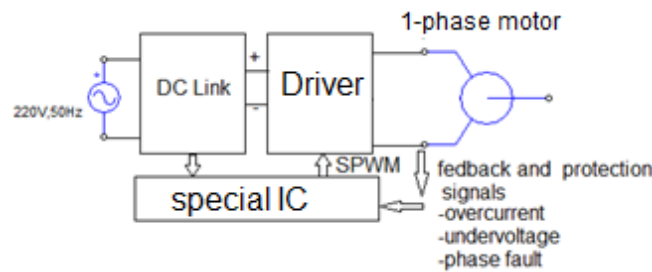


Fig. 1. Block diagram on 3-phase motor controlled by microcontroller.

SPWM signal which is a width modulated signal but with certain values on such a way that we could create a sine shape wave at the output. This with used on MOSFET or IGBT transistors could result in a sine wave inverter.

It is generally known that PWM signal is pulse width modulation. That means we modulate the width of a square signal and by that we could control power. But, this width in case of normal PWM is always the same. In case of SPWM or sinusoidal pulse width modulation, the width of the signal is increasing and decreasing and my that simulating the curve of the sine wave. With small width pulse, the output will increase a little bit and that represents the zone after the 0 cross of the sine wave. Then with bigger widths, the output is getting bigger and bigger and then it starts to get lower, just as a sine wave. Using two transistors switching, can could get both the positive and negative sides of the sine wave, Fig. 2.

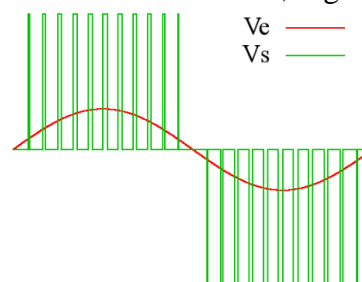


Fig. 2. Construction of SPWM signal.

In the Fig. 3 below can see a bit better how the width of the SPWM can create a good sinusoidal shape at the output. Will use Integral Circuit to generate this SPWM signal. We apply this signal to the power driver. These will be connected to the motor. In the Fig. 3 is shown SPWM signal and the current and voltage waveforms of the motor.

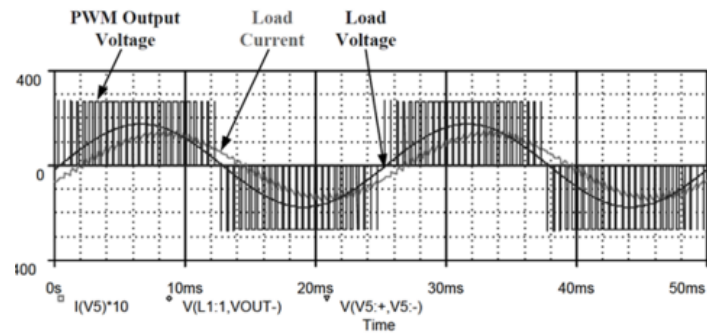


Fig. 3. SPWM signal and the current and voltage waveforms of the motor.

## 2. Characteristics of the EG 8010 Special Integral Circuit

This Integral Circuit allows to obtain the pure sine wave at 50/60 Hz with high precision and low harmonic distortion. It is also an external 12MHz crystal oscillator that allows you to adjust the system clock. Lastly there is a sinusoidal SPWM generator. We report below the block diagram and the electrical characteristics of the Integral Circuit. In the Fig. 4 is shown block diagram on this circuit. This circuit can operation in unipolar and bipolar mod. With unipolar modulation operation, only one of the two bridges (SPWMOUT3 and SPWMOUT4) will be used for the output modulated in SPWM, the other bridge will be used instead for the fundamental output (SPWMOUT1, SPWMOUT2). From the circuit point of view there will be an inductor and a capacitor, to create an LC filter, connected to the output port of the SPWM and there will also be a voltage feedback circuit connected to the output of the inductor.

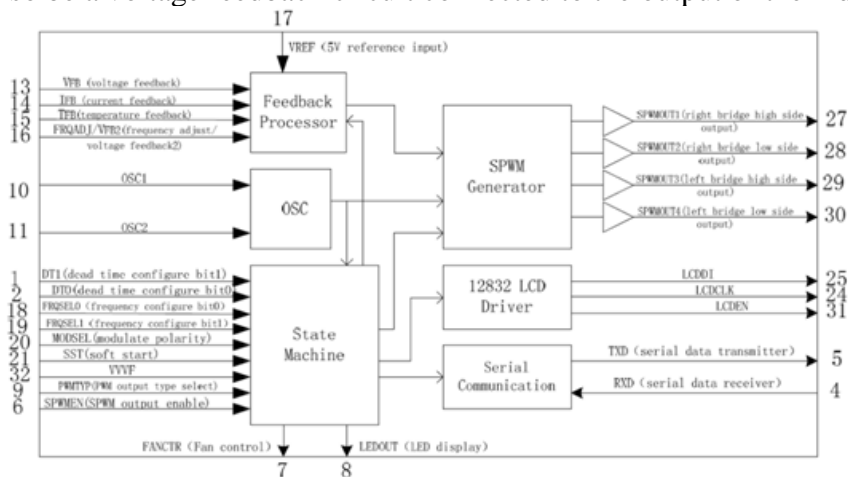


Fig. 4. Block diagram on EG 8010 circuit.

EG 8010 can ensure that the source (converter) operates in mode on variable output voltage and constant frequency, in mode on constant voltage and variable frequency and in mode on variable voltage and variable frequency. The first and second mode is used for AC voltage consumers and the third for AC motor speed regulation. In the Fig.5 is shown the physical appearance of the electronic board EG002 where they are embedded IC EG8010 and driver IRF2110. In the Fig. 6 is shown electrical circuit on the electronic board with build IC EG8010 and driver IRF2110.

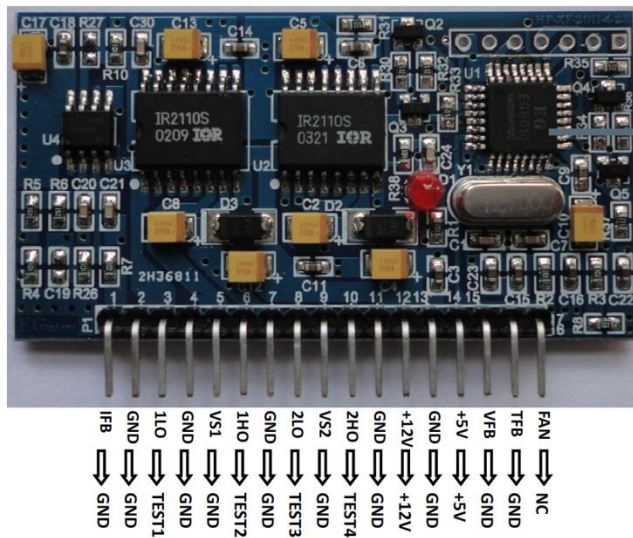


Fig. 5. Electronic board EGS002 with build IC EG8010 and driver IRF2110.

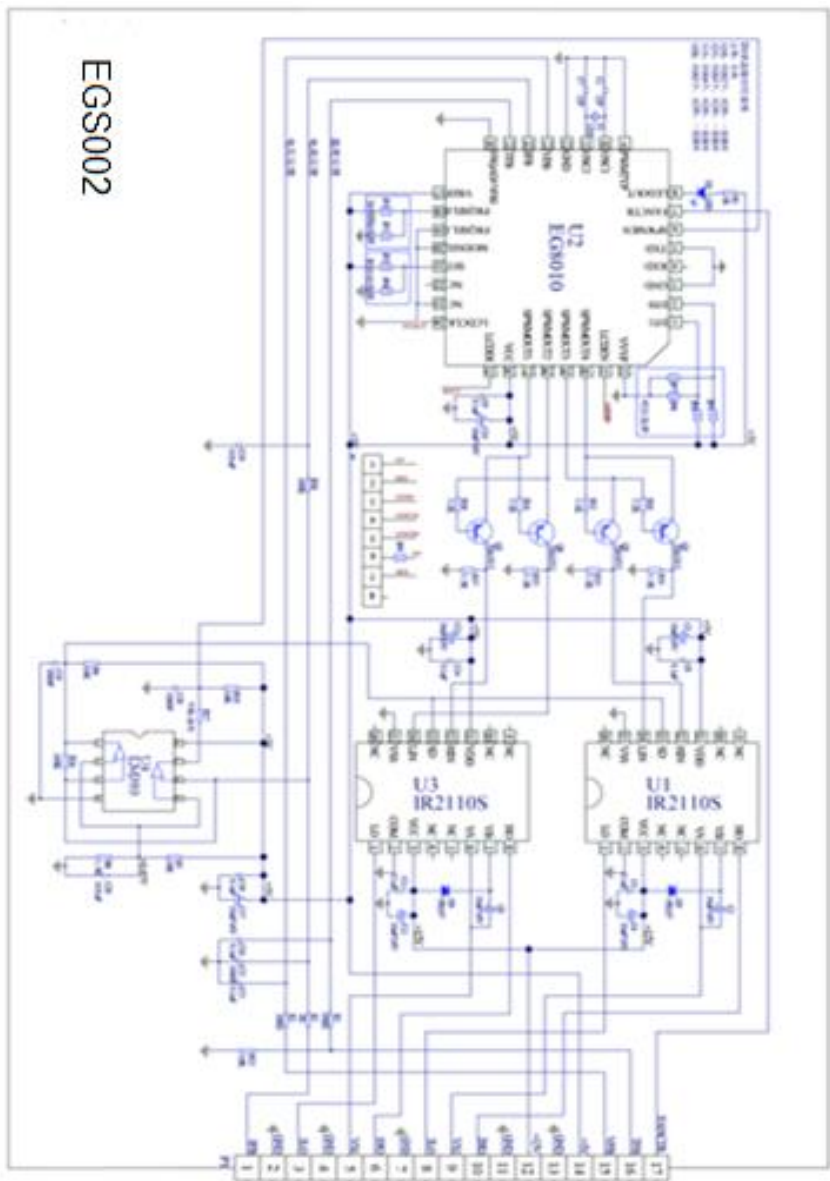


Fig. 6. Electrical circuit on the board EG002 with build IC EG8010 and driver IRF2110.

In this paper, a converter design based on EG 8010 in mode on constant voltage and variable frequency is made. In the Fig. 7 is shown electrical connected circuit where EG8010 operates as a source frequency controller.

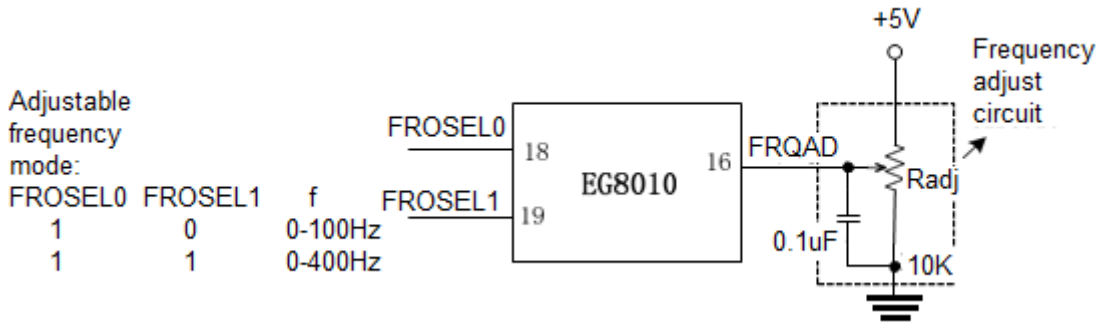


Fig. 7. Electrical connected circuit where EG8010 operates as a source frequency controller.

EG8010 has two frequency modes: constant frequency mode and adjustable frequency mode. In adjustable frequency mode, EG8010 only uses unipolar modulation, and pin (20)MODSEL has to connect to low level. Pins FRQSEL1 and FRQSEL0 set the frequency mode. In constant frequency mode, “00” outputs 50Hz frequency and “01” outputs 60Hz frequency. FRQADJ has no function in constant mode. Pin (16) is used as VFB2 voltage feedback circuit under bipolar modulation. In adjustable frequency mode, “10” outputs frequency in range of 0-100Hz and “11” outputs frequency in range of 0-400Hz. Pin FRQADJ adjusts the frequency as shown in figure 8.6a. Pin FRQADJ’s voltage varies from 0-5V, which is corresponding to the fundamental wave output frequency from 0-100Hz or 0-400Hz. This function accompanies with pin VVVF can be used in the single phase frequency transformer system.

### 3. Experimental results

The operation of the EG8010 circuit is experimentally illustrated in the mode of constant voltage and variable frequency. For this purpose the corresponding pins of the EG 8010 are set as follows: for source with 100Hz variable frequency pins FRQSEL1,FRQSEL0=10, or for source with 400 Hz variable frequency pins FRQSEL1,FRQSEL0=11, and pin VVVF is setting in logical 0. Variable frequency from 0 to 100 Hz (or 0 to 400 Hz) is setting with resistor connected to pin 16 on EG8010 shown in Fig. 7. AC output voltage is adjusted by the feedback resistor R23.

To illustrate the mode of constant voltage and variable frequency, a prototype of a frequency sine source was designed and practically realized. In the Fig. 8 is shown the prototype in the manufacturing phase and Fig. 8 b is shows the finished device.

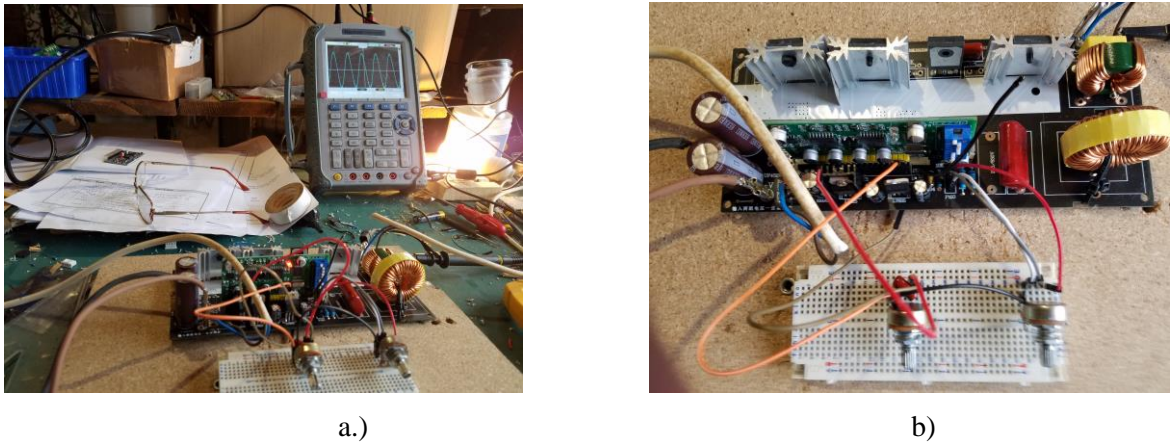


Fig. 8. Prototype of practically realized a frequency sine source: a.) in the manufacturing phase, b.) finished device.



In the Fig. 10a is shown PWM waveform on the output SPWMOUT3 and SPWMOUT4 on EG 8010.

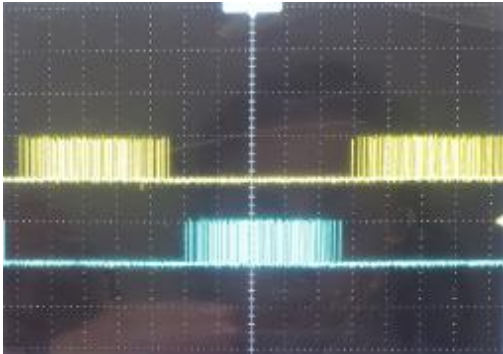
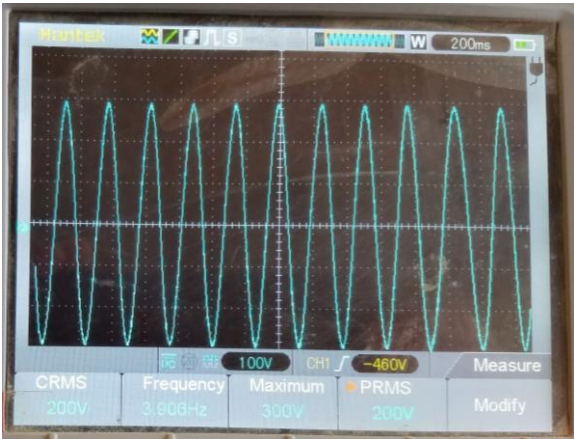


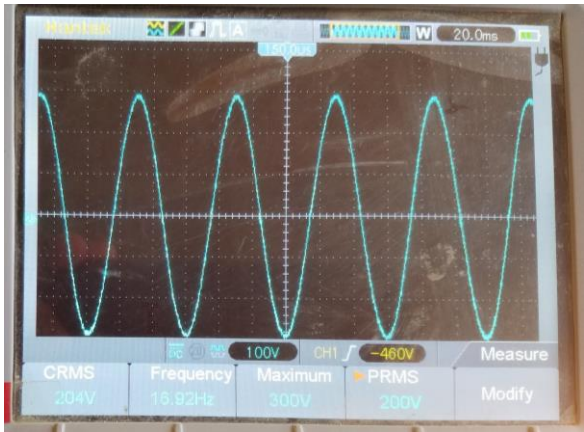
Fig. 10. PWM waveform on the output SPWMOUT3 and SPWMOUT4 horizontal is 4 ms/div and vertical is 5 V/div.

From Fig. 10 are see that the pulse on output SPWMOUT3 and SPWMOUT3 are phase shifted for 180. It provides orthogonal switching of IGBT transistors in one half bridge.

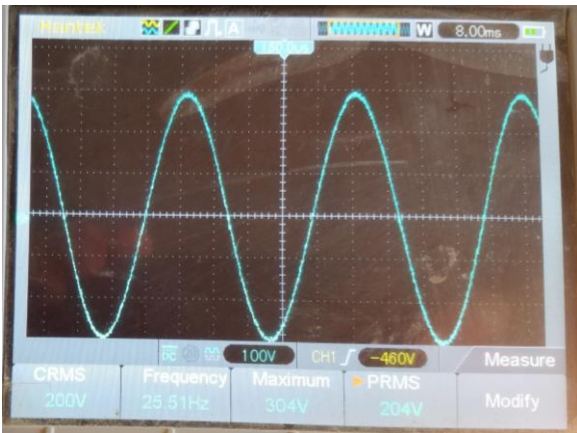
For verification of the work of the realized frequency sine source, are made oscillograms which are shown in the Fig. 9.



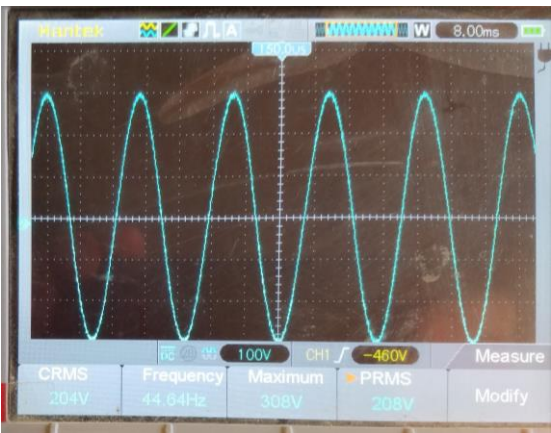
a.)



b.)



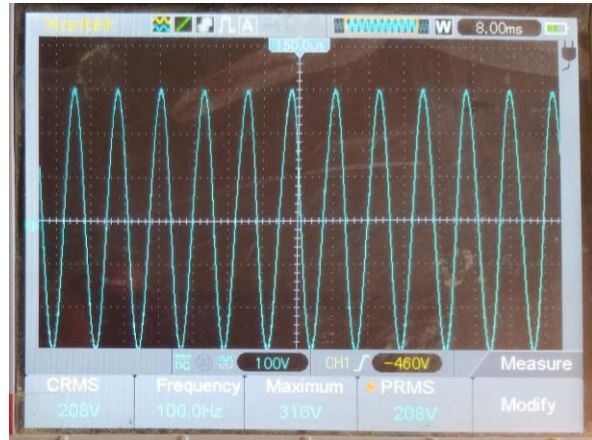
c.)



d.)



e.)



f.)

Fig. 9. Oscillograms from the work of the frequency sine source: a.) 3 Hz, horizontal div is 200 ms, b.) 16 Hz, horizontal div is 20 ms, c.) 25 Hz, horizontal div is 8 ms, d.) 44 Hz, horizontal div is 8 ms, e.) 69 Hz, horizontal div is 8 ms, f.) 100 Hz, horizontal div is 8 ms.

From Fig. 9 it can be seen that all oscillograms have a sine waveform, the vertical base is 100V/div and the sine wave amplitude is 300 V. The oscillograms in Fig. 9 are made when EG8010 works like source with 100Hz variable frequency and pins FRQSEL1,FRQSEL0=10. In the Fig 10 are shown the oscillograms when EG8010 works like source with 400Hz variable frequency and pins FRQSEL1,FRQSEL0=11.



a.)



b.)



c.)

Fig. 10. Oscillograms from the work of the frequency sine source: a.) 135 Hz, horizontal div is 2 ms, b.) 217 Hz, horizontal div is 2 ms, c.) 305 Hz, horizontal div is 2 ms.

## Conclusions

The paper analyzes the application of a special integrated circuit which controlling inverter to generate sine voltage. The characteristics of the circuit are given and the advantages of its application in relation to the inverters controlled by microcomputer are emphasized. Designed and experimentally is realized prototype on frequency sine source controlling by this circuit. The results of the work of the prototype confirmed by the oscillograms, show that the realized frequency sine source generates voltage with sine waveform with variable frequency and constant amplitude.

## References

- [1] Williams W. B., (2006). Principles and Elements of Power Electronics, University of Strathclyde, Glasgow.
- [2] Kumar A.A., (2014). Pulse and Digital Circuits, PHI.
- [3] Atmel AVR, (2018) 48A/PA/88A/PA/168A/PA/328/P, Microchip Technology Incorporated, All Rights Reserved.
- [4] Atmel ATmega, (2014), 640/V-1280/V-1281/V-2560/V-2561/V, Atmel Corporation, 1600 Technology Drive, San Jose, CA 95110 USA.
- [5] <https://www.theengineeringprojects.com/2018/06/introduction-to-arduino-nano.html>.
- [6] [https://www.lz2gl.com/data/power-inverter\\_3kW/eg8010\\_datasheet\\_en](https://www.lz2gl.com/data/power-inverter_3kW/eg8010_datasheet_en).
- [7] [https://www.egmicro.com/download/EGS002\\_manual](https://www.egmicro.com/download/EGS002_manual)





## MEASUREMENT ON COMPENSATION CAPACITANCE IN INDUCTIVE NETWORK BY MICROCONTROLLER

*Goce Stefanov<sup>1</sup>, Saso Gelev<sup>2</sup>, Todor Cekerovski<sup>3</sup>*

<sup>1</sup>Faculty of Electrical Engineering University Goce Delcev Stip R.Macedonia, goce.stefanov@ugd.edu.mk

<sup>2</sup>Faculty of Electrical Engineering University Goce Delcev Stip R.Macedonia, saso.gelev@ugd.edu.mk

<sup>3</sup>Faculty of Electrical Engineering University Goce Delcev Stip R.Macedonia, todor.cekerovski@ugd.edu.mk

### Abstract

*In the paper are presents the results of a practically realized prototype on an microcontroller circuit for determined on the compensation capacitance in inductive network. In energy networks with high inductive load the reactive energy is high and therefore these networks operate with a low power factor. In such networks to reduce the reactive energy are installed compensating capacitors. The solution in the paper determines the required capacitance in inductive networks to reduce reactive energy and increase the power factor to one unit. The realized measuring circuit, in addition to determining the value of the compensation capacitor, determines the current, voltage, active power, active energy and reactive energy. The circuit is based on Atmega 328 microcontroller and smart power meter PZEM004. The capacitance value is visualized on an LCD display, and the values of current, voltage, active power, compensation capacitance and power factor are displayed on a serial monitor on the computer.*

### Key words

*Power meter, Microcontroller, Measurement capacitance.*

### 1. Introduction

In power industrial plants, AC and DC motors are mainly used as actuators. They are inductive consumers and contribute to increasing reactive power (energy). The increase of reactive power is related to the decrease of the power factor and thus the decrease of the active power at the same apparent power. In power plants with AC or DC motors connected directly to the power network, the reason for the reduction of the power factor is the increase of the phase angle between the voltage and the current. This increase is caused by the inductive nature of electric motors.

The situation is similar at actuators supply by converters. Due to the change in the inductance of the load leads to a reduction of the power transfer from the converter to the load.

From interest is the power transferred from the power network (or converter) on the load be maximal. Often due to the change in the parameters of the output circuit of the converter, this power is not always maximal [1], [2], [3]. To maintain maximum transferred power from the converter to the load, is needed knowledge of the parameters that affect the power. Independent of the type of process controlled by the converter, motor drive or induction device, etc., causes leading to a reduction in the transferred power are related to increasing the phase difference between the voltage and the current of the converter as well the deviation of duty cycle of value 0.5. The change in the phase difference is caused by the change of parameters (inductance, resistance, and capacitance) of the output circuit of the converter. To changing the duty cycle on the output voltage of the converter comes as a result of the need to change the effective value of the output voltage, with target to controlling the output power of the converter. The change on the phase difference leads to an increase in reactive power and a reduction in the

active power of the converter. And reduction of the duty cycle from 0.5 increases the harmonic distortion of the output voltage and current of the converter. Both reasons reduced the output active power and efficiency of the converter [4], [5], [6] [7].

In Fig. 1 is shown the electrical scheme of inductive actuators which is supply from full bridge converter. A typical inductive actuator is a device for induction heating of metal materials. The nominal initial values of the actuator parameters are:  $R = 0.24 \Omega$ ,  $C = 26,6 \mu\text{F}$  and  $L = 26,5 \mu\text{H}$  [8].

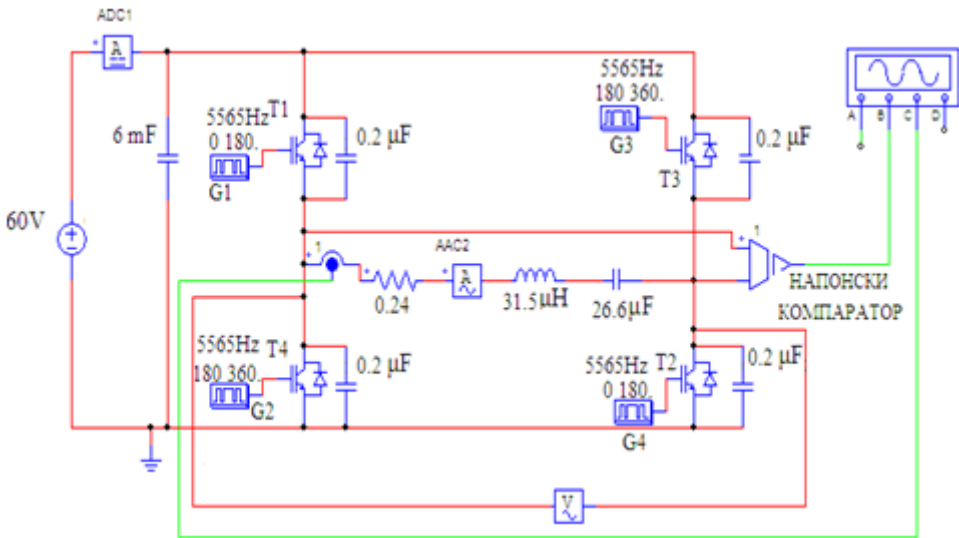


Fig. 1. Electrical scheme of inductive actuators which is supply from full bridge converter.

In Fig. 2 shows the output voltage and current waveforms on the converter from Fig. 1. In induction heating/melting and similar applications the heated workpiece equivalent electrical parameters are part of the resonant circuit. As the work-piece temperature increases, its equivalent resistance and inductance change, thus changing the circuit resonant frequency. Consequently, the deviation of the switching frequency from the resonant one is also changed, which results in undesired change of output power. The typical  $R$  and  $L$  change during metal-piece induction melting is in the range of 50%. These real values are used as an example in the following investigation giving the values for the resonant frequency  $\omega_0 = 37665 \text{ rad/s}$ ,  $f_0 = 5998 \text{ Hz}$  [9], [10].

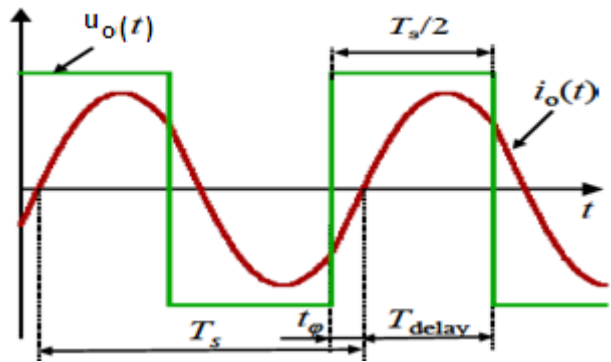


Fig. 2. Output voltage and current waveforms on full bridge converter loading with inductive load.

The mode of induction heating changes the value of the resistance and inductance of the resonant circuit of the converter. This leads to a change in the phase difference between the current and the voltage of the converter and the change of the output power. In Table I are given the values on the switching frequency  $f_{sw}$ , output voltage  $U_o$ , output current  $I_o$ , output power  $P_o$  and phase difference  $\varphi$  for change the inductance for 20 %, i.e.: change on  $L$  from

26.5  $\mu\text{H}$  on 31.5  $\mu\text{H}$ .

TABLE I: VALUE ON OUTPUT CONVERTER PARAMETERS FOR CHANGE ON INDUCTANCE FROM 20%

$L$ [ $\mu\text{H}$ ]	$R$ [ $\Omega$ ]	$\varphi_i$ [ $^\circ$ ]	$f_{sw}$ [kHz]	$I_o$ [A]	$U_o$ [V]	$P_o$ [kVA]
26,5	0,24	5,00	6.27	208	56	10,7
31,5	0,29	31,34	6.27	145	56	6,16

From Table I it can be seen that a change of  $R$  and  $L$  by 20% causes a change of the phase angle for 63 % and change on the power for 58 %. In the Table II is given value on compensation capacitance which is needed to compensate for the change in inductance and the phase angle  $\varphi$  and the power  $P_o$  to remain unchanged.

TABLE I: VALUE ON COMPENSATION CAPACITANCE AND POWER

$L$ [ $\mu\text{H}$ ]	$R$ [ $\Omega$ ]	$C$ [ $\mu\text{F}$ ]	$\varphi_i$ [ $^\circ$ ]	$f_{sw}$ [kHz]	$I_o$ [A]	$U_o$ [V]	$P_o$ [kVA]
26,5	0,24	26.6	5.00	6.27	208	56	10,7
31,5	0,24	21.28	5.00	6.27	208	56	10.7

From Table II it can be seen that if a capacitor is installed in the circuit whose value is changed by 20 %, it will compensate for the change in inductance and the circuit will operate with constant power.

2. Design on microcontroller circuit for measurement on compensation capacitance

In this part an microcontroller (microcomputer) power meter is designed. The designed solution will collect data for the current from current transformer and the voltage on which is connected device in industrial power process. In the Fig. 3 is shown block diagram of the specific microcontroller circuit, [8], [9], [10] [11].

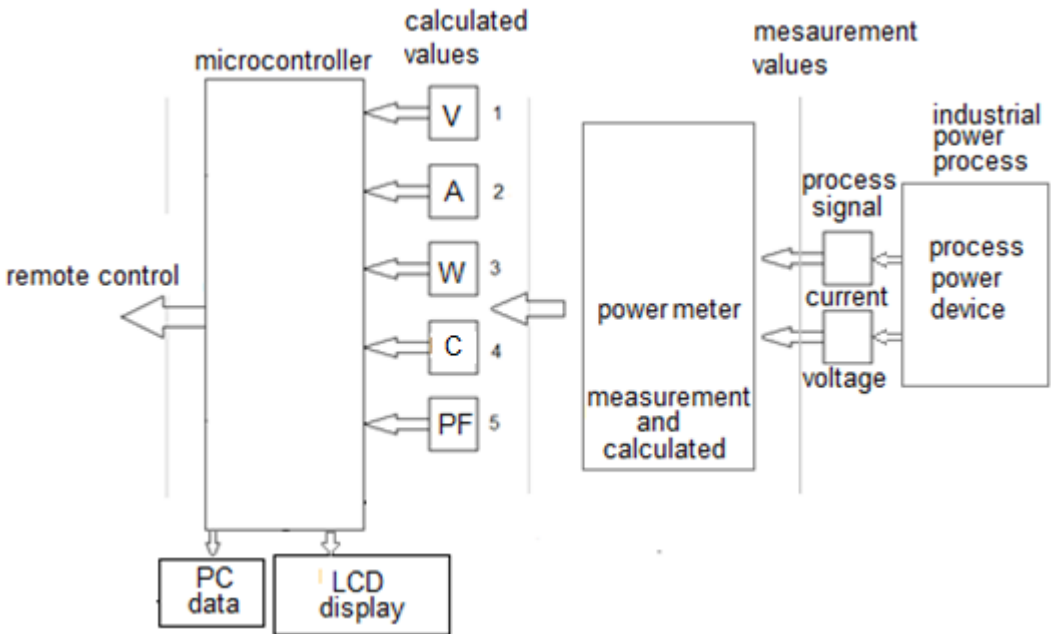


Fig. 3. Block diagram of the specific solution of an microcontroller power meter.

The main part of this power meter is the microcomputer. In the solution is selected the microcontroller Atmega 328P [12]. Microcontroller power meter takes data on the current and

the voltage from the power device. The current data is taken with a current transformer. The voltage data is obtained from the voltage of the device terminals. Based on the current and voltage, the power meter calculates power, capacitance and power factor and sends it to the microcomputer together with the current and voltage data. In the Fig. 3 calculated values are marked as: 1 is the data for voltage marked as V, 2 is the data for current marked as A, 3 is the data for power marked as W, 4 is the data for capacitance marked as C, and 5 is the data for power factor marked as PF. The power meter is connected to the microcomputer with the serial port. Based on the values of these parameters, the microcontroller according to the developed algorithm calculates the value of the compensation capacitance and displays it on the LCD display. Also the microcontroller sends data on the current values of the quantities, on a personal computer in serial monitor.

In the Fig. 4 is shown the connection diagram of the realized solution.

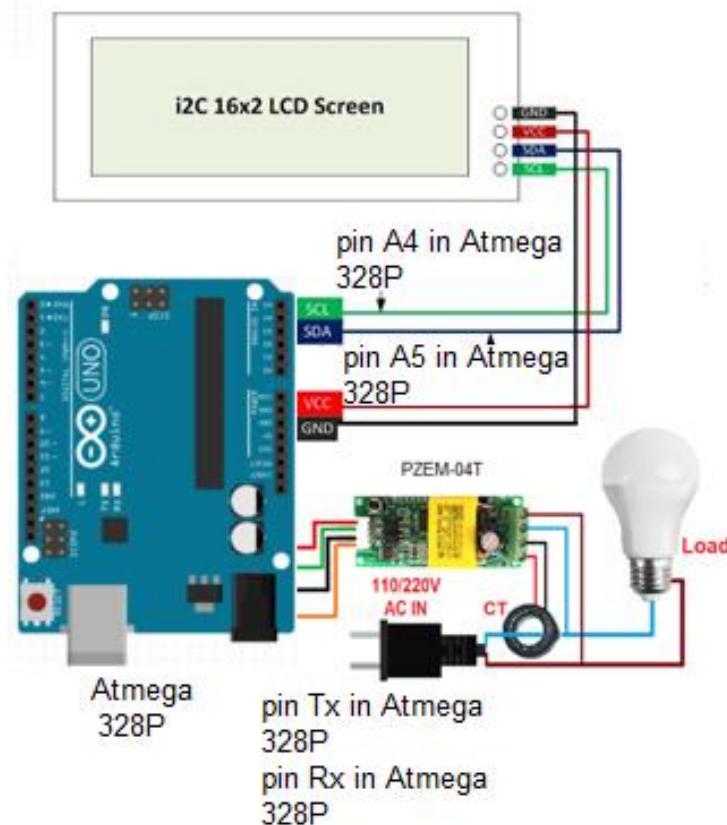


Fig. 4. Connection diagram of the realized solution.

Figure 4 shows that the solution was realized using Arduino Uno Atmega 328P and a power meter PZEM 004T, [13] .

## 2.1 Features of the used hardware

### a.)Microcomputer Atmega 3238P

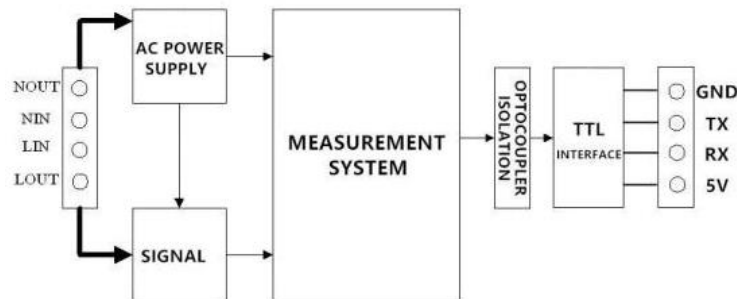
The Arduino Uno is an open-source microcontroller board based on the Microchip ATmega328P microcontroller and developed by Arduino.cc. The board is equipped with sets of digital and analog input/output (I/O) pins that may be interfaced to various expansion boards (shields) and other circuits. The board has 14 digital I/O pins (six capable of PWM output), 6 analog I/O pins, and is programmable with the Arduino IDE (Integrated Development Environment), via a type B USB cable. It can be powered by the USB cable or by an external 9-volt battery, though it accepts voltages between 7 and 20 volts. The word "uno" means "one" in Italian and was chosen to mark the initial release of Arduino Software.<sup>[1]</sup> The Uno board is







a.)



b.)

Fig. 6. a.) The board on PZEM-004T power meter, and b.) block diagram on this module.

### Function description

Voltage measuring range is 80~260V.

Current measuring range is 0~10A(PZEM-004T-10A); 0~100A(PZEM-004T-100A)

Active power measuring range is 0~2.3kW(PZEM-004T-10A); 0~23kW(PZEM-004T-100A)

Starting measure power is 0.4W. Resolution is 0.1W.

Display format: < 1000W, it display one decimal, such as: 999.9W. ≥1000W, it display only integer, such as: 1000W. Power factor measuring range is 0.00~1.00, resolution is 0.01.

Frequency measuring range is 45Hz~65Hz, resolution is 0.1Hz.

Active energy measuring range is 0~9999.99kWh, resolution is 1Wh.

Display format: < 10kWh, the display unit is Wh(1kWh=1000Wh), such as: 9999Wh

≥10kWh, the display unit is kWh, such as: 9999.99kWh

Over power alarm

Active power threshold can be set, when the measured active power exceeds the threshold, it can alarm. Communication interface is RS485 interface.

### Communication protocol

Physical layer use UART to RS485 communication interface. Baud rate is 9600, 8 data bits, 1 stop bit, no parity. The application layer use the Modbus-RTU protocol to communicate. At present, it only supports function codes such as 0x03 (Read Holding Register), 0x04 (Read Input Register), 0x06 (Write Single Register), 0x41 (Calibration), 0x42 (Reset energy).etc. 0x41 function code is only for internal use (address can be only 0xF8), used for factory calibration and return to factory maintenance occasions, after the function code to increase 16-bit password, the default password is 0x3721.

The address range of the slave is 0x01 ~ 0xF7. The address 0x00 is used as the broadcast address, the slave does not need to reply the master. The address 0xF8 is used as the general

address, this address can be only used in single-slave environment and can be used for calibration etc.operation.

The command format of the master reads the measurement result is(total of 8 bytes): Slave Address + 0x04 + Register Address High Byte + Register Address Low Byte + Number of Registers High Byte + Number of Registers Low Byte + CRC Check High Byte + CRC Check Low Byte.

The command format of the reply from the slave is divided into two kinds: Correct Reply: Slave Address + 0x04 + Number of Bytes + Register 1 Data High Byte + Register 1 Data Low Byte + ... + CRC Check High Byte + CRC Check Low Byte Error Reply: Slave address + 0x84 + Abnormal code + CRC check high byte + CRC check low byte.

### 3. Experimental results

The design of an microcontroller power meter are consists of hardware design and software design.

#### *Hardware design*

According to the description of the characteristics of the hardware components given above and the main purpose of the paper, in the Fig. 4 is shows the electrical circuit of the WI-FI smart power meter. The circuit consists of Arduino Uno, PZEM-004T power meter and LCD display.

#### *Software design*

The software is written in micro C. Arduino Uno software is compatible with the Arduino IDE platform. The software ensures that the microcomputer receives the signals from the power meter and, after processing, displays the current values on the voltage, current, power, energy, frequency and power factor on LCD display, sends them in serial monitor.

According to the above, the software consists of several steps.

*Defining on variables and libraries:*

```
#include <PZEM004Tv30.h>
#include <SimpleTimer.h>
#include <LiquidCrystal.h>
#include <Wire.h>
#include <LiquidCrystal_I2C.h>
```

*Reading data on Serial Monitor:*

```
float v = pzem.voltage(ip);
if (v < 0.0) v = 0.0;
Serial.print(v);Serial.print("V; ");
float i = pzem.current(ip);
if (i < 0.0) i = 0.0;
Serial.print(i);Serial.print("A; ");
float p = pzem.power(ip);
if (p < 0.0) p = 0.0;
Serial.print(p);Serial.print("W; ");
Serial.print(Cap);Serial.print("uF ");
Serial.print("PF= ");Serial.print((p)/(v*i));
```

*Building a data log file:*

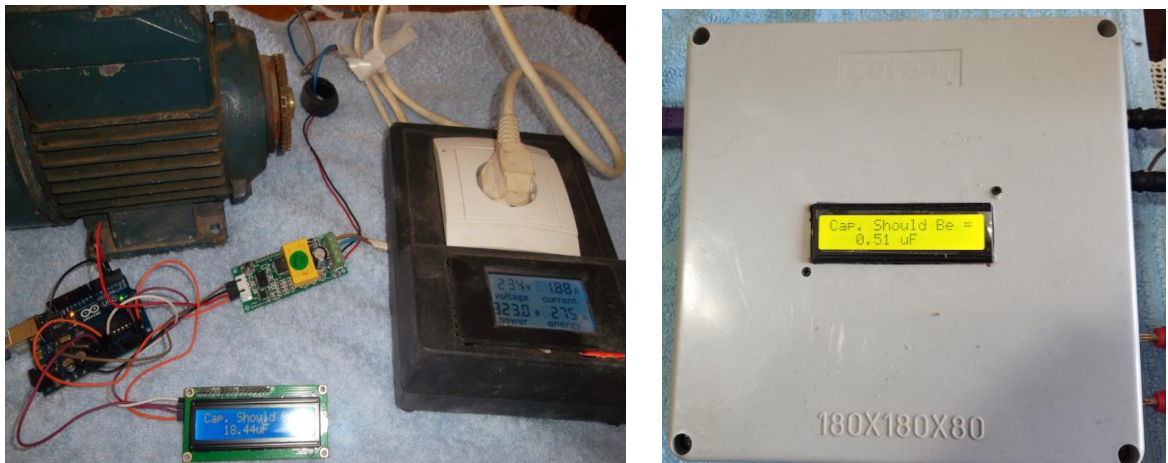
```
Serial.print(value()); // Read value from sensor and send its value to Excel
Serial.print(","); // Move to next column
```

*Reading data on display:*

```
lcd.print("name:");
lcd.print(variable);
lcd.print("unit");
```



In the Fig. 7a is shown the experimental prototype on microcontroller power meter, and the Fig. 7b is shown the complete process microcontroller power meter.



a.) b.)

Fig. 7. Experimental results: a.) prototype on the microcontroller power meter and b.) the complete process microcontroller power meter.

In the Fig. 8 is shown data for voltage, current, power, capacitance and power factor in serial monitor.

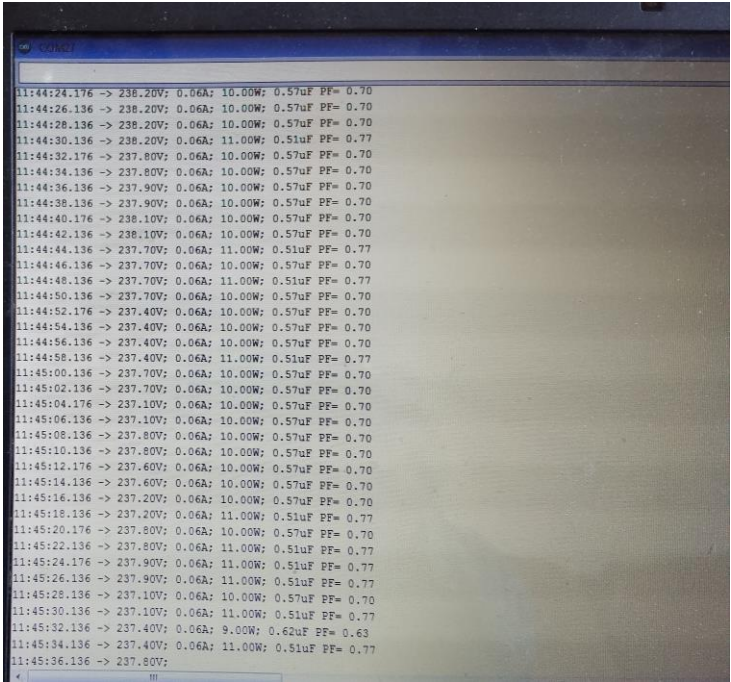


Fig. 8. The data for voltage, current, power, capacitance and power factor in serial monitor.

Conclusions

In the paper with theoretical analysis is designed and practically realized microcontroller power meter. The power meter allows data on power, compensation capacitance and power factor to be obtained only by measuring the voltage and current of a process device. Then these data are processed, the required compensatory capacity is visualized on an LCD screen and data for

voltage, current, power, capacitance and power factor are sent in serial monitor. The solution also provides the ability for upgrade to remote control on the process quantities.

## References

- [1] G.E.Totten, Steel Head Treatment, Portland State University, Oregon USA, Second Edition 2006.
- [2] W. B. Williams, Principles and Elements of Power Electronics, University of Strathclyde, Glasgow, 2006.
- [3] W. Shepherd, L. Zhang, Power Converter Circuits, Marcel Dekker, 2004, ch.15
- [4] D. Maksimovic, R. Zane, R. Erickson, "Impact of digital control in power electronics", In Proceedings of the IEEE 16th International Symposium on Power Semiconductor Devices and ICs. May: 13–22. 2004.
- [5] K. Harada, Analysis and Design of ZVS-PWM Half-Bridge Converter, IEEE PESC Record, 1995, pp. 280-285.
- [6] J. Shklovski, K. Janson, T. Sakkos, Natural Mode Constant Power Source for Manual Arc Welding, Elektronika Ir Elektrotehnika, Vol 18, No 9, 2012.
- [7] Y. Kwon, S. Yoo, D. Hyun, "Half-bridge series resonant inverter for induction heating applications with load-adaptive PFM control strategy", Applied Power Electronics Conference and Exposition, pp. 575–581, Dallas, TX, USA, 14–18 Mar 1999.
- [8] S. Bennett, S. Linkens, Computer Control of Industrial Processes, D.A. (Eds.), IEEE, 1982.
- [9] Ching-Lai Hor and Peter A. Crossley, Knowledge Extraction from Intelligent Electronic Devices, Lecture Notes in Computer Science pp. 82-111, January 2005.
- [10] Teen-Hang Meen, Wenbing Zhao and Cheng-Fu Yang Special Issue on Intelligent Electronic Devices Reprinted from: Electronics 2020, 9, 645.
- [11] By M.A. Matin and M.M. Islam, Wireless Sensor Network, <https://www.intechopen.com/books/wireless-sensor-networks-technology-and-protocols/overview-of-wireless-sensor-network> September 6th 2012, DOI: 10.5772/49376.
- [12] ATmega 328P 8-bit AVR Microcontroller with 32K Bytes In-System, [https://ww1.microchip.com/downloads/en/DeviceDoc/Atmel-7810-Automotive-Microcontrollers-ATmega328P\\_Datasheet.pdf](https://ww1.microchip.com/downloads/en/DeviceDoc/Atmel-7810-Automotive-Microcontrollers-ATmega328P_Datasheet.pdf)
- [13] PZEM004T V3.0 User Manual, <https://innovators-guru.com/wp-content/uploads/2019/06/PZEM-004T-V3.0-Datasheet-User-Manual.pdf>



## ИЗРАБОТКА НА ВЕШТ НАОД И МИСЛЕЊЕ ОД ОБЛАСТА НА ЕЛЕКТРОТЕХНИЧКИТЕ НАУКИ

**Ненад Поповиќ<sup>1</sup>, Сашо Гелев<sup>2</sup>**

<sup>1</sup>Студент на 2 циклус студии Електротехнички факултет Универзитет Гоце Делчев Штип Република  
Македонија [npopovic2@hotmail.com](mailto:npopovic2@hotmail.com)

<sup>2</sup>Електротехнички факултет Универзитет Гоце Делчев Штип Република Македонија,  
[saso.gelev@ugd.edu.mk](mailto:saso.gelev@ugd.edu.mk)

**Апстракт:** Во текот на досегашната практика во изработка на вештачења изработени од колеги вешти лица, можат да се воочат разлики, понекогаш и дијаметрални, не само во методологијата на изработка, туку и на форма на пристапот на проблемот. Ова може да предизвика забуна кај корисниците на овие наоди. Со овој труд се обидуваме да дадеме придонес кон методологија за изработка на професионален и објективен наод и мислење, посебно што за такво нешто досега нема изработено трудови, барем не кај нас во република Македонија.

Во трудот се обработува проблематика на опожарување на објекти предизвикани од ел.енергија. Трудот е составен од три дела. Во првиот е дадена методологијата на утврдување на причините на опожарувањето. Во вториот дел се обработени причините за настанување на истото. Во третиот дел се обработени неколку карактеристични примери. Во овој труд не се обработувани економски загуби и штети од причина што вештото лице од областа на електротехника не е овластено за економско-финансиски вештачења

**Клучни зборови:** пожар, куса врска, вешто лице, методологија, постапка, начин на изработка на вешт наод и мислење

### 1. Методологија на утврдување на причини на опожарување

Утврдување на причините за пожар е комплексно вештачење кое се изведува со преглед на опожарен објект од страна на вештаци за пожари од страна на МВР. Ова се спроведува со цел да се утврди примарна причина за пожарот, односно, да ли е до пожар дојдено поради технички дефект или неисправност, или се работи за намерно предизвикан пожар. Постапката на вештачење на пожарот, доколку се работи за електрична енергија како можеен причинител, се спроведува со преглед и испитување на електрична инсталација и електричните уреди, утврдување на место на настанување и видот на дефектот на дел од електрична инсталација или електричниот уред и врските помеѓу дефектот и причината за пожарот[6]. Утврдувањето се врши со увид на лице место, како и со вештачењето на материјалот земен од местото на опожарување.

Подготовката за увид се состои во добивање на сите релевантни информации во врска со настанувањето на пожарот: место и време на настанок, изјави на очевидците и пожарникари, изјава на сопственик или корисник на објектот, фотографии и на крајот, дали во објектот постоел некој вид на противпожарна заштита. Исто така, пожелно е да се прибави и техничка документација за објектот, доколку постои, од кои може да се утврди начин на приклучок и други параметри поврзани со електротехничките карактеристики на инсталацијата на опожарени објект.

## 2. Причини за појавување пожар

Пред да наведеме неколкуте случаи на опожарени објекти, ќе се задржиме на теориски дел, за причините поради кои електрична струја предизвикува пожар [1]. Според статистички податоц и места за појавување неисправност на електричните инсталации се:

- дефекти на проводници вградени во објект (преку 33%),
- кабли, вклучувачи (20%),
- сијалици и други извори на светлина (околу 20%),
- прекинувачи, продолжни кабли и утичници (10%),
- осигурачи, главни прекинувачи, разводни ормани(5%),
- мерни уреди и други места во рамките на електричен развод.

Кога струјата поминува низ електричните проводници се развива топлина. Согласно Џул-Ленцовиот закон, количина на развиена топлина  $Q(J)$  е пропорционална со квадратот на струјата  $I(A)$ , отпорот на проводник  $R(\Omega)$  и времето на протекнување  $T(s)$ .

$$Q = RI^2 T$$

Поради тоа со протекнување на електрична струја доаѓа до прегревање на проводници што предизвикува загревање и палење на изолацијата. Настанато преоптеретување најмногу влијае на контакти и на споеви на проводниците, посебно доколку не се правилно изработени. До прегревање на проводниците може да дојде и при нормални оптеретувања, под услов да на некој начин било спречено одведување на топлина. Во пракса најчесто се палат некавалитетни и преоптеретени продолжни кабли, како што ќе биде дадено во случај подолу.

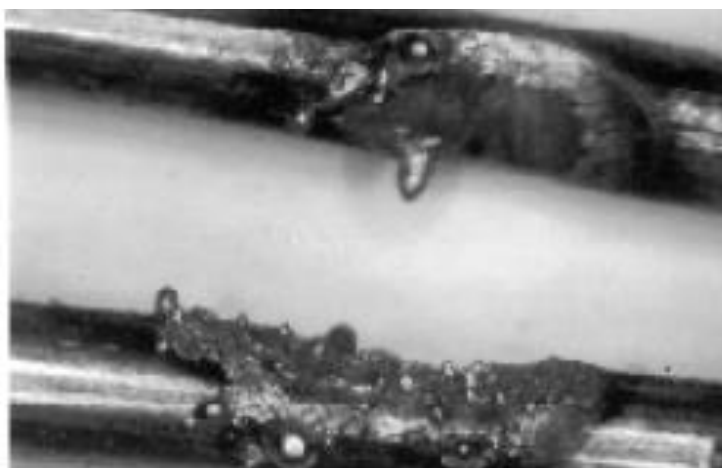


Слика 1. Запалени продолжителни кабли



Лош контакт има голема отпорност што како последица има локално загревање а со тоа и зголемена оксидација. Ова е неповртен процес, бидејќи отпорост на местото се зголемува а со тоа и уште поголемо ослободување на топлина, што резултира за палење на запаливи материјали во непосредна околина. Поради ова, може да дојде до опожарување на материјали со мала термичка инерција како што се постелнини, перници и друго, доколку се тие поставени блиску до изворот на топлина. Потребна моќност на дисипација изнесува 28W. За компоненти на електрична инсталација изработени од ПВЦ, моќноста на дисипација за опожарување е 30W, додека за дрвени предмети, таа изнесува 35-50W.

Друга причина за опожарување предизвикано од електрична инсталација е куса врска. Треба да се разликуваат два типа на куси врски. Примарна и секундарна. Примарна куса врска настанува во нормална средина и таа е најчесто причина за пожар. Секундарната кусаа врска настанува отпосле, во контаминирана средина полна со продукти на согорување и таа настанува секогаш како последица на опожарување. При настанување на куса врска, на место на допир на проводниците, се јавуваат ситни топчиња, како последица на топење на материјалот, предизвикано од електричен лак, кои што се разликуваат по големина од топчиња на проводникот настанати поради негово топење од пожарот [2].



Слика 2. Топчиња настанати од к.в.



Слика 3. Топчиња настанати поради топење од пожар

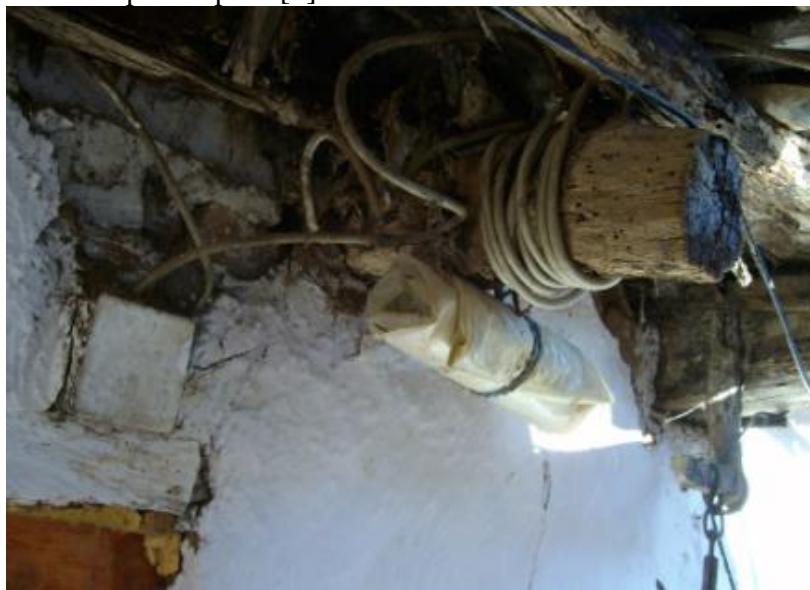


Слика 4. Изглед на внатрешноста на осигурачот од зависноста на видот на преоптеретување.

Често се на место на опожарување можат да најдат електрични решоа, греалки, и слични уреди, кои што можат да предизвикаат пожар[3]. За да предизвикаат пожар тие треба да се наоѓаат во центарот на опожарено место, да се во близина на материјал кој може да гори, а и мора да имаат грејни површини кои можат да развијат доволна топлина за запалување на материјалот.

### 3. Карактеристични примери на пожар

**Случај 1.** Во една индивидуална селска кука настанат е пожар во кој е уништена комплетна кровна конструкција, како и голем дел од покуќнина и мебелот. Останати биле само сидовите . Опожарен бил само еден од објектите, додека на старата кука, која била веднаш до неа, немало траги од опожарување. Со увид на лице место утврдено е крајно лоша изведба на инсталација, а корисникот извршил своеволно изместување на мерен уред од старата кука, во нов објект, кој сега е опожарен. Пожарот е настанат, најверојатно, како последица на куса врска на инсталација во новоизградениот објект, при изместување на мерна опрема[4].



Слика 5. Инсталација во стариот објект



Слика 6. Опожарен нов објект

**Случај 2.** Во пожар на еден мерен разводен орман во индивидуална стамбена кука, интервенирано е благовремено, поради што пожар не зафатил поголем дел од куќата, туку е локализиран на местото на настанување. Со увидот на лице место утврдено е дека пожар настанал во мерен разводен орман, од каде се проширил во просторија позади орманот опожарувајќи ги делови од електрична инсталација и просторијата позади орманот. Пожар е највероватно настанал како последица од куса врска во проводниците внатре во него. како последица од развиена топлина, стопено е броилото, а од настаната секундарна куса врска, оштетен е и доведен кабел од броилото до штендерот. Во овој случај, требало да се одвојат разводен од мерен орман, со што би се одбегнало групирање на проводници и нивната подобра прегледност. Да забележиме и дека се видливи карактеристични траги на дрво, т.н „крокодилска кожа“. Промени настанати со горење на површина на дрвото се манифестираат во облик на коцкички познати под како „крокодилска кожа“ Тие се поситни таму каде ватра подолго траела. огин по правило секој пат доаѓа од страна каде се коцкички помали и помеки



Слика 7. Типичен изглед на „крокодилска кожа“.





Слика 8. Траги на опожарување во орманот и ел.инсталација

Во горниот спрат немаше никакви траги од опожарување ниту оштетување на некој од апаратите.

**Случај 3.** Опожарена е трафостаница која се наоѓала во подрум во една деловна зграда. По дојава на пожар, интервенирале вработените и со помош на противпожарни апарати за електрични инсталации го изгасмале, без тој да се прошири надвор од трафостаница. увидот е извршен откако дежурната екипа веќе дошла на лице место и санирала оштетените уреди. Констатирано е дека пожар настанал како последица на лабави контакти (зголемен преоден отпор) на осигурачите за една група на потрошувачите во зградата. Ова довело до зголемување на температура се до точка на топење. Само со благовремена интервенција на вработените, спречена е поголема штета.



Слика 9. Слика со термална камера по извршена замена на оштетени постолја за осигурачите стопени поради голем преоден отпор. Се гледа нормална температура.

**Случај 4.** Опожарен е дел од мини трговски центар, поточно штанд каде што се продаваат санитарии. Од документација дадена на вешто лице, утврдено е дека единствен можен причинител е продолжен кабел со кој се напојувал сметач-фискална каса. Од извештај од крим техника, кој е дојден по изготвување на вештачењето, потврдено е дека причината за пожар е заборавена греалка вклучена на продолжен кабел[5].

Генерално, на секоја вредност на електрична струја, одговара соодветно зголемување на температура, кое мора да биде ограничено, односно температура не смее да достигне точка на палење на изолација, околни предмети и материјали, кои можат да бидат различни. Поголем дел на европски и национални прописи предвидуваат дека зголемувањето на температура на ел.спроводник на смее да биде поголема од 25° C во однос на амбијентална температура.

Чести се случајеви на преоптеретувањето на проводниците во домаќинствата каде електрична инсталација првично била димензионирана за помал број на потрошувачите, поради што и проводникот бил со помал напречен пресек. Со времето број на потрошувачите во домаќинства се зголемил и по број и по моќноста, без да се изврши реконструкција на инсталацијата. Последното има за последица прегревање на спроводниците и предизвикување на пожарот.

#### 4. Заклучок

Во овој труд е обработена проблематика на настанок и опожарување на кеон објекти. вештачење на причините за пожарот е мултидисциплинарно вештачење во кое најчесто учествуваат вештаци од електротехника, машинство, и хемиска струка, од кои секој врши увид во место на настанот, барајќи карактеристични трагови давајќи на тој начин одговор за причините на настанок на пожарот.

Во трудот е на примери од пракса прикажан начинот на работа на вештакот при утврдување на причините за пожар на објектите. Приказани се методи за утврдување на местото на настанок и причините за пожарот, а укажано е на некои карактеристични кварови кои можат да доведат до пожарот. На примерот на индивидуални станбени објекти прикажани се пожари предизвикани од стара или несоодветно изведена инсталација. Кај пожарот во трафо-станицаа се работи за слаб контакт помеѓу собирниците и држачи за осигурувачи, што резултирало со прекумерно загревање и топење на истите.

#### 5. Литература

- [1] Ненад Папиќ – Вјештачење узрока пожара индивидуалних објектата.
- [2] Д-р Милан Благојевиќ- Експертиза удеса шк.2016/2017.
- [3] Милан Благојевиќ, Сретен Рогановиќ и Радован Радовановиќ Форезничка истражувања кратког споја као узрока пожара.
- [4] Адријана Бјелановиќ, Понашање дрва и дрвених конструкција у пожару и отпорност на деловање пожара.
- [5] [https://www.scribd.com/document/339799094/Ekspertiza\\_pozara-odgovori](https://www.scribd.com/document/339799094/Ekspertiza_pozara-odgovori)
- [6] Младен Жилиќ Електрична енергија како могуќи узрок пожара или експлозије, доказивање таквог узрока или мјере превенције.



## SIMULATION OF AN INDUSTRIAL ROBOT WITH THE HELP OF THE MATLAB SOFTWARE PACKAGE

*Dusko Pleskov<sup>1</sup>, Saso Gelev<sup>2</sup>, Goce Stefanov<sup>3</sup>*

<sup>1</sup>Faculty of Electrical Engineering University Goce Delcev Stip R.Macedonia,  
dusko.20539@student.ugd.edu.mk

<sup>2</sup>Faculty of Electrical Engineering University Goce Delcev Stip R.Macedonia, saso.gelev@ugd.edu.mk

<sup>3</sup>Faculty of Electrical Engineering University Goce Delcev Stip R.Macedonia, goce.stefanov@ugd.edu.mk

### Abstract

Robotics is an applied technical science that is a link between machines and computer technology. Robotics includes various branches such as machine design, control and regulation theory, computer programming, artificial intelligence and theory of production. In other words, robotics is an interdisciplinary science that covers the fields of mechanics, electronics, informatics and automation. In this paper we will deal with industrial robots or industrial manipulators. The first part of the paper will explain the basic concepts of industrial manipulators. The different configurations of the industrial manipulators and their working space will be considered. The second (practical) part of this paper will explain the modeling and simulation of the Scara robot in Matlab. The movement of the robot from point to point will be simulated (application in palletizing, spot welding, assembly, etc.).

**Keywords:** industrial manipulators, modeling and simulation, Scara robot, Matlab,

### 1.Introduction

Robotics is an applied technical science that is a link between machines and computer technology. Robotics includes various branches such as machine design, management and regulation theory, computer programming, artificial intelligence and production theory. In other words, robotics is an interdisciplinary science that covers the fields of mechanics, electronics, informatics and automation. It deals primarily with the study of machines that can replace humans in the performance of tasks, such as various forms of human physical activity and decision making. The development of robotics is initiated by the desire of man to try to find a replacement for himself, which could be related in his capacity in different applications, taking into account the interaction with the environment around him. They replace man primarily with dangerous, monotonous and difficult jobs. Man is left with work tasks that require more intelligence, knowledge and creativity. In this way, robots contribute to increasing productivity, and at the same time to humanizing work. In all their applications, industrial manipulators perform certain movements to perform their work tasks. The drive system is responsible for the successful execution of the movements of the manipulator, together with the commands that are in accordance with the trajectory of the desired movement. Control the movement of the manipulator end effector requires an accurate analysis of the characteristics

of the mechanical structure, actuators and sensors that make up the robotic system of an industrial manipulator. The purpose of such an analysis is to determine the mathematical model of the components of the industrial manipulator. The application of software packages for modeling and simulation in robotics is of increasing importance in the design of robotic systems and the determination of a mathematical model and analysis of the components that make up the industrial manipulator. One of the most commonly used tools for modeling and simulation in robotics is the Robotics Toolbox for Matlab. This software tool enables working with vectors and matrices, homogeneous transformations, solving problems of direct and inverse kinematics, generating the trajectory of motion and the orientation of the robot. In this paper, a DH model of a SCARA robot with four degrees of freedom was developed, based on which a simulation of the robot's movement from point to point was performed. The paper practically demonstrates the capabilities of the Matlab software package with its Peter Corke Robotics Toolbox plugin for modeling, simulation, trajectory generation, and visual representation of the robot and its movement.

## 2. Robot kinematics

Regardless of the constructive performance of the robot, a way is needed that will fully describe the position and movement of the robot in space. There are two ways to define robot kinematics: Denavit Hartenberg analytical procedure and numerical procedure based on Rodrigues formulas. The first method is used to determine the kinematic equations of the robot, while the other method is used to determine the dynamic equations of the robot. There are two basic problems with formulating the kinematics of a robot: forward and inverse kinematic problems. To solve the problems of forward and inverse kinematics, a reference coordinate system is defined which is placed on the base of the robot, based on that reference coordinate system the external coordinates of the robot are determined, ie the position of the robot end effector in (x, y, z) space. Each joint of the robot is joined by a Cartesian coordinate system so that the z-axis of the coordinate system coincides with the axis of rotation. The robot's end effector is accompanied by a coordinate system of the robot tool, so that when solving the robot kinematics, the coordinates are transformed in relation to the reference coordinate system. The internal coordinates of the robot are scalar quantities that describe the position of one segment relative to the other segment of the kinematic pair that make it up. The number of internal coordinates depends on the number of degrees of freedom, ie the number of joints of the robotic manipulator. The internal coordinates are usually denoted by  $q_i$  and represent the vector  $q = [q_1, q_2, \dots, q_n]$ . External coordinates describe the position of the robotic manipulator end effector in space relative to the reference coordinate system. The position of the robot's hand is described by the coordinates  $(p_x, p_y, p_z)$ , and the orientations are described by the Euler angles  $(r_x, r_y, r_z)$ . Determining the vector of the external coordinates for a given vector of the internal coordinates is called a forward kinematic problem. By changing the internal coordinates, the position of the robot's hand in space changes, ie the external coordinates change. While the reverse process, determining the vector of internal coordinates for a given vector of external coordinates is called the inverse kinematic problem. The first step in solving the direct kinematic problem is to define a symbolic scheme (mathematical model) of the robotic manipulator in relation to the reference coordinate system and to define the zero position of the robotic manipulator. At zero position all the internal coordinates of the robot have a value of zero. The procedure of Denavit and Hartenberg will be explained below. The Denavit and Hartenberg procedure is a simple way to model the joints and segments of a robot and can be applied to any robotic configuration. To model an robotic arm according to the Denavit Hartenberg convention, an appropriate coordinate system is attached to each joint of

the manipulator. More specifically, the z-axis and the x-axis are joined while the y-axis is always normal to both axes, but it does not need to be determined because the DH model does not use the y-axis (Figure 1). The connection of the coordinate system to the joints is done as follows:

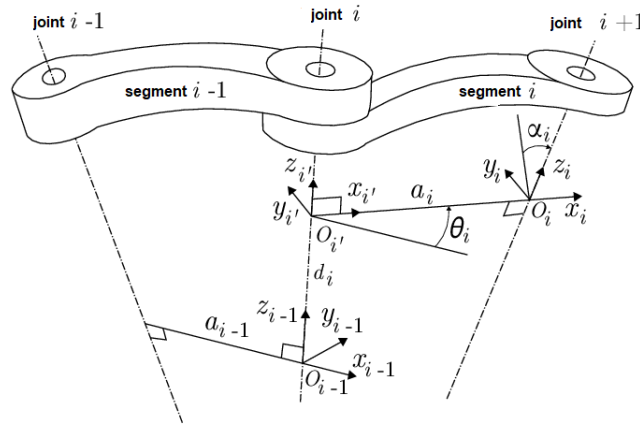


Figure1.DH parameters of kinematic pair of rotary joints

All joints are represented by a z-axis. If the joint is rotational, the z-axis is set in the direction of rotation as a rule of the right hand, while if the joint is translational, the z-axis is set in the direction of the translational movement.  $z_{n-1}$  denotes the z-axis associated with the n-th joint,  $z_n$  denotes the axis associated with the (n + 1) -th joint, and  $z_{n+1}$  denotes the z-axis of (n + 2)-th joint. If the joint is rotational its variable will be the angle of rotation  $q$ , about the z-axis, and if the joint is translational its variable will be the length of the segment along the z-axis denoted by  $d$ . In the general case, the joints do not have to be parallel or intersecting. As a crescent, their z-axes are generally divergent lines. It is known from geometry that for two lines that are intersecting, there is always a line that is normal to them and represents the shortest distance between the intersecting lines. This normal line is called the common normal line of the intersecting lines and the x-axis of one joint is always set in the direction of the common normal line of its z-axis and the z-axis of the previous joint. Consequently, if  $a_n$  is the common normal line between the  $z_{n-1}$  axis and the  $z_n$  axis, the direction of the  $x_n$  axis will be along  $a_n$ . Similarly if  $a_{n+1}$  is the common normal line between  $z_n$  and  $z_{n+1}$ , the direction of the  $x_{n+1}$  axis will be along  $a_{n+1}$ . If two adjacent z-axes are parallel then they have an infinite number of common normal line. In such a case, a joint normal line is chosen that is collinear with the joint normal line of the previous joint. If two adjacent z-axes intersect, they have no common normal line. The x-axis is then set in the direction of the normal line to the plane formed by the two z-axes.

To model any robot configuration according to DH notation and convention we need four parameters:

- Parameter  $a_i$  - distance between  $z_{i-1}$  and  $z_i$  axis along the  $x_i$  axis (segment length)
- Parameter  $d_i$  - distance along the  $z_{i-1}$  axis from  $\theta_{i-1}$  to the intersection of the  $x_i$  and  $z_{i-1}$  axes (moving the segment)
- Parameter  $\alpha_i$  - the angle between the  $z_{i-1}$  and  $z_i$  axis, measured around the  $x_i$  axis (angle of rotation of the segment)
- Parameter  $\theta_i$  - the angle between  $x_i$  and  $x_{i-1}$ , measured around the  $z_{i-1}$  axis (angle of rotation of the segment)



3. Scara robot with four degrees of freedom and DH parameters

The SCARA is a type of industrial robot. The acronym stands for Selective Compliance Assembly Robot Arm or Selective Compliance Articulated Robot Arm. By virtue of the SCARA's parallel-axis joint layout, the arm is slightly compliant in the X-Y direction but rigid in the 'Z' direction, hence the term: Selective Compliant. This is advantageous for many types of assembly operations, i.e., inserting a round pin in a round hole without binding. The second attribute of the SCARA is the jointed two-link arm layout similar to our human arms, hence the often-used term, Articulated (Figure 2).



Figure2.Scara(Selective Compliance Assembly Robot Arm)robot

The type of robot that will be the subject of modeling and simulation in this paper is the Scara robot configuration with four degrees of freedom. The robot that will be modeled is with RRTR configuration, ie seen from the base to the top, it has two rotational, translational and rotational joints. (Figure 3) shows the mathematical model of the Scara robot with associated coordinate systems to the joints according to DH notation. Based on this DH model, the four parameters that we will need to create and model our robot type with the help of a robotics tool in the Matlab environment are determined (Figure 4).

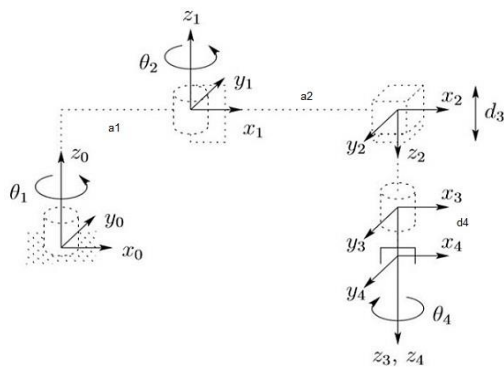


Figure3.Mathematical model of Scara robot with associated coordinate systems to the joints

Знак	$\theta$	$d$	$a$	$\alpha$	Начало $q$
1	$\theta_1$	0	$a_1$	$0^\circ$	$0^\circ$
2	$\theta_2$	0	$a_2$	$180^\circ$	$0^\circ$
3	$0^\circ$	$d_3$	0	$0^\circ$	$0^\circ$
4	$\theta_4$	$d_4$	0	$0^\circ$	$0^\circ$

Figure 4.DH parameters for Scara robot with four degrees of freedom

#### 4. Modeling and simulation of Scara robot in Matlab

Creating and modeling our Scara robot involves entering its parameters according to the Denavit Hartenberg notation into .m file that is created using a command from the File-New>Script menu. The modeling of the Scara robot with four degrees of freedom according to the model of (Figure 3) and according to the DH parameters from (Figure 4) is done by setting the dimensions of the segments and the dimensions of the robot tool (Figure 5). In our case  $a_1$  is the length of the segment that joins the first and second rotational joints,  $a_2$  is the length of the segment joining the second and third (translational) joints, while  $d_4$  represents the tool length of the Scara robot.

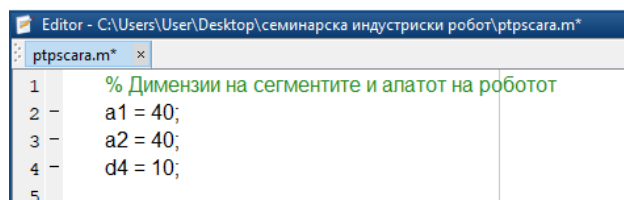


Figure 5. Enter the dimensions of the robot segments

The next step in modeling the robot is entering the Denavit Hartenberger parameters. We enter the DH parameters with the function  $L = \text{Link}([Th\ d\ a\ \alpha])$ . Depending on whether the joint is rotational or translational, we add 0 or 1 at the end, if the joint is rotational we add 0, if the joint is translational then we add 1. After entering the DH parameters, we create the serial connection, ie the kinematic chain that makes up the joints and segments of the robot with the SerialLink (L) function (Figure 6), where we can also give the name of the robot, in our case 2RTR Scara.

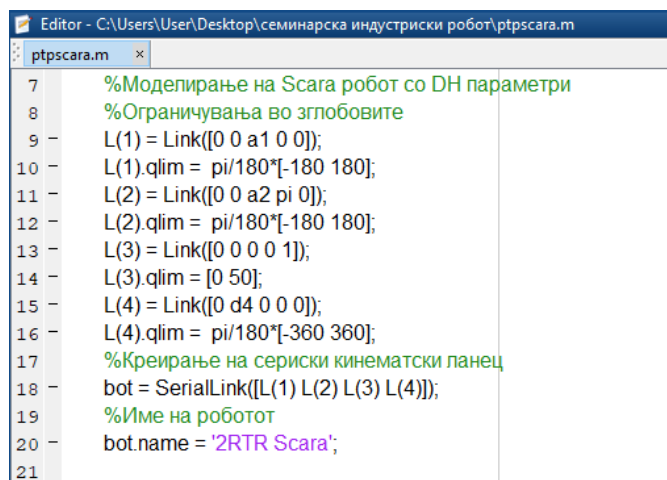


Figure 6. Enter DH parameters and create Scara robot

The robot modeled in this way can be represented graphically if we give the command `bot.plot(q0)` in the command window, where  $q_0 = [0\ 0\ 0\ 0]$  represents the vector of the zero position, ie the initial position of the robot. (Figure 7). A point-to-point movement simulation will be performed on the Scara robot modeled and created in this way. In point-to-point movement, the manipulator moves at discrete points in the workspace, and the trajectory between the points is not important, but the positioning accuracy is important. This mode of motion control is used for discrete operations such as: point finishing, moving objects, palletizing, etc.



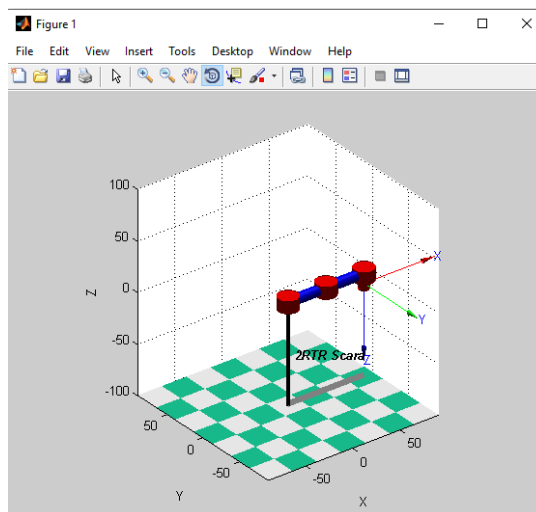


Figure 7. Graphic display of the Scara robot in the initial position

The simulation will be a simple example of positioning the robot in space, ie a circular plate will be given together with the positioning points. The drawing of the plate is done with the help of the `plot_circle` function, with given coordinates of the plate and the positioning points of the robot in the working space (Figure 8).

```

Editor - C:\Users\User\Desktop\семинарска индустриски робот\ptpscara.m
ptpscara.m x
24      %Координати на работната плоча и точките на дупчење
25      p0=[-40 35 -40];
26      p1=[-20 35 -40];
27      p2=[-60 35 -40];
28      %Исцртување на работната плоча и точките на дупчење
29      plot_circle(p0, 40, 'black');
30      plot_circle(p1, 5, 'black');
31      plot_circle(p2, 5, 'black');
32

```

Figure 8. Coordinates and drawing the contour of a plate

The robot in zero position and the contour of the circular plate together with the positioning points are given in (Figure 9).

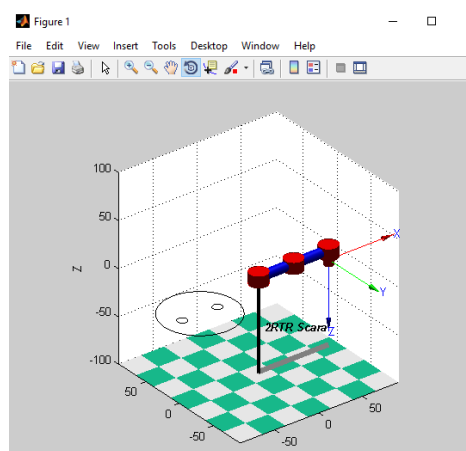
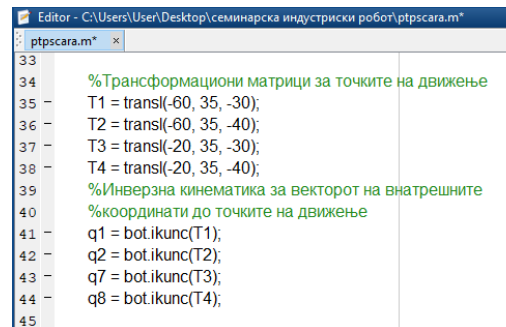


Figure 9. Graphic display of the Scara robot in the initial position and plate

The transformation matrices from the zero position to the points where the robot is to be positioned are given by the function  $T = \text{transl}(p_0)$ , where  $p_0(x, y, z)$  is a point in space (Figure 10). The transformation matrices have a dimension of  $4 \times 4$  and represent the position and orientation of the robot in space, for given internal coordinates of the robot joints. The Robotics Toolbox uses the `ikine` function to determine the inverse kinematic problem.



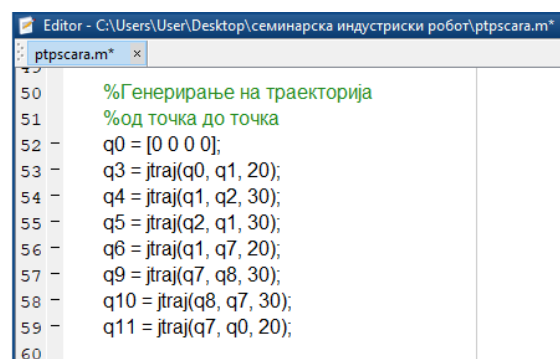
```

33
34 %Трансформациони матрици за точките на движење
35 T1 = transl(-60, 35, -30);
36 T2 = transl(-60, 35, -40);
37 T3 = transl(-20, 35, -30);
38 T4 = transl(-20, 35, -40);
39 %Инверзна кинематика за векторот на внатрешните
40 %координати до точките на движење
41 q1 = bot.ikunc(T1);
42 q2 = bot.ikunc(T2);
43 q7 = bot.ikunc(T3);
44 q8 = bot.ikunc(T4);
45

```

Figure 10. Forward and inverse kinematic problem

Point-to-point positioning in the Robotics Toolbox is done using the `jtraj` function ( $q_0, q_f, t$ ). The `jtraj` function generates the trajectory of the joints or internal coordinates so that the robot is positioned from the starting point  $q_0$  to the end point  $q_f$  during time  $t$  (seconds). (Figure 11).



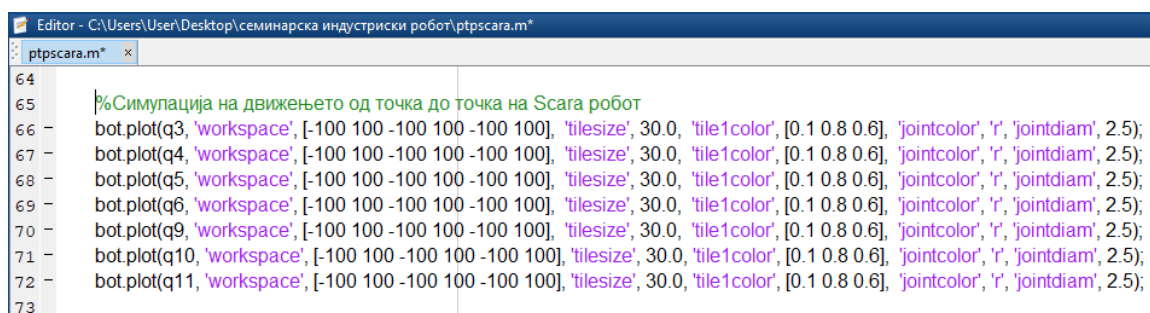
```

50 %Генерирање на траекторија
51 %од точка до точка
52 q0 = [0 0 0 0];
53 q3 = jtraj(q0, q1, 20);
54 q4 = jtraj(q1, q2, 30);
55 q5 = jtraj(q2, q1, 30);
56 q6 = jtraj(q1, q7, 20);
57 q9 = jtraj(q7, q8, 30);
58 q10 = jtraj(q8, q7, 30);
59 q11 = jtraj(q7, q0, 20);
60

```

Figure 11. Generating trajectory for positioning points

We visualize the simulation with the `plot` function, for all generated trajectories from the zero position to the points where the Scara robot should be positioned. (Figure 12).



```

64
65 %Симулација на движењето од точка до точка на Scara робот
66 bot.plot(q3, 'workspace', [-100 100 -100 100 -100 100], 'titlesize', 30.0, 'tile1color', [0.1 0.8 0.6], 'jointcolor', 'r', 'jointdiam', 2.5);
67 bot.plot(q4, 'workspace', [-100 100 -100 100 -100 100], 'titlesize', 30.0, 'tile1color', [0.1 0.8 0.6], 'jointcolor', 'r', 'jointdiam', 2.5);
68 bot.plot(q5, 'workspace', [-100 100 -100 100 -100 100], 'titlesize', 30.0, 'tile1color', [0.1 0.8 0.6], 'jointcolor', 'r', 'jointdiam', 2.5);
69 bot.plot(q6, 'workspace', [-100 100 -100 100 -100 100], 'titlesize', 30.0, 'tile1color', [0.1 0.8 0.6], 'jointcolor', 'r', 'jointdiam', 2.5);
70 bot.plot(q9, 'workspace', [-100 100 -100 100 -100 100], 'titlesize', 30.0, 'tile1color', [0.1 0.8 0.6], 'jointcolor', 'r', 'jointdiam', 2.5);
71 bot.plot(q10, 'workspace', [-100 100 -100 100 -100 100], 'titlesize', 30.0, 'tile1color', [0.1 0.8 0.6], 'jointcolor', 'r', 'jointdiam', 2.5);
72 bot.plot(q11, 'workspace', [-100 100 -100 100 -100 100], 'titlesize', 30.0, 'tile1color', [0.1 0.8 0.6], 'jointcolor', 'r', 'jointdiam', 2.5);
73

```

Figure 12. Simulation of point to point movement

In (Figure 13) you can see part of the simulation of the movement of the Scara robot, from point to point.

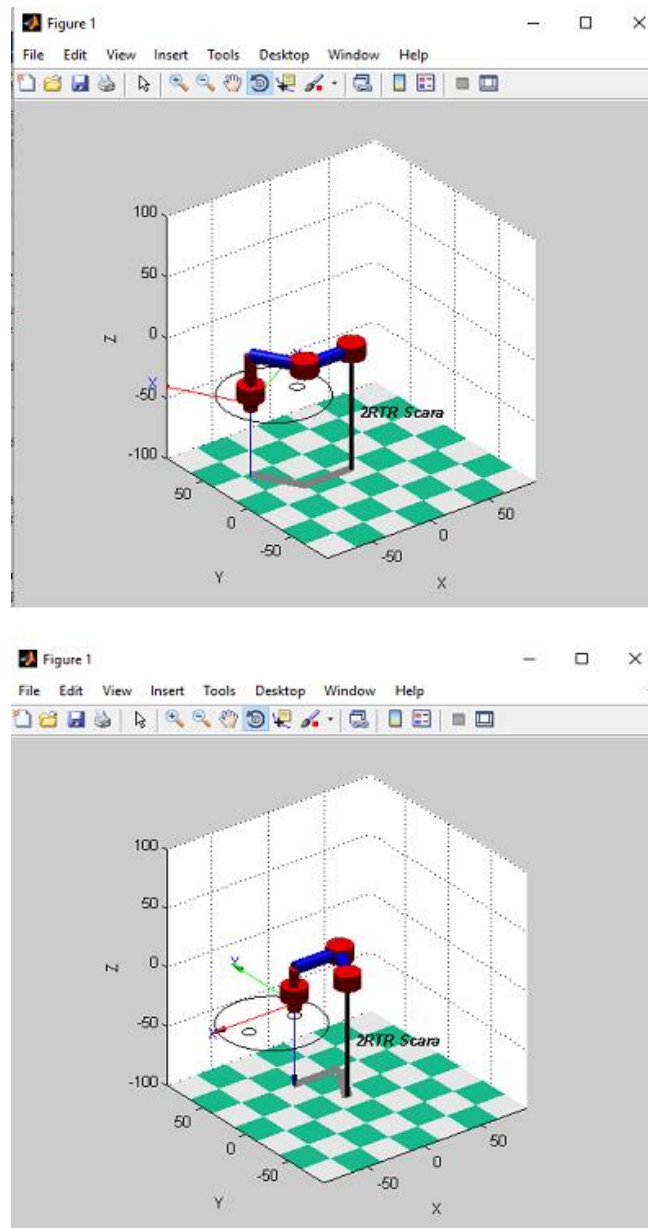


Figure 13.Simulation of Scara robot movement from point to point

#### 4.Conclusion

Industrial production today is almost unthinkable without automation. Industrial manipulators have greatly enhanced automation in industrial plants and raised it to a higher level. Old and slow machines become history over time and are replaced by new modern automated machines and manipulators. Robotic manipulators make the job easier, replacing the men in difficult and dangerous jobs, which makes the men feel more secure in the workplace and his work comes down to observing the technological process.

The first part of the paper will explain the basic concepts of industrial manipulators. The different configurations of the industrial manipulators and their working space will be considered. The second (practical) part of this paper will explain the modeling and simulation of the Scara robot in Matlab. The movement of the robot from point to point will be simulated (application in palletizing, spot welding, assembly, etc.).

## Literature

- [1] Saso Gelev "Robotika i avtomatizacija" Univerzitet "Goce Delcev" <http://e-lib.ugd.edu.mk/500>
- [2] Peter Corke "Robotics Toolbox for Matlab", Release 9  
<http://www.petercorke.com/RTB/robot.pdf>
- [3] Vlatko Dolecek, Isak Karabegovic "Robotika" Univerzitetska knjiga  
[https://www.ucg.ac.me/skladiste/blog\\_13268/objava\\_56688/fajlovi/robotika.pdf](https://www.ucg.ac.me/skladiste/blog_13268/objava_56688/fajlovi/robotika.pdf)
- [4] Zdenko Kovačić, Stjepan Bogdan, Vesna Krajči "Osnove Robotike"  
[http://www.graphis.hr/news/robotika/robotika\\_39.pdf](http://www.graphis.hr/news/robotika/robotika_39.pdf)



## BATTERY ENERGY STORAGE SYSTEMS AND TECHNOLOGIES: A REVIEW

*Marija Sterjova<sup>1</sup>, Dragan Minovski<sup>1</sup>, Vasilija Sarac<sup>1</sup>*

<sup>1</sup>Faculty of Electrical Engineering, University “Goce Delcev” - Stip

E-mails: marija.22512@student.ugd.edu.mk, dragan.minovski@ugd.edu.mk, vasilija.sarac@ugd.edu.mk, conf.etf@ugd.edu

### Abstract:

*With the fickle nature of the weather conditions upon which renewable energy sources mostly depend, as well as the changing consumer demand profile, the need for balance in the electric power system between supply and demand through a reliable energy storage system becomes essential. Besides most of the energy storage system technologies are not commercially viable at present due to some of their limitations, the battery energy storage system (BESS) carries out an increased role and frequency in energy markets and continuous improvements that serve a variety of energy optimization purposes, improving the quality, reliability, and affordability of electricity.*

*This topic covers and analyzes the different technologies of the battery system and their characteristics according to the type of battery, their adaptation, evolution, and functionality as key to the energy transition. Flexible options are necessary to overcome the overall variability between the interaction of systems and the regulation of their parameters. The battery energy storage system cannot become obsolete in the coming period, but on the contrary will contribute to faster realization of new energy trends, development of stationary markets, and the rise of a sustainable energy future.*

**Keywords:** *energy transformation, renewable energy, battery technologies, grid-level energy storage, energy sector trends, electrochemical design, battery model*

### 1. Introduction

Electricity storage is a sustainable option for current and future energy needs. It offers an efficient and economical solution as a central component in the energy infrastructure itself. Regulating the supply of electricity from renewable sources that can fluctuate owing to weather conditions, as well as daily and seasonal models, is a key concept that will help develop technologies that will enable this process. The power system requires capabilities to bridge the time gap between supply and demand, which is called the flexibility of the power system to match fluctuating production with also fluctuating demand [1] – [9]. Large-capacity energy storage facilities can meet the challenges of safe and secure operation resulting in reduced voltage fluctuations, improved electricity quality, and reduced costs [3].

This paper will review the research conducted on technologies, applications, and everything else related to electricity storage, with emphasis on battery-electrochemical energy storage systems. They are directly dependent on the readiness of technologies for various applications for electrical energy storage concerning the electricity grid. Battery energy storage systems (BESS) are growing rapidly due to their diversity, high energy density, and efficiency. More grid applications are adapting to these storage systems as the cost of battery technologies

decreases while performance and lifespan continue increasing. This, in turn, will reduce decarbonization costs in key sectors and accelerate the global energy transition above the expectations of major global energy trends (decarbonization, digitalization, decentralization).

**2. Applications of Battery Energy Storage Technologies**

The fundamental advantage provided by battery energy storage technologies represents the flexibility in providing a sufficient range of active and reactive power needs. The potential contribution of applications of such technologies is present at all levels of the electricity grid: production, transmission, distribution, and end consumers [10].

Using battery energy storage systems through distributed micro-grids (Figure 1) can improve the integration and enhance the utilization of the energy generated from photovoltaic systems, photovoltaics, and wind turbines. Through distributed micro-grids can also monetize assets through new revenue streams, increase asset utilization, improve yield, and reduce operating costs. It also improves safety by reducing fall current by up to five times. This happens due to the utilization of electronic devices that allow for lower fall current contribution to the rest of the electrical grid.



**Figure 1:** Fields of application of BESS

Other battery storage technology applications include renewable smoothing as we can see in Figure 2.



**Figure 2:** Technology applications of BESS

As shown in Figure 2 regarding the renewable smoothing, at a yellow-colored area we observe intermittent PV production during the daylight. By including energy storage systems and filling the gaps which are indicated by the green-colored area it can produce a smooth generation of renewable energy throughout the whole day. Another application or benefit of a battery energy storage system remains the ability to handle ramps or the frequently known duct curve (see Figure 2). The ramp or the duct curve is when the energy consumption increases dramatically in the predefined time. The ability to handle the loading ramp cannot be achieved through traditional, conventional generators, but it can be handled very quickly through battery energy storage devices.



BESS also supports diverse applications including firming renewable production, stabilizing the electrical grid, controlling energy flow, optimizing asset operation, and creating new revenue. Commercial and industrial end-users can mitigate demand charges, optimize the differential or time of day energy prices and benefit from additional on-site PV generation through the utilization of BESS. Some of the other applications are shown below in Figure 3:

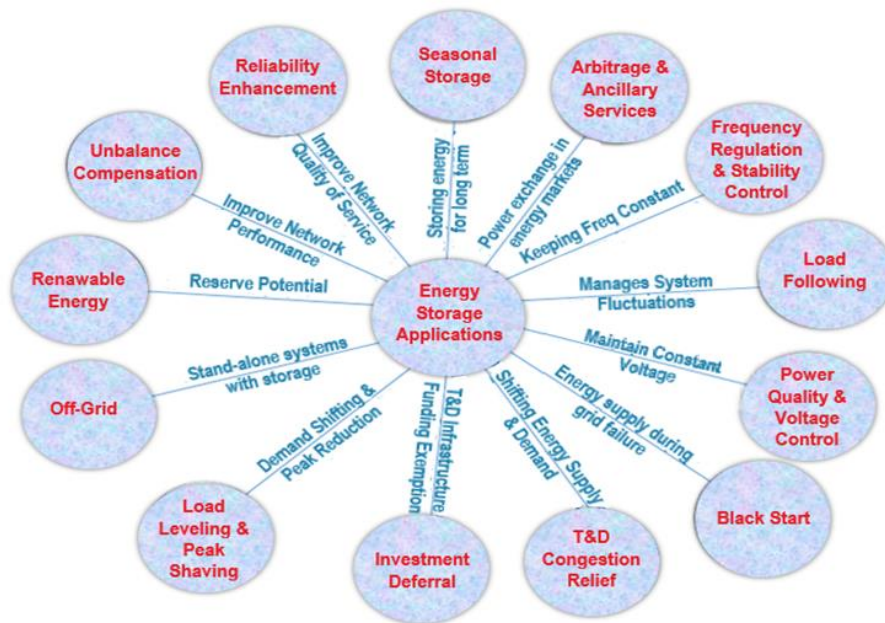


**Figure 3:** Some applications of battery energy storage systems

Among other applications, they include:

- **seasonal storage** such as the ability to store energy for a longer period,
- **energy arbitrage** (buying energy at a low price, storing it, and selling it later at a higher price on energy markets), and **ancillary services** (all services required by the transmission(distribution) system operator to enable them to maintain the integrity and stability of the transmission (distribution) system as well as energy quality),
- **frequency regulation** and **stability control** by maintaining constant frequency as much as possible throughout the network,
- **load following** capability that allows for system fluctuations to be managed,
- **power quality** and **voltage control** where we can maintain constant voltage through reactive power injection,
- **black start** capability where energy supply is done during grid failure and black start generators are not available or not possible to utilize,
- **transmission and distribution congestion relief** where the energy supply and demand is served locally,
- **investment deferral** for T&D infrastructure,
- **load leveling** and **peak shaving** where demand is shifted and the peaks are reduced,
- **off-grid** support where standalone energy systems are used with off-grid networks or standalone micro-grid systems,
- **the ability to improve the renewable energy penetration** and **network performance** by correcting any unbalance in the system, and finally
- **reliability enhancement** by improving network quality of service.

### 3. The Architecture of Battery Energy Storage Systems and Design

The utilization of any battery system needs to carefully consider all associated system components to be able to achieve the primary aim of a target application. Although the technology may look simple, involving a single battery type and a complete functional battery energy storage system requires a significant number of auxiliary components that need to be sized and designed all-around a specific storage technology [11].

The key components of battery storage systems are illustrated in Figure 4 [3].

- The battery system consists of the battery pack, which connects multiple cells to appropriate voltage and capacity,
- the battery management system (BMS) which protects the cells from a harmful operation, in terms of voltage, temperature, and current, to achieve reliable and safe operation, and balances varying cell states-of-charge (SOCs) within a serial connection, and
- the battery thermal management system (B-TMS) which controls the temperature of the cells according to their specifications in terms of absolute values and temperature gradients within the pack.

The components required for the reliable operation of the overall system are system control and monitoring, the energy management system (EMS), and system thermal management. System control and monitoring is general (IT) monitoring, which is partly combined into the overall supervisory control and data acquisition (SCADA) system but may also include fire protection or alarm units. The EMS is responsible for system power flow control, management, and distribution. System thermal management controls all functions related to the heating, ventilation, and air-conditioning of the containment system.

The power electronics can be grouped into the conversion unit, which converts the power flow between the grid and the battery, and the required control and monitoring components — voltage sensing units and thermal management of power electronics components (fan cooling, etc.).

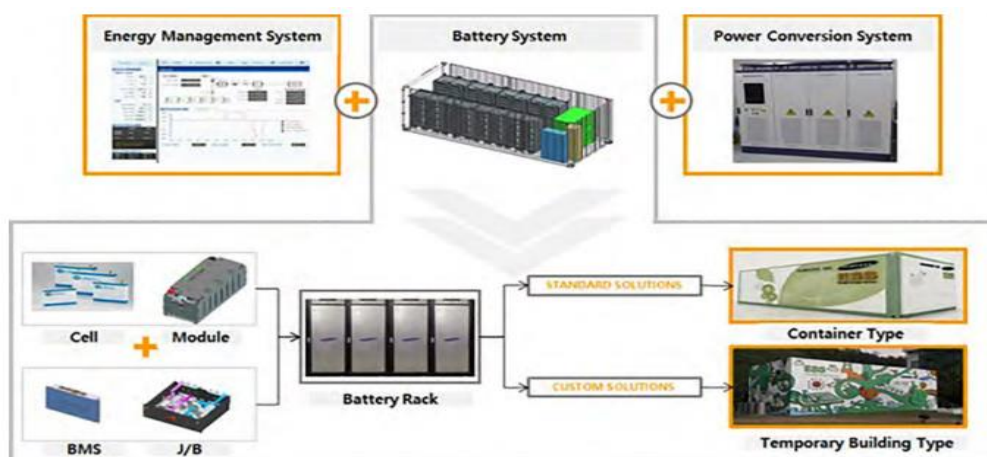


**Figure 4:** Schematic of typical BESS

*Source:* Korea Battery Industry Association 2017 “Energy storage system technology and business model”

#### 4. Grid Connection

A battery storage system involves seven major designs and hardware/software components. The unique and desirable functions of these components are briefly given in Figure 5 [11]:

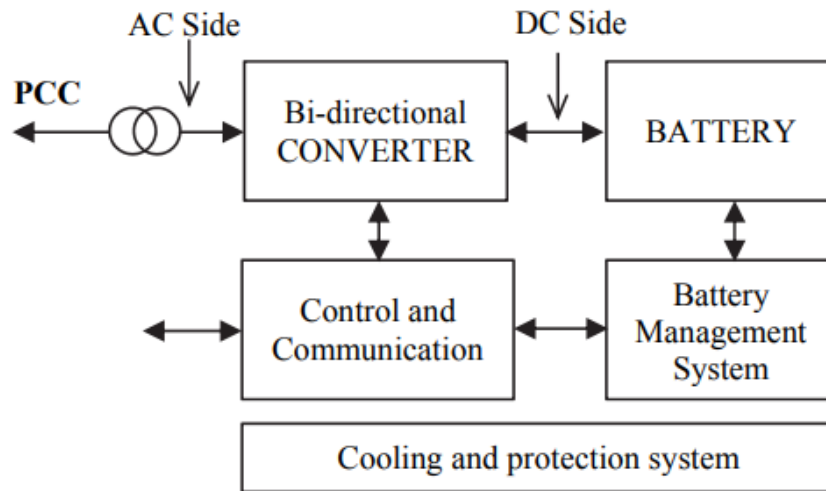


**Figure 5:** General block diagram of grid-connected energy storage unit which includes several key components: bi-directional converter, one or more battery modules, onboard sensors, and control components. The left-hand AC side shows the on-site power supply based on renewable energy. The right-hand side shows electrical DC connection to the battery bank.

- **CONVERTER:** Bidirectional and ideally 4-quadrant,
- **DC SIDE:** DC protections, DC voltage ranges, DC ripples, keep safe operating conditions,
- **AC SIDE:** System operator related, flexible, ancillary, reactive support, black start, ramp rate control, isolation and stepping up,
- **PERFORMANCE:** Harmonics, time response, efficiency, power deratings, cooling, safety, and protection,
- **CONTROL AND COMMUNICATIONS:** Frequency, power input/output in medium voltage, the state of charge, the control mode by the battery management system, historical view of data, alarms,
- **EPC (Engineering, Procurement, Construction) AND INTEGRATION:** Require companies and individuals with suitable and highly multidisciplinary skills,
- **GRID INTERCONNECTION:** Interconnection point (distribution line, transmission line, suburban, urban/rural), safety, noise, location, lighting, grounding, communication/protection requirements by the T/D providers, ability, and cost of interconnecting, size of the distributed generation system, voltage considerations.

The design of a battery energy storage system is a highly complex study. In addition to the desirable functionalities, the design work needs to consider the overall efficiency of BESS as well. The overall efficiency of a BESS is directly related to battery technology, type of converter used, protection and cabling, isolation transformer (at the output of the converter), and/or distributed/transmission transformer and point of common connection (PCC).

## 5. Classification of Battery Energy Storage Technologies

There exist electrochemical systems with internal and external storage. External storage systems have the advantage that energy content and power can be designed separately. Important examples are redox flow batteries. In internal storage systems, energy content and power depend on each other: higher energy content means higher power. A distinction is made between low-temperature and high-temperature batteries [12]. Classification of the major electrochemical energy storage systems is presented in Figure 6.

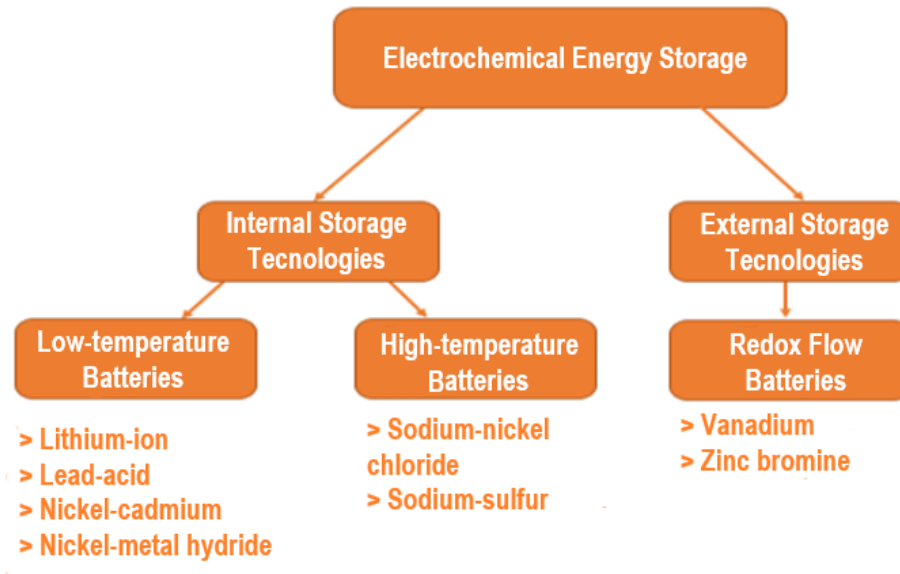


**Figure 6:** Classification of electrochemical energy storage systems

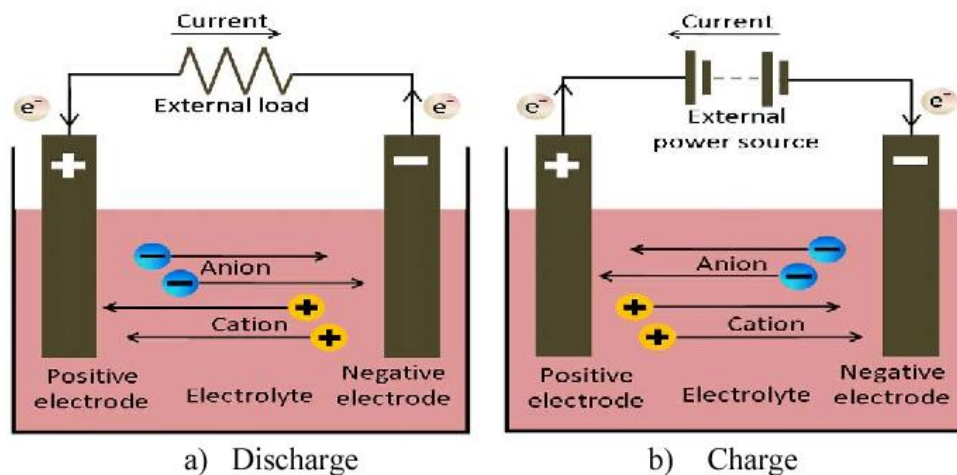


**Figure 7:** Schematic representation of the operation of electrochemical cell [13]

The basic design of an electrochemical cell (Figure 7) consists of a negatively charged electrode (anode), a positively charged electrode (cathode), and an electrolyte that serves as a medium for ion exchange between electrodes within a single cell. There is also a process of charging and discharging, i.e. oxidation-reduction reactions (redox reactions).

Electrochemical cells are a combination of metals and salt solutions. According to the structure of the electrodes and the electrolyte, electrochemical batteries are divided into several categories:

1. **Batteries with the liquid electrolyte and solid electrodes**, such as lead-acid (Lead-acid), nickel-cadmium (Ni-Cd), nickel-metal hydride (Ni-MH), and lithium-ion (Li-ion) batteries.
2. **Batteries with the solid ceramic electrolyte and liquid electrodes** (so-called high-temperature batteries), such as sodium-sulfur (Na-S) and ZEBRA (Zeolite Battery Research Africa) - sodium-nickel chloride (NaNiCl<sub>2</sub>) batteries.
3. **Batteries with two electrolytes that are separated from each other, and which are combined within the so-called regenerative cell during charging and discharging.** This group of batteries known as rechargeable batteries includes vanadium redox flow batteries (VRFBs), sodium bromine (Na-Br), and zinc-bromine (Zn-Br) batteries.

### 6. Comparison of Battery Energy Storage Technologies

Lead-acid batteries are considered the most mature technology currently available; Na-S, Li-ion, Zn-Br Ni-Cd, Ni-MH, and ZEBRA have commercial status, while that the technology of VRFB is nowadays in early commercialization. Li-ion is the most common battery chemistry used to store electricity in power systems worldwide. This is primarily due to their energy density, efficiency, cycle life, warranties, and cost. Although Li-Ion batteries can also offer a range of sub-chemistries with different operating characteristics and their safe operation.

Lead-acid technology is not only mature technology but also one of the cheapest storage options among other technologies. Its power and energy capital costs range from 50-200 (\$/kWh) and 300-600 (\$/kW), compared to the values for other technologies. ZEBRA also presents cost-effective solutions to those capital costs. Although the lead-acid battery is mature and a cheap energy storage option, it produces toxic waste, which harms the environment. Furthermore, Ni-Cd and VRF technologies are also toxic and harm the environment. One of the possible measures to solve the potentially negative effects is using an effective recycling system. It is the best approach to end-of-life management of spent batteries for the environment as well as for resource conservation and economic reasons.

**Table 1: Comparison of technical characteristics of energy storage technologies [14], [15]**

Technology	Operating temperature (° C)	Specific energy (Wh / kg)	Specific power (W / kg)	Efficiency (RTE - %)	Self-discharge (%/day)	Cycle life	Power cost (\$/kW)	Energy cost (\$/kWh)
Lead-acid	-40 - 60	30 - 50	75 - 300	70 - 90	0,1 - 0,3	500-1500	300-600	50-200
Nickel-cadmium	-20 - 45	50 - 75	150 - 300	60 - 70	0,2 - 0,6	2000-2500	500-1500	800-1500
Nickel–metal hydride	-20 - 60	70 - 100	250 - 1000	66 - 92	0,5	~2000	-	-
Lithium-ion	25 - 80	75 - 200	150 - 315	85 - 98	0,1-0,3	500-2000	175-4000	500-2500
Sodium–sulfur	300 - 350	150 - 240	150 - 230	75 - 90	0	~2500-4500	1000-3000	300-500



<b>Sodium–nickel chloride (ZEBRA)</b>	270 - 350	100 - 120	150 - 200	80 - 95	0	>2500	150-300	100-200
<b>Vanadium redox</b>	5 - 45	10 - 25	166	75 - 85	Low	10000-16000	600-1500	150-1000
<b>Zinc-bromine</b>	20 - 50	30 - 50	45	65 - 75	Low	>2000	700-2500	150-1000

**Table 2: Overview of benefits with the characteristics [14], [15]**

Benefits	Characteristics power requirement, response time, and storage/discharge time	Technology
Peak shaving	100 kW–100 MW, seconds to minutes, and 1–10 h	Lead-acid, Li-ion, VRF, Zn-Br, Na-S, and Ni-Cd
Energy management	<1 MW, milliseconds to seconds, and ~2–10 h	Na-S, Zn-Br, VRF, Li-ion
Load leveling	More than 100 MW, minutes, and up to 10 h	Lead-acid, Li-ion, VRF and Zn-Br
Power fluctuations	Few hundred kW, milliseconds, and few seconds	VRF
T&D upgrade deferral	10–100 MW, seconds, and 1–10 h	VRF
Frequency regulation	1–5 MW, milliseconds to seconds, and few minutes to 1	Na-S, Lead-acid, ZEBRA, Ni-Cd, и Zn-Br
Low voltage ride through	<10 MW, ~ milliseconds, and few seconds to a minute	Lead-acid, ZEBRA, Li-ion, and Na-S
Loss minimization	~100 MW, milliseconds, and few seconds	Na-S, Zn-Br, VRF, and Li-ion
Reliability improvement	~1 MW, milliseconds, and few minutes to ~5 h	Lead-acid, VRF и Na-S
Reserve application	1–100 MW, few seconds, and minutes to few hours	VRF, Zn-Br, and Ni-Cd
Demand response	<1 MW, seconds, and ~1–10 h	Li-ion, VRF, Zn-Br, and ZEBRA
EV vehicles	~50 kW, milliseconds, and minutes to hours	Li-ion, Lead-acid

**Table 3: Merits, demerits of battery energy storage systems [3], [6]**

Technology	Strengths	Weaknesses
Lead-acid	Acceptable energy and power density Inherent safety by controlled overcharge reaction No complex cell management needed Relatively low investment	Limited life cycle Ventilation required Recycling required
Nickel-cadmium	High reliability High energy density Very low maintenance required	Suffer from memory effect Relatively high cost ( \$1500 kWh)



<b>Nickel–metal hydride</b>	Environmentally friendly (without cadmium, mercury, or lead) 30 - 40% higher capacity than standard Ni-Cd Profitable for recycling mercury	High intensity of self-discharge Deteriorated performance at higher temperatures
<b>Lithium-ion</b>	High efficiency High energy density Long cycle life	High capital cost due to special packaging Internal over-charging protection circuits
<b>Sodium–sulfur</b>	Raw material cost is low High energy density High cycle and acalearlar lifetime	High operating temperature High thermal standby losses Maintenance requirements
<b>Sodium–nickel chloride (ZEBRA)</b>	High cell voltage High cycle and acalearlar lifetime	Low energy and power density High operating temperature High thermal standby losses
<b>Vanadium redox</b>	Low cost No maintenance Large storage capacity	Low energy and power density
<b>Zinc-bromine</b>	Low cost High reliability High energy efficiency	Low energy and power density Corrosion of material

## 7. Conclusion

The grid-level energy storage system is an integral part of the energy transformation process. It plays a crucial role in the balancing of power generation, utilization, and renewable penetration. By pairing with renewables, such as solar and wind, resource developers can smooth the output from these resources and ensure that renewable energy is injected onto the grid at the times when it is most needed.

In this paper, various battery energy storage technologies have been studied, and their various features are given. These technologies are desirable devices for stationary applications due to their modularization, fast response, flexible installation, and shorter construction cycles. An important role in providing energy services from these technologies must include four key components like integration, technological maturity, conceptual design, and maintenance.

Reducing global greenhouse gas emissions and the need to tackle climate change are dominant and vital for our sustainable future. The production of economically viable technology is the only way to achieve the energy transition and the development of the clean energy economy.

## References

- [1] Khan, M. I., Hassan, M. M., Rahim, A., & Muhammad, N.: *Flexible Batteries. Rechargeable Batteries*, 2020, pp. 41–60.
- [2] Figgenger, J., Stenzel, P., Kairies, K.-P., Linßen, J., Haberschusz, D., Wessels, O., Sauer, D. U.: *The development of stationary battery storage systems in Germany – A market review. Journal of Energy Storage*, 2020, 29, 101153.
- [3] Handbook on Battery Energy Storage System, 2018.
- [4] Energy Storage in Grids with High Penetration of Variable Generation, 2017.
- [5] Breeze, P.: *Power System Energy Storage Technologies. Power Generation Technologies*, 2014, pp. 195–221.
- [6] Dekka, A., Ghaffari, R., Venkatesh, B., & Bin Wu.: *A survey on energy storage technologies in power systems. IEEE Electrical Power and Energy Conference (EPEC)*, 2015, pp. 105-111.
- [7] Fan, X., Liu, B., Liu, J., Ding, J., Han, X., Deng, Y., Zhong, C.: *Battery Technologies for Grid-Level Large-Scale Electrical Energy Storage. Transactions of Tianjin University*, 2020.
- [8] Lachs, W. R., & Sutanto, D. (n.d.). *Application of battery energy storage in power systems. Proceedings of 1995 International Conference on Power Electronics and Drive Systems. PEDS 95*.
- [9] Jeroen Büscher, Charlotte Hussy, Kris Kessels, Michèle Koper *Support to R&D Strategy for battery based energy storage et al.* 2017.
- [10] Energy storage: *Tracking the technologies that will transform the power sector*, 2014.
- [11] Ertugrul, N.: *Battery storage technologies, applications and trend in renewable energy. 2016 IEEE International Conference on Sustainable Energy Technologies (ICSET)*.
- [12] Krivik, P., & BAC, P.: *Electrochemical Energy Storage. Energy Storage - Technologies and Applications*, 2013, pp. 79-100.
- [13] Li, S., Ke, B.: *Study of Battery Modeling using Mathematical and Circuit Oriented Approaches, 2011 IEEE Power and Energy Society General Meeting*, 2011, San Diego, California, pp. 1-8.
- [14] Sufyan, M., Rahim, N. A., Aman, M. M., Tan, C. K., & Raihan, S. R. S.: *Sizing and applications of battery energy storage technologies in smart grid system: A review. Journal of Renewable and Sustainable Energy*, 2019, 11(1), 014105.
- [15] Mohanty, P., Sharma, K. R., Gujar, M., Kolhe, M., & Azmi, A. N.: *PV System Design for Off-Grid Applications. Green Energy and Technology*, 2015, pp. 49–83.



## POWER-TO-X TECHNOLOGIES

**Sara Aneva**

Faculty of Electrical  
Engineering  
Goce Delcev University,  
Stip, R.N. Macedonia  
Sara.20551@student.ugd.edu.  
mk

**Dragan Minovski**

Faculty of Electrical  
Engineering  
Goce Delcev University,  
Stip, R.N. Macedonia  
dragan.minovski@ugd.edu.  
mk

**Vasilija Sarac**

Faculty of Electrical  
Engineering  
Goce Delcev University,  
Stip, R.N. Macedonia  
vasilija.sarac@ugd.edu.m  
k

### Abstract

*The transport, buildings and industry sectors, which still rely on gas and liquid fossil fuels, are the sectors with the highest carbon reduction costs. In this context, Power-to-X technologies, together with the development of low carbon electricity generation facilities look promising for full decarbonization by 2050. This paper describes three types of Power-to-X technologies, the basic principle of Power-to-X systems and the reactions that occur. Then the technical and economic parameters for Power-to-H<sub>2</sub>, Power-to-CH<sub>4</sub> and Power-to-Liquids are reviewed, followed by their advantages and disadvantages. An assessment is made of the conditions under which these technologies can compete with the alternative low-carbon production processes by 2050.*

**Key words:** *Power-to-X technologies, Power-to-H<sub>2</sub>, Power-to-CH<sub>4</sub>, Power-to-Liquids.*

### Introduction

All state-signatories to the 2015 Paris Agreement have pledged to reduce greenhouse gas emissions to zero by 2050. To achieve this goal, it is necessary to completely eliminate fossil fuels that pollute the environment. Renewable sources, such as the sun, water, wind, etc., have long been used to produce clean green energy. The production of electricity from renewable sources does not pollute the environment, but still most of the electricity in the world is produced from fossil fuels. However, if 100% of electricity is obtained from renewable energy sources, the problem of environmental pollution from fossil fuels is far from solved. Transport and aviation, as well as certain processes in the chemical industry, still depend on fossil fuels. Because of this, Power-to-X technology has emerged and it makes renewable energies compatible and applicable for these sectors and processes.

Power-to-X (PtX) is a new technology for the production of synthetic fuels and raw materials from electrical energy. X stands for methane, liquid fuels, or solid synthetic fuels.

### 1. Literature review

As mentioned earlier, this paper describes three types of P2X technologies. Section 2 describes the basic principle of P2X technologies. Then, sections 3, 4 and 5 describe the Power-to-H<sub>2</sub>, Power-to-CH<sub>4</sub> and Power-to-Liquids technologies along with the reactions that occur, their

advantages and disadvantages and their benchmark technologies, respectively. Finally, in section 6 is given a brief overview of the fields of application for Power-to-X.

## 2. Basic principle of Power-to-X technologies

The first step in Power-to-X technology is water electrolysis: using electricity as an input process, water decomposes to hydrogen and oxygen atoms. First, hydrogen is produced from water. This process requires electricity produced from renewable sources. Carbon dioxide is then used to convert hydrogen to gas or liquid to serve as fuel. There are several ways to get the carbon dioxide needed in this process: direct air capture, capture from biomass and capture from industry. However, the best way is to capture carbon dioxide directly from the atmosphere, which will reduce its emissions into the air, but this method is also the most expensive.

### Water electrolysis:



Each P2X conversion path is characterized by a specific combination of technologies that depends on the required inputs and outputs (Figure 1). Electrolyzers are a core component of all P2X systems. There are three main types of electrolyzers:

- Alkaline electrolyzers;
- Polymer electrolyte membrane (PEM) electrolyzers and
- Electrolyzers made of solid oxide electrolysis cells (SOEC).

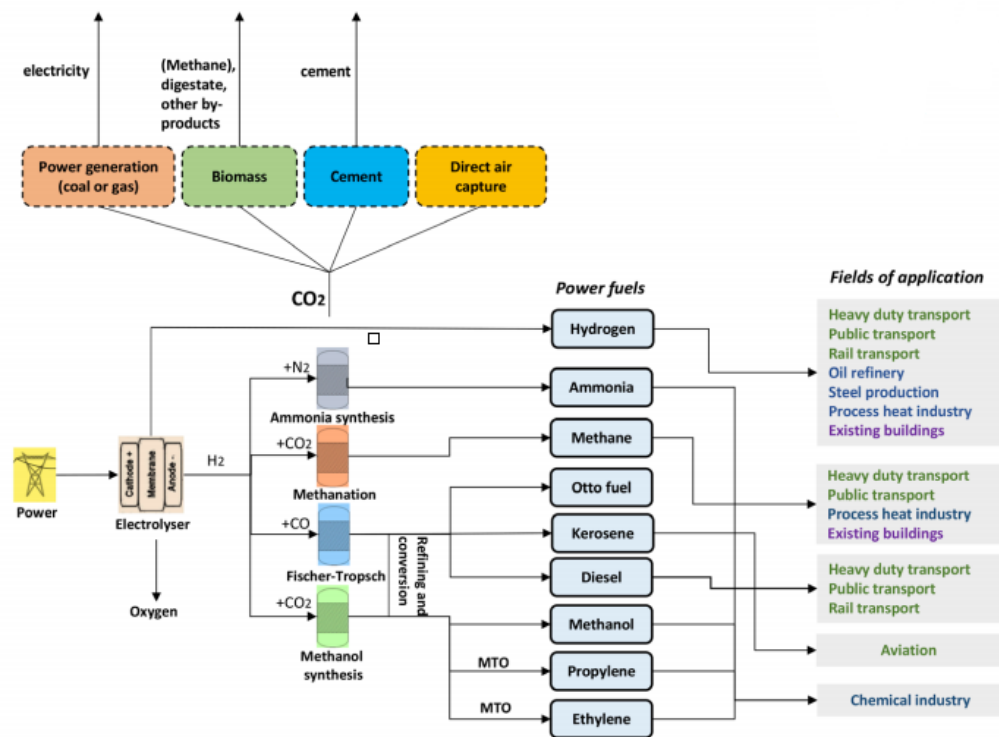


**Fig. 1 System diagram of different chains for P2X production with technological alternatives**

Source: Perspectives of Power-to-X technologies in Switzerland: A white paper

While alkaline electrolysis is the current water electrolysis technology and is widely used for large industrial applications, PEM electrolyzers are typically built for small applications but

have a comparatively higher power density and cell efficiency at a higher cost. SOEC, operating at high temperatures, are at an early stage of development with potential advantages of high electrical efficiency, low material cost and the ability to operate in reverse mode as a fuel cell or in co-electrolysis mode, producing synthetic gas from water steam and CO<sub>2</sub>. Although electrolysis is an endothermic reaction, heat transfer losses usually occur as a result of waste heat that can be used in other applications.

### **Synthesis of methane, other hydrocarbons or ammonia**

The production of synthetic gaseous or liquefied hydrocarbons in the following process steps after electrolysis requires various additional reactor systems, such as a metanation reactor (catalytic reactor or biological reactor), the Fischer-Tropsch catalytic reactor or a methanol synthesis reactor, which also can be used in combination with a further process for the production of oxymethylene ether (OME). In these reactors CO<sub>2</sub> is a raw material, in addition to hydrogen. During the completed P2X chains, each step of the process is associated with energy losses: typical efficiencies for the production of electricity-based synthetic fuels range from 20% (OME) to about 40% (methane). Depending on the thermodynamics of the processes, improved efficiency can be achieved if the waste heat (e.g. from the methanization reactor) is used to heat other processes within the P2X system.

## **3. Power-to-H<sub>2</sub> technologies**

This section describes the different technologies for the production of hydrogen, starting with Power-to-H<sub>2</sub> technology (i.e. different types of water electrolysis) and then explaining the conventional technologies.

### **3.1. Technical and economic parameters**

Power-to-H<sub>2</sub> is a chemical process that produces synthetic hydrogen using electricity. Water electrolysis is currently the main technique to achieve this process: H<sub>2</sub>O is broken down into H<sub>2</sub> and O<sub>2</sub> using electricity. There are 3 techniques for achieving this process: alkaline electrolysis, proton exchange membrane electrolysis (PEM), and solid oxide electrolysis cell (SOEC).

In addition, all three technologies, and especially SOEC, can be upgraded by leading the process of electrolysis at high temperatures, which will increase the efficiency of the process. However, as high temperature electrolysis and SOEC are not currently mature, there are still no technical and economic projections for these technologies. As a consequence, low temperature alkaline technology and PEM technology are the only two technologies whose data are analyzed in detail for Power-to-H<sub>2</sub>.

The cost of producing H<sub>2</sub> depends on four key parameters: service life, energy conversion efficiency, capital costs (CAPEX) and operating costs (OPEX).

#### **Alkaline electrolysis**

The following reactions occur in this process:



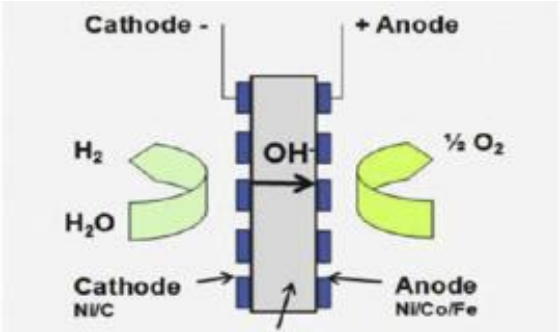


**Fig. 2 Illustration of the principle of operation of a cell for electrolysis of alkaline water**  
Source: METIS Studies: The role and potential of Power-to-X in 2050

**Table 1. Advantages and disadvantages of alkaline electrolysis**

Advantages	Disadvantages
Currently the cheapest electrolysis technology;	Low margin of improvement of CAPEX;
Fast response time enables provision of services of the power system (i.e. flexibility);	Dangerous corrosive electrolyte.
Longer life than PEM;	
High purity of hydrogen (some consumers have high standards of purity quality, such as the transport sector).	

Source: METIS Studies: The role and potential of Power-to-X in 2050

**PEM electrolysis**

The following reactions occur in this process:

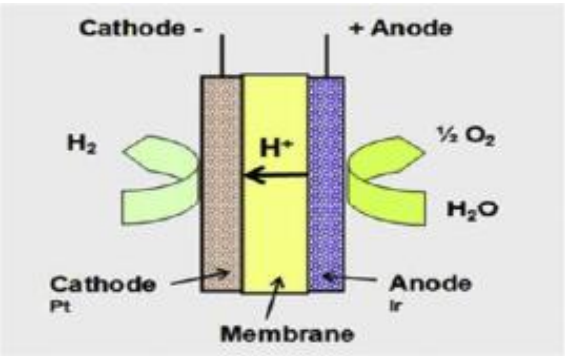


**Fig. 3 Illustration of the principle of operation of a PEM cell for water electrolysis**  
Source: METIS Studies: The role and potential of Power-to-X in 2050

**Table 2. Advantages and disadvantages of a PM electrolysis**

Advantages	Disadvantages
The absence of electrolyte allows easy handling of the technology compared to alkaline;	Use of precious metals (depending on costs);
Compactness, easy production;	Less mature than alkaline technology: not yet commercial on a large scale (higher CAPEX).
Less impact from input conditions;	



Fast response time to flexibility;	
High purity of hydrogen.	

Source: METIS Studies: The role and potential of Power-to-X in 2050

### SOEC electrolysis

The following reactions occur in this process:

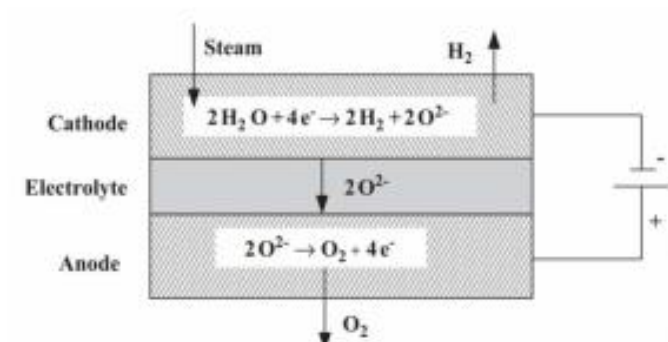


**Fig. 4 Illustration of the working principle of SOEC**

Source: METIS Studies: The role and potential of Power-to-X in 2050

**Table 3. Advantages and disadvantages of a SOEC electrolysis**

Advantages	Disadvantages
Better efficiency than other technologies;	Far from commercial;
Can be combined with other heat recovery processes at a low cost.	Less flexible than other technologies and unsuitable for intermittent operation.

Source: METIS Studies: The role and potential of Power-to-X in 2050

### 3.2. Alternatives for hydrogen production

In addition to electrolysis of water, H2 can be produced by alternative techniques such as: Steam Methane Reforming (SMR), Partial oxidation of fossil energy; Autothermal reforming: a combination of steam reforming and partial oxidation; Gasification of coal; Biomass gasification; Thermochemical cycles; Photocatalytic separation of water; Photo-biological separation of water; A by-product of the production of acetylene and olefins or refineries.

Assuming a high rate of decarbonisation in the gas sector and given current technological trends, the main competitor to Power-to-H2 will be SMR with CCS.

#### SMR/ SMR + CCS

SMR or steam methane reforming is a process in which methane from natural gas is heated by hot steam, in the presence of a catalyst, to obtain carbon monoxide and hydrogen used in organic synthesis and as a fuel.

CSS is the process of capturing waste carbon dioxide, transporting it to a storage site and depositing it where it will not enter the atmosphere.

#### SMR Method:

The following reaction occurs first:



Then, elimination of CO:



The result is:



and finally purification.

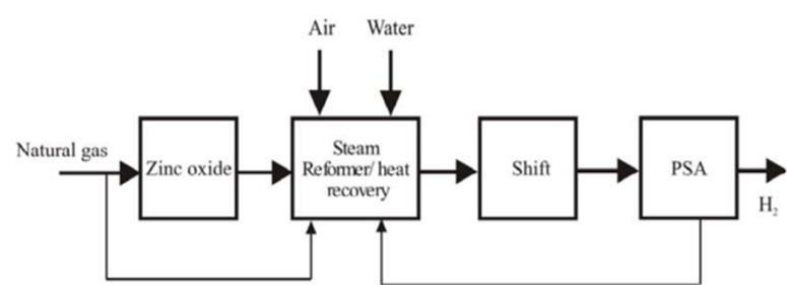


**Fig. 5 Block diagram of hydrogen flow through methane steam reform**

Source: METIS Studies: The role and potential of Power-to-X in 2050

**Table 4. Advantages and disadvantages of SMR + CCS**

Advantages	Disadvantages
SMR offers an efficient, economical and widely used hydrogen production process.	SMR is dependent on the price of natural gas and the price of carbon dioxide;
	CCS is not currently commercially available;
	The development of SMR + CCS depends on the progress of CCS and its ability to integrate into SMR plants.

Source: METIS Studies: The role and potential of Power-to-X in 2050

The SMR + CCS configuration has more significant costs (CAPEX and OPEX) than the simple SMR process. However, the CCS component can be cost effective if the cost of carbon and the number of hours at full load are high enough. In order to determine the break, the production costs (variable price + investment price) for both technologies are calculated. Production costs are calculated using the following equations:

$$productionCost(SMR) = \frac{annualisedCapex(SMR) + Opex(SMR)}{LoadHours} + CH_4Cost(SMR) + CO_2Price(SMR) \tag{3.2.4}$$

$$productionCost(SMR + CCS) = \frac{annualisedCapex(SMR + CCS) + Opex(SMR + CCS)}{LoadHours} + CH_4Cost(SMR + CCS) \tag{3.2.5}$$

4. Power-to-CH<sub>4</sub> technologies

4.1. Technical and economic parameters

After electrolysis, hydrogen can be converted to methane through a process called methanation. Methanation is the reaction of hydrogen with carbon monoxide (CO) or carbon dioxide to produce methane.

Carbon dioxide methanation can be described by the following reaction:



This reaction can occur through two different techniques: catalytic methanation or biological methanation.

Catalytic methanation

The catalytic reaction takes place inside the reactor in the presence of a catalyst such as nickel, rhodium or ruthenium, and nickel is more commonly used due to its low cost. Two types of reactors can be used: adiabatic reactor and isothermal reactor. There is no heat exchange between the adiabatic reactor and the reaction fluids resulting in an increase in temperature inside the reactor. The isothermal reactor includes a cooling circuit that allows heat to be dissipated and the temperature in the reactor to be controlled.

The reaction that takes place inside the reactor is as follows:



Table 5. Advantages and disadvantages of catalytic methanation

Advantages	Disadvantages
Technology well known in the industry;	Temperature control inside the reactor is required: high temperature can damage the catalyst;
Efficiency can be improved by returning the high temperature released during the reaction.	Longer response time than electrolysis.

Source: METIS Studies: The role and potential of Power-to-X in 2050

Biological methanation

The biological way is a new technology that uses methanogenic microorganisms that act as bio-catalysts. The reaction takes place under anaerobic (oxygen-free) conditions inside the so-called digester where there are two possibilities of process. Either H<sub>2</sub> is added directly to CO, initially stored in the digester by microorganisms or H<sub>2</sub> is first mixed with CO<sub>2</sub>, then the aggregated gas is sent to a water-filled digester containing the microorganisms.

Both methanation processes require a reliable source of CO.

- Operating temperature: between 35 ° C and 65 ° C depending on the type of microorganisms;
- Operating pressure: atmospheric pressure (1 bar);
- Methane rate in the exhaust gas: 98-99%;
- Efficiency: 78-80%;
- CAPEX: 1000 € / kW (for methane);

- OPEX: ~ 12% (capex);
- Flexibility: time of induced increase from 0 to 90%.

**Table 6. Advantages and disadvantages of a biological methanation**

Advantages	Disadvantages
Simple technology;	It is not yet mature technology;
No catalyst;	pH control inside the digester.
High purity of methane output;	
Better response time than catalytic methanation;	
Raw biogas can be used as a source of carbon dioxide (depending on the type of digester);	
Significant cost reductions are forecasts by professionals in the coming decades.	

Source: METIS Studies: The role and potential of Power-to-X in 2050

**4.2. Alternatives for methane production**

Methane production is currently dominated by fossil natural gas, with only a small proportion coming from biogas. Biogas refers to a mixture of different gases produced by the decomposition of organic matter (biomass), mainly methane and carbon dioxide, and secondarily H<sub>2</sub> (hydrogen), O<sub>2</sub> (oxygen), H<sub>2</sub>S (hydrogen sulfide) and N<sub>2</sub> (nitrogen). After further purification, biogas becomes biomethane which has the same quality as natural gas and whose production has increased significantly in recent years. Unlike biogas, biomethane can be used in vehicles and injected into the gas network.

Biomass-to-CH<sub>4</sub> (biomethane) has two main production techniques: anaerobic digestion and thermal gasification. Similar to biological methanation, anaerobic digestion carries out a series of biological processes in which microorganisms decompose into biodegradable material in the absence of oxygen. The process results in digest (decomposed material) and biogas (mainly CH<sub>4</sub> and CO<sub>2</sub>). To obtain biomethane, biogas must be added to methane by removing carbon dioxide (through a so-called purification process).

During thermal gasification, the thermal decomposition of wood biomass and consumer waste takes place in a gasifier, in the presence of a controlled amount of oxygen and steam. As a result of synthetic gases (containing CO, CO<sub>2</sub>, H<sub>2</sub> plus pollutants such as sulfur and chlorides) it is purified and upgraded to biomethane thanks to the methane metering unit (as a catalytic methane for power-to-methane).

As for the production of H<sub>2</sub>, the main competitor for the production of Power-to-CH<sub>4</sub> should be evaluated. Assuming a high cost of carbon dioxide, it is likely that Power-to-CH<sub>4</sub> will have to compete with Biomass-to-CH<sub>4</sub> as a carbon dioxide neutral alternative.

**5. Power-to-Liquids technologies**

**5.1. Technical and economic parameters**

By following the process of electrolysis of water, synthetic hydrogen can be converted to various liquid fuels such as diesel, ethanol, methanol, dimethyl ether or ammonia-like fuels. Each fluid has its own conversion process. In the remainder of item 5, the focus is on diesel /

gasoline-like fuels generated through Power-to-Liquids process chains, for two main reasons. First, these fuels are produced through Fischer-Tropsch synthesis or methanol synthesis, which are the most experimented processes of Power-to-Liquids and are thus characterized by the highest availability of data in terms of technical and economic parameters. Second, these fuels are likely to experience significant use in the future because of their ability to replace fossil fuels in specific segments of the transport sector where electric batteries or fuel cells can only be used to a limited extent, such as aviation.

**Production of liquid fuels through Fischer-Tropsch synthesis**

The Fischer-Tropsch process produces various hydrocarbons through the main reaction:



n is usually 10-20, resulting in crude liquid fuel being refined.

Other types of reactions occur inside the reactors. Carbon monoxide is obtained from carbon dioxide by using a reverse reaction to change water and gas.

**Table 7. Advantages and disadvantages of Fischer-Tropsch synthesis**

Advantages	Disadvantages
Relatively established technology, because it is already used for processes for conversion of coal into liquids	It is not yet fully mature technology for power conversion processes into liquids.

Source: Source: METIS Studies: The role and potential of Power-to-X in 2050

**Production of fuels through the synthesis of methanol**

The reaction for methanol synthesis is as follows:



- Methanol can also be produced by the reaction of H<sub>2</sub> and CO.
- Methanol can be supplemented by further conversion to synthetic gasoline, diesel or monomolecular fuels such as OME (oximethyl ether) or DME (dimethyl ether).

**Table 8. Advantages and disadvantages of synthesis of methanol**

Advantages	Disadvantages
The synthesis of methanol is a known process, but the raw materials are natural gas or coal.	There is currently no mature technology for Power-to-Liquids.

Source: Source: METIS Studies: The role and potential of Power-to-X in 2050

**5.2. Alternatives for fuel production**

Biofuels can be considered the most advanced sub-category of Biomass-to-Liquids conversion technologies. Among biofuel technologies, first-generation biodiesel and bioethanol are currently the most developed, but they have limited growth due to their competition with the food industry and their limited carbon emission benefits. Considering advanced biodiesel as a major competitor to Power-to-Liquids conversion technology seems to be increasingly relevant as Power-to-Liquids fuels should not be mixed with other fuels (they can be used directly in ICE).

## 6. Fields of application for Power-to-X projects

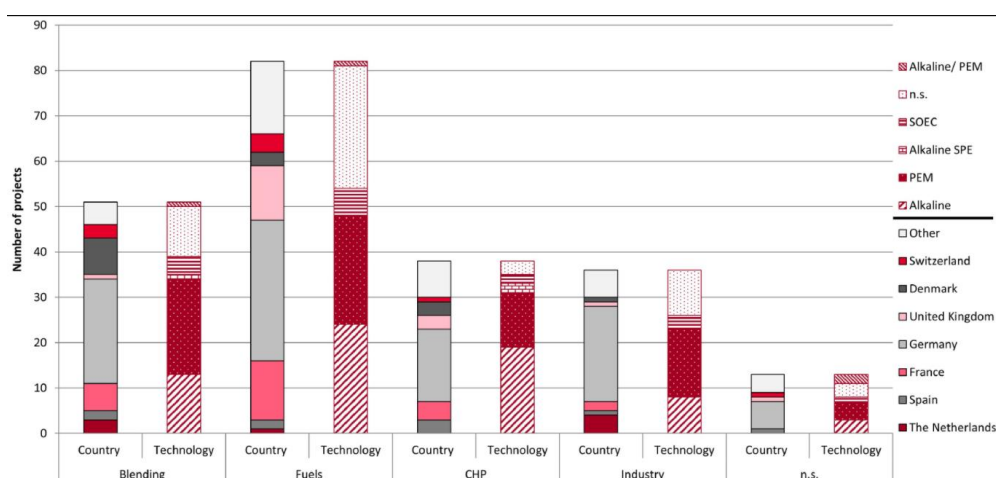


**Fig. 6 Fields of application for Power-to-X projects according to countries and technologies.**

Source: Demonstration Projects in Europe. Institute of Energy and Climate Research – Systems Analysis and Technology Evaluation

As can be seen in figure 6, in the context of fuel production, PtX is the most common field of application in Europe with a 37% share of all projects. As it can be seen from figure 6 certain types of electrolyzer are preferred for different fields of application. For CHP purposes, an alkaline electrolyzer is used in almost 50% of the projects, whereas for industrial applications, a PEM electrolyzer is used in 47% of the projects. However, the use of industrial applications and PEM electrolyzers has increased significantly in recent years.

## Conclusions

The development of P2X technologies is progressing quickly and will continue to do so in the near future due to its characteristics, applications and impact on the environment. The development of PEM and alkaline electrolyzer technologies has been good and these technologies are used very often, although there seems to be an apparent preference for the more mature alkaline technology in the future. Solid oxide electrolyzer cells are catching up in their technological development with multi-MW projects. Methanation is used in many applications and has proven its feasibility for hydrogen processing. As for the production of liquid fuels, it is safe to say that it is the fuel of the future. As much effort as possible should be made to utilize this technology, which will contribute to saving the planet from pollution.

## References

- [1] METIS Studies: *The role and potential of Power-to-X in 2050*, 2014
- [2] A White Paper: *Perspectives of Power-to-X technologies in Switzerland*, 2019
- [3] Wulf, Christina / Zapp, Petra / Schreiber, Andrea: Review of Power-to-X Demonstration Projects in Europe. *Institute of Energy and Climate Research – Systems Analysis and Technology Evaluation, Forschungszentrum Jülich, Jülich, Germany*, 2020.





## NEW INNOVATIVE TOURISM PRODUCT FOR REANIMATING RURAL AREAS

***Biljana Petrevska<sup>1</sup>, Risto Popovski<sup>2</sup>, Vlatko Chingoski<sup>3</sup>***

<sup>1</sup>Faculty of Tourism and Business Logistics, Goce Delčev University – Štip, North Macedonia, email:  
*biljana.petrevska@ugd.edu.mk*

<sup>2</sup>Faculty of Natural Sciences, Goce Delčev University – Štip, North Macedonia, email:  
*risto.popovski@ugd.edu.mk*

<sup>3</sup>Faculty of Electrical Engineering, Goce Delčev University – Štip, North Macedonia, email:  
*vlatko.cingoski@ugd.edu.mk*

### **Abstract**

*During the COVID-19 pandemic, the tourism industry was severely affected, and the travel patterns dramatically changed. Yet, the love for travel and leisure remained with a focus on the environment and rural areas. The paper presents new insights into the possibility of developing innovative tourism product based on the Earth's natural electromagnetic waves with an extremely low frequency of 7.83[Hz]. It discusses the option for using the Schumann resonance for tourism purposes. The main objective of the research is to demonstrate the way some rural areas have the potential to apply the therapeutic benefit of the Earth's magnetic field to tourists and visitors. Data measurements are collected in the village Lesnovo (North Macedonia) during 2019. It was found a presence of positive and harmonious energy vibrations, thus pointing to the possibility of creating a completely new dimension for rural areas. This may attract more visitors and boost the rural economy if raising the awareness that villages may offer much more than just an ordinary rural ambient. The paper adds to the scarce literature on Schumann's effects on tourists along with its practical contribution for proposing new frontiers and innovative solutions for tourism development based on positive vibrations of the rural areas.*

### **Keywords**

*Rural areas, Tourism, Positive effects, Earth's natural electromagnetic waves.*

### **Introduction**

Tourism was severely affected by the COVID-19 pandemic provoking changes in demand and travel patterns [4], [8], [25], [28]. Due to numerous safety restrictions, travel patterns dramatically changed. Yet, the love for travel and leisure remained but this time with a focus on the natural environment, unexplored and isolated destinations, and rural areas. This urged tourism policymakers to try to create a new dimension for attracting visitors by considering numerous constantly changing travel restrictions. The idea was to create a perception for a safe destination that offers a new leisure experience with the priority on the health issue. Thus, the rural areas emerged as one of the most required destinations for relaxation and vocation.

Besides the untouched nature, the breathtaking scenery, and the moment of isolation, the rural areas may offer another interesting and new aspect for developing a completely different rural tourism product. The symbiosis may be found in the potential for synchronizing the positive emotions and good vibrations to the cardiovascular, respiratory, immune, and nervous systems influenced by the Schumann resonance (SR) [24]. The Earth produces natural electromagnetic waves at an extremely low-frequency level of 7.83[Hz] spreading the signal and affecting everyone and everything in the natural environment. Though the literature on SR is continuously growing, the issue of the effects on tourists and visitors is barely discussed. Some exceptions for the use of the SR for tourism purposes are already discussed [5], [21]. This paper adds to the state of the art by arguing the potential to use the rural areas as destinations with

therapeutic benefit to tourists and visitors produced by the Earth's magnetic field. Moreover, it discusses the option for developing innovative rural tourism product by using the SR as a signal with positive effects on humans in the natural environment. The presented research is carried in a small village as a sample location in North Macedonia and offers some new frontiers for innovative tourism product based on harmonious energy present in the rural area.

The paper is divided into several sections. After the introduction, a brief literature review on the SR environmental effects is presented. This is followed by the research methodology explaining the study method. The next section discussed the results, being followed by the main conclusion of the study.

## **1. Literature review**

The issue of the SR [24] as a spectrum of resonant electromagnetic waves in the extremely low-frequency range in the Earth-ionosphere cavity [2] is vastly explored. The interest in the literature is still permanently growing offering a variety of interpretations. [16] - [18] explore the SR when evaluating the characteristics of the thunderstorm activity and the global lightning. Some research is focused on monitoring the global upper-tropospheric water vapor changes [22], on the monitoring of the planetary temperature [27], while some explored it on the lower ionosphere parameters on celestial bodies [19].

Furthermore, many scholars explain the effects of the Earth's magnetic field on living beings, starting from the fundamental frequency of 7.8[Hz] to the higher harmonic components at 14[Hz], 20[Hz], 26[Hz], 33[Hz], 39[Hz], and 45[Hz] [6]. These harmonics directly overlap with the central nervous system alpha waves being associated with the psychophysiological coherence of 0.1[Hz], the approximate 10-second cycle of ocean waves, and the hypothetical resonant frequency of the Earth [14], [15]. Furthermore, the postulation of feedback loops between all living systems and the Earth's magnetic field is discussed [3], which enables electromagnetic interactions within and between people [11], [13], [23]. This provokes implications for bone growth and ligament healing, capillary formation, fibroblast proliferation, and decrease skin necrosis [10]. Other numerous positive impacts of the SR on the human condition is already vastly discussed related to the heart rate, blood pressure, brain activity, nervous system activity, calming, athletic performance, memory, and other tasks [1], [7], [9], [12], [14], [20], [26].

## **2. Research methodology**

### **Case study – village Lesnovo (North Macedonia)**

Having in mind that North Macedonia has over 70% of rural areas rich with amazing natural scenery, it is selected as suitable for investigation. Lesnovo is a very small mountain village with only 40 inhabitants located in the northern part of the country. It is two hours drive from the capital city of Skopje, and 13 km from the nearest town Probištip. It is one of the oldest villages in the country laying in a well-preserved fossil volcanic crater being a natural geological monument in the western part of the Osogovo Mountains. The village is vastly visited due to the main monastery St. Gavril Lesnovski, constructed on the site of a much older monastery, and dating from 1347 or thereabouts. Many tourists, visitors, and pilgrims visit the main church and enjoy the fresco paintings and the iconostasis which are powerful and full of mystery. The village is also famous for its high-quality watermill rocks that have been made for centuries, traditional rural architecture, several cave churches, and many beautiful fountains built in traditional style with natural material (Figure 1).





**Fig. 1 Lesnovo**  
Source: Authors

### Study method

The study attempted to investigate the possibility of creating new innovative tourism product for rural areas based on a presence of positive and harmonious energy vibrations. For that purpose, it applied: (1) Qualitative method – A desk research with an in-depth review of literature on the SR is made, and (2) Quantitative method – Data were collected in the village Lesnovo on April 17<sup>th</sup>, 2019 with a 16 Bit AD converter as the main measurement instrument (Figure 2). Along with the original signal of the location, the low bandpass Butterworth filter 1-35[Hz] was applied, and the Fast Fourier Transform spectrum was done.

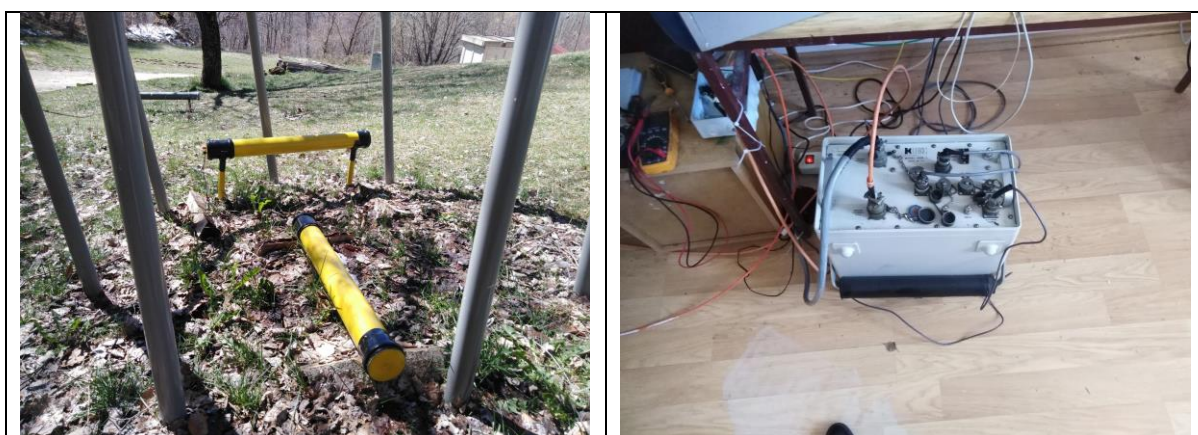




**Fig. 2 Measurement instruments**

Source: Authors

On the location, the measurements were repeated in different time momentums during the day since the effects of the solar wind and magnetization differ and vary on a range of timescales from minutes to hours.

### 3. Results

Collected data from the village Lesnovo are visually presented in Figures 3-5. Figure 3 presents the basic signal and the Butterworth filter 1-35[Hz], Figure 4 presents the spectrogram, and Figure 5 presents the spectrum. It is visible that village Lesnovo has a significant presence of the basic pulsation of the SR of 7.8[Hz] along with other harmonics.

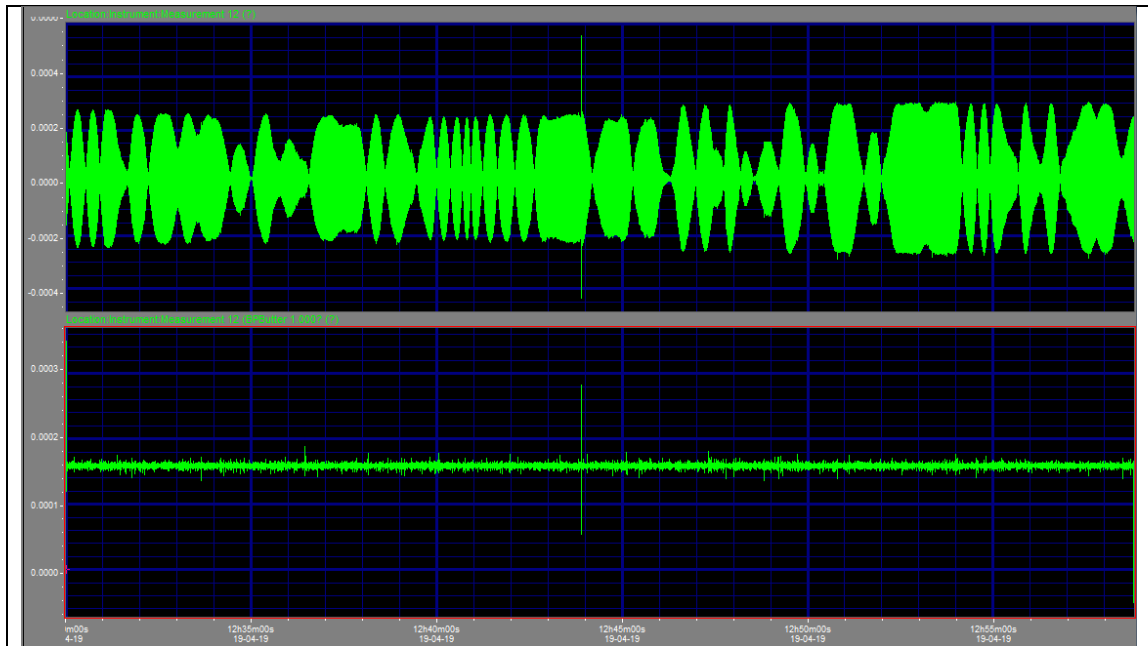


**Fig. 3 Basic signal and the Butterworth filter 1-35[Hz]**

Source: Authors



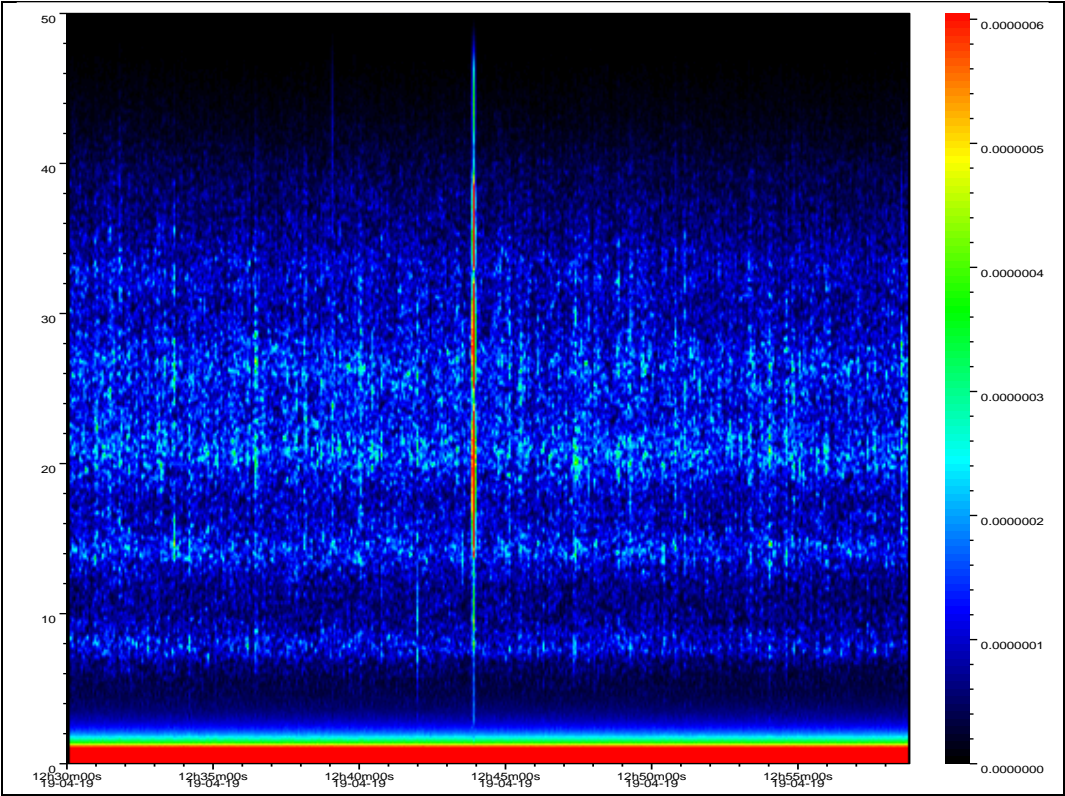


**Fig. 4 Spectrogram**

Source: Authors

A closer look at Figure 5 reveals many positive harmonics of the basic pulsation of the SR of 14.4[Hz], 20.5[Hz], 27.5[Hz], and 33.6[Hz]. Such impulses provoke positive therapeutic effects on the human body [1], [7], [20]. Moreover, bone growth and ligament healing may be supported by the frequencies between 7-8[Hz], and a capillary formation, fibroblast proliferation, and decrease skin necrosis by the frequencies between 14-15[Hz] [10]. Other detected positive harmonics of the registered magnetic field may positively affect tourists and visitors of the village Lesnovo by supporting the overall health condition, heart rate, blood pressure, and calming [9], [12], [14], [26].

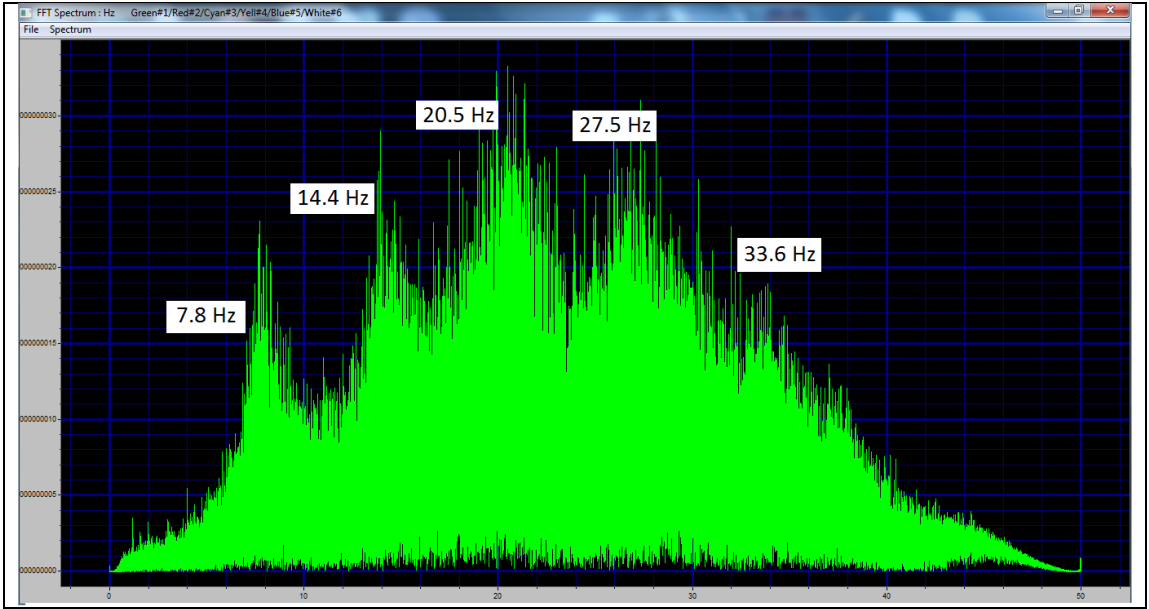


**Fig. 5 Spectrum**

Source: Authors

## Conclusion

The study measured the SR in a rural area to detect new frontiers for creating innovative rural tourism product. It found a presence of positive and harmonious energy vibrations, thus pointing to the possibility of creating a completely new dimension for rural areas. This may attract more visitors and boost the rural economy if introducing new product pointing that villages as recreational and leisure areas may offer much more than just an ordinary rural ambient. The results point that village Lesnovo may be promoted as a destination that offers positive and harmonious energy vibrations in addition to the well-known preserved environment. As such, tourism supply may be dramatically expanded thus attracting visitors, one-day trippers, excursionists, and nature-lovers. Yet, the awareness of the positive Earth's magnetic field on the psychological, physiological, and neurological health of tourists and visitors, is very low among locals and tourism-policy makers. One may presume that when tourists are going to be familiarized with the fact that Lesnovo offers symbiotic harmonics which positively encode and interact with their consciousness, emotions, and thoughts, they will be much interested in extending the stay and revisiting the destination.

Only when rural areas are promoted as locations that offer the therapeutic benefit of the electromagnetic field radiation on human's health, it is to expect to gain an added value. Then, a new dimension may be highlighted with a focus on a new product that may result in an ultimate satisfaction in a harmonious ambient fulfilled with energy vibrations. In this line, rural areas like the village Lesnovo, must develop a new tourism product based on the positive impulses from nature that has no seasonality, contributes to sustainability, and provokes zero negative impacts on the environment caused by tourism development. As such, traditional rural tourism may exceed the conventional approach and proactively offer a new solution for rejuvenation and overall wellbeing.

The paper adds to the scarce literature on how the SR affects tourists and visitors when recreating in a rural natural environment. Additionally, its practical contribution is in the fact that proposes new strategic dimensions for introducing an advanced solution for tourism development based on positive vibrations present in villages.

The research has several limitations. First, the data is collected only in one day, so additional time extension and measurement repetitions are needed. Second, the measurement is performed with only one mobile instrument, so more mobile induction antennas are advisable enabling data comparison. Finally, the research applied the case study which brings the risk for overrating generalization of the findings. All these notes suggest some further issues to be addressed. However, besides contributing to the current literature review on the SR, the paper posts new directions for rural tourism development.

## References

- [1] Babayev, S. E., Allahverdiyeva, A. A. (2005). Geomagnetic Storms and their Influence on the Human Brain Functional State. *Revista CENIC Ciencias Biológicas*, Vol. 36, 1-7.
- [2] Balser, M., Wagner, C. A. (1960). Observations of Earth-ionosphere cavity resonances. *Nature*, Vol. 188, No. 4751, 638.
- [3] Brizhik, L., Del Giudice, E., Jorgensen, S.E., Marchettini, N., Tiezzi, E. (2009). The role of electromagnetic potentials in the evolutionary dynamics of ecosystems. *Ecological Modelling*, Vol. 220, 1865-1869.
- [4] Brouder, P. (2020). Reset redux: possible evolutionary pathways towards the transformation of tourism in a COVID-19 world. *Tourism Geographies*, 1-7.
- [5] Cingoski, V. & Petrevska, B. (2019). From global Earth magnetic field to therapeutic experience: Towards a theoretical framework for developing tourism product. *Journal of Applied Economics and Business*, 7(3), 23-29.



- [6] Edwards, S. D. (2015). The global coherence initiative: Opportunities for scientific research and health promotion. *African Journal for Physical Health Education, Recreation and Dance*, <https://www.researchgate.net/publication/286869493>, (13 December 2018).
- [7] Gubbins, D., Herrero-Bervera, E. (2007). *Encyclopedia of Geomagnetism and Paleomagnetism*, Springer, Netherlands.
- [8] Hall, C. M., Scott, D., and Gössling, S. (2020). Pandemics, transformations and tourism: Be careful what you wish for. *Tourism Geographies*, Vol. 22, No. 3, 577–522.
- [9] HeartMath Institute, (2019). *Effects of Geomagnetic, Solar and Other Factors on Humans*, <https://www.heartmath.org/articles-of-the-heart/effects-geomagnetic-solar-factors-humans/>, (1 February 2019).
- [10] Human frequency blog (b). *Reiki Frequencies and Schumann Resonances*, <https://www.humanfrequencies.com/> (20 February 2019).
- [11] Lynch, J. J. (2014). Hidden therapeutic dialogue: Decoding the language of the human heart. *Neuropsychotherapist*, July, 49-70.
- [12] Mitsutake, G., Otsuka, K., Hayakawa, M., Sekiguchi, M., Cornélissen, G., Halberg, F. (2005). Does Schumann resonance affect our blood pressure?, *Biomedicine & Pharmacotherapy*, Vol. 59, S10-S14.
- [13] McCraty, R. (2003). *The energetic heart. Bioelectric interactions within and between people*. HeartMath Research Centre, Boulder Creek, CA: Institute of HeartMath.
- [14] McCraty, R., Deyhle, A. & Childre, D. L. (2012). The Global Coherence Initiative: creating a coherent planetary standing wave. *Global Advances in Health and Medicine*, Vol. 1, No. 1, 64-77.
- [15] McCraty, R., Deyhle, A. (2015). The Global Coherence Initiative: Investigating the dynamic relationship between people and the earth's energetic systems. In: P. J. Rosch (Ed.), *Bio-electromagnetic and Subtle Energy Medicine*, 2<sup>nd</sup> Edition (pp. 411-425). Boca Raton, FL: CRC Press.
- [16] Nickolaenko, A. P., Besser, B. P., Schwingenschuh, K. (2003). Model computations of Schumann resonance on Titan. *Planetary and Space Science*, Vol. 51, No. 13, 853-862.
- [17] Nickolaenko, A. P. (1997). Modern aspects of Schumann resonance studies. *Journal of Atmospheric and Solar-Terrestrial Physics*, Vol. 59, No. 7, 805-816.
- [18] Nickolaenko, A. P., Hayakawa, M. (2002). *Resonances in the Earth-Ionosphere Cavity*, Kluwer Acad., Norwell, Mass.
- [19] Nickolaenko, A. P., Rabinowicz, L. M. (1982). On the possibility of existence of global electromagnetic resonances on the planets of solar system1. *Earth*, Vol. 6, No. 10.6, 18-3.
- [20] Persinger, A. M., Saroka, S. K. (2015). Human Quantitative Electroencephalographic and Schumann Resonance Exhibit Real-Time Coherence of Spectral Power Densities: Implications for Interactive Information Processing, *Journal of Signal and Information Processing*, Vol. 6, 153-164.
- [21] Petrevska, B. & Popovski, R. (2019). Schumann resonance: new aspects for tourism development. Conference proceedings from the 4th International Scientific Conference "Tourism in the function of development", Vrnjacka Banja, Serbia, 31.05-01.06.2019, 705-722.
- [22] Price, C. (2000). Evidence for a link between global lightning activity and upper tropospheric water vapor. *Nature*, Vol. 406, No. 6793, 290.
- [23] Rosch, P. J. (2014). Why the heart is more than a pump. *Neuropsychotherapist*, July, 1-13.
- [24] Schumann, W. O. (1952). *On the radiation-free self-oscillations of a conducting sphere which is surrounded by an air layer and an ionospheric shell* (in German), *Z. Naturforsch.* A, 7, 149.
- [25] Wachyuni, S. S., Kusumaningrum, D. A. (2020). The Effect of COVID-19 Pandemic: How are the Future Tourist Behavior? *Journal of Education, Society and Behavioral Science*, 67-76.

- [26] Ward, P. J., Henshaw, L. D. (2016). *Geomagnetic Fields, their Fluctuations and Health Effects*, unpublished, <https://www.researchgate.net/publication/242259262>.
- [27] Williams, E. R. (1992). The Schumann resonance: A global tropical thermometer. *Science*, Vol. 256, No. 5060, 1184-1187.
- [28] Zenker, S., Kock, F. (2020). The coronavirus pandemic—A critical discussion of a tourism research agenda. *Tourism Management*, 81.



## PROPOSED MODEL FOR BETTER ENGLISH LANGUAGE ACQUISITION, BASED ON WEARABLE DEVICES

***Stojce Recanoski<sup>1</sup>, Simona Serafimovska<sup>2</sup>, Dalibor Serafimovski<sup>1</sup>***

<sup>1</sup>Faculty of Electrical Engineering, Goce Delčev University – Štip, Macedonia, email: [rechanoskistojche@gmail.com](mailto:rechanoskistojche@gmail.com)

<sup>2</sup>Faculty of Philology, Goce Delčev University – Štip, Macedonia, email: [simona.serafimovskai@ugd.edu.mk](mailto:simona.serafimovskai@ugd.edu.mk)

<sup>3</sup>Faculty of Electrical Engineering, Goce Delčev University – Štip, North Macedonia, email: [dalibor.serafimovski@ugd.edu.mk](mailto:dalibor.serafimovski@ugd.edu.mk)

### Abstract

*A solid English Language comprehension is a necessity in today's technology driven world. Furthermore, the significance of the English Language is only amplified by its presence in modern higher education. This paper presents a smartphone and wearable device oriented language learning model which can be used both during and after lectures. The model intends to gradually enrich the students' English language vocabulary as they proceed further with their lectures. Additional features are designed to help students improve their pronunciation of the newly discovered words. A key point that makes this model efficient is that students can advance their vocabulary and pronunciation skills paralleled with their study subjects.*

### Key words

*Language learning, Blended Learning, English vocabulary app.*

### Introduction

It goes without saying that the most of the available literature, that can be easily accessed today, is written in English. Furthermore, the English Language is well known for being present in every branch of science and technology, especially when it comes to scientific terms and engineering vocabulary. Establishing itself as one of the most widely spread languages across the world, it induces one's necessity for a certain level of language proficiency.

Fluency in English is not only needed because of its significance in the exhaustive study of any subject, but also for conducting research, different forms of formal communication, job interviews, etc.

In this context, the aim of this paper is to describe a mobile and wearable device oriented learning model that helps the students to comprehend the English Language better which is used in their lectures and study.

### 1. Literature review

As constant usage of smartphones becomes evident among students, various mobile learning applications have recently been developed. Many authors have seen the potential mobile devices promise in teaching. Concretely speaking, in a research [1], English language students have used 2D barcodes, namely Microsoft Tags, to learn new vocabulary more efficiently. Furthermore, in another paper [2], the potential of context-aware mobile language learning is presented, targeting German and Thai students.

Considering the many language learning apps widely available today across various platforms, an overview of some is presented in a rather interesting column (Godwin-Jones, R. (2011)), in which the author also explains the technologies used for developing such apps.

Language learning apps can seem effective in that they provide a personal and learner-centered learning opportunity with ubiquitously accessible and flexible resources and activities. This could encourage learners to develop a sense of individuality and develop life-long learning habits [4].

The Blended Learning approach to teaching a foreign language is taken into account by Sharma, P. and Barrett, B. In their book [5], they present technological tools which can be used in the classroom as well as instructions on how to use the Internet for teaching.

The effectiveness of smartphone usage has been tested in a different research where findings show that smartphone usage has a great impact on 99% of targeted students [6].

Smartphones are even being used for pronunciation learning. A rather efficient technique is presented in a paper by Lee et al. [7], where users can correct their pronunciation through listening to native pronunciations.

What was revealed in a study [8] is yet another point on the benefits of smartphone usage in the teaching process. Namely, the learner's positive learning mood.

Likewise, it has been concluded that through an app-based spelling learning, not only did students made progress in acquiring spelling ability, but developed learning habits as well.

To our observation, most of the current research, at least when it comes to vocabulary learning, is based on fixed set of words, while our model differs in the continuous expansion of the starting set of vocabulary words. That is, the initial number of words in the set of words grows proportionally to the new learning material of the respective subject. .

## **2. The model**

One way of making the process of learning a foreign language much easier for students is by making the language itself easily accessible to them at any given time. We firmly believe students should be regularly exposed to new vocabulary and they should be motivated to practice communicating in English with their peers more often. After all, practice makes perfect.

Having in mind the excessive use of mobile phones and wearable devices among students, we recommend a way of discovering and learning new words through the use of the very same mobile devices. Thus putting the smartphones to good use.

The suggested model consists of three main parts. The first, and foremost, being the front - end part of the model i.e. the application used by the students. The second part is the back – end, or server – side, part consisted of the network infrastructure and the servers used for data storage. Finally, the third part is the teachers' part, which includes a desktop application in which the students' activity and progress is being supervised. Because of technical similarities, and for descriptive purposes, the first and the third part of the model will be grouped in the next section. We would like to emphasize that the students (and their teachers) are themselves a huge part of this model.

The briefly discussed building blocks of this language acquisition model will be separately described in greater detail in the following sections.

## **3. The front-end part**

For us, one of the most important prerequisites for a language acquisition model is its usability and effectiveness. To achieve the set goals, we use a mobile application that serves as an interface between the students and the material they need to learn. The app is connected to multiple databases which will be discussed in the section dedicated to the description of the server - side part of this model.

The application used by the teachers is mainly designed to function as a simple, yet efficient, monitoring station. All data entered by the students is visible to the desktop app.

However, one may argue that for this kind of model it is of greater importance to more thoroughly describe the application that the students use. It itself, is constructed of multiple modules. Such module is the “Random word generator”, where students get a different word every time they click a button, alongside a task to translate that word. If the translation is done correctly by the student, the student receives in-app points. But, if the student doesn’t know the word he/she can save it to a personal “list of words” or simply ask a friend for help. In order to make the app more interesting, during this activity, groups of words are formed. An example of one of those groups is the “Most difficult words this week”. The goal is to form a list of words that can be reviewed over and over by the students, so ultimately they can remember the new vocabulary more easily.

In order to use the smartphone application, the student first needs to sign in using his/her student id and password. Figure 1 shows the Student sign in page.

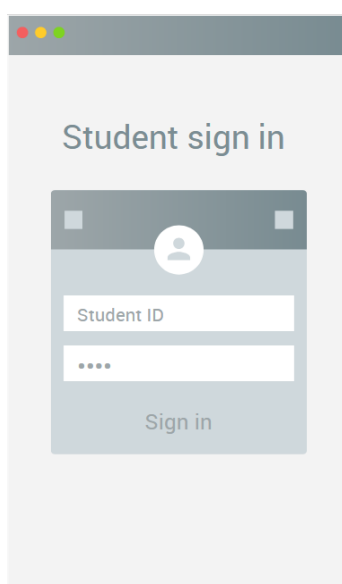


**Fig. 1 Student sign in page, part of the mobile application that the students use.**

Once the student has successfully signed in, he/she can practice and improve vocabulary skills through the use of the previously described “Random word generator” module. Figure 2 illustrates an example of the use of this module. Students get a new word with a click of a button. Afterwards, they have to fill in the correct translation and submit their answer.

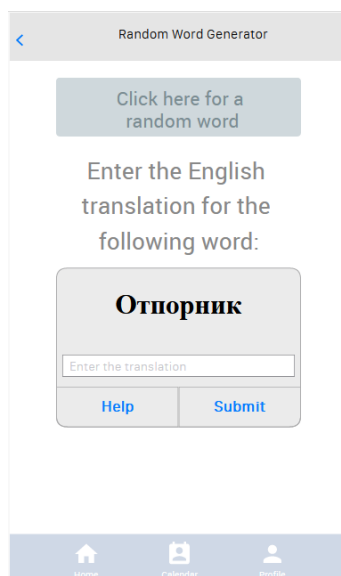


**Fig. 2 Random word generator page, part of the mobile application that the students use.**

The starting set of words is previously entered (hardcoded) into a database named “Word bank”. In the “Word bank” there are many English words with their corresponding translation. An algorithm is used to check whether the translation is correct or not. As an extension to this module, even the Google Translate API may be used so that students could translate other words and strings instantly. The point of this module is to get students familiarized with as many English words as possible.

Through the application each student can add any word of their choice. That word will be sent to the “Words added by students” database. Afterwards, each student can enter a translation for any of the words stored in that database. Later, the translation is sent to the teacher for approval. For each correct translation the student receives in-app points. This way students are motivated to continuously update the starting vocabulary of the app. This part of the model puts an emphasis on encouraging students to learn more freely from each other.

Another very useful module of the application is the “Words used in this lecture” module. Here, the goal is to find words unknown to the app and possibly to the students. Particularly, words that have been used in the students’ current lecture but have not been added to the “Word bank” nor the “Words added by students” database yet. The found words are then sent to the students via the app’s notification system. Please note that an algorithm scans for words written in the students’ native language. Despite being temporarily stored in a database, at that moment the words don’t have a suitable translation (or any translation at all). The students’ task for this part is to find and enter the English translation of each new word. Afterwards, the translation of the word is sent to the teacher. If the teacher approves the translation, the English translation is then instantly linked to the corresponding word. In the next step, the unknown word along with its translation is stored in the “Word bank” database. Finally, all students who have correctly done the translation receive in-app points for each correctly translated word.

The data flow between the presentation notes, the network and the databases is illustrated in Figure 3. Combined together, the previously described features of the app result in a real-time update of the current set of words whilst encouraging student activity. In other words, the beauty of this module is that the in-app vocabulary grows in proportion to the students’ own vocabulary.



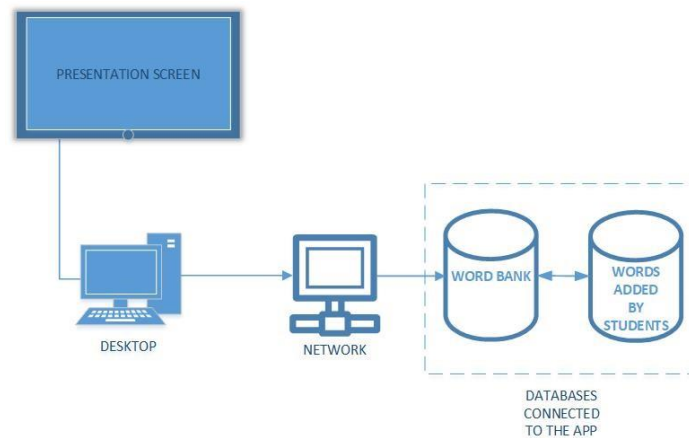


**Fig. 3 Real-time vocabulary update.**

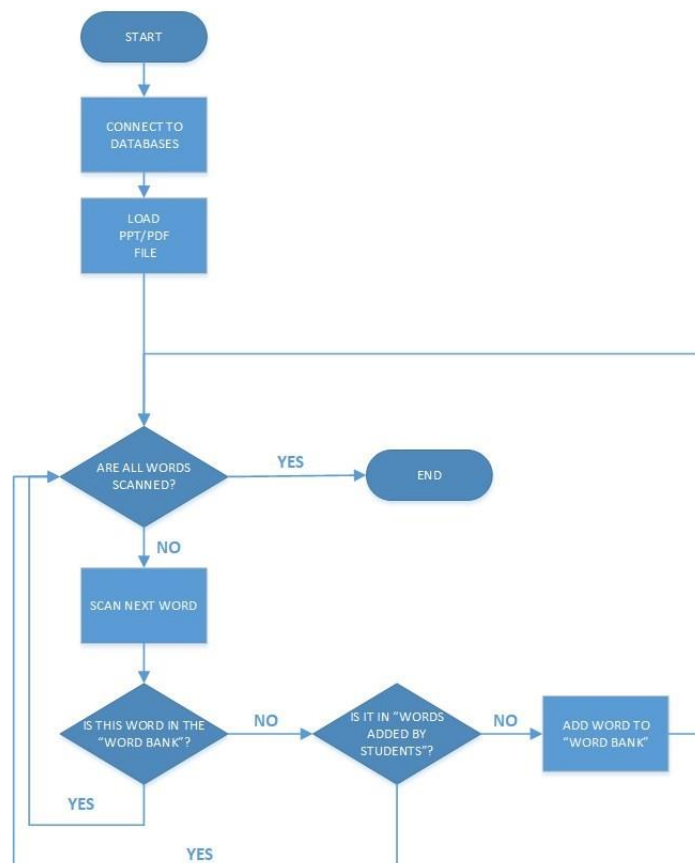
The working principle behind this module is based on simply scanning the PDF/PPT file that the lecturer uses for presentation purposes. This module can be modified to scan for words either in English or any other spoken language (students' native language), meaning that it is reversible.

Figure 4 presents the algorithm used for scanning the lecture notes and adding words to the "Word bank" in real-time.

In the first step, the app connects to the databases and then loads the file from which potentially unknown words can be acquired. The actual scanning for new words begins after the file is loaded.

Until all the words have been looped, the algorithm executes a series of if-else statements. First, a check is performed to determine whether all words in the file have been scanned. If not, the algorithm proceeds onto scanning the next word. At this point, another check is performed to see whether the word has already been added to either of the databases.

If the algorithm discovers that a word has already been added to a database, it skips that word and returns to the point where it checks whether there are any other words remaining to be scanned.



**Fig. 4 The algorithm used for performing real-time scan for unknown words.**

As a result of the wearable devices’ popularity, this model features a smartwatch application, similar to the previously described smartphone application. Figure 5 shows a screenshot of the menu featured in the smartwatch application. Again, the student can select the “Random word generator” module which is based on the same module used in the smartphone app. What’s interesting about the smartwatch app is that it uses a phonetic algorithm so that students can practice and work on their pronunciation. Speech-to-text technology is used to convert voice to text. If the student pronounces the given word correctly, he/she receives in-app points. Through the use of the “Practice saying the word” module, students receive tasks to pronounce the words from the “Word bank” which is regularly updated. This app uses the same databases and the same back-end technologies as the smartphone app uses.

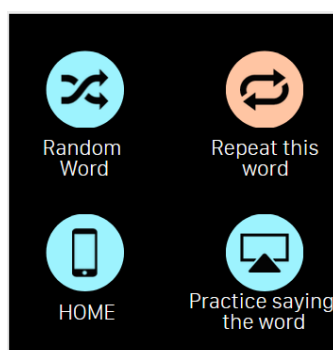


**Fig. 5 The smartwatch application.**

The “Practice saying the word” module is shown in Figure 6. Through a click of a button, the student is given one random word. Next, the student has to hold the other button and repeat i.e.

correctly pronounce the same word. For the purposes of this application a microphone has to be used. In that manner, the student can use either the smartwatch's built-in microphone or use a microphone from a headset.

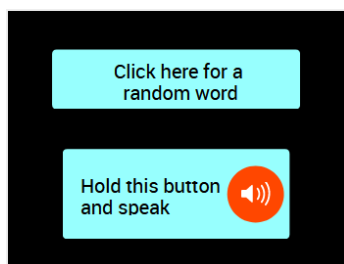


**Fig. 6 The smartwatch app, “Practice saying the word” module.**

#### **4. The back-end part**

For the purpose of this model, a fully functional network has been built. A simplified illustration of the network infrastructure that enables the communication between the students' mobile devices and the teacher's application is shown in Figure 7.

Even though only two databases have been introduced, the complexity of this model demands the use of other databases as well. To be more precise, one such database is used for storing the students' data (name, surname, year of study, etc.). Another database has to be used to store the teachers' data. Different databases for teachers and students are used because the entries in the teachers' database have rights to modify the content in other databases, while the entries in the students' database have limited, even read-only access to some databases, as was previously discussed.

As one might expect, all of the databases have to be stored somewhere on a server. We find that Amazon's cloud computing services, also known as Amazon Web Services (AWS) are ideal for such use. Indeed, AWS offers a variety of database storage plans. A few services, which are used in this English language acquisition model, will be briefly explained in the next few sentences.

For example, the Amazon EC2 service enables us to create and manage our own server on an operating system of our choice. Additionally, using the Amazon VPC service all data, which is stored in the databases, is kept secure and only available to those involved (students and teachers). Of course, privacy is important to both students and teachers.

The notification system used to notify students of newly added words that may be unknown to them is part of AWS as well. For this purpose, we use the Amazon SNS, a notification system which can be integrated with apps written in various programming languages, running on any platform (web, mobile, Android, iOS). This is particularly useful for the successful implementation of the model as it consists of applications that will run on smartphones and wearables which run on multiple operating systems.

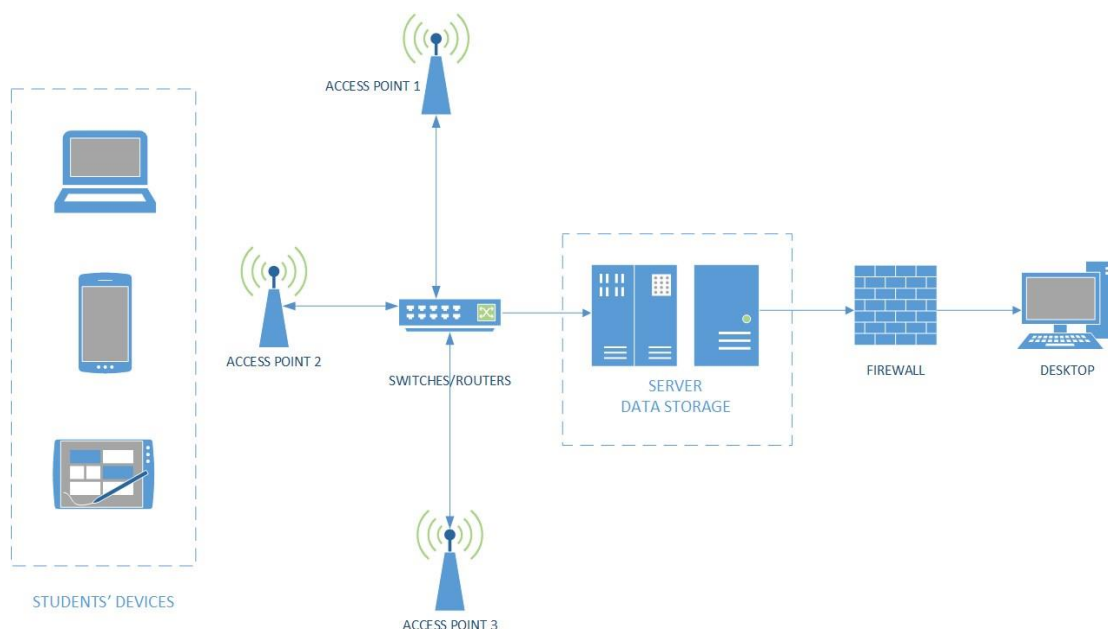


**Fig. 7 The network infrastructure**

As was previously stated, one feature of the application is grouping words by different categories. That is achieved by using Amazon's Data Analytics in the Cloud service. Moreover, among the vast range of tools offered by AWS, there are some that adequately meet the data gathering demands of the desktop application used by the teachers. To be more precise, data regarding the daily time spent in using the application by individual students as well as their current performance, progress of task completion etc.

Furthermore, different AWS networking products are used for the network infrastructure as well, making the network shown in Figure 7 only a small portion of the network used from Amazon's service – Network as a Service (NaaS).

Having all the data stored on the cloud will enable students to exploit this model's resources anywhere and anytime. Using their smartphones and smartwatches, through an already familiar user interface, students can learn new vocabulary and practice their pronunciation (or revise) at their own pace. This was actually one of the starting objectives of this model.

In our opinion, students should be exposed to the English Language vocabulary outside of the faculty if good results are expected in the process of language learning and acquisition.

## Conclusions

This model can be further modified and molded to serve as a teaching aid not only at the universities, but also in high schools and elementary schools, especially vocational secondary schools where knowledge of English Language terms and vocabulary is much needed.

As in the findings of other studies, the students' satisfaction of using mobile technology while learning was, as expected, at higher levels. The presented model is tested from a technical point of view in a university environment and gives satisfactory technical characteristics to all of the modules which creates secure perspectives for using in schools and universities from teachers and students. At the same time, it's also a good blended learning tool.

## References

- [1]. Agca, R. K., & Özdemir, S. (2013). Foreign language vocabulary learning with mobile technologies, *Procedia - Social and Behavioral Sciences*. 83 ( 2013 ) 781 – 785.
- [2]. Morales, R., & Igler, B. & Böhm, S. & Chitchaipoka, P. (2015). Context-Aware Mobile Language Learning. *Procedia Computer Science*. 56 ( 2015 ) 82 – 87.
- [3]. Godwin-Jones, R. (2011). Emerging Technologies: Mobile Apps for Language Learning. *Language Learning & Technology*, June 2011, Volume 15, Number 2, pp. 2–11.
- [4]. Kim, H., & Kwon, Y. (2012). Exploring smartphone applications for effective mobile-assisted language learning. *Multimedia-Assisted Language Learning*, 15(1), 31-57.
- [5]. Sharma, P., & Barrett, B. (2007). *Blended learning: Using technology in and beyond the language classroom*. Macmillan education.
- [6]. Muhammed, A. A. (2014). The impact of mobiles on language learning on the part of English foreign language (EFL) university students. *Procedia-Social and Behavioral Sciences*, 136, 104-108.
- [7]. Lee, J., Lee, C. H., Kim, D. W., & Kang, B. Y. (2016). Smartphone-assisted pronunciation learning technique for ambient intelligence. *IEEE Access*, 5, 312-325.
- [8]. Shih, R. C., Lee, C., & Cheng, T. F. (2015). Effects of English spelling learning experience through a mobile LINE APP for college students. *Procedia-Social and Behavioral Sciences*, 174, 2634-2638.



## OPEN SOURCE LEARNING PLATFORM – MOODLE

**Muamer Ozegovic<sup>1</sup> Jugoslav Ackoski<sup>2</sup>, Boban Temelkovski<sup>3</sup>**

<sup>1</sup> Military Academy “General Mihailo Apostolski”, email: [kadet.ozegovic.muamer@gmail.com](mailto:kadet.ozegovic.muamer@gmail.com)

<sup>2</sup> Military Academy “General Mihailo Apostolski”, email: [jugoslav.ackoski@ugd.edu.mk](mailto:jugoslav.ackoski@ugd.edu.mk)

<sup>3</sup> Military Academy “General Mihailo Apostolski”, email: [boban.temelkovski@ugd.edu.mk](mailto:boban.temelkovski@ugd.edu.mk)

### Abstract

*LMS Moodle platform has begun to be used during a military exercise for cadets, organized by the Military Academy “General Mihailo Apostolski” – Skopje in the Republic of North Macedonia. It was available to all cadets who participated in that exercise. Later, the platform has been started to be used in the academic part of teaching. Exploiting the platform, the analyses has been conducted in terms -of the results of cadets who have used it versus those who have not. Also, the platform is suitable for online learning, and it is completely safe for use within the university. The recent use of this platform pro-vides insight into the fact that in the future it will be increasingly used both in the field and in academic conditions due to its enormous benefits.*

### Key words

*analysis, online learning, LMS, Moodle, military exercise, academic, increasingly.*

### Introduction

Today in the world we can see the improvement of technology in every aspect of life. Education is one of that aspects. The using of e – learning in last few years is in increase.

Namely, the term "e-learning" was first used at a seminar on CBT systems in 1999, while at the beginning of the 21st century businesses adopted this type of learning as a central way of training and training workers [1]. When begun a COVID – 19 pandemic, we saw advantages of e – learning.

Currently, it is estimated that the online education industry is worth approximately 38 billion Euros. In the United States, 3.5 million students are enrolled in online degree courses [2]. Many students around the globe are learning on this way since pandemic start, and without e – learning they would be far behind with education. The goal of this paper is to review the most valuable option for online learning, the Moodle’s online learning platform, highlight its features and show how they influence in learners learning performance and make online learning environment a valuable asset in distributing knowledge. Moodle’s e-learning platform through its features gives students' greater access to education in comparison to traditional methods of teaching, as students can undertake their study from anywhere and at any time as well as being given the option to study part-time or full-time. Moodle platform in this moment is one of the most useful software in learning, on this platform student have many options like blogs, chats, database activities, glossaries. And due to the mentioned reasons, choosing a proper online learning platform is one of the keys to successful education, therefore, it is very important for educators to familiarize themselves with the features and options those platforms can offer.



1. Moodle

Moodle is a free software, a learning management system providing a platform for e-learning and it helps the various educators considerably in conceptualizing the various courses, course structures and curriculum thus facilitating interaction with online students. Moodle was devised by Martin Dougiamas and since its inception, its primary agenda has been to contribute suitably to the system of e-learning and facilitate online education and attainment of online degrees. Moodle actually stands for Modular Object-Oriented Dynamic Learning Environment and statistics reveal that about 14 million consumers are engaged in about 1.4 million courses propagated by this learning management system [3].

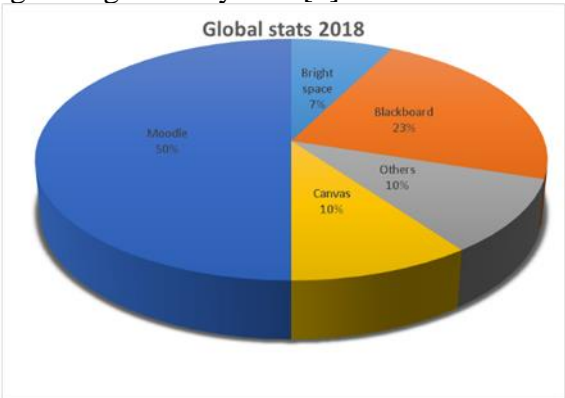


Figure 1 The figure shows usage of Moodle’s platform.

2.Advanced Distributed Learning – Military Academy “General Mihailo Apostolski”

The section title LMS Moodle platform at the Military Academy “General Mihailo Apostolski” as we early said, began to be used during the military exercise for hooking some material about military doctrine. On this exercise LMS Moodle platform was very useful for cadets and commanders. So they started to use this platform in academic part of learning and upload materials of some subjects. Since then LMS Moodle has proven to be successful in learning process. Especially when pandemic started, cadets from home could not reach the library at the Academy and all materials was on Moodle platform. Current learning on Military Academy cannot be imagined without Moodle platform. When they at the Academy, cadets could reach the platform from modem which is connected with internal protected military network, and from that internet to web server and to Moodle database server as is show on figure 2. should be relevant for the text content

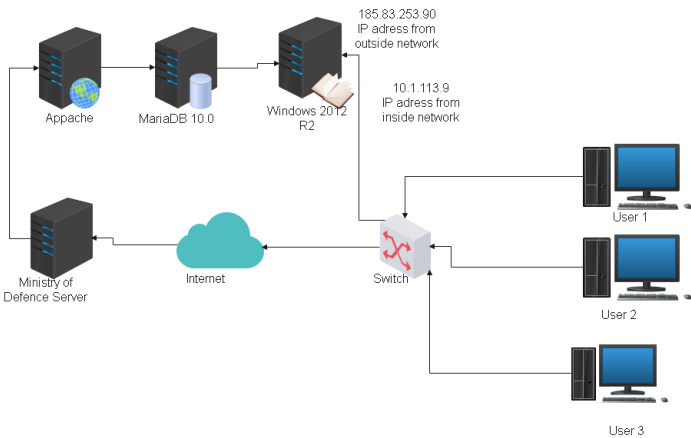
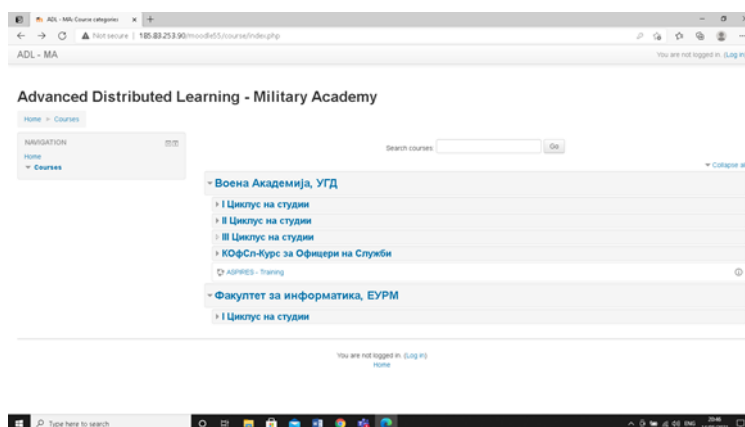


Figure 2 Moodle access scheme.

At this moment LMS Moodle platform is used by two universities, University „Goce Delcev“ - Shtip, Military Academy “ General Mihailo Apostolski” is part of this university and second is European University – Skopje. Faculty of Informatics, which is part of this university, use LMS Moodle platform. Current courses on LMS Moodle platform is one part of Military Academy program and part is from Faculty of Informatics. Military Academy has two study cycles and for officers in the service. While Faculty of Informatics has one study cycle for all four years of studying.



**Figure 3** LMS Moodle platform.

### **3.Installation and configuration of the LMS Moodle platform**

The LMS Moodle platform can be installed on several OS, such as Linux, Windows, Solaris and Mac. On Military Academy we installed LMS Moodle on Windows OS. Installation LMS Moodle on Windows is easy and practice. Before getting started with Moodle LMS installation, it is necessary to know which hardware is going to best support to users and data. Managed Moodle Cloud Hosting is the recommended option as it will support any amount of users and will ensure Moodle site doesn't crash if user exceed his capacity. When user knows his capacity, it is time to install database server. The three databases recommended by Moodle are MySQL, MariaDB, or PostgreSQL. Except database server, it is necessary to install web server. Apache 2 is the recommended web server to use with Moodle because it has been tested and verified. IIS 7/8 has also been used in the past but has not been tested for the same reliability as Apache 2. Also very important thing to do is install PHP. When installing a PHP on operating system, best practices need to be followed. Next thing is download and copy the Moodle files from download.moodle.org. There are a number of different places that user can obtain Moodle's open source code from. It is possible that user download the standard version from Moodle as his site will be better supported for security and bug fixes from a trusted Moodle Partner. Once downloaded, a directory called "Moodle" will appear which contains a number of files and folders. Moodle data directory and secure database should be created immediately after. It is necessary to create data directory to store all of Moodle files (this includes uploads, cache, session data, even temporary data). Once a Moodle data directory was created, it is important to take appropriate measures to secure this data. To begin, it is recommended to ensure that directory is NOT accessible directly via the web. If user is hosting Moodle internally, it is vitally to be create an empty database for the installation. If user is outsourcing hosting, he need to find a web-based administration page for databases as part of the control pane. It is recommended that user outsource his hosting to a specialized Moodle hosting vendor. After all of this it is time to begin installation. It is important to Run the installer to create Moodle database tables so user can configure his new site. It is also recommended to do

setup backups. There are countless errors that may cause Moodle site to crash resulting in the loss of courses, student data, and history. Ensuring that a proper backup and disaster recovery system is in place will be the difference between business failure or business continuity. It is important that Moodle courses are backed up in addition to Moodle data, Moodle directories and users Moodle site configuration. Backups should be performed hourly and stored in multiple geographic locations in the case of a natural disaster. With Managed Moodle Cloud Hosting, this is all taken care off. And last but not least thing is checking server security and performance. There are many factors to consider to ensure that Moodle operates with optimal performance and compliance with regulatory safety standards. A poorly executed Moodle site results in slow page loads, lagging videos, system crashes, and security / vulnerability threats. To accurately check server security and performance, the user will want to collect reference data from performance monitoring sites. It can then measure exactly how well its Moodle page is working. Examples of performance metrics for comparison are: scalability, server clusters, hardware configuration, operating system speed, web server performance, PHP performance, and database performance [4].

Also we can configure Moodle platform for some additional options. One of them is advanced features which is site that really extend the functionality of Moodle, but are not considered plugin based. These advanced features can be enabled or disabled as needed. There are quite a few features that the user has to choose from: Outcomes - These are goals that set up in a course and attach to learning activities, to help evaluate a learner's competence in a subject. Web Services - When enabled, these can be used to connect Moodle with other applications. Completion Tracking - It is possible to follow the criteria for courses, and the activities within those courses. Conditional Access - Here user can restrict the access users have to the learning resources and activities within a course, based on their different qualifications such as grades, completion status (of other activities), profile fields, and groups they belong to. Second additional option is users. User accounts are the profiles created for the learners in the Moodle site, that require the person to login to his or her account using a username and password. There are quite a few different ways to create users. Once the accounts are created, users can then begin enrolling in courses. Registration, Authentication, And Enrollment for the sake of simplicity, it will break registration into 3 main categories: User-based, Manager- or Administrator-based, and Automated. This can use a combination of multiple authentication methods. And the fourth and last additional option is course enrolment. Enrollment is the method of adding users to a course so that they can participate and engage within the course. Moodle is modular in nature, so it offers many different ways to enroll a user in a course: Self-enrollment is the method that allows users to manually enroll themselves in a course. This is a great option if teacher want learners to be able to choose which courses they would like to take, or if the courses are optional; Manual enrolment is done by an administrator, manager, or instructor. This method works well when there are a small number of users A Cohort Sync allows a manager or administrator to add users into a group called a "Cohort." They can then enroll an entire cohort into a course, thus adding multiple, grouped users; There is a PayPal method of enrollment, that allows users to browse courses, enroll in a selected course, and pay for it through PayPal. This is the method to use when access to content is being sold, and when students are picking their own courses. It is also well suited for client training, and/or partner training where the list of users is unknown [5].

#### **4. BigBlueButton in Advanced Distributed Learning – Military Academy**

The Moodle platform on Military Academy provides professors opportunity to create online courses with access that only registered students have.

Moodle facilitates the exchange of information to educational communities, develops a student-centered approach, and ultimately strengthens social interaction. The flexibility of the

Moodle platform allows students to access uploaded materials at any time and from anywhere. It also allows for a range of interactions between teachers and students. Students have ample time to thoroughly discuss and exchange ideas. This platform allows teachers and students living in different geographical areas to exchange information through synchronous and asynchronous communication. Professors who use Moodle will have complete control over their students' records. Activities are checked online. Professors can see what students have been doing during a given time frame [6].

BigBlueButton is an open source web conferencing system for online learning. The goal of the project is to enable instructors to effectively engage remote students. The project supports live online classes, virtual office hours, and group collaboration with remote students.

BigBlueButton supports real-time sharing of slides (including whiteboard), audio, video, chat, emojis, breakout rooms, and screen. It also records all content for later playback. Like Moodle, BigBlueButton is open source. The BigBlueButton project was started in 2008 by Blindside Networks. In addition to our work on BigBlueButton core, we created this BigBlueButtonBN Moodle plugin so you can fully leverage BigBlueButton's capabilities from within your Moodle site.

For example, for this pandemic situation it is better to use BBB than Microsoft Teams, because Teams record every conversation and store it in Microsoft database, to which we do not have access. And with using of BBB we have complete control over our conversation. The BigBlueButtonBN plugin enables you to: Create multiple activity links to online sessions within any course, Restrict students from joining a session until a teacher (moderator) joins the session, Launch BigBlueButton in a separate window, Create a custom welcome message that appears at the top of the chat window when joining the session, Specify join open/close dates for the session that appears in the Moodle's calendar, Record a session, Access and manage recordings [7].

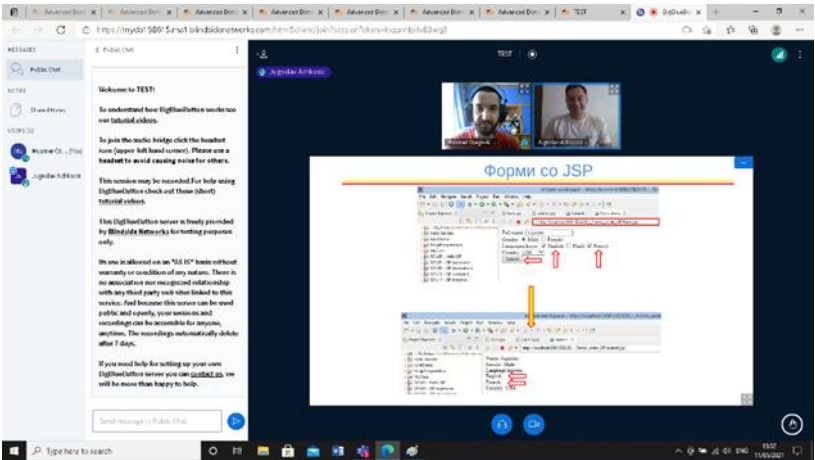


Figure 4 An example of learning through BBB.

5. Testing implemented system

In this first graph we can see an example of data that professor can see about a student. This is data from military exercise in 2019 (we said earlier that LMS Moodle platform began to use in military exercise). The graph shows the student who joined to Moodle platform on June 10th to look three different materials. First material which student opened was training plan on June 10th at 9:29 p.m. Second material was instructions for shooting with infantry weapons also on June 10th at 9:30 p.m.

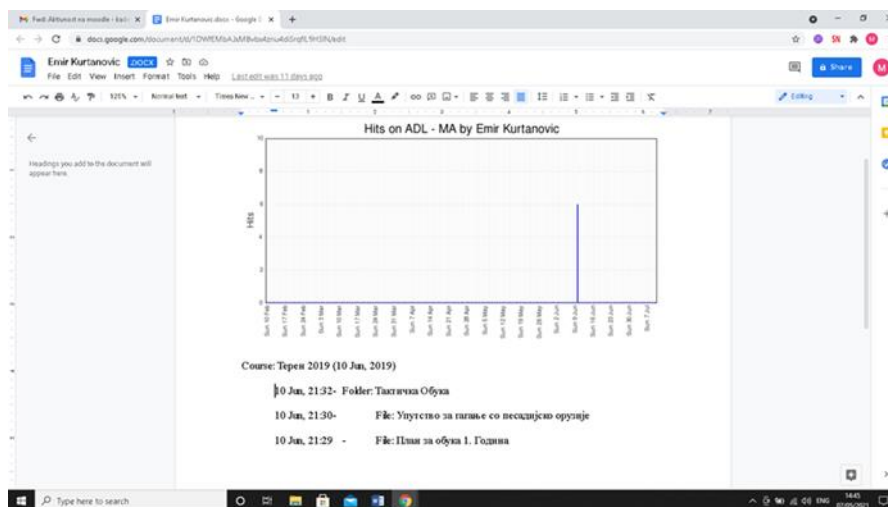


Figure 5 Graph number 1.

The second graph shows a different student, these data are also from the 2019 military exercise. This student first joined the LMS Moodle platform in March, when the materials were uploaded. He joined for the second time in April, and the third time on June 10 when the exercise began. First material which second student opened was on March 2019 but we don't have information for the materials in that period. He opened instructions for shooting with infantry weapons on June 10<sup>th</sup> at 02:24 a.m. Also he opened second year training plan and tactical training at 02:27 a.m.

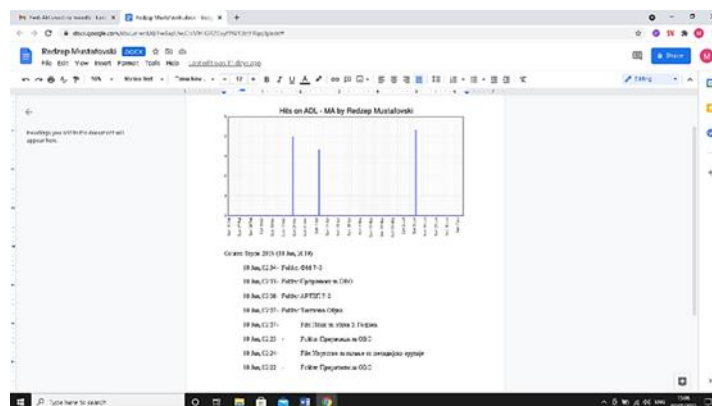


Figure 6 Graph number 2.

## Conclusions

The LMS Moodle platform, as we have seen, has a number of advantages and this platform is an educational future. Some advantages are collaborative tools and activities, easy to install, easy to use interface, users can have a large number of materials, learning in a state when it is impossible in college, etc. Many students and professors did not recognize Moodle as a useful learning platform, but when the pandemic began, professors uploaded many books, materials, and quizzes for students at home to Moodle. It was the LMS Moodle platform at the Military Academy that helped many students study. In the future, LMS Moodle will be used even more, because technology is evolving every day, also our need for technology will be greater and it is logical that we want to develop our education system. This pandemic shows us that online learning is as feasible and well-done as convection learning. As Moodle has spread and the community has grown, more input is being drawn from a wider variety of people in different teaching situations. Moodle development is increasingly influenced by its community of developers and users. Moodle is an active work in progress and constantly

evolving to a better state, and due to its open source nature it allows its huge community to contribute and change the platform towards a better state. All in all, combining all of the above, similar features are hard to find for no charge and that is what makes Moodle the perfect advanced distributed learning platform intended for every use.

## References

- [1] Gogos, Roberta: “A brief history of e-learning”. EFront blog: 2013.
- [2] Lungu, Monica: “What is MOODLE? What are Online Learning Managements Systems?”. Studyportals: 2021.
- [3] Lungu, Monica: “What is MOODLE? What are Online Learning Managements Systems?”. Studyportals: 2021.
- [4] Young, Ben: “How To Install Moodle (Windows And Mac)”. eLearning Industry: 2018.
- [5] Young, Ben: “Moodle Site Configuration, Part 1: Features, Users, And Course Enrollment”. eLearning Industry: 2018.
- [6] Tchello, Kasse / Triastuti, Anita: “The implementation of the Moodle platform to help teachers develop blended learning in the field of Teaching English as a Foreign Language (TEFL)”. In: English Linguistics, Literature, and Language Teaching in a Changing Era: Proceedings of the 1st International Conference on English Linguistics, Literature, and Language Teaching (ICE3LT 2018). Yogyakarta, Indonesia 2019 (p. 300). Routledge.
- [7] Dixon, Fred / Federico, Jesus. “BigBlueButtonBN”. Moodle.





## СПОРЕДБЕНА ТЕХНО-ЕКОНОМСКА АНАЛИЗА ПОМЕЃУ ТЕРМИЧКИ ИЗОЛИРАН И ТЕРМИЧКИ НЕИЗОЛИРАН СТАНБЕН ОБЈЕКТ

*Тамара Димова<sup>1</sup>, Марија Чекеровска<sup>2</sup>, Тодор Чекеровски<sup>3</sup>*

<sup>1</sup> Дипл. маш. инж., Машински факултет Универзитет „Гоце Делчев“ - Штип, Северна Македонија:  
tamara.19498@student.ugd.edu.mk

<sup>2</sup> Машински факултет Универзитет „Гоце Делчев“ Штип, Северна Македонија:  
marija.cekerovska@ugd.edu.mk

<sup>3</sup> Електротехнички факултет Универзитет „Гоце Делчев“ Штип, Северна Македонија:  
todor.cekerovski@ugd.edu.mk

### Апстракт

Во овој труд се прикажани пресметки на потребна енергија за греење на изолиран и неизолиран станбен објект за една грејна сезона. Се работи за веќе постоечки станбен објект за еден спрат од куќа. Станбениот објект сè уште не е надворешно изолиран, но има избран вид на изолација, предложен од страна на градежен изведувач. Системот за греење кој треба да се инсталира е етажно топловодно греење и вклучува: печка на пелети, цевен развод и панелни радијатори како оддавачи на топлината. Најпрво се пресметани коефициентите на премин на топлина на преградите, потоа загубите на топлина и потребната енергија за греење. Направена е пресметка на трошоци во однос на есенската цена на пелетите, и споредба на трошоците за изолиран и неизолиран објект. Пресметан е и периодот на исплатливост, односно периодот по кој ќе се врати инвестицијата за надворешна топлотна изолација. Цел на овој труд е да се укаже на придобивките од топлотната изолација.

### Клучни зборови

*греење, термоизолација, инвестиција;*

### Вовед

Денес човекот живее во организирани т.н. урбани средини. При тоа постои стремеж да се овозможи висок комфор т.е. чувство на удобност, кое не може да се реализира ако не се користат соодветни материјални добра и потрошувачка на енергија. Еден од условите за чувство на удобност кај човекот е температура на воздухот во просторот во кој живее и работи. Бидејќи температурата на надворешниот простор се менува како во текот на денот, така и во текот на годината се појавува потреба за зголемување или за намалување на температурата на воздухот во кој човекот престојува.

Заштита од големите промени на температурата на надворешниот воздух првобитниот човек наоѓал во пештерите, во кои промената на температурата во текот на годината е занемарлива. Големо подобрување на условите за живеење човекот

постигнал со откривање на огнот. Најпрво палеле оган во пештерите, а потоа и на отворен простор, кои со време еволуирале во примитивни покриени живеалишта. Кај овие живеалишта подоцна бил решен и проблемот за извлекување на чадот од просторот за живеење, најпрво низ разни отвори, а потоа низ специјално вградени оџаци.

Со понатамошниот напредок, во поглед на загревање на воздухот во просторот за живеење е пронаоѓањето на печката, како уред за загревање. Во почетокот печката е користена за загревање на една, а подоцна и на повеќе простории. Следен напредок во поглед на загревање на воздухот во просторот за живеење е примената на етажно или централно греење на еден кат. По него доаѓа примената на централното греење за една зграда поединечно, за повеќе згради заедно, за цели градски подрачја и за цел град.

Денес сè поактуелна е енергетската ефикасност во процесот на греење, односно подобрувањето на истата. Тоа подобрување се постигнува со користење на обновливи извори на енергија, на енергетско ефикасни уреди и со користење на топлотна изолација на објектите со користење на соодветни термоизолациони материјали. При разгледување на карактеристиките и параметрите за енергетска ефикасност кај згради и објекти, од првостепена важност се вредностите за термичките карактеристики и параметри на материјалите[1].

Со македонскиот стандард детално се утврдуваат сите методи за пресметка на топлински отпори и коефициенти на премин на топлина за градежни компоненти и градежни елементи, со разгледување на отворите (врати, прозорци и други стаклени елементи), делови од згради во непосредна близина на земја и елементи за вентилација[2].

Цените на грејните средства, особено фосилните горива како што се јагленот, нафтата и гасот, нагло растат на светскиот пазар. Ова зголемување на цените доведува до зголемена употреба на изолациски материјали со цел намалување на потрошувачката на вакви фосилни горива како извори на енергија. Во истражувањето и со помош на пресметката е докажано дека дебелината на изолацијата силно влијае на термичката преносливост на конструкцијата и специфичната годишна потрошувачка на топлина на зградата. Загубите на топлина се под силно влијание на линеарните термички мостови, кои најчесто се случуваат на балконите, аглите и столбовите и топлинските мостови [3].

Намалувањето на потрошувачката на топлинска енергија се постигнува со примена на соодветни технички решенија. Со цел да се намалат загубите на топлина во индустријата, се применува топлинска изолација на опремата и инсталациите. При дизајнирање, изборот на соодветен изолациски материјал и дебелина на изолацијата е од посебно значење. Покрај основната задача за намалување на загубата на топлина со изолација, се постигнуваат и други ефекти, како што се: звучна изолација, заштита од пожар и заштита на погонските работници од изгореници, и сл. [4].

Во овој труд направена е техно-економска споредба на потребната енергија и трошоци за загревање на изолиран и неизолиран објект кој се состои од веќе постоечки спрат од кука.

Топлотна изолација

Топлотната изолација се користи со цел да се зголеми енергетската ефикасност на објектот односно да се намали потребната енергија за греење и ладење на објектот. Со намалување на потребната енергија за греење или ладење се намалуваат и трошоците. Топлотната изолација се монтира на површините на објектот кој се изолира, и тоа:

- топлотна изолација на подот,
- топлотна изолација на кровот, и
- топлотна изолација на надворешните сидови.

Пресметка на потребна топлина за проектни услови

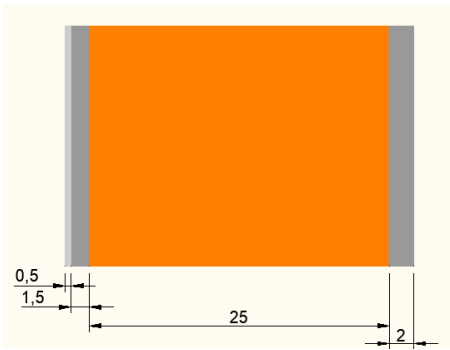
Во понатамошниот текст се прикажани табелите со коефициенти на топлинопредавање за соодветните прегради како и градежни отвори кои се потребни во понатамошните пресметки, како и приказ на соодветните сидови со соодветните слоеви од сидовите без и со топлотна изолација.

Табела 1. Коефициенти на топлинопредавање

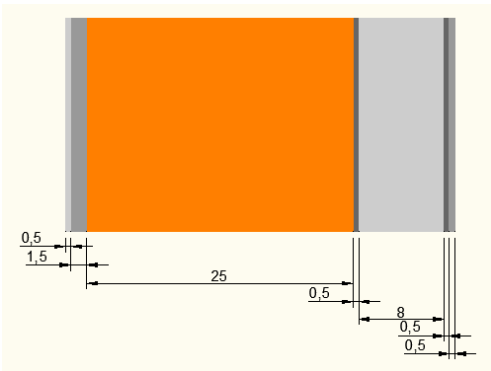
Услови	Коефициенти на топлинопредавање (W/m²K)
<b>Внатрешна страна</b>	<b><math>\alpha_v</math></b>
Вертикални прегради, сидови, прозорци, врати	8,0
За тавани и подови при пренесување на топлината од долу нагоре	8,0
За тавани и подови при пренесување на топлината од горе надолу	6,0
<b>Надворешна страна</b>	<b><math>\alpha_n</math></b>
Вертикални прегради, сидови, прозорци, врати	23,0

Пресметка на коефициентот на премин на топлината на надворешните сидови без топлотна изолација се врши според следната формула:

$$k = \frac{1}{R} = \frac{1}{\frac{1}{\alpha_v} + \sum \frac{d}{\lambda_i} + \frac{1}{\alpha_n}} = \frac{1}{\frac{1}{8} + 0,528 + \frac{1}{23}} = \frac{1}{0,696} = 1,436 \rightarrow \text{се зема } 1,45[W/m^2K] \text{ (1)}$$



Слика 1. Пресек на надворешен сид без надворешна топлотна изолација



Слика 2. Пресек на надворешен сид со надворешна топлотна изолација

На Сл. 1 даден е пресек на надворешен сид со слоевите со соодветните дебелини без изолација, додека на Сл. 2 даден е пресек на ист таков сид но со топлотна изолација. Во

Табела 2 дадени се поединечните слоеви со соодветната дебелини и коефициентите на топлинотспроведување.

Табела 2. Коефициент на премин на топлина низ надворешен сид без топлотна изолација

Надворешен сид без топлотна изолација				
Материјал	Дебелина (d)	Коеф. (λ <sub>i</sub> )	d/λ	Коеф. (k)
	cm	W/mK	m <sup>2</sup> K/W	W/m <sup>2</sup> K
Надворешен малтер	2	0,87	0,023	
Керамички блок	25	0,52	0,481	
Продолжен малтер	1,5	0,87	0,017	
Глет маса	0,5	0,7	0,007	
Вкупно:	29		0,528	1,45

Пресметка на коефициентот на премин на топлината низ преградите се пресметуваат според равенката (2):

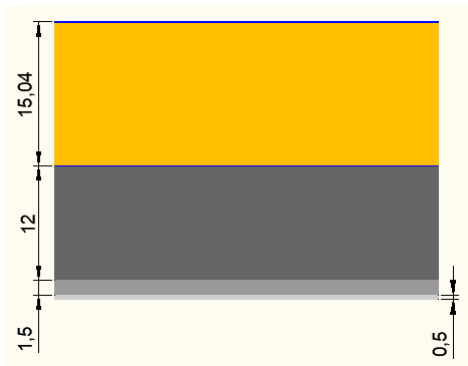
$$k = \frac{1}{R} = \frac{1}{\frac{1}{\alpha_v} + \sum \frac{d}{\lambda_i} + \frac{1}{\alpha_n}}$$

(2)

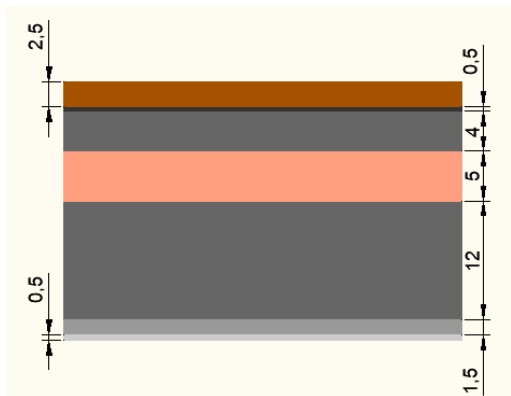
Табела 3. Коефициент на премин на топлина на надворешен сид со надворешна топлотна изолација

Надворешен сид со надворешна топлотна изолација				
Материјал	Дебелина (d)	Коеф. (λ <sub>i</sub> )	d/λ	Коеф. (k)
	cm	W/mK	m <sup>2</sup> K/W	W/m <sup>2</sup> K
Надворешен малтер	0,5	0,87	0,006	
Полимерно цементно лепило со мрежа	0,5	0,40	0,013	
Стиропор	8	0,04	2	
Лепило за стиропор	0,5	0,40	0,013	
Керамички блок	25	0,52	0,481	
Продолжен малтер	1,5	0,87	0,017	
Глет маса	0,5	0,7	0,007	
Вкупно:	36,5		2,537	0,38

На Сл. 3 даден е пресек на таванската плоча, додека на Сл. 4 даден е пресек на под. Во Табелите 4 и 5 дадени се поединечните слоеви со соодветната дебелини и коефициентите на топлинотспроведување.



Слика 3. Пресек на таванската плоча



Слика 4. Пресек на под

Табела 4. Коефициент на премин на топлина на таванска плоча


Таванска плоча				
Материјал	Дебелина (d)	Коеф.( $\lambda_i$ )	d/ $\lambda$	Коеф. (k)
	cm	W/mK	m <sup>2</sup> K/W	W/m <sup>2</sup> K
Парна брана	0,02	0,17	0,001	
Тервол	15	0,038	3,947	
Парна брана	0,02	0,17	0,001	
АБ плоча	12	2,3	0,052	
Продолжен малтер	1,5	0,87	0,017	
Глет маса	0,5	0,70	0,007	
Вкупно:	29,04		4,025	0,25

Табела 5. Коефициент на премин на топлина на под

Под				
Материјал	Дебелина (d)	Коеф.( $\lambda_i$ )	d/ $\lambda$	Коеф. (k)
	cm	W/mK	m <sup>2</sup> K/W	W/m <sup>2</sup> K
Паркет	2,5	0,21	0,119	
Лепак	0,5	0,93	0,005	
Цементна кошулица	4	1,6	0,025	
Стиродур	5	0,035	1,429	
АБ плоча	12	2,3	0,052	
Малтер	1,5	0,87	0,017	
Глет маса	0,5	0,7	0,007	
Вкупно:	26		1,654	0,57

Коефициентот на премин на топлината низ прозорец, односно врата со ПВЦ рамки се добиваат директно од нивниот производител.

Табела 6. Коефициент на премин на топлина на прозорци и балконски врати

Прозорци и прозорец-врати со ПВЦ рамки, со тројно застаклување, со исполна со воздух или благороден гас, со или без ниско-емисивен премаз	Коеф. (k)	
	W/m <sup>2</sup> K	
	1,7	

Пресметка на потребната топлина на греење на секоја просторија одделно

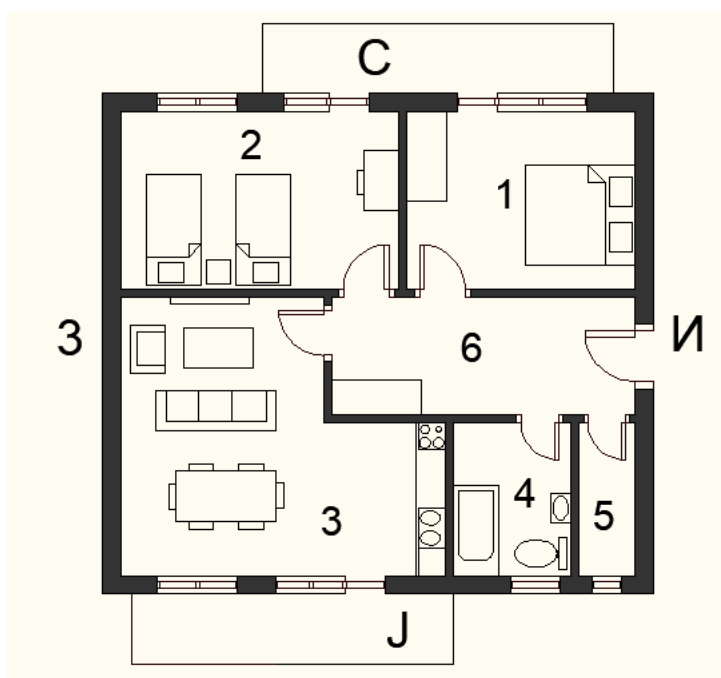
Вкупната топлина за греење т.е. потребната топлина за проектни услови на една просторија е поголема од загубите поради пренесување на топлината низ преградните површини  $Q_0$  за големината на додатоците на топлина и се определува според релацијата (3). За подот и таванот се земаат чистата внатрешна должина и ширина, за вратите и прозорците се земаат димензиите на отворите во сидовите [5].

За сидовите се зема чистата внатрешната ширина, а за висина се зема катната димензија т.е. висинска разлика помеѓу подот на едниот во однос на подот на станот над

него. На вака пресметаните топлински загуби се додаваат додатоците на загуба на топлина изразени во проценти [%]. На тој начин се добива вкупната потребна топлина за греење на еден стан. Шематски приказ на катот од куќата е даден на Слика 5.

$$Q_p = Q_0 \cdot Z [W]$$

$$Q_p = Q_0 \cdot (1 + Z_D + Z_s + Z_v)[W] \quad (3)$$



Слика 5. Спрат од куќа за кој се вршат пресметките

### Пресметка на потребна топлинска енергија за затоплување и сезонски трошоци

Во овој дел се пресметува потребната топлинска енергија во текот на една грејна сезона и трошоците за гориво, во нашата анализа тоа е дрвен пелет. Откако ќе се пресметаат трошоците за неизолиран и изолиран станбен објект, ќе направиме споредба на истите.

Најпрво се пресметува средногодишниот искористлив капацитет  $Q$ :

$$Q = Q_p \cdot (t_{vp} - t_{sr}) / (t_{vp} - t_{np}) [kW] \quad (4)$$

$Q_p [W]$  – потребна топлина за проектни услови;

$t_{vp} [^{\circ}C]$  - внатрешна проектна температура;

$t_{np} [^{\circ}C]$  - надворешна проектна температура;

$t_{sr} [^{\circ}C]$  - средна надворешна температура во текот на грејната сезона.

За градот Штип, средната надворешна температура во текот на грејната сезона изнесува:  $t_{sr} = 4,3 [^{\circ}C]$

Потоа се пресметува потребната енергија на греење  $E$ :

$$E = Q \cdot \tau [KWh/sez] \quad (5)$$



$Q[kW]$ - средногодишниот искористлив капацитет;

$\tau[h/sez]$ – времетраење на грејната сезона;

Времетраењето на грејната сезона се мери во часови и истото може да се добие како производ на бројот на месеци во кои се користи греењето ( $Mg = 6$ ), бројот на денови во месеците ( $Nm = 30$ ) и времетраењето на греењето во еден ден изразено во часови ( $Vc = 15$ ). Времетраењето на греењето во текот на еден ден се зема да изнесува 15 часа бидејќи станбените објекти генерално се греат со прекин од 9 до 12 часа ( $24 - 9 = 15$ ). Соодветно, времетраењето на грејната сезона за овој станбен објект изнесува:

$$\tau = 6 \cdot 30 \cdot 15 = 2700[h/sez] \tag{6}$$

Потрошувачка на гориво  $B$ , се пресметува според следната релација:

$$B = \frac{E}{H_d \cdot \eta_k} [kg/sez] \tag{7}$$

$E [KWh/sez]$  - потребната енергија на греење;

$\eta_k = 0,85$  – степен на корисно дејство;

$H_d [KWh/kg]$  – калорична вредност на горивото;

За долна калорична вредност на горивото, во нашиот случај станува збор за дрвени пелети од класа A2, земаме дека  $H_d = 5,51 [KWh/kg]$ .

Следен чекор е пресметка на трошоци за гориво во текот на грејната сезона  $C$ , според дадената релација (8):

$$C = c \cdot B [\text{Денари}] \tag{8}$$

При тоа, земаме есенска цената на дрвени пелетите ‘‘Шишарка A2’’ која изнесува 200 денари за количина од 15 kg. Соодветно, цената за еден килограм од овие дрвени пелети изнесува  $c = 13,33$  денари.

**Табела 7. Пресметки на потребната топлинска енергија на греење, трошоците за гориво на сезона на станбениот објект без сидна изолација**

Пресметка на потребна топлинска енергија без изолација			
Потребна топлина [W]		Средногодишен искористлив капацитет Q[kW]	
Qp1	2.175,77	$Q = Q_p \cdot (t_{vp} - t_{sr}) / (t_{vp} - t_{np}) [kW]$	4,77
Qp2	2.492,00	Потребна енергија за греење E [kWh/сезона]	
Qp3	3.391,13	$E = Q \cdot \tau [KWh/sez]$	12.877,42
Qp4	705,42	Потрошувачка на пелети B [kg/сезона]	
Qp5	893,71	$B = \frac{E}{H_d \cdot \eta_k} [kg/sez]$	2.745,72
Qp6	940,67	Трошоци за пелети за една грејна сезона C [МКД]	
Qp	10.598,7	$C = c \cdot B [\text{Денари}]$	36.600,43

**Табела 8. Пресметки на потребната топлинска енергија на греење, трошоците за гориво на сезона на станбениот објект со сидна изолација**

Пресметка на потребна топлинска енергија со изолација	
Потребна топлина [W]	Средногодишен искористлив капацитет Q[kW]

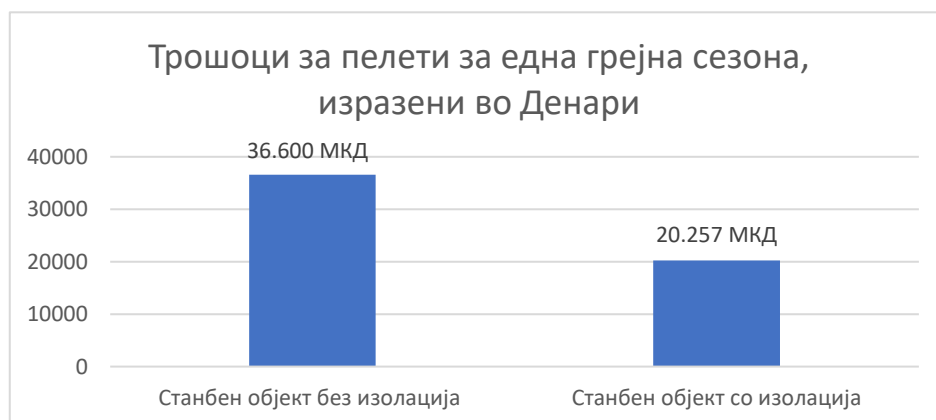
Qp1	1.172,76	$Q = Q_p \cdot (t_{vp} - t_{sr}) / (t_{vp} - t_{np}) [kW]$	2,64
Qp2	1.381,76	Потребна енергија за греење E [kWh/сезона]	
Qp3	1.896,88	$E = Q \cdot \tau [KWh/sez]$	7.127,13
Qp4	364,28	Потрошувачка на пелети B [kg/сезона]	
Qp5	322,27	$B = \frac{E}{H_d \cdot \eta_k} [kg/sez]$	1.519,64
Qp6	728	Трошоци за пелети за една грејна сезона C [МКД]	
Qp	5.865,95	$C = c \cdot B [\text{Денари}]$	20.256,85

## Инвестиција во надворешна топлотна изолација

Во изолацијата која е предложена за овој станбен објект, како термоизолационен материјал е избран стиропор со дебелина од 8 [cm]. Стиропорот е синтетички производ поволен за животната средина, кој се произведува со полимеризација на стирен и претставува цврст пенест материјал исполнет со воздух. Иако има многу мала густина, има релативно висока механичка јакост, како и многу ниска топлотна и ниска акустична спроводливост, со што се сврстува во категоријата на најдобрите термички и акустични изолатори. Термоизолациониот ефект на 1[cm] е еднаков на 15 [cm] шуплива тула.

Стиропорот исто така има многу ниска апсорпција на вода и висока отпорност на микроорганизми и водена пареа, што му даваат предност во однос на другите материјали за топлинска изолација при употреба во подрачја изолжени на влага. Не подлежи на гниење (исчезнување), долготраен е и незапалив. Овие карактеристики се должат на специфичниот состав на овој производ, кој содржи 98% заробен воздух и 2% полистирен. Голема предност е што има поедноставна монтажа и пониска цена од другите изолациони материјали. Единствен недостаток на стиропорот е неговата паро-непропустливост т.е. не дише.

Во пресметките се добива дека доколку станбениот објект е со предложената надворешна топлинска изолација, трошоците за пелети за една грејна сезона се помали за 16.343 МКД, или приближно за 45%. На дијаграмот 4.1 е дадена споредбата на трошоците за пелети за една грејна сезона кога станбениот објект е без и со надворешна топлотна изолација.



Дијаграм 1. Споредба на трошоците за пелети

## Пресметка на инвестицијата во надворешната топлотна изолација и периодот на повраќање на истата

Пресметка на надворешната сидна површина што треба да се изолира  $A_i$  е дадена со следната релација:

$$A_i = a \cdot b \cdot h = 10 \cdot 11 \cdot 2.90 = 121.80 \text{ [m}^2\text{]} \quad (9)$$

$A_i [\text{m}^2]$  - надворешна сидна површина што треба да се изолира;

$a [\text{m}]$  – надворешна должина на спратот од куќата;

$b [\text{m}]$  – надворешна ширина на спратот од куќата;

$h [\text{m}]$  – катна димензија т.е. висина на спратот од куќата

Во нашата анализа користиме само катна димензија бидејќи станува збор за изолација само на еден спрат од куќа т.е. се пресметува само надворешната сидна површина на спратот за кој се вршени пресметките. Од оваа површина не се одбива површината на прозорците, вратите и другите отвори во сидовите. При формирањето на цената за изолацијата и нејзината изведба се користи целата надворешна површина на сидовите.

Откако ја знаеме површината што треба да се изолира и цената за изолација за 1  $\text{m}^2$  површина заедно со цената за монтажа, се добиваат вкупните трошоци (инвестицијата) за надворешната топлотна изолација.

Конечно, периодот за кој ќе се врати инвестицијата за надворешна изолација претставува количник од вкупните трошоци за поставување на надворешната изолација и разликата на трошоци за огревен материјал, т.е. пелети за една грејна сезона за греење помеѓу надворешно неизолиран и надворешно изолиран станбен објект. Периодот е изразен во години, а добиените резултати се дадени во Табела 9.

**Табела 9. Инвестиција за надворешна топлотна изолација**

Инвестиција за надворешна топлотна изолација	
Надворешна сидна површина што треба да е изолирана $[\text{m}^2]$	121,8
Цена на предложена сидна изолација за 1 $\text{m}^2$ [МКД]	1.200
Вкупни трошоци за надворешна изолација [МКД]	146.160
Вкупни трошоци за пелети за една грејна сезона [МКД]	16.343
Период на враќање на инвестицијата [години]	8,9

## Заклучок

Топлотната изолацијата на станбените објекти е еден од начините да се подобри енергетската ефикасност на истите. Овој станбен објект има веќе изолиран кров и под, но нема надворешна топлотна изолација. За надворешна топлотна изолација е избран стиропор со дебелина од 8  $[\text{cm}]$ . Стиропорот е најмногу користен термо-излоационен материјал со оглед на лесната монтажа, поволната цена и добриот коефициент на премин на топлина. Најпрво е направена пресметка на коефициентите на премин на топлина на преградите (под, таван, надворешни сидови). За надворешните сидови пресметани се и коефициентот на премин на топлината со и без надворешна топлотна изолација. Потоа се пресметани топлотните загуби и потребната топлина на секоја просторија одделно, со и без надворешна топлотна изолација.

По направените пресметки за потребната енергија може да се увиди колку всушност се подобрува енергетската ефикасност на станбениот објект, кога истиот ќе се изолира. Трошоците за пелети за една грејна сезона се помали за околу 16.500 денари, а инвестицијата за надворешна топлотна изолација се враќа за околу 9 години. Освен овие трошоци, топлотната изолација ги намалува и почетните вложувања за системот за греење т.е. помала печка (котел), помалку или помали грејни тела. Како кај овој станбен објект така и кај другите објекти, доколку е возможно, најдобро е истите најпрво термички да се изолираат, а потоа да се инсталира системот за греење. Сите овие факти укажуваат на важноста на топлотната изолација и придобивките од истата.

### Користена литература

- [1] Тромбев, Ѓ.: Градежна физика, Битола, 2014
- [2] Цветковска, М.: Градежна физика, Обука за енергетски контролори, 2014
- [3] Prezelj, J.: Raziskovalna naloga: ANALIZA TOPLOTNE IZOLACIJE fasade, Celje, 20. 4. 2006
- [4] Simic, S., Orasanin G., Golubovic, D., Blagojevic, J., Milic, D.: Uticaj toplotne izolacije na smanjenje gubitaka energije u industrijskim i energetskim postrojenjima, Procesna tehnika, June, 2017
- [5] Арменски, С.: Термотехнички машини и уреди, Скопје
- [6] Атанасоски, С.: ОСНОВЕН МАШИНСКИ ПРОЕКТ – За машинска опрема и инсталација за греење и ладење на просториите во објектот, Скопје, Мај 2017.
- [7] Schramek, E. R.: Taschenbuch für Heizung + Klimatechnik
- [8] EN – 12 831 Инсталации за греење во згради;



## COMPARISON OF PERT AND MONTE CARLO SIMULATION

*Maja Kukuseva Paneva<sup>1</sup>, Goce Stefanov<sup>2</sup>, Biljana Citkuseva Dimitrovska<sup>3</sup>, Dejan Milcevski<sup>4</sup>*

<sup>1</sup>Faculty of Electrical Engineering University Goce Delcev Stip R. N. Macedonia, maja.kukuseva@ugd.edu.mk

<sup>2</sup>Faculty of Electrical Engineering University Goce Delcev Stip R.N. Macedonia, goce.stefanov@ugd.edu.mk

<sup>3</sup>Faculty of Electrical Engineering University Goce Delcev Stip R.N. Macedonia,  
biljana.citkuseva@ugd.edu.mk

<sup>4</sup>SOU Kosta Susinov, Radovis, R. N. Macedonia, dejanmilcevski@gmail.com

### Abstract

*Risk management is critical issue for successful competition of any project. In order to complete a project within predefined schedule it is crucial to estimate the probability of project completion precisely. The aim of project management when dealing with large and complex projects is to identify the critical path and one or several subcritical paths. In this paper a comparison between two most widely used project planning and scheduling techniques PERT (Program Evaluation and Review Technique) and Monte Carlo simulation is made. PERT considers the uncertainties in activity duration by considering three estimates of time, while in Monte Carlo simulations the distribution for activity duration can be uniformed, triangle, normal etc. The analysis made in this paper is based on same project using classical PERT and Monte Carlo simulation with uniform distribution of time activity. The model used in this paper is developed in C++ programming language.*

### Key words

*PERT, Monte Carlo simulation, project scheduling, activity duration.*

### Introduction

A typical modern- day project requires coordination of numerous complex activities, so the project risk and uncertainty have to be considered. Project management consists of planning, designing and implementation a set of activities that needed to be completed in order project to end successfully. The main aim in project management is identification of the critical path of the project. The critical path is defined as longest path through the project network so that the project is completed in shortest possible duration. If any activity on the critical path is delayed, the completion of the project will be delayed. The most popular technique for identification of the critical path used in project management is Project Evaluation and Review Technique (PERT). PERT is a network based technique developed by US Navy for the POLARIS Missile Program, [1]. PERT overcomes the disadvantages of Critical Path Method (CPM) so that, activity duration is a random variable calculated by three points estimation as an average heavily weighted toward the most like time.

When the project is large and complex, the project manager has to identify one critical path and several subcritical paths. The subcritical path is a set of activities that are almost critical or are at risk of becoming critical if delayed past their expected competition time. This rises the project sensitivity and the risk of delaying the project. In order to overcome the disadvantages of PERT [2-3], Monte Carlo simulations are used. Monte Carlo simulation identifies not only the critical path, but subcritical paths that may become critical.

This paper is organized as follow. In section 3 overview of PERT approach is given, while in section 4 Monte Carlo simulations are represented. The used methodology is given in Sector 5. In Sector 6 numerical illustration of a given project is represented. Sector 7 concludes this paper.

## 1. Project Evaluation and Review Technique (PERT)

In practice, it is not always possible to determine the exact duration of the activities, so the projects include variability in time required to complete the activity due to various factors such as lack of experience, equipment breakdown, late delivery, unpredictable weather conditions and etc. Therefore, PERT uses three point estimates to determine the average weighted duration of the activities: optimistic time (a), most likely time (m) and pessimistic time (b) as represented on Figure 1. All the activity times are random independent variables having beta distribution with probability density function:

$$f(x) = \frac{\Gamma(\alpha+\beta)}{\Gamma(\alpha)\Gamma(\beta)} \frac{(x-a)^{\alpha-1}(b-x)^{\beta-1}}{(b-a)^{\alpha+\beta-1}} \quad (1)$$

Where  $\alpha$  and  $\beta$  are shape parameters,  $a < x < b$  and  $\alpha, \beta > 0$ .  $\Gamma(\cdot)$  is gamma function.

The expected time (mean) to complete each activity is calculated as:

$$t_e = \frac{0+4m+b}{6} \quad (2)$$

With variance  $\sigma_x^2 = \left(\frac{b-a}{6}\right)^2$ .

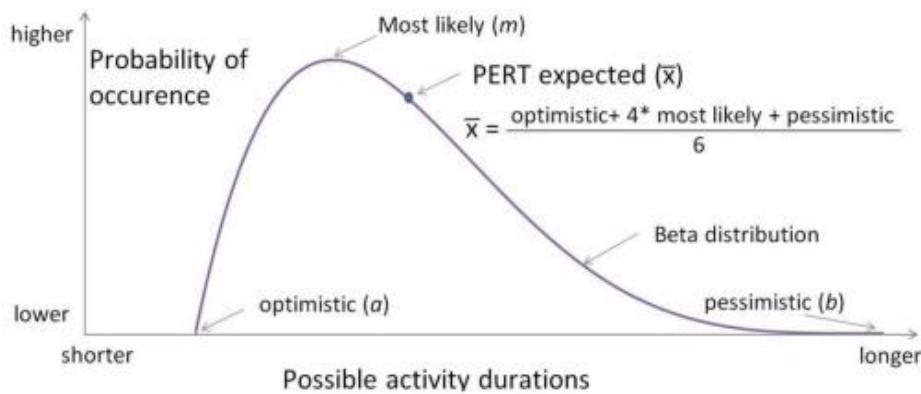


**Fig. 1. Density function of PERT- beta distribution**

According to central limit theorem if the network is large enough than the project duration follows a normal distribution with mean  $\mu$  and variance of the distribution of the project duration defined as:

$$\sigma^2 = \sum_x \sigma_x^2 \quad (3)$$

Where  $x$  represents the activities on the critical path. Knowing the expected project duration and standard deviation of the critical path, the probability of completing the project earlier or later than  $\mu$  can be calculated using normal distribution as:

$$Z = \frac{T-\mu}{\sigma} \quad (4)$$



Where T is desired completion time of the project.

## 2. Project Evaluation and Review Technique (PERT)

The term Monte Carlo was first introduced by Von Neumann and Ulam during World War II, [4], as a code for the secret development of Los Alamos atomic bomb that included behavior simulation of accidental neutron diffusion. Today, Monte Carlo method is one of the most commonly used powerful tool for analysis of complex projects. This method initially used random or pseudo random numbers with uniform distribution in the interval [0;1].

The PERT method discovers one critical path and other possible subcritical paths are ignored. If the duration of the critical path is around its most likely time completion time and if the subcritical path ends around its optimistic time, the project will be delayed. That's the main reason why techniques like Monte Carlo are used. Monte Carlo simulations are used to calculate the entire network diagram and obtain one critical path and possible subcritical paths.

In this paper, the simulations are performed with a uniform distribution (figure 2) where the most likely time to complete the activity is a random number in range between the optimistic and pessimistic time. The probability density function of a uniform distribution is defined as:

$$f(x) = \begin{cases} \frac{1}{b-a}, x \in (a,b) \\ 0, x \notin (a,b) \end{cases} \quad (5)$$

With cumulative distribution function defined as:

$$F(x) = \begin{cases} \frac{x-a}{b-a}, x \in (a,b) \\ 1, x > b \\ 0, x < a \end{cases} \quad (6)$$

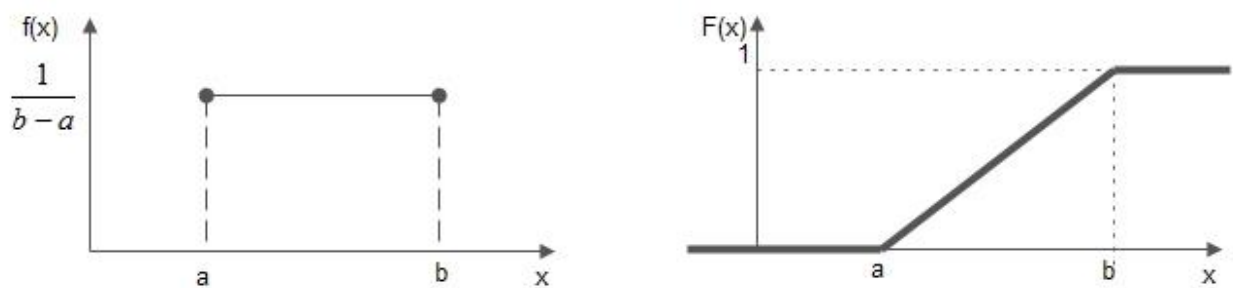
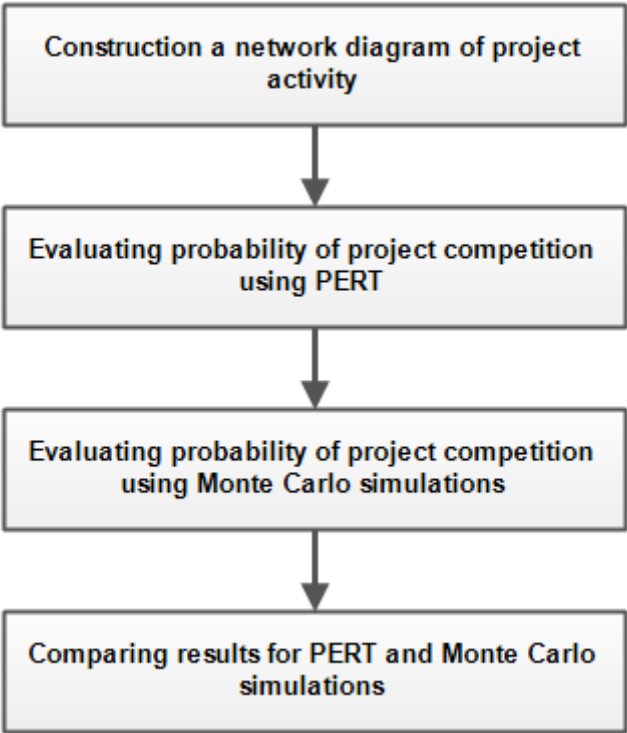


Fig 2. Probability density function and cumulative distribution function of uniform distribution

## 3. Methodology

A network diagram is formed for the given project. First, the PERT is applied to the project to evaluate the probability of project completion for a given time unit (day, months). The results obtained identifies only one critical path. After that, Monte Carlo simulations are performed on the same project in order to obtain probability of project competition. Results from these

simulations identifies same critical path and one or more subcritical path with percentage of occurrence. At the end, a comparison of PERT and Monte Carlo simulations is made.



**Fig 3. Methodology**

**4. Numerical illustration**

In this paper the project [5] given with data represented in Table I is analyzed. The starting activity of the project is denoted as activity1 and end activity is denoted as activity 7. Project due date is set to 37 time units. The network diagram of this project is given in Figure 5.

**Table 1 Time estimates for project activities**

Activity	(a,m,b)	Activity	(a,m,b)
(1-2)	(5,6,8)	(3-6)	(3,4,5)
(1-4)	(1,3,4)	(4-6)	(4,8,10)
(1-5)	(2,4,5)	(4-7)	(5,6,8)
(2-3)	(4,5,6)	(5-6)	(9,10,15)
(2-5)	(7,8,10)	(5-7)	(4,6,8)
(2-6)	(8,9,13)	(6-7)	(3,4,5)
(3-4)	(5,9,19)		

The code for PERT calculations is developed in Program Language C++. After executing the program, the differences of the output from the procedures forward and backward pass gives the floating time for every project activity. If the activity has zero floating time any delays in completing this activity will delay project completion, so thus this activity is part of the critical path.

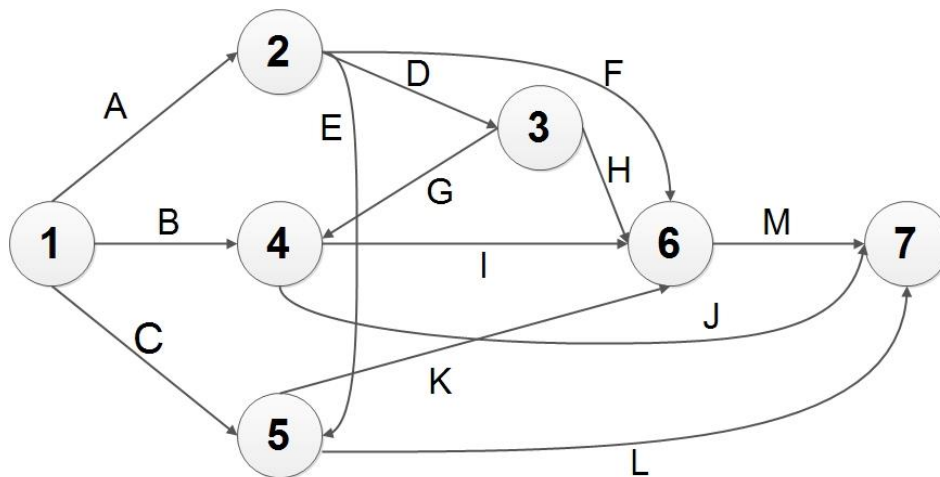


**Fig. 4. Network diagram**

**Table 2 Floating times for project activities**

Activity	(i,j)	Floating time $S_{ij}$	$t_e$	$\sigma_x^2$
A	(1-2)	0	6.17	0.25
B	(1-4)	18.33	2.83	0.25
C	(1-5)	14.34	3.83	0.25
D	(2-3)	0	5.00	0.11
E	(2-5)	3.83	8.17	0.25
F	(2-6)	13.17	9.50	0.69
G	(3-4)	0	10.00	5.44
H	(3-6)	13.17	4.00	0.11
I	(4-6)	0	7.67	1.00
J	(4-7)	22.83	6.17	0.25
K	(5-6)	3.83	10.67	1.00
L	(5-7)	12.5	6.00	0.44
M	(6-7)	0	4.00	0.11

The results represented in Table 2 shows that the critical path is A-D-G-I-M. This means, that the completion of activities B, C, E, F, H, J, K and L can be delayed up to their floating time and not affect the duration of the project. Since all activities through the path must be completed sequentially without overlapping, the project duration is calculated as the sum of the times required critical path to be completed. The simulations show that the probability distribution of project duration has mean  $\mu=32.83$  time units and standard deviation  $\sigma^2=2.63$  time units.

The confident coefficient  $z$  is calculated as:

$$z = \frac{37 - 32.83}{2.63} = 1.58$$

Thus, the probability that project will be completed in 37-time unit is calculated as:

$$P(T \leq \mu) = P(z \leq 1.58) = 0.94295$$

Project activities duration have uncertainties that have to be considered in order to evaluate project completion probability The code for Monte Carlo simulations is developed in program language C++. Random activity durations for the simulations were generated through pseudo random number generator on the range from optimistic to pessimistic time. The number of Monte Carlo iteration defined in the program is 10000. After analysis of the obtained data, one critical path and two subcritical paths are identified. Results from the simulations are represented in Table 3.

**Table 3 Results from Monte Carlo Simulation**

	Critical Path	Subcritical Path	
	1-2-3-4-6-7	1-2-3-6-7	1-2-5-6-7
Number of occurrence	6941	573	2486
Occurrence (%)	69.40%	5.73%	24.86%
Mean path duration	33.43	28.72	29.43
Standard deviation	4.45	1.31	2.19

The confident coefficient z for the critical path is calculated as:

$$z = \frac{37 - 33.43}{4.45} = 0.802$$

Thus, the probability that project will be completed in 37-time unit is calculated as:

$$P(T \leq \mu) = P(z \leq 0.802) = 0.77884$$

### Conclusion

In this paper, a comparison of PERT and Monte Carlo was represented. From the results represented above can be concluded that Monte Carlo is giving a better identification of the risk. The output of PERT simulation is only one identified critical path, while Monte Carlo identifies not only the critical path, but two subcritical paths. The subcritical paths influence the project completion expected time which lead probability of ending the project on schedule to be decreased. Moreover, Monte Carlo simulations offers a choice of various probability distributions like triangle, normal, gamma etc.

The project completion time calculated by PERT was found to be 32.83 time units, while with Monte Carlo it was found that the completion time is 33.43 time units. The difference between these two approaches is 1.74%.

## References

- [1] Malcom, D., Roseboom, J., Clark, C., “Application of a Technique for Research and Development Program Evaluation”, *Operational Research*, 7, 646-669, 1959.
- [2] Tysiak, W. Risk Management in Projects: The Monte Carlo Approach versus PERT. *The 6th IEEE International Conference on Intelligent Data Acquisition and Advanced Computing Systems: Technology and Applications*, 2011, Czech Republic.
- [3] Milian, Z., Monte Carlo Simulation with Exact Analysis for Stochastic PERT Networks, *The 25<sup>th</sup> Symposium on Automation and Robotics in Construction*, 2008.
- [4] Metropolis, N., The Beginning of the Monte Carlo Method, *Los Alamos Science Special Issue*, 1987.
- [5] Taha, H. A., Operation Research: An Introduction, 10<sup>th</sup> Edition, Pearson, 2017.



## E-LEARNING – CYBER SECURITY CHALLENGES AND PROTECTION MECHANISMS

*Dimitar Bogatinov<sup>3</sup> Goce Stevanoski,<sup>2</sup> Monika Kachurova<sup>1</sup>*

<sup>1</sup>Military academy “General Mihailo Apostolski” – Skopje, University “Goce Delcev” - Stip, N.Macedonia,  
monikakachurova@hotmail.com

<sup>2</sup>Military academy “General Mihailo Apostolski” – Skopje, University “Goce Delcev” - Stip, N.Macedonia,  
goce.stevanoski@ugd.edu.mk

<sup>3</sup>Military academy “General Mihailo Apostolski” – Skopje, University “Goce Delcev” - Stip, N.Macedonia,  
dimitar.bogatinov@ugd.edu.mk

### Abstract

*In the successful functioning of modern society, the traditional educational methods are not enough, and new methods must be introduced. Given the constant development of technology today, a high-quality workforce is needed as much as possible. The fast changes in the modern way of living are forcing a life in virtual spaces, in which smart devices are an essential part.*

*The e-learning concept offers several advantages to educational organizations that use this technology, including short and effective training, flexibility, and modulation. The Internet is increasingly used for a variety of online courses, so one of the essential tasks is understanding the e-learning security issues. The security aspect is very important for the companies creating e-learning platforms, which should consider the safety of the instructors, the students, as well as the companies / educational institutions that use the services. In this paper, we will look at the threats to the security and privacy of the most popular e-learning systems and suggest methods for overcoming those challenges.*

**Keywords:** e-learning, threats, security and privacy.

### Вовед и преглед на литература

Денес, кога станува збор за образованието, напредувањето во дигиталната технологија станува суштинска ставка во нашето секојдневие. Бидејќи сè повеќе начинот на пренесување на знаења се сведува преку интернет, треба да ги разбереме безбедносните проблеми на електронското учење. Безбедносниот аспект е уште поважен за компаниите кои користат системи за е-учење за да испорачуваат курсеви за обука на своите вработени. Е-учењето е нов метод на учење кој зависи од Интернет при неговото извршување и е добро познато дека интернетот стана место за нов пакет на незаконски активности, така што околината за е-учење е изложена на многу ризици и закани. Ризикот се појавува при електронски пренос на информациите, додека заканата подразбира предвидена опасност. Вообичаени закани за компјутерите се вируси, мрежни продирања, кражби и неовластено модифицирање на податоците, прислушување и достапност на сервери и персонални компјутери.

За време на преносот, оригиналните документи можат да бидат изменети, поправени или уништени од активните и пасивни напади на хакерите. Како произложена технологија на вообичаени закани и ризици е електронското учење.



## Електронското учење

Е-учење е обединувачки термин за да се опише учењето преку Интернет, обука базирана на веб-страници и упатства засновани на технологија. Обично, поимот е - учење подразбира курсеви, настава или обуки преку Интернет [1].

Подолу се дадени некои карактеристики на системите за е-учење:

- Процесот на учење се врши во виртуелна училница;
- Едукативниот материјал е достапен на Интернет и вклучува текст, слики, врска до други мрежни ресурси, слики, аудио и видео презентации;
- Виртуелната училница е координирана од инструктор кој ја планира активноста на учесниците во работните групи, дискутира за аспектите на курсот со помош на форум за разговор или разговор, обезбедува помошни ресурси, итн.;
- учењето станува социјален процес;
- поголемиот дел од системите за е-учење овозможуваат следење на активностите на учесниците, а некои од нив, исто така, вклучува и симулации и работа на подгрупи.

Концептот на е-учење нуди неколку предности на образовните организации што ја користат оваа технологија, вклучувајќи кратка и ефикасна обука, флексибилност и модулизација. Повеќето иновации за е-учење се фокусираат на развојот на курсот и начинот на презентирање, со малку или воопшто посветување на внимание на приватноста и безбедноста како потребни елементи. Сепак, од горенаведените трендови, јасно е дека ќе има поголема потреба од високи нивоа на доверливост и приватност во апликациите за е-учење и дека мора да се воспостават безбедносни технологии за да се задоволат овие потреби. Исполнувањето на безбедносните барања во системот за е-учење е исклучително комплексен проблем затоа што е неопходно да се заштитат содржината, услугите и личните податоци, не само за надворешните корисници, туку и за внатрешните корисници, вклучително и администраторите на системот.

## Закани и ризици

Загубата на средството е предизвикана од реализација на закани или ризици. Сите закани се реализираат преку медиум на ранливост [2].

Главните закани се:

- Прекршување на доверливоста;
- Повреда на интегритетот;
- Одбивање на услугата: Спречување на легитимни права за пристап со нарушување на сообраќајот за време на комуникацијата меѓу корисниците на системот за е-учење.
- Нелегитимна употреба: Експлоатација на привилегии од легитимни корисници;
- Злонамерна програма: Код за оштетување на програми;
- Одредување: Лица што негираат учество во пренос на документи;
- Анализа на сообраќајот: протекување на информации со злоупотреба на комуникацискиот канал;

- Brute force attack: Обид со сите можни комбинации да се открие лозинката.

### **Можни ризици на креаторите на содржини**

Современата технологија им овозможи на креаторите на содржини да обезбедат пристап до материјали како книги, списанија, итн. Креаторите на содржини се одговорни да ја развиваат и имплементираат содржината. Причината зошто многу креатори на содржини се воздржуваат од обезбедување е стравот дека нивниот составуван материјал може да биде предаден и обработен без нивно знаење. Должноста на креаторот на содржини е да се заштити од неовластена употреба, модификација и повторна употреба на податоците во различни контексти поврзани со е-учење.

Белешките на креаторите на содржини може да бидат модифицирани / уништени од хакерите преку напади. Затоа, во интерес на креаторот на содржини е да се осигура дека корисниците ја добиваат содржината непроменета и дека корисниците можат да го проверат интегритетот на текстот.

### **Можни ризици на професорите**

Професорите се одговорни за обезбедување на секоја можна поддршка на студентите во врска со академската материја. Професорите можат да ја следат или да купат содржината на курсот, презентации од трето лице според барањата на курсот. Сите ризици од е-учењето не треба да бидат ограничени на техничкиот систем. Неопходно е да се опфатат целокупните методи на предавање, испитување и оценување. Методологиите на наставата се менуваат од еден наставник на друг, но ќе има вообичаени ризици во настаните како што се предавање, испраќање белешки и задачи, прифаќање и обележување листови со одговори, подготвување и дистрибуирање на тестови. Дискусиите се основна компонента на наставата на кој било курс. Една форма на дискусија може да биде преку онлајн форумот.

Предност на дискусиите на форумите преку Интернет во однос на усните дискусии е тоа што сите пишани документи се чуваат електронски на серверот, но дигиталното складирање на материјали претставува голем ризик за приватноста на студентите, како и на Професорите.

Покрај тоа, постои ризик во системот за испити што вклучува стандардизација на прашањата за испит и список на прашања што може да ја ограничат академската слобода на одделни наставници. Мора да постои тим што ќе се грижи за сите овие ризици. Ризикот поврзан со испитување е директно поврзан со мамење. Освен мамењето, Професорите мора да бидат загрижени за достапноста на оценките. Исто така, за време на испитувањето студентите се повеќе сакаат да соберат материјали за проучувањето на содржината. Сите наставници мора да бидат свесни за ризикот студентите да добијат непроменет прашалник пред почетокот на испитите и сите одговори да се чуваат на непроменет начин. Иако предавањето е наједноставна и природна форма на комуникација, останува секогаш ризикот од модификација на предавањето на час (говор) за време на предавањето.

### **Можни ризици кај студентите**

Максимален број на корисници во системот Е-Учење се студентите кои учат и го споделуваат своето знаење со други во системот. Студентската група може да се класифицира на различни нивоа од низок степен, дипломски, постдипломски, до ниво на докторски студии. Но, секој корисник мора да биде свесен за секој материјал добиен од институтот, Професорите или другите студенти. Од друга страна, доколку натрапниците ги уредувале документите со прашања или други важни документи, потоа студентите ќе треба да се соочат со проблеми во моментот на испитувањето.

Покрај тоа, постои ризик од зачувување на информации за најава (корисничко име и лозинки). Сите студенти мора да бидат свесни за злоупотреба на информации за најава, во спротивно напаѓачот може да се обиде да го спречи овластениот ученик да пристапува до серверот за Е-учење со горенаведените напади. Професорите не се секогаш достапни за да им помогнат на студентите, така што тие треба да бидат дисциплинирани да работат самостојно без помош на наставникот.

Студентите треба да имаат добри вештини за пишување и комуникација. Кога Професорите и другите студенти не се состануваат лице в лице, можно е да не се разберат, т.е. погрешно да се протолкуваат. Како механизам за повратна информација од постои ризик од страна на студентите да ги испратат истите повратни информации до раководството на институтот за е-учење. На крај, сите ученици треба да бидат свесни за фишингот каде напаѓачот поставува лажни веб-страници кои изгледаат како вистинска веб-страница за е-учење, така што тешко може да прави се разлика помеѓу вистинската и страната на напаѓачот. Овде често од студентите се бара да внесат некои доверливи информации.

### **Други закани и ризици при е-учење**

Покрај горенаведените ризици, постојат и разни други закани присутни во системот на е-учење, како:

Природни закани – може да бидат предизвикани од природни непогоди, како што се пожар, невреме, вулканска ерупција, земјотрес, поплави и др. Системот за електронско учење може да биде под влијание на овие закани.

Промислени– Заканите може да бидат од измама, уцена, кражба итн.

Ненамерни – Може да има некои неизбежни закани како компјутерска грешка, прекинување на електрична енергија, грешка во ракување итн.

### **Начини за справување со ризици**

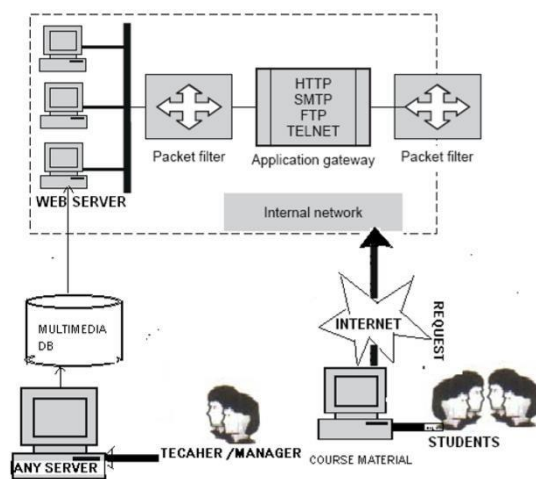
Учесниците на системот за е-учење се соочуваат со различни ризици или закани, како што беше дискутирано во претходниот дел. Следниве алатки или техники може да бидат наметнати за да се минимизираат овие ризици[3].

### **Контрола на пристап со помош на “Firewall”**

Заштитен сид (Firewall) е комбинација на хардверски и софтверски систем за безбедност, воспоставен за да се спречи неовластен пристап до корпоративната мрежа од надвор во организацијата. Технички, заштитниот сид е специјализирана верзија на рутерот. Покрај

основните функции за рутирање и правила, рутерот може да се конфигурира за да ја изврши функционалноста на заштитниот сид, со помош на дополнителни софтверски ресурси.

Главниот принцип заснован на правилото е дека целиот сообраќај од внатре кон надвор и обратно, мора да помине низ заштитниот сид. За да се постигне ова, целиот пристап до локалната мрежа мора прво физички да се блокира, а пристапот само преку заштитниот сид треба да биде дозволен. Само сообраќајот овластен според локалната политика за безбедност треба да се дозволи да помине. Самиот заштитен сид мора да биде доволно силен, за да ги направи сите напади извршени врз него бескорисни. Во практични имплементации, заштитниот сид обично е комбинација на филтри и апликации. Еден таков заштитен сид е прикажан на сликата подолу. Пософистицираните заштитни сидови можат да блокираат извесен сообраќај од надвор, но да им дозволи на корисниците на Е-Учење (може да бидат студенти, наставници, итн.) да комуницираат слободно.



Слика 1: Организација на безбедносен сид базиран во е-учење

Значи, должноста на сите администратори на системот е да имаат знаење и вештини за спроведување на заштитниот сид, да го конфигурираат заштитниот сид и да ги следат и решаваат проблемите со заштитните сидови.

## Криптографија

Целта на доверливоста е да се осигура дека информациите и податоците не се откриваат на кое било неовластено лице или субјект. Исто така, читателите мора да се потпрат на точноста на курсот. Една од техниките во овој аспект е криптографијата. Различни криптографски алатки и техники се потребни за примена на безбедноста во трансакциите базирани на интернет. Постојат два вида на алгоритми во криптографијата:

- Алгоритми на таен клуч
- Алгоритми со јавен клуч
- Алгоритми на таен клуч

Во алгоритмите со таен клуч, клучот за криптирање и декрипција е ист, тој бара испраќачот и примачот да се договорат за клучот пред комуникацијата, главната функција на овој алгоритам е криптирање на податоците. Примери на вакви алгоритми

се Стандард за криптирање на податоци (DES), Меѓународни алгоритми за криптирање на податоци (IDEA) и Напреден стандард за криптирање (AES).

### **Алгоритми со јавен клуч**

Крипто-системите на јавниот клуч, од друга страна, користат еден клуч (јавниот клуч) за криптирање на пораки или податоци и втор клуч (тајниот клуч) за декриптирање на тие пораки или податоци. Тука главно се користат три математички модели – Факторизација, дискретни логаритми и елипсовидна крива. Различни алгоритми со јавен клуч се RSA, El-Gamal, DiffieHellman. Можеме да ги користиме овие техники за време на испраќање на хартија за прашања и примање на листови со одговори. За автентикација на учесник, можеме да ги користиме следниве технологии користејќи алгоритам за јавен клуч:

- Дигитален потпис
- Дигитален сертификат

### **Криптографија базирана на невронски мрежи**

Криптографија базирана на невронски мрежи е нов пристап заснован на вештачки невронски мрежи (АНН) за безбедност на податоците во електронската комуникација. Претставува крипто-систем, кој се заснова на биолошки идеи, вклучително и мрежна архитектура, биолошки операции и процес на учење. Значи, сложеноста на генерирање на обезбедениот канал е линеарна со големината на мрежата. Овој биолошки механизам може да се користи за изградба на ефикасен систем за криптирање со употреба на клучеви кои се менуваат. Многу е едноставен и брзо може да се спроведе во случај на можен напад во моментот на пренесување на документ за е-учење.

### **Биометриска автентикација**

Меѓу сите техники за автентикација како лозинки, паметна картичка, дигитален потпис и дигитален сертификат, не постои гаранција дека студентите ќе ја чуваат својата лозинка во тајност. Лозинката може да биде злоупотребена за време на поднесување на задача, примање на трудови, преземање на материјали од курсот и сл, каде што биометриската автентичност би давала поголема безбедност. Но, за ова треба малку повеќе инвестиции.

## Заклучок

За успешно функционирање на современото општество и следење на трендовите на пазарот веќе не се доволни традиционални методи на образование, туку веќе има потреба од нови форми на стекнување со знаење. Со оглед на постојаниот развој на технологијата во денешно време, потребата за високообразована работна сила е се поголема. Постојаното забрзување на темпото на живот нè насочува кон виртуелниот свет и компјутерот станува дел од нашиот секојдневен живот. Важна карактеристика на учење од далечина е употреба на информациска и комуникациска технологија и од ден на ден се повеќе влијае на животот на поединецот, но и на целото општество и на тој начин и на нивниот образовен процес.

Развојот на системите за е-учење треба да се направи со користење на меѓународно признати методи и стандарди за безбедност. Системот треба да спроведе безбедносни механизми како што се автентикација, криптирање, контрола на пристап, управување со корисници и нивни дозволи. Безбедната платформа за учење треба да ги вклучи сите аспекти на безбедноста и да ги направи повеќето процеси потранспарентни за наставникот и ученикот.

Поради постојано забрзување на темпото на живот, кој оди заедно со технологијата, учењето на далечина се повеќе станува неопходност на денешното општество. Учењето од далечина станува препознатливо како многу важен и моќен начин за успешно управување со современото општество ширум светот, вклучително и кај нас.



## Користена Литература

1. Creswell, J. W. „*Conducting Risk Assessments* 1 (2): 1-95. [10] Sugiyono. (2014) *Metode Penelitian Manajemen* “[Title in English: *Research Method in Management*], Bandung, Alfabeta. (2016)
2. Dobre, I., „The standard model of an e-learning platform“. Bucharest, Romania, (2010). (Chapter 2)
3. Edgar, R. W. „Critical Study of the present e-learning systems“, Academia Romana, Romania, (2005). (Chapter 2).
4. Jalal, A. & Ahmad, M. „Security in e-learning“. Springer. Vienna University of Technology, Austria, (2008). (Chapter 1).
5. Kritzinger, E. & Solms S „Security Enhancement for E-Learning“ Portal. Proceedings of International Journal of Computer Science and Network Security“, Department of Computer Science City University, Peshawar, Pakistan, (2006). 41-45.
6. Kumar, S. & Kamlesh, D. “Information Security Management System Based on ISO/IEC 27001: 2005,” E-learning: Incorporating Information Security Governance, Proceeding of Informing Science and IT Education Conference, Salford (Greater Manchester), England, (2011 Chazar, C. (2015), 319-325.
7. Norwood, Herry T., and P. Sandra. Catwell. *Cybersecurity, Cyber analysis and Warning*, New York, Nova Science Publisher, Inc (2009)
8. Pustaka Pelajar, *Research Design:., Quantitative, Qualitative Method*“, 4th Ed., SAGE Publication, Yogyakarta.



## SECURITY AND PRIVACY WITH E-LEARNING SOFTWARE

**Monika Kachurova<sup>1</sup>, Goce Stevanoski<sup>2</sup>, Dimitar Bogatinov<sup>3</sup>**

<sup>1</sup>Military academy "General Mihailo Apostolski" – Skopje, University "Goce Delcev" - Stip, N.Macedonia,  
monikakacurova@hotmail.com

<sup>2</sup>Military academy "General Mihailo Apostolski" – Skopje, University "Goce Delcev" - Stip, N.Macedonia,  
goce.stevanoski@ugd.edu.mk

<sup>3</sup>Military academy "General Mihailo Apostolski" – Skopje, University "Goce Delcev" - Stip, N.Macedonia,  
dimitar.bogatinov@ugd.edu.mk

### Abstract

*E-learning is becoming an increasingly common form of teaching process. It is most often used in holding courses, seminars, conferences, and similar lectures, but it can also be effectively implemented for the teaching process in high schools and colleges. The increase in demand for tools that would enable this process also raises the development of concepts and practical solutions to these problems. A number of tools and services are available for the practical realization of e-learning. An important aspect of these solutions is data security and privacy. Implementation approaches and policies are individual to the providers of such services. But not completely. However, they are also subject to legal regulations. Within the European Union, the GDPR (General Data Protection Regulation) privacy policy is in force, which obliges private companies to have an ethical attitude towards the user data they own. In essence, this regulation calls for transparency. In that sense, the company must clearly state what type of user data it has, how it collects it, how it protects its privacy and for what purpose it uses it. The user must be notified of this in a timely manner and give his consent. Additionally, if the user requests a report at any time and for any reason for the data that the company has about him, the company is obliged to submit it. If the company does not offer such transparency to customers in the European Union, it may be subject to legal sanctions. Because online services generally operate worldwide, these privacy policies are widely accepted, and because of the good ethical practice they imply, some companies implement them for users around the world.*

*This paper will analyze 4 potential e-learning software solutions: ZOOM, Microsoft Teams, BigBlueButton and BlueJeans. An overview of their general functionalities, policies and functionalities within the security, policies, and functionalities within the protection of user data privacy, as well as the GDPR compliance of each of these platforms will be given.*

**Keywords:** cyber security, e-learning, videoconference, GDPR compliance

### Вовед

Електронското учење станува се почеста форма на наставен процес. Овој процес и имплементација значително се зголеми со Covid19 пандемијата, при што од март 2020 година, скоро сите образовни институции во светот на свој сопствен начин преминаа на електронско учење. Овој премин откри мноштво на проблеми како слаба интернет

конекција, безбедносни проблеми<sup>1</sup>, лимитирани педагошки ресурси и познавања на методологии и проблеми со видео стриминг технологијата.<sup>2</sup>

Еден значаен аспект на овие решенија е безбедноста и приватноста на податоците, имајќи во предвид дека употребата на интернетот за време на Covid19 пандемијата е зголемен за преку 70%<sup>3</sup> и безбедносните ризици постојано се зголемуваат, а посебно делот заштита и приватност на личните податоци и почитување на стандардите поврзани со заштита и приватност на лични податоци.<sup>4</sup> Во литературата може да се најдат неколку објавени трудови за безбедноста на податоците на електронско учење кои се потпираат на околности каде учеството во е-учење е опционално и се дефинирани систематски мерки за да се избегнат ризиците со што би се заштитиле личните податоци.<sup>5</sup>

Употребата на стандарди како што е GDPR кај платформите за електронско учење е нешто што во последните години постојано се имплементира но сеуште го нема постигнато посакуваното ниво и сеуште има проблеми со крадење на кредитијали, лични податоци и непочитување на стандардите од страна на компаниите кои ги имаат креирано солуциите за електронско учење.

При поставувањето на платформа за е-учење, безбедноста е клучен аспект од системот. Имплементацијата на безбедносни механизми може да се реализира на повеќе нивоа.

Заштита на самата платформа за е-учење – поставување на соодветни улоги и пермисии за секој кој би учествувал во наставниот процес.

## 1. Видеоконференциски решенија за електронското учење

### 1.1. Zoom платформа

Во суштина, ZOOM платформа е наменета за комуникација, но како што се покажа истата е и важна алатка за електронско учење. Најважната карактеристика на ZOOM би била тоа што е многу едноставна и лесна за користење. На почетокот на 2020 кога голем дел од компаниите и јавните институции беа приморани да работат од дома, ZOOM беше еден од најчестите избори за остварување работа од дома и онлајн часови. Но тоа што платформата доби толку многу внимание имаше и лоша страна: стана цел на хакери, и со месеци беше изложена на голем број на безбедносни пропусти.

Но и покрај скандалот, ZOOM остана една од најкористените платформи за видео конференција.

---

<sup>1</sup> 1. Pandey, Neena, and Abhipsa Pal. "Impact of digital surge during Covid-19 pandemic: A viewpoint on research and practice." *International journal of information management* 55 2020, 102171.

<sup>2</sup> 2. Baeva, Liudmila V. "The "Black Swan" of COVID-19 and the Security Issues in Digital Learning." *Galactica Media: Journal of Media Studies* 3.2, 2021, pp 110-140.

<sup>3</sup> 3. De Oliveira Dias, Murillo, R. D. O. A. Lopes, and Andre Correia Teles. "Will virtual replace classroom teaching? Lessons from virtual classes via zoom in the times of COVID-19." *Journal of Advances in Education and Philosophy* 4.05, 2020, pp 208-213.

<sup>4</sup> 4. Beech, M. (2020). COVID-19 pushes up internet use 70% and streaming more than 12%, first figures reveal. [www.forbes.com/sites/isabeltogo/2020/04/24/united-just-ordered-flight-attendants-to-wear-masks-heres-why-passe-fingers-could-be-next](http://www.forbes.com/sites/isabeltogo/2020/04/24/united-just-ordered-flight-attendants-to-wear-masks-heres-why-passe-fingers-could-be-next).

<sup>5</sup> 5. Cvitić, Ivan, et al. "Methodology for Detecting Cyber Intrusions in e-Learning Systems during COVID-19 Pandemic." *Mobile networks and applications*, 2021, pp 1-12.

<sup>6</sup> 6. Chigada, Joel, and Rujeko Madzinga. "Cyberattacks and threats during COVID-19: A systematic literature review." *South African Journal of Information Management* 23.1, 2021, pp 1-11.

<sup>7</sup> 7. F.A. Muqtadiroh, E.W.T. Darmaningrat, and R.N. Savira, "Risk assessment and risk mitigation of E-Learning Implementation in the middle school using failure modes and effects analysis (FMEA)," *Semin. Nas. Teknol. Inf. Komun. Dan Ind.*, vol. 0, no. 0, Art. no. 0, May 2017.

- Политики за безбедност:
  - Енкрипција на податоци во транзит и пасивни податоци со AES 256 GCM алгоритам;
  - Контрола врз рути за пренос на податоци – корисниците можат да одберат кои податочни центри да ги користат;
  - Заштита на состаноците со цел да се спречи влез и прислушување од страна на трети лица:
    - 11 цифрени уникатни идентификатори за состанок;
    - Комплексни лозинки;
    - Имплементација на чекални со можност автоматско пропуштање само на регистрирани корисници или корисници од специфични емаил домени;
    - Заклучување на состанокот и спречување на влез.
  - Аудио снимки со електронски потпис кој покажува кој ја снимил содржината. Со ова, доколку снимката е споделена без соодветна дозвола, може да се најде кој ја споделил;
  - Доколку некој од присутните го слика екранот на кој е споделена некаква содржина, адресата на тој корисник директно се додава на сликата;
  - Енкрипција на локални снимки и зачувување на снимки на сервер
    - Снимките може да бидат енкриптирани, заштитени со лозинка и достапни само за одредени домени;
    - Иницијално може да бидат достапни само на организаторот на состанокот и администраторот кои може да управуваат со тоа кој има пристап до нив и каков пристап: спуштање, копирање, споделување, читање итн
    - Доколку се овозможи размена на документи во текот на состанокот, тие може да бидат енкриптирани и сочувани на сервер до 31 ден од состанокот.
- Политики за приватност:
  - Нема профитирање од кориснички податоци. Ништо од податоците не се продава на трети лица.
  - Нема мониторинг на состаноци. Единствен пристап до состаноци имаат доколку организаторот на состанокот експлицитно побара снимање на истиот. Кога корисниците влегуваат на таков состанок, тие добиваат известување дека состанокот се снима и самите може да одлучат дали ќе присуствуваат на истиот или не;
  - Организаторот може да одлучи дали снимката од состанокот ќе ја зачува локално или на Zoom сервер и може да одреди кому и колку ќе му биде таа снимка достапна;
  - Zoom прибира кориснички податоци за целите за функционирање на услугите и за нивно подобрување. Пример, се зема IP адресата на корисникот и детали за оперативниот систем;
  - Податоците од корисниците не се користат за маркетиншки цели и не се собираат такви податоци при посета на zoom.us или zoom.com страната. На тие страни дополнително има политика за користење на колачиња кои корисникот може да ги исклучи;
  - Отстранета е опцијата со која организаторот можеше да следи дали некој од присутните работи и нешто друго за време на состанокот;
  - Проверка на видео: пред корисникот да се вклучи со камера, може прво да ја провери сликата и да намести позадина пред целото тоа да биде видно за сите присутни;
  - Автентикација преку повеќе автентикациски провајдери. <sup>6</sup>

<sup>6</sup> Wagenseil, Paul. "Zoom security issues: Here's everything that's gone wrong (so far)." Toms guide, 2020, pp 1-3.

Сертификати за приватност и безбедност

- SOC 2 (Type II);
- FedRAMP (Moderate);
- GDPR, CCPA, COPPA, FERPA и HIPAA согласност (со BAA);
- Privacy Shield Certified (EU/US, Swiss/US, Data Privacy Practices);
- TrustArc Certified Privacy Practices and Statements ;
- UK National Cyber Security Centre's (NCSC) cloud security principles.

Zoom е GDPR сертифицирана платформа, што значи дека ги исполнува условите за приватност на европската унија.

Сервисите кои Zoom ги нуди немаат никакви тракери или колачиња. Политиката за користење на колачиња се однесува само за нивните веб страници: zoom.us и zoom.com. Податоците од овие колачиња се користат за маркетиншки цели и тоа за подобро разбирање на потребите и интересите на корисниците, за доставување порелевантни понуди, како и за евалуација на успешноста на кампањите. Овие колачиња може да се онеспособат преку пребарувачот. Типот на информации кои се собираат се IP адреса, приближна локација, оперативен систем, следење на кликови и посетени страници.

## 1.2. Microsoft teams

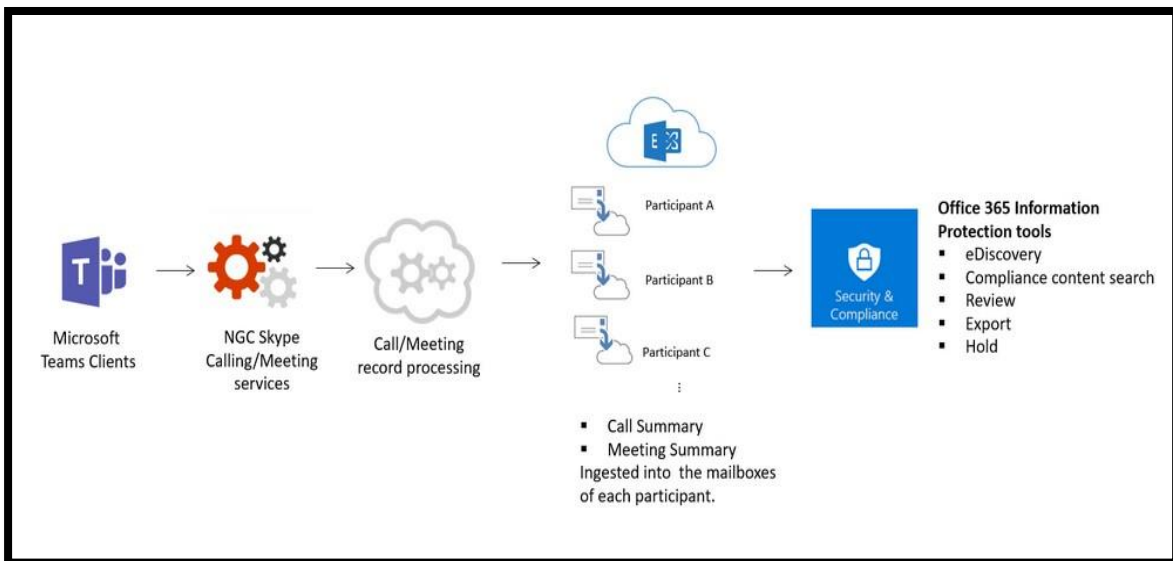
Платформа за комуникација од Microsoft. Беше конструирана да го замени Skype for Business и да ги задоволи потребите за бизнис комуникација, и тоа состаноци, колаборација Платформата е континуирано одржувана што значи дека подобрувања и нови функционалности редовно се доставуваат на корисниците.

Она што вреди да се спомне во однос на Teams е дека има интеграција со апликации. Microsoft има обезбедено интеграција со апликации кои се во нивна сопственост, како што се OneNote, Planner, Office и други. Но постои и отворен пазар за апликации, што значи дека секој би можел да напише екстензија на Teams и да ја објави за широка употреба, бесплатно или со наплата. На страната на Teams се достапни ресурси наменети за програмери кои содржат упатства како да се напише апликација за Teams. Со ова платформата веќе не може да се третира како едноставна апликација за комуникација или социјална алатка.<sup>7</sup>

- Политики за безбедност
- Teams обезбедува two-factor автентикација, single sign-on преку Active Directory на ниво на организација.
- Податоците се енкриптирани и во транзит и во мирување.
- Документите се чуваат на SharePoint каде што безбедноста е на товар на таа платформа, односно енкрипцијата на истите е во склоп на SharePoint.
- Белешките се чуваат на OneNote и нивната безбедност е во склоп на правилата за безбедност на OneNote.

---

<sup>7</sup> Ilag, Balu N. "Microsoft Teams Overview." Understanding Microsoft Teams Administration. Apress, Berkeley, CA, 2020. 1-36.



**Слика 1: Комуникација помеѓу Teams и Exchange за размена на документи за време на состанок**

Извор: Официјална страна на Микрософт

- Политики за приватност
- Опции за состаноци – организаторот на состанокот може да одлучи кој ќе влезе на состанокот а кој ќе може да остане на чекање во чекална.
- Улоги во склоп на состанок – учесниците на состанокот може да добијат свои улоги, како презентер или слушател, со што се контролира кој може а споделува содржини за време на состанокот.
- Согласност за снимање – за време на состанокот доколку некој го снима истиот, сите присутни добиваат нотификација за ова. Дополнително, организаторот може да одлучи кои од присутните смеат а кои не смеат до го снимаат состанокот.
- Споделување на снимката од состанокот – снимената содржина по принцип е достапна за присутните и поканетите на состанокот, но администраторот може да ги промени овие права.
- Модерирање и контрола на канал – сопствениците на каналот може да ги модерираат споделените содржини, така што се овозможува само дозволени содржини да бидат достапни во каналот.
- Teams не ги користи корисничките податоци за достава на реклами.
- По принцип, податоците се заштитени и не се дозволува целосен пристап ниту на владини барања.
- Дозволен е пристап до сопствените податоци во било кое време и од било која причина.
- Редовни извештаи за транспарентност во кои стои на кои трети страни биле доставени податоци, и кои податоци се во прашање.
- Безбеден пристап за гости – дозволен пристап на корисници надвор од организацијата, но под контролиран пристап до организациски документи и други содржини.
- GDPR согласност



Teams исполнува преку 90 политики на безбедност и сигурност од земји и организации од целиот свет. General Data Protection Regulations – е една от тие. GDPR не е аплициран само за корисниците од Европа туку за целиот свет. Во таа смисла, Microsoft не ги доставува корисничките податоци на трети лица за профилирање, маркетинг, реклами, продажба или други цели. Не им се помага на владини тела преку отварање на скриени врати, достава на клучеви за енкрипција или било каква помош за рушење на енкрипција.

Податоците кои Microsoft ги собира за корисникот се зависат од контекстот на сервисот и корисникот може да не дозволи да се собираат во секој момент. Доколку сервисот или легалниот договор зависи непосредно од тие податоци, договорот нема да биде склучен или сервисот нема да биде достапен за тој корисник.

Податоците кои се собираат се користат за таргетиран маркетинг, персонализација на продуктите и препораки, надградба и подобрување на постоечките продукти и услуги, како и корисничка поддршка. Анализата на податоците може да биде автоматизирана преку услуги со вештачка интелигенција или рачно.

Microsoft користи колачиња и beacons за следење на активноста на корисникот. Достапни се повеќе различни механизми со кои корисникот може да ја запре употребата на овие.

Бидејќи Teams не е само апликација за комуникација, освен што самите тие се согласни со GDPR имаат доста документација, чек-листи, водичи и алатки со кои им помагаат на своите бизнис клиенти да остварат GDPR согласност во склоп на нивната компанија, односно спрема нивните клиенти.<sup>8</sup>

За заштита на корисниците Teams дополнително користи можности за:

- Communication Compliance – анализа на комуникацијата која се одвива во рамките на Teams со тоа што ќе се бара согласност со поставената политика за однесување, во смисла на употреба на вулгарни или навредливи зборови, чувствителни информации и слично.
- Retention Policies – политики за зачувување и бришење на податоци. Содржините кои не се релевантни за организацијата може да се маркираат за отстранување, додека они важните може да се чуваат подолго време.
- DLP (Data Loss Prevention) – системот за заштита од ненамерно губење податоци кој е имплементиран за Office 365 е достапен и за Teams.
- eDiscovery и Advanced eDiscovery – систем за пребарување на содржини во случај на судски спор или било каква потреба од документи, извештаи и анализи. Исто така и алатка која овозможува клиентската компанија да постигне GDPR согласност. Напредната варијанта овозможува анализа на неструктурирани податоци и анализа на релевантност со машинско учење.
- Legal Hold – маркирање на податоци кои треба да останат непроменети во случај на судски спор.

### 1.3. Bigbluebutton

Ова е платформа за комуникација која во преден план има да ги задоволи потребите на студентите и професорите, а имаат инкорпорирано функционалности за споделување на аудио, презентации, видео и екран, чат можност за гласања (poll) и сл услуги. Она што е посебно удобно е што има заеднички достапна бела табла на која во реално време

---

<sup>8</sup> Kyncl, Libor, et al. "Personal Data Processing In The Academic Conditions Using The Modern Instruments Of Group Electronic Communication." European Scientific Conference of Doctoral Students. 2020.

може да пишуваат презентерите или група од присутните. За тимска работа (работа во групи) постои можноста за breakout rooms.

Бидејќи ова е апликација чија намена е online училница, повеќето функционалностите се ориентирани околу организаторот (презентерот). Тој ја има целосната контрола врз пристапот на учениците, може да им додава, одзема права, да ги контролира нивните инпути во смисла на аудио, видео, што тие гледаат, пишување на табла, дозволи за презентирање и слично.

BigBlueButton е open source платформа. Тоа значи дека може било кој да го подигне BBB серверот. Негативната страна е што за поставување на серверот е потребно машина со Ubuntu и луѓе што знаат како да го одржуваат истиот. Алтернативата е да се користи преку еден од провајдерите кои го хостираат кај нив и го нудат како сервис по различни цени.<sup>9</sup>

#### - Политики за безбедност

Апликацијата е достапна преку веб пребарувач. Податоците се доставуваат преку обезбедена конекција (TLS), што значи дека податоците во транзите се енкриптирани. Стримовите од податоци се пуштаат во вид на RTP (real time protocol packets) преку UDP со Datagram Transport Layer Security (DTLS), додека медиа пакетите се праќаат со Secure Real-Time Protocol (SRTP).

Бидејќи BBB е само сервер, безбедноста на податоците во мирување и заштита на серверската машина зависи од хостинг провајдерот.

Политики за приватност. Во BBB може да се постави код за пристап до училницата или полиса за одобрување на учениците пред да влезат од страна на модераторот.

Чувањето на снимките, кеш фајловите, логовите и други податоци е на хостинг серверот. Хостинг провајдерот е одговорен за приватноста и безбедноста на овие податоци.

GDPR согласност, Хостинг провајдерот е задолжен за GDPR согласноста на BigBlueButton кој го нуди. Се што BBB може да направи во оваа смисла е да обезбеди начела и помош околу идентификација на податоците, типот на податоците кои се собираат, а кои би биле од интерес за GDPR, и каде истите се чуваат. Администраторите може да наместат локација на чување на логови, кеш документи, снимки и презентации, и самите се одговорни за тоа колку време и како ќе ги чуваат истите. Согласноста со политиката на приватност треба да биде обезбедена од фронт ендот, каде што GreenLight се уште не поддржува таков дијалог. Самата политика на приватност треба да биде изработена и формулирана од страна на хостинг провајдерот.

#### 1.4. BlueJeans

Ова е платформа за комуникација која дава посебно значење на интероперабилноста. Тоа значи дека акцент става на компатибилност со вариетет од уреди, од компјутери и мобилни уреди до комплексни канцелариски конференциски системи.<sup>10</sup>

<sup>9</sup> Kumar, Krishan, et al. "An analysis of Big Blue Button remote teaching tool in an Information Systems undergraduate course." (2021).

<sup>10</sup> Bloom, N., Davis, S. J., & Zhestkova, Y. (2021, May). Covid-19 shifted patent applications toward technologies that support working from home. In AEA Papers and Proceedings (Vol. 111, pp. 263-66).

Интересна алатка е Meeting Highlight каде може да се додаваат забелешки за состанокот кои се поврзани со временска линија од снимката од состанокот. Така може лесно да се прегледаат само најбитните моменти од целата снимка.

- Политики за безбедност
  - Секој состанок има клуч од рандомизирани 9 цифри;
  - Второ ниво на безбедност може да е овозможување на лозинка за секој од поканетите учесници;
  - Состанокот може да се заклучи, со што се оневозможува влез на дополнителни учесници;
  - Учесниците може да се исклучат од состанокот од страна на модераторот;
  - Видео состаноците се енкриптирани;
  - Нотификации за неуспешна најава;
  - Двофакторска автентикација;
  - Авторизација базирана на улоги.
- Политики за приватност

Корисничките податоци кои се прибираат може да дојдат директно од корисникот бидејќи тој или фирмата за која работи ги користат сервисите од BlueJeans, или соработуваат со BlueJeans за да понудат сервиси. Исто така се прибираат податоци и од трети извори поради истите причини.

Исто така, се користат и колачиња за собирање податоци, но корисникот може да ги исклучи преку пребарувачот или преку формата за согласност.

Причините за собирање податоци се за маркетиншки цели, за следење на употребата на софтверот со цел подобрување на самиот софтвер или корисничкото искуство, за согласност со правните барања, за корисничка поддршка и за основно функционирање на постоечките сервиси.

Повеќето податоци се чуваат додека корисникот е клиент на BlueJeans, но некои податоци може да се задржат подолго заради правни причини или решавање на евентуални спорови. Податоците може да се споделат со трети страни доколку истите се контрактори и се соработува со нив за да се обезбедат сервиси на корисниците. Други околности се правни обврски, заштита на правата и сопственоста на BlueJeans и/или нивните корисници, како и евентуални околности кога е во прашање безбедноста на на корисниците или јавноста. Во случај на продажба на сопственост на BlueJeans, може да се случи податоците да поминат во нова сопственост, но ако се случи тоа корисниците добиваат нотификација преку меил и може да не го одобрат трансферот на нивните податоци. Друга околност за споделување податоци е со цел спречување на сајбер криминал.

Снимањето на состаноците е под контрола на организаторот, што значи дека ако некој од присутните не сака да биде снимен, ќе мора да го побара тоа директно од него, бидејќи BlueJeans не поседува механизми за да го оневозможи тоа.

- GDPR согласност.

BlueJeans е согласна со GDPR политиката со тоа што е транспарентна околу типот на податоци кој се собира, начинот на нивното чување како и намената на податоците. Дополнително има дедицирана служба која одговара на барања за извештаи за корисничките податоци.

## Заклучок

Бидејќи станува збор за компании кои ги нудат своите сервиси на корисниците од целиот свет, сите овие платформи се GDPR согласни, со исклучок на BigBlueButton кој е open source софтвер а не сервис. Безбедноста и приватноста се сериозни прашања и секоја од компаниите има одговорен пристап кон истите. Секоја од нив ги имплементира основните технички стандарди за безбедност, како што е SSL и енкрипција на податоци во мирување и уште барем неколку специфични функционалности кои одат во прилог на безбедноста и приватноста.

## Користена литература

1. Pandey, Neena, and Abhipsa Pal. "Impact of digital surge during Covid-19 pandemic: A viewpoint on research and practice." *International journal of information management* 55 2020, 102171.
2. Baeva, Liudmila V. "The "Black Swan" of COVID-19 and the Security Issues in Digital Learning." *Galactica Media: Journal of Media Studies* 3.2, 2021, pp 110-140.
3. de Oliveira Dias, Murillo, R. D. O. A. Lopes, and Andre Correia Teles. "Will virtual replace classroom teaching? Lessons from virtual classes via zoom in the times of COVID-19." *Journal of Advances in Education and Philosophy* 4.05, 2020, pp 208-213.
4. Beech, M. (2020). COVID-19 pushes up internet use 70% and streaming more than 12%, first figures reveal. *www.forbes.com/sites/isabelitogo/2020/04/24/united-just-order-ed-flights-attend-dance-towear-masks-heres-why-passe-fingers-could-be-next*.
5. Cvitić, Ivan, et al. "Methodology for Detecting Cyber Intrusions in e-Learning Systems during COVID-19 Pandemic." *Mobile networks and applications*, 2021, pp 1-12.
6. Chigada, Joel, and Rujeko Madzinga. "Cyberattacks and threats during COVID-19: A systematic literature review." *South African Journal of Information Management* 23.1, 2021, pp 1-11.
7. F.A. Muqtadiroh, E.W.T. Darmaningrat, and R.N. Savira, "Risk assessment and risk mitigation of E-Learning Implementation in the middle school using failure modes and effects analysis (FMEA)," *Semin. Nas. Teknol. Inf. Komun. Dan Ind.*, vol. 0, no. 0, Art. no. 0, May 2017.
8. M. Ilkan, M. Beheshti, M. Behendish, E. Atalar, and M. Ilkan, "Managing interaction related risks on the development of E-Learning it Projects: A Case Study of a Language Institute E-Learning Platform Design in Iran," vol. 5, no. 2, p. 9, 2017.
9. J. Demchak, "Global risks abound for higher education institutions," <https://www.marsh.com>, Aug. 22, 2019. <https://www.marsh.com/us/insights/risk-in-context/global-risks-higher-education.html> (accessed Jun. 20, 2020).
10. Cvitić, Ivan, et al. "Methodology for Detecting Cyber Intrusions in e-Learning Systems during COVID-19 Pandemic." *Mobile networks and applications*, 2021, pp 1-12.
11. Mohamed, Khaled Salah. "Introduction to Cyber Security." *New Frontiers in Cryptography*. Springer, Cham, 2020. 1-12.
12. Wagenseil, Paul. "Zoom security issues: Here's everything that's gone wrong (so far)." *Toms guide*, 2020, pp 1-3.
13. Williams, Christina Meilee, Rahul Chaturvedi, and Krishnan Chakravarthy. "Cybersecurity risks in a pandemic." *Journal of medical Internet research* 22(9), 2020, 23692.
14. Chigada, Joel, and Rujeko Madzinga. "Cyberattacks and threats during COVID-19: A systematic literature review." *South African Journal of Information Management* 23(1), 2021, pp 1-11.
15. Stevens, Rock, et al. "It Lurks Within: A Look at the Unexpected Security Implications of Compliance Programs." *IEEE Security & Privacy* 18.6 (2020): 51-58.
16. Ilag, Balu N. "Microsoft Teams Overview." *Understanding Microsoft Teams Administration*. Apress, Berkeley, CA, 2020. 1-36.
17. Kyncl, Libor, et al. "Personal Data Processing In The Academic Conditions Using The Modern Instruments Of Group Electronic Communication." *European Scientific Conference of Doctoral Students*. 2020.
18. Kumar, Krishan, et al. "An analysis of Big Blue Button remote teaching tool in an Information Systems undergraduate course." (2021).
19. Bloom, N., Davis, S. J., & Zhestkova, Y. (2021, May). Covid-19 shifted patent applications toward technologies that support working from home. In *AEA Papers and Proceedings* (Vol. 111, pp. 263-66).



## ROOTKITS – CYBER SECURITY CHALLENGES AND MECHANISMS FOR PROTECTION

*Goce Stevanoski,<sup>1</sup> Monika Kachurova,<sup>2</sup> Dimitar Bogatinov,<sup>3</sup>*

<sup>1</sup>Military academy “General Mihailo Apostolski” – Skopje, University “Goce Delcev” - Stip, N.Macedonia,  
*goce.stevanoski@ugd.edu.mk*

<sup>2</sup>Military academy “General Mihailo Apostolski” – Skopje, University “Goce Delcev” - Stip, N.Macedonia,  
*monikakacurova@hotmail.com*

<sup>3</sup>Military academy “General Mihailo Apostolski” – Skopje, University “Goce Delcev” - Stip, N.Macedonia,  
*dimitar.bogatinov@ugd.edu.mk*

### Abstract

*A rootkit is a collection of computer software, typically malicious, that has the intention to infiltrate the operating system (OS) or database, avoiding detection, resist removal and maintain privileged access to the system. Many rootkits are designed to attack the "root", or kernel, of the OS and therefore work without disclosing their presence to the computer owner.*

*A rootkit is one of the most dangerous malware programs because it allows any program to gain access to different levels of the operating system. Rootkit's detection is difficult because a rootkit may be able to subvert the software that is intended to find it, and usually the only effective way to remove it is to perform a clean reinstallation of the operating system. Because rootkits can hijack or subvert security software, making it likely that this type of malware could live on your computer for a long time causing significant damage, with that positioning as one of the biggest concerns for IT administrators.*

*This paper aims to review the types of rootkits, their attack methods, as well as to describe the detection and prevention methods against this type of malware.*

**Key words:** Rootkit, Backdoor, prevention, security

### Вовед и преглед на литература

Огромниот број на податоци во дигиталниот свет претставува неисцрпно богатство на информации интересни за многу светски актери како што се владини агенции, невладини организации и различни криминални групации. Нивниот мотив постојано продуцира нови начини како да се искористи сајбер просторот за добивање на свежи и навремени доверливи податоци за предметот на интерес. Тоа е порив кој нема да исчезне и во иднина.

Ваквата состојба предизвикува постојан развој на различни вектори за напад на компјутерските мрежи и системи. Во множеството на сајбер закани како единствени по карактеристиките на софистицираност се јавува класа на малициозни софтвери наречена руткитови. Главна цел на руткитовите е да остане што подолго неоткриен во нападнатите системи, овозможи пристап на напаѓачите и сокрие докази за преземените активностите. На повеќето руткитови им се потребни привилегии на административно ниво за да се инсталираат во системот. Тоа најчесто се остварува со искористување на



различни ранливости на системот кои може да овозможат највисок пристап на администраторски права (ring 0). Целосна контрола врз системот значи дека постоечкиот софтвер во системот може да се модифицира, брише и деактивира, тука вклучувајќи го и софтверот кој инаку би можел да се користи за откривање или бришење на истиот.

Детекцијата на нови руткит софтвери во последните 10 години е во опаѓање. Причини за тоа се: сложеноста за да се развие ваков тип на софтвер, па напаѓачите развиваат поедноставни решенија и преземените мерки на развојните компании за отстранување на можностите за инсталација на руткит софтвери директно во дизајнот на системската архитектура. Но последните детекции на овој тип на софтвер, во 2018 на LoJax и во 2020 на MosaicRegressor, покажаа дека неоткривањето на руткитовите во „дивината“ на сајбер просторот се должи и на софистицираноста на напаѓачите при развој на руткит софтверите.

Појавата на LoJax во 2018 година, како прв детектиран UEFI руткит ја потврди веќе започнатата дебата за безбедноста на компјутерските системи од ваков тип на напади. Истражувањата на ASERT и ESET покажаа дека LoJax руткит се користел од страна на групата Sednit на владини компјутерски системи на Балканот и во Централна и Источна Европа. LoJax е предвесник на новиот UEFI руткит софтвер детектиран во 2020 година од страна на Касперски а наречен MosaicRegressor. Овој руткит се наоѓал во компјутерски системи на дипломатски и невладини организации во Азија, Африка и Европа во периодот од 2017 до 2019 година. Истражувањата на собраните податоци и употребен јазик во MosaicRegressor покажале дека доминира кинескиот јазик а се таргетирани организации кои на различни начини биле поврзани со Северна Кореја.

Овие примери покажуваат дека руткитовите софтверите не се изумрени или во опаѓање истите стануваат пософистицирани во нивото присуство и делување а тоа придонесува за потешко детектирање на истите.

### **Опис на руткитовите и начин на функционирање**

Како се појавувале руткит софтверите така нивата дефиниција се менувала. Повеќето дефиниции се однесуваат на тоа дека руткит е злонамерен софтвер, или колекција на злонамерни софтвери, во компјутерските системи, но не го опфаќаат целиот дијапазон на негово единствено делување. Поради тоа во трудот ќе ја прифатиме дефиницијата на (Bill Blunden) дека „Руткит софтвер воспоставува интерфејс за далечински пристап на нападателен систем со кој се овозможува да се манипулира системот и да се собираат податоци на начин на кој е тешко да се открие“.

Терминот руткит е комбинација на "root" (традиционалното име на привилегираниот корисник на оперативните системи слични на Unix) и зборот "kit" (кој се однесува на софтверските компоненти кои ја спроведуваат алатката). Овој термин има негативни конотации поради неговата употреба како софтвер за малициозни активности. Првично, руткитовите претставувале легитимна колекција на алатки што овозможувала административен пристап до компјутер или мрежа. Денес, руткит софтверите се поврзуваат со малициозните видови на софтвери кои обезбедуваат привилегиран пристап на највисоко ниво во компјутерските системи, притоа криејќи го своето постоење и дејствие. Напаѓачите користат руткит за да се сокријат сè додека не одлучат да го нападат системот. Нападите вклучуваат активности за деактивација на анти-малициозен софтвер и антивирусен софтвер, оштетување на инсталирани апликации, собирање на чувствителни информации и информации за однесувањето на корисникот, започнување на DDoS напади и слично. Со цел отстранување на закана од руткитовите, од витално значење е да се разбере како истите се кријат и како се детектираат во еден систем.

За да се откријат руткивите и да се заштитат системите од истите, треба да се објасни нивното функционирање. Во понатамошниот текст во чекори е прикажано како тие работат.

### Чекор 1: Инфекција на таргетираниот систем

Првиот чекор на напад со руткит е инсталирањето на руткитот во таргетираниот систем. Притоа, се користи еден од следните методи за инсталирање на малициозен софтвер:

- **Phishing** – напад со испраќање на електронски пораки кои го наведуваат корисникот да преземе документ или да пристапи кон линк кој инсталира руткит во позадина без негово знаење.
- **Преземање на лажни софтвери/апликации:** Навидум легитимен софтвер кој претставува апликација која го наамува корисникот да преземе руткит.
- **Drive by Downloads:** Во некои случаи, самата посета на веб страница со слаба веб-безбедност може да инсталира руткит во системот.
- **Malvertising:** Напаѓачите дизајнираат реклами кои содржат малициозен софтвер за да инсталираат руткит кога ќе се кликне на нив.
- **Baiting:** Напаѓачот остава УСБ со инсталиран руткит на јавно место. Ако некоја жртва го поврзе со неговиот компјутер, руткитот ќе биде инсталиран.
- **Tailgating/ Evil maid attacks:** Напаѓачот сам инсталира руткит софтвер на компјутери кои што се без надзор.
- **Exploit Kits:** Напаѓачите ги користат овие комплекти за скенирање на системи/ апликации/ IoT уреди за пронаоѓање на ранливости во системите и за инјектирање на руткивите.

### Чекор 2: Тајни активности

Откако ќе се инсталираат, руткивите остануваат скриени во системот без знаење на корисникот. Руткивите ги избегнуваат антивирусните програми, анти – малициозните софтвери и други софтвери за безбедност, бидејќи се подигнуваат во исто време, пред или после подигнувањето на системот. Исто така, руткивите манипулираат со размена на податоци за време на системските процеси за да го сочуваат неговото постоење.

### Чекор 3: Креирање на задна врата

Руткит создава задна врата за обезбедување на напаѓачот со привилегиран пристап до компјутерот и/или мрежата.

### **Можни последици од напад со руткит**

Употребата на руткивите често се држи во тајност, а со нивна употреба се инсталираат други малициозни софтвери во системот. Руткивите работат во позадина на системот и често се поддршка на малициозниот софтвер кој се инсталира преку деинсталирање на антивирусната програма, повторна инсталација на малициозниот софтвер и слично.[1] Можни последици од напади со руткивите се:

**Крадење на чувствителни податоци:** Руткивите им овозможува на хакерите да инсталираат дополнителни малициозни софтвери кои крадат чувствителни кориснички информации, како што се броеви на кредитни картички, кориснички лозинки и слично.

Инфекција со малициозен софтвер: Напаѓачите користат руткивовите за да инсталираат малициозен софтвер на компјутерите и системите без да бидат откриени. Руткивовите го кријат малициозниот софтвер од кој било постоечки антивирус, честопати деактивирајќи го безбедносниот софтвер без корисничко знаење. Како резултат на деактивацијата, руткивовите им овозможуваат на напаѓачите да инјектираат штетни датотеки на нападнатиот систем.

Отстранување на датотека: Руткивовите овозможуваат пристап до сите датотеки и команди на оперативниот систем. Напаѓачите кои користат руткивовите можат лесно да ги избришат директориумите на Linux и Windows, клучевите од регистарите и датотеките.

Прислушување: Сајбер криминалците користат руткивови за искористување на необезбедени мрежи и пресретнување на лични кориснички информации и комуникации, како што се е – пошта и пораки разменети преку разговор.

Далечинско управување: Напаѓачите користат руткивови со далечински пристап за промена на системската конфигурација. Тогаш напаѓачите можат да ги променат отворените TCP порти во внатрешноста на firewall – от или да ги променат скриптите за стартување на системот.

### **Видови на руткивови**

Руткивовите може да се класифицираат според местото на нивното инјектирање. Подолу се прикажани видовите на руткивови, согласно тежината на откривање и отстранување до најсофистицирани и многу потешки за откривање и отстранување.[2]

### **Апликациски руткивови**

Едноставните руткивови работат во режим на корисник. Таквите руткивовите модифицираат процеси, мрежни врски, датотеки, настани и системски услуги. Притоа можат да инфицираат стандардни апликации како Microsoft Office, Notepad, или Paint. Тоа е единствениот вид на руткив што може да се открие со обична антивирусна апликација. Руткивовите во корисничкиот режим се извршуваат во ring 3, заедно со други апликации како корисник, наместо системски процеси на ниско ниво. Тие имаат голем број на можни инсталациски вектори за пресретнување и менување на стандардното однесување на програмските интерфејси (API) на апликацијата.

Некои инјектираат динамички поврзана екстензија (како што е .DLL датотека во Windows или екстензија .dylib на Mac OS X) во други процеси и со тоа можат да навлезат во било кој целен процес за да ја измамат; други со доволно привилегии едноставно за да се пребрише меморијата на целната апликација. Механизмите за инјектирање вклучуваат:

Употреба на проширувања на апликација обезбедена од добавувачи. На пример, Windows Explorer има јавни интерфејси кои им овозможуваат на трети страни да ја прошират својата функционалност.

- Следење на пораките.
- Debuggers.
- Експлоатација на безбедносни слабости.

- Функционирање на најчесто користените API-ја, на пример, за да се скрие процес или датотека што работи во податочниот систем.

### **Јадрени руткитови**

Руткитовите кои работат во јадрото, исто така познати како руткитовите во режим на кернел, можат да го модифицираат целиот оперативен систем. Руткитовите на јадрото се извршуваат со највисоките привилегии на оперативниот систем (Ring 0) со додавање на код или замена на делови од јадрото на оперативниот систем, вклучувајќи ги и Кернелот и соодветните двигатели на уредот. Повеќето оперативни системи ги поддржуваат драјверите за уредот на режимот на јадрото, кои ги извршуваат со истите привилегии како самиот оперативен систем. Оваа класа на руткит има неограничен безбедносен пристап, но е потешко да се напише. Комплексноста прави грешки и сите грешки во кодот што работат на ниво на кернелот може сериозно да влијаат на стабилноста на системот, што доведува до откривање на руткит. Roots може да ги модифицира структурите на податоци во кернелот на Windows користејќи метод познат како манипулација на директен кернел (DKOM). Овој метод може да се користи за да се сокријат процеси. Roots на кернелот исто така може да ја закачи табелата за системска дескрипторска услуга (SSDT) или да ги модифицира портите помеѓу корисничкиот режим и режимот на кернелот, со цел да се скрие самата себе. Честопати, руткит создава скриен, шифриран датотечен систем во кој може да скрие друг малициозен софтвер или оригинални копии на датотеки.

### **Bootkits**

Модификацијата руткит која се вика bootkit може да го инфицира кодот за стартување како Master Boot Record (MBR), записник за гласовно запишување (VBR) или секторот за подигнување, и на тој начин може да се користи за напад на системи за шифрирање со целосен диск.

### **Hypervisor level (Ниво на хипервизори)**

Руткитовите се создадени како Тип II Хипервизори како доказ за концептот. Со искористување на функциите за виртуелизација на хардвер како што се Intel VT или AMD-V, овој тип на руткит работи во Ring-1 и го хостира целниот оперативен систем како виртуелна машина, со што му овозможува на Руткит да интервенира со хардверски повици направени од оригиналниот оперативен систем. За разлика од нормалните хипервизори, тие не мора да се вчитаат пред оперативниот систем, но можат да се вчитаат во оперативен систем пред да го промовираат во виртуелна машина.

### **Firmware and hardware (Основен софтвер хардвер)**

Руткит во основниот софтвер го користи истиот за кај уредот или платформата да создаде постојана слика на малициозен софтвер во хардверот, како што е рутер, мрежна картичка, хард диск или системски BIOS. Руткит-от се крие во основниот софтвер, бидејќи истиот обично не го проверува интегритетот на кодот. Технологијата Intel Active Management, дел од Intel vPro, имплементира управување надвор, давајќи им на администраторите далечна администрација, далечинско управување и далечинска контрола на компјутери без вклучување на процесор или BIOS, дури и кога системот е исклучен. Далечинската администрација вклучува далечинско вклучување и исклучување, далечинско ресетирање, пренасочено подигнување, пренасочување на конзолата, пристап до подигнување на BIOS-те, програмирање за филтрирање за влезните и излезни мрежни сообраќаи, проверка на присуството на агентот, алармирање, пристап до информации за системот, информации за хардверските ресурси, постојани

дневници за настани и други информации кои се зачувани во меморијата. Хардверските руткитови вградени во чипсетот можат да помогнат во враќањето на украдени компјутери, да ги отстранат податоците или да ги направат бескорисни, но исто така претставуваат и загриженост за приватноста и безбедноста на незабележливо шпионирање и пренасочување од страна на раководството или напаѓачите кои би можеле да добијат контрола.

### **Начини за заштита од руткитовите**

Руткит нападите се опасни и штетни, но тие го инфицираат системот или компјутерот само доколку на било кој начин се стартува малициозниот софтвер што го носи руткит. Во понатамошниот текст се наведени чекори што треба да се следат за да се спречи инфекцијата со руткит. [3]

Скенирање на системите: Руткит скенирањата со помош на софтверски програми обично се ефикасни во откривањето и отстранувањето на руткит апликации. Сепак, тие се неефикасни против другите видови на напади.

Скенирањата на ниво на јадро можат да детектираат малициозен код само кога руткит е неактивен. Ова значи дека мора да се запрат сите процеси на системот и да се стартува компјутерот во безбедносен режим за ефикасно скенирање на системот. Потребно е да се направи резервна копија од податоците, а потоа повторно да се инсталира целиот систем.

Избегнување на фишинг напади: Фишинг е вид на напад од социјален инженеринг во кој што напаѓачите користат е – пошта за да ги измамат корисниците да кликнат на малициозен линк или да превземат инфициран прилог. Инфицираните прилози можат да бидат Word или Excel документи, апликација или програма или инфицирана слика.

Ажурирање на софтвер: Тековните ажурирања на софтверот се од суштинско значење за безбедност или спречување на напаѓачите да инјектираат малициозен софтвер. Сите програми и оперативниот систем треба да бидат ажурирани и на тој начин може да се избегне напад на руткит кој ги користи ранливостите.

Користење на антивирус од следната генерација: Авторите на малициозниот софтвер секогаш се обидуваат да бидат чекор пред индустријата за сајбер безбедност. За спротиставување на неговиот напредок, треба да се користат антивирусни програми кои ги користат модерните безбедносни техники. Притоа, може да се одреди потеклото на руткитот врз основа на неговото однесување, да се открие малициозен софтвер и да се изврши блокирање од инфицирање на системот.

Следење на мрежниот сообраќај: Техниките за следење на мрежниот сообраќај ги анализираат мрежните пакети со цел да се идентификува потенцијален малициозен мрежен сообраќај. Анализата на мрежата исто така може побрзо да ги ублажи заканите додека ги изолира мрежните сегменти кои се под напад за да се спречи ширењето на нападот.

Континуирано образование на корисниците: Напаѓачите ја користат најслабата алка во сајбер безбедноста – човечката компонента – за да постигнат системска инфекција и инсталација на руткис. Најдобар начин да се спречи инфекцијата со руткит е преку континуирано образование на корисниците, особено оние со административни привилегии. Тие треба да разберат како да ги идентификуваат обидите за фишинг, важноста од превземање само на легитимен софтвер, а не со кликување на сомнителни датотеки кои го идентификуваат потенцијално малициозниот мрежен сообраќај.

## Заклучок

Руткит е една од најопасните малициозни програми, поради тоа што дозволува која и да е програма да добие пристап до различни нивоа од оперативниот систем. Сè додека постојат експлоатации на софтвер, руткитовите ќе ги користат овие експлоатирања. Тие работат заедно. Сепак, дури и ако таквите експлоатации не се можни, руткитовите сепак ќе постојат.

Во следните неколку децении, напредокот на технологиите за виртуелна машина ќе нанесе огромен удар врз оние кои се потпираат на далечинска експлоатација. Ова не значи дека експлоатациите ќе исчезнат. Новиот свет на експлоатација ќе се заснова на логички грешки во програмите наместо на архитектурните недостатоци.

Со или без далечинска експлоатација, руткит-ите ќе опстојуваат. Руткитовите може да се сместат во системите во многу фази, од развој до инјектирање. Сè додека има луѓе, луѓето ќе сакаат да дознаваат информации за други луѓе. Ова значи дека руткитовите секогаш ќе имаат место во нашата технологија. Програмите и технолошките субверзии се безвременски.

Руткит најчесто се внесуваат на крајот од процесот на напад. Затоа и се нарекуваат post-exploit алатки.



## Користена литература

- [1] A. Todd, J. Benson, G. Peterson, T. Franz, M. Stevens, and R. Raines, “Analysis of tools for detecting rootkits and hidden processes,” in Proceedings of the IFIP International Conference on Digital Forensics, P. Craiger and S. Sheno, Eds., Orlando, FL, 2007, pp. 89–105.
- [2] J. A. Dawson, J. T. McDonald, J. Shropshire, T. R. Andel, P. Luckett, and L. Hively, “Rootkit detection through phase-space analysis of power voltage measurements,” in Proceedings of the International Conference on Malicious and Unwanted Software (MALWARE), Oct. 2017, pp. 19–27.
- [3] L. Zhang, S. Shetty, P. Liu, and J. Jing, “RootkitDet: Practical end-to-end defense against kernel rootkits in a cloud environment,” in Proc. 19th Eur. Symp. Res. Comput. Secur., 2014, pp. 475–493.
- [4] J. Joy, A. John, and J. Joy “Rootkit Detection Mechanism: A Survey” in Chapter in Communications in Computer and Information Science · January 2011 pp. 367-373
- [5] Arati Baliga, Liviu Iftode :” Automated Containment of rootkits Attacks” 2018, pp.2-5
- [6] Hyde, D. (2009). A Survey on the Security of Virtual Machines. St. Louis, MO: Washington University in St. Louis. Retrieved 9.2.2020 from <https://www.cse.wustl.edu/~jain/cse571-09/ftp/vmsec.pdf>
- [7] Jana, A. P. (2019). Keysniffer [Software]. Retrieved 8.12.2019 from <https://github.com/jarun/keysniffer>
- [8] Kim, S., Park, J., Lee, K., You, I., & Yim, K. (2012). A Brief Survey on rootkit Techniques in Malicious Codes. Journal of Internet Services and Information Security (JISIS), 2(3/4), pp. 134-147.
- [9] Kleiman, I., Gao, J., Khan, I. & Song, D. (2019). Honey Pot Bears rootkit [Software]. Retrieved 28.1.2020 from <https://github.com/shortland/Honey-Pot-Bears-Pymkum>
- [10] Lehti, R., & Virolainen, P. (2019). AIDE - Advanced Intrusion Detection Environment [Software]. Retrieved 31.1.2020 from <https://github.com/aide/aide>



## TOOLS AND TECHNIQUES FOR MITIGATION AND PROTECTION AGAINST SQL INJECTION ATTACKS

*Dimitar Bogatinov,<sup>1</sup> Goce Stevanoski,<sup>2</sup> Monika Kachurova<sup>3</sup>*

<sup>1</sup>Military academy “General Mihailo Apostolski” – Skopje, University “Goce Delcev” - Stip, N.Macedonia,  
monikakacurova@hotmail.com

<sup>2</sup>Military academy “General Mihailo Apostolski” – Skopje, University “Goce Delcev” - Stip, N.Macedonia,  
goce.stevanoski@ugd.edu.mk

<sup>3</sup>Military academy “General Mihailo Apostolski” – Skopje, University “Goce Delcev” - Stip, N.Macedonia,  
dimitar.bogatinov@ugd.edu.mk

### Abstract

*Most of the services we enjoy on the Web are provided by database applications. Web-based email, online shopping, forums, corporate web sites, and portals are all database-driven. To build a modern web site, you need to develop a database application, usually a SQL database, which is responsible for managing data in a structured way. Recent attacks can lead to the conclusion that web applications are insufficiently protected and are the biggest threat to database security. The most popular form of attacks is the SQL injection attacks that use the data entry, search and username or password fields to inject code into the SQL database.*

*These attacks can detect sensitive data, alter database data, or destroy an entire database. An attacker could even damage the operating system. Usually, the SQL injection attacks are just an introduction to some other attacks, so preventing these attacks can also mean protection from other potentially more dangerous attacks. The purpose of this paper is to review the most common SQL Injection attacks, as well as to propose technical solutions and measures that can contribute to the mitigation of this kind of attacks.*

**Key words:** SQL injection, vulnerabilities, security, privacy

### Вовед и преглед на литература

Со напредувањето на технологијата, современото општество постигна многу незамисливи цели. Сепак, како што се развива технологијата, така се зголемува и ризикот вклучен во нејзиното користење. Ист е случајот со веб – апликациите. Од 2003 година, SQL Injection останува на списокот на OWASP безбедносни ризици со кои се борат компаниите. Нови случаи на ранливост на веб апликациите стануваат се потешки за да се пронајдат и да се искористат. Секоја веб апликација има база на податоци во позадина, и најмногу поради тоа нападите врз бази на податоци се случува преку слабостите во веб апликациите. Може слободно да заклучиме дека веб апликациите се недоволно добро заштитени, и се најголемата закана за безбедноста на базите на податоци кои се во нивната позадина на серверот.

Најсериозните напади на веб апликациите се оние во кои се доаѓа до чувствителни податоци или се добива пристап до системите што работат во позадината на апликацијата. За многу компании, било каков напад на системот што предизвикува прекин во работењето е критичен.

Според многу написи и споделени искуства, токму во областа на безбедносните веб апликации се одвива голема битка помеѓу напаѓачите и оние кои се бранат со податоци и ресурси.

### **Карактеристики на “SQL”**

“SQL” е кратенка за “Structured Query language” и широко се користи како јазик за бази со податоци, обезбедувајќи средства за манипулација со податоците (чување, превземање, измена, бришење) и креирање на бази со податоци. Скоро сите модерни системи за управување со релационите бази со податоци како што се MS SQL Server, Microsoft Access, MSDE, Oracle, DB2, SyBase, MySQL, Postgre,

Informix, користат “SQL” како стандарден јазик за работа со базите на податоци. Прашалниците (Query) се примарни механизми за превземање на информации од базите со податоци и се состојат од прашања кои ја презентираат базата со податоци во соодветен формат. Во “SQL”-от постојат два вида на прашања:

- Data Definition Language (DDL)
- Data Manipulation Language (DML)

DDL прашалниците ја менуваат структурата на базата со податоци, додека DML прашалниците манипулираат со содржината на базата со податоци. “SQL Injection” се напади со вметнување на код во кој се вклучени влезните податоци во динамички конструиран “SQL” прашалник и се третира како “SQL” код. На Веб страните кај кои се користат бази со податоци, “SQL Injection” ранливоста е посебно изразена, затоа што напаѓачите лесно ги наоѓаат и продираат во базата со податоци. Едно истражување направено од “Gartner Group” дошло до сознание дека од преку 300 тестирани веб страни, дури 97% од нив биле ранливи на “SQL Injection”. Со откривањето на “SQL Injection” ранливоста, напаѓачите обично ги извлекуваат и ги менуваат податоците со правење на DDL и DML прашалници.

Со мала измена во програмскиот код т.е. со воведување на додатни проверки е можно да се одбрани страната од поголем број напади со вметнување на SQL код. Секако, упорниот напаѓач и покрај тоа може да изведе SQL напад. Сепак ако некоја страна (и нејзината база на податоци) е добро заштитена, повеќето напаѓачи, ќе се откажат брзо и ќе пристапат кон напад на друга страница која не е толку добро заштитена.

### **Извори на напад на SQLI**

Ранливоста на SQL инјектирањето може да се најде во кој било параметар на апликациите што можат да се користат во базата на податоци. Во понатамошниот текст наведени се четири извори, преку кои може да се започне SQL [1]:

Инјектирање со корисничка улога: Веб апликациите, генерално, користат форми за собирање на податоци од корисници (како што се регистрирање, најава итн.) или да дозволат на корисниците да ги специфицираат податоците што треба да се превземат (како што се пребарување, адаптиран приказ итн.). Овие форми што содржат „поле за текст“ може да ги искористат напаѓачите за да инјектираат малициозен код што резултира со добивање тајни податоци.

Инјектирање преку колачиња: Неодамнешните веб-апликации користат колачиња за складирање на преференциите на корисниците. Колачињата се датотеки зачувани на клинската машина кои содржат информации генерирани од веб апликациите. Напаѓачот може да вметне злонамерен код во содржината на колачињата зачувани во

неговиот компјутер, користејќи ја содржината на колачињата за да изгради SQL пребарувања кои се ранливи на напади.

**Инјектирање преку сервер варијабилите:** Сервер варијабилите се збир на параметри кои содржат мрежни заглавија, HTTP податоци и варијабилите на околината. Веб апликациите ги користат овие варијабилите на серверот за ревизија на статичките податоци за употреба и идентификување на трендовите на прелистување. Ако овие променливи се зачувани во базата на податоци без валидација, напаѓачите можат да ја искористат оваа ранливост со поставување на SQLIA директно во варијабилите на серверот.

**Зачувано инјектирање:** Во зачуваното инјектирање напаѓачите вметнуваат малициозни влезови во базата на податоци за индиректно да вметнат SQLIA секој пат кога ќе се користи влезот [2].

## **Видови на напади на SQL**

SQL нападот може да биде во неколку форми и во следниот дел се класифицираат главните типови на напади на SQLI[3].

**Tautology:** Општата цел на нападот базиран на tautology, е да внесе код во една или повеќе условени изјави, така што тие секогаш се проценуваат како вистинити. Најчестите начини на употреба се заобиколување на страниците за автентикација и извлекување на податоци.

**Bling SQL инјекција:** вид на напад на SQLI што ја прашува базата на податоци точни или погрешни прашања и го одредува одговорот врз основа на одговорот на апликацијата. Овој напад често се користи кога вел – апликацијата е конфигурирана да прикажува генерички пораки за грешки, но не го ублажила кодот што е ранлив на SQL инјекција

**Union query:** Во овој вид на напад, напаѓачот го користи операторот на UNION за да се приклучи на злонамерно барање до оригиналното барање, дозволувајќи му на напаѓачот да ги добие вредностите на колоните на другите табели.

**Piggy-backed query:** Во овој вид на напад, напаѓачот има намера да инјектира дополнителни пребарувања за да извлече податоци или да измени/додаде податоци. Напаѓачите инјектираат дополнителни пребарувања на оригиналното пребарување и како резултат, DBMS добива повеќе SQL пребарувања.

**Зачувани процедури:** Напаѓачот има за цел да преработува зачуваните процедури кои се веќе зачувани во базата на податоци. Притоа, повеќето постојни бази на податоци се проширени со стандарден сет на имплементирани функции наречени складирани процедури кои овозможуваат дури и интеракција со оперативниот систем. Овие зачувани процедури генерално го избегнуваат повторното пишување на стандардни функции.

**Алтернативно кодирање:** Во алтернативното кодирање, напаѓачот се обидува да го скрие вметнатиот текст со цел да избегне откривање со дефанзивни практики за кодирање и техники на автоматска превенција. Поточно, алтернативните кодирања овозможуваат техники со кои напаѓачите ги избегнуваат контрамерките за откривање. Овие техники на затајување се широко користени од натрапникот, затоа што тие знаат дека повеќето IDS го скенираат барањето за одредени познати „лоши карактери“, како што се единечните понуди.

Нелегални/логичко неточни пребарувања: Во нелегално неточни пребарувања, напаѓачите имаат намера да внесат манипулиран пребарувач во базата на податоци за да генерираат порака за грешка која содржи некои информации за причината за грешката.

### **Валидирање на податоците**

Најважен совет за заштита од напади со вметнување на SQL код е да се валидираат сите податоци коишто корисникот ќе ги внесе. Всушност, проследување на внесените податоци кон базата со податоци, без нивна претходна валидација, овозможува напади со вметнување на SQL код дури и на напаѓачите аматери. Во продолжение се наведени некои совети во врска со проверките на податоците пред да се проследат на базата со податоци:

Проверка на податоците би требало да се прави на серверската страна. Имено, доколку проверката се извршува на клиентската страна, напаѓачот може едноставно да ја добие веб страната како “.html” датотека и да го преработи делот со кодот каде што се прави проверката. После тоа напаѓачот може да ја стави веб страната локално и да праќа прашалници без притоа тие прашалници да се проверуваат.

Да се прилагоди типот на податоци кој се очекува. На пример, проверката на корисничкото име е различна од проверката на бројот на кредитната картица коишто корисникот ги внесува при интернет купивањето. Кај проверувањето на бројот на кредитната картица, треба да се провери дали навистина сите внесени карактери се броеви. Додека кај проверката на корисничкото име таква проверка нема смисла, затоа што корисничкото име може да се состои од букви, од броеви, од специјални знаци. Доколку добиените карактери не одговараат на очекуваниот тип на податоци, тогаш прашалникот не смее да се проследи кон базата со податоци.

Проверка на бројот на карактерите. Доколку бројот на карактери во полињата за внес на податоци не е ограничен, тогаш е потребно да се провери колку карактери има внесено корисникот. Преголем број на внесени карактери може да укажува на потенцијален напад. На пример, познато е колку карактери содржи бројот на кредитната картица. Доколку бројот на карактери што ќе ги внесе корисникот го преминуваат тој број, прашалникот во базата со податоци не би смеел да се изврши. Дополнително, 100 карактери во корисничкото име исто така треба да предизвикаат сомнеж дека е тоа регуларен внес на податоци.

Проверка на наводници. Во повеќето случаи корисниците немаат потреба од внесување на наводници (единечни или дупли). За разлика од нив, напаѓачите користат наводници во своите напади, како што е покажано претходно во претходниот дел. Заради тоа е добра пракса да се направи проверка дали постојат наводници пред да се обработат влезните податоци од корисниците.

Проверка на постоење на процедури. Процедурите може да им бидат на напаѓачите многу корисни алатки. Доколку се користи база со податоци Microsoft SQL Server, се препорачува да се провери постоење на низата „xp\_“ во корисничките податоци. Нивното постоење може да укаже на обид за напад со вметнување на SQL код кој ги користи претходно направените процедури како xp\_cmdshell.

## Техники за детекција и превенција

Проверувач на tautology: Статичката анализа се користи за да се спречи нападот на tautology. Аритметичките и логичките јамки се користат за да се провери можната SQL инјекција. Особено, сетот на SQL пребарувања кои програмата може да ги генерира како автомат со конечна состојба се приближни. Овој метод не е погоден за откривање на други напади на SQL инјекции.

AMNESIA: Техника која детектира и спречува напади со инјектирање на SQL. Комбинира статичка анализа и мониторинг на runtime. Овој метод е многу ефикасен и ефективен против SQL инјектирањето. Како прв чекор е идентификација на критичните точки во апликацискиот код и потоа се гради моделот за SQL пребарувања. После секоја идентификувана критична точка се испраќа повик за мониторинг.

SQL проверка: Пристапот е потврден со SQLCHECK кој што претставува имплементација за поставување на команди занатади за инјектирање. SQLCHECK се оценува на реални веб-апликации со реални податоци за напади како инпут кои се системски составени. Времетраењето е кратко и може да се примени директно на веб-апликации напишани со употреба на различни програмски јазици.

Спречување на напади со зачувани процедури: Овој метод ја елиминира појавата на SQL напади со комбинирање на статичка анализа, а кодот за апликација со валидација на времето на траење. Главната цел на овој метод е да се спореди оригиналната структура на SQL изјава со изјавата која што вклучува кориснички инпут. Користењето на оваа техника може да бие автоматизирано и може да биде само кога е потребно.

Машинско учење: Машинското учење се користи за да се откријат малициозни веб побарувања добиени преку логови, кои успешно откриваат малициозни логови. Покрај тоа, совпаѓањето на низата се користи за да одговара на карактеристиките во фазата на класификација. „Машинското учење се заснова на алгоритми кои можат да учат од податоците без да се потпираат на програмирање засновано на правила“. Оваа дефиниција значи дека машинското учење е техника за давање дозвола на машината да донесе своја одлука со имплементација на алгоритми за машинско учење без употреба на програмибилни кодови. Ова истражување ќе се насочи кон еден од видовите на машинското учење, а тоа е надгледувано учење чија што цел е да обезбеди предвидувања за откривање на SQL напади. Надгледуваното учење може да се категоризира како:

Регресија: Анализа на регресија е предвидување на следната вредност врз основа на статистиката на претходните податоци за тестот со набљудување на примерокот. Идејата е податоците да бидат распределени на линеарен график, за да се извлече праг од активностите за да се разликува резултатот што ќе се категоризира.

Класификација: Техниката на класификација е вид на надгледуван метод за класифицирање на атрибутот на податоците за време на фазата на обука, така што може да се класифицира атрибутот за следната одлука. Овој метод е добро позната техника и најшироко се користи кај истражувачите. Се користи овој пристап како класификатор за детекторот да ги класифицира логовите на URL – адресите, без разлика дали истите се малициозни[4].



## Заклучок

Нападите со вметнување на SQL код претставуваат голема закана за секоја веб страна која користи база со податоци. Бројни веб страни се нападнати на ваков начин, а од нападите не биле поштедени ни “големите” страни како страните на Microsoft или страната на MySQL. Со нападите може да се откријат осетливи податоци, да се менуваат податоците во базите или пак да се уништи цела база со податоци. Напаѓачот дури може да му наштети и на оперативниот систем. Некои од нападите со вметнување на SQL код се само вовед во некои други напади, па затоа спречувањето на овие напади може да значи и заштита и од други потенцијално поопасни напади. Доколку не е воведена никаква заштита од вметнување на SQL код и напаѓачите без големо искуство можат да изведат успешен напад со несогледливи последици. На Интернет постојат бројни примери на злонамерно обликуван SQL код со кој може да се креираат напади. Доколку страницата не е осигурана со основните проверки на корисничките внесови на податоци, напаѓачот може едноставно да ископира некој од SQL кодовите и да проба дали може да изведе напад. Со воведување на основните проверки на корисничкиот внес на податоци, како што е проверката на постоење на наводници, знакот точка-запирка или SQL клучните зборови, на повеќето злонамерни корисници доволно им се отежнува нападот за да се откажат од него. За дополнителна сигурност потребно е да се воведат измени во самата база со податоци или на серверот. Такви измени секако се препорачуваат, затоа што штетата предизвикана со нападот може во потполност да ја уништи веб страната или базата со податоци. Како и кај другите сигурносни ранливости, потребно е постојано да се надгледува сигурноста на системот. Не е доволно еднаш да се воведат измени и да се заклучи дека страната е доволно заштитена. Напаѓачите се сè повеќе спремни и креативни, па затоа и администраторите на базите со податоци мора постојано да го надоградуваат својот систем како би бил отпорен на напади како што се вметнување на SQL код.

Со оглед дека одржувањето и подигнувањето на нивото на сигурноста на апликациите и базите со податоци е обемна работа, затоа треба да се ангажираат сите структури од развојниот тим, како што е претставено, потребна е тимска работа, за да програмерите превентивно делуваат на сигурноста, тестерите да ги воочат пропустите во развојот и да ги поправат истите, и на крајот администраторот кој ја одржува апликацијата да се бори со нападите во реално време, а сè со цел заради зголемување на сигурноста на податоците.

## Користена литература

1. Kuldeep Rana, "Classification of SQL Injection Attacks And Using Encryption As A Countermeasure", Bhagwan Parshuram Instt. of Technology (GGSIPU) 2008
2. M. Howard and D. LeBlanc "Writing Secure Code" , Redmond, Washington : Microsoft Press second edition 2003
3. E. M. Fayo, "Advanced SQL Injection in Oracle Databases". Black Hat USA : Technical report, Argeniss Information Security, Black Hat Briefings, 2005
4. Y. Huang, F. Yu, C. Hang, C. H. Tsai, D. T. Lee, and S. Y. Kuo, "Securing Web Application Code by Static Analysis and Runtime Protection", In Proceedings of the 12<sup>th</sup> International World Wide Web Conference (WWW 04) 2004
5. SQL Injection, <http://php.net/manual/en/security.database.sql-injection.php>, 2011
6. AltexSoft. (2019). Web Application Architecture: How the Web Works. AltexSoft. <https://www.altexsoft.com/blog/engineering/webapplication-architecture-how-the-web-works/>
7. Chaturvedi, V. A., Bagdi, S., & Choudhary, V. (2016). Analysis of SQL Injections Attacks and Vulnerabilities. International Journal of Advanced Research in Computer Science and Software Engineering, 6(3), 106-110.
8. Choi, J., Kim, H., Choi, C., & Kim, P. (2011, September). Efficient malicious code detection using n-gram analysis and SVM. In 2011 14th International Conference on Network-Based Information Systems (pp. 618-621). IEEE. <https://doi.org/10.1109/NBiS.2011.104>
9. GeeksforGeeks. (2019). Supervised and Unsupervised learning. GeeksforGeeks. <https://www.geeksforgeeks.org/supervised-unsupervised-learning/>
10. GeeksforGeeks. <https://www.geeksforgeeks.org/clustering-in-machine-learning/>
11. Greene, D., Cunningham, P., & Mayer, R. (2008). Unsupervised learning and clustering. In Machine learning techniques for multimedia (pp. 51-90). Springer, Berlin, Heidelberg. [https://doi.org/10.1007/978-3-540-75171-7\\_3](https://doi.org/10.1007/978-3-540-75171-7_3)
12. Halfond, W. G., Viegas, J., & Orso, A. (2006, March). A classification of SQL-injection attacks and countermeasures. In Proceedings of the IEEE international symposium on secure software engineering (Vol. 1, pp. 13-15). IEEE. <https://www.cc.gatech.edu/~orso/papers/halfond.viegas.orso.ISSSE06.pdf>
13. Jansen, B. J. (2006). Search log analysis: What it is, what's been done, how to do it. Library & Information Science Research, 28(3), 407-432. <https://doi.org/10.1016/j.lisr.2006.06.005>
14. Joshi, A., & Geetha, V. (2014, July). SQL Injection detection using machine learning. In 2014 International Conference on Control, Instrumentation, Communication and Computational Technologies (ICCICCT) (pp. 1111-1115). IEEE. <https://doi.org/10.1109/ICCICCT.2014.6993127>



## INFLUENCE OF ROTATION ANGLE OF LUMINAIRES WITH ASYMMETRICAL LUMINOUS INTENSITY DISTRIBUTION CURVE ON CALCULATED PHOTOMETRIC PARAMETERS

*Marek Mokráň, Dionýz Gašparovský, Roman Dubnička,*

Faculty of electrical engineering and information technology

Slovak University of Technology in Bratislava

Bratislava, Slovakia

marek.mokran@stuba.sk

### Abstract

*Lighting systems often use square LED panels or spherical luminaires, which may not always have an exactly symmetrical luminous intensity curve, even if they appear to be symmetrical. A problem with these luminaires can already arise when measuring luminous intensity distribution curves in a photometric laboratory due to incorrect symmetry determination. For design reasons, many times it is very complicated or even impossible to determine the photometric axes of the luminaire in the case of both spherical and square luminaires. This fact may cause a difference in the angle of rotation of the luminaire in light design software and real lighting systems and thus can cause a situation that the lighting system does not meet the requirements of standard STN EN 12464-1. Such a situation is, of course, undesirable and can cause considerable financial losses. Considering the uncertainties of measuring the parameters entering the lighting system calculation and other influences that cause the difference between the calculated and measured parameters, it is necessary to oversize the system to a certain extent, but there is an upper limit defined by Act no. 555/2005 on the energy performance of buildings. This article deals with the problem that can be caused by an incorrect angle of rotation of the luminaire with an asymmetrical luminous intensity curve when installing the lighting system.*

### Key words

*LED, Lighting design software, luminaire.*

### Introduction

When designing lighting systems, it is necessary to respect valid legislative and normative requirements within a comprehensive set of quantitative and qualitative lighting parameters. The basic parameters include the illumination and the uniformity of illumination, but the same importance is attached to the requirements to prevent glare. From the lighting point of view, spaces with workplaces have a special position in interiors, where it is necessary to create suitable conditions for the working environment. During the building inspection, the photometric parameters of the lighting are verified by measurement and must comply with the requirements of the Decree and the Standard. It is, therefore, necessary to pay increased attention to the design of lighting. Normative requirements for indoor workplaces are prescribed by the standard STN EN 12464-1. The lighting system must be in accordance with Act no. 555/2005 Coll. also efficient and economical. The design and calculation of artificial lighting are associated with a large number of lighting technical calculations. The aim of this process is, on the one hand, to determine the power and the total number of luminaires or light sources and, on the other hand, to verify the required photometric parameters of the illumination. Proper lighting has a significant effect on the overall focus and speed of object

recognition. For correct calculation of lighting system parameters, it is necessary to know sufficiently precise parameters entering the calculation. A critical input parameter for square luminaires not only in the calculation of lighting but also in the realization of the lighting system is the luminous intensity curve. An example of a square luminaire that does not have to have a completely symmetrical luminous intensity distribution curve is shown in Figure 1. [1, 2].



**Fig.1. An example of a square luminaire with a not completely symmetrical luminous distribution curve**

### **Luminous intensity distribution curve of square luminaires**

The luminous intensity curves are a very important input parameter in the lighting calculation, therefore it is very important to measure this photometric parameter of the luminaire as accurately as possible. The basic photometric data of luminaire consist of a set of values of the luminous intensity in different directions, produced by direct photometric measurements. For such photometric measurements involving direction, it is necessary to define a spatial framework around the luminaire. The determination of the intensity distribution of a luminaire in space involves the use of a coordinate system to define the direction in which the intensity measurements are made. The system used is a spherical coordinate system with the centre coincident with the photometric centre of the luminaire. In general, the luminous intensity of luminaire is measured in a number of planes. Square luminaires intended for indoor installation are usually measured in a system of planes C. The system of C-planes (see Fig. 2) is a bundle of planes whose intersection is a vertical line passing through the photometric centre of the luminaire. C - planes are denoted by angles  $C_x$  in the range  $0^\circ - 360^\circ$ . In a given plane, the directions are determined by angles  $\gamma$  in the range  $0^\circ - 180^\circ$  [3] [4].

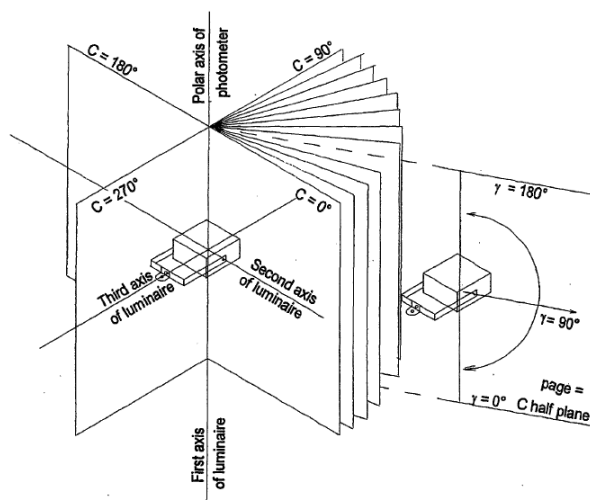


**Fig.2. Luminaire orientation for C,γ goniophotometry**

The first axis usually going through the photometric centre of luminaire and perpendicular to the light emitting area. The second axis lies within the plane  $C=0$ . The third axis is the long

axis of the luminaire. According to standard 13032-1 + A1, the axis of the luminaire is determined by the manufacturer or the photometric laboratory to clearly determine the location of the luminaire in the coordinate system for photometric measurements and for lighting calculations. In practice, we often encounter that the luminaire manufacturer does not specify the photometric axes of the luminaire. If specific instructions are not provided, then the plane containing the lower edge of the luminaire canopy should be taken as one reference and the longitudinal axis, determined from the outer edges of the luminaire when viewed in plan, should be taken as the second reference. In the case of square luminaires, there is a problem in determining the photometric axes of the luminaires. The photometric laboratory may identify and mark photometric axes before measuring the luminaire. Without such marking of the photometric axes on the luminaire, it is practically impossible to install the luminaire in a lighting system with the correct rotate. The measurement of photometric parameters is performed on 1 sample and it may happen that based on the marking of the axes of this sample it is not possible to mark other manufactured luminaires of this type. This is due to the use of optical materials whose directional orientation is not visible. Examples of such materials may be microprismatic diffusers or opto-mechanical nanostructures [5, 6].

The measurement accuracy is influenced by several possible sources of errors, which can be caused, for example, by the construction of the measuring instrument (goniophotometer), the conditions in the laboratory and, last but not least, by the accuracy of the lighting technician. The last-mentioned fact is closely related to one of the problems of square and spherical luminaires. The curves of these luminaires may at first glance look like rotationally symmetrical, and the lighting technician can simply erroneously evaluate that it will be sufficient to measure only 1 plane C as allowed by the standard STN 13032-2 and subsequently to make the curve symmetry. Such measurement saves a lot of time but at the cost of measurement accuracy. As shown in Figure 3, these luminaires may not always have a luminous intensity distribution curve symmetrical [7, 8].

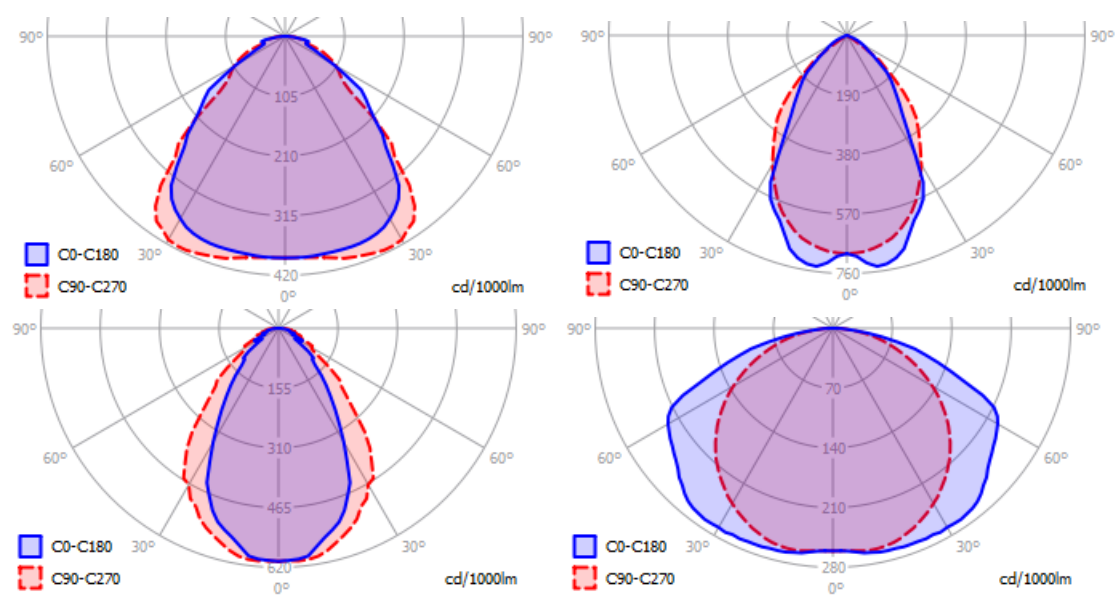


**Fig.3. An example of luminous intensity distribution curve of square luminaires 1-4**

### Design of lighting systems

The procedure for designing the lighting system is clearly given and based on normative requirements. The first step of the design is to model a certain space (interior or exterior) with all the necessary parameters such as the reflectance of surfaces, the positioning of objects and



windows, and the determination of the maintenance factor. The second step is usually the placement of computational areas or points, for example at the place of visual activity. In the third step, the luminaires are inserted into the modeled space. Computing software offers various luminaire arrangement options:

- rectangular arrangement
- polygonal arrangement
- circular arrangement
- line arrangement
- place individual luminaire
- automatic arrangement for space

In addition to the "circular arrangement" option, all other types of luminaires insertion add the luminaires to the room so that the angle of rotation about the vertical Z-axis is 0 °. In the case of square luminaires with an asymmetrical luminous intensity curve, the rotation of the luminaire shall be determined according to the luminous intensity curve, for example in a 3D view. This view is shown in Figure 4.

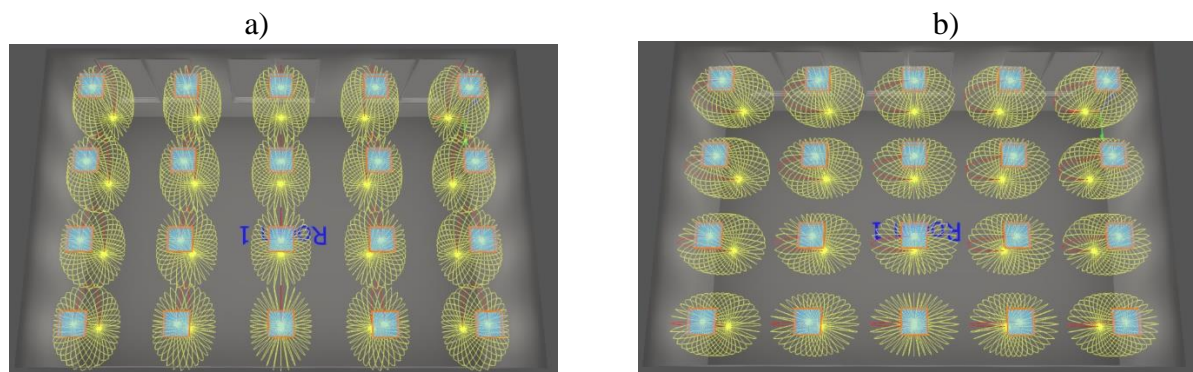


**Fig.4. a) Luminaires with Z-axis rotation = 0° b) Luminaires with Z-axis rotation = 90°**

The previous figures also show that the designer can turn the luminaires in the calculation software. However, in the case of square luminaires, the resulting rotation cannot be clearly determined from the lighting system documentation. In the documentation, which is generated by the calculation software, the arrangement of the luminaires as well as their rotation is usually mentioned. An example of such output is given in Table 1. The information about the rotation of a square or spherical luminaire has no telling value since it is often not possible to determine its axes with this type of luminaire.

**Table 1. Information on the position and rotation of luminaires**

Luminaire	Position [m]			Rotation [°]		
	X	Y	Z	X	Y	Z
1	9,9	1,04	3,2	0	0	0
2	3,24	1,04	3,2	0	0	0

Figures 5 and 6 show the arrangement of square luminaires. This output is generated by lighting design software. The images are the same, so it is not possible to determine the rotation of the luminaire.



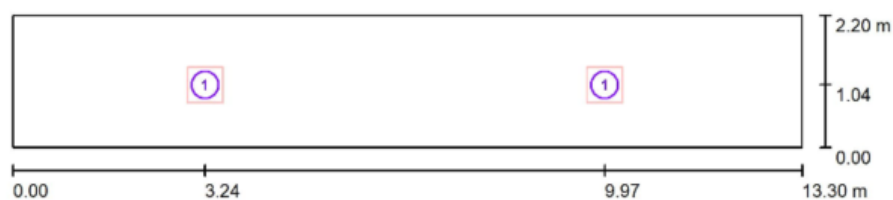


Fig.5. Arrangement of luminaires with rotation about Z-axis = 0 °

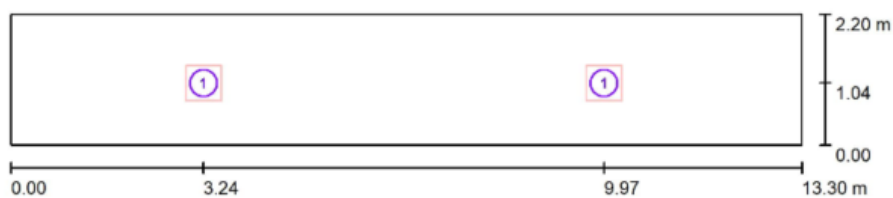


Fig.6. Arrangement of luminaires with rotation about Z-axis = 90 °

### Simulation results

To compare the influence of 90° rotation of the luminaires around the Z-axis, simulations were performed in three calculation software. The visualizations of the rooms in each software are shown in Figure 7.

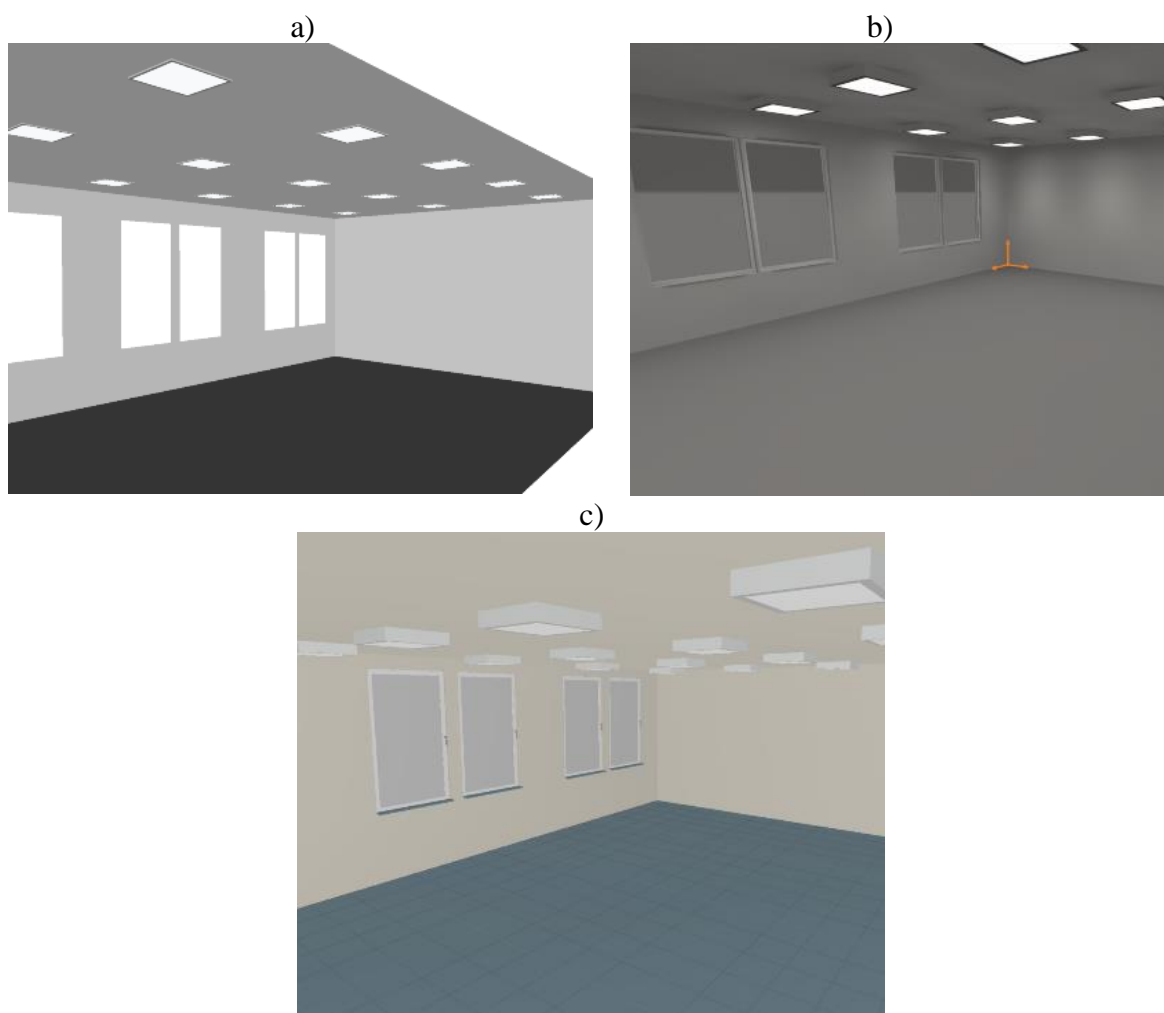


Fig.7. Visualisation of modelled room

A narrow corridor and a wide classroom were modeled in each computational software. The same dimensions, surface reflectivity, maintenance factors, dimensions and position of the windows were set in the rooms. Square luminaires were inserted into each project, the luminous intensity distribution curves of which are shown in Figure 2. A narrow corridor and a wide classroom were modeled in each computational software. The same dimensions, surface reflectivity, maintenance factors, dimensions and position of the windows were set in the rooms. Square luminaires were inserted into each project, the luminous intensity distribution curves of which are shown in Figure 2.

The calculated parameters were:

- average maintained illumination  $\bar{E}_m$
- uniformity of illumination  $U_0$
- UGR

Tables 2 to 8 show the results of the simulations.

**Table 2. Calculated parameters of the lighting system in the corridor where was used the luminaire no. 1**

LUMINAIRE 1									
	Tool 1			Tool 2			Tool 3		
	Z=0°	Z=90°	Δ (%)	Z=0°	Z=90°	Δ (%)	Z=0°	Z=90°	Δ (%)
$\bar{E}_m$ (lx)	132	136	2,9	132	137	3,6	129	133	3
$U_0$ (-)	0,53	0,56	5,4	0,53	0,57	7	0,51	0,53	3,8
UGR (-)	20	20	0	19,5	19,6	0,5	20,6	20,4	-1

**Table 3. Calculated parameters of the lighting system in the corridor where was used the luminaire no. 2**

LUMINAIRE 2									
	Tool 1			Tool 2			Tool 3		
	Z=0°	Z=90°	Δ (%)	Z=0°	Z=90°	Δ (%)	Z=0°	Z=90°	Δ (%)
$\bar{E}_m$ (lx)	125	133	6	126	134	6	125	134	6,7
$U_0$ (-)	0,67	0,69	2,9	0,74	0,75	1,3	0,71	0,71	0
UGR (-)	19	23	17,4	18,7	22,2	15,8	21,1	25,1	15,9

**Table 4. Calculated parameters of the lighting system in the corridor where was used the luminaire no. 3**

LUMINAIRE 3									
	Tool 1			Tool 2			Tool 3		
	Z=0°	Z=90°	Δ (%)	Z=0°	Z=90°	Δ (%)	Z=0°	Z=90°	Δ (%)
$\bar{E}_m$ (lx)	148	145	-2,1	149	146	-2,1	145	142	-2,1
$U_0$ (-)	0,4	0,34	-17,6	0,4	0,33	-21,2	0,39	0,32	-21,9
UGR (-)	20	18	-11,1	19,7	17,8	-10,7	20,6	18,3	-12,6

**Table 5. Calculated parameters of the lighting system in the corridor where was used the luminaire no. 4**

LUMINAIRE 4									
	Tool 1			Tool 2			Tool 3		
	Z=0°	Z=90°	Δ (%)	Z=0°	Z=90°	Δ (%)	Z=0°	Z=90°	Δ (%)
$\bar{E}_m$ (lx)	139	126	-10,3	140	126	-11,1	135	122	-10,7
$U_0$ (-)	0,43	0,34	-26,5	0,43	0,33	-30,3	0,43	0,33	-30,3
UGR (-)	21	17	-23,5	20,1	16,4	-22,6	20,8	18,1	-14,9

**Table 6. Calculated parameters of the lighting system in the classroom where was used the luminaire no. 1**

LUMINAIRE 1									
	Tool 1			Tool 2			Tool 3		
	Z=0°	Z=90°	Δ (%)	Z=0°	Z=90°	Δ (%)	Z=0°	Z=90°	Δ (%)
$\bar{E}_m$ (lx)	527	525	-0,4	517	515	-0,4	522	523	0,2
$U_0$ (-)	0,67	0,67	0	0,64	0,64	0	0,82	0,85	3,5
UGR (-)	19	19	0	18,7	19,5	4,1	20,2	20,9	3,3

**Table 7. Calculated parameters of the lighting system in the classroom where was used the luminaire no. 3**

LUMINAIRE 3									
	Tool 1			Tool 2			Tool 3		
	Z=0°	Z=90°	Δ (%)	Z=0°	Z=90°	Δ (%)	Z=0°	Z=90°	Δ (%)
$\bar{E}_m$ (lx)	524	521	-0,6	515	517	0,4	553	550	-0,5
$U_0$ (-)	0,63	0,66	4,5	0,65	0,62	-4,8	0,81	0,72	-12,5
UGR (-)	16	17	5,9	16,7	16,9	1,2	19,9	22,3	10,8

**Table 8. Calculated parameters of the lighting system in the classroom where was used the luminaire no. 4**

LUMINAIRE 4									
	Tool 1			Tool 2			Tool 3		
	Z=0°	Z=90°	Δ (%)	Z=0°	Z=90°	Δ (%)	Z=0°	Z=90°	Δ (%)
$\bar{E}_m$ (lx)	605	608	0,5	593	597	0,7	580	588	1,4
$U_0$ (-)	0,71	0,65	-9,2	0,69	0,59	-16,9	0,79	0,89	11,2
UGR (-)	18	19	5,3	18,5	18,5	0	19,4	19,3	-0,5

## Conclusion

From the calculated values it follows that the rotation of the square luminaire by 90 degrees has a significant influence on the calculated parameters of the lighting system. The biggest change in average maintained illumination was achieved with the luminaire no. 4 which was used in the corridor. This change was -11,4%. Changes of the average maintained illumination in the classroom were minimal. The significant influence of luminaire rotation was on parameter U0 too. In the corridor, there was the biggest difference of this parameter after turning the luminaire by 90 degrees - 30.3% and in the classroom -16.9%. The UGR parameter was also influenced by changing the rotation of the luminaires around the Z-axis. The biggest change in UGR was recorded in a narrow corridor where there was a difference 23,5%. The results show that the designer must also consider the possibility that the lighting system will be realized with luminaires turned 90 degrees. Especially for square and spherical luminaires where it is not possible to determine the longitudinal axis of the luminaire, the designer should verify the effect of the rotation of these luminaires. The consequent financial costs associated with rotating the luminaires in the finished lighting system can be high.

## References

- [1] STN EN 12464-1. Light and lighting. Lighting of work places. Part 1: Indoor work places.
- [2] Act no. 555/2005 Coll. on the energy performance of buildings
- [3] CIE 121:1996 The Photometry and Goniophotometry of Luminaires.
- [4] Schwanegel, Ch. Comparison of techniques for measuring luminous intensity distribution overall and across segments. s.l. : TechnoTeam Bildverarbeitung GmbH.
- [5] Light and Lightings – Measurement and Presentation of Photometric Data of Lamps and Luminaires – Part 1 : measurement and File Format.
- [6] Ing. Mácha, M. Opto-mechanical Nanostructures for Overcoming Fundamentals in Optics Design. Lumen V4, 2014, Visegrád, Hungary.
- [7] CIE 198:2011. Determination of Measurement Uncertainties in Photometry. ISBN 978-3-902842-00-8.
- [8] STN EN 13032 - 2. Light and lighting. Measurement and presentation of photometric data of lamps and luminaires. Part 2: Presentation of data for indoor and outdoor work places.



## PHOTOMETRIC PARAMETERS OF LED LUMINAIRES WITH SWITCHABLE CORRELATED COLOUR TEMPERATURE

*Marek Mokráň, Roman Dubnička, Peter Janiga*

Faculty of electrical engineering and information technology

Slovak University of Technology in Bratislava

Bratislava, Slovakia

marek.mokran@stuba.sk

### Abstract

*At present, there are lights on the market that are capable of emitting white light with an adjustable correlated color temperature. The advantage of these luminaires is the possibility of changing the correlated color temperature, for example, due to a change in the function of the room in which they are installed, with no replacement of the lamps. The disadvantage of such a correlated color temperature setting is that this setting is performed directly on the luminaire and it is not possible to set the correlated color temperature with the control system. When changing the color temperature, in most cases, it is undesirable to change the other photometric parameters. In this paper, attention is paid to changes of the photometric parameters caused by changing the correlated color temperature.*

### Key words

*LED, correlated colour temperature, luminous flux, tunable-white*

### Introduction

In the past, the colour temperature was fixed to a light source. Tunable-white lighting is one of the biggest trends in commercial lighting. Emerging studies on health, comfort, and productivity suggest that being able to change, or tune, the colour temperature of a light source to match the needs of the application, event, or occupant preference has significant benefits. Luminaires with switchable correlated colour temperature are determined where the future is expected a change in the functionality of the room. Sometime in the future, you might have plans to redecorate your living room and go from an ordinary, homely ambient tone to something whiter and more modern. Rather than replacing all of your lights to keep up with their new environment, you just change their colour temperature and keep them. When changing correlated colour temperature, it is expected that other photometric parameters will change only minimally. Luminaire manufacturers often indicate photometric parameters for only one correlated colour temperature. Change of photometric parameters can be dependent on the method used for changing correlated colour temperature and installed light sources [1].

### Methods used to change the correlated colour temperature

There are several methods used to change the correlated colour temperature. Each method has its advantages and disadvantages. Selecting luminaire with a suitable method of change correlated colour temperature is the designer's job and depend on the function of the room.

- **Tunable whites use color mixing**

Standard LED color-mixing uses red, green and blue channels that are adjusted to deliver the entire range of the color spectrum. Tunable-whites work in a similar way, using a number of controllable channels to adjust the color temperature of the luminaires white light output. The channels in a tunable-white system all produce white light, but with varying colour temperatures, from a warm tone to a cool tone. [1]

- **Simple system use two or more lines of LEDs**

The most basic tunable linear systems use LED strips mounted side-by-side. One channel has a correlated colour temperature close to 2700K, with the other one has correlated colour temperature around a 6000K. The LED strips can be mount inside an aluminium extrusion fitted with an opal diffuser, which does the colour mixing as the light passes through it [1].

- **Multi-chip versions do the mixing at chip level**

More products are using ‘multi-chips’ where a number of tiny LED chips are combined into the same module. This means that the color mixing occurs as the light leaves the module. Their very small size means that tunable-white products can be made much smaller. These multi-chips tend to have a higher performance specification than the individual LED strips [1].

Changing the color temperature is done differently on each luminaire. Some luminaires with switchable correlated color temperature are adjustable by small dip switches that are located either on the front or on the back of the luminaire. Also known as CCT (correlated colour temperature) adjustable downlights, these types of lights provide you with the ability to change the colour temperature. Within one downlight, you have multiple colour temperatures that range from warm white to cool white. The variation of colour temperature ranges from each brand. The dip switch design should be called CCT select-able. The luminaire with dip switch is shown in the figure 1 and 2. Luminaires with a switch in the front have the advantage that the user is able to make a colour change. Luminaires with a switch located at the rear can have a more attractive design, but to switch correlated colour temperature is necessary to remove the luminaire [1] [2]. Figure 3 shows a typical spectral radiant flux distribution curves of LEDs used for adjusting correlated colour temperature.



**Fig. 1. Luminaire with dip switch on the front**





**Fig. 2. Luminaire with dip switch on the back**

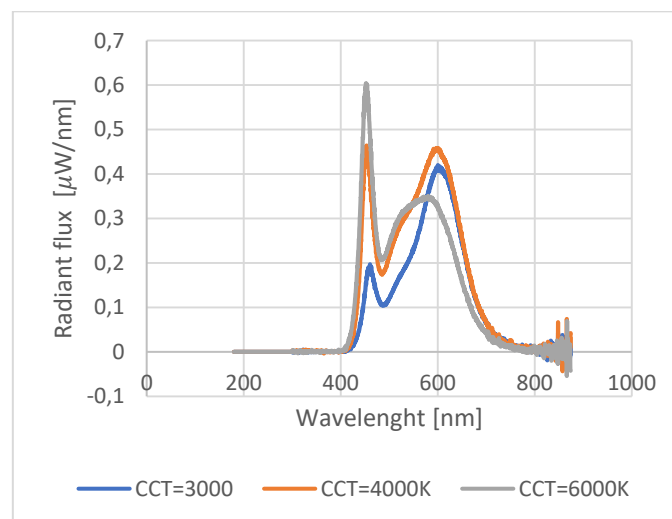


**Fig. 3. Spectral radiant flux distribution curves**

## Measurement

Devices under test were luminaire with switchable correlated color temperature. The luminaires use three lines of LEDs with different correlated colour temperature. Switching between correlated color temperature was performed by the dip switch placed on the back of the luminaire. Measurement of luminous intensity distribution curves was measured on the far-field goniophotometer. The goniophotometer used for the measurement is shown in figure 4. Luminous flux was measure in photometric integrator spherical with a diameter of 3 meters. Photometric integrator spherical is shown in figure 5. The measurement was performed according to STN EN 13032-4 - Light and lighting - Measurement and presentation of photometric data of lamps and luminaires. Part 4: LED lamps, modules and luminaires [3].

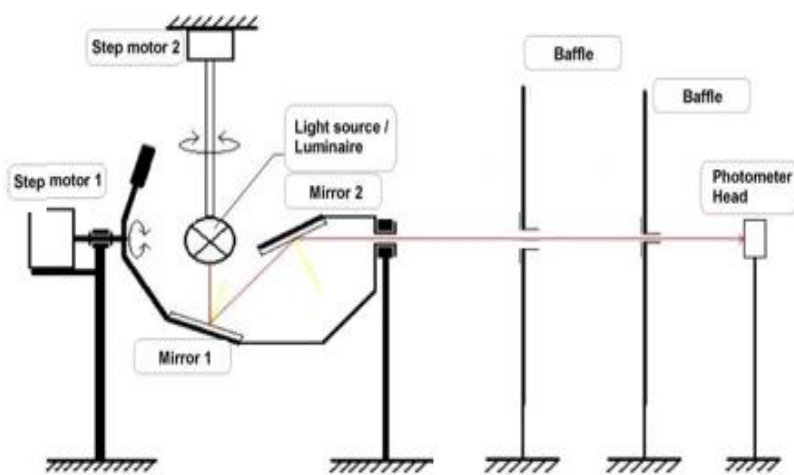


Fig. 4. Farfield goniophotometer

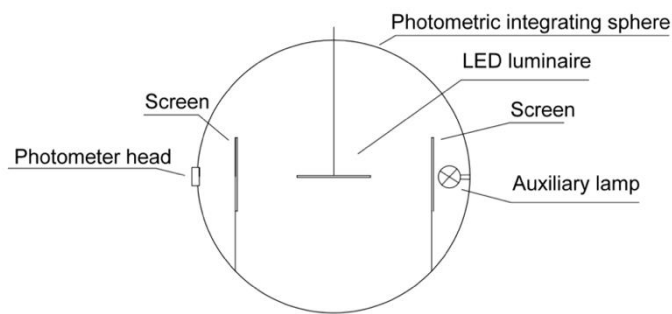


Fig. 5. Fotometric spherical integrator

The measurement results are shown in tables 1, 2 and in figures 6, 7 and 8.

Expanded uncertainty of measurement is shown in table 3. The reported expanded uncertainty of measurement in table 1 is stated as the standard uncertainty of measurement multiplied by the coverage factor  $k=2$ , which for a normal distribution corresponds probability of approximately 95%.The standard uncertainty of measurement has been determined in accordance with EA-4/02 [4].

Table 1. Measurements results I

Tested samples	Measured parameters			
	$Ra$ [-]	$CCT$ [K]	$\phi$ [lm]	Luminous efficacy [lm/W]
LED 1 / 3000K	82	2858	959	58,96
LED 1 / 4000K	88	3905	1223	80,67
LED 1 / 6000K	87	5937	1104	67,44
Declared by the manufacturer	> 80	-	1200	-
LED 2 / 3000K	83	2796	431	50,68
LED 2 / 4000K	87	3738	521	65,06
LED 2 / 6000K	87	5425	491	58,05
Declared by the manufacturer	> 80	-	600	-
LED 3 / 3000K	82	2836	914	54,87
LED 3 / 4000K	87	3865	1137	71,07

Tested samples	Measured parameters			
	<i>Ra</i> [-]	<i>CCT</i> [K]	$\phi$ [lm]	<i>Luminous efficacy</i> [lm/W]
LED 3 / 6000K	86	5970	991	57,3
Declared by the manufacturer	> 80	-	1200	-
LED 4 / 3000K	83	2889	1663	69,34
LED 4 / 4000K	88	3910	2012	90,72
LED 4 / 6000K	87	6231	1742	72,52
Declared by the manufacturer	> 80	-	2000	-

Table 2. Measurement results II

Power of tested samples	Correlated colour temperature of luminaires		
	3000K	4000K	6000K
LED 1 P [W]	16,27	15,16	16,37
LED 2 P [W]	8,51	8,01	8,46
LED 3 P [W]	16,66	16,01	17,11
LED 4 P [W]	23,99	22,18	24,02

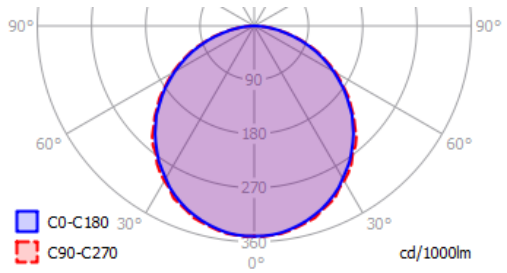


Fig.6. Light distribution curve / CCT=3000K

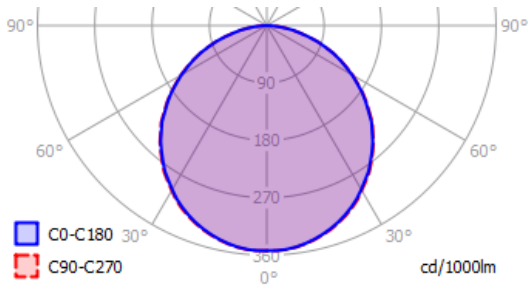


Fig. 7. Light distribution curve / TCC=4000K

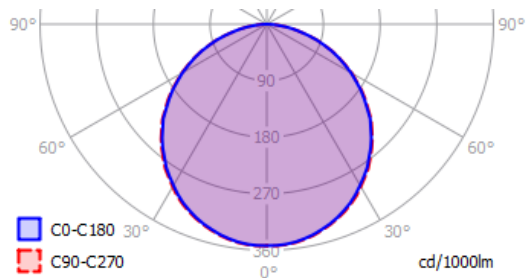


Fig. 8. Light distribution curve / TCC=6000K

Table. 3. Expanded uncertainty of measurement

<i>Parameter</i>	<i>Expanded uncertainty U (k=2)</i>
$\phi$ [lm]	7,5%
P [W]	1,0%
Ra [-]	2
TCC [K]	200K
Luminous efficacy [lm/W]	6,6%

### Simulations in software Dialux evo

The problem that may occur when using the photometric parameters specified by the manufacturer is described in this chapter. Photometric parameters of the luminaires with switchable correlated colour temperature are often given for only one correlated colour temperature or generally for the luminaire. The measurement results in the previous chapter show that the photometric parameters are different for each correlated colour temperature. In our case, the parameters declared by the manufacturer correspond to the measured parameters only at a correlated colour temperature of 4000K. The problem that arises from the above is shown in simulation in the Dialux software. The office visualization used to compare simulations is shown in figure 9. The office project has been designed according to STN EN 12464-1 Light and work lighting. Part 1: Indoor work places [5]. In the first design, were used luminaires LED 4 with a correlated colour temperature of 4000k because of their photometric parameters correspond to photometric parameters declared by the manufacturer. The number of luminaires and their location are chosen to meet the lighting requirements of the aforementioned standard. In the next designs, the luminaires were replaced with luminaires with another correlated colour temperature without changed place and number of luminaires. The simulation results are shown in table 4.



Fig. 9. Office visualization in Dialux Evo 8

**Table 4. Calculated parameters with Dialux software**

Calculated parameters	Correlated colour temperature of luminaire			Required parameters
	3000K	4000K	6000K	
Vertical illuminance of visual task $\bar{E}_m$ [lx]	457	549	478	> 500
Vertical Illuminance of surrounding area [lx]	457	551	479	> 300
Vertical Illuminance of background area [lx]	435	526	456	> 100
$U_0$ [lx]	0,88	0,89	0,88	> 0,6

## Conclusion

The main advantage of luminaires with switchable correlated colour temperature is that you do not depend with one colour temperature and you can change it depending on the function of the room. Providing you with the flexibility to make a change whenever you want to. Without needing any electricians and without any additional costs. When designing the lighting system, the designer must consider that during the operation the lamps will changing the correlated colour temperature and thus the other photometric parameters as a luminous flux and colour rendering index. The measurement results show that the change in luminous flux can be more than 20%. The manufacturer of the samples tested gave uniform photometric parameters for all correlated colour temperature however it is necessary to specify the photometric parameters separately for each correlated colour temperature. As figures 6, 7 and 8 show light distribution curves did not change their shape when changing correlated colour temperature. The shape of the light distribution curves does not change due to the use of a microprismatic optical system and a suitable LED lines layout. The simulation results confirmed that the designer must not rely on the photometric parameters declared overall for the luminaire with switchable correlated colour temperature.

## References

- [1] C. Horridge, "Colour temperature switchable downlights compared." Internet: <https://www.downlightsdirect.co.uk/advice/downlights/colour-temperature-switchable-downlights/>, Feb. 1, 2018 [June 26, 2018]
- [2] I. Goswami, (2016, Oct.) "Explore and control LED-based tunable-white lighting." LEDs Magazine, [Online]. 13 (8), pp. 45-47. Available: <http://digital.ledsmagazine.com/ledsmagazine/201610?WS1016&pg=49#pg49> [July 3, 2018]
- [3] STN EN 13032-4. 2017. Light and lighting - Measurement and presentation of photometric data of lamps and luminaires.
- [4] EA-4/02 M. 2013. Evaluation of the uncertainty of measurement in calibration.
- [5] STN EN 12464-1. 2012. Light and lighting. Lighting of work places.Part 1:Indoor work places



## ENERGY-EFFICIENT STREET LIGHTING SYSTEM OF THE CITY OF SHTIP USING SOLAR ENERGY AND LED TECHNOLOGY

*Filip Majstorski<sup>1</sup>, Vlatko Chingoski<sup>2</sup>*

<sup>1</sup>Faculty of Electrical Engineering, University “Goce Delcev” Shtip, Macedonia,  
filip.20248@student.ugd.edu.mk

<sup>2</sup>Faculty of Electrical Engineering, University “Goce Delcev” Shtip, Macedonia,  
vlatko.cingoski@ugd.edu.mk

### Abstract

*This paper deals with two currently very important energy issues, the increase of energy efficiency and sustainable energy development. For living standards, street lighting is unavoidable conformity that, in general, consumes a significant amount of electric power due to prolonged utilization period, and many lighting sources with significant-rated power and modest life expectancy.*

*In this paper, the authors proposed the replacement of the existing street lighting system of the part of the city of Shtip with a new, energy-efficient, and environmentally friendly, and energy sustainable system. The proposed system utilizes renewable solar energy sources and the replacement of the existing and obsolete streetlight bulbs with new and highly efficient light bulbs based on LED technology. The comparative analysis is given from technological and financial viewpoints proving that this new system could easily repay investments in the period less than two years. Although the initial investments might look too large, the operation and maintenance of the proposed system including payment for consumed electricity justify not partial, but replacement of the entire city street lighting system.*

**Keywords:** *renewable energy sources, solar energy, street lighting, LED bulbs*

### Introduction

The gradually growing requirement of energy and the limited resource of traditional energy sources has become a challenge for both developed and developing countries. Until now, people around the globe depend on fossil fuels for their energy needs. Fossil fuels are limited in amount, expensive, and polluting the environment. Therefore, a lot of research and developments have been proposed to solve those serious problems. One of the ways is to utilize renewable energy resources. Such resources are free of cost and available in abundance. Solar energy is the amplest, direct, and clean form of renewable energy. Total solar energy absorbed by the Earth is about 3,850,000 (EJ) in one year, which is even twice as much as all the non-renewable resources on the earth found and used by a human being, including coal, oil, natural gas, and uranium. [1], [5].

Taking this idea into consideration, we are proposing the replacement of the existing street lighting system of the part of the city of Shtip with a new, energy-efficient, and environmentally friendly, and energy sustainable system. In this project, we are incorporating an “all-in-one” light monitoring system. [3], [2]

A solar street lighting system is a system consisting of LED lamps, and they can be dimmed or illuminated to any certain level depending on the user’s profile. The following are some of the present advantages of the use of solar street lighting over conventional lighting: [9], [10].



- 80% less energy use in addition to savings from high-efficiency lamps.
- 50% or more savings per year in operating and maintenance costs.
- Better living environments with more reliable and safer lighting.
- The ability to mix lamp technologies to suit the needs of the city and accommodate new lamp types.
- A tremendous reduction in CO<sub>2</sub> emissions.
- Longer lifespan of LED lamps compared to HPS lamps.
- Does not take any time for dimming and it is an instant process.

The solar street lighting system also has disadvantages which are as follows:

- The higher initial investment cost for upgrading from conventional lamps to LEDs.

### 1. Literature review

Macedonia has a very favorable geographical position where solar irradiation is large and convenient for installing solar systems for the use of solar energy, but unfortunately, it is rarely used. With about 280 sunny days per year and about 1,500 kWh/m<sup>2</sup> of solar irradiation, Macedonia is one of the countries with the highest solar irradiation in Europe, but not in the countries using that energy the most. For example, Germany and Austria produce 100 times more electricity from solar energy, though they have 30-40% less solar irradiation compared to Macedonia [13].

The Municipality of Shtip is in the central-eastern part of the Republic of Macedonia between 41°31'15 " and 41°44'25 " north latitude and 22°10 'and 22°13' east longitude. The area of the Municipality of Shtip is characterized by increased duration of the solar irradiation. On average, there are 2,370 sunny hours per year or an average of 6.5 sunny hours per day. The maximum number of sunny days is observed in July and the minimum in December. The distribution of sunny days and other meteorological data for this region are given in Table 1, [13].

**Table 1: Meteorological data including solar insolation at the location of city of Shtip [13]**

Shtip Macedonia	I	II	III	IV	V	VI	VII	VIII	IX	X	XI	XII
Insolation [kWh/m <sup>2</sup> /day]	1.69	2.33	3.31	4.09	5.20	6.14	6.38	5.58	4.09	2.66	1.69	1.37
Clearness, 0-1	0.44	0.44	0.45	0.43	0.48	0.53	0.57	0.56	0.50	0.44	0.40	0.40
Temperature, °C	-2.65	-0.89	3.70	9.26	14.76	18.52	21.01	21.06	16.37	10.36	3.68	-1.61
Wind speed, m/s	4.12	4.24	4.02	3.89	3.51	3.33	3.57	3.57	3.67	3.92	3.93	4.21
Precipitation, mm	34	33	38	42	61	53	42	36	35	43	55	44
No. of Wet days	8.9	9.0	9.6	10.6	11.9	9.6	6.7	6.4	5.6	7.1	9.2	10.3

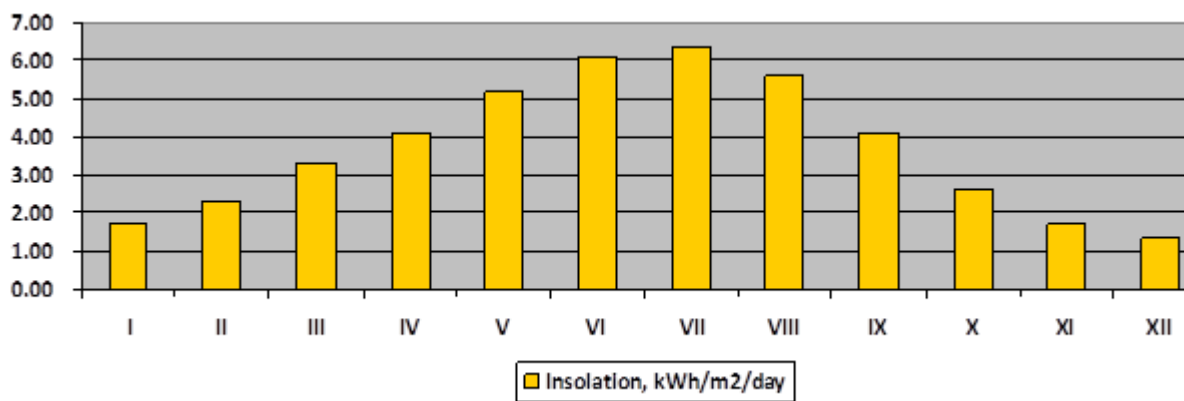


Fig. 1: Average kWh/ m² per day by months of 2016, the city of Shtip [13]

## 2. Data collection and analysis

In this project, we are investigating the potential replacement of the existing street lighting system at the central part of Shtip with an energy-efficient photovoltaic (PV) LED lighting system. This street represents the city/center area, along the river Otinje. Besides this part are the building of the Municipality of Shtip, Basic Court Shtip, Rectorate of UGD, Hotel Oaza, and many other buildings and institutions, where there is constant movement and where the conditions for the street lighting should be without any defects and interventions and to be constant in function [4].



Fig. 2. Aerial view of the location under investigation.

Source: <http://www.google.maps.com>

Table 2: Basic data for the investigated location.

Street	Poles	Lamps
2,030m length	68 poles; Height 10m each; Distance between them: 30m	68 lamps; HPS = 23 (400W) Mercury bulbs = 45 (250W)

3. Technical data for the SSL system under investigation

For replacing the existing traditional solar lighting system based on mercury/HPS lamps, we are providing LED lamps with solar panels and battery attached or built into it, shortly called solar street lighting system (SSLS).

The proposed high-quality LED lamps powered by a solar panel shown in Fig. 3, are made of high-quality materials and can be rotated and adjusted according to local needs, i.e., to be in a position where most of the day the sun's rays can fall on it. Other main properties of this streetlight system are: [14]

- Connector for rain protection - Aluminum cable output screw with a rubber plug, 2-level water protection that allows the lamps to withstand even the heaviest rain for a long period.
- Solar panels are made of high-quality material with a lifespan of about 25 years.
- Diamond Reflector - a glossy base that is made of light aluminum material and at the same time increases the light intensity by 30%.
- Li LiFePO4 battery - a very durable battery. About 2000 times charge and discharge cycle, 4 times more than lithium battery, 8 times more than a lead-acid battery.



Fig. 3: Proposed LED street lights with solar panels.

Source: <http://www.minsenslight.com/sale-12389543-remote-control-integrated-solar-led-street-light-50w-100w-200w-300w-longlife.html>

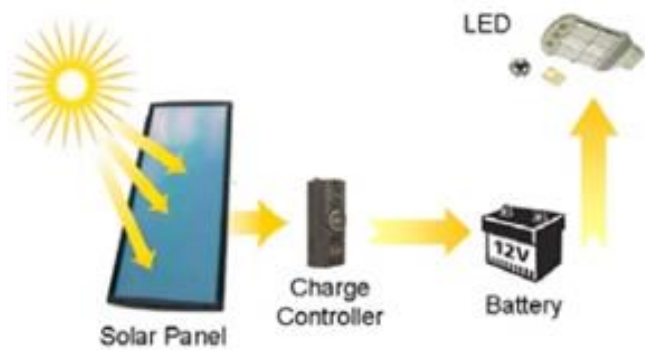
The main technical characteristics of the proposed equipment for this SSLS system are given in Table 3: [6], [7], [14].

Table 3: Technical data for the proposed SSL system including solar panels.

Model	MINSENS MS 32 C - 50W
Lamp	50W
Solar panel	High-efficiency polysilicon Solar Panel – 6V 20W
Lithium iron phosphate build-in battery	LiFePO4 battery – 18AH
Lighting angle	120 degrees
Number of working hours	12-14 hours per day
Battery discharge time	3-5 days without sun
Lamp life expectancy	50,000 hours

<b>Operation at low/high temp.</b>	From -20 to 60
<b>Battery charging time</b>	6-8 hours
<b>Price</b>	115euro / 7049.5denars
<b>Guarantee provided</b>	3 years

According to the principle of the photovoltaic effect, these solar panels receive solar radiation during the daytime and then convert it into electrical energy through the charge and discharge controller, which is finally stored in the battery. When the light intensity is reduced to about 10 lx during the night and the open-circuit voltage of the solar panels reaches a certain value, the controller has detected voltage value and then acts. The battery offers the energy to the LED light to drive the LED to emit visible light in a certain direction. Battery discharges after a certain time passes, the charge and discharge controller will act again to end the discharging of the battery to prepare the next charging or discharging again [6], [8].



**Fig. 4: Basic operation principle of the proposed street lighting system.**

Source: <https://www.elprocus.com/solar-powered-led-street-light-control-circuit/>

#### 4. Project economics

Table 4 presents the cost for the operation of the existing (traditional) lighting.

**Table 4: Existing cost for operation of the existing lighting system.**

Traditional street lighting consumption	Quantity	Consumption [kWh] Monthly / Annual	Costs Annual
Mercury lamps	45 (250W)	3.37 / 41.06 MWh	228,307.5 MKD /3,724.4 euro
HPS lamps	23 (400W)	2.76 / 33.58 MWh	186,704.8 MKD / 3,045.7 euro
Maintenance & repairing	57,120 MKD / 931.8 euro		
<b>Total</b>	<b>68 lamps</b>	<b>74.64 MWh</b>	<b>472,132.3 MKD / 7,701.9 euro</b>

We can see from Table 4, that the annual consumption and costs from traditional street lighting are 74.64 MWh, or 472,132.3 denars (app. 7,701.9 euro). These costs are constant each year with changes in the amount of app. 1-2%. due to year-by-year changes in the maintenance & repairing costs.

To be able to make a comparison and calculate what is a difference between the existing traditional street lighting system and our new proposed SSL, we projected that in the last 3 years there was already installed our new SSL system [4].

Data from our research, e.g., number of sunny days, sunny hours, and rainy days in Shtip in the last 3 years, have been considered and it has been calculated how many days per year we will need electricity from the distribution network. The estimated data is presented in Table 6, including the initial investment cost for the replacement of the existing street lighting system with the proposed SSL system in 2018.

**Table 5: Projected operation characteristics for the newly proposed lighting system.**

	2018			2019			2020		
	Sunny days	Sunny hours	Duration of the day	Sunny days	Sunny hours	Duration of the day	Sunny days	Sunny hours	Duration of the day
January	23	200	10	14	117	10	25	250	10
February	15	138,5	11	22	170,5	11	21	237,5	11
March	10	229	13	26	286	13	13	175,5	13
April	13	336,5	14	18	297	14	16	216	14
May	18	378	15	14	333,5	15	15	247	15
June	16	347	15	13	334,5	15	7	232,5	15
July	22	378,5	15	15	347	15	14	278,5	15
August	27	387,5	13	24	377	13	18	347,5	13
September	29	305	12	19	279	12	22	285	12
October	26	251	10	25	224	10	22	274	10
November	20	187	9	16	145	9	26	327	9
December	24	209,5	9	16	140	9	17	257	9

**Table 6: Estimated data for the proposed SSL system.**

SSL System	2018	2019	2020
Number of days the system needs electricity from a distribution network	15	11	11
Annual consumption [kWh]	669.39	608.6	489.59
Annual cost	3,705.15 MKD (60.44 euro)	3,383.85 MKD (55.2 euro)	2,722.17 MKD (44.4 euro)
Procurement & installation cost	479,366 denars 7820 euro	/	/
Annual total cost	483,071.15 MKD (7,880.55 euro)	3,383.85 denars / 55.2 euro	2,722.17 denars / 44.4 euro

**Table 7: Cost comparison between both street lighting systems for three years period.**

	2018	2019	2020
Proposed SSLS	483,071.15 MKD (7,880.55 euro)	3,383.85 MKD (55.2 euro)	2,722.17 MKD (44.4 euro)
Conventional SLS	472,132.3 MKD (7,701.9 euro)	472,132.3 MKD (7,701.9 euro)	472,132.3 MKD (7,701.9 euro)

<b>Difference:</b> (- loose, + gain)	<b>-10,938.85 MKD</b> (-178.4 euro)	<b>468,748.4 MKD</b> (7,646.7 euro)	<b>469,410 MKD</b> (7,657.5 euro)
---	--	--	--------------------------------------

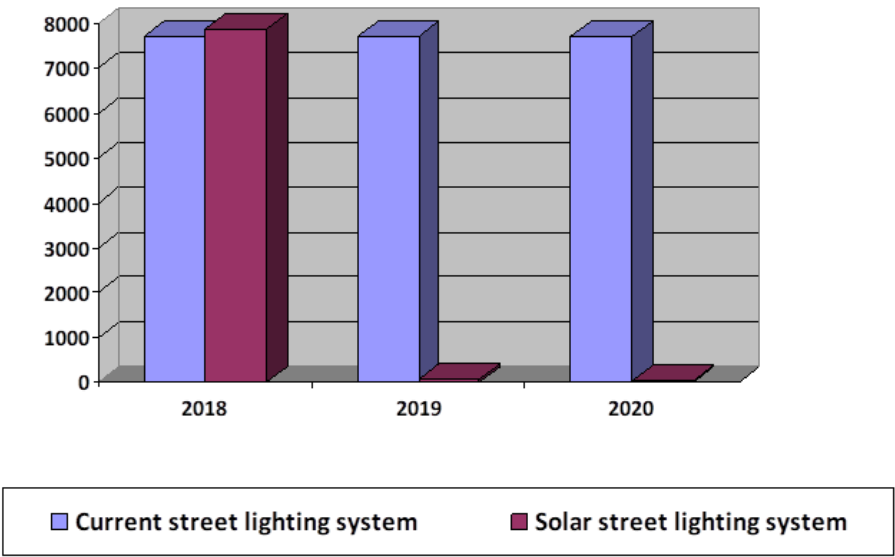


**Fig. 5: Comparison between conventional (existing) SLS and the proposed SSLS for a projected period of 3 years including initial investments during the first year.**

### 5. Conclusions

According to all projections, analyzes, and calculations, one can see that our proposed SSLS in place of the traditional sodium and mercury bulbs, is a very good investment.

The proposed SSL system provides the following benefits:

1. Reduce electricity consumption, and thus bills will be lower. This means that the funds can be saved or reallocated to other purposes.
2. Reduce the percentage and frequent breakdowns, and thus dark and unsafe streets.
3. Increased Street safety. In addition to traffic safety, reducing traffic accidents also reduces the number of thefts due to good lighting.
4. Significantly reduced the number of emissions of polluting particles, and thus cleaner air in the winter, where there is a lot of polluted air due to heating and exhaust fumes from cars.

Speaking about the investments, the Municipality of Shtip can easily manage and deal with this whole project. In respect of funding the project, the Municipality of Shtip can afford this investment. Additionally, there are other ways for partial or entire financing this project such as NGO’s grants, various Embassies, and other international organizations that approve funding for projects related to the use of renewable energy and solar energy, or through a public-private partnership, as is the case for some other cities in Macedonia for such and similar projects realized in the past.



## References:

- [1] Cingoski, Vlatko: Renewable energy sources, Lecture 1-12, 2018.
- [2] Boyle, Godfrey: *Renewable energy*. U.K Oxford University Press, May 2004.
- [3] M. Masters, Gilbert: *Renewable and Efficient Electric Power Systems*. New Jersey, 2004.
- [4] Strategy for rural development of the Municipality of Shtip 2012-2017. Available online at: [http://bregalnica-ncp.mk/wp-content/uploads/2016/07/pod\\_strategija\\_za\\_ruralen\\_razvoj\\_na\\_Opstina\\_Stip\\_2012\\_2017.pdf](http://bregalnica-ncp.mk/wp-content/uploads/2016/07/pod_strategija_za_ruralen_razvoj_na_Opstina_Stip_2012_2017.pdf)
- [5] “Alternative Energy”, Available online at: <http://www.altenergy.org/renewables/solar.html>
- [6] “HPS: How it Works”. Available online at: <http://www.edisontechcenter.org/SodiumLamps.html>
- [7] “Comparison Chart LED Lights vs. Incandescent Light Bulbs vs. CFLs”. Available online at: [https://igpny.com/wp-content/uploads/2017/11/LL88-LED-vs-Incandescent-Comparison-Chart-page-link\\_.pdf](https://igpny.com/wp-content/uploads/2017/11/LL88-LED-vs-Incandescent-Comparison-Chart-page-link_.pdf)
- [8] Y. Fujii, N. Yoshiura, A. Takita, and N. Ohta: “*Smart streetlight systems with energy-saving function based on the sensor network*”. Berkeley, CA, United States, 2013.
- [9] Cost benefits of Solar-powered LED street Lighting system. Available online at: [https://www.researchgate.net/publication/328125462\\_Cost\\_Benefits\\_of\\_Solar-powered\\_LED\\_Street\\_Lighting\\_System\\_Case\\_Study\\_AUS](https://www.researchgate.net/publication/328125462_Cost_Benefits_of_Solar-powered_LED_Street_Lighting_System_Case_Study_AUS)
- [10] The PV Led Engine. Available online at: [https://www.researchgate.net/publication/282909459\\_PV\\_LED\\_ENGINE\\_characterization\\_lab\\_for\\_standalone\\_light-to-light\\_systems](https://www.researchgate.net/publication/282909459_PV_LED_ENGINE_characterization_lab_for_standalone_light-to-light_systems)
- [11] Solar Street Lighting – Department of Energy. Available online at: <https://www.energy.gov/sites/prod/files/2018/11/f57/Allery-2018-solar-street-lighting.pdf>
- [12] Ultimate Guide for Solar Street Lights. Available online at: <https://www.lightinus.com/wp-content/uploads/2017/06/Ultime-Guide-for-Solar-Street-Lights.pdf>
- [13] Solar electricity production. Available online at: [https://www.qsl.net/z33t/solarna\\_energija\\_mkd.html](https://www.qsl.net/z33t/solarna_energija_mkd.html)
- [14] Remote Control Integrated Solar LED Street Light. Available online at: <http://www.minsenslight.com/sale-12389543-remote-control-integrated-solar-led-street-light-50w-100w-200w-300w-longlife.html>



## NANOTECHNOLOGY-BASED BIOSENSORS IN DRUG DELIVERY SYSTEMS: A REVIEW

*Mihail Aleksandrov<sup>1</sup>, Maja Kukuseva Paneva<sup>2</sup>*

<sup>1</sup>Faculty of Medical Sciences, Goce Delcev University of Stip, Krste Misirkov, No. 10-A, 2000 Stip, Republic of North Macedonia; e-mail: [aleksandrovmihail32@gmail.com](mailto:aleksandrovmihail32@gmail.com)

<sup>2</sup>Faculty of Electrical Engineering, Goce Delcev University of Stip, Krste Misirkov, No. 10-A, 2000 Stip, Republic of North Macedonia; e-mail: [maja.kukuseva@ugd.edu.mk](mailto:maja.kukuseva@ugd.edu.mk)

### Abstract

*Going nano means not only the size of a matter will be reduced but also the matter can be manipulated on the molecular and atomic levels. As a result, it will bring many benefits. In the case of a nanoparticle or a quantum dot, for example, reducing the size will increase the surface activity and induce unique quantum effects (e.g., confinement of electrons or photons by controlling the densities of electron states or photon states). This in turn will lead to unprecedented electronic, optical, and magnetic properties of the nanoparticle and quantum dot. Furthermore, the ability to arrange and rearrange atoms and molecules at will in a material will help render novel physical and chemical properties for the material. In today's definition, biosensors are analytical devices that combine a biological-sensitive element with a physical transducer to selectively and quantitatively detect the presence of specific compounds in a given biological environment. The biological-sensitive element consists of biological receptors (as probes) made of molecular species such as antibodies, enzymes, or nucleic acids for binding the target analytes, and the physical transducer is for converting the biological recognition or binding event into an electrical or optical signal. Thus, from a material's viewpoint, today's biosensors consist of two major components: an organic part as the sensitive element and an inorganic part as the transducer element. Many progresses have been made in the development of lab-on-a-chip microscale devices, and surely these devices will become more compact and more functional with higher sensitivity, specificity, and reliability in terms of sensing and with higher controllability in terms of drug delivery as the field of nanobiotechnology advances, but full-fledged autonomous systems of biosensors for drug delivery applications may still be years away. Currently, the development of biosensors for drug delivery takes a slightly different route. As discussed in the Introduction, drug delivery systems have been evolving from the totally passive drug-carrying vehicles of the first-generation systems, the environmental-sensitive drug-carrying vehicles of the second-generation system, to the target-specific and bioactive drug-carrying vehicles of the third-generation systems. Following this route, one can see that by adding sensitive components to the drug delivery systems, integrated capabilities of biosensing and drug delivery can be realized. Thus, it is conceivable that the next-generation drug delivery systems could be biologically sensitive drug-carrying vehicles incorporated with an underlying transducer (e.g., optical or image based) for signal detection and communication. This route may eventually converge with the lab-on-a-chip route, leading to an autonomous system with both the diagnostic and therapeutic functionalities. But for now, one of the challenges in developing biosensitive drug delivery vehicles is to devise drug carriers that are biocompatible, resistive to biodegradation, resistive to host inflammatory and immunologic responses, and sensitive to specific targets, among other things. In addition, the drug carrier constructs should be highly effective in prolonged drug retention, especially for water-soluble drugs. Biological constructs such as liposomes are potentially good drug carrier materials due to their abilities to protect drugs from degradation and to target the specific site for action.*

**Key words:** analytical devices, biosensors, drug delivery, nano-biotechnology, nanoparticle, physicochemical properties, transducer.

## 1. Introduction

Nanotechnology is not a single technology or discipline but it encompasses various technologies that crosses sectors, such as nanomaterials, medicine, devices, fabrication, electronics, communication and energy. It is the ability to measure and to control matter at the nanometer scale. Nanotechnology deals with the generation and alteration of materials to nanosize ( $10^{-9}$  m) [1]. Nanomaterials based biosensors which represents the integration of material science, molecular and electrical engineering, chemistry and biotechnology can markedly improve the sensitivity and specificity of biomolecule detection, hold the capability of detecting or manipulating atoms and molecules, and have great potential in application such as biomolecular recognition, pathogen diagnosis and environment monitoring.

As per IUPAC, biosensor is defined as “A self-contained integrated device which is capable of providing specific quantitative or semi-quantitative analytical information using a biological recognition element which is in direct spatial contact with a transducer element”. Biosensor is a device that combines a biological recognition element with a physical or chemical transducer detects a biological product [2]. It is a probe that integrates a biological component with an electronic component to yield a measurable signal. These biosensors consists of five components: (1) bioreceptors that bind the specific form to the sample; (2) an electrochemical interface where specific biological processes occurs giving rise to a signal; (3) a transducer that converts the specific biochemical reaction in an electrical signal; (4) a signal processor for converting the electronic signal into a meaningful physical parameter and finally and (5) a proper interface to display the results to the operator [3].

Going “Nano” means not only the size of a matter will be reduced but also the matter can be manipulated on the molecular and atomic levels. As a result, it will bring many benefits. In the case of a nanoparticle or a quantum dot, for example, reducing the size will increase the surface activity and induce unique quantum effects (e.g., confinement of electrons or photons by controlling the densities of electron states or photon states). This in turn will lead to unprecedented electronic, optical, and magnetic properties of the nanoparticle and quantum dot. Furthermore, the ability to arrange and rearrange atoms and molecules at will in a material will help render novel physical and chemical properties for the material [4]. In the case of biosensing, at the component level going “Nano” means that the capability to sense and detect the state of biological systems and living organisms will be radically transformed by the emerging ability to control the patterns of matter on the nanometer scale. Such a radical transformation is expected to enable sensing at the single-molecular level and with parallel detection of multiple signals in living cells. At the systems level, going nano will help decrease the size of the active sensing element to the scale of the target species (to increase the sensitivity and decrease the lower detection limit), reduce the required volumes of the analyte reagent, and minimize the detection time [5]. Reducing the size of biosensors can also result in tiny devices which maybe deployable to any desired location in the body.

Biosensors can provide feedback control by recognizing changes in its surrounding physiological or biological fluid and then taking “action”, either in terms of simple movement of a device component or release of one or more drugs. In recent years we have seen an explosion in the field of such novel sensors and microfabricated devices for drug delivery [6]. Such devices provide a platform for well-controlled functions in the micro- or nano-level. They include nanoparticulate systems, recognitive molecular systems, biosensing devices, and

microfabricated and microelectronic devices. The synthesis and characterization of biomimetic gels for drug and protein delivery systems is a significant focus of recent research. There are numerous techniques for microfabrication of patterned polymer surfaces and microchips for medical devices [7]. While silicon has been the choice material for much of the research done, the methacrylates and acrylates could provide an inexpensive base for future work. Several applications have already been suggested including patterned surfaces for cell adhesion, biosensors, microfluidic devices, and arrays for chemical screening.

The physicochemical understanding of such hydrogels under the conditions of application is neither simple nor well developed. Considering that all these carriers are ionic hydrogels, and that several ionic and macromolecular components are involved, with associated thermodynamically non-ideal interactions, it is evident that analysis and prediction of their swelling and response behavior is rather complex [8].

Environmentally responsive hydrogels lend themselves naturally to utilization in microfabricated devices. Polymerization of the required monomers and crosslinking agents can be done by free-radical polymerization using UV light, thus enabling photolithographic techniques to be adjusted to pattern these materials on the microscale. When hydrogels are immobilized within microstructures, the ability of the hydrogel to function is improved. There are many advantages of utilizing hydrogels in this way. First, hydrogels can be deposited permanently in specific locations of a substrate where they can exhibit their unique physiologically responsive characteristics repeatedly. Second, the hydrogels mechanical failure is less of an issue when the primary action is swelling against a well-defined structure. While biosensors and sensing devices are usually made of nonbiodegradable sensing materials and substrates, environmentally sensitive hydrogel networks whose crosslinks are degradable by hydrolysis can have a significant advantage over their nondegradable counterparts [9].

## **2. Hydrogel-based biosensing**

Several decades of research have contributed to our understanding of stimuli-responsive hydrogels so that they can now be utilized in an abundance of sensing applications. A comprehensive knowledge of their physical and chemical properties exists along with how the materials interact with living systems [10]. Alongside, theory has evolved to explain the unique interaction of these systems with their environment and other external stimuli. Engineers are now poised to develop and utilize novel sensing systems that allow the biological processes of life to be monitored like never before.

Hydrogels are water-swollen hydrophilic crosslinked polymers, that do not dissolve in water or biological fluids because of chemical or physical crosslinks [11]. Certain hydrogels can sense changes in their environment on a molecular level, which lead to changes in their swollen volume. These are commonly referred to as environmentally responsive hydrogels. Large changes in the swelling ratio of these hydrogels can be observed with changes in the pH, temperature, ionic strength, nature of the swelling agent, and electromagnetic radiation [12]. Biomolecules are commonly immobilized within environmentally responsive hydrogels to yield biosensing materials. The most common of these is the immobilization of glucose oxidase within pH-responsive hydrogels to make glucose-sensitive materials.

pH-Responsive hydrogels are anionic, cationic, or amphiphilic. Anionic hydrogels exist in a collapsed state at low pH. When the pH of the external environment is raised above the pK<sub>a</sub> of the gel, they begin to swell. This is due to ionization of the side groups and repulsion of the like-charged chains. The charge repulsion is more powerful than other forces such as hydrogen bonding which exist between the chains in the collapsed state. At the molecular level and if the swelling is isotropic, this increase in volume corresponds to an increase in the network

mesh size. The reduced size of these hydrogel microstructures leads to faster mass transfer and chemomechanical response [13]. To better understand the kinetic response of hydrogel-based sensors, we must understand the kinetic response of the hydrogel itself. The swelling and shrinking of hydrogels requires transport of the stimulus into the network followed by water transport into or out of the network [14]. An interesting complexity in this system is that shrinking of the gel can generally occur more rapidly than its swelling. The characteristic response time in a hydrogel sensor is dependent on the square of the distance, so the hydrogel thickness should be as small as possible [15]. This is why microfabrication techniques are actively investigated with hydrogels. It is interesting to note that the type of transducer can further slow the kinetics of the sensor. If the method of transduction is based on measurement of the changes of the optical transparency or conductivity of the material, then free swelling kinetics can apply. If the volume change of the gel must be transduced mechanically, such as by the use of microcantilevers, then the sensor will be inherently slower. The external force required slows the sensor performance versus our free swelling models [15].

### *2.1. Application of hydrogels in biosensing – Hydrogels as immobilizing scaffold for biomolecules*

The first examples of hydrogels in biosensing employed hydrogels for the immobilization of biomolecules to measure biospecific interactions. In one such example, *Fagerstam et al.* [16] covalently attached biomolecules to thin hydrogel films atop surface plasmon resonance chips to measure biomolecular interaction kinetics and concentration. Solutions containing biomolecules of interest were flowed over the hydrogel and small mass changes were measured with a sensitivity of 10 pg/mm<sup>2</sup>. Some advantages of this early biosensor include that it did not require any biomolecular labeling and the sensor chip could be used repeatedly.

Immobilization of nucleic acids on solid supports has been widely used in the detection of DNA and other biomolecules in sensor technology. Because three dimensional hydrogel matrices offer significant advantages for capturing probes over more conventional two dimensional rigid substrates and the ability to provide a solution-mimicking environment, they are becoming increasingly attractive as desired supports for bio-analysis [17]. The use of hydrogels to immobilize enzymes for improved and sustained activity of biomolecules is not limited to the microscale. While commonly employed in lab-on-a-chip technologies, these materials also perform favorably in large-scale bioreactors as well. Hydrogel microspheres containing immobilized enzymes were used to monitor packed-bed bioreactor by *Guisseppi-Elie et al.* [18]. Enzyme activity was tested after the materials were stored in buffer at 4°C for one year. The materials retained 80% of their initial activity. This high stability shows promise towards the utilization of hydrogel-based biosensing materials on a variety of scales. Since scale-up is of common concern in the practice of chemical engineering, it is important to note that hydrogel-based biosensing elements have shown desirable performance at a variety of scales.

## **3. Drug Delivery Systems**

Drug delivery system platform is a rapidly expanding market for pharmaceutical and biomedical engineering. In terms of pharmaceuticals, the need for drug carriers that will offer targeted drug delivery is of vital importance. This is of great value as it reduces the side effect profile by allowing usage of low dosage drugs, site specific activity and increased bioavailability. Non-targeted systemic drug administration leads to the bio-distribution of pharmaceuticals across the entire body [19]. This distribution causes toxicity effects on non-target tissues and wastage of pharmaceutical compounds since they are used by non-target



tissues. For biomedical engineering, design of devices that will offer better diagnosis and therapeutics is required to ensure better illness management. Biomedical engineering will aid in targeted drug delivery, selective targeting of imaging contrast agents, delivery of nucleic acid and genetic therapies, and prediction of pharmacokinetics and pharmacodynamics patterns of the drug [20].

Biomaterials are needed to design a stable and biocompatible drug delivery system. These can vary from natural polymers, metals compound, modified and synthetic polymers. Biocompatibility and biodegradation of these play a vital role in the toxicity effect of the system and its mode of action. A beneficial drug delivery system must have an effect on drug absorption, distribution, and metabolism levels [21]. This can be achieved by controlling drug delivery system. Controlled drug delivery systems function by means of controlling where and when the therapeutic agent will be released. The major features of controlled drug delivery system include the rate of drug release and mode of activation. Drug release may be rapid or may occur over a prolonged period of time depending on the required action and the location of the device in the body.

The mode of release and the rate is related to the biomaterial constituting the major part of the system. Depending on the location where the system is directed to release the drug, the biomaterial that make up the system play a role in terms of reacting with the physiochemical compounds to protect the therapeutics, sense the activator and also allow binding to the target site for localized drug release.

Targeted drug delivery can be done by means of using natural organic compounds. These natural compounds interact with surface of the synthetic/modified polymers and peptides. The use of sugar molecules which can be mucoadhesive allows targeting of the intestine. These will be stimulated by temperature (e.g., poly (N-isopropylacrylamide)) and pH level (polyacrylic acid and chitosan) for drug release. There are different kinds of polymers that can be used for this purpose; anionic (polyacrylic acid), cationic (chitosan), non-ionic (polyethylene glycols) and thiolated polymers (cysteine conjugates) [22].

Depending on the mode of action required for the drug delivery system, these biomaterials can be modeled into different forms such as spheres for carrying therapeutics and film/hydrogels layers for physiochemical response. For therapeutic implication, nanoparticles and liposomes are primarily used to adsorb and absorb drugs of interest and even for encapsulating the sensitive therapeutics. Targeted drug delivery requires binding of biochemical molecules which offer directed control of therapeutic action. For continuous and responsive drug delivery system, thin films and even nanoparticles may be used as they can respond to the physiochemical changes that may occur in the body. Hydrogels form a three-dimensional structure consisting of cross-linked networks of water-soluble polymers, which can undergo conformational changes once they interact with water [23]. They can further be modified to react at a certain temperature, detection of analyte based on interaction with functional groups or pH in relation to their mode of action and target site. Upon reaching a certain site of action, the swelling dynamics will change, allowing for the diffusion of a therapeutic from the network matrix. The fabrication of these systems relates to their chemical properties. If a system is designed for targeting the gastric intestinal tract, it must withstand physiochemical changes such as pH and temperature before it reaches its required site of action.

Polymers such as chitosan, polyvinyl alcohol and ethylene glycol, can be used for both targeted and responsive action. Chitosan as a drug carrier has been used for various administration routes such as oral, bucal, nasal, transdermal, parenteral, vaginal, cervical, intrauterine and rectal [24]. As a responsive or targeted drug delivery vehicle, these biomaterials can be cross-linked or conjugated to other compounds to offer a responsive and



improved targeting. Synthesis can be conducted by means of modifying temperature, ionic strength and pH during formulation. Physiochemical interactions such as hydrophobic/hydrophilic interactions, charge condensation, and hydrogen bonding have effects on the physiological interactions of the device.

#### **4. Integration of Biosensors with Drug Delivery Systems**

Biosensors are the tools that can shape illness treatment by increasing accuracy of diagnosis, illness monitoring and prognosis. The advantages of biosensors are that they are easy to use, inexpensive, rapid, robust and can allow analysis of different biomarkers simultaneously [25]. The other main advantage is that there is no sample preparation since the biosensor can detect the biomarker within a pool of other bimolecular substances and this makes the integration of biosensors with current drug delivery systems feasible. Microneedles are painless minimally invasive drug delivery systems that do not contact with blood thereby reducing infection and risk of device contamination. In drug delivery, these microneedles are used to inject a therapeutic transdermally whilst for biomedical sensing they aid in fluid extraction for analysis. Utilizing such and many other tools the current research in illness management focuses one of its aspects on integration of biosensors with drug delivery systems. Many such systems that have been studied and published are based on responsive drug release, biocompatibility, biofouling, self-regulatory implants and refillable reservoirs [26, 27].

##### *4.1. Bio-Micro-Electro-Mechanical Systems (Bio-MEMS)*

The development of Micro-Electro-Mechanical Systems (MEMS) devices is accomplished the process of micro-fabrication, where silicon, glass and plastic are used. The initial stage for designing MEMS device is patterning technique where photolithographic process is used to design desired patterns on the wafer surface. The wafer is photoresist and then exposed to radiation through a mask which contains the pattern of interest. Once a pattern has been formed the photoresist is removed. The next step is deposition process where a thin film of material (bioelectrics, polymers (polydimethylsiloxane (PDMS) and polymethylmethacrylate (PMMA)), silicon dioxide, silicon nitride, metals (electrodes) or biomolecules is deposited on the surface of the wafer [28]. This is followed by the process of etching which can be either wet where etching is due to liquid chemicals or dry where gas-phase chemistry is used. In both the phases etching processing can occur in all directions equally leading to mask undercutting and a rounded etch profile (isotropic) or be directional (anisotropic) due to either chemical or physical induction [29]. The final step is bonding where the two substrates are bound together by anodic or fusion bonding [30]. The use of MEMS has led to the development of microfluidics which is a field of the design and development of miniature devices that can sense, pump, mix, monitor and control flow of small volumes of fluids [31].

BioMEMS technology has allowed fabrication of both disposable (external application) and implantable drug delivery systems and diagnostic tools. Solid durable, solid degradable and hollow microneedles can be used for delivery of insulin (JewelPump, Debiotech) and for vaccination (Intaza, Sanofi Pasteur) [32]. Implantable drug delivery microdevices designed by means of BioMEMS technology can reduce conventional implantable drug delivery devices disadvantages. Most implantable drug delivery devices have unintended drug dumping events which cause side effects and reduce patient compliance as this causes health risk to patients [33]. Implant lifetime also affects compliance as this increases cost of implant replacement. These implants have further problems such that the implant drug release rate and drug contents cannot be changed without invasive procedure.

Conventional pumps are usually osmotically, electrolytic or peristaltic driven [34]. By means of BioMEMS, a piezoelectric pump controlled drug delivery system was made for transdermal delivery of insulin by means of using microneedle, which improved precision and accuracy in relation to mechanical controlled pumps [35]. For longer lifetime and improved biocompatibility, the BioMEMS device will require use of biodegradable polymers or compounds that mitigate tissue response to the implant such as antibiotics or anti-inflammatory agents [36].

#### *4.2.Smart Polymers*

Smart polymers represent a group of polymers that function in the same manner as biological systems. Stimuli responsive hydrogels can undergo structural changes when exposed to external stimuli such as pH, temperature and ionic changes. The polymers are divided into three groups based on their physical form. Linear free chains in solutions are when the polymer undergoes a reversible collapse after a stimulus is applied, covalently cross-linked reversible gels are when swelling/shrinking are triggered by environmental changes and chain adsorbed/surface-grafted form represent polymers that have reversible swelling/collapse on the surface once a trigger is changed [37, 38]. Similar to affinity biosensors a hydrogel has been designed by grafting an antigen-antibody complex onto polymer network that will lead to competitive binding of the free antigen triggering a change in the network structure of the hydrogel [39]. Such behavior allows long term use of the system unlike affinity biosensors that get saturated over time as reversible binding is not favored. In another approach the entrapment of glucose oxidase within a pH responsive hydrogel (gluconic acid increase due to oxidation of glucose) and attachment of insulin allowed the smart polymers to act as both drug delivery vehicles for insulin in addition to being a biosensor of glucose concentration [40].

Other reversible systems include desthiobion/biotin and concanavalin in immobilized systems. Desthiobion/biotin-binding protein complex can be dissociated under physiological conditions by either biotin or desthiobiotin (analogue of biotin) [41]. Since biotin can be used to label a variety of proteins, this can be conjugated to either antibodies or antigens to serve as a reversible biosensor. Immobilization of Con A has shown to lead to a reversible sol-gel phase in the presence of free glucose again due to competitive binding with insulin conjugated to glucose [42].

#### *4.3.Microfabricated Devices*

Most of the microfabricated devices are in the form of biosensors. There is a time limitation to the use of microfabricated implantable biosensors due to their short time of functionality. Designing an implantable biosensor that has long term functionality can be a critical component of the ideal closed-loop drug delivery or monitoring system, without considering issue of implant biocompatibility and biofouling which must be addressed in order to achieve long-term in vivo sensing [43]. By use of a thermal, pH, ionic strength or biomolecular sensitive hydrogel as a transducer this can be implied in integration of drug delivery system and biosensor technology with better biocompatibility and reduced biofouling.

A cantilever can be employed as a lid on a reservoir whereby a sensing molecule embedded in a responsive hydrogel can stimulate the opening and closing of the lid in relation to analyte quantity. Furthermore the electrically responsive hydrogel can be used as components of MEMS-based sensors or drug delivery devices whereby the external electrical current can be applied on an implant to stimulate drug release intramuscularly. For drug delivery MEMS technology has been applied to formulate microparticles and micro-reservoirs.

Microparticles have been formed by means of generating a pattern of wells ranging in size from 25 to 100 $\mu$ m inside silicon squares ranging from 80 to 150 $\mu$ m in size [44]. These

wells are then filled with a drug of interest and then sealed with a dissolvable cap that has bioadhesive properties for targeted delivery. These microparticles can be further improved by use of smart polymers that can shrink when an analyte is detected as caps to facilitate responsive drug release, thus integrating with biosensor. Instead of voltage, smart polymers can be used to collapse in response to analyte concentration or by means of generating conductive polymers that can be stimulated during redox reactions. Microfabricated devices have led to the development of controlled release microchips [45].

## 5. Conclusions

In this paper a potentialities of various novel nanotechnologies- based sensors in drug delivery systems have been represented. Nanotechnology is new emerging technology that is assumed to take an essential role in drug delivery systems since it would change the treatment of diseases. The latest development in nanomaterial production techniques as well as the development of analytical technologies have led to establishing more effective methods for drug delivery of various therapeutic treatments.

## References

- [1] Suravi, Pandit / Debaprotim, Dasgupta / Nazneen, Dewan / Prince Ahmed: „Nanotechnology based biosensors and its application". *The Pharma Innovation Journal* 5(6), 2016, pp. 18-25.
- [2] Akifumi, Kawamura / Takashi, Miyata: „4.2 – Biosensors". In *Biomaterials Nanoarchitectonics*. 2016, pp. 157-176.
- [3] Chen, Jianrong / Miao, Yuqing / He, Nongyue / Wu, Xiaohua / Li, Sijiao: „Nanotechnology and biosensors". *Biotechnology Advances* 22, 2004, pp. 505–518.
- [4] Sandeep, Kumar, Vashist / Konstantinos, Mitsakakis / Gregor, Czilwik / Günter, Roth / Felix, von Stetten / Roland, Zengerle: „Nanotechnology-Based Biosensors and Diagnostics: Technology Push versus Industrial/Healthcare Requirements". *BioNanoSci.* 2, 2012, pp. 115–126.
- [5] Venkataramani, Anandan / Yeswanth, L., Rao / Guigen, Zhang: „Nanopillar array structures for enhancing biosensing performance". *International Journal of Nanomedicine* 1(1), 2006, pp. 73-79.
- [6] Bayer, C.L. / Peppas, N.A.: „Advances in cognitive, conductive and responsive delivery systems". *J Controlled Release* 132, 2008, pp. 216-221.
- [7] Heller, A.: „Integrated Medical Feedback Systems for Drug Delivery". *AIChE Journal* 51, 2005, pp. 1054-1066.
- [8] Kryscio, D.R. / Peppas, N.A.: „Critical Review and Perspective of Macromolecularly Imprinted Polymers". *Acta Biomaterialia* 8, 2012, pp. 461-477.
- [9] Doyle, F.J. / Dorski, C. / Harting, J.E. / Peppas, N.A.: „Control and modeling of drug delivery devices for the treatment of diabetes". *Proceed. Amer. Control Confer.*, 1996, pp. 776-780.
- [10] Hilt, J.Z. / Gupta, A.K. / Bashir, R. / Peppas, N.A.: „Ultrasensitive BioMEMS sensors based on microcantilevers patterned with environmentally responsive hydrogels". *Biomed Microdev* 5, 2003, pp. 177-184.
- [11] Lowman, A.M. / Peppas, N.A.: „Solute transport analysis in pH-responsive, complexing hydrogels of poly(methacrylic acid-g-ethylene glycol)". *J Biomat Sci-Polym E* 10(9), 1999, pp. 999-1009.
- [12] Peppas, N.A. / Hilt J.Z. / Khademhosseini A. / Langer R.: „Hydrogels in biology and medicine: From molecular principles to bionanotechnology". *Adv Mater* 18(11), 2006, pp. 1345-1360.
- [13] Lei, M. / Ziaie B. / Nuxoll, E. / Kristof I. / Noszticius Z. / Siegel, R.A.: „Integration of hydrogels with hard and soft microstructures". *J Nanosc Nanotechn* 7(3), 2007, pp. 780-789.
- [14] Dicker, M.P.M. / Bond, I.P. / Rossiter J.M. / Faul C.F. / Weaver P.M.: „Modelling and Analysis of pH-Responsive Hydrogels MRS". *Proceedings*, 2015, published on line, DOI: <http://dx.doi.org/10.1557/opi.2015.20>
- [15] Richter, A. / Paschew, G. / Klatt, S. / Liening, J. / Arndt, K.F. / Adler H.J.: „Review on hydrogel-based pH sensors and microsensors". *Sensors* 8, 2008, pp. 561-581.
- [16] Fagerstam, L.G. / Frostell-Karlsson, A. / Karlsson, R. / Persson, B. / Ronnberg, I.: „Biospecific interaction analysis using surface-plasmon resonance detection applied to kinetic binding-site and concentration analysis". *J Chromatogr* 597, 1992, pp. 397-410.

- [17] Tang, J. / Xiao, P.F.: „Polymerizing immobilization of acrylamide-modified nucleic acids and its applications”. *Biosens Bioelectron* 24(7), 2009, pp. 1817-1824.
- [18] Guiseppi-Elie, A. / Sheppard, Jr. N.F. / Brahim, S. / Narinesingh, D.: „Enzyme microgels in packed-bed bioreactors with downstream amperometric detection using microfabricated interdigitated microsensor electrode arrays”. *Biotechno Bioeng.* 75(4), 2001, pp. 475-484.
- [19] Sijja, H.K. / East, M.P. / Mao, H. / Wang, Y.H. / Nie, S. / Yang, L.: „Development of multifunctional nanoparticles for targeted drug delivery invasive imaging of therapeutic effect”. *Curr. Drug Discov. Technol.* 6, 2009, pp. 43–51.
- [20] Pierige, F. / Rossi, S.S. / Magnani, M.: „Cell based drug delivery”. *Adv. Drug Deliv. Rev.* 60, 2008, pp. 286–295.
- [21] Deo, S.P. / Moschou, E.A. / Peteu, S.F. / Bachas, L.G. / Daunert, S.: „Responsive drug delivery system”. *Anal. Chem.* 75, 2003, pp. 207–213.
- [22] Inzelt, G. / Pineri, M. / Scheltze, J.W. / Vorotyntsev, M.A.: „Electron and proton conducting polymers: Recent developments and prospects”. *Electrochim. Acta* 45, 2000, pp. 2403–2421.
- [23] Deligkaris, K. / Tadele, T.S. / Olthuis, W. / Berg van den, A.: „Hydrogel-based devices for biomedical applications”. *Sens. Actuators B Chem.* 147, 2010, pp. 765–775.
- [24] Denkbass, E.B. / Odabasi, M.: „Chitosan microspheres and sponges: Preparation and characterization”. *J. Appl. Polym. Sci.* 76, 2000, pp. 1637–1643.
- [25] Tothill, I.E.: „Biosensor for cancer diagnosis”. *Semin. Cell Dev. Biol.* 20, 2009, pp. 55–62.
- [26] Anderson, J.M. / Langone, J.J.: „Issues and perspectives on the biocompatibility and immunotoxicity evaluation of implanted controlled release systems”. *J. Control Release* 27, 1999, pp. 107–103.
- [27] Maloney, J.M.: „An implantable microfabricated drug delivery system”. *Am. Soc. Mech. Eng.* 70, 2003, pp. 115–116.
- [28] James, T. / Mannoor, M.S. / Ivanov, D.V.: „BioMEMS-Advancing the frontiers of medicine”. *Sensors* 8, 2008, pp. 6077–7107.
- [29] Voldman, J. / Gray, M.L. / Schmidt, M.A.: „Microfabrication in biology and medicine”. *Annu. Rev. Biomed. Eng.* 1, 1999, pp. 401–425.
- [30] Roberts, H.Q. / Steyn, J.L. / Turner, K.T. / Carretero, J.A. / Yaglioglu, O. / Saggere, Y. / Su. Y. / Hagood, N.W. / Spearing, S.M. / Schmidt, M.A.: „A piezoelectric microvalve for compact highfrequency, hug-differential pressure hydraulic micropumping system”. *J. Microelectromech. Syst.* 12, 2003, pp. 81–92.
- [31] Nisar, A. / Afzulpurkar, N. / Mahaisavariya, B. / Tuantranont, A.: „MEMS-based micropumps in drug delivery and biochemical applications”. *Sens. Actuators B* 130, 2008, pp. 917–942.
- [32] Zhou, C. / Liu, Y. / Wang, H. / Zhang, P. / Zhang, J.: „Transdermal delivery of insulin using microneedle rollers in vivo”. *Int. J. Pharma.* 392, 2010, pp. 127–133.
- [33] Nuxoll, E.E. / Siegel, R.A.: „BioMEMS devices for drug delivery”. *IEEE Eng. Med. Biol. Mag.* 28, 2009, pp. 31–39.
- [34] Meng, E. / Hoang, T.: „MEMS-enable implantable drug infusion pumps for laboratory research, preclinical, and clinical applications”. *Adv. Drug Deliv. Rev.* 64, 2012, pp. 1628–1638.
- [35] Ma, B. / Liu, S. / Gan, Z. / Liu, G. / Cai, X. / Zhang, H. / Yang, Z.: „A PZT insulin pump with a silicon microneedle array for transdermal delivery”. *Elec. Comp. C.* 56, 2006, pp. 677–681.
- [36] Cheung, K.C. / Renaud, P.: „BioMEMS for medicine: On-chip cell characterization and implantable microelectrodes”. *Solid-State Electron.* 50, 2006, pp. 551–557.
- [37] Tomar, L. / Tyagi, C. / Lahiri, S.S. / Singh, H.: „Poly(PEGDMA-MAA) copolymeric micro and nanoparticles for oral insulin delivery”. *Polym. Adv. Technol.* 22, 2011, <http://onlinelibrary.wiley.com/doi/10.1002/pat.v22.12/issuetoc22> , pp. 1760–1767.
- [38] Kumar, A. / Srivastava, A. / Galaev, I.Y. / Mattiasson, B.: „Smart polymers: Physical forms and bioengineering applications”. *Prog. Polym. Sci.* 32, 2007, pp. 1205–1237.
- [39] De, S.K. / Aluru, N.R. / Johnson, B. / Crone, W.C. / Beebe, D.J. / Moore, J.: „Equilibrium swelling and kinetics of pH responsive hydrogels: Models, experiments and simulations”. *J. Microelectromech. Syst.* 11, 2002, pp. 544–555.
- [40] Traitel, T. / Cohen, Y. / Kost, J.: „Characterization of glucose-sensitive insulin release systems in simulated in vivo conditions”. *Biomaterials* 21, 2000, pp. 1679–1687.
- [41] Hirsch, J.D. / Eslamizar, L. / Filanoski, B.J. / Malekzadeh, N. / Haugland, R.P. / Bechem, J.M. / Haugland, R.P.: „Easily reversible desthiobiotin binding to streptavidin, avidin, and other biotin-binding proteins: Uses for protein labeling, detection and isolation”. *Anal. Biochem.* 308, 2002, pp. 343–357.
- [42] Qiu, Y. / Park, K.: „Environment-sensitive hydrogels for drug delivery”. *Adv. Drug Del. Rev.* 53, 2001, pp. 321–339.

- [43] Grayson, A.C. / Shawgo, R.S. / Johnson, A.M. / Flynn, N.T. / Li, Y. / Cima, M.J. / Langer, R.: „A BioMEMS review: MEMS technology for physiologically integrated devices”. *Proc. IEEE* 92, 2004, pp. 6–21.
- [44] Ahmed, A. / Bonner, C. / Desai, T.A.: „Bioadhesive microdevices for drug delivery: A feasibility study”. *Biomed. Microdevices* 3, 2001, pp. 89–95.
- [45] Tsai, A.H. / Moschou, E.A. / Daunert, S. / Madou, M. / Kulinsky, L.: „Integrating biosensors and drug delivery; a step closer toward scalable responsive drug-delivery systems”. *Adv. Mater.* 21, 2009, pp. 656–660.





## IOT SYSTEM FOR SHORT-CIRCUIT DETECTION OF DC MOTOR AT EKG-15 EXCAVATOR

*Milutin Radonjić<sup>1</sup>, Božo Krstajić<sup>2</sup>, Žarko Zečević<sup>3</sup>*

<sup>1</sup>University of Montenegro, Faculty of Electrical Engineering, Podgorica, Montenegro, email: [mico@ucg.ac.me](mailto:mico@ucg.ac.me)

<sup>2</sup>University of Montenegro, Faculty of Electrical Engineering, Podgorica, Montenegro, email: [bozok@ucg.ac.me](mailto:bozok@ucg.ac.me)

<sup>3</sup>University of Montenegro, Faculty of Electrical Engineering, Podgorica, Montenegro, email: [zarkoz@ucg.ac.me](mailto:zarkoz@ucg.ac.me)

### Abstract

*In this paper, we present a concept of an IoT system that monitors the DC motor at the EKG-15 excavator. The proposed system is designed for the coal mine "Rudnik uglja Pljevlja", which uses this type of excavator for surface mining. Due to the type of excavation and the work procedures of the excavator, it often happens that the DC motors that drive the bucket of the excavator are in the so-called short circuit. During that time, a large current flow through the motor, which is electronically limited to a value of 2kA. However, there is no limitation in the time domain, which means that this current can flow for an unlimited time. If the operator keeps the excavator control lever in the active position for too long, during a short circuit, the DC motor will burn out. In that case, large repair costs are generated, and the excavator is out of order for a long time. Therefore, there is a need to alarm the operator that the motor is short-circuited, as well as to keep records of such events, to determine the causes of motor burnout and liability. The proposed system is based on a microprocessor hardware platform for short-circuit detection of DC motor and perform the mentioned functions. Experimental and implementation results showed that this IoT platform provides the collection of data that can be useful in the process of analyzing the operation and predictive maintenance of the excavator.*

### Keywords

*DC motor, Excavator, IoT.*

### Introduction

Working on the surface mine of a coal mine is a challenging job, both for the people and the machines. In the winter, the temperature drops far below 0°C, while in the summer, tropical heat is a common case. There is no shelter from the cold or heat on the surface mine, so the workers are exposed to the extreme ambient conditions. It is similar to the machines that these workers use or operate. Therefore, predictive maintenance becomes a very important task, to cut maintenance costs of an ordinary industrial plant [1] – [4]. A proactive approach can save a lot of effort, especially by avoiding unnecessary delays in the production and use of human resources. However, such prediction is not an easy task and is possible only by continuous observation of the machine's parameters. We are dealing with this very important and challenging topic within the framework of the international project Faster [5]. The focus of this project is predictive maintenance of the rotating machines. Working on this topic in the coal mine "Rudnik uglja Pljevlja" (RUP) [6] we found some more important and challenging aspects to be considered about maintenance of machines. For this purpose, a modification and adjustment of the device that was already developed within the Faster project were performed.

One of the key machines for working on the surface mine of coal mines is a suitable excavator. The EKG-15 excavator is used for this purpose in the "Rudnik uglja Pljevlja" (Fig. 1). It is a



machine in which the loading bucket is controlled by a high-power DC motor. In normal operation, these motors are designed to provide a long excavator life. However, when the loading bucket gets stuck due to the extremely hard terrain, the motor can be overloaded. Namely, if the operator does not release the lever that controls the movement of the loading bucket, the motor still tries to move the bucket. In these moments, a so-called short circuit occurs, when a high amount of current passes through the motor. If the operator does not react quickly and releases the lever, the short-circuit current threatens to damage the motor. If this happens, the motor will be out of use, and so will the excavator. Repair of these motors is very expensive and cannot be performed in a very short time. It is clear what this means for the surface mining process in the mine.

For these reasons, there is a need to solve the problem of short circuit current flow through the motors. In the case of excavators located in the company "Rudnik uglja Pljevlja", the manufacturer limited the short-circuit current to an amount of 2kA, as prevention. This means that the current flowing through the motor windings will not exceed this value. However, there is no protection provided concerning the duration of the short-circuit condition. In other words, a current of 2kA will flow through the motor windings as long as the operator activates the bucket control lever. If the operator keeps the motor active for a long time, the conductor will heat up and the motor will burn out.

Less experienced operators can unintentionally cause a condition that leads to a short-circuit current on the motors and often do not recognize in time that such a situation has occurred. This inevitably leads to motor burnout. However, since there is no protection, nor control, or records of the excavator's working mode, the operator can also intentionally cause a short-circuit current and consequently the motor to burn out for some of its reasons.

Therefore, there was a need to find a solution that would prevent the occurrence of a short-circuit current or at least reduce its probability. When designing a system that would lead to solving this problem, the requirement was that the original operation mode of the excavator is not affected in any way, nor that its control electronics are changed. In other words, a clear warning to the operator should be activated when a short-circuit current occurs. Also, it is necessary to record and store for later processing information related to the occurrence of the short-circuit current. Based on this information, the behavior of the operator can be determined, and errors can be pointed out to him if they are found. This provides prevention and extends motor life. In addition, this information can be used to analyze the cause of motor burnout, when it occurs.

Since the funds for the design of a prototype device that would perform described function were not planned in the company's budget, the device had to be inexpensive. Therefore, we decided to base this IoT system on the widely known Arduino open hardware platform [7], [8]. For authorities to have an immediate overview of the situation regarding the short-circuit current of the excavator motors, the data collected by the Arduino platform is immediately sent to the cloud platform. We used the open LiveGate platform for this purpose [9].



**Fig. 1 Excavator EKG-15**

Source: <https://uralmash-kartex.ru/en/electric-rope-shovels#&gid=1&pid=1>

The paper is organized as follows. In Section 1, we analyze the control of the excavator's DC motors and discuss possible techniques for short-circuit detection. Section 2 describes the proposed architecture of the system for detection and indication of the short-circuit current. Preliminary results of the system testing through laboratory simulations are presented in Section 3. Finally, in the conclusion, we summarize important aspects of this paper.

## 1. Analysis of the short-circuit detection of DC motor

To monitor the motor load in the excavator, the manufacturer implemented the system that allows the operator to have information about the current flowing through the DC motor windings. Namely, in the circuit of each of the two DC motors, there is one resistor, the so-called shunt. A voltage of 75mV is generated on this resistor during a short circuit current of 2kA. The voltage from the shunt is brought to an analog voltmeter with a symmetrical scale since the motor can move in both directions, so the current can also flow in both directions. One such voltmeter is in the machine part and another in the operator cabin of the excavator. Of course, the scale is calibrated in (kilo)amperes since the strength of the current flowing through the motor is important. This means that the operator, in addition to the mine surface where he works, should also continuously observe an analog instrument. This is inconvenient both from the point of safety or from the point of work efficiency. Therefore, it would be convenient for the operator to be somehow warned when the motor overloads.

The electronics that manage and control the excavator is a closed system that we did not have insight into. Therefore, the modification on the control electronics itself, to protect against overload, i.e., to prevent long-term short-circuit current, was not possible. Also, the maintenance engineers in RUP requested that the manufacturer's electronics of the excavator should not be modified or influenced in any way. Therefore, the only way to prevent frequent motor overload, and thus its burnout, was to warn the operator clearly and reliably that an undesirable situation had occurred, and that motor activity should be stopped.

The motor short-circuits current detection system, which is the subject of this paper, aims to continuously monitor the voltage from the shunt located in the motor circuit. As long as the current flowing through the motor does not exceed the critical value, i.e., the voltage on the shunt does not exceed the predefined value, the system does not take any action. When the voltage on the shunt above the critical value is detected (in the current version of the prototype it is set to 65mV), the timer that measures the duration of the excessive current is started. There is some time during which it is considered that the current flow of about 2kA is not dangerous

for motor failure (in the current version of the prototype it is set to 3 seconds). If this time elapses, actions are taken to warn the operator and to store information about critical event.

## 2. Architecture of the proposed IoT system

After consulting with the engineers in charge of machine maintenance in RUP, we decided that the system for short-circuit detection of DC motor at EKG-15 excavator has a principal scheme shown in Fig. 2. Instead of messing up with the control electronics of the excavator, the warning signal to the operators will be generated by a strong siren (alarm). It will serve not only as a warning but also as an incentive for the operator to stop the overcurrent motor mode. The sound intensity and frequency have been chosen to be an inconvenience to the operator when exposed even for a short time. Since this siren is supplied with electricity taken from the power supply unit of the excavator, its activation is performed utilizing a common relay.

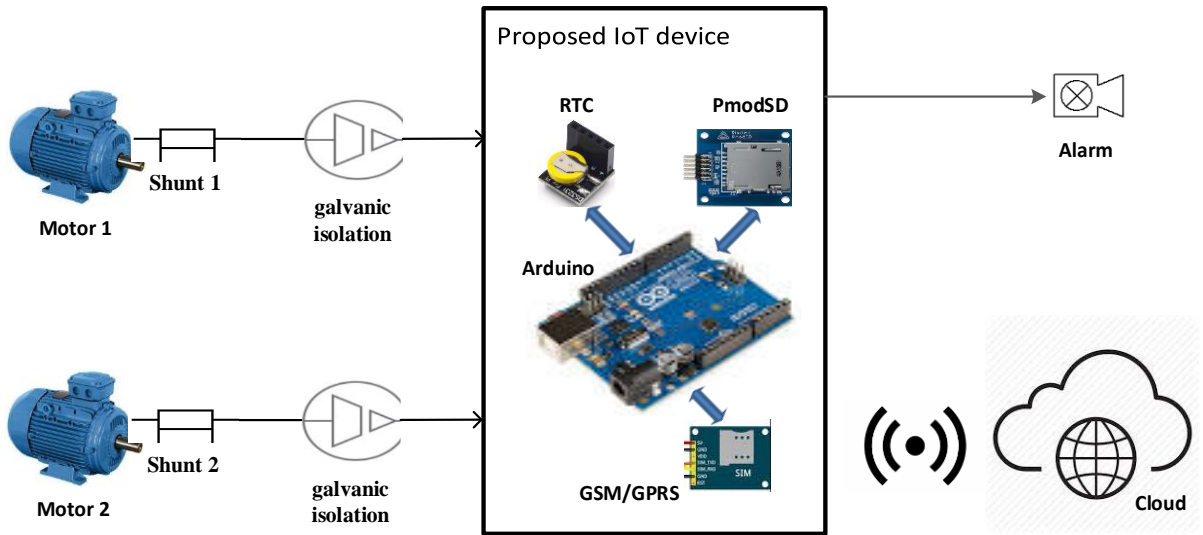


Fig. 2 Block diagram of the proposed solution

### 2.1 Short-circuit detection of excavator's DC motor

Monitoring the voltage on the shunt in the motor circuit is the most critical part of the designed system. Since we have taken the Arduino microcontroller platform as the basis of the system, voltage monitoring is performed using a built-in A/D converter. Inside each excavator, it is necessary to monitor two DC motors, so an Arduino with at least two A/D converters is needed, to complete the job for the entire excavator with one microcontroller platform.

The voltage on the shunt to be monitored changes polarity during motor operation. When the motor rotates in one direction the voltage has one polarity, and when the motor rotates in the other direction the voltage has the opposite polarity. This is a challenge for the acquisition process because the microcontroller is powered by DC voltage, as well as its A/D converter. Therefore, it is not possible to measure the voltage that is "negative" from the point of the microcontroller. On the other hand, it is mandatorily required for the implementation of the shunt voltage monitoring system to be galvanically isolated from the monitored circuit. This means that it is not possible to directly apply voltage from the shunt to the input of the A/D converter of the microcontroller.

We solved the problem with galvanic isolation by using a TLP7920 optically isolation amplifier from Toshiba Corporation [10]. Voltage from the shunt is applied to the input of TLP7920. A voltage proportional to the input voltage is generated at the output, but galvanically isolated. This output voltage can also be negative from the point of the microcontroller, and its range is quite small. We have experimentally determined that in the case of the maximum voltage on

the shunt ( $\pm 75\text{mV}$ ), i.e., voltage at the input of the TLP7920 circuit, a voltage of about  $\pm 570\text{mV}$  is obtained at its output. This means that output voltage must be translated into a range that will have a single polarity from the point of the microcontroller. It should also be amplified to utilize the entire input range of the A/D converter and thus get a more accurate reading. We performed the translation and the amplification using appropriate operational amplifiers, which is beyond the scope of this paper. Finally, the inputs of the A/D converter receive a voltage in the range of  $0.13\text{V}$  to  $2.98\text{V}$  when the shunt voltage changes in the range from  $-80\text{mV}$  to  $+80\text{mV}$ . Since the range of acceptable input signal on the A/D converter is from  $0\text{V}$  to  $3.3\text{V}$ , we considered this design to be appropriate.

## ***2.2 Communication between microcontroller platform and the cloud***

As mentioned earlier, at the moment of detecting a critical short-circuit current, in addition to the audible alarm, the system must save information about the event. This information is of multiple importance. On the one hand, maintenance engineers need to have continuous insight into potentially critical situations related to excavator motors, to take preventive actions for better maintenance. This means that it would be convenient to transmit information about the detected event immediately after the event occurred. The simplest way to perform this action is to use a GPRS connection. Namely, the RUP coil mine is covered by the signal of the mobile telephony operator. Therefore, in regular conditions, it is possible to transmit information about the critical event via GPRS. Within our system, a GSM/GPRS module based on the SIM808 chip was used (Fig. 3).



**Fig. 3 GSM/GPRS module SIM808**

The information transmitted via the GPRS module must be stored somewhere and made easily visible and noticeable for those people who should observe the events on the excavator system. Since it has become common to use cloud services for such purposes, we opted for one such service, called LiveGate [9]. It is a free service developed at the Faculty of Electrical Engineering, University of Montenegro. In addition to providing data storage, this service offers visualization of the stored data.

## ***2.3 Data storage at the platform itself***

Although the GPRS connection is quite reliable in the case of good coverage of the mobile operator's signal, it can still fail when trying to transfer data to the cloud. Failure may occur either due to the current unavailability of the mobile operator's signal due to an interruption in its operation, or some other error in the process of establishing or maintaining a GPRS connection. In any case, the data transfer failure may occur when there is an urgent need for the data transfer. If the system relies solely on data transmitted by a GPRS connection, some important data may not be available for later processing. For this reason, we decided that the data of the motor overload are, in addition to the cloud, also stored on the SD memory card,

which is an integral part of the device installed in the excavator. For this purpose, we used a PmodSD adapter from Digilent (Fig. 4).



**Fig. 4 Digilent PmodSD module**

Source: <https://store.digilentinc.com/pmod-sd-full-sized-sd-card-slot/>

### ***2.3 Real-time clock***

When sending data to the cloud via a GPRS connection, the cloud platform keeps track of the time at which the data arrived. This means that the device does not have to take care of the exact time and transmits the timestamp to the cloud platform. However, when it comes to writing data to the SD memory card, things are different. Namely, the information that there was a motor overload does not mean much if it is not known when that overload occurred. Only based on information on the time in which the overload occurred, conclusions can be drawn about the behavior of individual operators or the mode of operation of the excavator in certain parts of the coal mine. Therefore, this means that the designed system must take care of the exact time. The easiest way to deal with the exact time is to use the Real-Time Clock (RTC) circuit. We used the DS3231 chip in our design (Fig. 5).

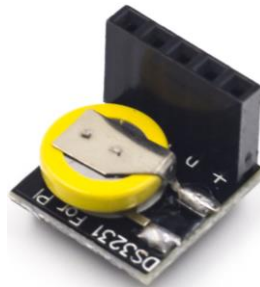


**Fig. 5 RTC module DS3231**

When a motor overload occurs, the RTC is read, and a file named by the date read from the RTC is created (if it does not already exist). In this way, it is easier to reach the necessary information when it is needed. The duration of the motor overload and the time in which the overload occurred are recorded inside the file. Of course, regardless of the writing to the SD card, the duration of the motor overload is also sent to the cloud.

## **3. Simulation results**

After careful consideration of all aspects of the proposed DC motor short-circuit current detection system, the prototype shown in Fig. 6 was developed. As can be seen from the figure, the current version of the prototype, in addition to the previously mentioned components, also has an LCD. In the development phase, we use this display to show important information about the current operation of the system and thus facilitate the design and development of the system itself. In the final version, this LCD is not required, because the device is mounted in the drive part of the excavator, where the operator does not have access while working with



the excavator. Therefore, it is not necessary to show any information on the display, especially since important information is sent to the cloud and saved to the SD memory card.

Before the installation and commissioning of the proposed system on the excavator itself, we performed extensive testing of the device in laboratory conditions. Instead of voltage from the shunt in the DC motor circuit, we applied voltages from galvanically isolated power sources with the voltage regulation to the system inputs. By applying various voltages, we also simulated the events of the short-circuit current, i.e., the corresponding shunt voltage. At that moment, as previously explained, the system saves data to the memory card and sent it to the LiveGate cloud service. Figure 7 depicts diagrams that visualize part of the data received from the designed system.

The diagrams labeled as “duration of overload” show the lengths of the detected overloads expressed in seconds, for each motor individually. These are data that are important for persons who perform the analysis and determine the behavior of the operator regarding the motor overload.

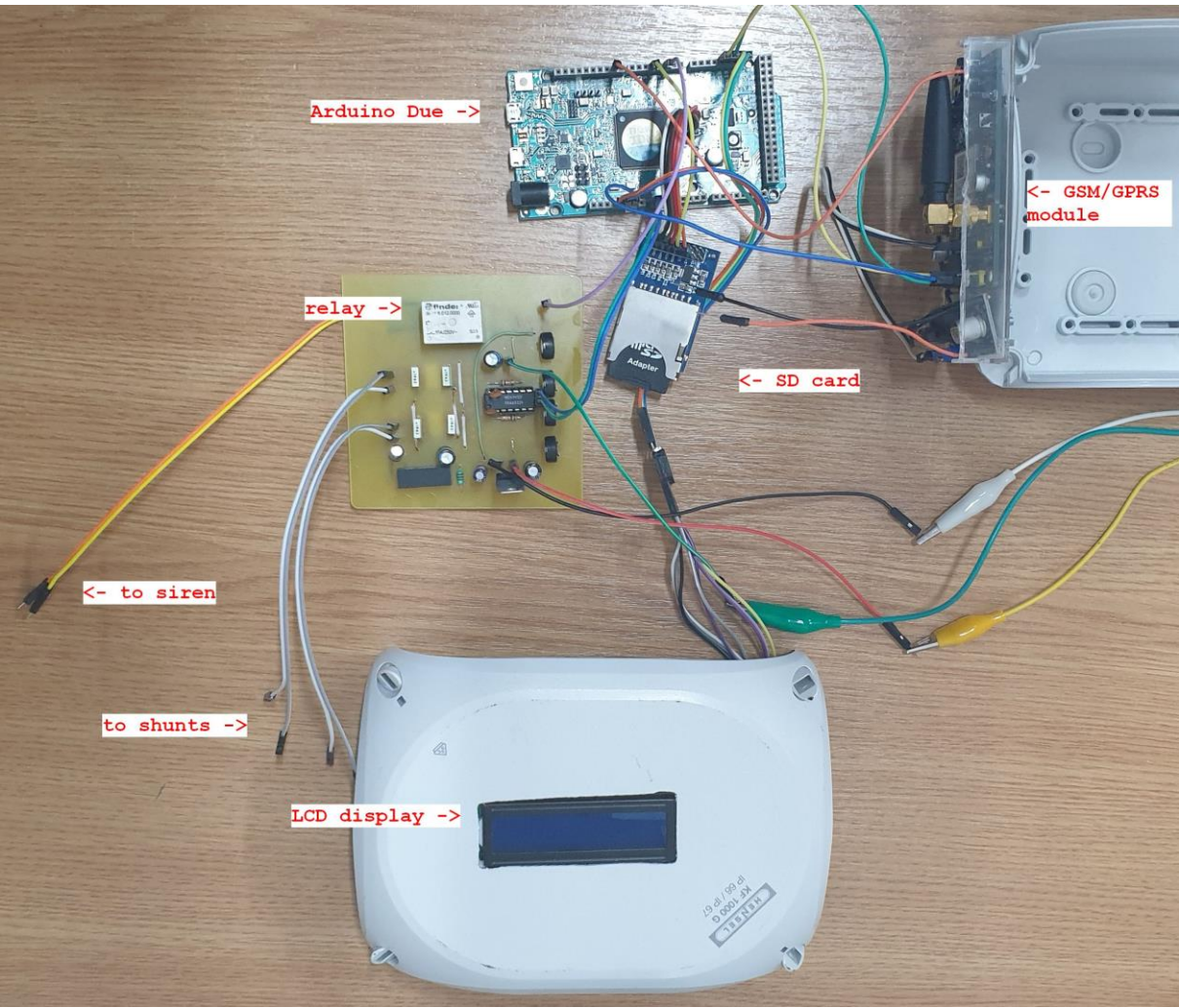


**Fig. 6 Prototype of an excavator’s DC motor short-circuit detection system**

However, in addition to this data, we decided to send two more pieces of information to the cloud. The first of them is the information that the device has started (diagram labeled as “Power on”). Namely, when the microcontroller platform is powered on (or restarted), one data is sent (an arbitrary number - in our case ‘1’) to the cloud to register that event and append the time stamp. The information about restarting the device can be significant in many ways. If a



reboot occurs frequently, this may indicate various problems with the system. In any case, from the moment the device shuts down until it responds to the cloud again, the system does not perform its function of detecting the short-circuit current of the motor.

Another additional information that we send to the cloud is the indicator that the device is active, i.e. that it performs its function. We send this information every hour in the form of the current time read from the RTC. If it is noticed that the device has not sent this data for more than an hour, it is necessary to check its functionality.



**Fig. 7 Data visualization within LiveGate cloud service**

## Conclusions

The paper presents an IoT system that was implemented within the FASTER project, to solve one of the challenges of predictive maintenance in the coal mine "Rudnik uglja Pljevlja". This system upgraded and improved the closed control system of the considered industrial machine with the microcontroller-based device described in the paper.

The simulation results show that the developed prototype works following the functional requirements, and additional adjustments will be performed based on the results in real operation conditions. Testing of this device on the considered excavator in real operating conditions is in progress. After that, we will analyse collected data and, if necessary, upgrade the device. In addition to the functional requirements, the ambient and other conditions in which the IoT device will work will be considered in the final design phase.

This solution is an example of the wide use of IoT systems in various industrial and home applications that enable the development of new or improvement of existing devices and systems. Modifications or upgrades of this device are feasible and simple, both in the existing application or some similar implementation, which is an added value of this solution. This confirms that the availability, openness, and interoperability of such systems are the main advantages that nominate them for the already proven wide application.

## References

- [1] Radonjic, M., Kvascev, G., Radulovic, M. and Krstajic, B., "One Example of Mobile Hardware Platform for Sound Acquisition in Industrial Environment", Proc. 24th Conference on Information Technologies IT 20, Žabljak, Montenegro, February 2020.
- [2] R. K. Mobley. An introduction to predictive maintenance (2nd ed.), Amsterdam: Butterworth-Heinemann, 2002.
- [3] G. Vachtsevanos, F. Lewis, M. Roemer, A. Hess, and B. Wu. Intelligent fault diagnosis and prognosis for engineering systems, Hoboken, NJ, USA: Wiley, 2006.
- [4] S. Vujnovic, Z. Djurovic, and G. Kvascev, "Fan mill state estimation based on acoustic signature analysis," Control Engineering Practice, vol. 57, pp. 29 – 38, 2016.
- [5] Faster project home page, <http://www.faster.ucg.ac.me/eng/index.php> (accessed on 01.05.2021.)
- [6] Web page of "Rudnik uglja Pljevlja", <https://www.rupv.me/en> (accessed on 01.05.2021.)
- [7] Gardašević, G., Veletić, M., Maletić, N. et al. The IoT Architectural Framework, Design Issues and Application Domains. Wireless Pers Commun 92, 127–148 (2017). <https://doi.org/10.1007/s11277-016-3842-3>
- [8] Arduino, <https://www.arduino.cc/>, (accessed on 12.05.2021).
- [9] LiveGate, Cloud platform, <http://www.livegate.ac.me/> (accessed on 12.05.2021.)
- [10] TLP 7920 datasheet, Toshiba Electronic Devices & Storage Corporation, <https://toshiba.semicon-storage.com/ap-en/semiconductor/product/optoelectronics/isolation-amplifiers-isolated-delta-sigma-modulators/detail.TLP7920.html> (accessed on 12.05.2021.)



## DESIGN OF A PHOTOVOLTAIC POWER PLANT

**Sara Aneva**  
Faculty of Electrical Engineering  
Goce Delcev University,  
Stip, R.N. Macedonia  
Sara.20551@student.ugd.edu.mk

**Todor Cekerovski**  
Faculty of Electrical  
Engineering  
Goce Delcev University, Stip,  
R.N. Macedonia  
todor.cekerovski@ugd.edu.mk

**Marija Cekerovska**  
Faculty of Mechanical  
Engineering  
Goce Delcev University,  
Stip, R.N. Macedonia  
marija.cekerovska@ugd.edu.mk

### Abstract

*The largest source of renewable energy is the Sun. The energy from the Sun, called solar energy, is free, safe and least harmful to the environment. Solar energy is converted into electricity by devices based on semiconductor materials, called photovoltaics. If the production of electricity from fossil fuels is replaced by the production of electricity from sunlight there will be much lower emissions of carbon dioxide. This paper analyzes the location, solar radiation and network connection for the provided location for the photovoltaic power plant. For collecting data on solar radiation, satellite data at a specific location were used. Based on these analyzes, the technical characteristics of the photovoltaic power plant with a total installed power of 201.6 kW are dimensioned and selected. The principal scheme of the photovoltaic power plant and the scheme of the AC Junction box are drawn in the software package Edraw max. Finally, the economic and financial profitability of the photovoltaic power plant is reviewed and proven.*

**Key words:** solar energy, solar radiation, network connection, Photovoltaic Power Plant, AC Junction box, economic and financial profitability.

### Introduction

One of the biggest problems facing the world today is the increase in electricity consumption globally and the pollution of the environment from burning fossil fuels (coal, oil, natural gas, etc.) for electricity production. Climate change is now more pronounced than ever before. Temperatures are rising globally due to greenhouse gases trapping more heat in the atmosphere. As a result of the increased temperature, fires occur and the ice melts. It is a well-known fact that many prehistoric viruses are hidden in the frozen parts of our planet, which will be reactivated if the ice melts. The threat is clear, and one of the main causes of climate change is the burning of fossil fuels to generate electricity. Combustion of fossil fuels releases carbon dioxide into the air, resulting in global warming. Increasing the production of electricity from renewable sources, such as solar energy, wind energy, hydroelectric energy, etc. will significantly reduce the effects of climate change and will help save our planet.

The prices of solar technology are currently much lower than before, and the implementation of solar power plants and systems is very simple. The Republic of North Macedonia is located in a very good geographical location, where solar radiation is large and suitable for installation of solar (photovoltaic - PV) systems and power plants and is one of the countries with the

highest solar radiation in Europe, but unfortunately it's not one of the countries that use solar energy the most. However, the production of solar energy does not pollute the environment, so we can conclude that, at the moment, the installation of photovoltaic systems for the production of electricity is the best choice. Due to this, in this paper researches have been made for installation of a photovoltaic power plant in the Republic of North Macedonia, in the city of Shtip. Based on the research, a 201.6 kW Photovoltaic Power Plant has been designed.

7. Literature review

When designing a photovoltaic power plant, several steps should be observed, given below in chronological order:

- Location selection;
- Determination of solar radiation and
- Network connection.

If the selected location proves to be good for installing a photovoltaic power plant (good solar radiation, has a transformer station or has the opportunity to build a new one, enough space, etc.), the following activities to be undertaken are:

- Selection of solar panels;
- Selection of connectors;
- Inverter selection and
- Selection of cables.

Once the technical characteristics of the power plant have been selected, the next step is to design the AC and DC junction box and finally make a financial analysis of the photovoltaic power plant.

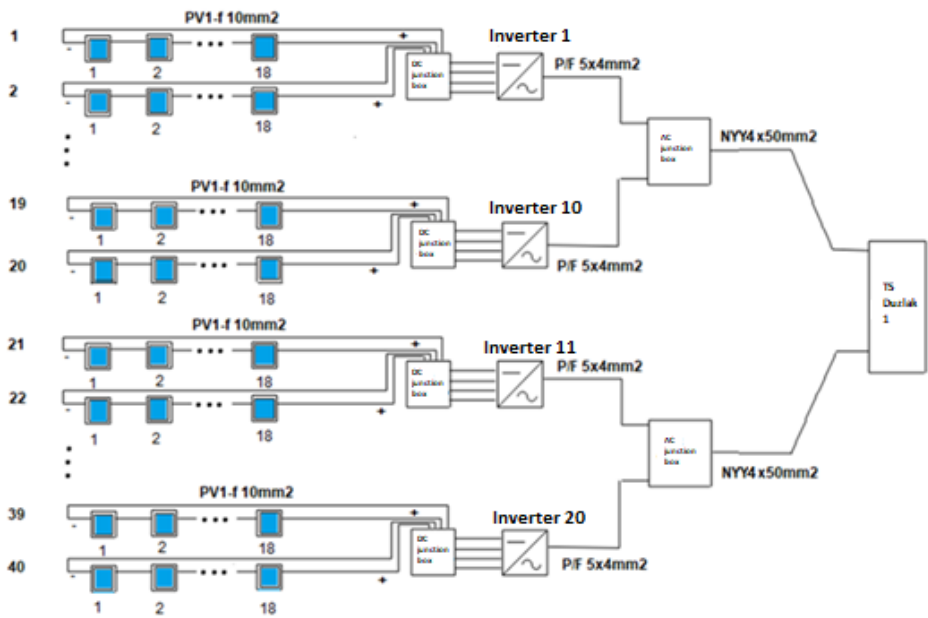


Fig. 1 Principle scheme of the proposed PV power plant  
Source: Author made this scheme in the software package Edraw max

The photovoltaic power plant designed in this paper has a total installed power of 201.6kW, and its principle scheme is shown in figure 1. This power plant consists of 40 PV arrays, each with 18 solar panels. Solar panels are interconnected by solar cables. Each of the two PV arrays is connected in parallel to a DC junction box. DC junction boxes have four 10A fuses and are connected to an inverter. The power plant has 20 inverters. 10 inverters are connected to one AC junction box and the other 10 inverters are connected to the other AC junction box. The two AC junction boxes are connected to the existing transformer station at the selected location and the produced electricity goes to the grid.

The total average annual electricity production from this power plant can be calculated as follows:

$$E_{total} = I_{daily,avg} \cdot P_{PV,total} \cdot 365 = 3.6 \cdot 201.6 \cdot 365 = 264902.4kWh / year \quad (1.1)$$

Where:

$I_{daily,avg}$  - daily average radiation in the city of Shtip;

$P_{PV,total}$  - total installed power of the photovoltaic power plant.

## 8. Location selection

The first step in designing a PV power plant is location selection. Choosing the right location is a key component to developing a sustainable photovoltaic project. The location selection process should take into account the constraints and the impact that the location will have on the price of the produced electricity. This means that the selected location should have an accessible area as much as will be needed for the implementation of the project, the solar radiation should be satisfactory, there should be no objects that will shade the modules, it should be easily accessible, there should be a transformer station nearby or to have a place for construction of a new transformer station, etc.

The selected location for the photovoltaic power plant in Stip is a place that is located near the neighborhood Sunny City. This location was chosen because it is located close to the transformer station Duzlak 1, so there will be no need to build a new transformer station. Another reason why this location is suitable is that there are no buildings that would do shading. This place has a lot of space, but most of it has trees. To build this power plant on that place, the trees will have to be cut down. Due to this, the location of the power plant is subject to change. The site for the power plant is state-owned and its use will require a long-term lease or purchase agreement.

## 9. Determination of solar radiation

In order for a photovoltaic project to be approved, we need to have data on solar radiation at the selected location. The solar resource expected during the entire service life of the photovoltaic power plant is estimated by analyzing the historical data on solar resources for the location. The total annual solar radiation in R.N. Macedonia varies from a minimum of 1250  $kWh/m^2$  in the north to a maximum of 1530  $kWh/m^2$  in the southwest. The area of the municipality of Shtip is characterized with increased duration of the solar radiation. On average, there are 2,370 hours of solar radiation per year, or an average of 6.5 hours per day. The maximum is in July and the minimum in December. The average daily radiation in Shtip is 3.6  $kWh/m^2$ . In the region of Shtip there is a good potential for utilization of the solar energy which can be seen from the map of solar resources of R.N. Macedonia presented in figure 2.

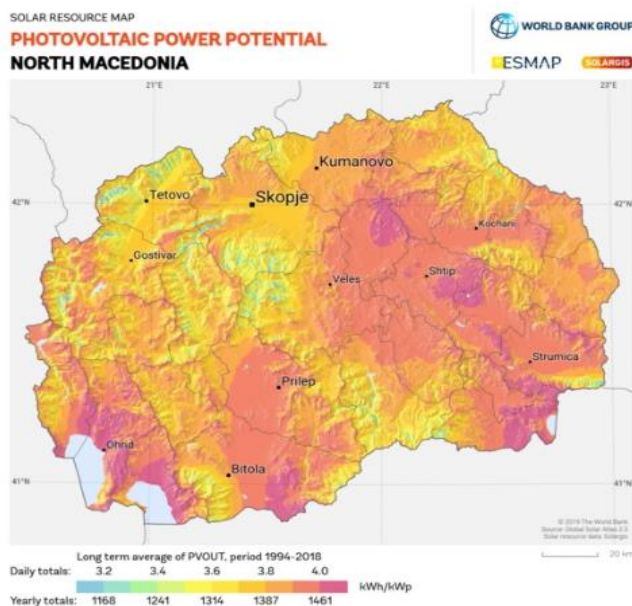


**Fig. 2 Map of solar resources of R.N. Macedonia**  
Source: [www.solargis.com](http://www.solargis.com)

### 10. Network connection

A grid connection with sufficient capacity is required to enable energy exports. The viability of the network connection depends on factors such as capacity, proximity, order, network stability and network availability.

This power plant will be connected to the transformer station Duzlak 1 (10 / 0.4 kV).

### 11. Solar panels

The solar panels that we will use for this power plant are from the company Pikcell Group, polycrystalline, type PIK280P (60), with installed power of 280 W. The company Pikcell Group is the first and only company in R.N. Macedonia that produces solar panels.

**Table 1. Electrical characteristics of solar panel PIK280P (60)**

ELECTRICAL CHARACTERISTICS	
STC (radiation: $G = 1000W / m^2$ , module temperature: $T = 25^{\circ}C$ , air mass: $AM = 1.5$ )	
Rated power ( $P_{rated}$ )	280 W
Short circuit current ( $I_{sc}$ )	9.45 A
Open circuit voltage ( $U_{oc}$ )	38.40 V
Current at MPP ( $I_{MPP}$ )	8.85 A
Voltage at MPP ( $U_{MPP}$ )	31.61 V
Solar panel efficiency	18.66 %

Source: PiKCELL Group LTD Skopje



Table 2. Mechanical characteristics of solar panel PIK280P(60)

MECHANICAL CHARACTERISTICS	
Dimensions	1640mm x 990mm x 40mm
Solar cells	60 polycrystalline
Weight	17.2 kg
Junction box/ Connectors	5 bypass diodes / MC4 compatible
Glass	3.2 mm antireflective

Source: PiKCELL Group LTD Skopje

The solar panels will be placed at an angle of 30° to the south. This angle is the angle at which the solar panels will produce maximum electricity at the selected location.

The total installed power of the photovoltaic power plant is 201.6 kW. Through the data on the installed power of the power plant and the power of the solar panels we can calculate the number of panels that we will need through the following equation:

$$N_{solarpanel} = \frac{P_{vk}}{P_{solarpanel}} \tag{5.1}$$

Where:

$P_{vk}$  - total installed power of the photovoltaic power plant;

$P_{solarpanel}$  - rated power of one panel.

$$N_{solarpanel} = \frac{201.6kW}{280W} = \frac{201600W}{280W} = 720 \tag{5.2}$$

The total area occupied by all the panels is obtained through the following equation:

$$A = N_{solarpanel} \cdot A_{solarpanel} = 720 \cdot 1.9305m^2 = 1389.96m^2 \tag{5.3}$$

Where:

$A_{solarpanel}$  - area of one solar panel.<sup>11</sup>

12. Connectors

According to the specifications of the solar panels, a compatible connector for those panels is the MC4 connector, type SY-CC4G for solar cables.

13. Inverter

Inverters are a particularly important part of the sizing of photovoltaic systems. Although the main function of the inverter is to convert DC energy to AC, its role is much larger. Inverters enable system monitoring for designers and owners, because they show how much electricity the system produces. There are different types of inverters and they differ according to how

<sup>11</sup> The dimensions of the solar panel are given by the manufacturer.

they are connected to the system. For this PV power plant we will use string inverters. We will have a total of 20 inverters, and on each inverter will be connected two PV arrays.

The chosen inverter for this PV power plant is three-phase, from the manufacturer Steca, type StecaGrid 10000 + 3ph.

**Table 3. Input characteristics of the inverter StecaGrid 10000 +3ph**

DC input side (PV generator connection)	
Maximum input voltage ( $V_{\max}$ )	845 V
Minimum input voltage ( $V_{DC,\min}$ )	350 V
Rated input voltage ( $V_{DC,\text{rated}}$ )	600 V
Maximum input current ( $I_{DC,\max}$ )	32 A
Rated input current ( $I_{DC,\text{rated}}$ )	17.3 A
Maximum input power at maximum active output power ( $P_{DC,\max}$ )	10 800 W

Source: StecaGrid

**Table 4. Output characteristics of the inverter StecaGrid 10000 +3ph**

AC output side (mains grid connection)	
Output voltage ( $V_{AC}$ )	320 V ... 480 V  (The output voltage depends on the network of each country, in our country the EVN network operates at 380V)
Maximum output current ( $I_{AC,\max}$ )	16 A
Rated output current ( $I_{AC,\text{rated}}$ )	14.3 A
Output power ( $P_{AC}$ )	10 000 W
Frequency	50 Hz
Grid type	$L_1 / L_2 / L_3 / N / PE$
Maximum efficiency ( $\eta_{\max}$ )	96.3 %

Source: StecaGrid

**Maximum number of modules in a PV array**

$$\eta_{\max} = \frac{V_{\max(INV)}}{V_{oc(module-10^{\circ}C)}}$$
(7.1)

Where:

$V_{\max(INV)}$  - maximum input voltage of the inverter;

$V_{oc(module-10^{\circ}C)}$  - open circuit voltage at  $-10^{\circ}C$ .

$$\eta_{\max} = \frac{845}{42.43} = 19.9 \quad (7.2)$$

With this solution it was determined that the maximum number of modules in a PV array is 19.

#### Minimum number of modules in a PV array

$$\eta_{\min} = \frac{V_{MPP(INV \min)}}{V_{MPP(module 70^{\circ}C)}} \quad (7.3)$$

Where:

$V_{MPP(INV \min)}$  - minimum voltage of the inverter at MPP;

$V_{MPP(module 70^{\circ}C)}$  - minimum voltage of the module at MPP at a temperature of  $70^{\circ}C$ .

$$\eta_{\min} = \frac{350}{27.34} = 12.8 \quad (7.4)$$

The number of modules in a PV array should range between the borders of maximum number of modules in a PV array and the minimum number of modules in a PV array.

$$\eta_{\min} < \eta < \eta_{\max} \quad (7.5)$$

$$12.8 < 18 < 19.9$$

## 14. Cables

Cables can be divided into solar cables and non-solar (standard cables). Solar cables connect the modules to the junction box or directly to the inverter. Standard cables are used on the AC side.

## 15. DC junction box

The two PV arrays are connected in parallel with a DC junction box. 4 cables from both arrays of solar panels (2- and 2+) are connected to this junction box. Hence, in the DC junction box we will have 4 fuses, one for each cable. These fuses will be 10 A because the current in each of the cables is 8.85A. Fuses should have either the same or greater current than the current in the cables (equation (12)).

The current of the DC junction box can be calculated by the following equation:

$$I = I_{MPP} \cdot N_{string} \quad (9.1)$$

$I_{MPP}$  - PV array current at MPP;

$N_{string}$  - number of PV arrays at MPP;

$$I = 8.85 \cdot 2 = 17.7 A \tag{9.2}$$

$$I_{Zcable} \leq I \tag{9.3}$$

$$8.85 A \leq 10 A$$

### 16. AC junction box

We will use two AC junction boxes for this power plant. The first 10 inverters will be connected to the first AC junction box, and the second 10 inverters will be connected to the second AC junction box. In one AC junction box we will have ten 22 A fuses for each cable of the 10 inverters, 3 main fuses of 220 A on the three main cables L1, L2 and L3, zero and ground - FeZn30x4mm strip. The fuses should have a current equal to or greater than the current in the cables, and from equation (13) we can see that this condition is met.

$$I_{cable} = I_{MPP} \cdot N_{string} = 8.85 \cdot 2 = 17.7 A \tag{10.1}$$

$$I = 22 A$$

$$17.7 A < 22 A \tag{10.2}$$

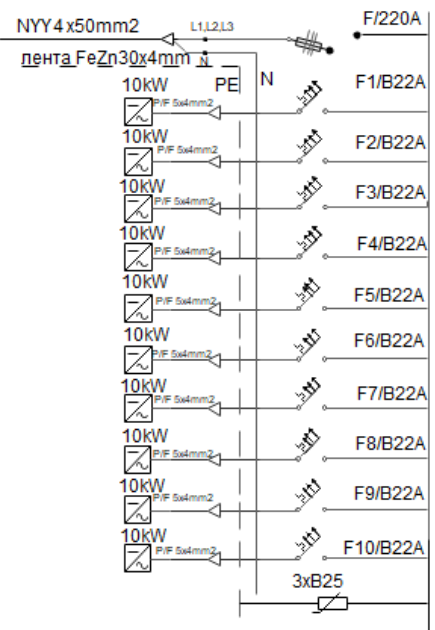


**Fig. 3 Single circuit diagram of AC junction box of the photovoltaic power plant**  
Source: Author made this scheme in the software package Edraw Max.

### 17. Financial analysis

If it is assumed that a loan with a repayment period of 10 years with an interest rate of 6% is taken for this investment, then the annual repayment installments will be calculated with the following formula:

$$A = P \cdot GRF(i, n) \tag{11.1}$$

Where:

$A$  - annual repayment for taken loan;

$P$  - value of borrowed capital;

$i$  - interest rate (%);

$n$  - years of loan repayment;

$GRF(i,n)$  - return on equity factor.

$$GRF(i,n)=\frac{i(1+i)^n}{(1+i)^n-1}=\frac{0.06(1.06)^{10}}{(1.06)^{10}-1}=0.13 \tag{11.2}$$

$$A=100000 \cdot 0.13 = 13000 \text{ € / year} \tag{11.3}$$

**Table 5. Economic analysis of the designed power plant**

Economic analysis	
Equity	98085.49 €
Credit	100000 €
Interest rate	6%
Annual repayment	13000 €
Preferential tariff <sup>12</sup>	0.16 € / kWh

Source: author based on the actual policies of the banks in Republic of North Macedonia

The total profit from the photovoltaic power plant can be obtained by multiplying the total annual electricity production and the feed-in tariff (Table 10):

$$C_{vk} = E_{vk} \cdot FiT = 264902.4 \cdot 0.16 = 42384.384 \text{ € / year} \tag{11.4}$$

The time required for the return on investment will be given as a quotient of the total costs for the photovoltaic power plant and the annual earnings:

$$\frac{198085.49}{42384.38} = 4.67 \text{ years} \tag{11.5}$$

The investment for this photovoltaic power plant will return in 4.67 years, which means that the project for photovoltaic power plant of 201.6 kW in the city of Stip is profitable.

<sup>12</sup> This preferential tariff in R.N. Macedonia was valid until 2018. The preferential tariff has been used in the calculations because a premium tariff is now used.

## Conclusions

According to the financial analysis, the project for the photovoltaic power plant in Shtip is profitable and with its realization 112,647 kg / year of carbon dioxide emissions will be avoided. The construction of this photovoltaic power plant will open a new path to a cleaner environment and clean energy will be obtained.

The consciousness in the world is indisputably mature and the desire is clearly expressed, the ecological heritage that we will leave to future generations not to be less than what we have inherited. Saving on the costs of preserving the environment will significantly increase the costs that future generations will pay for its restoration.

## References

- [1] Jager, Klaus / Isabella, Olindo / H.M. Smets, Arno / A.C.M.M. van Swaaij, Rene / Zeman, Miro: *Solar Energy. Fundamentals, Technology, and Systems*. Delft University of Technology, 2014, pp. 326-327.
- [2] Mitanski, Dragan: *Utilization of the potential from renewable energy sources in the Republic of Macedonia for electricity production. Master thesis*. Bitola, 2016, pp. 50-51.
- [3] *Training Manual for Engineers and Technicians - Design and Installation of Photovoltaic Systems*, Skopje 2019





## DEVELOPMENT OF COMPUTER SOFTWARE FOR CREATING CHOREOGRAPHY

**RISIMA RISIMKIN, PhD**

Film Academy, Dance Department University of Goce Delchev, Stip, North Macedonia,  
risima.matevska@ugd.edu.mk

### Abstract

*This paper is based on research into the connection between computers and the process of documenting and creating choreography as part of the performing arts. The possibilities for creating a software program that will digitize the creation of choreographic record and will go a step further, a program that will be able to create works based on those digital records and will support the artistic expression in the creation process, ie. will enable the creation of software for the articulation of artistic expression. To develop such a program that will have the functionality to create computer-generated choreography.*

### Key words

*Computer-generated choreography, dance, contemporary dance, software, digitalize*

### Introduction

The paper is based on research into the use of digitalization in the performing arts, namely, the art of dance, as well as the possibility of programming software to create computer-generated choreography, with a focus on contemporary dance, its justification and use in a broader sense. Given the huge development of technology, especially in the field of computer science and technology, the question arose as to how to make a program for computer-generated choreography, which will support the creation process and what will be its justification in terms of creating works of art by artists 'live' (in-person), or the beginning of a process in which choreography can be created through software, which belongs to the field of artificial intelligence.

Research shows that initial attempts in this direction are based on the need to create digital records of choreographic works, given that in contemporary dance, there is no official vocabulary, as in the classical ballet technique, but each choreographer creates their own vocabulary. Throughout the history of the development of contemporary dance in the 20th century, attempts have been made to create an effective system for recording choreographic works, but the results are complicated writing systems, such as Labanotation (considered one of the most successful systems), then notation systems by Benesh, and Eshkol-Wachman. The development of technology provides an opportunity to create digital records and a number of artists and computer engineers are beginning to research in that direction. Exploring the historical development of this issue, we came to specific projects and programs that connect computers and choreography, at the beginning of the second half of the 20th century. During this period, the term 'computer-generated choreography' is formulated, and the development of technology directly affects the digitization and documentation of works of art. We are interested in how this process of computer-generated choreography can help in the creation of choreography, whether and how these programs will help in digitalization and technology in the educational process in the field of dance; determining the need for the art processes to keep up with and follow technological progress; studying the way of creating art programs and the impact that those programs will have on real-world situations, ie. their

use and justification. The paper explores the possibility of creating software for the articulation of artistic expression, based on a particular existing language for notation of dance (Labanotation).

## Literature review

The history of the development of the performing arts, especially contemporary dance, has been linked to the development of technology since the early 20th century, when Loie Fuller and her innovations in the use of light and light effects on stage appeared as she danced. The art of dance has developed extremely fast in the last years of the 20th century and the beginning of the 21st century and in its development, it introduces technological elements, which enrich the stage space and visualization of the works that are performed. Sometime in the middle of the 20th century, the first articles appeared in which computers were connected with choreography, and later through the development of this process the term 'computer-generated choreography' was developed, which means a technique for using algorithms to create a choreographic text, i.e. dance / choreography. The process began with the work of American dancer and professor Jeanne Beaman [1] in 1964, when with the help of computer scientist Paul LeVasseur she created the work "Random Dances" [2]. Her ventures are considered pioneering in terms of connecting computers and choreography. In 1966, Michael Noll [3], for the Philadelphia Art Alliance, wrote a paper titled "Choreography and Computers" (published in Dance Magazine in 1967), in which he spoke about the use of computers in the direction of writing and notation of choreography, i.e. how a computer program could recognize and transcribe the movements, leaving a permanent record of the choreography / choreographic text (dance notation typewriter). Noll assumes that if the traditional way of creating choreography is avoided, the time for rehearsing the choreographic text would be better used and the process of creation in the studio would be used to the maximum. He imagines that the choreographer has in front of him a "tool" ("digital computer with some form of visual display") through which he will create and write the choreography, which he will then only transmit to the dancers. Between 1968- 1974, Francisco Sagasti [4] and William Page attempted an interaction between dance and computers, i.e. worked on a program to "create and stage a computer-generated choreography for multiple dancers" [5]. Their work, on the one hand, is based on the need to use technology in creating dance sequences, which would bring the technology closer to the artists, but, on the other hand, to point out the fact that technology and computers cannot take the living artistic creations, no matter how sophisticated the software that will produce the program.

The first world-famous choreographer to connect computers to the process of creating choreography was Merce Cunningham. He used the "LifeForms" program to determine the position of dancers on stage and in 1991 created the first computer-generated choreography "Trackers", which he then staged. Cunningham also used "Dance Forms", the successor to "LifeForms", to create the "CRWDSPCR" choreography. This work remained on the company's repertoire until 1999.

The process of computer creation of choreography develops in parallel with the development of computer technology itself, algorithms, and neural network systems. Attempts and interest in combining technologies and computer advances in the programming of choreographic text sentences are increasingly appearing on the world stage. Most significant are the work of computer scientist Thomas W. Calvert from the eighties of the 20th century, the Choreology Project of the University of Sydney, based on Benesh notation [6], then the work of Robert John Lansdown [7], whose experiments were based on understanding the possibilities of creating computer-generated choreography / dance with the help of "various procedural techniques for generation" and "established notations for scoring". He realizes that in order to create a sophisticated program that will at least produce a choreographic text close to the work of a human choreographer, a remarkably sophisticated program needs to be created. Therefore, he, in a way, "limits" the program, in order to set only the basic movements of the dance sequences, "the peaks, not the complete movement", i.e. makes a framework, in which it allows choreographers to insert their ideas. Brazilian choreographer Analivia Cordeiro works on creating a computer program that uses computers and television to design and perform dance. According to her "by selecting components and establishing formal relationships between them, the choreographer structures an interactive dance-TV system. In this way he creates the algorithm which will generate the choreography he imagined". The computer program devised by Cordeiro generated a set of instructions for the dancer, the cameramen, and the TV director, with the dancer using his or her individual expression to define additional elements, such as muscular effort and fluidity of movement, that remained unspecified by the computer program.[8]

Considering that this paper aims to help develop software for creating choreography in the field of contemporary dance, special attention was drawn to the work of the Ohio State University, which in collaboration with world-renowned choreographer William Forsythe, through the Advanced Computing Center for the Arts and Design (ACCAD). They create the "Synchronous Objects" project, which seeks to answer certain questions, such as "What are the organizing structures behind a piece of choreography? How can these be made visible using interactive screen-based media? And what is the best way to communicate them?" [9]. Forsythe is making an effort to create digital platforms for storing choreographies, such as "Improvisation Technologies: A Tool for the Analytical Dance Eye", then "Synchronous Objects", and "Motion Bank", a research platform for creating and researching online digital scores in collaboration with guest choreographers.

Over the past twenty years, there appear authors who want to link computer-generated choreography to artistic dance expression, such as the project of Wayne McGregor, a world-renowned choreographer from the UK, and his collaboration with Google Arts & Culture Lab, followed by Luka Crnkovic-Friis and Louise Crnkovic. Friis in their paper "Generative Choreography using Deep Learning" and others.

### **Development of computer software for creating choreography**

The creation of a choreographic work can be defined as a complicated mental and artistic process, which is related to the conditionality of several elements needed to achieve the goal - dancer / body, space, choreographic thought / idea and process of the work itself, i.e. creation of movements in continuity, which would create a composition of movements, which will grow into a reflection of the choreographic thought, i.e. a process of creating a choreographic text. The original choreographic text is autochthonous and is part of the stylistic expression and poetics of each artist separately. In order to create a choreography with artistic expression, the choreographer works in a space in which he or she is together with the dancers (bodies) who are instruments in the creation of the choreographic text, which revives the choreographic thought.

To develop such a program that will have the functionality to create choreography, means to

digitalize the idea and the process of creating choreographic text. If we want to make a sophisticated computer program, which will initially write, i.e. document the process of creating dance sequences, and for that we take as a basis Labanotation, which through a complicated system of symbols, makes records for a certain choreography, it is necessary to get acquainted with the kinetic theories of dance by Rudolf Laban. In his system for the description of human movement, called “Laban movement analysis (LMA)”, Laban defines four basic categories, through which he makes his analysis of the movements: Body, Form, Strength and Space (Categories, according to the LMA, are capitalized). Laban, in his theories, gives an interpretation of the relations of the four categories: Body, Form, Strength and Space. He explains the connections and conditionality of these four basic categories, which are at the heart of dance, as well as their sub-categories and relations. At the same time, Laban creates a codified system for recording movements, Labanotation, which consists of symbols and is quite complicated, but can be taken as a basis on which to create the computer program.

All previously known tools / software programs for computer-generated choreography are based on the creation of formations and eventual positioning of bodies in space. Therefore, it can be said that if we look at the Laban Motion Analysis (LMA), as well as the categories Laban analyzes in his kinetic theories, the hitherto known types of computer programs for computer-generated choreography deal with the relationship between Body and Space. In order to achieve a real process of creating computer-generated choreography it is necessary to initially develop software that will cover the following categories individually: Body, Form and Strength. Then it will be possible to develop software that will generate the relationships between the categories, which, more precisely, will be able to obtain ‘original’ movements, which will be combined in the creation process.

Until we succeed in producing software programs that will break down and support the categories according to Laban, their subcategories and relationships in a software program, it is almost impossible to talk about the process of creation with computer-generated choreography which will reflect the real-world process of creating choreography.

Initially, it is necessary to create a digital model of the human Body (bodies). An example is a physical body, which will be connected to the computer body through sensors: Alter-body [10] of the original. In this way it will be possible to copy the movements and ‘write them down’ in the algorithm of movements, which we would divide into basic (basic), definite (individual) and interactive (duet). We will call this vocabulary of movements the Global Digital Vocabulary of HighAlterBodies.

### **Library of basic movements**

To clarify the process of creating the Global Digital Vocabulary, we will say that the software for the development of motions of the AlterBody, if based on LMA, should rely on biokinetics and the way the body moves. The program should initially be ‘fed’ by the Library of basic movements, which will consist of the well-known, specific movements of the Body category.

To complete the process of creating this library, an algorithm should be developed, in which

the categories - Body, Effort and Shape, and their sub-categories will be inserted, as well as defining the movements that contain the interactive reactions between these categories and sub- categories.

Effort has four subcategories (effort factors) - Space, Weight, Time and Flow, each of which has two opposite polarities (Effort elements); Direct/Indirect; Strong/Light; Sudden/Sustained; Bound/Free.

Shape has three Modes of Shape Change: Shape Flow, Directional & Carving.

Effort has a model of Action drive which includes Space, Weight, and Time with the combinations, named Float, Punch (Thrust), Glide, Slash, Dab, Wring, Flick, and Press.

These elements should be projected for each body segment separately.

The program created for the AlterBody will be able, we assume, to support 'real' human movement in dancing with greater credibility. Then, a program for the interaction between Space and the AlterBody should be developed, i.e. the ways of interaction of these two categories should be predicted. In combination with the software for AlterBody (with a completely generated Library of basic movements) and Space (with generated basic directions of movements), it will be possible to complete the movement of the computer-generated

AlterBody, which will be able to fulfill the tasks of creating certain movements through space, which would be closest to the terms dance and choreography. The program should define a basic digitized vocabulary of movements, supported by the categories and their software, which will represent the database of elements to be worked with.

### **Particular movements**

In order to realize the idea of complementing computer-generated choreography, with artistic expression, during further development, we need to create a prototype of an upgraded model of AlterBody with artificial intelligence, which we will call HighAlterBody. This model should have a program that combines, designs, and upgrades elements from the basic digitized vocabulary with individual interpretation and sequencing. Given that when creating live choreographic text (in-person), there is an interactive reaction between the choreographer and the dancers, which greatly facilitates the creation itself, such software should have a tool (brain), which will consist of algorithms and neural networks, with which it will be able to program the necessary interaction. Technology will help us feed this system, through programs that use neural networks and sensory interactions, as tools to support movements, according to certain human examples. Thereby, a library of special-defined-individual movements will be created, which will serve for further development of the HighAlterBody model.

### **Duet movements**

This part of creating the program will be the most complex, because it means the interaction of two HighAlterBodies. Each HighAlterBody will need to be able to maintain individuality and not produce symmetrically-synchronized movements, but individually-segmented movements, which will perform in interactive harmony. This duet movement will be programmed as an algorithm for connecting segmented and precisely defined parts of two HighAlterBodies.

The process of motion detection will again have to be combined with 'feeding' by simulating duet movements of real human bodies, recognizing and segmenting them. This phase can be developed when the first two phases of creating the Global Digital Vocabulary of HighAlterBodies to support the process of creating a choreographic text are fully formed.



The development of artificial intelligence will be crucial to finish this program, which will help create a model for the creation of mutual dance, which includes not only forms and formations throughout space, but ways of functioning that are transversal, three-dimensional and special.

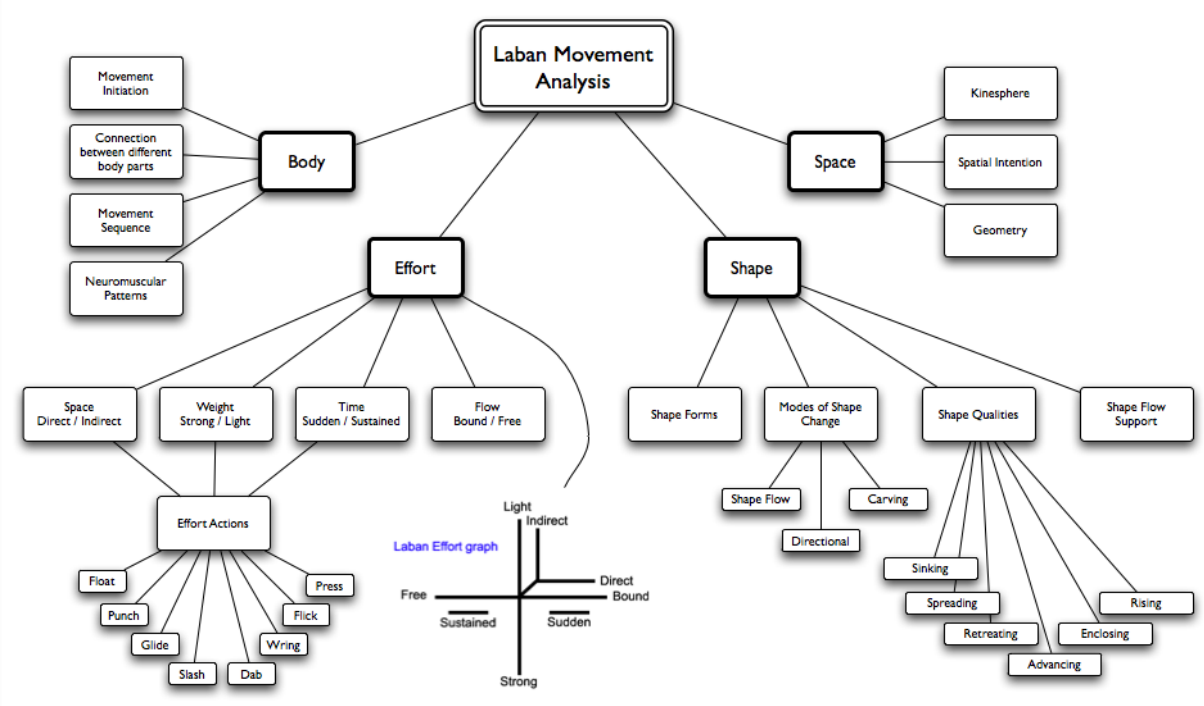


**Fig. 1 Key parameters of Laban Movement Analyses**

Source: Debaig, Clemence, *Using Laban Movement Analysis to create a framework of interactions*; <https://medium.com/@demzou.art>

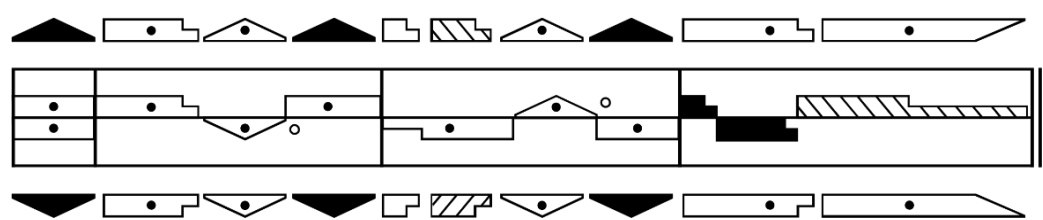


**Fig. 2 Labanotation, example, graphic score**

Source: <https://commons.wikimedia.org/wiki/File:Labanotation.svg>



## Conclusions

For the past 60 years, the development of computer-generated choreography programs has grown exponentially. The beginning is inspired, above all, by the desire to document and write down existing choreographies, ie. facilitating that process. With the development of computer technology and advances in software development, achievements are being accelerated. Today we have programs which are supported by artificial intelligence, which support the movement, which through sensors and holograms create an interaction of artificial AlterBodies and physically present bodies.

The original idea was to create a tool that would help shorten the creation process in the studio, thus saving time and resources, a tool that would allow the choreographer to try out certain

situations and experiment, without involving other participants and to work more effectively in a studio, 'live' (in-person). Now, that idea has been developed to a much higher level, as state-of-the-art programs are used to determine motion and create body avatars that move and reproduce computer-generated motion. By creating the Global Digital Vocabulary of HighAlterBodies program, the development of computer-generated choreography will be elevated one level higher. Creating a dance is still a thought, but we are approaching the moment when a program will be created that can upgrade itself and 'think'.

Here, we can ask ourselves the question of the ethical justification of the development of such technology and its use, as well as the replacement of people with their digital AlterBody and HighAlterBody counterparts. The dilemma is philosophical, we wonder if such programs can completely replace the creativity that is born through the interaction of two living beings - the choreographer and the dancer. The 'artistic' dimension will be difficult to achieve until artificial intelligence reaches the peak of its development. This advancement of technology will completely change the understanding of Man and his environment, will develop and technologically overcome the social, anthropological segments of the social order. Dance, since ancient Greek times, is considered a free (perhaps the oldest) art. It was originally associated with the term 'expressive art', as opposed to 'constructive art', a term that Nietzsche [11] later defined as 'Dionysian' and 'Apollonian' art. It is a dualism that has permeated the definitions of artistic categories for centuries. Dance is considered a part of the fine arts, which has a universal language, with strong individual features. When talking about the future of dance and choreography and their connection to technology, as well as the development of computer programs, the advantage that dance has as a free, expressive, Dionysian art, becomes an obstacle, which in the future, through technology will have to be determined through the 'dose' of constructiveness it carries, which takes away expression, the main individual feature of contemporary dance and contemporary dance choreography. What started out as a need for a 'tool' to help document choreographic performances can take precedence and develop into a process that will completely replace the existing notion of artistic values and needs. The development of technology is unstoppable and necessary in many segments of modern life, because it facilitates and simplifies the daily process of existence. However, there is a dose of doubt, simply, here, today, we are not sure how technology will succeed in replacing the process of interaction between two human beings and the individuality of their expression in contemporary dance. And, the question is, if that succeeds, what will happen to Man and his creativity, what will happen to art?

## References

- [1] Jeanne Hays Beaman (1919 – 2020) was an American pioneer of computational choreography, creating the piece *Random Dances* in 1964 by using an IBM 7070 computer to select and order movement instructions from three lists. Her 1965 article, "Computer Dance", was widely cited by later practitioners, as was a 1968 exhibition of her process at the Institute of Contemporary Arts in London. In her early career she studied with Martha Graham and danced with the San Francisco Ballet; she was also Professor Emeritus at the University of Pittsburgh, where she taught from 1961-74.
- [2] J. Beaman, "Computer Dance: Implications of the Dance," *Impulse: The Annual of Contemporary Dance*, 1965, 27–28.
- [3] A. Michael Noll (born 1939) is an American engineer, and professor emeritus at the Annenberg School for Communication and Journalism at the University of South California. He was a very early pioneer in digital computer art and 3D animation and tactile communication.
- [4] FRANCISCO SAGASTI is a professor at the Pacifico Business School of the Universidad del Pacifico and a senior researcher emeritus at FORO Nacional Internacional, Lima, Peru.
- [5] Francisco Sagasti and William Page, "Computer Choreography: An Experiment on the Interaction between Dance and the Computer," *Computer Studies in the Humanities and Verbal Behavior* 3 (January 1970): 46–49. This short-lived academic journal, printed by Mouton & Co. in The Hague, saw the publication of five volumes between 1968 and 1974.
- [6] Benesh Movement Notation (BMN), also known as Benesh notation or choreology, is a dance notation system used to document dance and other types of human movement. Invented by Joan & Rudolf Benesh in the late 1940s, the system uses abstract symbols based on figurative representations of the human body. It is used in choreography & physical therapy and by the Royal Academy of Dance (UK) to teach ballet.
- [7] Robert John Lansdown (1929 – 1999) was a British computer graphics pioneer.
- [8] Analivia Cordeiro, "The Programming Choreographer," *Computer Graphics and Art Magazine* (February 1977): 29, <http://analivia.com.br/analivia-cordeiro-theprogramming-choreographer/>.
- [9] 60. Steve Sucato, "The Science Inside a Dance: What Can Choreography Do for Scientific Research? William Forsythe and Ohio State University Team Up to Find Out," *Dance Magazine*, May 2009, 50.
- [10] In the text below, when describing the software program, we will use this term to denote the end-product that we want to get.
- [11] Friedrich Nietzsche, *Die Geburt der Tragödie aus dem Geiste der Musik*, Publisher E. W. Fritzsch, 1872.



## AUTOMATED SYSTEM FOR SMART METER TESTING

*Peter Janiga<sup>1</sup>, Boris Cintula<sup>2</sup>*

<sup>1</sup>Slovak University of Technology in Bratislava, Faculty of Electrical Engineering and Information Technology,  
email: [peter.janiga@stuba.sk](mailto:peter.janiga@stuba.sk)

<sup>2</sup>Slovak University of Technology in Bratislava, Faculty of Electrical Engineering and Information Technology,  
email: [boris.cintula@stuba.sk](mailto:boris.cintula@stuba.sk)

### Abstract

*Smart metering is debated issue currently. It is a consequence of the introduction of this technology into practice, a many of pilot operations and the effort find the optimum technology for each area. The aim of the paper is a system for testing of selected functionalities of smart meters. In particular, the ability to evaluate the power quality parameters such as waveform distortion, detection of maximum and minimum values and other parameters defined in the standard STN EN 50160. Described system is under development and testing, so some functionality will put the finishing touches according to current requirements.*

### Key words

*Smart meter, measuring, harmonics, testing*

### Introduction

Incoming technology of smart metering brings new opportunities for power system operation. Smart metering provides in addition to measurement of voltage, current, and then calculating other indicators, for example distortions, interruptions, etc.

Functionalities adding to the meter a makes question about validity of obtained data. Not all parameterizations of smart meters are set correctly and identifying incorrect setting is not easy. If the problem with incorrect settings is appear after installing to the network, then many problems arise with subsequent disposal problems. Therefore, precision testing is the pursuit of prior to commissioning. Developed measuring system allows testing the most common errors in parameterization of smart meter and variability of the system allows adjusting the measuring system to identify any problems.

Between the problems which the system wants to identify include, for example, influence current flow and data transfer error. In the case specify distorted current flow may cause the increasing the error rate of data transmission. The proposed system allows generating currents up to 100th harmonic distortion.

A further possibility of presented system is the use when smart meters are tested at different operating temperatures. For example, the smart meter verification of accuracy of measurements of limitary low and limitary high temperature by placing smart to the conditioning chamber, using high precise power supply source and reference standard using an accurate measurement can be verified by measurement bias and quantify uncertainty smart meter.

### 1. Components of testing system

Developed system consists of a programmable source, reference standard, measuring the stand and control software. Programmable source Applied Precision 8325B has a separate current and voltage circuits. If necessary, there is possible to connect these circuits but it is necessary to carry out to safety. Output circuits of power source can generate the signal in the range of 0-

300 V and 0-120 A. Signal generator, which generates shape of voltage and current, can generate a waveform with 100 harmonics.

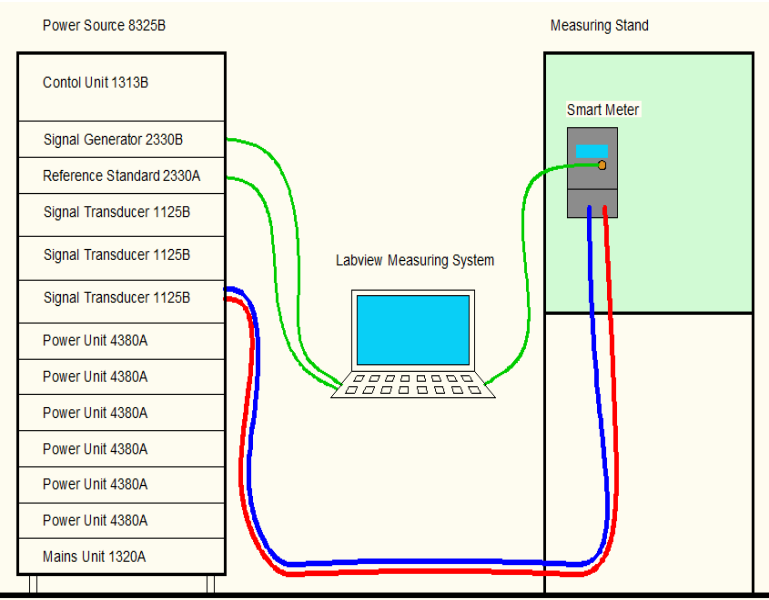
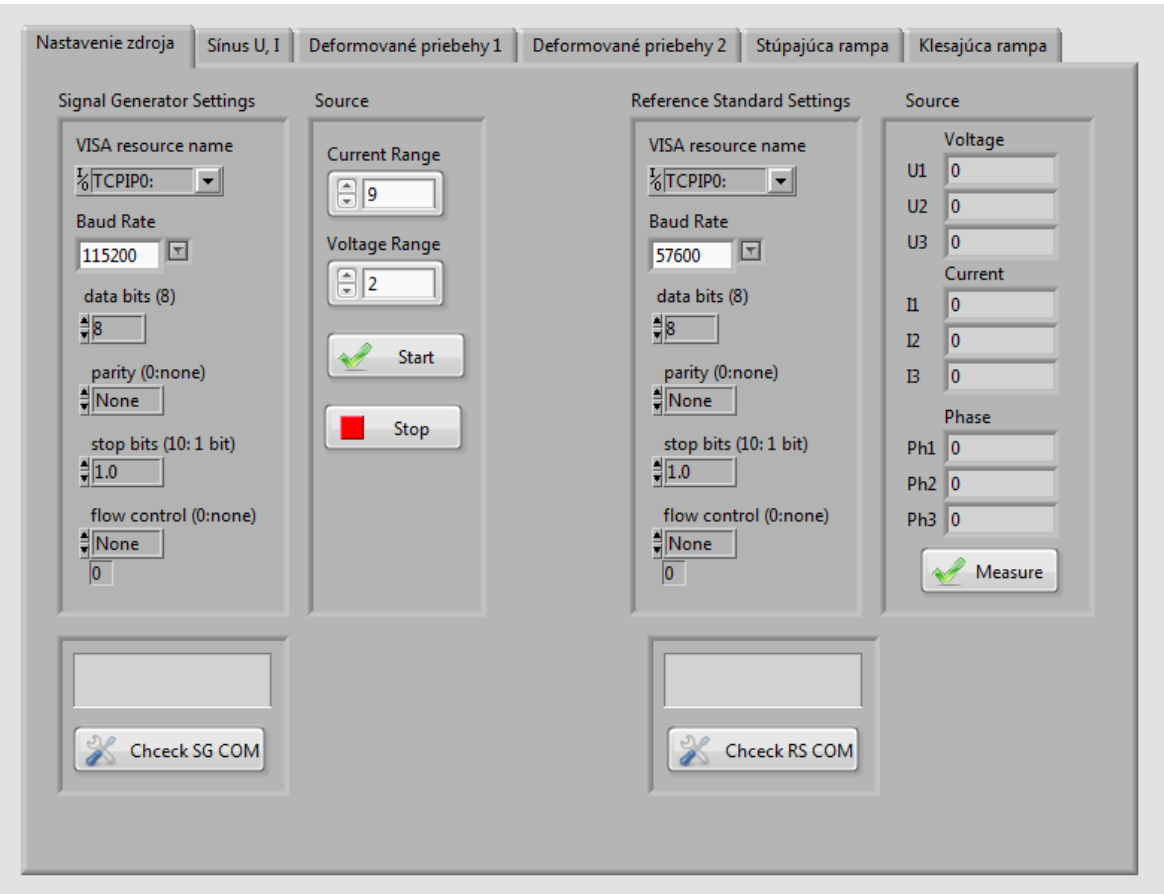


Fig. 1 Scheme of measuring system

Programmable source Applied Precision 8325B has a separate current and voltage circuits. If necessary, there is possible to connect these circuits, but it is necessary to carry out to safety. Output circuits of power source can generate the signal in the range of 0-300 V and 0-120 A. Signal generator, which generates shape of voltage and current, can generate a waveform with 100 harmonics.



**Fig. 2 Main window of software**

Source has separate three phases of voltage and current circuits. This allows verifying the meters with indirect measurement. On the other hand, if is necessary to measure more than two meters with interconnected current and voltage circuits (disconnection is not technically possible) then use isolation transformers is required.

The main program window Fig. 2 shows a set of communication paths with signal generator and the reference standard. Those are standard serial port settings. At the bottom there is a button to test communication. For correct communication window lists the name of the signal generator and the reference standard.

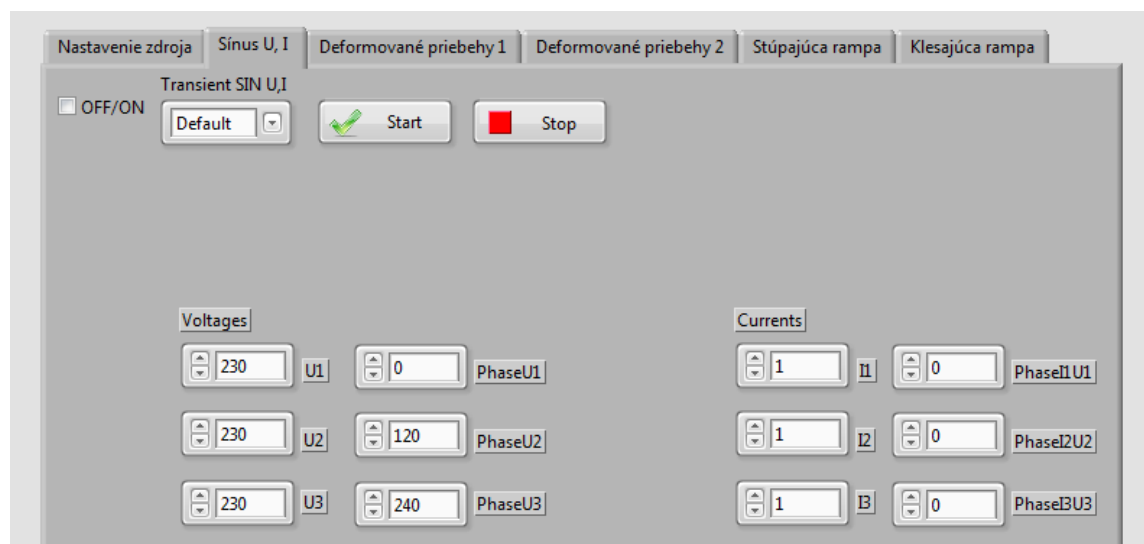


**Fig. 3 Window for testing with sinusoidal signal**

Second window Fig. 3 allows setting voltages and currents to generate sinusoidal signals. On the top of the window is transient option set, which means how will run output source. It is possible to choose between three options: default (signal will be generated according to the default setting source), generate soft (gradual onset signal under the curve, which is defined in the source) and immediate (ramp signals will be immediate). If there is immediate set, then must be careful about shocks. In some cases, must be range chose with a margin that starting do not disconnect internal resource protection.

Created system allows generating distorted waveforms of voltages and currents. System in conjunction with the above described source can generate harmonics up to order 100. For each harmonic can also enter the angle, which can change the shape of the resulting waveform. When entering the deflection voltage parameter can be entered manually or choose from predefined signals. Harmonic distortion of predefined signal based on EN 50160th. The options are All harmonics (0 to 100th harmonic of EN 50160) Even harmonics (0 to 100 odd harmonic of EN 50160) Odd harmonics (0 to 100 odd harmonic of EN 50160) Tripplen harmonics (0 to 100 tripplen harmonic of EN 50160).

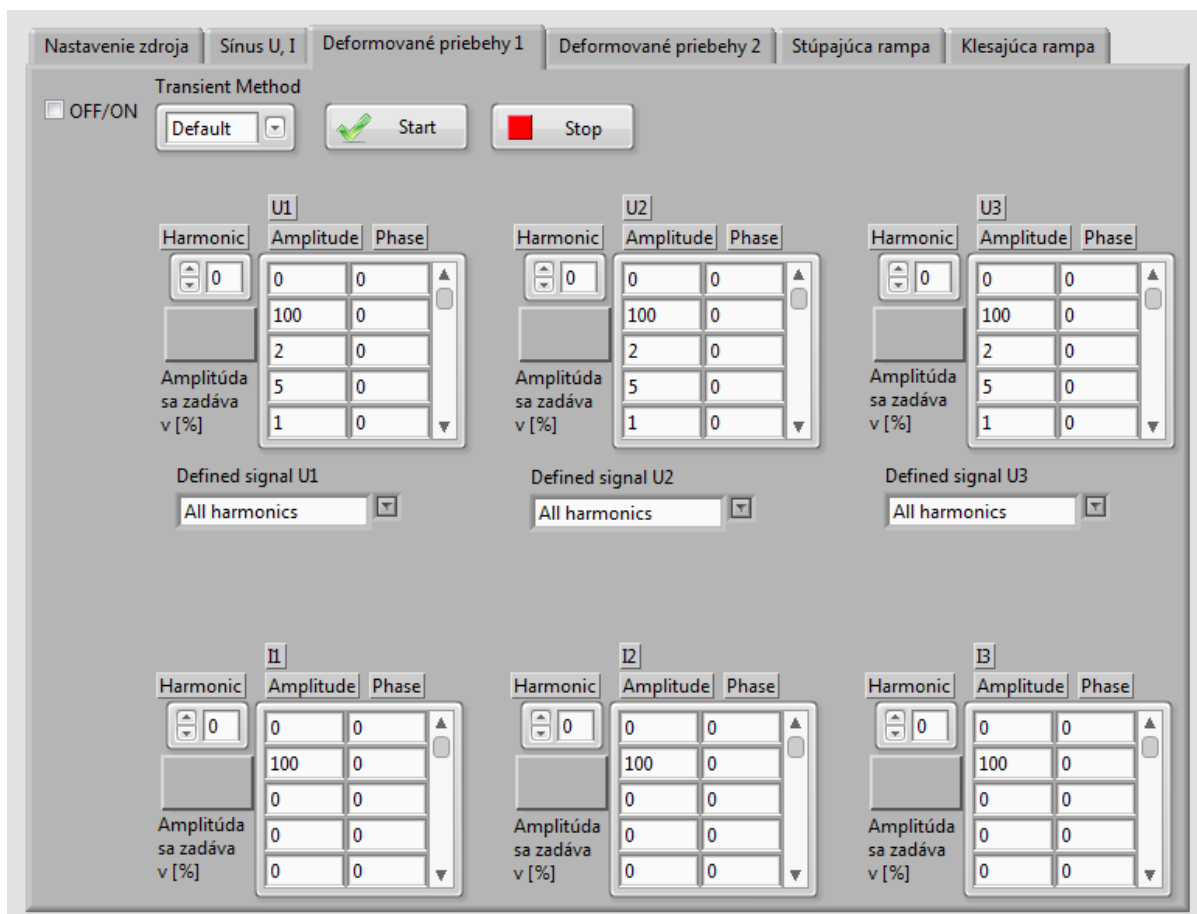


Fig. 4 Window for testing with distorted signal

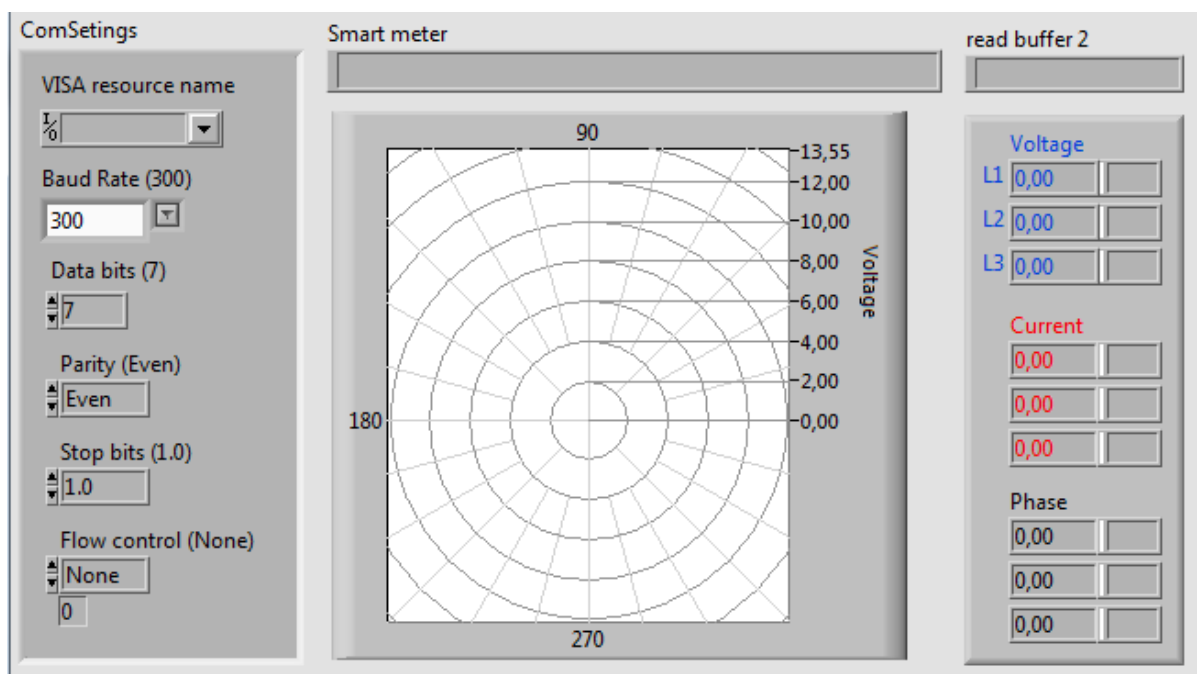


Fig. 5 Smart meter data window

Test panel allow comparing the values measured by reference standard and read from smart meter by optic head. Before communication start with smart meter is necessary to set



communication parameters for optic head adapter. This is particularly the speed of communication, which can be in a variety of smart meters is defined differently. Smart meter data window reads the actual values recorded to smart meter. Phase diagram can be created from the values. All measured values are shown numerically. A graphical representation is showed for better orientation in the results.

### 3. Testing the measuring set

The system has been tested only on simple tests when running sine and also when running distorted waveforms. Test and subsequent consultation with distribution network operators showed justify the system and the requirement from technical practice. Based on the responses to the created system will be modified next steps for the tests were focused on the most common problems.

During tests are compared values from the Main window and Window Smart metering data. Form and expression of the measured differences can be defined arbitrarily due to variability of Labview.

Block of Smart metering data currently read 9 registers:

- 32.25(),52.25(),72.25() for voltages
- 31.25(),51.25(),71.25() for currents
- 33.25(),53.25(),73.25() for phases

The registers mentioned above correspond to the actual measured values. In case that were analyzed other values that can detect the smart meter, a simple method adds read registers and values are displayed.

The important thing is to have the exact address of the register to be read. The values obtained can be compared with the reference standard outputs or with data from other measuring devices.

The system could be made for the case that the data were compared with those consigned to the data centers. Such a solution but requires parameterized settings headquarters and create a working data connection created with the database system. At this stage, the aim of verifying the measured data and they are stored in memory registers.

### Conclusions

Developed system is under debugging. Highlights include established software modularity and easy adaptability according to current requirements. This variability is given variability of LABVIEW program, through which the whole system is created. Even in developing parts of the program, emphasis was placed on creating blocks that can be configured as a different edit.

Developed system has great potential for testing smart meters and supports the different parties to deploy the technology and also to eliminate some problems.

Additional steps that could finalize the generation of power interruption and monitoring how these interruptions evaluates the smart meter.

Since it is possible for smart meters to define many functionalities, it is also necessary to leave the system in an optimal manner designed to be customizable open to emerging needs.

## References

### Standards

- [1] IEC 736 Testing equipment for electrical energy meters
- [2] IEC 387 Symbols for alternating-current electricity meters
- [3] STN EN 60521 Class 0.5, 1 and 2 alternating-current watt-hour meters
- [4] STN 35 6111 Induction var-meters. Technical requirements and test methods
- [5] STN 35 6113 Maximum demand indicators for electricity meters. Technical requirement and test methods



## INFLUENCE DIMING OF LED LAMPS TO ELECTRICAL PARAMETERS

*Peter Janiga<sup>1</sup>, Marek Mokran<sup>2</sup>*

<sup>1</sup>Slovak University of Technology in Bratislava, Faculty of Electrical Engineering and Information Technology,  
email: [peter.janiga@stuba.sk](mailto:peter.janiga@stuba.sk)

<sup>2</sup>Slovak University of Technology in Bratislava, Faculty of Electrical Engineering and Information Technology,  
email: [marek.mokran@stuba.sk](mailto:marek.mokran@stuba.sk)

### Abstract

Lighting systems are currently one of the main uses of electricity. The most popular option for reducing of electricity consumption is the use of dimming. Dimming is a type of regulation in which we can regulate luminous flux of a lamps and luminaires. This system of regulation is used in the road lighting industry, but also in households. Dimming allows adaptation of the lighting system according to specific requirements and various ambient conditions such as traffic density, daylight, etc. The regulation of the luminous flux de-pending on the dimming system can affect the electrical parameters of the luminaires such as the power factor. The article deals with the electrical parameters of luminaires with various lamps at different types of dimming.

### Key words

LED, Power factor, total harmonic distortion

### Introduction

In recent years LED luminaires play a decisive role in the field of lighting systems. Among their most important benefits are luminous efficiency, various correlated color temperature, color rendering index and energy efficiency that leads to energy savings. LED luminaire consists of a main body, light sources, power supply (LED driver) and an optical distribution system. LED driver is a non-linear load. Designing the LED drivers is a challenging task where many problems need to be solved. The most frequently solved problems are currently harmonics reduction and power factor correction (PFC). Power supplies without power factor correction generated and reflected back to the AC power lines many unwanted harmonic currents which degrade the power quality.

The presence of harmonics in power system can cause various problems such as reducing the power factor and so on [1].

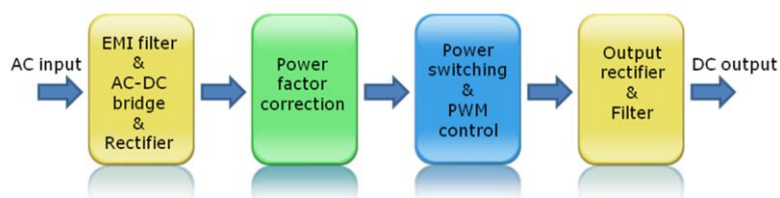


Fig. 1 Block diagram of LED driver with power factor correction

Power factor is simply defined as the ratio of real power to apparent power:

$$PF = \frac{P[W]}{S[VA]}$$

If both current and voltage are sinusoidal and in phase the power factor is 1. If both current and voltage are sinusoidal but not in phase, the power factor is the cosine of the phase angle.

$$THD_i[\%] = 100 \times \sqrt{\sum_{p=2}^{\infty} \frac{I_p^2}{I_1^2}}$$

### 1. Literature review

Total harmonic distortion is quadratic sum of the unwanted harmonics over the fundamental that gives the relative weight of the harmonic content with respect to the fundamental. [2] Electrical equipment in Europe must comply with the EN 61000-3-2 “Electromagnetic compatibility (EMC). Part 3-2: Limits. Limits for harmonic current emissions (equipment input current up to and including 16 A per phase)”. [3] There are 4 different classes (A,B,C,D) in the EN 61000-3-2 that have different limit values. It should be taken into consideration that these limits are for individual harmonics (from 2 to 40) and do not specify total harmonic distortion (THD). Class A are Balanced 3-phase equipment, household appliances excluding equipment identified as class D, tools, excluding portable tools, dimmers for incandescent lamps, audio equipment, and all other equipment, except that stated in one of the following classes. Class B are Portable tools, arc welding equipment which is not professional equipment Class C are Lighting equipment. (Table I.) Class D are PC, PC monitors, radio, or TV receivers. Input power  $P \leq 600$  W. [4] If a power supply output power is grated than 25W, it must meet class C. Otherwise it can be test withed the class D standard. To pass Class C and Class D, power supply must have power factor correction.[5]

**Table 1 Harmonic current limits for LED driver > 25W**

Harmonic order n	Maximum permissible harmonic current expressed as a percentage of the input current at the fundamental frequency %
2	2
3	30.λ *
5	10
7	7
9	5
11 ≤ n ≤ 39	3
* λ is the circuit power factor	

### 2. Power factor correction

When choosing a PFC it is important to recognize that the low power factor that occurs in LED drivers is different from the power factor of traditional load. Low power factor of traditional load requires a different correction approach. This type of low power factor can be easily corrected by adding the reactive component of the opposite sign in parallel with the load. Low power factor of LED drivers is caused by nonlinear circuit elements. Low Power Factors can be improved by PFC circuits. We know the two basic types active and passive PFC. Active PFC is more efficient, a little more expensive, generally integrated into a power supply, and can achieve a PF of about 0.98 or higher. Passive PFC is less expensive and usually corrects PF to lower values.

### 2. Measurement of electrical parameters

For the measurement were selected three luminaires with different drivers and powers.

**Table 2 Electrical parameters of luminaire with driver 1**

Driver 1					
Dimm [%]	S [VA]	P [W]	Q [Var]	PF [-]	THDi [%]
10					
20	6,32	1,60	6,12	0,250	16,56
30	7,40	2,43	6,98	0,328	21,06
40	7,99	3,14	7,35	0,390	21,57
50	8,55	3,91	7,61	0,456	18,49
60	8,95	4,58	7,68	0,513	15,86
70	9,46	5,52	7,67	0,584	13,91
80	9,85	6,43	7,59	0,654	12,15
90	10,56	7,25	7,43	0,693	10,81
100	10,90	8,04	7,35	0,737	10,09

**Table 3 Electrical parameters of luminaire with driver 2**

Driver 2					
Dimm [%]	S [VA]	P [W]	Q [Var]	PF [-]	THDi [%]
10	11,14	3,05	10,70	0,271	15,42
20	12,21	5,94	10,67	0,483	16,27
30	15,14	8,95	12,31	0,597	17,53
40	15,14	11,10	10,23	0,734	10,70
50	17,25	14,11	9,92	0,817	9,73
60	20,69	18,20	9,77	0,881	8,68
70	23,12	21,09	9,46	0,907	8,12
80	25,57	23,79	9,34	0,930	7,55
90	28,42	26,86	9,15	0,944	7,31
100	31,07	29,76	8,94	0,957	7,11

**Table 4 Electrical parameters of luminaire with driver 3**

Svietidlo 3					
Dimm [%]	S [VA]	P [W]	Q [Var]	PF [-]	THDi [%]
10	23,98	9,88	21,76	0,413	86,70
20	41,15	18,63	36,64	0,453	87,65
30	32,85	30,14	13,06	0,917	24,35
40	41,06	38,82	13,47	0,945	21,35
50	49,86	47,82	13,91	0,960	18,44
60	59,56	57,80	14,37	0,970	15,86
70	68,86	67,22	14,83	0,977	13,86
80	78,70	77,14	15,59	0,980	12,77
90	89,44	87,92	16,42	0,983	11,75
100	98,69	97,19	17,10	0,985	10,98

Luminaire 1 has a driver 1 with rated power 18W with range of load 3 - 18 W. Luminaire 2 has a driver 2 with rated power 35W with range of load 15 - 35 W. Both have been controlling by DALI. Luminaire 3 has a driver 3 with rated power 100W. It has been controlling by 1~10Vdc, 10V PWM, resistance and contain built-in active power factor correction function. Drivers 1 and 2 have a declared power factor of 0.95 and Driver 3 has declared power factor > 0.96 at rated power. The load of the drivers 1 (44% of rated power) and 2 (85% of rated power) is lower than rated power of drivers which are used in the selected luminaires. The load of the driver 3 is approximately equal to the rated power (97% of rated power). Electrical parameters were measured during dimming in the range of 10 - 100% of luminous flux for all luminaires. During the measurement were luminaires supplied from a stabilized AC power supply with nominal voltage 230 V. At each level of dimming were the samples stabilized for 15 minutes. Measurement of electrical parameters was performed using the precision meter for electrical power and energy measurement Applied Precision reference standard rs 2330A. The measured values of active, apparent, reactive power, power factor and total harmonic distortion of current during the dimming are shown in the tables 2 - 4. A comparison of the individual measured parameters for the selected ballasts is shown in the figures 2 - 6.

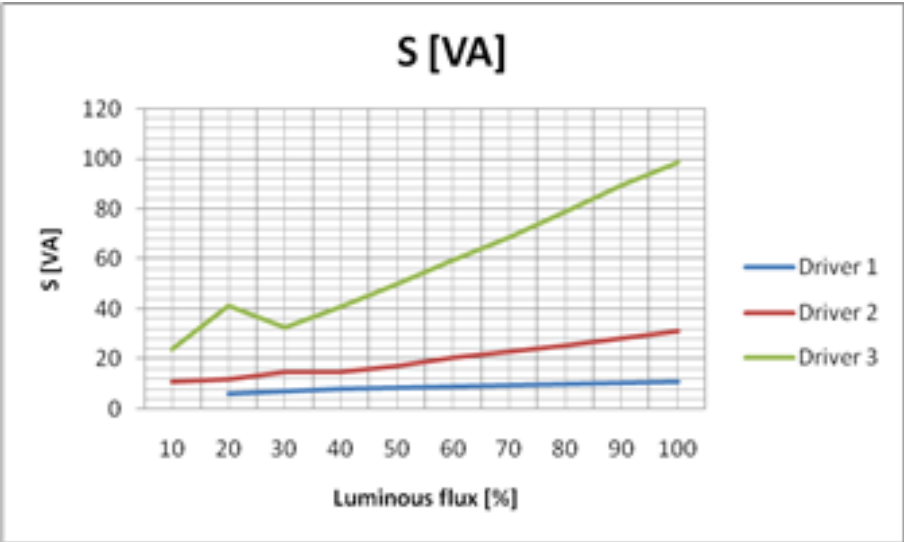


Fig. 2 Apparent power dependence on dimming

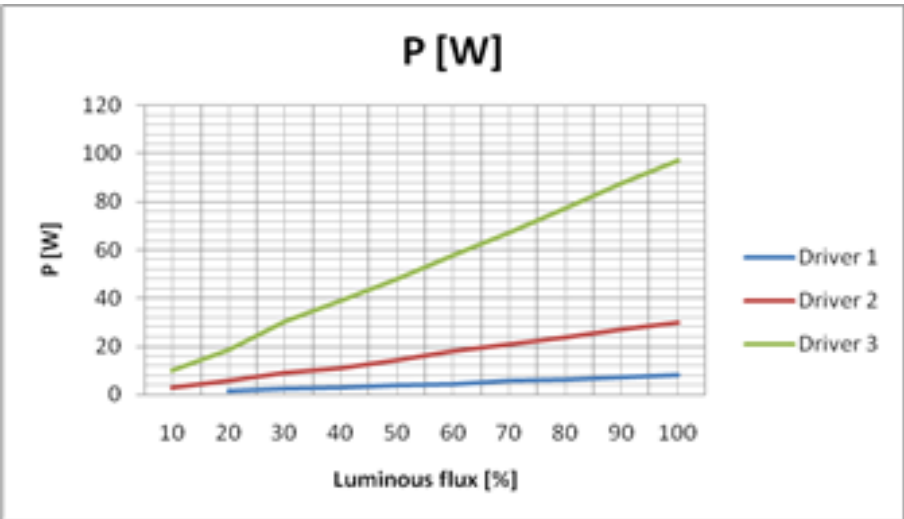


Fig. 3 Active power dependence on dimming



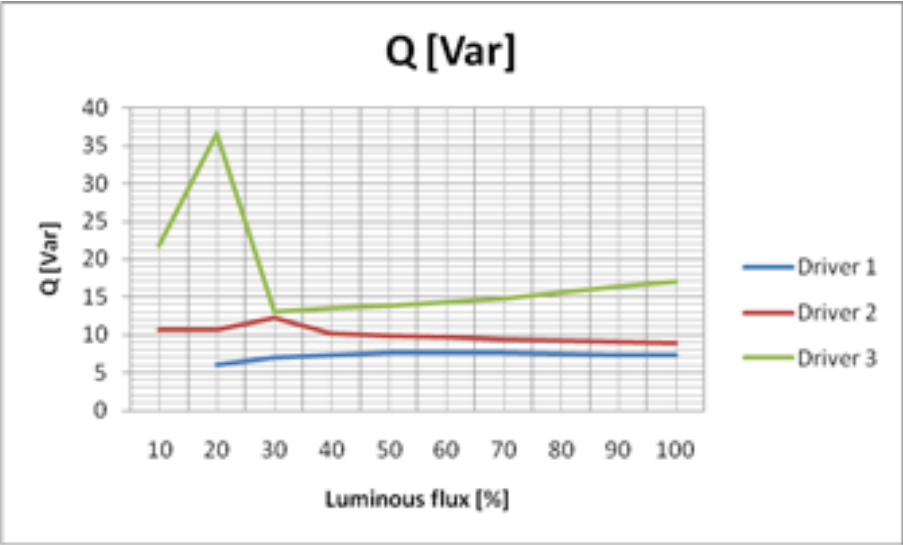


Fig. 4 Reactive power dependence on dimming

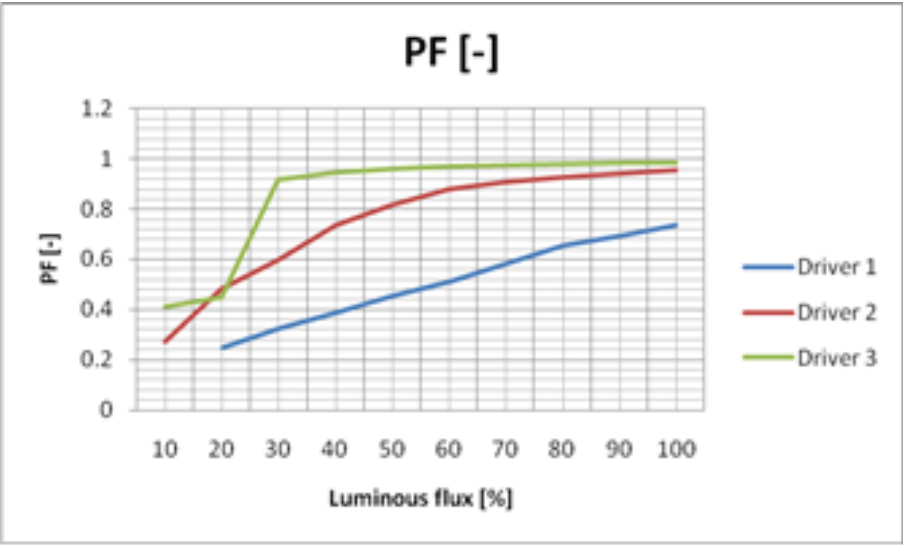


Fig. 5 Power factor dependence on dimming

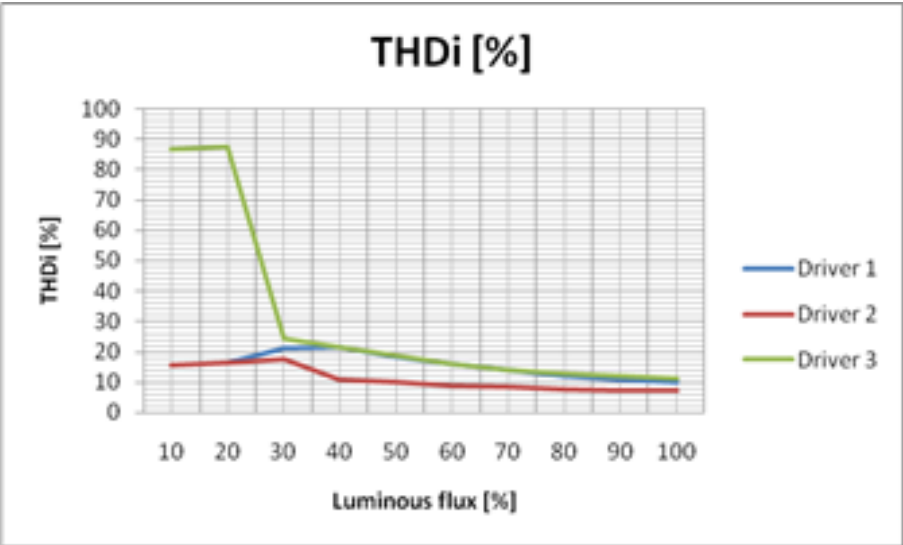


Fig. 6 Total harmonic distortion dependence on dimming

Driver 1 has a declared power factor of 0.95 at rated power. The load of the drivers 1 was 44% of rated power. This caused that at 100% (8.04W) was the maximum power factor 0.737. Driver

1 was dimmed in the range of 20 - 100%, because less power than 1.6 watts could not be set. Driver 2 has also declared power factor of 0.95 at rated power. The load of the drivers 2 was 85% of rated power. At 90% dimming (26.86 watts) was the power factor 0.944 which is less than declared 0,95. Driver 3 has declared power factor  $> 0.96$  at rated power. The load of the drivers 3 was 97% of rated power. Measured values show that the use of dimmable drivers with power factor correction is better because it can correct power factor values better than 0.95 in the range 50 - 100% of dimming.

## Conclusions

Dimming allows control of the lighting system according to specific requirements and various ambient conditions. Dimming allows to reduce the power consumption of public lighting systems at nighttime when there is a low traffic also allows the control of interior lighting systems in dependence on the availability of daylight. During dimming are electrical parameters that can affect the power quality and the electromagnetic interference changing. One of the parameters that change significantly is the power factor. In Slovakia is power factor evaluated monthly for electricity consumers. It assesses the amount of active and reactive electricity taken off. If the users or company does not comply with its tolerance values of 0.95 to 1 than the special mark-ups on the invoice apply. Lighting systems with regard to the operating time of the dimming and the used luminaires may significantly affect the value of the power factor. The solution of this problem is compensating devices which by their activity maintain the optimal values of the power factor.

## References

### Standards, handbooks and reports

- [1] T.A. Kneschke, "Distortion and Power Factor of Nonlinear Loads", IEEE Power Engineering Society Summer Meeting, 1999, pp. 457-462.
- [2] ON Semiconductor, Power Factor Correction (PFC) Handbook, HBD853/D Rev.5, 2014
- [3] K IEC 61000-3-2, Electromagnetic compatibility (EMC) – Part 3-2: Limits – Limits for harmonic current emissions (equipment input current  $\leq 16\text{A}$  per phase), 2018.
- [4] European power supply manufacturers association, Harmonic current emissions, 2010
- [5] MEAN WELL ENTERPRISES, LED power supply technical manual, 2009



## INRUSH CURRENT OF LAMP

*Peter Janiga<sup>1</sup>, Marek Mokran<sup>2</sup>*

<sup>1</sup>Slovak University of Technology in Bratislava, Faculty of Electrical Engineering and Information Technology,  
email: [peter.janiga@stuba.sk](mailto:peter.janiga@stuba.sk)

<sup>2</sup>Slovak University of Technology in Bratislava, Faculty of Electrical Engineering and Information Technology,  
email: [marek.mokran@stuba.sk](mailto:marek.mokran@stuba.sk)

### Abstract

*Lighting systems pass through big change in terms of light source recently. LED replace discharge lamp and this change represent change of electrical parameters and influence to installations. Lighting systems with discharge lamp use inductive ballasts with choke and starter or electronic ballasts. Lamps with LED use drivers which are switching sources. The drives include rectifier, high frequency oscillator, transformer and capacitors. Typically, rectifier has impact to distortion of luminaire current and capacitor has impact to inrush current. Over the last years, problem increases with inrush current. Public lighting networks reconstruct with LED luminaires. Often increase inrush current and circuit-breaker must be changed for stronger. This change cause increasing of payment for energy distribution and sometime is necessary change installation. Aim of this paper is describe difference between luminaires from point of view inrush current. Size and duration of inrush current depends on construction of driver and on phase of supply voltage. In paper are analyzed amplitudes, durations and behavior of electrical parameters various LED luminaires.*

### Key words

*LED, lamp, driver, inrush current*

### Introduction

Describes Lamps are quantitatively important group of consumers. Therefore, the question about optimizing their operations is still topical problem. In this context, operator efforts to reduce consumption and costs associated with maintenance and lighting system. In the past, thermal light source was dominated and for start it or operation of this lamp was not necessary driver or ballast. With discharge lamps using appear ballasts and later to reduce losses classic ballast pass to electronic ballast. Recently, LED light sources entered to using in interior and exterior lighting systems. When LED lamp is powered up from distribution network (for example 230 V AC) then lamp need driver for voltage and current stabilization.

### 1. Literature review

Driver is electronic circuit shown schematically in the figure below. In term of transients the peaks of current are during start up. Switching affects depend on size of the capacitor in DC side of bridge rectifier. His rapid charging cause increased value of start up current.

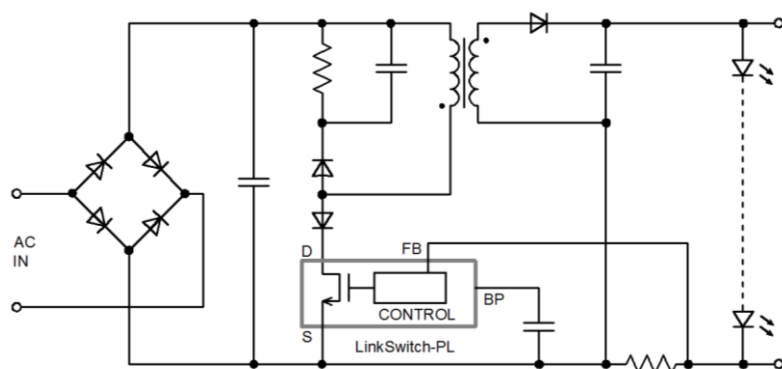
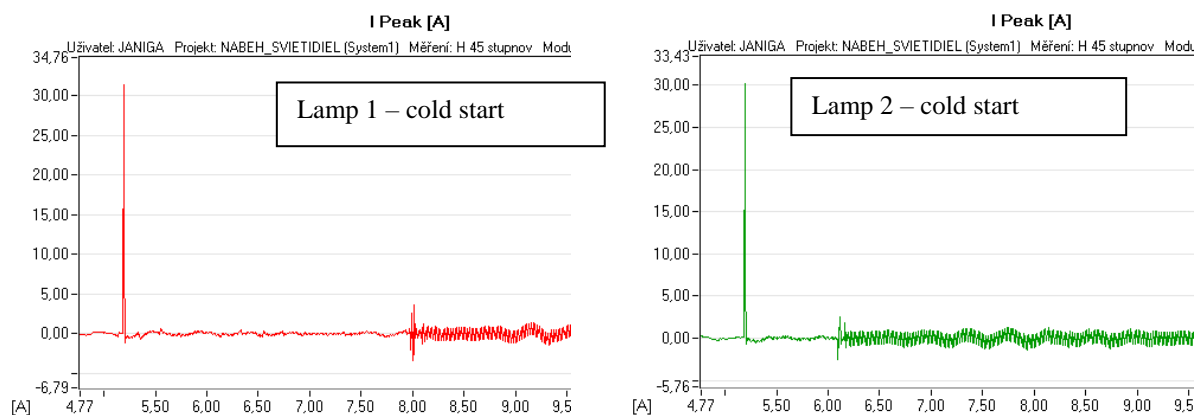


**Fig. 1** Scheme of components in driver for LED lamp

Next transient is during driver output LED load connection. This transient is much smaller and its size and delay depending on lamp type. Delay between first and second transient is less than one second usually. The second current increase is about half of first transient. Size and time when current peaks come are depending on the driver construction, used LED modules, capacitor discharge (re-start) and phase of voltage when turning on the lamp. In the case driver with harmonic filter may be the size of starting current depends on inductance and capacitance of this filter also [5].

## 2. Inrush current LED lamp with driver

During the start of a lamp with LED driver occur two transients. Fig 2 shows behavior of two different lamps starts and shows what a difference may be when lamp start from normal status (cold start) and when lamp is restarted (hot start). The upper waveforms show start from cold status and bottom waveforms show start from warm-up lamp. During these measurements were phase and size of voltage identical. The aims of these measurements are show the differences of delay between first and second current peak.



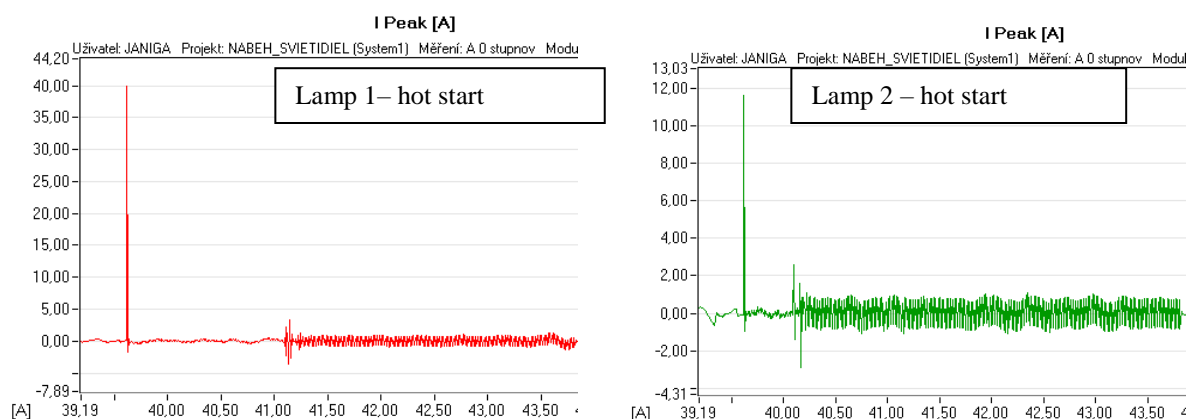
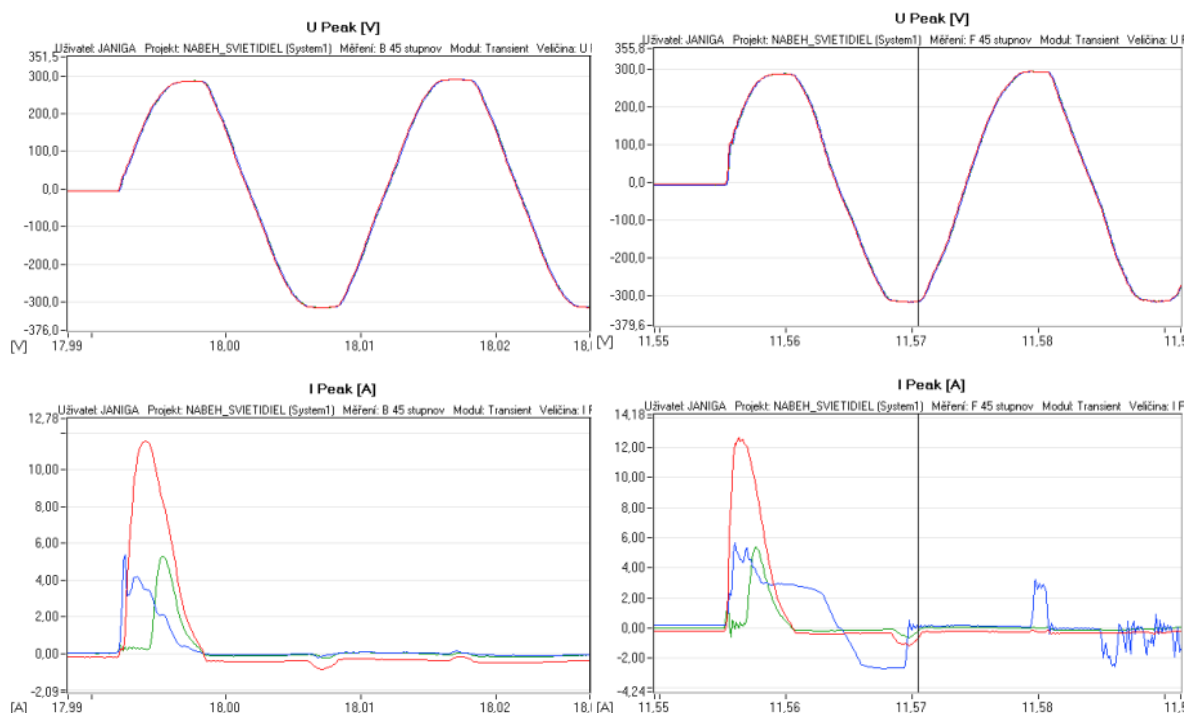


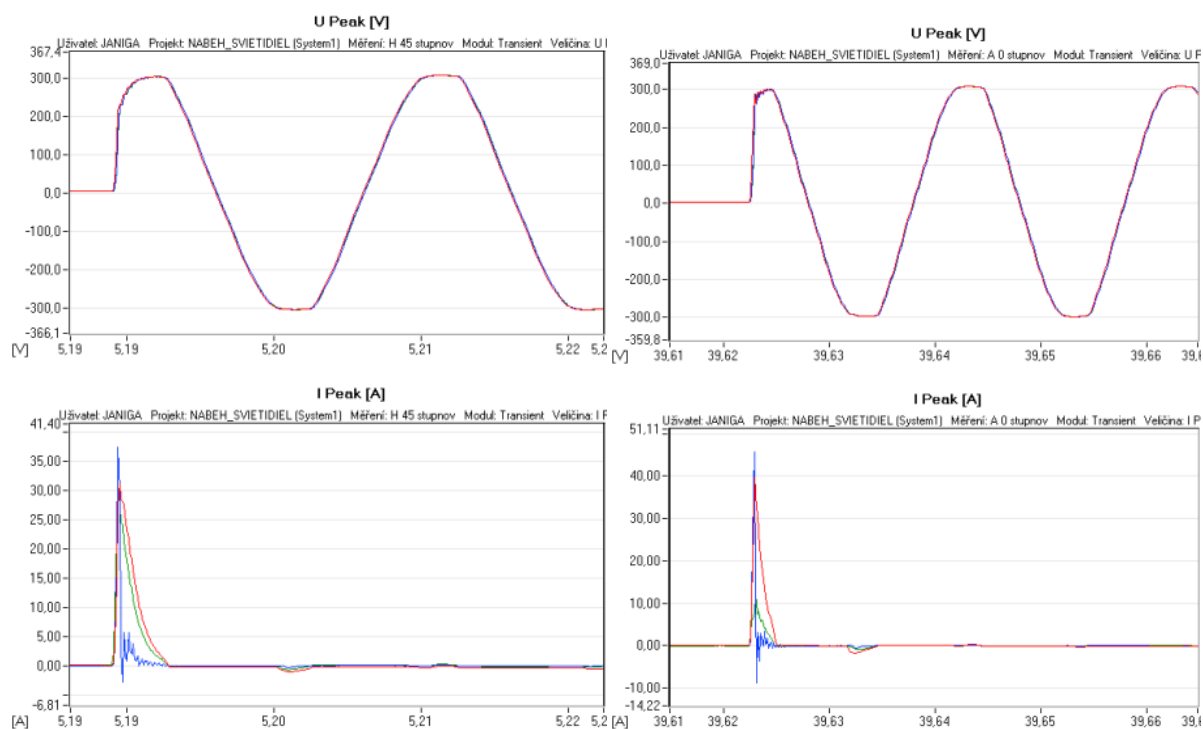
**Fig. 2 Current during start. Cold start on upper figures and hot start on bottom figures**

Repeated starts may cause overloading and design of installations has switched off protection. These transients may bring about problems with power quality and other device function [2]. In case of repeated starts shortly consecutive, the current peaks increase stress on internal circuit of driver and lamp. This overloading is caused by repeating current peaks. The Fig. 2 shows decreased first current peak during hot start in the case of 2nd lamps.

### 3. Current peak during lamp start

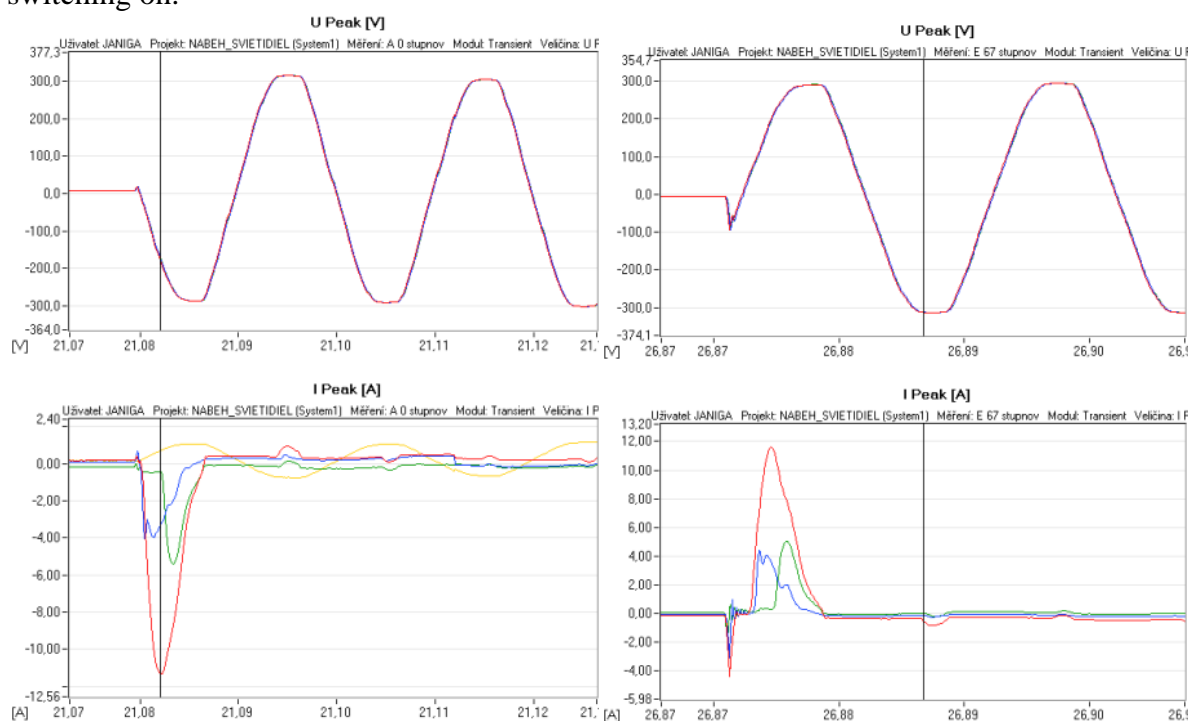
During the analysis were investigated three different LED lamps and they were analyzed during the switching on transient. Voltages and currents are plot in figures below. Curves of voltages and current are colored, where lamp1 is red, the lamp 2 is green and the lamp 3 is blue. The figures show the impact of voltage phase at start to current behavior. If voltage phase is near 90 degree, the current peak is maximal. Duration of current peak is dependent on capacitor but for reliable operation is no possible to decrease capacity of this capacitor.





**Fig. 3 Change current peak in dependence on phase of voltage**

The voltage phase depends on turn on lamp moment. Greater instantaneous voltage during start moment cause greater current peak. Results of measuring shows behavior of lamps with drivers but from measurement is not possible provide general information about start up current. Different drivers generate different behavior of current. If we try to find formula for behavior description during start up, then it is possible to describe like as transient during capacitive load switching on.





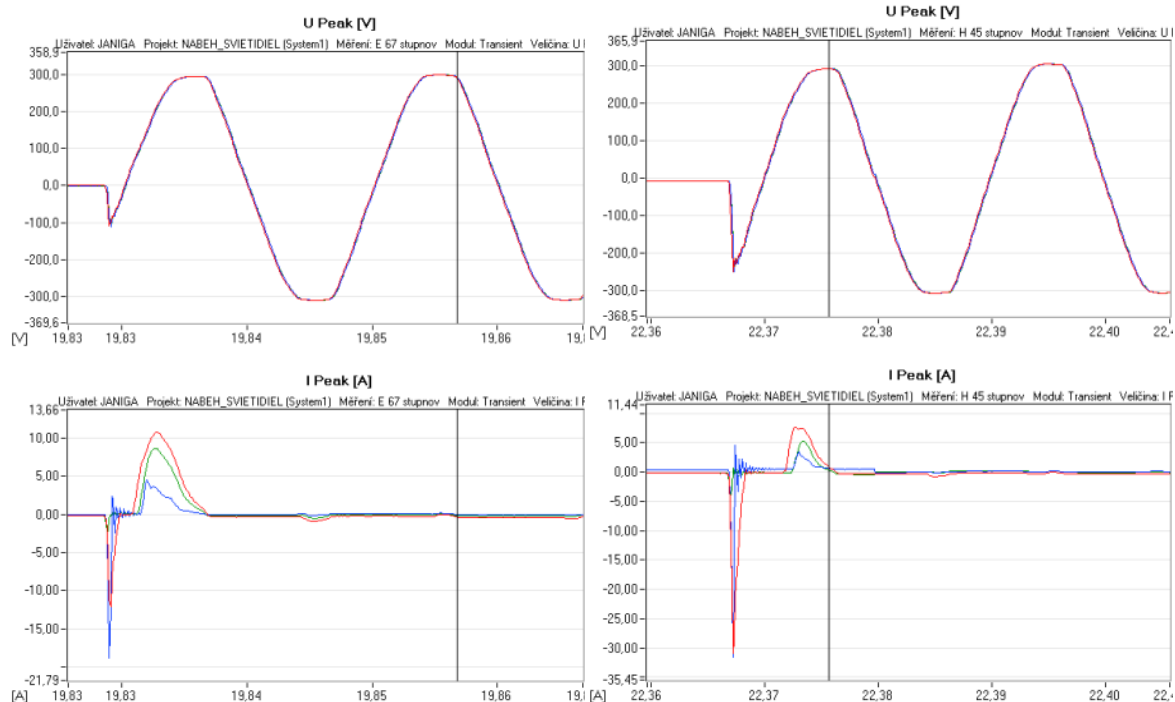


**Fig. 4** Change current peak in dependence on phase of voltage (angle from 270 to 360 degree)

Results of investigation of start up current with phase voltage from 180 to 360 degree are showed on Fig. 4. There is interested the behavior around the 180 degree, where voltage cross the axis. In this case is current peak divide to two small peaks. It can decrease current peak during start up of lamp driver.

#### 4. Switching flash

Switching of lamp is solved by switching elements with mechanical switching contacts most often. In consequence the mechanical property of switching contacts is switching flash very often. It is small oscillations of contacts and it cause oscillations of voltage. On Fig. 5 is possible to view these oscillations and oscillations of current too.

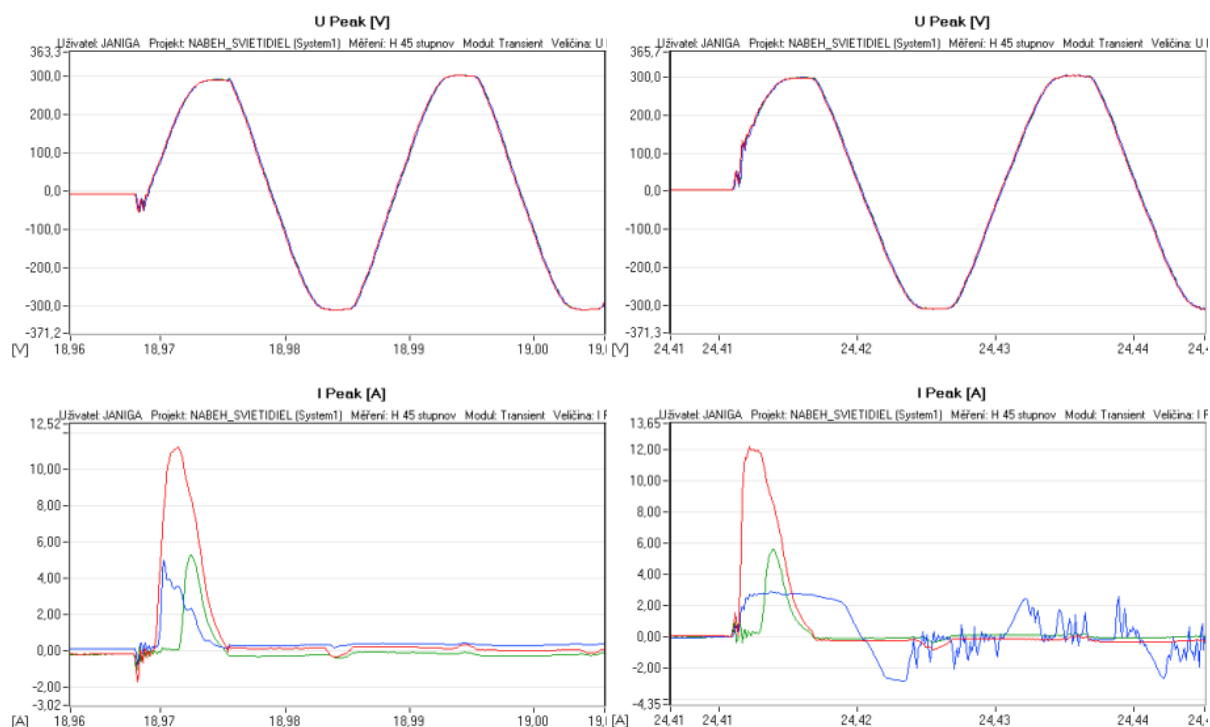


**Fig. 5** Change current peak in dependence on relay contact

Semiconductor switching elements can eliminate the problem about switching flash but now is used rarely.[1]

## 5. Mathematical description of start up current

Calculation of the start up current of LED lamp can be solved in two ways. Comprehensive method is by modelling whole electrical circuit of driver and LED modules. Simply method for start up current calculation is by modelling lamp like capacitive load (capacitor) or inductive load (transformer). This simplification reduces calculation to solving problem switching inductive or capacitive load. Current waveforms during inductive or capacitive load switching are calculated using differential equations. [5]

### Inductive load switching

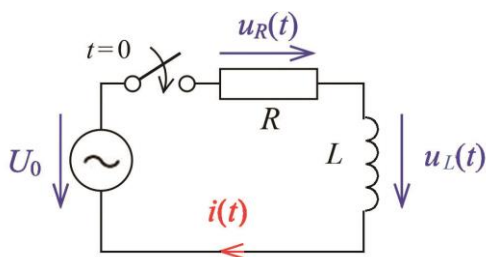


**Fig. 6** Simple circuit with switching RL load

Resultant current formula  $i(t)$  is calculated:

$$i(t) = \frac{U_{0m}}{Z} \left[ \sin(\omega t + \alpha - \delta) - \sin(\alpha - \delta) e^{-\frac{R}{L}t} \right]$$

where  $U_{0m}$  – maximum voltage of power supply,  
 $Z$  – circuit impedance,

$\omega$  – angular speed  $2\pi f$ ,  
 $\delta$  – phase difference.

### Capacitive load switching

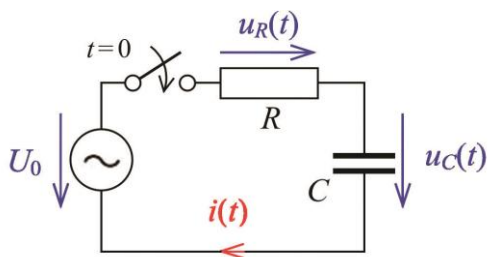


Fig. 6 Simple circuit with switching RC load

$$i(t) = \frac{U_{0m}}{Z} \sin(\omega t + \alpha - \delta) - \frac{\cos(\alpha + \delta)}{\omega RC} e^{-\frac{t}{RC}}$$

Although capacitor and transformer are located in the DC part of the circuit, description of transient is preferable with formulas for AC circuits. It is due, the voltage in DC circuit copy the voltage on AC during start up (half of period). At the rise time the voltage is in half of period, it is still unidirectional, and it has sinusoidal shape.

### Conclusions

LED lamps using is increasing in field of interior and exterior lighting. It is reason why is LED lighting topic more often discussed. Exercitation of LED lamp shows problems of this technology. Some problems have electrical character. One of them is startup current. It is difficulty identifiable by electrical engineering without special measuring equipment because startup current is very fast with high current peak. This paper show results of measuring of startup current and it give information about this problem.

Aim of this paper is also describe methodology of calculation startup current. Exactly calculation of current peak is difficult and for calculation is necessary information about all components of lamp. Paper describes simplified calculation which gives information about current behavior during startup.

## References

### Conference proceedings

- [1] Cintula, Boris / Beláň, Anton: “Riadené spínanie výkonových vypínačov” In: ŠVOČ 2009 : Študentská vedecká a odborná činnosť. Zborník víťazných prác. Bratislava, Slovak Republic, 29.4.2009. - Bratislava : STU v Bratislave FEI, 2009. - ISBN 978-80-227-3094-5. - CD-Rom
- [2] Eleschová, Žaneta / Beláň, Anton / Smola, Miroslav: “Monitoring of Electric Power Quality in Administrative Building” 3rd International Scientific Symposium `Elektroenergetika 2005`, Stará Lesná, Slovak Republic, 21.-23.9.2005. In: Elektroenergetika 2005 : 3rd International Scientific symposium. Stará Lesná, Slovak Republic. 21.- 23. 9. 2005. - Košice : Technická univerzita v Košiciach, 2005.
- [3] Koval', Peter / Liška, Martin: “Smart Metering” In: Power Engineering 2011. Energy - Ecology - Economy 2011 : Tatranské Matliare, Slovakia, June 7-9, 2011. - Bratislava : Slovak University of Technology in Bratislava, 2011. - ISBN 978-80-89402-40-3. - USB flash
- [4] Liška, Martin: “Solving the Transients Event In Electric Circuits Using a Mathematical Model of Differential Equations” In: Technical Computing Bratislava 2010 : 18th Annual Conference Proceedings. Bratislava, Slovak Republic, 20.10.2010. - Bratislava : RT Systems, 2010. - ISBN 978-80-970519-0-7. - CD-Rom

### Articles in journals

- [5] Liška, Martin: “Kvalita elektriny, štandardy a ich plnenie”. In: EE časopis pre elektrotechniku, elektroenergetiku, informačné a komunikačné technológie. - ISSN 1335-2547. - Roč. 16, mimoriadne č. : ELOSYS. Trenčín, 5.-8.10.2010 (2010), s. 230-233



## COMPLEX EVALUATION MODEL OF A SMALL-SCALE PHOTOVOLTAIC INSTALLATION PROFITABILITY

*František Janíček<sup>1</sup>, Ján Poničan<sup>1</sup>, Matej Sadloň<sup>1</sup>*

<sup>1</sup>Slovak University of Technology in Bratislava, Faculty of Electrical Engineering and Information Technology, Ilkovičova 3, 812 19 Bratislava, Slovakia  
frantisek.janicek@stuba.sk, jan.ponican@stuba.sk, matej.sadlon@stuba.sk

**Abstract:** *Number of small-scale photovoltaic installations grows rapidly every year. A decade ago, this was motivated solely by the attempt to reduce greenhouse gas emissions, because the investment itself was not economically viable. Nowadays, the table is turning. Small-scale installations are becoming profitable, if selected wisely. Therefore, the article discusses, what are the factors that need to be taken into consideration when selecting the photovoltaic installation, what data must be collected beforehand and how to proceed in their analysis. To sum up, the article provides an in-depth methodology for the small-scale photovoltaic installation assessment that is aimed to be used in household's or small commercial consumer's profitability appraisal of such an investment.*

**Keywords—** *photovoltaic systems; profitability; price; electricity consumption; electricity generation; renewable energy sources support; energy storage; optimization; standard consumption diagram*

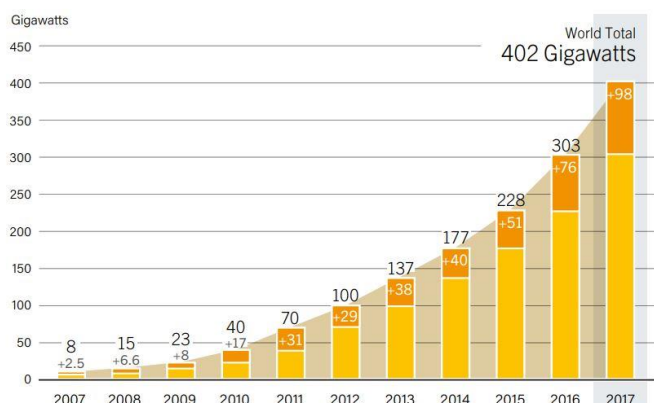
### Introduction

Renewable energy sources (RES) development is a major tool in climate change combat within the power engineering sector. These technologies however represent a significant shift that may be seen like a threat both in terms of grid technologies and in terms of finances. Despite these assumptions, the photovoltaic (PV) market is growing rapidly. This is naturally connected with obligations of states under the international law to decrease their carbon footprint. Some countries focus on large-scale projects in sunny locations. [1] These are not suitable for each geographical region. This might be seen in the European trend of small-scale household installations. They have several advantages. Firstly, they usually do not occupy land and could easily be installed on the rooftop. Secondly, they are financed by private entities and do not require a complicated state administration. Although, support schemes might still be relevant in terms of profitability in some regions or for some consumer categories. Thirdly, they constitute a much less significant threat for the electricity grid since they are spread all over the grid and thus their generation output is usually different and distributed to various node areas. And finally, if optimized properly, a majority of the generated electricity could be consumed in a real time or stored in an energy storage device. Thus, the amount of transported electricity would be minimalized. However, battery systems are still very expensive and unprofitable. Therefore, the real-time consumption supported by some support schemes such as net metering constitutes a way forward in many European countries. [2]

Household customers usually do not know what factors to take into consideration when selecting the PV installation. Nevertheless, the market is quite competitive and there are many PV suppliers, installers and many companies operating on various markets connected with both electrical appliances and energy services that offer turnkey projects. PV design optimization is a complicated process and large-scale project designers usually use various expensive softwares.

On the other hand, household customers deciding upon the PV installation usually follow the recommendations of the supplier. However, these do not necessarily have to be relevant. There are many factors that should be considered, and an in-depth analysis should always be performed before an installation purchase. Choosing a suitable PV installation is crucial for the profitability of an investment. Too expensive installation with an overly set installed capacity would cause the investment not to return at all, because the majority of electricity would not be utilized and would only be sent to the grid as a surplus. An installation with an insufficient installed capacity would not be profitable either, because the installation costs and the equipment costs would not be proportional to the energy savings related to low installed capacity. As the findings show, the starting point of each PV optimization should be the electricity consumption, i.e. both its curve and its volume should be considered. It is important to understand that households' consumption peaks are usually located before and after the working hours, whereas the PV generation peak is located during the working hours. On the other hand, in case of the small commercial consumers it is vice versa. This has a significant impact on the amount of surplus electricity that cannot be consumed in a real time and thus creates a need for a battery storage, what makes the installation far more expensive. The conclusion is that the consumption data allows for the PV installation optimization that leads towards the profitability maximization.

Due to the above mentioned, the aim of the article is to identify a small-scale PV installation profitability assessment methodology that would be clearly answering the question, what PV installation is the most profitable for a specific electricity consumer. However, the article only discusses Slovak market conditions and focuses mostly on the household customer categories. Nevertheless, the proposed methodology may be used for other small-scale customer categories, too.



Global PV Capacity and Annual Additions, 2007-2017. [3]

## Methodology

### Categorizing the final consumer

First of all, a detailed consumption data is needed. As it was already stated above, the PV generated electricity is utilized in the most profitable way only when consumed immediately without any energy storage solutions. Thus, it is important to adjust the PV installation according to the consumption volume and its curve.

There are two options in defining the consumption of a specific electricity consumer. First and much more accurate approach is to collect a real data. The easiest would be to collect these from a smart meter or its online database. Another option might be to use the data collected by the consumer himself. However, this data might not be that accurate. Second option, used if the real data is unavailable, is to use the standard consumption diagram (SCD) provided by the local distribution system operator. These usually divide the small-scale final consumers into several categories according to their load profiles. Basic categories usually distinguish residential and



commercial customers. This also applies to SCDs used by Západoslovenská distribučná a.s. (ZSD). Seven consumer categories are defined by ZSD. Three of these are specified for households, three for commercial customers and one for public lighting. [4] The load profile is then combined with the annual consumption volume in order to calculate a consumption diagram of the particular final consumer. This procedure results in a complex consumption data covering all hourly, daily and monthly details. These constitute a solid platform for the optimization.

### **Defining the PV technology**

Secondly, the PV technology should be defined. Each PV panel type has different results under different conditions. Therefore, it would not be correct to select one of the existing PV technologies and to use it solely. Hence, the calculations are based only on an installed capacity, an efficiency and a surface area of the considered panel. The respective details can be found in datasheets and are used in further process in order to calculate exact amounts of electricity generated by the PV installation. This method allows for a simple and quick technology comparison. Nevertheless, polycrystalline panels are globally used the most. The reason is economical. They are the cheapest to produce and majority of PV producers focus only on this technology. However, it is important to state that their efficiency is slightly lower. [5]

When assessing the profitability, the installation investment ( $P_i$ ) is a cornerstone. This price is however made up of two items. A panel price ( $P_{1P}$ ) defines the market price of one selected PV panel. An equipment price ( $P_e$ ) defines the costs of a wiring, switchgear, inverter, installation work and connected fastening material. All this information can be found in a pricelist of a selected PV panel producer or installer. Market survey showed that the ratio among these two installation price components has usually an exponentially decreasing trend. Higher the panel number, lower the equipment price specified for an installed capacity unit, i.e. consumers installing a bigger PV installation have more favorable equipment price.

To sum up, installed capacity, surface area, efficiency, and complex price details of the specified panel must be gathered in order to proceed into the next stage of the analysis.

### **Collecting the radiation data**

Another factor that needs to be considered is the amount of radiation ( $G$ ). Naturally, radiation depends on the locality of installation and is affected by weather, shading obstacles, panel orientation etc. All these aspects need to be considered when calculating the PV production. To sum up, it is difficult to predict the radiation amounts. Therefore, various predicting softwares are used. Their calculations are usually based on historical data collected in a specific locality. It might be anticipated that their predictions may not be fully accurate. With a more accurate data more accurate results would be achieved. Majority of the respective softwares are provided only commercially. However, a sufficiently accurate data can be gathered from PVGIS software provided by the European Commission for free. [6] In addition to that, the respective software provides both hourly and monthly average radiation data inevitable for the complex PV production calculation.

### **Defining the PV installation**

With the aforementioned consumption, solar radiation and PV panel data an optimization of the installation can be performed. Thus, the aim of this stage is to define the most profitable PV installation for a specified electricity consumer. This is achieved by consumption and production simulations performed in order to assess the profitability of a PV investment.

The first step is to identify the hourly production values of a selected panel within an average day of each month ( $E_{1P}$ ). Primary input of this calculation is the hourly radiation amounts of an average day within the month. Other inputs are related to the selected PV panel, i.e. the surface

area ( $S$ ), performance factor ( $p_F$ ) and efficiency ( $\eta$ ). The performance factor represents losses related to an inverter efficiency, dust, snow, wiring and switchboard losses, shading, panel orientation etc. The number usually fluctuates around 0,8 and can be set precisely if needed. The temperature coefficient ( $c_t$ ) represents monthly adjustments of the calculation related to the temperature disturbances of the PV production. The installed capacity of the PV panel may only be achieved under standard test conditions (STC). Usual datasheet STC temperature is defined to be 25° C. Each deviation influences the PV production. Therefore, it is important to cover a performance increase or decrease related to the temperature. [7]

$$E_{1P} = G * S * p_F * c_t * \eta * t \quad (1)$$

$$\eta = \frac{P_{TC}}{S * G_{TC}} \quad (2)$$

The above stated formulas had to be adjusted, because these results are required to be collected not only for each single hour of the average day in the month, but for each single relevant installed PV capacity that can be considered, i.e. a cumulative hourly production value of the whole PV installation ( $E_{PV}$ ) needs to be defined for various installed capacities. Thus, an equation (3) was introduced. The number ( $n$ ) represents the installed capacity of the PV installation. Here it is important to understand that the installed capacity is adjusted by simply increasing or decreasing the amount of PV panels in the installation. A small-scale installation is according to Slovak law an installation with an installed capacity of up to 10 kW. [8] If standard polycrystalline panels with a 270 Wp installed capacity are considered, their number should not exceed 37. Therefore, the simulation data should cover a PV production of 1 to 37 panels. However, if other panels are considered, the number of panels should be altered accordingly.

$$E_{PV} = n * E_{1P} \quad (3)$$

Next step is to define hourly surplus electricity ( $\Delta E$ ) values. These again need to be calculated for each single hour of an average day of the month and for each single relevant installed PV capacity. The surplus electricity represents the amount of electricity that cannot be consumed by the consumer in a real time and thus needs to be sent to the grid or to be stored in an energy storage device or to be utilized in other way that is always more expensive for the consumer than the real time consumption. In order to define the respective data, hourly consumption values ( $E_C$ ) of an average day in a month are needed. With these details, the amount of surplus electricity generated in a PV installation can be identified for each single hour of 12 average days representing the average conditions of the respective month. The comparison needs to be at least this complex, because both the consumption and the PV production are significantly different throughout the year. The most accurate method would be to calculate these numbers for each single hour of the year based on real consumption data from previous years and on exact solar radiation predictions defined for a concrete upcoming year and its weather conditions. Consumption is largely dependent on household's habits, heating and cooling needs that usually remain very similar throughout the years. The PV generation is mostly affected by the radiation amounts and the weather character. These are predictable with only a certain amount of accuracy. Thus, a prosumer energy optimization always requires an in-depth analysis.

$$\Delta E = E_{PV} - E_C \quad (4)$$

Result of the calculations is a specific number of charts with 12 average days, each with 24 values representing the hourly consumption, production and surplus data. The number of charts depends on the number of considered PV panels. Such complex data allows for daily, monthly and yearly sums of PV production, consumption and surplus and thus constitute a solid platform for comparison of PV installation options.

However, defining the installation's scale is just a part of the optimization process. Potential prosumer has several choices when deciding upon the installation. Three major ones can be distinguished under conditions of the Slovak market. Firstly, opting for a cheapest option, installing solely a PV installation and thus relying only on a real-time consumption of the PV generated electricity. Secondly, increasing the investment and spending extra money on energy storage in order to utilize a higher portion of generated electricity. Commonly used are battery systems usually sold in a bundle with the PV installation. And thirdly, subscribing to a novel service on Slovak market offered by Západoslovenská energetika, a.s. (ZSE), a virtual battery. Respective service provides a theoretical storage of PV generated electricity that cannot be utilized in a real time. It is basically a net metering allowing prosumers to virtually use the surplus electricity generated by their PV installation in periods when their PV generation is insufficient. This is in fact done only through invoicing, i.e. no physical energy storage is included.

Major tool used for analyzing the profitability is a profitability index. It compares the investment costs with the future earnings arising from the investment and thus mathematically expresses the investment suitability. [9] Higher the profitability index, higher the ratio of future cash flows in comparison to its costs. For the purposes this article, the investment represents all the PV installation costs and the future earnings represent the electricity savings related to the PV installation. However, these are significantly different for the above mentioned three scenarios and thus the next step has to be divided into three options.

### Real-time consumption scenario

The optimization is crucial especially in case of an installation without a physical or virtual energy storage, because the lack of flexibility in the utilization of the PV generated electricity constitutes a significant barrier in the use of the PV installation. As it was stated above, the installation investment ( $P_i$ ) can be divided into two elements, the panel price ( $P_{1P}$ ) and the equipment price ( $P_e$ ). However, this does not concern a case when only bundles provided by a supplier or installer are considered. Then, the division would be irrelevant and only the provided bundle installations and their costs would be considered. Due to the fact that the aim of the methodology is the profitability index comparison of potential PV installations, the installation price has to be defined for each of the potential installed capacities ( $n$ ).

$$P_i = n * (P_{1P} + P_e) \quad (5)$$

Renewable energy sources (RES) are often subject to a state support. This concerns PV installations, too. Thus, in case of an investment contribution eligibility, it is important to include this fact in the calculations. This can be done by simple deducting the contribution from the installation price. However, it is important to keep in mind that the contribution may change according to the installation details, usually according to the installed capacity and thus may be different for various considered PV installations.

Next step is to identify the annual savings ( $P_s$ ), i.e. the financial value of electricity savings. For this purpose, the hourly PV generation data and hourly surplus electricity data connected to each considered scale of the PV installation are used. These numbers are needed to identify the real time consumption within each hour. These amounts are subsequently summed and multiplied by the electricity price ( $P_{1kWh}$ ) set by a tariff relevant for the particular customer. All

the electricity generated in times when the production is higher than the consumption constitutes a surplus that does not provide any electricity savings for the prosumer and is only donated to the electricity supplier, in other words absolutely worthless for the prosumer. Therefore, the optimization needs to ensure its minimizing.

$$P_s = (E_{PV} - \Delta E) * P_{1kWh} \quad (6)$$

The last step is to define the profitability index (PI) for each single assessed installed capacity of the PV installation. These are then compared and the highest is selected as the optimal installation for the real-time consumption scenario.

$$PI = \frac{P_s}{P_i} * 100\% \quad (7)$$

### Accumulation scenario

The most frequently used energy storage technology connected with the small-scale PV power plants is the Lithium-ion (Li-Ion) battery storage. Method used in assessing the accumulation possibilities is very similar to the first scenario. However, several adjustments needed to be done. The profitability analysis is slightly more complicated, because it does not only compare various PV installed capacities, but it also compares various battery capacities. In spite of the fact that the Li-Ion batteries are usually sold as preset products and thus cannot be sized to specific capacities, the methodology is aimed towards selecting the most profitable battery capacity irrespective of the offered products. However, assessing the standardized capacities only is an option, too.

When defining the installation investment ( $P_i$ ) the accumulation price needs to be considered, too. A price of 1 kWh battery storage ( $P_{1B}$ ) can be defined after an up to date market analysis. With this value, battery system investments related to each considered capacity can be identified by multiplying the respective 1 kWh price with a specific number of kWh ( $x$ ), i.e. considered capacity. Naturally, this constitutes an accuracy deviation, because higher battery capacities are usually connected with discounts, i.e. the price / capacity ratio is not entirely linear. However, this method can be easily adjusted for standardized offered products and thus to ensure more accurate results. Moreover, the described method can be used for other energy storage technologies, too.

$$P_i = n * (P_{1P} + P_e) + (P_{1B} * x) \quad (8)$$

Major difference in comparison with the real-time consumption scenario is related to the energy savings calculation. The difference is that the electricity that cannot be consumed in a real time has to be divided into two categories, the electricity that can be stored in the battery ( $\Delta EB$ ) and the electricity that cannot be utilized ( $\Delta ED$ ), because there is not a sufficient battery capacity in a relevant time, i.e. the electricity donated to the supplier. Their definitions are pretty straight. The surplus electricity, or in other words the electricity that cannot be consumed in a real time, represents the electricity that can be utilized up to a point when the battery capacity is reached. All the subsequently generated electricity that cannot be consumed in a real time is donated to the supplier without any remuneration. Both values can be defined from the hourly consumption, PV production and battery capacity data. This difference results in an adjustment to the annual savings ( $P_s$ ) formula that needs to include the PV generated electricity stored in a battery.

$$P_s = (E_{PV} - \Delta E + \Delta E_B) * P_{1KWh} \quad (9)$$

After both the installation investments and the annual savings are defined for each considered number of PV panels and for each considered battery capacity option, the profitability indexes for individual combinations can be identified and the highest can be selected using the same technique as in the previous scenario.

### Virtual battery scenario

A precondition of the virtual battery service is a smart meter capable of measuring both the amount of electricity purchased from the electricity supplier and the amount of electricity send back to the grid in times when the PV generated electricity is not needed. This allows ZSE to motivate potential prosumers to opt for one of their PV installations by offering a service consisting of a virtual storage of the surplus electricity. The idea is to allow customers to utilize the surplus electricity sent to the grid later when the PV installation does not provide enough energy. This is however performed only financially via an annual electricity invoice. Price representing the annual amount of the virtually stored surplus electricity is deducted in the settlement invoice from the costs of the consumed grid electricity. This means that the service subscription is not reflected in the monthly bill and the customer is monthly charged in the same manner as any other customer without the respective service. On the other hand, the deduction does not include the whole electricity price, but only one of its components, the electricity supply. This represents approximately only 30 to 40 % of the electricity price, depending on customer's tariff. In addition to that, the service in question is a subject to a monthly fee of 2 €. All these characteristics have to be included in the methodology.

Firstly, the installation investment ( $P_i$ ) has to be identified for each considered PV installed capacity. This is done in the same manner as in the real-time consumption scenario.

Secondly, the annual savings ( $P_s$ ) definition has to be distinguished into two variants. First for a case when the electricity sent to the grid is fully utilized in the virtual battery service, as described in equation (10). Second in case this is not possible. Here, the surplus electricity has to be divided into two categories, the electricity that can be virtually stored ( $\Delta E_{VB}$ ) and the electricity that cannot be virtually stored and has to be donated to supplier ( $\Delta E_D$ ). The reason is that the amount of PV generated electricity sent to the grid can only be deducted from the annual electricity price up to the amount of consumed grid electricity. Thus, if the amount of electricity sent to the grid is higher than the amount of grid electricity consumed, only a part of the surplus electricity sent to the grid can be utilized in the virtual battery service. The amount of virtually stored electricity under the second variant can be defined as a portion of consumed electricity that does not include the real-time consumption of PV generated electricity. The rest of the surplus electricity represents the amount that is only donated to the supplier and thus does not stand for any electricity savings. This is expressed in formulas (11) and (12).

$$E_{VB} = \Delta E \quad (10)$$

$$E_{VB} = E_C - (E_{PV} - \Delta E) \quad (11)$$

$$E_D = E_{PV} - E_C \quad (12)$$

The next step is to sum the hourly electricity amounts of the real-time consumption, of the virtual storage and of the donated surplus in order to calculate their annual values. This data is subsequently used for the annual savings identification. In this process, electricity price per kWh ( $P_{1kWh}$ ) has to be known together with its component representing the electricity supply price



( $P_{SC-1kWh}$ ). Moreover, the flat rate subscription fee of 24 € per year ( $P_F$ ) has to be deducted from the savings.

$$P_S = [(E_{PV} - \Delta E) * P_{1KWh}] + [E_{VB} * P_{SC-1KWh}] - P_F \quad (13)$$

Finally, the last step is to calculate the profitability index for each considered PV panel capacity using the same formula as in both previous scenarios in order to identify the most profitable installation.

## Conclusion

The aforementioned methodology results in three profitability indexes. Each of them represents a specific option for the potential prosumer. Profitability index is a universal financial characteristic that is widely used to compare investments. Thus, it can be used to identify, which of these options is the most profitable.

PV optimization service is globally offered by dozens of companies that have either developed their own software or use a licensed version of another provider. The main advantage of the discussed approach is the fact that it is tailor-made for the purposes of the current Slovak market and that it can be easily adjusted according to existing conditions, in other words extended to include novel services, price fluctuations, PV or accumulation technologies etc. In addition to that, the defined process is a methodology and thus can be included in a software that could after providing customer's data, answer the question, which PV installation is optimal.

On the other hand, a significant drawback represents the fact that it is fully dependent on the consumption and production data. These are rarely fully accurate. However, novel weather and solar radiation prediction softwares are being developed every year. Therefore, it might be assumed that the amount of error will only decrease in the future. With more accurate data a more accurate optimization may be performed with the respective methodology.

To sum up, a complex assessment model was developed in order to quickly and easily define an optimal small-scale PV installation for a potential prosumer under conditions of the Slovak market.

## Acknowledgements

This publication was created thanks to support under the Operational Program Integrated Infrastructure for the project: International Center of Excellence for Research on Intelligent and Secure Information and Communication Technologies and Systems – 2. stage, ITMS code: 313021W404, co-financed by the European Regional Development Fund.



## References

- M. Huo, D. Zhang. "Lessons from photovoltaic policies in China for future development." *Energy Policy*, vol 51, pp. 38-45, May. 2012
- František Janíček, Ján Poničan, Matej Sadloň, "Modified Discounted Payback Period of various small-scale photovoltaic installation.", in press.
- Renewable Energy Policy Network for the 21st Century. "Renewables 2018 Global Status Report" Internet: [http://www.ren21.net/wp-content/uploads/2018/06/17-8652\\_GSR2018\\_FullReport\\_web\\_final\\_.pdf](http://www.ren21.net/wp-content/uploads/2018/06/17-8652_GSR2018_FullReport_web_final_.pdf) [Mar. 22, 2019]
- Západoslovenská distribučná, a. s. "Aktuálne Typové diagramy odberu." Internet: <https://www.zsdis.sk/Uvod/Dodavatelia/Typove-diagramy-odberu/Hodnoty> [Jan. 24, 2019]
- František Janíček, Ján Poničan, Matej Sadloň, "Modified Discounted Payback Period of various small-scale photovoltaic installation.", in press.
- European Commission. "Photovoltaic Geographical Information System (PV-GIS)." Internet: [http://re.jrc.ec.europa.eu/pvg\\_tools/en/tools.html#PVP](http://re.jrc.ec.europa.eu/pvg_tools/en/tools.html#PVP), [Feb. 25, 2019]
- E. Ghiani, F. Pilo, S. Cossu, "On the performance ratio of photovoltaic installations." [IEEE 2013 IEEE Grenoble PowerTech - Grenoble, France (2013.06.16-2013.06.20)] 2013 IEEE Grenoble Conference - On the performance ratio of photovoltaic installations, pp. 1-6, Jun. 2013.
- Slovak energy Act n. 251/2012 Z. z. as amended.
- R. Higgins, "Analýza pro finanční management." Grada Publishing, Issue 1, pp. 202, 1997.



## IMPACT OF FAULTS IN TRANSMISSION AND DISTRIBUTION NETWORK ON VOLTAGE SAGS

***Boris Cintula<sup>1</sup>, Peter Janiga<sup>1</sup>***

<sup>1</sup>Slovak University of Technology in Bratislava, Institute of Power and Applied Electrical Engineering,  
email: [boris.cintula@stuba.sk](mailto:boris.cintula@stuba.sk)

### **Abstract**

*This article deals with the issue of evaluation of voltage sags based on the analysis of the impact of different fault types in power systems. The aim is to identify a range of influences of considered faults on voltage sags in the industrial low voltage network. The analysis is based on the simulation calculation of selected faults to classify negative effects causing potential improper operation of industry equipment due to faults in the power system. In the paper are also described options of proposed measures for minimization of these phenomena.*

### **Key words**

Short-circuit, earth fault, voltage sag, industrial network, distribution system, simulation.

### **Introduction**

In general, electrical appliances are dependent on the power supply, mainly on actual voltage magnitude in the electric network. Voltage sags or interruptions in the power supply could result in a negative influence on the operation of appliances. The appliance's ability to withstand voltage sag, respectively outage depends on the internal structure and topology of electrical appliances. [5], [7]

The electric network provides in the context of measures for the protection of sensitive customers' equipment very limited possibilities. The duration of voltage sags and short-term interruptions can be reduced by increasing the capacity of the loop of power lines or improved realization of elements of power system; the depth of voltage sags can be reduced by increasing the short-circuit power of supply network. [7], [8]

Most voltage sags and short-term interruptions are caused by short circuits or earth faults occurring in the power supply. These failures cannot be eliminated, but the number can be significantly reduced. Restriction of the number of short-circuits results in less negative impact on electrical appliances and can be achieved by, e.g. improved realization of elements of the power system, replacing the overhead lines in cable lines, cleaning insulators, as more consistent and more frequent elements controls of the supply network, etc. [5], [7]

Malfunctioning equipment on a large scale in industrial enterprises can have significant economic impacts on their operation. Such facts may ultimately lead to e.g. to change the electricity supplier or other changes, but the origin of the problems may be based on the electrical topology, the specific location of the company in this topology. [1], [2]

The following research is based on this assumption, where the aim is to assess the impact of various faults in the transmission and distribution electrical networks on the voltage conditions in the distribution of an industrial enterprise. The range of the impact of selected faults will be identified by quantifying voltage sags that could cause malfunction of industrial equipment such as inverters, etc.

A suitable tool for an assessment of voltage conditions in the industrial network is a simulation analysis of various faults in the power system.

The research is performed on a mathematical model based on the real topology of a part of the transmission and distribution system with all devices, which is complemented by a detailed topology of the industrial power system.

## 1. Literature review

In recent years, the increase of automation in the industrial sector has brought problems with power quality. These problems are mainly associated with using of electronic control circuits, e.g. production technology sensitive to voltage sags. These devices are an important part of the production and their failure can result in production restriction for a long time and cause significant technological and financial losses for consumer. [1], [2], [4]

Overvoltage, voltage sags and interruptions are usually the reason of the faults in electrical networks. Unpredictable load change or production change could cause the any voltage deviations. It is not possible to eliminate all transient events in power system, and thus it is not possible to maintain the constant value of voltage in low voltage networks. Despite, producers should ensure that their products are able to withstand the operation within the defined limits. [3], [5]

Another point of view, the distribution system operators should keep the power quality according to standard EN 50160 "Voltage characteristics of electricity supplied by public electricity networks. In practice, it often happens that the distribution system operators comply with the power quality requirements, but sensitive equipment installed at the customer do not have to work properly. It is not possible to guarantee permanently constant value of voltage in the distribution system due to various sources causing these sags. And therefore, sensitive equipment should be capable to withstand the voltage changes in exactly defined limits in terms of depth and duration of the voltage sag. [6], [8]

To analyze the range of voltage sags, there were modeled a part of high and medium voltage network. Both models were created based on the real data of distribution and industrial network regarding simulation of the impact of different fault types in distribution network on the low voltage level.

Based on the simulation calculations, there are analysed potential causations of voltage sags with appropriate measures proposed for elimination of these phenomena in the industrial low voltage network.

## 2. Model description

Voltage sags assessment in industrial network is based on the simulation calculations for different types of faults (short circuits and earth faults) in the power system at different voltage levels.

In the first part, assessment of voltage sags in industrial network is performed using a model of HV distribution network (110kV) according to Fig.1. This area is supplied via a transformer 400kV/110kV, nominal power 350MVA, short-circuit power in that node is 5.5GVA. Transmission power system is modeled using a model of equivalent network with given short-circuit power.

In the second part, assessment of voltage sags in industrial network is performed using a model of MV distribution network (22kV) according to Fig.2. This area is supplied via transformers T1.1 and T1.2 (T1.2 je turned off, both busbars in present substation are supplied from transformer T1.1).

Present models are based on real data of power system included given values of consumption, i.e. topology of high (HV) and medium voltage (MV) level, transformers parameters, types and lengths power lines and cables, loads.

### 3. Simulation scenarios

Analysis and impact of considered faults on the voltage conditions (voltage sags) in industrial network are performed for the following simulation scenarios:

- Line-to-line short-circuit, line-to-line short-circuit with earth connection and line-to-earth short-circuit in the transmission network near the transformer 400kV/110kV,
- Three-phase short-circuit, line-to-line short-circuit, line-to-line short-circuit with earth connection and line-to-earth short-circuit in HV network (110kV),
- 1<sup>st</sup> earth fault at different locations in MV network (22kV),
- 1<sup>st</sup> earth fault and following 2<sup>nd</sup> earth fault at different locations in MV network (22kV).

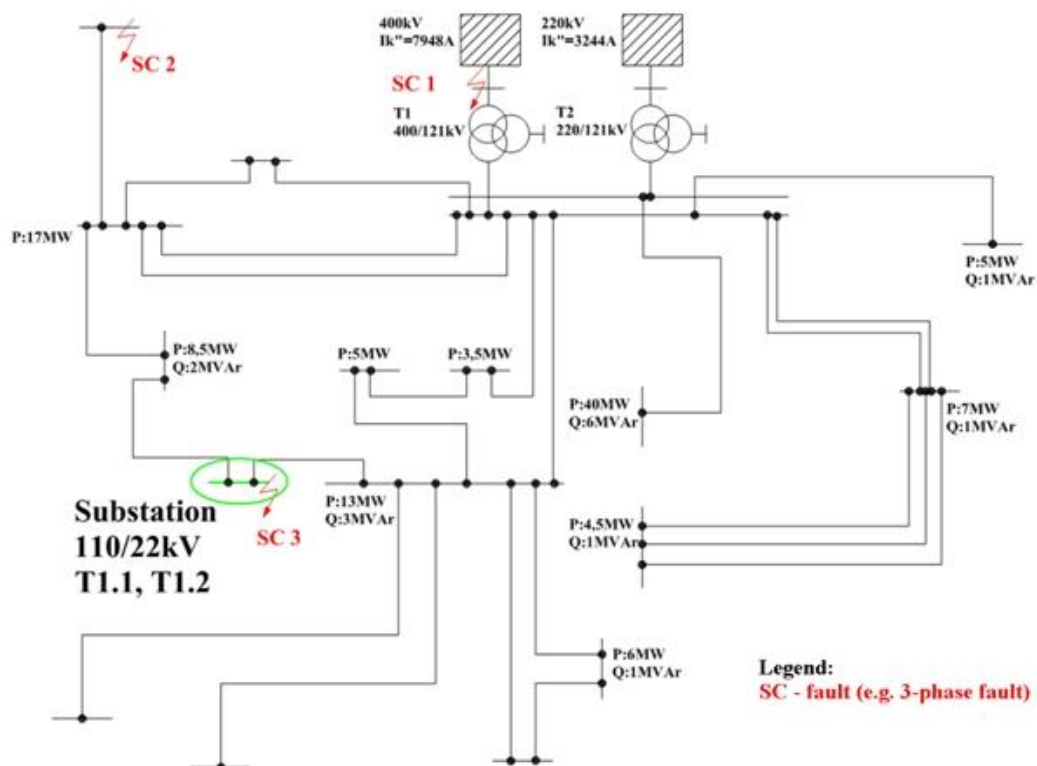


Fig. 1 Simplified model of HV distribution network

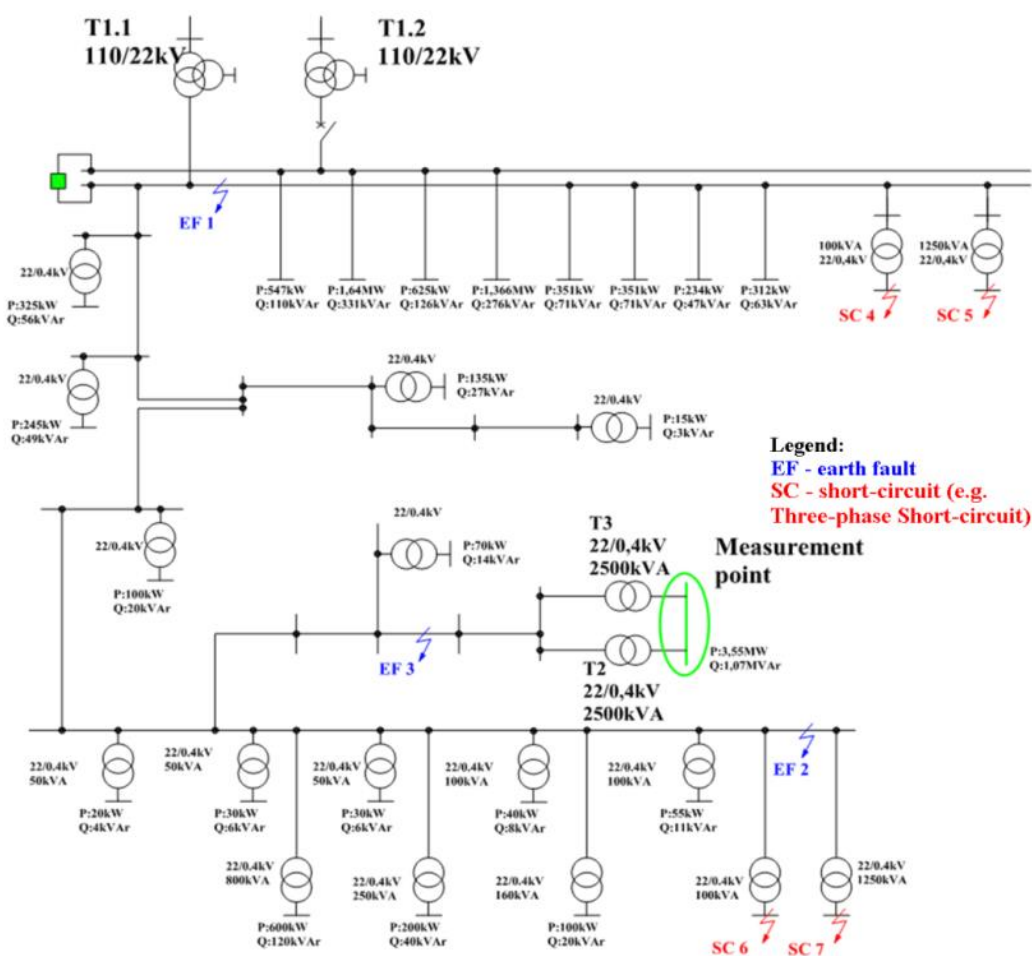


Fig. 2 Simplified model of MV distribution network

Table 1 Simulation scenarios list

Voltage level	Fault type	Fault position
400kV	Line-to-earth short-circuit, Line-to-line short-circuit, Line-to-line short-circuit with earth connection	SC1
110kV	Line-to-earth short-circuit, Line-to-line short-circuit, Line-to-line short-circuit with earth connection, Three-phase short-circuit	SC2
	Line-to-earth short-circuit with the resistance of 100Ω	SC2
	Line-to-earth short-circuit, Line-to-line short-circuit, Line-to-line short-circuit with earth connection	SC3
22kV	1 <sup>st</sup> earth fault with following 2 <sup>nd</sup> earth fault in the same substation	EF1
	1 <sup>st</sup> earth fault with following 2 <sup>nd</sup> earth fault in the same substation	EF2
	1 <sup>st</sup> earth fault with following 2 <sup>nd</sup> earth fault in the same substation	EF3
	1 <sup>st</sup> earth fault with following 2 <sup>nd</sup> earth fault in another substation	EF1-EF2
	1 <sup>st</sup> earth fault with following 2 <sup>nd</sup> earth fault in another substation	EF1-EF3
	1 <sup>st</sup> earth fault with following 2 <sup>nd</sup> earth fault in another substation	EF2-EF3
0.4kV	Line-to-earth short-circuit, Line-to-line short-circuit, Line-to-line short-circuit with earth connection, Three-phase short-circuit (transformer with ratio 22kV/0.4kV and nominal power of 100kVA)	SC7
	Three-phase short-circuit (transformer with ratio 22kV/0.4kV and nominal power of 100kVA)	SC6

	Three-phase short-circuit (transformer with ratio 22kV/0.4kV and nominal power of 1250kVA)	SC5
	Three-phase short-circuit (transformer with ratio 22kV/0.4kV and nominal power of 100kVA)	SC4

All considered faults were performed as zero-resistance faults except one case of simulation of line-to-earth short-circuit with fault resistance ( $100\Omega$ ) in HV network (110kV).

Simulated scenarios in MV network (22kV) were performed for the 1<sup>st</sup> earth fault and following the 2<sup>nd</sup> earth fault in the same substation and also for the 1<sup>st</sup> earth fault and following the 2<sup>nd</sup> earth fault in another substation.

Fault in LV network (0.4kV) (Fig. 2 – SC6) were performed on the secondary side of transformer 22kV/0.4kV with small and large nominal power.

Selection of fault locations were determined in order to identify an impact significance of near, far and earth faults on voltage sags in the assessed low voltage (LV) network (0.4kV) in the industry.

Simulation experiment is assessed separately based on the results of simulation calculations in power system as follows:

- HV network (110kV) supplied from transformer T1 400kV/110kV and transformer T2 220kV/110kV;
- MV network (22kV) supplied from transformers 110kV/22kV T1.1 and T1.2;
- Transformers 22kV/0.4kV T1 and T2 with measurement of phase voltage at LV side of transformer.

#### 4. Simulation results

The aim of simulation scenarios is to evaluate of voltage on MV and LV side of transformer T2 and T3 and to assess an impact on possible voltage sags. Therefore, on LV side the values of phase voltages are evaluated: absolute voltage change, percentage voltage changes related to nominal voltage (230V). On MV side the values of phase-to-phase voltages are evaluated.

##### 4.1 Line-to-earth Short-circuit and Line-to-line Short-circuit with Earth Connection in Transmission Network

Faults located in the transmission network were simulated on the busbar of primary transformer side T1 400kV/110kV. In the following figures are shown occurred phase voltage sags in LV network for cases: line-to-earth short-circuit, and line-to-line short-circuit with earth connection (fault location in Fig.1- SC1).

From the voltage waveforms, it results that fault in the transmission network near to the transformer 400kV/110kV has a significant impact on the voltage sag in LV voltage network. In case of the line-to-line short-circuit with earth connection the voltage in phase L1 dropped in LV network to the zero value. Due to power supply HV network (110kV) from the only one transformer (T1 400kV/110kV), faults near to the transformer significantly affect the voltage conditions in HV and thus in LV network.



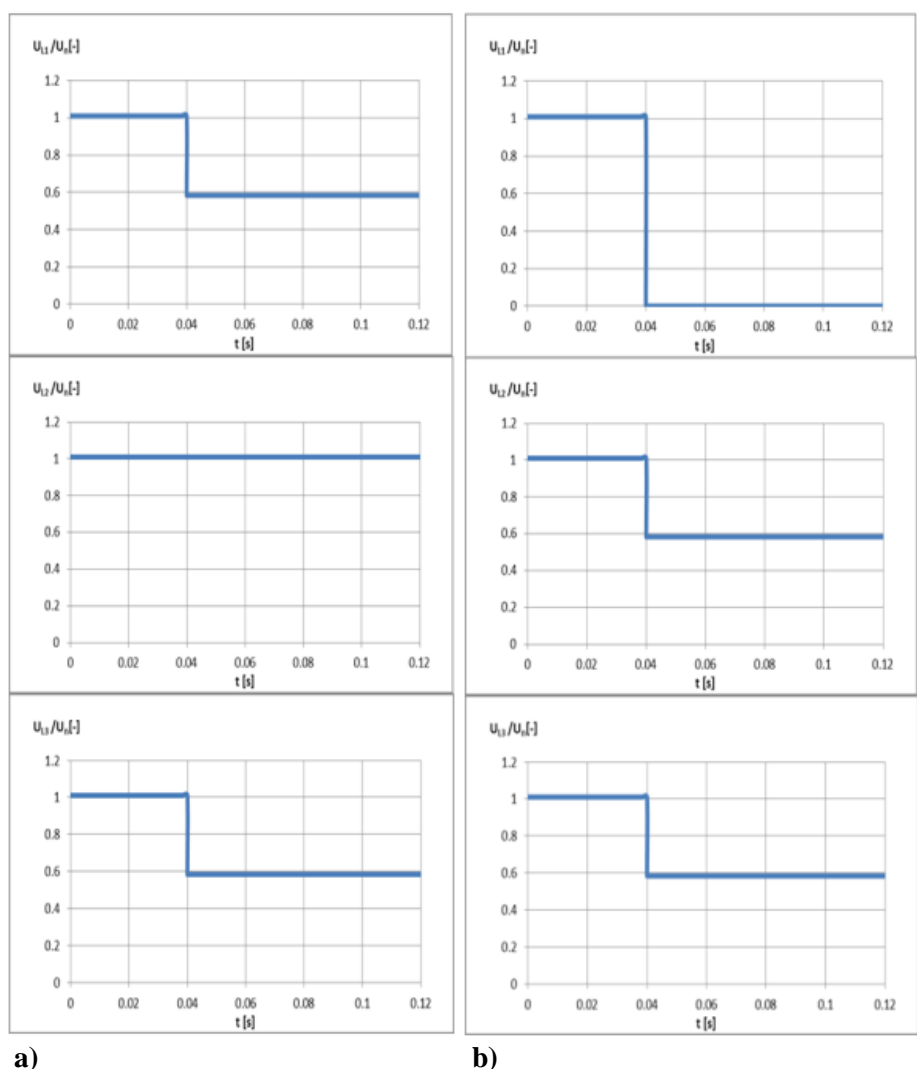


**Fig. 3 a) Phase voltage (p.u.) in LV network for case: line-to-earth short-circuit in transmission network, b) Phase voltage (p.u.) in LV network for case: line-to-line short-circuit with earth connection in transmission network**

#### 4.2 Line-to-line Short-circuit and Line-to-line Short-circuit with Earth Connection in 110kV Network near to Transformer 110kV/22kV

This simulation scenario is focused on the analysis of impact of near faults to the assessed point in HV network. Fault location point SC3 (Fig.1) is near to the transformer 110kV/22kV which supplies the MV network (22kV). In the following figures are shown simulation results of phase voltage sags in LV network for cases: near line-to-line short-circuit and line-to-line short-circuit with earth connection in HV network (110kV).

Results of present simulation scenarios for case line-to-line short-circuit and line-to-line short-circuit with earth connection in the near 110 kV substation confirmed an occurrence of phase voltage sags in LV network. In case of the line-to-line short-circuit, the voltage sag was lower, equal to value 0.86 (p.u). The line-to-line short-circuit with earth connection caused the voltage sag in LV network, equal to value 0.63 (p.u).

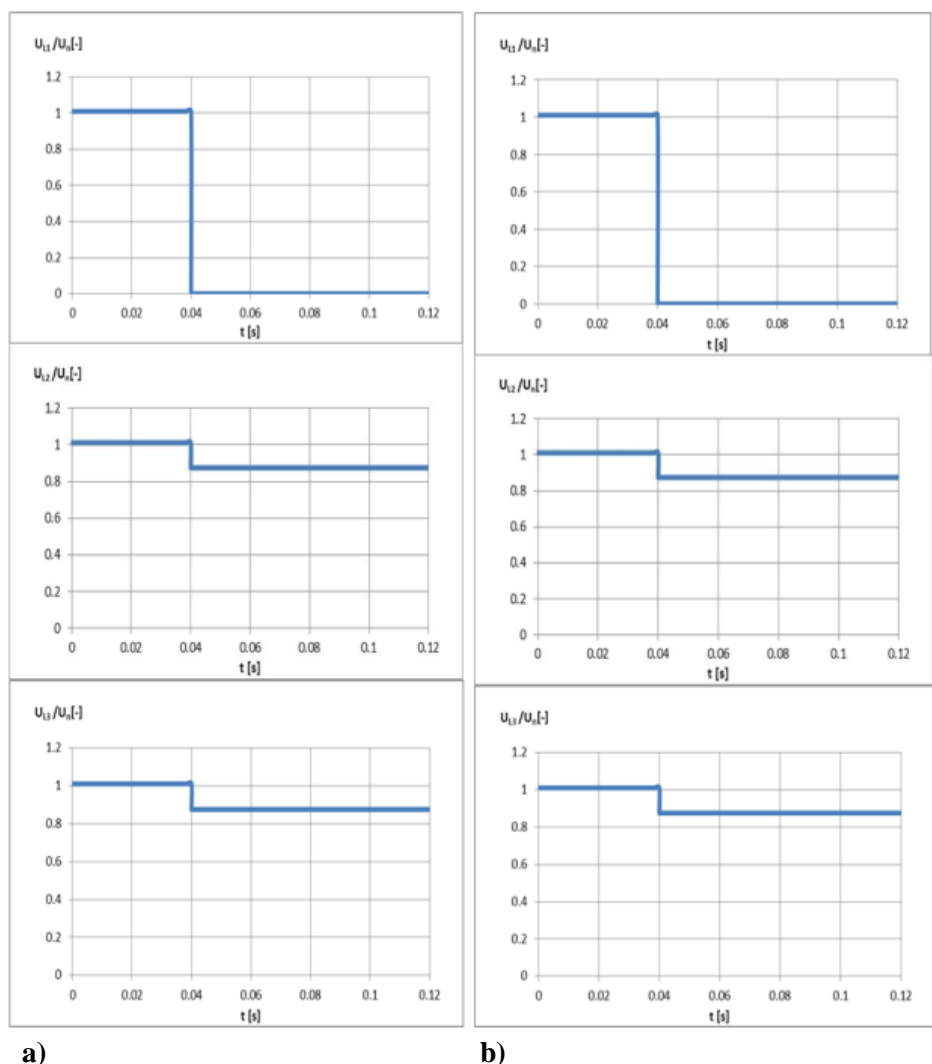


**Fig. 4 a) Phase voltage (p.u.) in LV network for case: near line-to-line short-circuit in 110kV network, b) Phase voltage (p.u.) in LV network for case: near line-to-line short-circuit with earth connection in 110kV network**

#### 4.3 Electrically Far Line-to-line Short-circuit and Line-to-line Short-circuit with Earth Connection in 110kV Network

In this case, considered fault was simulated in HV network (110kV) in electrically far point SC2 (Fig.1) from the transformer T1.1 supplying MV network (22kV). The aim of this simulation calculation is to analyze an impact of far fault in the HV network on voltage sags in LV network. In the following figures are shown simulation results of phase voltage sags in LV network for cases: electrically far line-to-line short-circuit, and line-to-line short-circuit with earth connection in HV network (110kV).

From the voltage waveforms, it results that electrically far faults cause almost the same magnitude of voltage sags in LV network as the near faults.

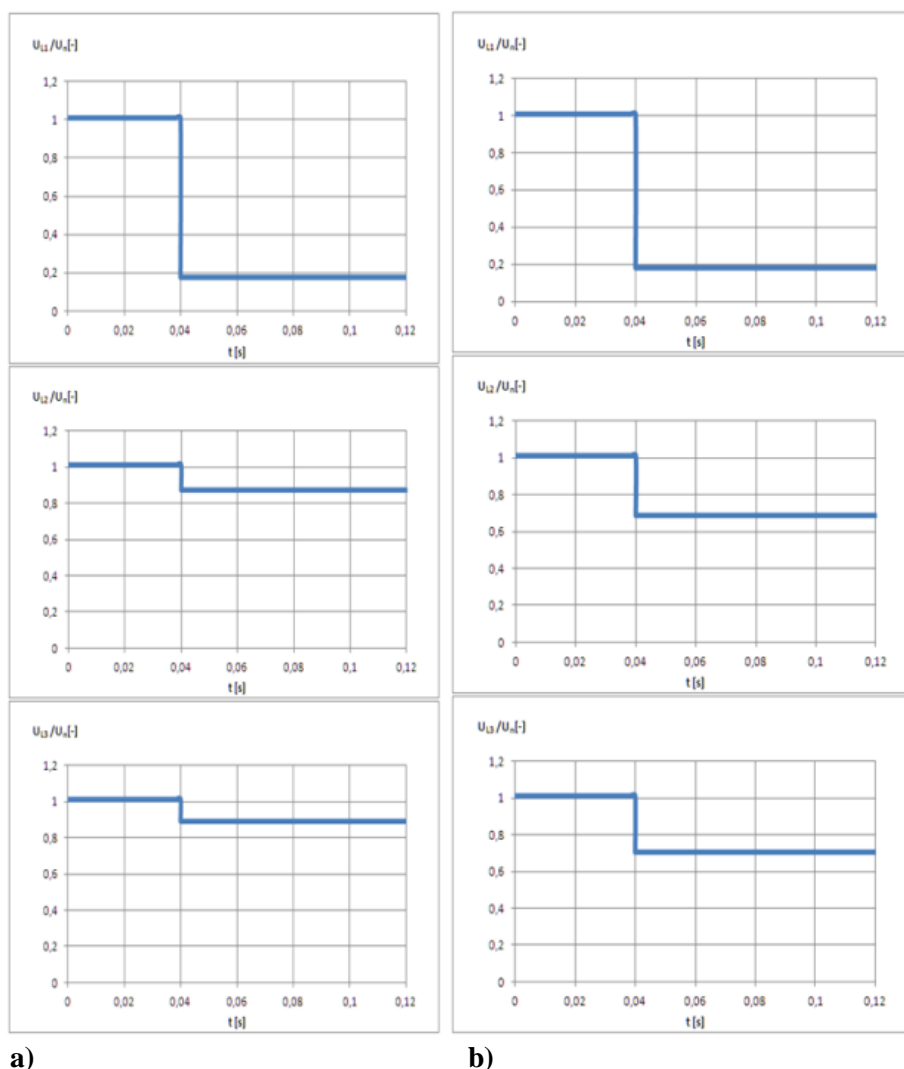


**Fig. 5 a) Phase voltage (p.u.) in LV network for case: far line-to-line short-circuit in 110kV network, b) Phase voltage (p.u.) in LV network for case: far line-to-line short-circuit with earth connection in 110kV network**

#### 4.4 Electrically Far Line-to-earth Short-circuit in 110kV Network with and without considering Fault Resistance

This simulation calculation is focused on the analysis of impact of fault resistance on voltage sags. In the following figures are shown simulation results of phase voltage sags in LV network for cases: line-to-earth short-circuit without a fault resistance and with a fault resistance 100Ω in SC2 (Fig.1).

From the comparison of simulation results, it clearly results the fault resistance significantly affects the impact of fault considering a fault resistance in HV network on the voltage sags in LV network.

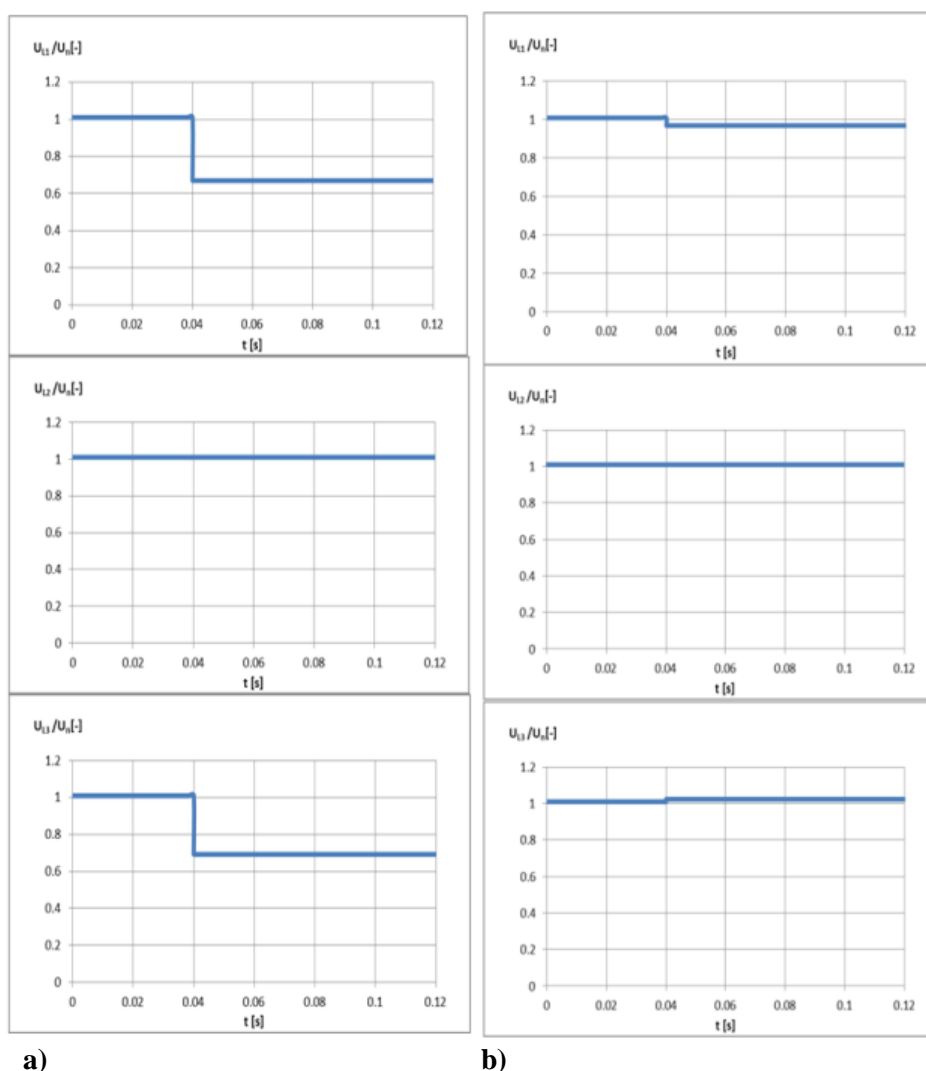


**Fig. 6 a) Phase voltage (p.u.) in LV network for case: near line-to-earth short-circuit in 110kV network without fault resistance, b) Phase voltage (p.u.) in LV network for case: near line-to-earth short-circuit in 110kV network with fault resistance 100Ω**

#### **4.5 1<sup>st</sup> and the 2<sup>nd</sup> Earth Fault in Main Substation 110kV/22kV and near to Transformer 22kV/0.4kV T2 and T3**

In MV network (22kV) were simulated different scenarios of earth faults. From given a large number of simulated scenarios of earth faults, this article shows results only of selected scenarios.

The first scenario represents the 1st earth fault in phase L1 in time 0.04s and the 2nd earth fault in time 0.08s in phase L2. The earth faults were simulated in the substation 110kV/22kV supplying a part of MV network (behind the transformer T1.1 on the 22kV busbar EF1 in Fig.2).

The second scenario represents the same type of fault in point EF3 near to assessed LV network. In the following figures are shown simulation results of phase voltage change for cases: earth fault in points EF1 and EF3 (Fig.2).

From the simulations results the 1st earth fault (in phase L1) in main 22kV substation does not affect voltage conditions in LV network. The 2nd earth fault (in phase L2) represents a line-to-line short-circuit with earth connection with a significant voltage sag in phase L1 in LV network.

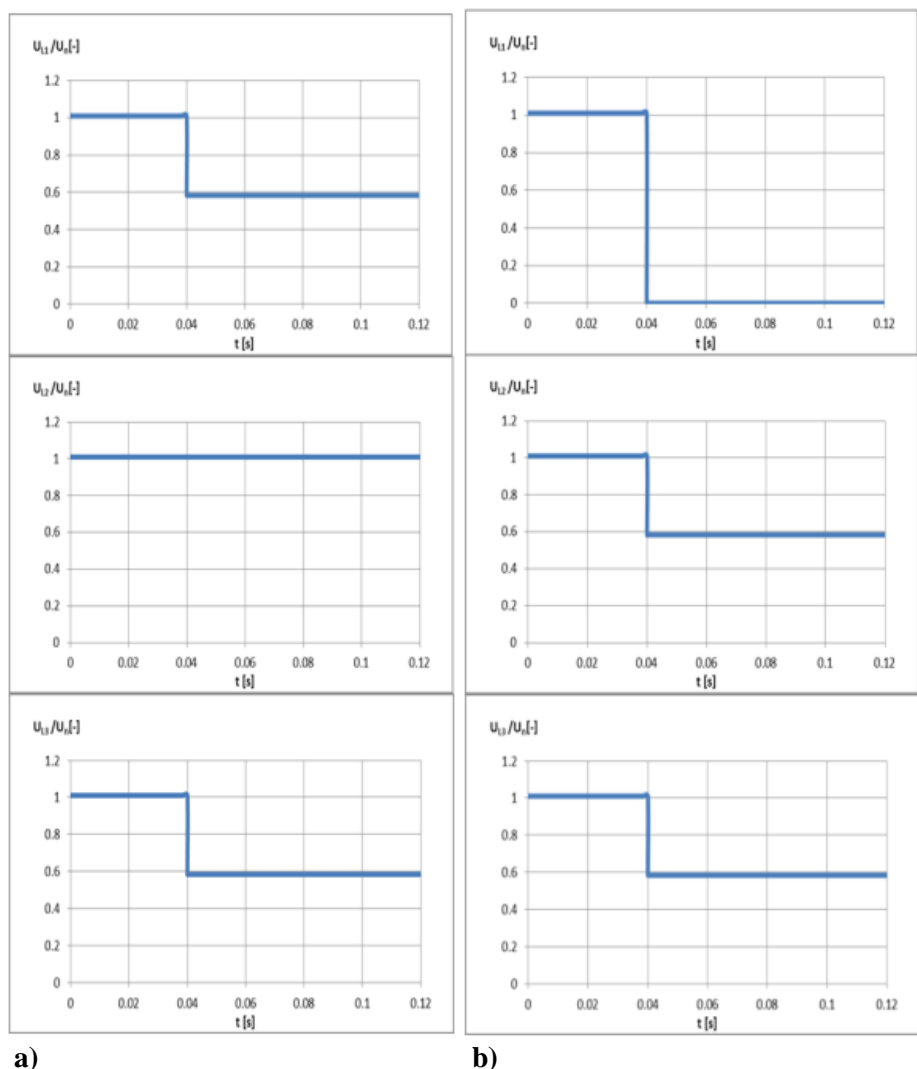


**Fig. 7 a) Phase voltage (p.u.) in LV network for case: near earth fault in 22kV network (EF1), b) Phase voltage (p.u.) in LV network for case: near earth fault in 22kV network (EF3)**

#### 4.6 Three-phase Short-circuit in 0.4kV Network

Present calculation is focused on the evaluation of impact of three-phase short-circuits located in LV network supplied from the same 22kV network as the assessed low voltage network.

In the first case, three-phase fault was simulated on LV side of transformer 100kVA (see SC6 in Fig.2) and the second case on LV side of transformer 1250kVA (see SC7 in Fig.2). These calculations were selected in order to analyze fault impacts in different LV network supplied from transformer with high impedance (100kVA) and low impedance (1250kVA) on voltage sags, concretely on the transmission of failure into the assessed LV network.

From the voltage waveforms, it results the fault in LV network supplied from the same MV network does not have a significant impact on the voltage sags in the assessed LV network. On the other side, simulations confirmed an impact of different value of nominal power of transformer on the transmission of failure into the assessed LV network. Transformer with nominal power 1250kVA (with lower impedance) has more significant impact on the voltage conditions than transformer with nominal power 100kVA (with higher impedance).

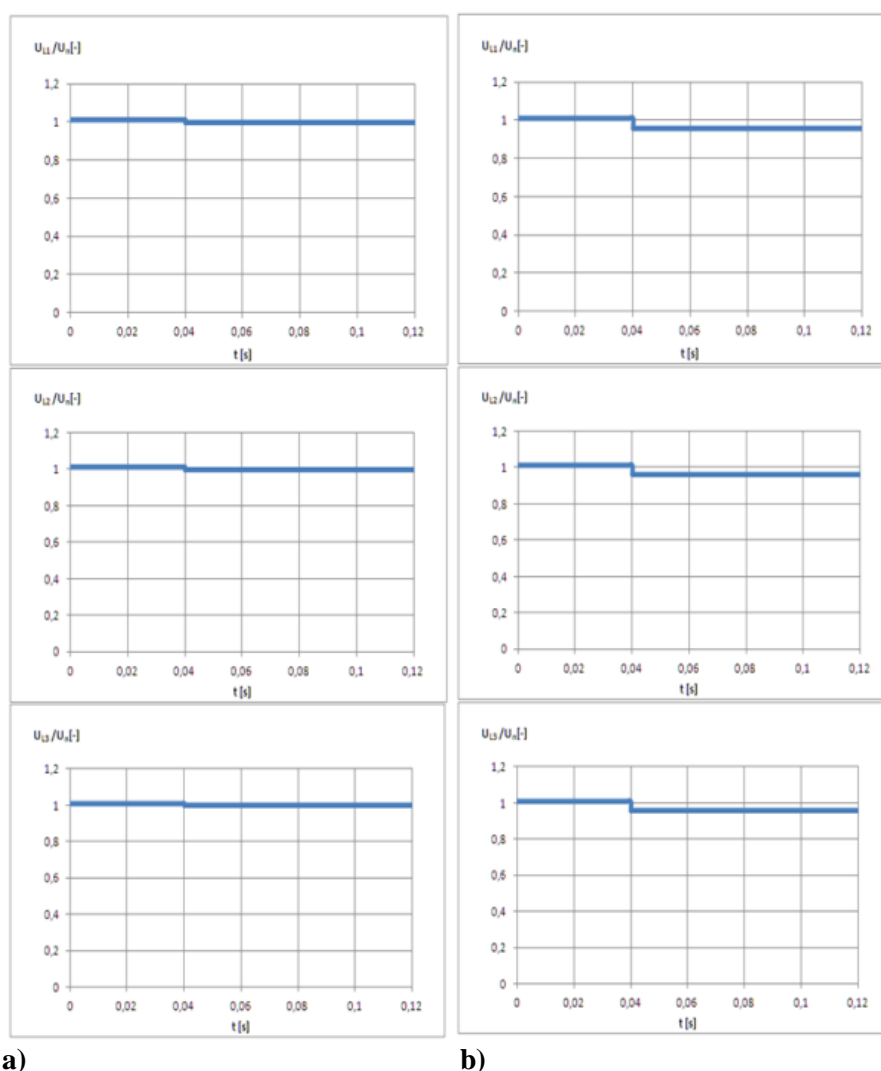


**Fig. 8 a) Phase voltage (p.u.) in LV network for case: three-phase short-circuit in LV network supplied from transformer 100kVA (SC6), b) Phase voltage (p.u.) in LV network for case: three-phase short-circuit in LV network supplied from transformer 1250kVA (SC7)**

## 5 Conclusion

The submitted paper deals with issue of analysis of impact of selected fault types located at different points in power system on voltage sags in the industry. Increase of automation in industrial sector brought problems related to voltage sags associated with wide using of electronic control circuits, i.e. technology sensitive to voltage sags. Failures of this equipment can lead in negative case to production restriction and cause significant technological and financial losses for consumer.

A suitable tool to avoid voltage sags is an assessment of voltage conditions using simulation analysis of selected various faults potentially most contributing to occurrence of voltage sags in the industrial distribution.

Assessment of voltage sags in industrial network is based on the simulation calculations for different types of faults (short circuits and earth faults) in the power system at different voltage levels.

The aim of simulation scenarios was to point out voltage response in industrial LV network considering different types of faults in selected locations in power system. From the simulations result the voltage response significantly depends on the type and impedance of fault.



In general, manners of elimination of voltage sags have to be implemented on the side of consumer as well as the system operator. The elimination of cautions of voltage sags from the distribution or transmission system is not completely possible due to an impact of variable unpredictable factors, such as meteorological factors (lightning, strong wind, frost, increased humidity), equipment age, fauna influence, the impact of operational factors such as overvoltage and so on. These phenomena are therefore necessary to minimize at the possible lowest level. In order to avoid the production restriction in the industry area, it is necessary to do more steps on both sides. The transmission and distribution system operators should perform proper and regular maintenance service in their networks. On the other side, industrial customers should perform the measurements in order to select the most sensitive equipment and increase their ability to withstand any potential voltage sags.

And therefore, it is possible to use one application of the following methods:

- Immunity increase of the sensitive equipment or process (technology),
- Installation of special devices between the sensitive equipment (technology) and power supply network,
- Elimination methods at the distribution or transmission grid.

## References

Muzi, F. / Passacantando, L.: “A real-time monitoring and diagnostic procedure for electrical distribution networks”. *International Journal of Energy*, Vol. 1, No. 1, 17-21.

Karthikeyan, S. P. / Raglend, J. / Pratyusha, P. / Kothari, D. P.: “A New Methodology for Distribution System Feeder Reconfiguration.” *International Journal of Energy*, Vol. 2, No. 1, 8-15.

Boutora, S. / Bentarzi, H. / Ouadi, A.: “Analysis of the Disturbances in Distribution Networks using Matlab and ATP”. *International Journal of Energy*, Vol. 5, No. 1, 9-16.

Djalel, D. / Rezaiguia, A. / Abada, Z.: “Improving the Electric Power Quality by UPFC Systems in Electrical Networks”. *International Journal of Energy*, Vol. 6, No. 4, 115-122.

Patne, N. R. / Thakre, K. L.: “Factor Affecting Characteristic of Voltage Sag Due to Fault in the Power System”. *Serbian Journal of Electrical Engineering* 5(1), 2008, pp. 171-182.

Otcenasova, A. / Bodnar, R. / Regula, M. / Hoger, M. / Repak, M.: “Methodology for Determination of the Number of Equipment Malfunctions Due to Voltage Sags”. *Energies* 2017 10(3), 2017.

Magalhães de Oliveira, Marcio: *Power Electronics for Mitigation of Voltage Sags and Improved Control of AC Power Systems*. Royal Institute of Technology: Stockholm 2000, p. 281.

Faisal, Mohamed F.: *Voltage Sag Solutions for Industrial Customers*. Tenaga Nasional Berhad, 2018, p. 153.



## ON APPLICABILITY OF BLACK-SCHOLES MODEL TO MSE

*Toni Stojanovski*

*Vodno Pty Ltd, Melbourne Australia, toni\_stojanovski@ieee.org*

**Abstract** *In this paper we test the accuracy of assumptions of Brownian motion model for stock pricing process for the Macedonian Stock Exchange (MSE) ), which serves as an example of an emerging incomplete market. For this purpose we use historical prices data for three traded companies on the MSE with the highest market capitalisation: Alkaloid (ALK), Makpetrol (MPT) and Komercijalna banka (KMB). We also evaluate the accuracy of Black-Scholes (BS) options pricing model for stocks traded on MSE. For this purpose we define a hypothetical trader whose investment strategy is to buy a fixed number of options every day. Our analysis proves that BS model is not suitable for evaluation of out-of-the-money options on incomplete markets since the assumptions of its underlying stock pricing process model are not satisfied. The BS model has limited value only for in-the-money options whose value is not significantly overestimated by leptokurtic nature of the distribution of daily returns.*

**Key words** *Financial Derivatives, Options, Black-Scholes Formula*

### Introduction

At the turn of the 20th century Louis Bachelier [1] proposed using random walk as a model for stock pricing processes - all subsequent price changes represent random departures from previous prices. This model for stochastic process, now called Brownian motion, has since become the dominant model for stock pricing processes and is at the core of pillars of modern finance: Markowitz portfolio theory [2], capital asset pricing model [3], and option pricing theory [4]. Efficient market hypothesis is dominant theory in financial economics associated with the idea of random walk. The logic of the random walk idea is that when the flow of information is unconstrained and information is immediately built in stock prices, then tomorrow's price change will reflect only tomorrow's news and will be independent of the former price changes. News is by definition unpredictable, hence, resulting price changes must be unpredictable and random [5].

Criticisms of random walk model are numerous. Benoit Mandelbrot [6] elaborates that random walk and Gaussian daily returns simply do not correspond to reality, and grossly underestimate the risk of huge market swings. Historical data from many markets indicate that the daily changes in stock prices do not follow Gaussian distribution. Huge changes in market prices occur much more frequently than predicted by the Gaussian distribution, which is popularly known as "heavy tails".

In this paper we test the accuracy of assumptions of the random-walk model, and of one of its most popular derivations – Black-Scholes (BS) model. Accuracy of BS model for option pricing has already been subject of several empirical investigations, indicating that BS model is biased in its estimation. Duan [7] suggests the tail properties of the underlying lognormal distribution are too small, and thus the assumption of an underlying lognormal distribution does

not hold. In [8], authors analyse error in BS model for valuation of European call options derived from the CAC-40 money-market index. Dependence of estimation error on moneyness and due-term of options is analysed, discovering error for both out-of-the-money (OTM) and in-the-money (ITM) options. McKenzie *et al.* in [9] evaluate the probability of an exchange traded European call option being exercised on the ASX200 Options Index. They conclude that the BS model is relatively accurate. More precisely, BS model is significant at the 1% level in estimating the probability of an option being exercised.

This paper extends previous results in the following direction. Statistical analysis of historical data on stock prices is given for the Macedonian Stock Exchange (MSE) as an emerging stock market with low liquidity. The aim is to determine the parameters for the model for the stock pricing process. Then, we address the following research questions: How accurate can we expect the BS option pricing models to be for MSE? This question is especially important for the process of introduction of options trading on MSE and other emerging markets. Traders need a working model for option valuation which they can reliably use to estimate the value of options. While we draw our conclusions from the historical data on MSE only, we argue that our results are valid for other emerging stock markets too.

The paper is organised as follows. In Section 0 we give summary of concepts used in the remainder of the paper: introductions to financial derivatives, option valuation models, and derivations of stochastic parameters make the paper self-contained and define the concepts and notation. Section 0 gives the results on the derivation of stochastic parameters from the analysis of historical data from MSE. Section 0 analyses the accuracy of BS formulae for MSE stocks. Section 0 gives conclusions and possible directions for future research.

## Background

### *A. Financial derivatives*

A financial derivative [10] is a financial instrument whose price depends on the price of the underlying asset such as oil, gold, stocks, interest rates, or currencies. Traders are using forwards, futures, options and swaps, and various combinations of these fundamental derivative instruments both (i) to manage or reduce risk, (ii) and to increase returns.

Options are very popular financial derivatives. A call/put option is a contract which gives the holder the right to buy/sell an asset at a certain time for a certain price (strike price). Deciding a fair value for an option is an extremely difficult task: the stock pricing process depends on many parameters; the option payoff can be greatly influenced by difficult-to-predict events in the future; options can be simple (European or American) but their payoff can also depend in a very complex way on price movements (exotic options). Several models have been developed for option pricing, most notably the Black-Scholes (BS) model [4], the Binomial option pricing model [11], the Trinomial Model [12], the Barndorff-Nielsen – Shephard model [13], and jump-diffusion model [14]. Using these models to value an option is a computationally intensive task, except for vanilla European options where BS model provides a closed-form solution. Additionally, calculating the Greek parameters for an option is an adamant requirement for traders: the Greek parameters quantify the sensitivity of the option value to changes in market conditions. Calculation of option value and Greek parameters involves parameters derived from historical or current market prices. Correct estimation of these parameters is of utmost importance for option valuation.

### *B. Economic impact of derivatives market*

The objective of a derivatives market is to maximize investor risk protection by offering hedging and risk management mechanisms. Additionally, derivatives markets have a significant economic role in price discovery. Price discovery is the way in which a market establishes the price for items traded in that market, and then disseminates those prices as information throughout the market and the economy as a whole [15]. Derivatives markets provide the links amongst cash markets, hedgers, and speculators and thus contribute to the development of the national financial infrastructure, stimulate national economic growth, and help development of financial markets. Organized markets for derivatives were typical of developed economies until the late 1980s, but the last two decades of the 20th century witnessed an increased interest in the launch of derivative markets in emerging economies. Financial derivatives are currently not traded on MSE and the stock exchanges in neighbouring countries. The process of globalization of world economy implies the need for developing countries to establish and develop financial derivatives trading, as a condition for further development of the national economy. Introduction of financial derivatives on stock exchanges in developing countries might attract foreign investments in listed companies, will stimulate further development of stock exchanges, will have a positive impact on stock trading and stock liquidity, and might even motivate new IPOs.

This paper aims to discover whether the option pricing models are valid for emerging financial markets.

### *C. Models for valuation of options*

At the heart of the BS model [4] for option valuation are the following assumptions:

- Market direction cannot be predicted. Geometric random walk is assumed in the BS model.
- Risk-free interest rate  $r$  remains constant over option duration.
- Stock returns are normally distributed
- Volatility  $\sigma$  of stock prices is constant over time.

The assumptions underlying the BS model are widely considered as being too strict and even unrealistic [16] [17]. Fisher Black [16] admits that BS formula depends on unrealistic assumptions, but there is no other formula that gives better results in a wide range of circumstances. Fallout of Long Term Capital Management (LTCM) hedge fund in 1998 [17] was mostly due to small-arbitrage trading strategies combined with high leverage. Myron Scholes and Robert C. Merton were amongst the partners of LTCM, and their mathematical risk models were used by LTCM. The inaccuracies in these models were amplified by the high leverage ratio of more than 250-to-1 [17] used by LTCM, and most certainly contributed to the fallout of LTCM.

BS option pricing formulae use  $r$  and  $\sigma$ . Stock's expected return doesn't appear in the BS formula (see Eq.(6)-Eq.(9)), and it doesn't affect the option's valuation according to the BS formula. However, it is intuitive that a higher (lower) expected return on the stock means a higher (lower) expected return on the option. Therefore, in the next sections 0.D and 0.E we describe the process of derivation of parameters  $r$ ,  $\sigma$  and return rate on stock prices  $\mu$  from stock pricing data.

Then, in section 0 we test the calculated statistics of  $r$ ,  $\sigma$ , and  $\mu$  for MSE against the assumptions of BS formula.

#### D. Derivation of stochastic parameters

Valuation of financial derivatives depends strongly on volatility estimates of the underlying stock. There are two broad approaches: *historical* and *implied* volatility [18] [19]. The historical approach assumes that past holds predictive power for the future. On the other hand, *implied* volatility is calculated from the assumption that the market prices implicitly contain a consensus estimate of volatility.

Even for historical volatility there exist several models. Different models can result in different estimates. For example, GARCH model and its special case - EWMA incorporate the dynamic structure of volatility, and are capable of forecasting future behaviour of risk. Historical approaches have two steps in common: (i) Calculate the series of periodic returns; (ii) Apply a weighting scheme.

First, for each day, we take the natural log of the ratio of stock prices.

$$\mu_i = \ln \frac{s_i}{s_{i-1}} \quad (1)$$

This produces a series of  $m-1$  daily returns e.g. from  $\mu_2$  to  $\mu_m$ , if there are price measurements for  $m$  days  $s_1, s_2, s_3, \dots, s_m$ . Daily returns are expressed in continually compounded terms. Then we calculate the average return for the whole measurement period

$$\mu = \frac{1}{m-1} \sum_{i=2}^m \mu_i \quad (2)$$

Second step estimates the variance from the same series of daily returns. We are using the exponentially weighted moving average (EWMA), in which more recent returns have greater weight on the variance. EWMA is more commonly used in risk management calculations, and the variance is given by the square root of

$$\hat{\sigma}_{t+1}^2 = \lambda \hat{\sigma}_t^2 + (1 - \lambda)(\mu_t - \mu)^2 \quad (3)$$

where  $\lambda$  is the decay factor, also known as the smoothing constant. In this method, the weights are geometrically declining, hence giving more weight to the most recent observation compared to older ones. This weighting scheme helps to capture the dynamic properties of the data. Commonly, the smoothing constants are 0.94 for daily data and 0.97 for monthly data [19].

#### E. Kurtosis

Kurtosis [20] characterises the relative peakedness or flatness of a distribution compared with the normal distribution. For a random variable  $x$  kurtosis is defined as

$$\text{Kurt}[x] = \frac{E[(x - \bar{x})^4]}{\sigma^4} - 3 \quad (4)$$

where  $E[(x - \bar{x})^4]$  is the fourth moment around the mean, and  $\sigma$  is the standard deviation of  $x$ . For a data series e.g. daily returns  $\{\mu_i\}$ , kurtosis  $\text{Kurt}[\mu_i]$  is calculated as

$$\text{Kurt}[\mu_i] = \left( \frac{n(n+1)}{(n-1)(n-2)(n-3)} \sum_{i=2}^m \frac{(\mu_i - \mu)^4}{\sigma^4} \right) - \frac{3(n-1)^2}{(n-2)(n-3)}$$

Distributions with zero kurtosis are called *mesokurtic*. Normal distribution has zero kurtosis. Distributions with high kurtosis are called *leptokurtic*, and tend to have a distinct peak near the mean, decline rather rapidly, and have heavy tails. Distributions with negative kurtosis (*platykurtic*) have a flat top near the mean and shorter, thinner tails.

In the following sections histograms will be calculated for daily stock returns, and then kurtosis will be used to measure accuracy of the assumption that the stock returns are normally distributed.

### Analysis of real market data

Capital market in Macedonia is relatively young compared with capital markets in developed countries. Trading on the MSE ([www.mse.com.mk](http://www.mse.com.mk)) started in 1996. Market’s short history makes challenging the calculation of historical averages for market risk premium, as well other market data like beta, industry averages. MSE’s short history means short time series, which has significant negative influence on calculation of indicators and ratios necessary for security valuation such as: beta calculation, historical risk premiums determination, rates of growth, industry averages etc. Historical trading data are available from the following link <http://www.mse.com.mk/Statistics.aspx?MenuId=9>.

Following set of figures give the stochastic parameters for the three stocks from MSE. **Figure 2** presents the histograms of daily returns for ALK, MPT and KMB. Solid violet line with cross markers gives the Gaussian distribution. Histograms of the daily return series for all stocks are leptokurtic and do not follow the Gaussian curve, which is a significant blow to the BS model [16]. This means that significant variations in the daily prices are much more common than estimated by the Gaussian distribution. The impact of higher curtosis for MSE stocks will become more obvious in the section on accuracy of BS formulae.

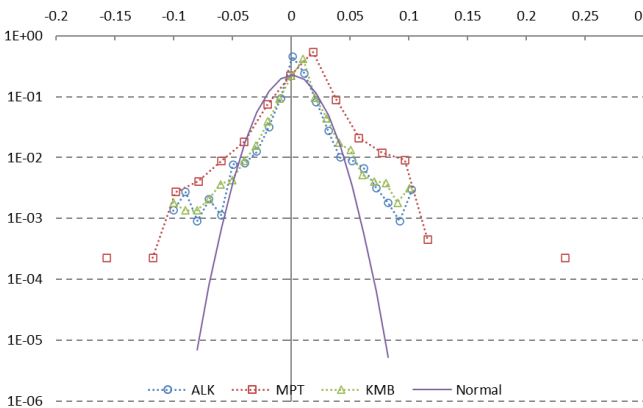


**Figure 2. Histogram of daily returns for ALK, KMB and MPT.**

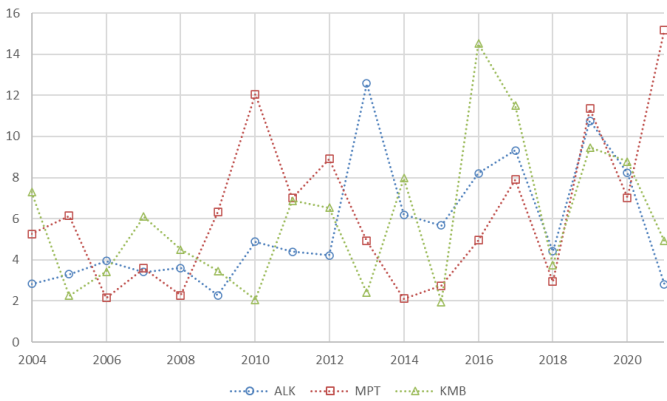


**Figure 3. Kurtosis vs. time for ALK, KMB and MPT.**

gives the kurtosis for daily returns for the period June 2003 to May 2021 calculated annually. We do not observe any downward trend in kurtosis values for the past 18 years, which means that the daily returns did not become more Gaussian-like during the past 18 years.



Following figure depicts EWMA estimator of the volatility  $\sigma_{EWMA}$ . As we can see in the following figure, volatility varies with time, which is in collision with the assumptions of the BS model. Over the past 18 years there were several periods of significant increases in volatility e.g. first half of 2020 which coincides with the Covid-19 outbreak and quarantine measures.

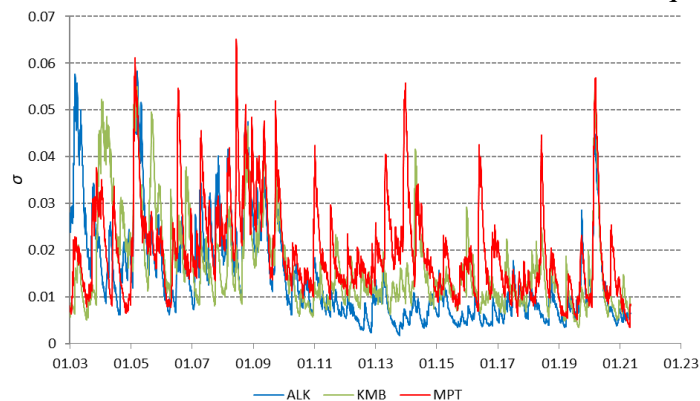


**Figure 4.** EWMA estimator of the volatility  $\sigma_{EWMA}$  for KMB stock on MSE.

### Accuracy of Black-Scholes formulae

In this section, we evaluate applicability and accuracy of BS formulae for stock options on MSE. BS formulae for pricing European call and put options at time  $t=0$  are:

$$C = S_0 N(d_1) - X e^{-rT} N(d_2) \quad (5)$$

$$P = X e^{-rT} N(-d_2) - S_0 N(-d_1) \quad (6)$$

$$d_1 = \frac{\ln\left(\frac{S_0}{X}\right) + \left(r + \frac{\sigma^2}{2}\right)T}{\sigma\sqrt{T}} \quad (7)$$

$$d_2 = \frac{\ln\left(\frac{S_0}{X}\right) + \left(r - \frac{\sigma^2}{2}\right)T}{\sigma\sqrt{T}} = d_1 - \sigma\sqrt{T} \quad (8)$$

where  $C$  is value of a call option,  $P$  is value of a put option,  $N()$  is Cumulative Normal Distribution function,  $S_0$  is current price of the underlying asset,  $X$  is exercise price,  $T$  is expiry time,  $r$  is continuously compounded risk-free interest rate, and  $\sigma$  is historical volatility for the underlying asset. As a risk-free interest rate we take the interest rate of treasury bonds issued by the National Bank of the Republic of Macedonia (NBRM). Data is available for download from the NBRM web site <https://nbstat.nbrm.mk/>.

For the purpose of measuring the accuracy of BS formulae, assume a hypothetical trader that uses those formulae to value options. Every day the trader uses historical market data to calculate volatility  $\sigma$  using Eq. (3) and then invests a certain amount in buying options. From trader's point of view, trading is discontinuous in time with time step 1 day. Trading times will be denoted as  $t = \{1, 2, 3, \dots\}$ . Trader pays no trading charges. If the assumptions of the BS formulae are valid, then in the long run the return of this investment strategy will be equal to the risk-free interest rate. But we know for a fact that many of these assumptions are not valid [16], and they serve only to simplify the model for the stock pricing process. Then, what is the profit or loss the trader will make on real markets? What is the impact of the expiry period on the profitability of this strategy? Does the ratio between the exercise price and spot price has a consistent impact on the profitability of the investment strategy? These are the questions that we address in the remainder of this section.

Our hypothetical trader uses an investment strategy where every trading day a fixed number of options is bought. For sake of simplicity we assume that 1 option is bought every trading day. Without losing any generality of the obtained results, we also assume that

- the trader always buys options with same expiry period  $T$ ,
- exercise price is calculated as a multiple of the spot price  $X_{t+T} = kS_t$  by a fixed factor  $k$ .

Total investment at time  $t$  is calculated as the sum of present value of all previous investments

$$I_t = I_{t-1}e^{rT_M} + C_t; I_0 = 0 \quad (9)$$

where  $C_t$  is the premium for a call option at time  $t$ ,  $T_M = 1/252$  is one trading day.

Earning at time  $t$  for an option with expiry time  $t$  and exercise price  $X_t = kS_{t-T}$  is calculated as  $\max(S_t - X_t, 0)$ . Total earning up to time  $t$  is calculated as

$$E_t = E_{t-1}e^{rT_M} + \max(S_t - X_t, 0); E_0 = 0 \quad (10)$$

Profit at time  $t$  is calculated as  $\max(S_t - X_t, 0) - C_{t-T}e^T$ , and total profit at time  $t$  is calculated as the sum of present value of all previous profits

$$P_t = P_{t-1}e^{rT_M} + \max(S_t - X_t, 0) - C_{t-T}e^T; P_0 = 0 \quad (11)$$

Finally, we calculate the return-on-investment  $ROI = P_t/I_t$ . Similar equations are valid for put options.

We repeat above calculations for  $T \in \{0.0183, 0.25, 0.5, 0.75, 1\}$  and  $k \in \{0.6, 0.7, 0.8, 0.9, 1, 1.1, 1.2, 1.3, 1.4\}$ .  $T = 1$  means expiry period of 1 year. We use the calculations to analyse the profitability of call and put options for stocks traded on MSE. **Figure 5** gives the return-on-investment  $ROI(t, k) = P_t(T, k)/I_t(T, k)$  as a function of  $k$ , and parameterised for the expiry period  $T$  for KMB call and KMB put options. For ITM options, that is,  $k < 1$  for call options and  $k > 1$  for put options, the profit is moderate, which means that BS formula gives a reasonable estimate of option's value. However, our trader is making significant profits for all OTM options, except for put options with expiry period of 1 month ( $T = 0.0183$ ) and  $k = 0.6$ . This is a direct consequence of the leptokurtic nature of the daily returns distribution. The heavy tails of the distribution of the daily returns will cause the deep OTM options to be exercised more frequently than expected according to the BS model. The deeper an option is out of the money, the more it is underestimated by the BS model. As a consequence, ROI grows as  $k$  approaches 1.5 for call options, and as  $k$  decreases towards 0.6 for put options.

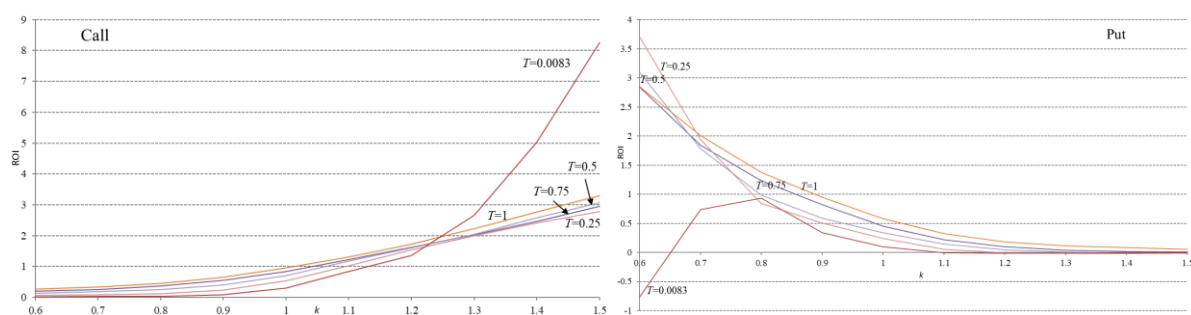


**Figure 5.** ROI vs strike price for KMB call and put options.  $T \in \{0.0183, 0.25, 0.5, 0.75, 1\}$  is curves' parameter.

How can both call and put options be highly profitable in the same time period? The explanation is actually very simple. Namely, KMB stock price experienced strong rises and drops in several periods between 2003 to 2010, and then again around February-March 2020 coinciding with the Covid 19 outbreak. As a consequence deep OTM call and put options were exercised more frequently than anticipated by the Brownian motion model and the log-normal distribution for the stock price changes. To emphasise this phenomenon, in **Figure 6** we give the earning of individual call and put options for  $T = 1$  month. Several periods of strong 1-month stock price rises in 2004-2006 make the call options highly profitable. In mid-2008 a bubble burst occurred which made the 1-month put options very profitable. At the end of February 2020, there was a Covid-19 induced drop in the share price, and consequently the OTM put options were exercised. Only a month later, the KMB prices recovered strongly, and hence the OTM call options were exercised.



**Figure 6.** Daily KMB prices, and daily earning of individual KMB call and put options for  $k = 1.3$  and  $k = 0.8$ , respectively. Expiry period is  $T = 1$  month.

Phenomena depicted in **Figure 5** were observed for ALK and MPT stocks too, as illustrated in **Figure 7** and **Figure 8**, respectively. Namely, deep OTM options are heavily undervalued and can raise significant ROI for the option owners. ITM options are correctly valued by the BM formulae, and do not favour neither the option buyer nor the option seller.

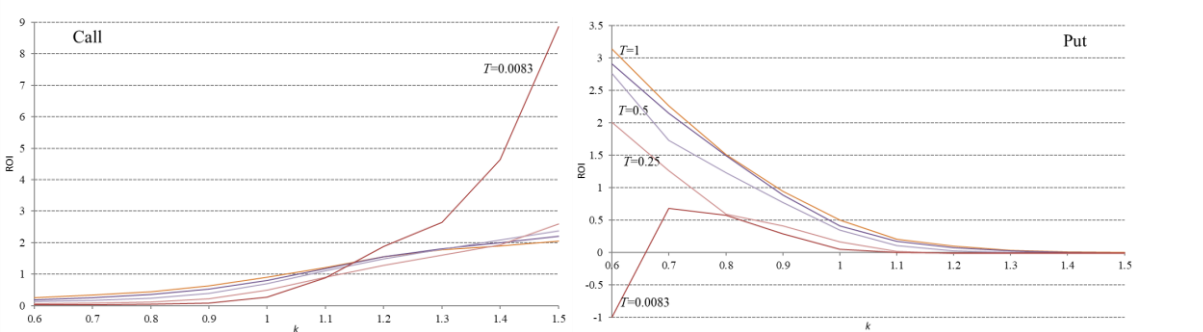


**Figure 7.** ROI vs strike price for ALK call and put options.  $T \in \{0.0183, 0.25, 0.5, 0.75, 1\}$  is curves' parameter.

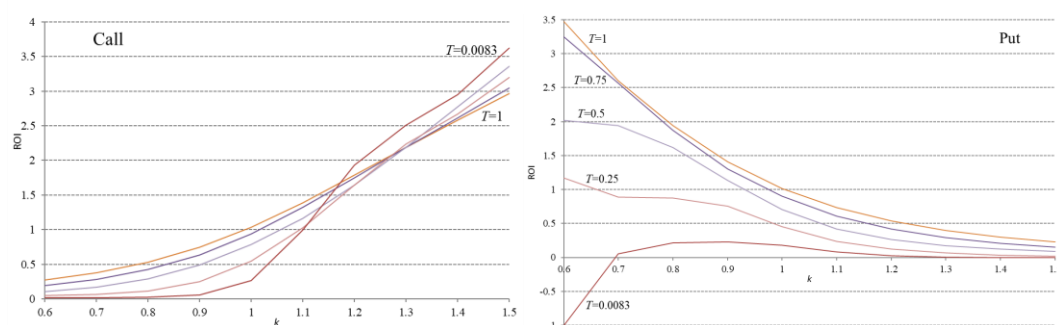


**Figure 8. ROI vs strike price for MPT call and put options.  $T \in \{0.0183, 0.25, 0.5, 0.75, 1\}$  is curves' parameter.**

## Conclusion

Accuracy of assumptions of Brownian motion model for stock pricing process are tested in this paper. We conclude that the two main assumptions of the stock pricing model underlying the BS formula are not valid for MSE and in general for developing markets. First, daily returns do not follow log-normal distribution, with high kurtosis values. Significant positive (bullish) runs and significant negative (bearish) runs are more likely on MSE than expected by the Brownian motion model. Second, volatility of daily returns is not constant over time. The invalidity of the main assumptions has severe consequences on the applicability of the BS model on MSE.

When applied to MSE, BS formulae severely underestimates the likelihood of occurrence of significant jumps and drops in stock prices. Deep OTM call and put options, which can be bought for very low premiums, are frequently exercised and bring extremely high earnings to the owner. Thus, on incomplete and developing stock exchanges BS formula puts options holders in a winning position.

We recommend that the BS formulae can be reliably used only for ITM options e.g.  $k > 1.1$  for put options and  $k < 0.9$  for call options. For the valuation of the OTM options at incomplete emerging stock markets, whose representative is MSE, one needs to use a model for stock pricing process which takes into account high likelihood of significant drops and jumps in stock prices e.g. jump-diffusion process, and occurrence of long positive and negative runs. Another option for the evaluation of ITM options is to use Monte-Carlo simulations based on the distribution of daily returns is derived from the historical stock prices.

## References

- [1] L. Bachelier, "Théorie de la spéculation," Phd Thesis, Sorbonne, 1900.
- [2] H. Markowitz, *Portfolio Selection: Efficient Diversification of Investments*, New York: John Wiley & Sons, 1959.
- [3] W. F. Sharpe, "Capital Asset Prices: A Theory of Market Equilibrium Under Conditions of Risk," *Journal of Finance*, vol. 19, pp. 425-442, 1964.
- [4] F. Black and M. S. Scholes, "The pricing of options and corporate liabilities," *Journal of Political Economy*, vol. 81, no. 3, pp. 637-654, May-June 1973..
- [5] B. G. Malkiel, "The Efficient Market Hypothesis and Its Critics," *CEPS Working Paper No.91*, 2003.
- [6] B. B. Mandelbrot and R. L. Hudson, *The (Mis)behavior of Markets*, Basic Books, 2006.
- [7] J. C. Duan, "Conditionally fat tailed distribution and the volatility smile in options," University of Toronto, Toronto, 1999.
- [8] E. Vasile and D. Armeanu, "Empirical Study on the Performances of Black-Scholes Model for Evaluating European Options," *Romanian Journal of Economic Forecasting*, vol. 10, no. 1, pp. 48-62, 2009.

- [9] S. McKenzie, D. Gerace and Z. Subedar, "An empirical investigation of the Black-Scholes model: evidence from the Australian Stock Exchange," *Australasian Accounting Business and Finance Journal*, vol. 1, no. 4, pp. 71-82, 2007.
- [10] J. C. Hull, *Options, Futures, and Other Derivatives*, 8th ed., Prentice Hall, 2011.
- [11] J. Cox, S. Ross and M. Rubinstein, "Option pricing: A simplified approach," *Journal of Financial Economics*, vol. 7, no. 3, pp. 229-263, September 1979.
- [12] P. Boyle, "Option valuation using a three jump process," *International Options Journal*, vol. 3, pp. 7-12, 1986.
- [13] O. Barndorff-Nielsen and N. Shephard, "Non-gaussian Ornstein–Uhlenbeck-based models and some of their uses in financial economics," *Journal of the Royal Statistical Society. Series B*, vol. 63, no. 2, pp. 167-241, 2001.
- [14] R. Merton, "Option Pricing when Underlying Stock Returns Are Discontinuous," *Journal of Financial Economics*, vol. 3, no. 1-2, pp. 125-144, January-March 1976.
- [15] R. Dodd, "Derivatives Markets: Sources of Vulnerability in U.S. Financial Markets," Financial Policy Forum - Derivatives Study Center, Washington D.C., 2006.
- [16] F. Black, "How to use the holes in Black-Scholes," *Journal of Applied Corporate Finance*, vol. 1, no. 4, pp. 67-73, 1989.
- [17] R. Lowenstein, *When Genius Failed: The Rise and Fall of Long-Term Capital Management*, Random House Trade Paperbacks, 2001.
- [18] S. Figlewski, "Forecasting Volatility Using Historical Data," New York University - Stern School of Business, May 1994.
- [19] R. Suganuma, "Reality Check for Volatility Models".
- [20] J. F. Kenney and E. S. Keeping, *Mathematics of Statistics*, 2nd ed., vol. 2, Princeton, NJ: Van Nostrand, 1951.



## ACOUSTIC SIGNAL DENOISING BASED ON ROBUST PRINCIPAL COMPONENT ANALYSIS

*Sanja Vujnović<sup>1</sup>, Aleksandra Marjanović<sup>2</sup>, Željko Đurović<sup>3</sup>*

<sup>1</sup>School of Electrical Engineering, University of Belgrade, Serbia, email: [svujnovic@etf.bg.ac.rs](mailto:svujnovic@etf.bg.ac.rs)

<sup>2</sup>School of Electrical Engineering, University of Belgrade, Serbia, email: [amarjanovic@etf.bg.ac.rs](mailto:amarjanovic@etf.bg.ac.rs)

<sup>3</sup>School of Electrical Engineering, University of Belgrade, Serbia, email: [zdjurovic@etf.bg.ac.rs](mailto:zdjurovic@etf.bg.ac.rs)

### Abstract

*Robust principal component analysis (RPCA) is a powerful procedure which decomposes a matrix into its low-rank and sparse matrix components. As such it can be used for signal denoising in situations where useful part of the signal can be represented as a low-rank matrix, which is usually the case in acoustic signals with some inherent periodicity. This paper examines the applicability of RPCA for cyclostationary acoustic signal denoising by decomposing the Short-time Fourier transform of a signal and eliminating its sparse component. The main purpose of this approach is improvement of the signal-to-noise ratio in acoustic signals obtained in noisy industrial surroundings for the purpose of fault detection or machine state estimation. The procedure is tested on artificially generated signals as well as on real acoustic recordings.*

### Key words

*Acoustic signals, Noise removal, RPCA, Industrial state estimation.*

### Introduction

With the rise of accessibility of smart hardware devices and inexpensive sensors, acoustic signals are starting to be used for the purposes previously reserved for some other, highly specialized, sensor systems. From ambient event detection, classification of movement, musical instrument detection, all the way to industrial predictive maintenance and state estimation, sound has become a medium which is capable of absorbing various information quite efficiently. It has been long known in the literature [1] that sound can be used to detect fault in rotating actuators sometimes faster than vibration signals which have been traditionally used for solving this issue. The problem, however, lies in the same feature of acoustic signal which makes it so attractive for diverse application: sound is capable of detecting even the slightest changes in the environment, which makes it prone to severe noise contamination. This is especially true in real industrial settings which are generally very noisy and which consist of large amounts of machines working simultaneously. With this in mind, identifying a single actuator in an industrial plant and performing sound analysis for that particular machine is more than challenging.

One of the popular algorithms in the last decade which has been used on acoustic signals, usually for the purpose of vocal extraction, is Robust Principal Component Analysis (RPCA). It is an extension of a widely used statistical data analysis tool called Principal Component Analysis (PCA) and is used to decompose any matrix into its low rank and sparse matrix components. This has proven to be very useful for diverse applications such as background removal from video surveillance cameras, instrument extraction and vocal extraction from musical compositions, etc. One example of musical application is given in [2] where Short Time Fourier Transform (STFT) of the musical composition is observed and it is concluded that musical instruments have a repetitive appearance on the time-frequency plot, which should



correspond to the low rank matrix presentation, while vocal segments are chaotically scattered in time and frequency, corresponding to the sparse matrix. Even though authors have not yet seen the application of RPCA decomposition for preprocessing of acoustic signals obtained from industrial surroundings, arguments for its potential use in this area are quite compelling. Bearing in mind the successful application of RPCA approach on music signals, we can analogously conclude that the expected behavior of rotary actuator signals in time-frequency domain can correspond to a low rank matrix (due to its cyclostationary behavior which leads to discrete number of peaks in the frequency domain), and the surrounding noise is expected to behave as a sparse matrix, similarly to vocal components in music.

The main idea of this paper is to test the aforementioned assumption: that RPCA decomposition of acoustic signal of a rotary actuator made in noisy industrial surroundings will yield a low rank matrix corresponding to the sound of the actuator and sparse matrix corresponding to the unwanted noise. This will be done on artificially generated signals first. These signals will be created to have similar properties as real signals from rotary actuators, with added noise, so that signal-to-noise ratio (SNR) can be controlled. After that the algorithm will be tested on real signals in three scenarios: 1) when the background noise is stationary, which is the most common case, and the source of the background noise are just the sounds of other machines in the plant; 2) when impulse disturbance is added to the background noise in a form of the hammer hitting the metal surface periodically; and 3) when speech contamination is present, i.e. people are speaking near the microphone which records the sound of the actuator. Since the nominal sound of the actuator is unknown, SNR cannot be measured for the real industrial scenario, so the performance of the algorithm will be assessed by analyzing the time-frequency representation of the filtered signal and by listening to the obtained recordings.

This paper is structured as follows. In Section 1 a short literature review is presented which introduces the way RPCA algorithm is used in the literature and the use of acoustic signals for predictive maintenance in real industrial surroundings. The RPCA based noise reduction algorithm is presented in Section 3, while the specific rotary fan mill on which the test has been done is described in Section 4. Results both on artificial and real signals are given in Section 5, while the conclusion of the paper is given in the last section.

## 1. Literature review

The initial attempt to robustify the PCA method, which is severely influenced by intensive noise, dates back to 1970s and 80s [3]; however, due to inability to implement it in polynomial time and the fact that there were no performance guarantees, the approach has not been popular until around 2010. During that time idealized version of that problem has been examined by [4] and has shown promising results. From then onward applications of RPCA methods have been diverse, from image processing applications such as background removal or recovery in video surveillance [5], to cyber security [6]. The application most interesting in the light of this paper is the use of RPCA for acoustic signals. By far the most popular subject in this area has been instrument and singing voice separation from musical compositions. This application has shown great potential, starting with a simple masking procedure in time-frequency domain, proposed by [2], this simple algorithm has been adopted and upgraded by using repeating pattern extraction [7]. There was even an attempt to implement this procedure in real time using bilateral random projection to reduce the amount of necessary computing [8]. It is evident that the applicability of RPCA approach is vast, and new practical applications are emerging every day.

This paper is concentrated on the problem of separating useful sound of the rotary actuator from the surrounding noise in acoustic signals recorded in industrial surroundings, and as such,

this issue is quite similar to separation of vocal component from instruments, as proposed by [2]. Even though it has been long shown that acoustic signature of rotary actuators is cyclostationary and that sound can be used for state estimation [1] the authors are yet to see the RPCA factorization used for such purposes in the literature. For that reason, the aim of this paper is to test the assumption that RPCA factorization can be used for preprocessing of acoustic signals for the use for state estimation algorithms such as the one proposed in [9].

## 2. RPCA based noise removal

Robust principal component analysis is a modification of one of the most widely used statistical algorithms for data analysis – PCA. The goal of RPCA is to recover low rank and sparse components of severely corrupted matrix  $M$ . Procedure itself, as stated in [4] is defined as an optimization problem:

$$\begin{aligned} & \text{minimize} \quad \|L\|_* + \lambda \|S\|_1 \\ & \text{subject to} \quad L + S = M \end{aligned} \quad (1)$$

Here,  $L \in \mathbb{R}^{n \times m}$  represents a low rank component of matrix  $M \in \mathbb{R}^{n \times m}$ , and  $S \in \mathbb{R}^{n \times m}$  represents its sparse component. Nuclear form of the matrix (sum of all singular values) is denoted as  $\|\cdot\|_*$  and the L1-norm of the matrix is denoted as  $\|\cdot\|_1$ . The parameter  $\lambda$  is used to balance between the rank of  $L$  and sparsity of  $S$ . A good choice of that parameter is offered in [4] as  $\lambda = 1/\sqrt{\max(n, m)}$  and this value has been used in this paper as well.

Bearing in mind the problem we are aiming to solve, i.e. denoising acoustic signals obtained in industrial surroundings, we should examine what kind of behavior is expected in a signal. First of all, the recorded signals are obtained with the goal of state detection of rotary actuators. That means that the acoustic signal is expected to have cyclostationary signature [1] with dominant frequency components related to rotating frequency and its higher harmonics. By observing the STFT of the signal it is expected to contain several peaks in frequency domain which corresponds to straight lines parallel to time-axis in time-frequency presentation, i.e. the STFT matrix is expected to have low rank. Intense surrounding noise, however, is expected to exist on all the frequencies and should have the behavior which corresponds to sparse matrix in time-frequency domain. As such, the STFT of acoustic signal can be decomposed into informative cyclostationary component,  $L$ , and noise which is expected to be contained in the matrix  $S$  from Eq. (1).

The algorithm which will be used for testing this hypothesis will be a modified version of the work proposed in [2] for separation of vocal components from musical compositions. Here vocal components have similar attributes as the surrounding noise, while musical instruments have the behavior which is expected in rotary actuators. The procedure consists of five steps:

- 1) Separating recorded acoustic signal into smaller frames 10 s long
- 2) Calculating matrix  $M$  which is a STFT of a frame (using Hamming window 1024 samples long, with 1000 samples overlap)
- 3) Using RPCA to decompose STFT into low rank matrix  $L$  and sparse matrix  $S$
- 4) Depending on the type of algorithm which will be implemented in this step one of two actions can be taken
  - a. Denoising without a mask: matrix  $L$  is adopted as the filtered signal,  $M_{\text{filtered}} = L$ ;
  - b. Denoising with a mask: masking is performed to obtain the filtered signal,  $M_{\text{filtered}}$  from the original matrix  $M$ ;

- 5) Inverse STFT of  $M_{filtered}$  is obtained as a reconstructed filtered signal in time-domain

Masking procedure in step 4) b. has been proposed by [2] to improve the separation results. The masking is used to indicate which part of the original matrix  $M$  is useful and should be kept in filtered signal. Binary time-frequency mask is obtained as

$$B(i, j) = \begin{cases} 1, & |L(i, j)| > k \cdot |S(i, j)| \\ 0, & \text{otherwise} \end{cases}, \quad (2)$$

for all  $1 \leq i \leq n$  and  $1 \leq j \leq m$ . Parameter  $k$  has been set to the value of 0.3, which is the value that yields best signal-to-noise (SNR) ratio for artificially generated signals. After calculating this mask, the filtered signal STFT is determined as

$$M_{filtered}(i, j) = B(i, j)M(i, j). \quad (3)$$

### 3. Case study

Acoustic signal denoising algorithm presented in the previous chapter has been created for the purpose of noise removal in industrial surroundings, and as such it will be tested both on artificially generated signals and on real acoustic recordings. The problem which we aim to tackle in this paper is related to predictive maintenance of coal grinding fan mill in thermal power plant Kostolac A1 in Serbia.

The main purpose of coal grinding subsystem is to pulverize coal into fine powder so that it can be transferred to the boiler where it is used as a fuel. The grinding process is achieved with fan mills which have an impeller within them with 10 impact plates placed around the center in circular fashion. Mill is filled with coal as the impact plates rotate with the speed of around 12.5Hz, and the friction between chunks of coal and the plates pulverizes the coal. Unfortunately, one side effect of this process is that the impact plates themselves get worn as the number of working hours increases. While they become depleted their performance and efficiency suffer and if the maintenance is not conducted on time this can lead to failures and shutdowns of the entire subsystem. For that reason periodical maintenance of the mills is usually conducted and recently there is an attempt to automate the process using acoustical recording obtained in the vicinity of the mill [9].

Acoustic signals are recorded by placing the microphone near the mill. The sampling frequency is 48kHz and is later downsampled to 4.8kHz due to the fact that the most important frequency components are lower than 2000Hz. It is shown that acoustic signals are informative enough to detect whether the impact plates are functioning properly or the maintenance needs to be conducted [9]; however, any unexpected noise in the acoustic recording can severely influence any similar state detection algorithm [10]. For rotary actuators such as fan mills, the acoustic signature is quite predictable in the frequency domain. There are dominant peaks at characteristic frequencies and several higher harmonics are usually visible as well. In the case of fan mill in thermal power plant Kostolac A1 in Serbia, the frequency signature is shown in Fig. 1. (left). The dominant peak is at the rotating frequency of  $f_r = 12.5\text{Hz}$  and its higher harmonics, as well as at the frequency at which the impact plate passes near the microphone (since there are 10 impact plates, that frequency is at  $f_p = 125\text{Hz}$ ) and its higher harmonics. STFT of the signal is typical for stationary behavior, i.e. there are dominant constant lines at specific frequencies. What is notable is that the signal shown in Fig. 1 (left) is naturally noisy

due to the fact that even in nominal working conditions the real industrial surroundings is such that the acoustic noise is unavoidable.

Since real acoustic signals are naturally corrupted by noise, it is hard to experiment with them and to determine signal-to-noise ratio. For this reason artificial signal is generated which mimics the behavior of the real signal in frequency domain, but without the noise. The idea is not to model the signal exactly, just to mimic the shape in the frequency domain so that the RPCA based algorithm is similar and we can control and test for the signal-to-noise ratio. The proposed signal  $x(t)$  is phase modulated so that the higher harmonics are generated in the frequency domain

$$x(t) = \sin(2\pi \cdot f_r t + \sin(2\pi \cdot f_r t)) + 3 \sin(2\pi \cdot f_p t + \sin(2\pi \cdot f_p t)). \quad (4)$$

Frequency domain and STFT of the signal are shown in Fig 1. (right) and we can see that the behavior sufficiently coincides with the recorded one.

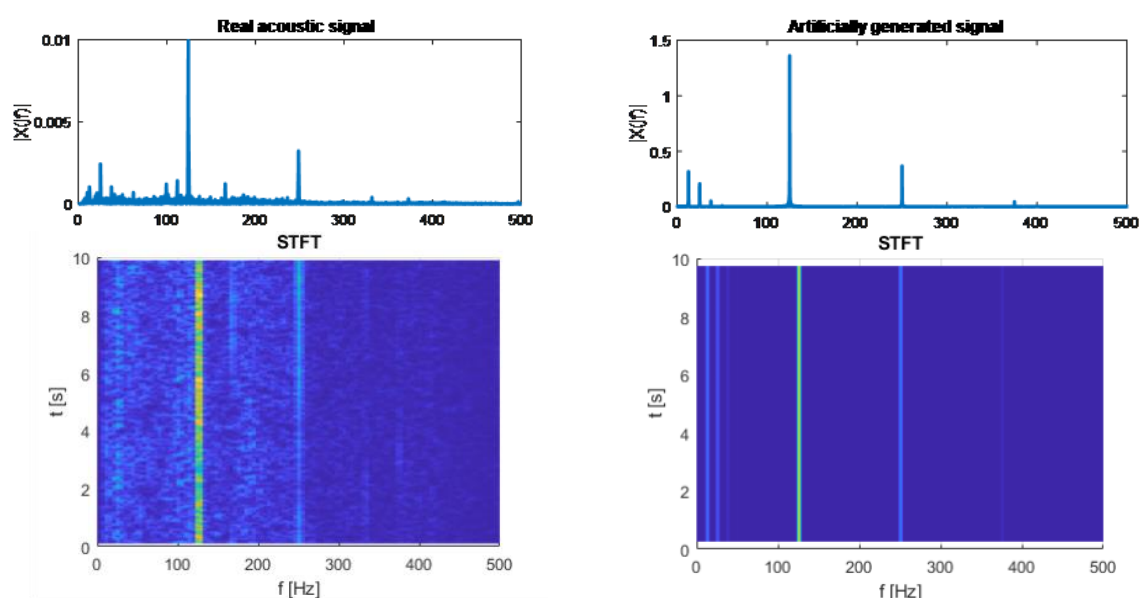


**Fig. 1** Real signal recorded near the mill in frequency domain (upper left) and STFT (lower left), as well as the artificially generated signal in the frequency domain (upper right) and STFT (lower right).  
Source: authors generated these images using Matlab.

## 4. Results

The aim of this paper is to examine whether RPCA noise reduction algorithm proposed in Section 2 can be used for noise removal of acoustic signals recorded in real industrial surroundings without significantly damaging the useful part of the signal. This was tested in two ways. First the artificial signal was corrupted with Gaussian noise and signal-to-noise ratios were measured before and after filtration to determine whether the proposed algorithm has any applicability. After that the real acoustic signals were used, and the algorithm was tested in three scenarios: 1) in nominal working conditions when stationary background noise is present; 2) when there is an impulse disturbance as sound of a hammer hitting a metallic surface; and 3) when there is noise from people talking near the microphone. While testing on real signals measuring signal-to-noise ratio is not possible, so the algorithm is tested by visual inspection of the behavior of signal in time-frequency domain as well as by listening to the resulting audio.

Artificially generated signal

Signal described in Eq. (4) was polluted with artificial Gaussian noise of different intensities, and the algorithm was tested with and without the application of mask. The results can be seen in Table 1 and shows a promising behavior of the RPCA method. First of all, in all instances denoising without the mask has shown better results than the one with mask, which is a compelling argument that while implementing this procedure on real signals the mask should not be used. Furthermore, when the signal-to-noise ratio is quite good (i.e. greater than 0dB) the algorithm does not enhance the quality of the signal significantly. Not only that, but when the noise is weak enough (SNR of 10 dB) this algorithm tends to corrupt the signal more than it enhances it. The true power of this procedure becomes evident when the noise is stronger than the signal, which is the case in the industrial surroundings. When SNR is lower than 0 dB this procedure significantly recovers the corrupted signal and furthermore the bigger the noise, the better relative increase in signal quality is achieved.

To visually inspect the performance of the algorithm it is informative to observe matrices  $S$  and  $L$  obtained with RPCA. In Fig. 2 it can be seen that the sparse matrix  $S$  has indeed gathered most of the noise, while in the low rank matrix  $L$  are all the dominant components of the original signal. It is evident as well that some components of the original signal are partly in matrix  $S$  as well (mainly those at the frequency of 125 Hz) and that is probably the reason why this procedure does not perform very well when the noise is negligible – the sparse component which is eliminated takes some useful information from the signal. Figure 3 shows the original, noisy and reconstructed signal in time domain.

Table 1 Signal-to-noise ratio before noise reduction, after noise reduction without a mask and after noise reduction with mask

SNR before denoising	10	5	0	-5	-10	-15	-20
SNR after denoising without mask	5.6	5.5	5.2	3.9	1.1	-3.7	-8.9
SNR after denoising with mask	4.2	3.2	0.4	-1.6	-5.8	-10.9	-15.7

Source: authors generated this data using Matlab.

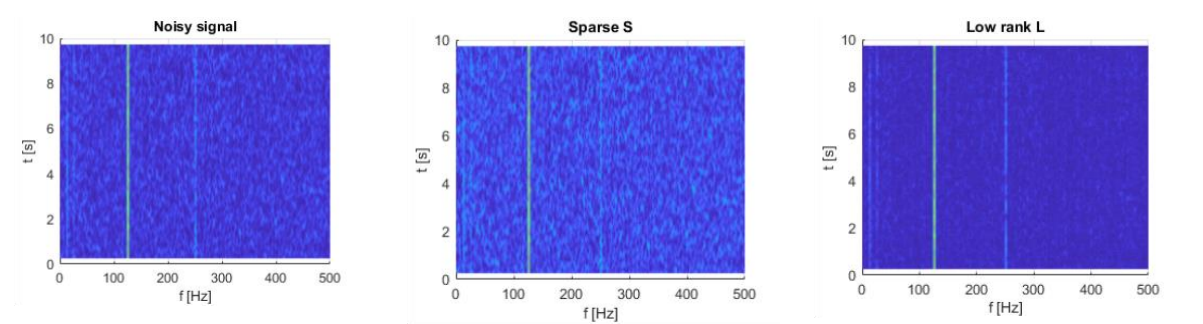
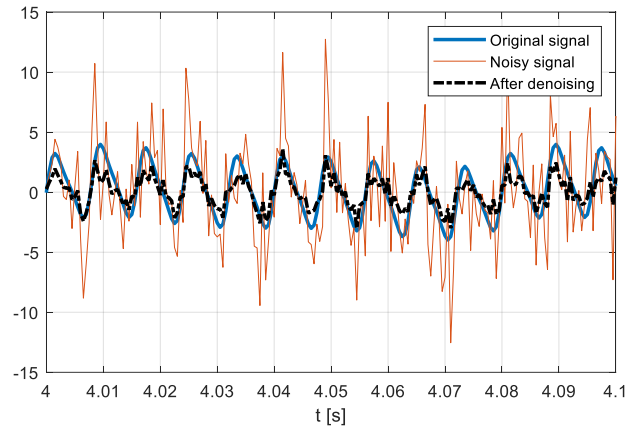


Fig. 2 STFT of artificially generated noisy signal for SNR value of -5dB (left), sparse matrix  $S$  (center) and low rank matrix  $L$  (right) obtained after RPCA decomposition.

Source: authors generated these images using Matlab.





**Fig. 3** time domain representation of the original signal, noisy signal with SNR value of -5dB and the signal obtained after denoising procedure without the mask.

Source: authors generated this image using Matlab.

### Real acoustic signals

As noted from Fig. 1, the acoustic recordings obtained from the real industrial surroundings are naturally noisy and as such it is quite difficult to extract the useful signal from the noise. Applying the RPCA denoising procedure on such signal we get the similar results as with artificially generated ones. Figure 4 shows STFT of an original signal and low rank matrix  $L$  (which also represents reconstructed signal without mask). It is evident that low rank matrix has managed to extract all the dominant frequency components; however, some of the components on lower frequencies, which originally had lower amplitude, are missing. This is due to the fact that there is a more severe noise pollution on lower than on higher frequencies.

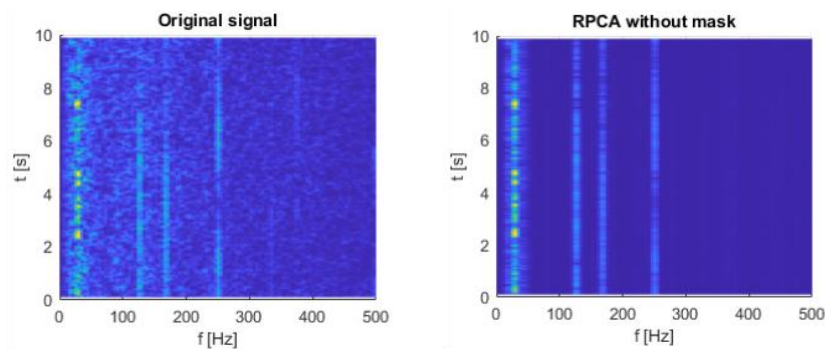


**Fig. 4** STFT of real acoustic signal (left) and RPCA reconstruction (right).

Source: authors generated these images using Matlab.

These results indicate that RPCA method can remove nonstationary noise from loud industrial surroundings, while keeping stationary features of the signal (i.e. dominant frequency components). The next test is to check whether additional disrupting noise can be filtered out as well. As it is shown in [10] dominant noise such as impulse disturbance in time domain or added speech signal can significantly damage state detection algorithms. Figure 5 shows the behavior of this denoising procedure when loud impacts of hammer to metal can be distinctly heard on the recording. As can be seen, impulse disturbance in time domain is presented as dominant component on all frequencies, in the frequency domain. After RPCA procedure all of those nonstationary sounds are removed. Also, subjectively, while listening to the resulting sound signal, the impacts of hammer have indeed been eliminated and cannot be heard in the resulting recording. Final test is the signal corrupted with added speech. This problem is quite elusive due to the fact that speech signal changes in intensity in time, and dominant frequency



components change as well. As shown in Fig. 6, RPCA denoising procedure manages to suppress this kind of contamination as well.

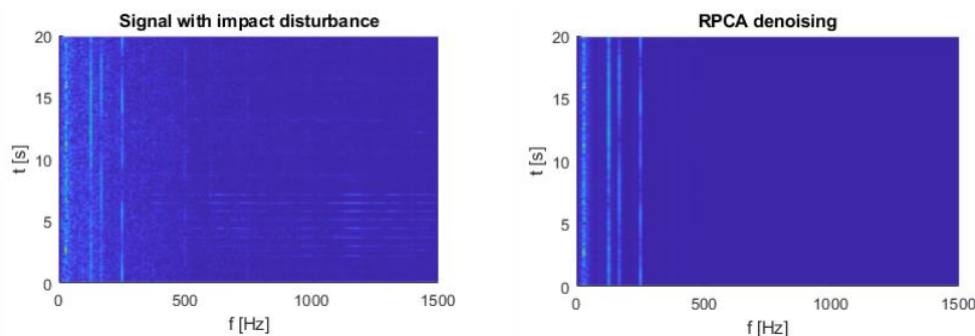


**Fig. 5 STFT of acoustic signal with impulse disturbance (left) and RPCA reconstruction (right).**  
Source: authors generated these images using Matlab.

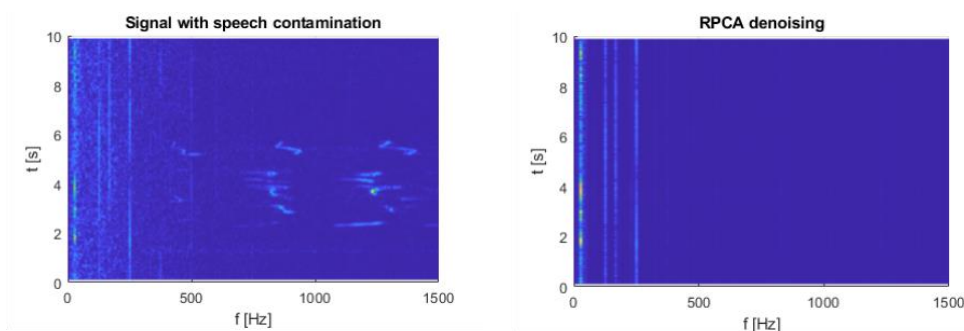


**Fig. 6 STFT of acoustic signal with speech contamination (left) and RPCA reconstruction (right).**  
Source: authors generated these images using Matlab.

## Conclusions

In this paper an RPCA denoising procedure has been proposed for the use on real acoustic signals obtained in industrial surroundings, as a preprocessing step for the purpose of state estimation. This algorithm has been tested on artificially generated signals, as well as on real acoustic recordings of a fan mill in thermal power plant Kostolac A1 in Serbia.

The results obtained on artificial signals seem promising. Since the signal is generated so that its behavior in time-frequency domain mimics the behavior of rotary actuator acoustic signature, results obtained here should indicate the applicability of this algorithm in real industrial surroundings. The noise used to pollute the signal is Gaussian, and signal-to-noise ratio was varied. The results show that the algorithm performs exceptionally well when the noise is severe; however it tends to degrade the useful signal if the noise is not significant (SNR larger than 5dB).

As far as the real recordings are concerned, subjective examination shows that all the added noise, in the form of speech contamination and impulse disturbance are eliminated effectively. What is not yet determined is whether the useful part of the signal is degraded using this procedure and whether that degradation (if any) influences the following steps of state estimation, which are the main reason for implementing this factorization.

Further work on this subject should aim to improve the quality of the algorithm. Since masking procedure is shown to be ineffective, some other approaches such as repeating pattern extraction could yield better results. On the other hand, real time implementation is something

that can be useful in the industry, so improving the speed of the algorithm (which is currently far from real time) can be beneficial. Finally, a detailed analysis of the performance of state detection algorithms with and without the preprocessing step of RPCA factorization should be examined to verify the initial assumption that indeed the procedure removes mostly noise, and that the informative part of the signal is unscathed.

## Acknowledgments

This paper is a result of activities within Eureka project E!13084 and the projects supported by Serbian Ministry of Education and Science.

## References

- [1] Baydar, Naim / Ball, Andrew: “A comparative study of acoustic and vibration signals in detection of gear failures using Wigner-Ville distribution”. *Mechanical Systems and Signal Processing*, 15(6), 2001, pp. 1091-1107.
- [2] Huang, Po-Sen et al.: “Singing-voice separation from monaural recordings using robust principal component analysis”. 2012 IEEE International Conference on Acoustics, Speech and Signal Processing (ICASSP), 2012, pp. 57-60.
- [3] Huber, P.: *Robust statistics*. Wiley, New York, 1981.
- [4] Candes, Emmanuel J. et al.: “Robust Principal Component Analysis?”. *Association for Computing Machinery*, 58(3), 2011, pp. 1-37.
- [5] Leow, Wee Kheng et al.: “Background Recovery by Fixed-Rank Robust Principal Component Analysis”. In: Wilson, Richard et al. (eds.): *Computer Analysis of Images and Patterns*. Springer Berlin Heidelberg, 2013, pp. 54-61.
- [6] Paffenroth, Randy C. et al.: “Space-time signal processing for distributed pattern detection in sensor networks”. In: Drummond, Oliver E. / Teichgraber, Richard D (eds.): *Signal and Data Processing of Small Targets*. 2012.
- [7] Doğan, Sait Melih / Salor, Özgül: “Music/singing voice separation based on repeating pattern extraction technique and robust principal component analysis”. 5th International Conference on Electrical and Electronic Engineering (ICEEE), 2018, pp. 482-487.
- [8] Mirbeygi, Mohaddeseh / Mahabadi, Aminollah / Ranjbar, Akbar: “RPCA-based real-time speech and music separation method”. *Speech Communication*, 126, 2021, pp. 22-34.
- [9] Vujnovic, Sanja / Djurovic, Zeljko / Kvascev, Goran: “Fan mill state estimation based on acoustic signature analysis”. *Control Engineering Practice*, 57, 2016, pp. 29-38.
- [10] Vujnovic, Sanja / Marjanovic, Aleksandra / Djurovic, Zeljko: “Acoustic contamination detection using QQ-plot based decision scheme”. *Mechanical Systems and Signal Processing*, 116, 2019, pp. 1-11.



## INVESTIGATION OF EFFICIENCY ASPECTS IN 3×3 PHOTOVOLTAIC PLANT USING MODEL OF SHADING

***Biljana Citkuseva Dimitrovska<sup>1</sup>, Roman Golubovski<sup>2</sup>, Hristina Spasevska<sup>3</sup>, Goce Stefanov<sup>4</sup>,  
Maja Kukuseva Paneva<sup>5</sup>***

<sup>1</sup>Faculty of Electrical Engineering University Goce Delcev Stip R.N. Macedonia,  
biljana.citkuseva@ugd.edu.mk

<sup>2</sup>Faculty of Natural Sciences and Mathematics University Ss. Cyril and Methodious Skopje R.N. Macedonia,  
roman.golubovski@t.mk

<sup>3</sup>Faculty of Electrical Engineering and Information Technologies University Ss. Cyril and Methodious Skopje  
R.N. Macedonia, hristina@feit.ukim.edu.mk

<sup>4</sup>Faculty of Electrical Engineering University Goce Delcev Stip R.N. Macedonia, goce.stefanov@ugd.edu.mk

<sup>5</sup>Faculty of Electrical Engineering University Goce Delcev Stip R. N. Macedonia, maja.kukuseva@ugd.edu.mk

### Abstract

*Solar irradiation is the most affordable renewable energy source, implementable even on household level. The considerably lower cost of setup and maintenance compared to the other renewable energies makes it a preferable choice in regions with lot of sunny days throughout the year. One of the main R&D aspects of interest of the Photovoltaic (PV) technologies is the efficiency of the PV conversion, which is dealt with on material level. Additional efficiency aspects could be a field of research in support to higher energy production. One of them is the land use efficiency of the utilized plot surface. Namely, the usual approach in populating the plot used by the plant is with row and column distances that guarantee no inter-shading among the panels. This paper presents results of research proposing use of denser panel population in the plot, with allowed inter-shading which under some approximation provides calculations of lower individual panel efficiency but much higher overall land use efficiency. The research project proposes an inter-shading model in a 3×3 PV plant, which can be validated in CAD applications. A clear-sky irradiation model is then used to estimate plant's power at certain moment in the year, and calculation of energy production. Sun position and its incidence angle are calculated using a verified model. The analytical software uses the following input parameters - plant geo-location (latitude, longitude, time zone); panel geometry (width, height); plant geometry (inter-row and inter-column distances, panel inclination angle); and date and time. The inter-shading model results in total plant exposed PV surface to direct solar irradiation, as well as in the total shaded PV surface receiving diffuse (and reflected) radiation. The energy model can then be used for power and energy calculations, as well as optimal inclination, inter-row and inter-column estimations. If panel technologies allow small segmentation with protective diodes implementing approximation that whole directly exposed surface performs PV conversion, then allowed inter-shading and thus denser panel populated plant plot may prove cost-effective.*

### Key words

*solar irradiation, photovoltaic conversion, intershading, land use efficiency.*

### Introduction

The energy consumption overall is in continuous increase with the increasing world population, so the energy issues raise major and fundamental challenges for the technological trends. The nonrenewable energy sources are depleting, and mankind needs to switch to the

renewable sources, which can be defined as geothermal (resulting from earth's core activity), sun related (direct solar irradiation, wind) and gravitationally related (tide, water flow) [1,2,3]. From all renewable sources, the Sun is one of the most used. Photovoltaic cells are devices that use semiconductor materials to convert sunlight into electricity. Photovoltaic technologies offer a large number of advantages which include producing clean energy; offering high reliability, because it does not employ moving/rotating parts; operating cost is very low due to non-demanding maintenance and because it does not require fossil fuel; modular structure allowing simple and flexible assembly [4].

The objective of this paper is implementation of a standard shading model used for a plant of photovoltaic panels to optimize its geometry for more efficient use of the land. The standard shadow model is applied to a plant consisting of nine photovoltaic panels, arranged in three rows and three columns (3×3). The goal is to determine analytically the inter-shading and consequently how the shading affects energy production emphasizing the efficiency of the land utilization. This paper is organized as follows. In section 1 overview of solar geometry and shading model is given, while in section 2 the used methodology is given. In Section 3 the analytical algorithms are described and presented. Section 4 presents results, and Section 5 concludes this paper.

## 1. Model of shading

The model of inter-shading among the PV panels in the 3×3 configuration as detailed in [5] determines how each panel shades the columns behind, after which the total exposed plant surface  $S_{dir}$  and the total shaded plant surface  $S_{dif}$  are calculated.

The inter-shading model uses a sun position model [6] that provides required momental sun seasonal altitude and daily azimuth along with the sun incidence angle based on a geolocation (latitude and longitude) as well as date and time.

The model of shading is based on trigonometric functions that determine the geometry of inter-shading. These mathematical relations are verified with CAD software.

Parameters taken for shadow calculations are the angle of inclination  $\beta$ , the panel width  $P_x$ , the panel length  $P_y$ , the inter-row distance  $r_y$  and the inter-column distance  $r_x$ .

Typical shaded moment is depicted in figure 1:

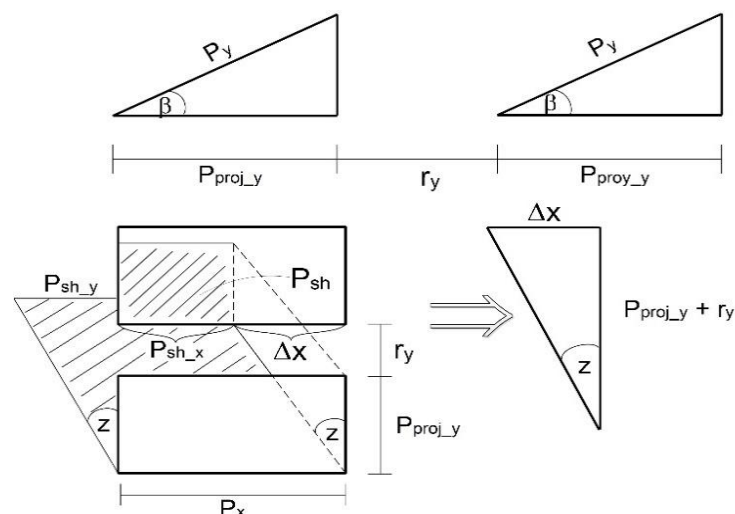


Fig. 1. Elements of inter-shading

This algorithm determines the total area  $S_{dir}$  directly exposed to solar radiation  $G_b$ , as well as the total area  $S_{dif}$  which is exposed to diffuse solar radiation  $G_d$ .

## 2. Calculation of power using Clear-sky irradiation model

After calculation of the solar parameters, the shadow geometry and consequently the exposed and shaded surfaces, the power output of the entire power plant can be calculated for every moment in time with the following equation [1,2]:

$$P_i = (G_b \cdot S_{dir} + G_d \cdot S_{dif}) \cdot \eta \tag{2.1}$$

$G_b$  is direct solar radiation,  $G_d$  is diffuse solar radiation,  $S_{dir}$  is surface of the panel exposed to direct radiation and  $S_{dif}$  is surface of the panel under shadow.

The proposed irradiation model simplifies the context with the assumption that all days of the year are sunny. Even on sunny days, there is some diffuse radiation, mainly due to the refusal of direct radiation by the molecules of the air. The total solar radiation is a sum of the direct, the diffuse and the ground reflected component of radiation. In this model the ground reflected component is insignificant because the location of the solar power plant is assumed to be in isolated rural areas [6,7,8,9].

The effects of the atmosphere in scattering and absorbing radiation are variable with time as atmospheric conditions and air mass change. It is useful to define a standard “clear” sky and calculate the hourly and daily radiation which would be received on a tilted surface under standard test conditions. Hottel (1976) has presented a method for estimating the beam radiation transmitted through clear atmospheres which considers zenith angle and altitude for a standard atmosphere and for four climate types.

Correction types are applied to  $a_0$ ,  $a_1$ ,  $nm$  to allow changes in climate types. The correction factors are given in Table 1.

**Table 1** Correction factors for climate type

<i>Climate type</i>	$r_0$	$r_1$	$r_k$
Tropical	0.95	0.98	1.02
Midlatitude summer	0.97	0.99	1.02
Subarctic summer	0.99	0.99	1.01
Midlatitude winter	1.03	1.01	1.00

The atmospheric transmittance  $\tau_b$  for beam radiation and the other factors  $a_0$ ,  $a_1$ ,  $k$  are given in the following form:

$$\tau_b = a_0 \cdot r_0 + a_1 \cdot r_1 \cdot \exp\left(\frac{-k \cdot r_k}{\cos(\Phi)}\right) \tag{2.2}$$

$$a_0 = 0,4237 - 0,00821 \cdot (6 - nm)^2 \tag{2.3}$$

$$a_1 = 0,5055 - 0,00595 \cdot (6.5 - nm)^2 \tag{2.4}$$

$$k = 0,2711 - 0,01858 \cdot (2 - nm)^2 \tag{2.5}$$

where  $nm$  is the altitude of the targeted geolocation in kilometers.

The clear sky beam normal radiation is then:

$$G_{bn} = G_{atm} \cdot \tau_b \quad (2.6)$$

where  $G_{atm}$  is extraterrestrial solar radiation given in the following form:

$$G_{atm} = G_{sc} \cdot (1 + 0,033 \cdot \cos(\frac{360 \cdot n}{365})) \quad (2.7)$$

and  $G_{sc} = 1367 \text{ W/m}^2$  is a **solar constant**,  $n$  is the day in a year.

Similarly, the  $\tau_d$  factor can be calculated, which tells the amount of diffuse radiation on a sunny day at the same location.

$$\tau_d = 0.271 - 0.294 \cdot \tau_b \quad (2.8)$$

The clear-sky diffuse normal radiation can be calculated as:

$$G_{dn} = G_{atm} \cdot \tau_d \quad (2.9)$$

Direct radiation changes throughout the day and is calculated according to the cosine rule:

$$G_b = G_{bn} \cos \theta \quad (2.10)$$

The diffuse solar radiation is:

$$G_d = G_{dn} \frac{1 + \cos \beta}{2} \quad (2.11)$$

The total solar radiation per  $m^2$  panel is given with the formula:

$$G_t = G_{bn} \cos \theta + G_{dn} \frac{1 + \cos \beta}{2} \quad (2.12)$$

where  $\theta$  is incidence angle,  $G_{bn}$  is normal direct solar radiation,  $G_{dn}$  is normal diffuse solar radiation and  $\beta$  is tilted angle.

Solar radiation models are essential for predicting average daily, monthly and seasonal radiation, beam radiation and diffuse radiation.

The energy produced for a day is calculated with:

$$Ei = \int_0^{interval} Pi \cdot di \quad (2.13)$$

The model of the solar position, the model of shading and the model of solar radiation (Clear-sky radiation) are mutually connected and implemented into application software for energetic analysis of photovoltaic plant of 3×3 panels. The output power and the cumulative energy for a given period (day, month, year) can be calculated using this software.



## 5. Methodology

The software is implemented in VBA (Visual Basic for Application). All algorithms which are used in the software are described using diagrams.

The input parameters which are used in the software are given in Table 3.1.

Submodels that are used in software: the model of geometry of solar position, model of a shadow and a model of a solar radiation (Clear-sky radiation). Model of geometry of solar position describes the correct position of the sun at a given moment of the time in relation to geolocation of the photovoltaic grid. The algorithm which describes the model of the solar position takes into consideration the following parameters: The geolocation of the photovoltaic plant ( $L, LOD$ ), the day in the year, the moment in the day ( $N, LMT$ ) and the geometric relations which are calculated from them. The parameters of the solar position are calculated on the basis of these relations: the altitude angle  $\alpha$ , the angle of solar azimuth  $z$  and the incidence angle  $\theta$ .

**Table 3.1** Input parameters used in software for energetic analysis

Input parameters	Symbol
Geographic latitude (°)	$L$
Geographic longitude (°)	$LOD$
A day in a year	$N (1 \sim 365)$
Local standard time in a day (min)	$LMT$
Width of a panel (m)	$Px$
Length of a panel (m)	$Py$
Efficiency of a panel (PV conversion)	$\eta$
Angle of inclination (°)	$\beta$
Azimuth angle of the panel orientation (°)	$azp$
Distance between rows (m)	$r_y$
Distance between columns (m)	$r_x$
Height above sea level (km)	$nm$
Time interval for integration of energy (min)	$\Delta t$

The model of shading considers the solar angles ( $\alpha, z$ ), the panel geometry ( $Px, Py$ ), the plant geometry ( $r_x, r_y, \beta$  и  $azp$ ). The whole illuminated area  $S_{dir}$  of the plant and the whole shadow area  $S_{dif}$  are determined on the basis of them.

If we know the areas  $S_{dir}$  and  $S_{dif}$  we can make an analytic valuation of the energetic aspects of the photovoltaic grid using the model of solar radiation (Clear-sky model).

The calculation of the power  $P_i$  (equation 3.1) enables calculation of cumulative produced energy at a given period (day, month, year etc.)

The calculation of energy is fundamental for precise determination of the optimal parameters of the photovoltaic grid: angle of inclination  $\beta_{opt}$  and the distances ( $opt_{rx}$ ;  $opt_{ry}$ ) between the photovoltaic panels.

The optimal daily inclination of the panels  $\beta_{opt}$  is that for which maximal energy is produced by the panels with optimal orientation of panels ( $azp=0^\circ$ ) towards local noon.

The optimal distances  $opt\_rx$  and  $opt\_ry$  are those for which the photovoltaic grid produces energy at least equal to some predefined reference energy at optimal daily angle of inclination  $\beta_{opt}$  and allowed intershading. According to that, distances between rows  $r_y$  and distances between columns  $r_x$  are in the range until overcoming the intershading. Algorithm for determining the optimal distances ( $opt\_rx$ ;  $opt\_ry$ ) is shown in Fig. 2.

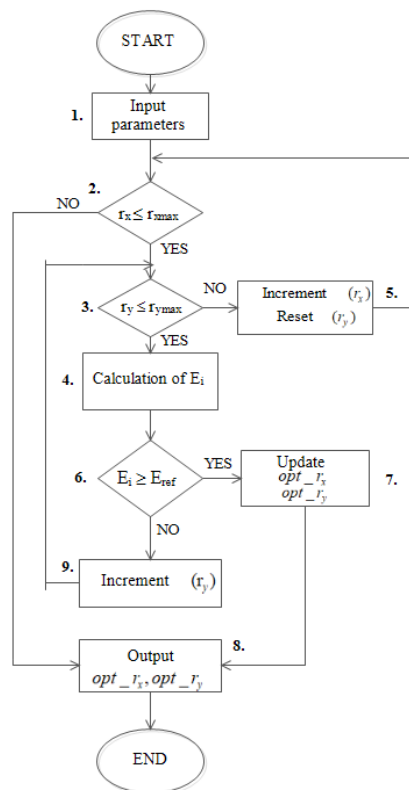


**Fig. 2. Algorithm for determining optimal interpanel distances**

The software enables energetic analyses for the defined photovoltaic plant and comparative analyses in relation to its essential parameters. The essential parameters which influence the production of electric energy are the parameters that describe the geometry of the photovoltaic plant, in other words, the interpanel distances  $r_x$  and  $r_y$  as well as the angle inclination of the photovoltaic panels  $\beta$ .

The input parameters in the software for energetic analysis of the photovoltaic plant are the following: width  $P_x=1\text{m}$  and length of the panel  $P_y=1,64\text{m}$ , efficiency of the panel  $\eta=20\%$ , angle of panel inclination  $\beta$ , azimuth angle of the panel orientation  $azp=0^\circ$ , height above sea-level  $nm=0,3\text{ m}$  and time interval for energy integrating  $\Delta t_E=15\text{ min}$ .

It is necessary to optimize the inclination angle  $\beta$  to get maximal production of electrical energy. The optimal angle of inclination  $\beta_{opt}$  is defined as inclination for which maximal energy is provided at a certain period (typical date day). In this way, daily tracking can be provided for the panels of the photovoltaic plant.

The tracking of the panels is updated at a daily base for the needs of this research. The optimal angle of inclination is calculated at avoided intershading, by testing the whole interval of the inclination angle  $\beta$  ( $0^\circ \sim 90^\circ$ ) with selected step  $1^\circ$ . Maximal daily energy production is achieved by choosing the optimal angle of inclination  $\beta_{opt}$  for a specific day. Algorithm for determine optimal angle of inclination  $\beta_{opt}$  is shown on Fig. 3.

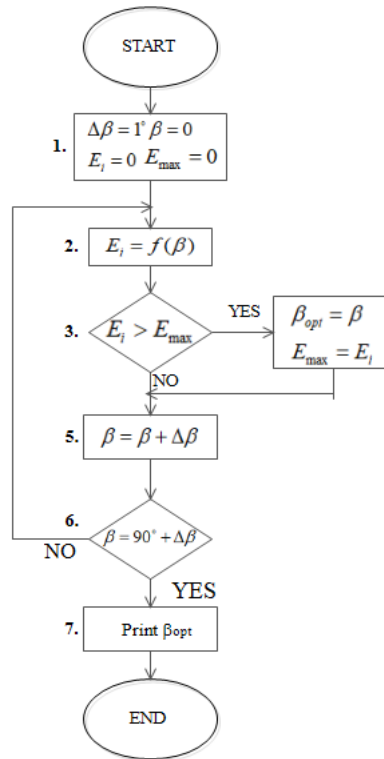


**Fig. 3. Algorithm for determination of optimal angle  $\beta_{opt}$**

The following analysis is made for geographic latitudes from  $0^\circ$  to  $65^\circ$  for the North hemisphere. Comparative analysis for the produced energy is made in relation to the shortest day of the year 21<sup>st</sup> December,  $N=355^{\text{th}}$  day of the year. This day is chosen because the shadows are the longest. As a result of this there is a need of the greatest values of the distances between the panels in order to avoid them. This day 21<sup>st</sup> December marked with  $N=355$  is taken as reference day. Besides the reference day 21<sup>st</sup> December other 7 days are selected: 9<sup>th</sup> February ( $N=40$ ), 21<sup>st</sup> March ( $N=80$ ), 1<sup>st</sup> May ( $N=121$ ), 21<sup>st</sup> June ( $N=172$ ), 7<sup>th</sup> August ( $N=218$ ), 21<sup>st</sup> September ( $N=264$ ) and 5<sup>th</sup> November ( $N=309$ ).

## 6. Numerical results and discussion

Analysis for the produced daily energy  $E$ , comprised area of the land and the surface efficiency of the land  $Eff$  for the reference day - the shortest day (21<sup>st</sup> December) is presented in the table 4.1.

**Table 4.1 Calculation of reference parameters: the distance between the columns  $ref\_rx$ , the distance between rows  $ref\_ry$ , comprised area of the land  $Sref$ , daily energy  $Eref$  and efficiency of the land  $Eff\_ref$  for 21 December (N=355).**

$L$ (°)	$ref\_rx$ (m)	$ref\_ry$ (m)	$Sref$ (m <sup>2</sup> )	$Eref$ (kWh)	$Eff\_ref$ (kWh/m <sup>2</sup> )
0	3,1	0,3	46,871	12,119	0,259
5	3,3	0,5	50,91	11,877	0,233
10	3,4	0,7	53,693	11,505	0,214
15	3,5	0,9	56,236	11,291	0,201
20	3,4	1,1	56,244	10,852	0,193
25	3,7	1,5	64,769	10,97	0,169
30	4,1	1,9	74,949	10,589	0,141
35	4,2	2,4	83,607	9,943	0,119
40	4,6	3,1	101,953	9,191	0,09
45	5,1	4	128,874	8,305	0,064
50	6,1	5,6	190,853	7,045	0,037
55	6,9	8	284,571	5,578	0,02
60	9,1	11,9	515,463	3,886	0,008
65	9,4	29,9	1305,15	1,805	0,001

According to table 4.1, the following parameters are calculated for the reference day (21<sup>st</sup> December): The distances between the columns  $ref\_rx$  and the rows  $ref\_ry$ , the comprised area of the land  $Sref$ , the daily energy  $Eref$  and the surface efficiency of the land  $Eff\_ref$ .

After calculating the reference and optimal distances between the panels of the defined photovoltaic plant, the annual energy  $GE$  is calculated for each obtained distance pair: reference distances ( $ref\_rx$ ;  $ref\_ry$ ), optimal distances ( $opt\_rx$ ,  $opt\_ry$ ) for each latitude from the range ( $0^\circ \sim 65^\circ$ ) respectively, as well as surface efficiency of the land  $Eff$ , with daily setting of the angle of inclination  $\beta$  on the optimal obtained angle  $\beta_{opt}$ .

Based on performed analysis, optimal distances ( $opt\_rx$ ;  $opt\_ry$ ), lowest energy loss  $\Delta GE$  and increased surface efficiency of the occupied land  $Eff$  are obtained in relation of the reference parameters. Conclusions about the optimal distances for a given value of the latitude with optimal placement of the panels and results provided from the calculated values for optimal distances ( $opt\_rx$ ;  $opt\_ry$ ) for each geographic latitude from the range ( $0^\circ \sim 65^\circ$ ) are given in table 4.2.

For all tested dates (corresponding optimal distances) and daily tracking of the  $\beta_{opt}$  angle of inclination of the photovoltaic panels, the annual energies  $GE$  for each latitude of the interval ( $0^\circ \sim 65^\circ$ ) are calculated. From the comparative analysis with the annual energies, it can be concluded that the relative change of the energy  $\Delta GE$  obtained at optimal distances, in

relation to the reference distances, changes and increases with the increase of the latitudes in the range from 1.27% to 15.2% for latitudes ( $0^{\circ} \sim 65^{\circ}$ ).

**Table 4.2 The values of optimal distances for the given value of the latitude at the optimal placement of the panels**

<i>L</i> (°)	<i>opt_rx</i> (m)	<i>opt_ry</i> (m)	<i>GE</i> (MWh)	<i>Eff</i> (MWh/m <sup>2</sup> )	$\Delta GE$ (%)
0	0	0	3,962	0,268	1,27
5	0	0,1	4,005	0,26	1,38
10	0	0,2	4,027	0,252	1,54
15	0	0,2	4,006	0,251	2,17
20	0	0,4	3,997	0,233	2,13
25	0	0,5	4,074	0,229	2,72
30	0	1,4	4,094	0,177	0,9
35	0	1,4	3,99	0,172	1,65
40	0	1,4	3,862	0,167	2,57
45	0	1,3	3,695	0,164	3,9
50	0	0,9	3,458	0,172	6,44
55	0	0	3,019	0,205	13,87
60	0	0	2,789	0,189	14,60
65	0	0	2,515	0,17	15,32

## Conclusion

The comparative analysis is performed with daily tracking of the angle of inclination  $\beta_{opt}$  of the photovoltaic panels, during which, a protocol is implemented, according to which the analysis of the values obtained on the daily energies is performed. According to the protocol, distances ( $max_{rx}$ ;  $max_{ry}$ ) are determined, during which the maximum daily energy  $E_{max}$  is obtained and the occupied land area  $S_{max}$ . These parameters apply when shading is negligible or completely avoided. In relation to the reference day, certain optimal distances ( $opt_{rx}$ ;  $opt_{ry}$ ) are determined, at which energy  $E_{opt}$  is obtained approximately equal to the reference energy  $E_{ref}$ , and the area of the covered land area is  $S_{opt}$ . The ratio between the reference area of the plot  $S_{ref}$  and the optimal area  $S_{opt}$  on it, defines the efficiency of the given land area. Based on the comparative analysis of the reference day, it can be concluded that the distances between the photovoltaic panels  $r_x$  and  $r_y$  and the optimal angle of inclination  $\beta_{opt}$  affects the change in the efficiency of the occupied land. The results show that the optimal parameters i.e., the optimal distances ( $opt_{rx}$ ;  $opt_{ry}$ ) are relative and depend on the selected reference date. If another date is chosen as the reference date or a higher reference energy is set, then the optimal distances in relation to that reference date will be greater than the distances obtained for December 21.

After the energy analyzes are made by days, it is determined that by allowing shading, there is reduction in the production electric energy on the plant and the average efficiency of photovoltaic panels is decreased, but at the expense of the efficiency of the used land containing the photovoltaic panels, which is increased many times.

Based on the obtained values for the annual energies  $GE$  and the change of the annual energy  $\Delta GE$ , recommendations are given for optimal placement of the photovoltaic panels in the grid, considering the latitude range, according to the most favorable day from the tested dates. One such example is Table 4.2 which gives the optimal distances by latitudes that results from the conducted comparative analysis for the reference day, December 21st.

After the optimization, the efficiency of the given land area is significantly increased, at the expense of the reduced annual electricity production, which means the existing site maximized for the reference date can accommodate many more panels (multiple 3x3 photovoltaic plants) on its surface.

## References

- [1] J. A. Duffie, W. A. Beckman, “*Solar Engineering of Thermal Processes, Fourth Edition*”, John Wiley and Sons, 2013.
- [2] T. Demsar, “Optimisation of quantity of electric energy from solar power plant regarding its layout”, University of Ljubljana, Master Thesis, 2015.
- [3] H. Spasevska “Solar energy in Macedonia: policy, perspectives and challenges for application”, *Proceedings of World Renewable Energy Congress- XI*, Abu Dhabi, p-p. 1409-1414, 2010.
- [4] B. Citkuseva Dimitrovska, R. Golubovski, H. Spasevska, J. Veta Buralieva, “Computational methodology in determining shading among photovoltaic panels”, *Balkan Journal of Applied Mathematics and Informatics (BJAMI)*, 4(1). Pp 41-50. ISSN 2545-4803, 2021.
- [5] B. Citkuseva Dimitrovska, M. Cepin, R. Golubovski, H. Spasevska, “Modeling photovoltaic grid inter-shading”, *Thermal Science*, May 2020.
- [6] Soteris A. Kalogirou, “*Solar Energy Engineering Process and Systems*”, Elsevier, 2009
- [7] C. Stanciu, D. Stanciu, “Optimum tilt angle for flat plate collectors all over the World—A declination dependence formula and comparisons for three solar radiation models”, *Energy Conversion and Management*, Elsevier, Volume 81, pages 133-143, 2014.
- [8] A. K. Yadav, S. S. Chandel, “Tilt angle optimization to maximize incident solar radiation: A review”, *Renewable and Sustainable Energy Reviews*, Elsevier, Volume 23(C), pages 503-513, 2013.
- [9] D. Stanciu, C. Stanciui, I. Paraschiv, “Mathematical links between optimum solar collector tilts in isotropic sky for intercepting maximum solar irradiance”, *Journal of Atmospheric and Solar – Terrestrial Physics*, Volume 137, Pages 58-65, Elsevier, 2015.
- [10] M. P. Mitkovic, J. P. Djekic, M. Z. Igic, P. B. Mitkovic, M. M. Dinic Brankovic, “Analysis of Electric power production in South Serbia: Recommendations for improvement of Operation of First Mini Photovoltaic Power Plants”, *Thermal Science*, Volume 22, Pages 1205-1216, 2018.





## PROGRESS OF NO-INSULATION HTS MAGNET DEVELOPMENT TOWARDS ULTRA-HIGH MAGNETIC FIELD GENERATION

*Takanobu Mato<sup>1</sup>, Syumpei Mori<sup>1</sup>, So Noguchi<sup>1</sup>*

<sup>1</sup>Graduate School of Information Science and Technology, Hokkaido University, email: [mato@em.hokudai.ac.jp](mailto:mato@em.hokudai.ac.jp)

### Abstract

*In this paper, we present the progress of the development of a No-Insulation (NI) winding technique. The NI technique is recognized as a technology necessary for the ultra-high magnetic field generation, because the NI technology drastically improves the thermal stability of High Temperature Superconducting (HTS) magnets. Many researchers have presented several types of the NI coils, such as Metal-as-Insulation (MI), Conductive-Epoxy-Resin-Covered (CERC), and intra-Layer No-Insulation (LNI) coils. However, the thermal stabilities of these coils are not clarified nor compared. Hence, in this paper, we systematically investigate the thermal stabilities and conduct the thermal stability comparison among these coils.*

### Key words

*HTS magnets, No-insulation winding technique, thermal-stability, ultra-high field.*

### Introduction

High Temperature Superconducting (HTS) magnets have a potential to revolutionize high field applications; such as Magnetic Resonance Imaging (MRI) **Error! Reference source not found.**, Nuclear Magnetic Resonance (NMR) **Error! Reference source not found.**, and particle accelerators **Error! Reference source not found.** Rare-Earth Barium Copper Oxide (REBCO) coated conductor, which is one promising high temperature superconducting wire, has the higher critical current and critical magnetic field than other superconductors.

In general, superconducting magnets have any electrical insulation between turns and layers. One well problem of turn-insulated REBCO coils is a high possibility to be burned-out or mechanically damaged at an event of “quench” **Error! Reference source not found.** However, in 2011, a breakthrough winding technique has been proposed, which is called No-Insulation (NI) winding technique **Error! Reference source not found.** The NI winding technique dramatically improves the thermal stability of REBCO pancake coils, because the operating currents can bypass a local hot spot through turn-to-turn contacts to reduce Joule heating. At National High Magnetic Field Laboratory of US, on 2017, an NI REBCO pancake coil showed its great potential by generating a world-record highest DC magnetic field of 45.5 T **Error! Reference source not found.**

Towards higher magnetic field generation, the thermal stability improvement is more important. To date, many researchers have proposed several different types of the NI winding technology, such as Metal-as-Insulation (MI) **Error! Reference source not found.**, Conductive-Epoxy-Resin-Covered **Error! Reference source not found.**, and intra-Layer No-Insulation (LNI) **Error! Reference source not found.** These coils are simply categorized into two groups from the viewpoint of the electrical equivalent circuit: 1) *conventional-based NI* including conventional NI and MI and 2) *supplementary-based NI (SNI-)* including CERC and LNI. For the conventional-based NI REBCO coils, the thermal stability has been well investigated in experiments and simulations. Meanwhile, for the SNI REBCO coils, the thermal stability has not been investigated well, although the different thermal stabilities and electrical behaviors have been reported **Error! Reference source not found.** Towards further i

improvements in thermal stability, it is necessary to clarify the thermal stability dependence on the characteristic parameters of SNI REBCO coils. In this paper, we investigated the thermal stabilities of SNI HTS coils systematically in simulations. The simulation results are compared with that of the conventional-based NI REBCO coils.

## 1. Electrical equivalent circuit of conventional-based NI REBCO coils

Fig. 1 shows the schematic view of the conventional NI and the MI REBCO pancake coils, which are categorized to the conventional-based NI REBCO pancake coils. In the case of the conventional NI REBCO pancake coil, an insulator between turns is removed. In a normal operation, the operating current flows through a REBCO layer in the circumferential direction without electrical resistance, because the turn-to-turn contact resistance is much higher than the superconducting zero resistance. When a local hot spot appears, the current escapes into the radial direction to reduce the Joule heating, as shown in Fig. 1 (a). If a current keeps passing through a normal-transitioned REBCO layer, a REBCO pancake coil would be burned out due to its high electrical resistance. For the MI REBCO pancake coils, although the REBCO tape is cowound with stainless steel tapes, a current can also bypass a local hot spot as shown in Fig. 1 (b). The current shortcut-paths of NI and MI REBCO pancake coils are identical despite their different structures.

The electrical equivalent circuit of the conventional-based NI REBCO pancake coils are shown in Fig. 2 [8]. The azimuthally directional elements are composed of the inductance  $L$ , the REBCO layer resistance  $R_{re}$ , and the copper matrix resistance  $R_{mt}$ . The REBCO layer resistance  $R_{re}$  exhibits a strong nonlinearity and the calculation model given in [13] is adopted. The radially directional element consisting of the radial turn-to-turn contact resistance  $R_r$  is connected in parallel to the azimuthally directional elements. It is well known that the radially directional turn-to-turn contact resistance characterizes the thermal stability of the conventional

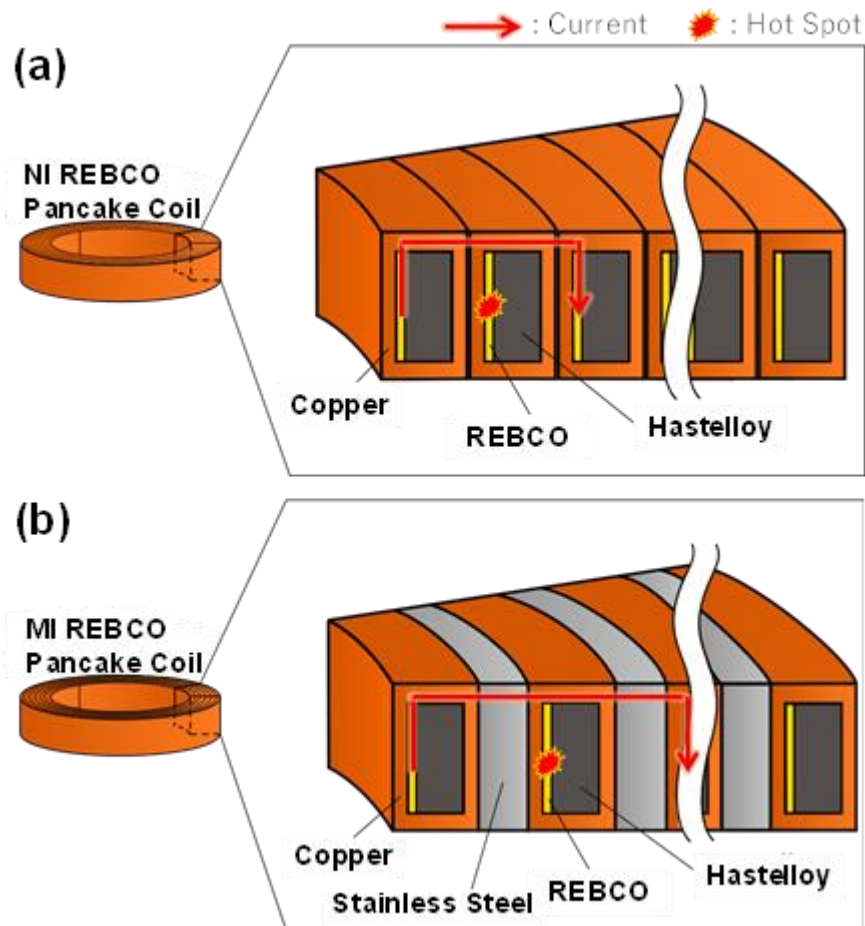


Fig. 1 Schematic views of (a) NI REBCO pancake coil and (b) MI REBCO pancake coil.

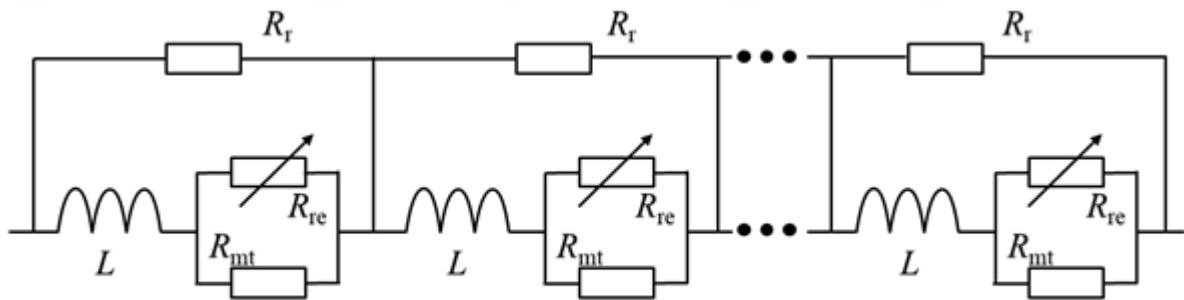


Fig. 2 Electrical equivalent circuit of conventional-based NI REBCO pancake coils. Radial turn-to-turn contact resistance  $R_r$  determines thermal characteristics.

NI REBCO pancake coil **Error! Reference source not found..** It is noted that each coil turn is modeled as an element circuit of Fig. 2.

## 2. Electrical equivalent circuit of SNI REBCO coils

The schematic views of the LNI and the CERC REBCO pancake coils are shown in Fig. 3. The LNI REBCO coil, as shown in Fig. 3 (a), is composed of a solenoid coil embedding supplementary copper sheets and insulators between layers. For the CERC REBCO pancake coil, the REBCO coated conductor is wound with insulator, and conductive epoxy is coated onto the top surface as a supplementary conductor. These coils are categorized into SNI REBCO coils, based on its bypassing current paths. For instance, in the case of the CERC REBCO pancake coil, a bypassing current flows into conductive epoxy when a local hot spot appears, and the bypassing current flows back into the adjacent turn.

Fig. 4 shows the electrical equivalent circuit for the supplementary-based NI coils. The azimuthal elements are the same as these of the conventional NI coils. The radially directional elements, which are connected in parallel to the azimuthal elements, represent the

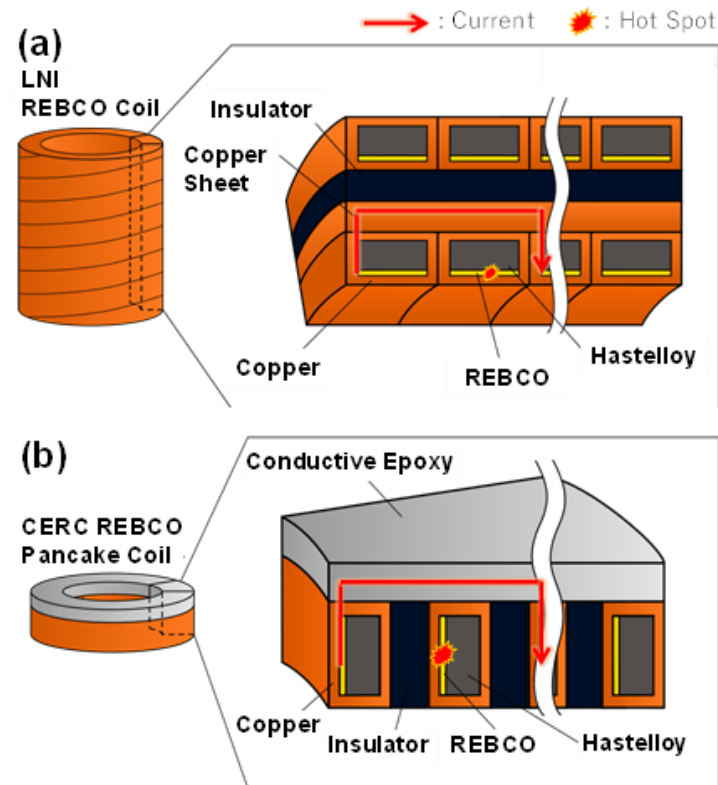


Fig. 3 Schematic views of (a) LNI REBCO coil and (b) CERC REBCO pancake coil

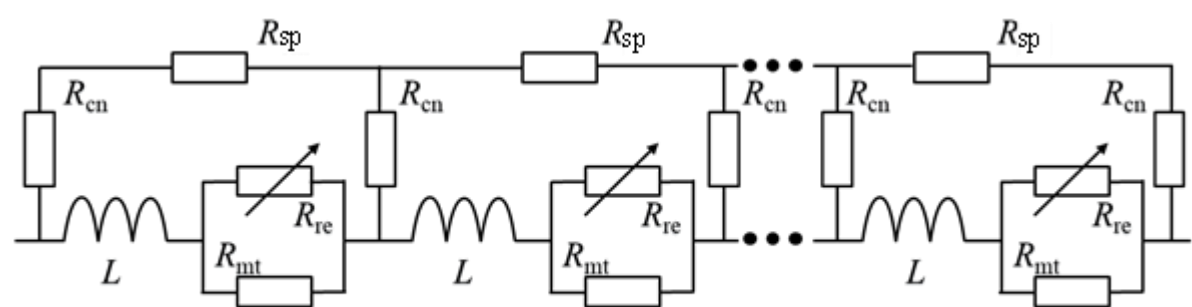


Fig. 4 Electrical Equivalent Circuit of Supplementary-Based NI REBCO Coils. Each Coil Turn Is Modeled as an Element Circuit.

supplementary conductor resistance  $R_{sp}$ . The supplementary conductor resistance is obtained based on the volume and resistivity of the supplementary conductor such as copper and conductive epoxy. The contact resistance  $R_{cn}$  between the REBCO coated conductor and the supplementary conductor is also modeled based on the contact area. The supplementary conductor resistance and the turn-to-turn contact resistance are the parameters to characterize the thermal stability of the SNI REBCO coils.

From the equivalent circuit, the electrical behavior is easily simulated. The heat diffusion along the radial direction is also simulated with a finite element method to correctly grasp the quench phenomenon. In this simulation, the heat generation on the contact surface between the supplementary conductor and the REBCO coated conductor is assumed to be equivalently divided to the supplementary conductor and the REBCO coated conductor.

### 3. Simulation Results

To compare the thermal stability of the conventional NI and the CERC REBCO pancake coils, the temperature rise was investigated when whole one turn of the REBCO coils turns from superconducting to normal state at  $t = 0$ . The simulation conditions are listed in Table 1.

Fig. 5 shows the temperature rise in 2 s after the occurrence of the local normal state transition. The nonlinear dependence of the temperature rise against the different supplementary conductor resistances is depicted (red, blue and green line). The high supplementary conductor resistance or contact resistance results in high temperature rise. Whereas, in the case of the conventional-based NI REBCO pancake coils (black line), the temperature linearly rises with the turn-to-turn contact resistance. It is noted that the temperature rise of the SNI REBCO coil in the dashed red-circle is lower than that of the conventional NI REBCO pancake coil. That is, the SNI REBCO coils with sufficiently small contact resistance are thermally more stable than the NI REBCO pancake coils.

The actual resistances gained in experiences are also plotted in Fig. 5, for the conventional NI [14], the MI [5], the LNI [12], and the CERC coils [6]. The high temperature rises of the CERC and the LNI REBCO pancake coils are observed. Whereas the temperature rise of the conventional NI REBCO pancake coils is much smaller than the others. Thus, the thermally most stable coil is the conventional NI REBCO pancake coil. To achieve the development of

**Table 1 Tape and Coil Conditions and Operating Conditions**

Parameters	Values
<b>REBCO coated conductor</b>	
Tape width [mm]	4.1
Tape thickness [mm]	0.15
Copper matrix thickness (each side) [ $\mu\text{m}$ ]	20
REBCO layer thickness [ $\mu\text{m}$ ]	2.0
Critical current at 77 K, self-field [A]	140
<b>Pancake coil</b>	
Inner and outer diameters [mm]	100; 136
Number of turns [-]	100
(MI, CERC) Insulator thickness [ $\mu\text{m}$ ]	30
(CERC) Conductive epoxy thickness [mm]	1.0
(LNI) Copper sheet thickness [ $\mu\text{m}$ ]	7.0
Supplementary conductor resistivity [ $\Omega\text{m}$ ]	variable
Contact resistivity [ $\Omega\text{m}^2$ ]	variable
<b>Operating conditions</b>	
Operating temperature [K]	50
Operating current [A]	300
Turn number of turning to normal state [-]	50th (middle turn)



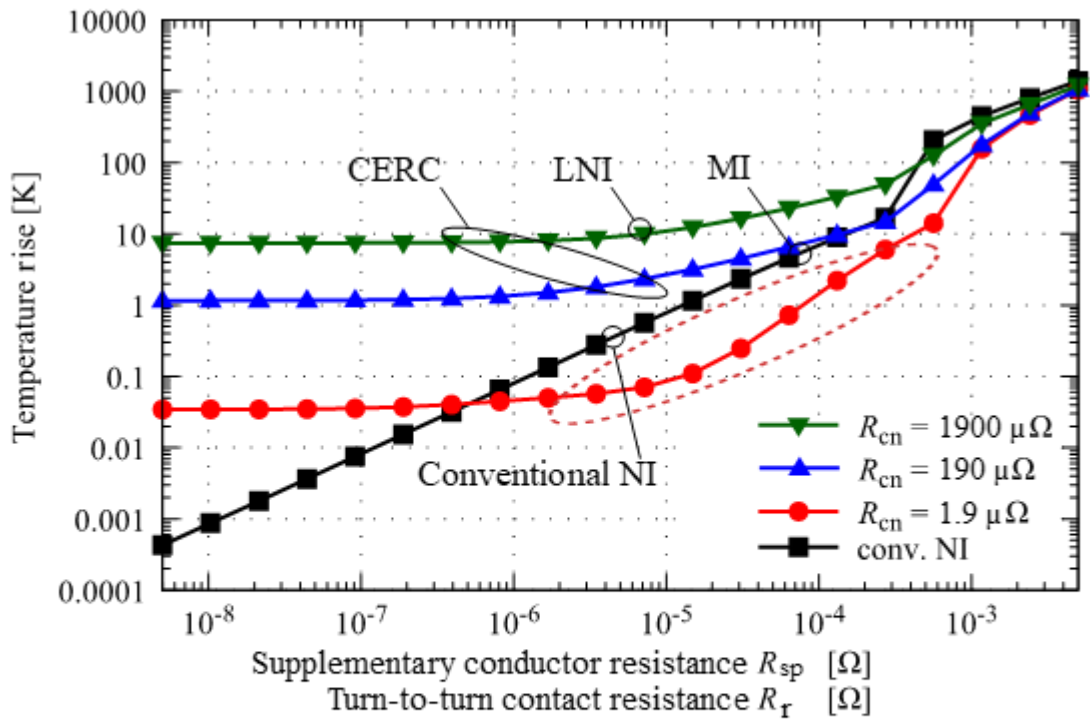


**Fig. 5** Temperature rise in 2 s after local normal state appearance as function of supplementary conductor  $R_{sp}$  or turn-to-turn contact resistance  $R_r$ . Red, blue and green line shows in case SNI REBCO coils for different contact resistance, and black line shows conventional-based NI REBCO pancake coils.

thermally more stable NI REBCO coils for ultra-high magnetic field generation, the important task is to decrease the contact resistance.

## Conclusions

In this paper, we investigated the thermal stability of several No-Insulation (NI) Rare-Earth Barium Copper Oxide (REBCO) coils, such as the conventional NI [1], the Metal-as-Insulation [5], the intra-Layer NI (LNI) REBCO [12], and the Conductive-Epoxy-Resin-Covered (CERC) REBCO coil [6]. We modeled the electrical equivalent circuit of these coils and categorized them based on the equivalent circuit; 1) the conventional-based NI for the conventional NI and the MI REBCO coils, and 2) the supplementary-based NI (SNI) for the CERC and the LNI REBCO coils. The thermal stability dependences on the supplementary conductor resistance and the contact resistance together with the radial turn-to-turn contact resistance are systematically investigated. As the result, the SNI REBCO coil exhibits the nonlinear thermal stability, whereas the conventional-based NI REBCO pancake coil shows linear dependence. Also, it is found that the SNI REBCO coils are thermally more stable than the conventional-based NI REBCO pancake coils when the contact resistance is sufficiently small. The thermal stability comparison among the four types of NI REBCO coils was also conducted. The conventional NI REBCO pancake coils are the best in the thermal point of view. However, the CERC and the LNI REBCO coils are thermally unstable due to their large contact resistivity, compared to the conventional NI REBCO pancake coil. A technology to reduce the contact resistivity is required.



## References

- [1] Hahn, Seungyong et al.: “HTS pancake coils without turn-to-turn insulation,” *IEEE Trans. Appl. Supercond.* 21(3), 2011, pp. 1592–1595.
- [2] Hahn, Seungyong et al.: “45.5-tesla direct-current magnetic field generated with a high-temperature superconducting magnet”. *Nature*, 570, 2019, pp. 496-499.
- [3] Katsumata, Kazuki et al.: “Influence of the turn-to-turn contact electrical resistance on the thermal stability in meter-class No-Insulation REBCO pancake coils during a local normal-state transition”. *IEEE Trans. Appl. Supercond.* 27(4), 2017, Art. no. 4602005.
- [4] Kim, Kwang Lok et al.: “400-MHz/60-mm All-REBCO nuclear magnetic resonance magnet: magnet design”. *IEEE Trans. Appl. Supercond.* 26(4), 2016, Art. no. 4302604.
- [5] Lécresse, Thibault / Iwasa, Yukikazu: “A (RE)BCO pancake winding with metal-as-insulation”. *IEEE Trans. Appl. Supercond.* 26(3), 2016, Art. no. 4700405.
- [6] Mato, Takanobu / Noguchi, So: “Sudden discharging and overcurrent simulations of REBCO coils coated with conductive epoxy resin”. *IEEE Trans. Appl. Supercond.* 31(5), 2021, Art. no. 4600705.
- [7] Miyazaki, Hiroshi et al.: “Over-current test of REBCO pancake coils impregnated with electrically conductive epoxy resin under conduction-cooled conditions”. *IEEE Trans. Appl. Supercond.* 29(5), 2019, Art. no. 4602805.
- [8] Noguchi, So: “Electromagnetic, Thermal, and mechanical quench simulation of NI REBCO pancake coils for high magnetic field generation”. *IEEE Trans. Appl. Supercond.* 29(5), 2019, Art. no. 4602607.
- [9] Paasi, Jaakko et al.: “Stability and quench of a HTS magnet with a hot spot”. *Supercond. Sci. Technol.* 13(7), 2000, pp. 949-954.
- [10] Parkinson, Ben: “Design considerations and experimental results for MRI systems using HTS magnets”. *Supercond. Sci. Technol.* 30(1), 2016, Art. no. 014009.
- [11] Rossi, Lucio et al.: “The EuCARD2 future magnets program for particle accelerator high-field dipoles: review of results and next steps”. *IEEE Trans. Appl. Supercond.* 28(3), 2018, Art. no. 4001810.
- [12] Suetomi, Yu et al.: “A novel winding method for a no-insulation layer-wound REBCO coil to provide a short magnetic field delay and self-protect characteristics”. *Supercond. Sci. Technol.* 32(4), 2019, Art. no. 045003.
- [13] Ueda, Hiroshi et al.: “Numerical simulation on magnetic field generated by screening current in 10-T-Class REBCO coil”. *IEEE Trans. Appl. Supercond.* 26(4), 2016, Art. no. 4701205.
- [14] Wang, Xudong et al.: “Turn-to-turn contact characteristics for an equivalent circuit model of no-insulation ReBCO pancake coil”. *Supercond. Sci. Technol.* 26(3), 2013, Art. no. 035012.



## GRID-CONNECTED HYBRID PV SYSTEM WITH BATTERY STORAGE

*Aleksandar Bogatinov<sup>1</sup>, Vlatko Chingoski<sup>2</sup>*

<sup>1</sup>Faculty of Electrical Engineering, University "Goce Delcev" Shtip, Macedonia,  
*aleksandar.20548@student.ugd.edu.mk*

<sup>2</sup>Faculty of Electrical Engineering, University "Goce Delcev" Shtip, Macedonia, *vlatko.cingoski@ugd.edu.mk*

### Abstract

*Photovoltaic systems (PV) are an integrated set of photovoltaic modules with all the necessary components that are dimensioned to receive solar energy and convert it into electricity that would be adequately powered by some DC and/or AC consumers. Depending on how they work, photovoltaic systems can be divided into stand-alone PV systems (off-grid), grid-tied PV systems connected to the electricity distribution network (on-grid), and hybrid PV systems as a combination of the previous two systems.*

*In this paper, we will consider the operation of a hybrid grid-connected PV system with battery storage which transforms solar energy into electricity and allows the storage of excess generated electricity in the batteries. Additionally, this system provides, if needed, the excess generated electricity to be delivered directly to the power grid. The proposed hybrid system could optimize all three energy sources PV modules, batteries, and power grid, and continuously deliver quality power to connected consumers. Properly sized and controlled hybrid PV systems significantly increase the use of so-called green energy from renewable energy sources and increase the independence and continuous power supply of the consumers.*

**Keywords:** *renewable energy sources, PV systems, inverters, batteries, hybrid systems*

### Introduction

The energy potential of the Sun as a renewable energy source is very large and the use of solar energy can be realized by converting it into heat and electricity. Solar energy can be converted into electricity in many ways, but the simplest way is that one with photovoltaic (solar) cells which is based on the photovoltaic effect. Converting solar energy into electricity using properly sized photovoltaic systems not only provides economically viable and overtime free electricity, but it also protects the environment from the pollution that accompanies the production of electricity from conventional energy sources, reduces CO<sub>2</sub> emissions into the environment which is one of the benefits of using solar energy.

The *photovoltaic effect* (PV) is a quantum-mechanical process wherein photovoltaic cells the energy of solar radiation is converted into electricity, or more precisely, it is the occurrence of the creation of voltage or adequate electricity in a semiconductor material, usual silicon with appropriate impurities added to its atoms, under its exposure to light-photons as the smallest carriers of solar energy packets.

PV cells are made with a certain technological procedure where a very thin layer of *n*-type semiconductor is applied to a *p*-type semiconductor and thus creating a so-called *pn*-junction with a shape that allows light to fall spatially on a larger surface and with the help of the photovoltaic effect produces electricity.

PV systems are systems designed to receive solar energy and convert it into electricity in a form that can be used by consumers, sent to the distribution network, or stored in appropriate power batteries and used when the need for energy arises, usually when the solar radiation is reduced, at night or due to problems with the electricity distribution. For a PV system to function flawlessly, it needs to be properly selected, sized, and integrated. The basic components of a photovoltaic system are the PV *module* (as a system of PV cells), the *inverter*, and the *batteries*.

The PV cell is a major part of the photovoltaic system. The output power of a cell is quite small; therefore several cells are properly connected in modules to provide adequate usable output power. Photovoltaic cells in the module can be connected in series or parallel. In practice, cells are connected in series because the serial connection of the cells increases the magnitude of the module voltage, and the current through them remains the same.

The PV module as a system of interconnected PV cells can further be used as a stand-alone or connected in a system with other modules with the same characteristics with the main task of the module converting solar energy into electricity. Multiple modules mounted on a common load-bearing structure constitute a PV *panel*. The panels can further be properly connected in an array or grid. The array can be consisting of one to several thousand modules, depending on the required output power, making a PV power plant. For the modules to give optimal results in converting solar energy into electricity, they are usually connected in series, facing south at a certain angle that corresponds to the local latitude. It is recommended that during the day there is no shading on the modules, the length of the so-called sundial at that location is maximum and there is good ventilation under and around the panels to avoid major overheating while exposed to the sun. The most practical application is monocrystalline and polycrystalline modules that are characterized by high durability of about 25 years.

In addition to the PV modules when dimensioning a photovoltaic system, *inverters* are also of great importance. These two components, PV modules, and inverters are crucial for the optimal functionality and the cost of a PV generation project. They constitute 70% of the total investment costs of the PV system. The inverter is the most exploited part of a PV system, and its main function is to convert direct current into alternating current, as well as to maintain appropriate power, to control the quality of electricity production (e.g. voltage and frequency) that is delivered to the grid, and for communication with the power network.

Several types of inverters differ in how they are connected to the system and are responsible for the efficiency of the system:

- central inverters (for the whole system),
- string inverters,
- micro-inverters,
- hybrid inverters, etc.

Each of these four types has its advantages and disadvantages. Which type will be chosen depends on the type of system and compatibility with other components of the PV system, as well as on several other factors such as site temperature, product safety, sustainability, altitude, servicing, and total costs. To ensure optimal efficiency and durability of the system, proper sizing is very important, and therefore when choosing an inverter the ratio between the power

of the photovoltaic system and the power of the inverter should be 1: 1, it should be adjusted to the operating parameters of the module. If the inverter is overloaded, the results could be power loss and premature aging of the devices.

In addition to PV modules and inverters, more and more systems use *batteries* as an additional source of energy according to the needs of the system, especially in areas where there is an unstable electrical network or stand-alone systems. Properly sized and connected batteries form a battery energy storage system (battery bank) which provides power storage and improves the reliability in systems that require more power. Also, they provide better energy stability of its network and savings of clean energy that will be stored during the day and will be used in the evening or case of power outages. Batteries are a good investment especially in systems that produce more energy than they can consume; however, utilization of batteries means higher investment costs and therefore the batteries should be well-chosen according to their capacity and quality and according to the real needs and expectations of the system. Installing batteries within the system can be a great way to get the most out of photovoltaic modules. There are many different types of batteries on the market, however, lead-acid and lithium-ion batteries are mostly used to store energy generated by photovoltaic systems [1], [2], [3], [4].

### 1. Types of photovoltaic systems

PV systems are an integrated set of photovoltaic modules with all the necessary components that are dimensioned so that they can receive solar energy and convert it into electricity that would be adequately powered by several DC or AC consumers.

Depending on how they work, PV systems can be divided into:

- **Stand-alone PV systems** (autonomous or Off-Grid PV systems),
- **Grid-tied PV systems**, (PV systems connected to the electricity distribution network or On-Grid PV systems), and
- **Hybrid PV systems** (PV systems that are a combination of the previous two systems).

#### Stand-alone (autonomous) PV systems (Off-Grid)

Stand-alone PV systems are systems that are not connected to the power grid, thus operate separated from the electricity distribution network. In these systems, the production and consumption of electricity the system should be well-balanced because the production of energy depends on weather conditions. These systems usually require an additional battery system for energy storage that can be used at night or during bad weather. The charge controller takes care of the proper charging and discharging of the battery, and the inverter enables the use of the produced energy in standard household appliances with standard electrical installation. Such systems are suitable for powering isolated and lonely buildings, for example in rural areas, locations far from the electrical grid where connection to the grid is very expensive, as well as for individual buildings where there is no electrical grid such as remote buildings for signaling, warnings, telecommunication transmitters, lighthouses, systems for monitoring, etc.

Advantages of these stand-alone networks are that they are energy independent of the distribution network, they can supply even the most remote places for which there is no possibility to connect to the electrical grid, there are no bills for payment of electricity, etc. It is also an advantage that for a start if the energy needs are modest, a smaller system can be dimensioned, which can be later upgraded over time if the need for electricity increases. For larger systems, the system should be well sized from the very beginning to cover 100% of the loads expected in the system. In case of prolonged inconvenience because of the stability of

the power supply, it is advisable to add a generator (running on diesel, gasoline, etc.) as the backup energy generator. It would be switched on when the batteries could not cover all the needs of the consumers of that system. This method may be a better and cheaper choice instead of investing in a huge battery bank that would rarely be fully utilized).

The main disadvantage of this system is that the energy from this system cannot be sent to the grid, thus the whole system cannot be subsidized if there are such incentive programs. Another disadvantage is that this system has more expensive components and thus higher initial costs. Batteries themselves are more expensive and reduce the efficiency of the system because their capacity degrades over time. However, sometimes, despite this higher initial cost, it may be cheaper to go with the installation of a battery bank than to pay a very expensive fee for connecting to a remote power distribution line [1], [3], [4].

### **PV systems connected to the electricity distribution network (On-Grid PV system)**

PV systems connected to the electricity distribution network use the distribution network as a backup power source (virtual battery), or as a consumer for the excess energy generated by PV modules. These systems work interactively and in parallel with the electricity distribution network, and despite the PV modules, additionally, they contain only an inverter. The direct current from the PV modules with the help of an inverter is converted into alternating current and with adjusted voltage through a distribution board and electrical installation supplies the consumers that are supplied in two ways. In periods when the photovoltaic modules produce less power than required, the control device also includes the grid as a backup source, so that the electricity consumption is always satisfied. In periods when the modules produce more than the required electricity, the surplus is taken over by the electrical grid. Overnight consumption by the system (usually home appliances), is provided exclusively by the distribution network. The control device adjusts the operation of the PV modules with variable consumption so that the operating point of the IU characteristic is closest to *the maximum power point* (MPP), to achieve the most efficient operation of the module. This device that enables optimal operation of the system in different operating modes regardless of the intensity of solar radiation or changes in loads is called *the maximum power point tracker* (MPPT). MPPT works on the principle of adjustment on the resistance of the circuit to extract maximum power from the system.

On-grid PV systems are very efficient because they have fewer components and thus the initial investment is lower than stand-alone systems. Another advantage is that by connecting to a distribution network, this network acts in a kind of virtual battery where the excess generated energy can be transferred, or energy can be withdrawn, in case of need of the network system. This system also affects the mitigation of the peak load of the distribution network itself. If there is a subsidy program, the surplus can be sold to the electricity distribution system and some profit can be made. Additionally, the delivered and/or withdrawn energy can be compensated, and thus a smaller electricity bill will be obtained. The transmitted and withdrawn energy from the distribution network is registered and monitored through the two-way energy meters that are installed in the network system.

The disadvantage of the on-grid PV systems is that when the power supply from the electrical grid is disconnected due to some problems in the grid, this system will be turned off at the same time. The inverters are automatically disconnected from the grid and to protect people who try to eliminate the problem of the grid. This means that you cannot have a power supply during a power outage. Thus, in return, you cannot store energy for later use, and you cannot use the energy generated by the photovoltaic system until the problem in the distribution network is overcome and reconnected. This is the so-called anti-islanding protection [1], [3], [4].



## Hybrid photovoltaic system

A hybrid photovoltaic system (HPV) is a system that combines the best of both above-described systems, the stand-alone and grid-tied PV systems. Descriptively speaking, these systems are PV systems with auxiliary (backup) power supply (one or more) or grid-tied PV systems with a battery storage system that provide the uninterrupted continuous power supply.

The HPV battery system connected to the power grid ensures maximum autonomy in terms of power supply. The system uses solar energy at the same time and allows the storage of the excess energy generated in the batteries of the battery energy storage system, except if there is an extra surplus of generated energy that should be delivered to the EE network. The consumers connected to such HPV battery system primarily use the energy generated by the PV modules. In case more energy is required than the energy currently generated by PV modules, this excess energy is provided from the electrical grid and/or from the energy previously stored in the batteries. When the batteries are depleted due to higher demand or when the production of electricity from the PV modules is not sufficient, then the system supplies the load needs with electricity from the electrical distribution network.

This hybrid type of system not only provides greater security in the delivery of the required electricity to consumers, but by being connected to the electrical grid reduces the need for large capacities of the battery system, extends the life of existing batteries, and reduce the costs for battery maintenance and replacements. If due to some technical problems, there are interruptions of power supply from the electrical grid, during sunny hours, the system enters the mode of operation disconnected from the grid. In this case, the loads will demand and receive energy directly from the PV modules. However, if there is a shortage of energy generated by the PV modules, the equilibrium energy will be extracted from the battery system.

As recapitulation, we can see that the hybrid system could be pre-programmed to optimize the three energy sources, the PV modules, batteries, and electrical grid, and to deliver continuous quality power to the consumers. In some hybrid systems that have critical consumers, the system could be programmed to power these critical consumers first, disconnecting the less important ones. Also, for other non-sunny hours, it can be programmed to draw power from either the grid or the battery, as desired, or even by setting a percentage shared supply from both.

The basic parts of this hybrid system are PV modules, hybrid inverter, and batteries (Figure 1).

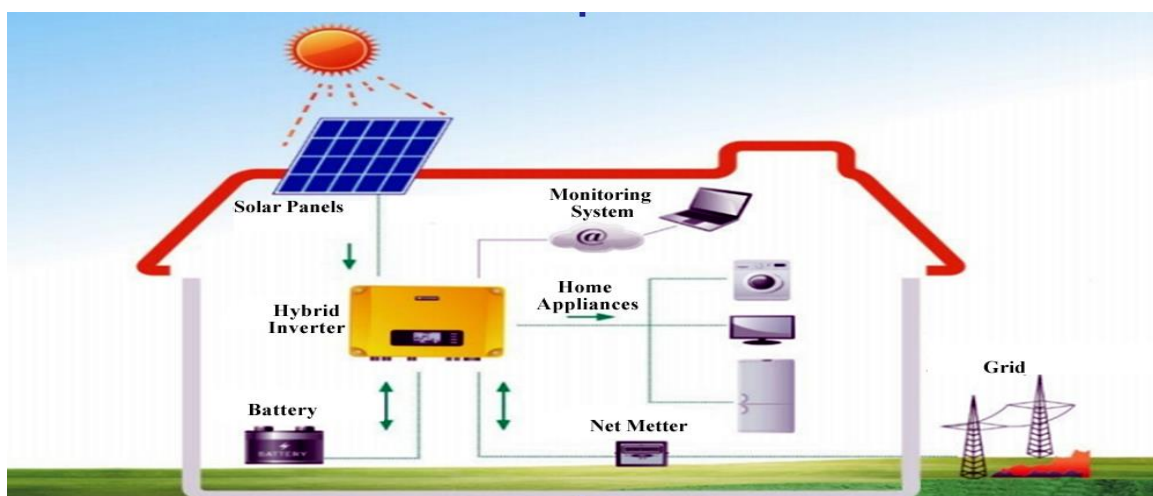


Figure 1. The HPV battery system connected to the power grid.

Nowadays, so-called intelligent hybrid inverters have been used that combine the functions of grid-tied, autonomous inverters, and MPPT controllers. They are real-time programmed to



automatically monitoring and analyzing the supply and demand of energy to their customers and to properly synchronize the energy sources in the system and thus contribute to energy savings. The inverters give priority to the use of solar energy and the electrical grid is used only in case of power shortage, and the use of batteries is somewhere in between, thus extending their lifespan. Most modern hybrid inverters have a built-in battery charger and connector that makes it easy to add batteries in the future. There are also hybrid systems with an integrated or suitable battery.

Some of the advantages of hybrid systems are:

- they are cheaper than stand-alone PV systems, and do not need an additional generator and a large battery backup system,
- they provide storage of excess electricity in the battery system which can later cover energy requirements at peak energy demand,
- they provide greater autonomy and security of electricity supply. During periods of insufficient sunlight (non-sunny days, at night, or when the electrical grid becomes unstable), the system will automatically switch to battery power and continue to operate independently of the grid (usually in just a few seconds),
- they have reduced energy demand from the grid and could deliver the excess energy from the system to the electrical grid which would later be compensated or subsidized accordingly.

The major disadvantages of hybrid systems are:

- higher initial costs from network systems due to battery system installation,
- longer payback period of the initial investments, and
- there might be a limit to how many devices can be started simultaneously depending on the type of hybrid inverter and its capabilities [1], [3], [4].

## **2. Topologies of HPV-battery system connected to the power grid**

The HPV battery system itself could be highly versatile, automated, and programmable, providing possibilities for energy sources and energy consumers to be prioritized and optimized accordingly. As already mentioned, in this system in case the energy generated by the PV modules is not sufficient for the supply of consumers, the differential energy can be drawn from the electrical grid or the batteries as previously programmed. If the grid is available, it can be extracted from it or it can be extracted from the battery if the grid is not available. On other occasions, the system can be programmed to take part of the needed energy from the battery and the rest from the electrical grid. In other words, this is a very versatile and very configurable power generation system.

To better understand the characteristics of such a system we will consider a configuration of a simple HPV battery system with an installed power of 1000 W and connected to the power grid and batteries. In total, eight common cases (topologies) are investigated.



Figure 2. Case #1.

In the first case (Figure 2), we do not have consumers who demand energy, and the entire energy generated from the PV modules in the amount of 1000W is delivered to the electrical grid (as pre-programmed).

Delivered energy to the grid is registered on the bi-directional energy meter.

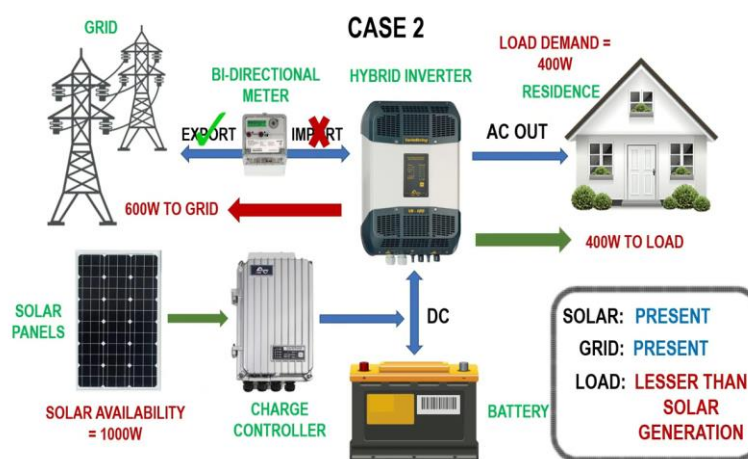


Figure 3. Case #2.

In this case (Figure 3), we have active consumers who demand part of the energy in the amount of 400W generated by the PV modules. Since PV modules generate 1000W, the excess generated energy again is delivered to the electrical grid, however this time in the amount of only the remaining 600W.

Again, delivered energy to the grid is registered on the bi-directional energy meter.

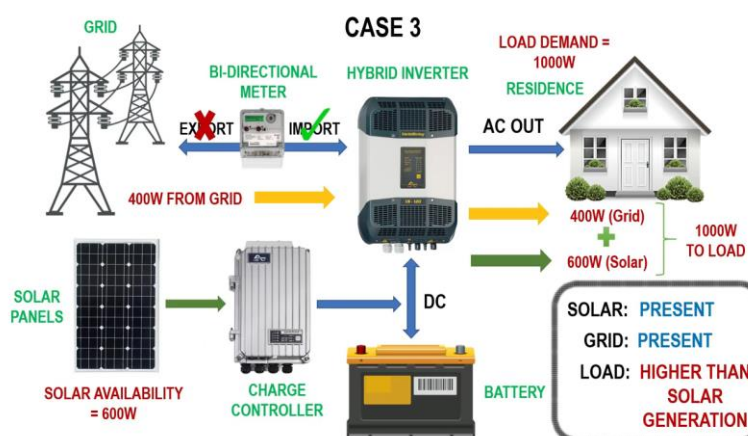


Figure 4. Case #3.

In this case #3 (Figure 4), compared to the previous two cases we have reduced energy production from PV modules, only 600W. Since consumers demand 1000W, more energy than produced by PV modules, the energy disbalance is covered by drawing energy from the electrical grid in the amount of 400W and thus the needs of consumers are met. Again, the bi-directional energy meter is used.

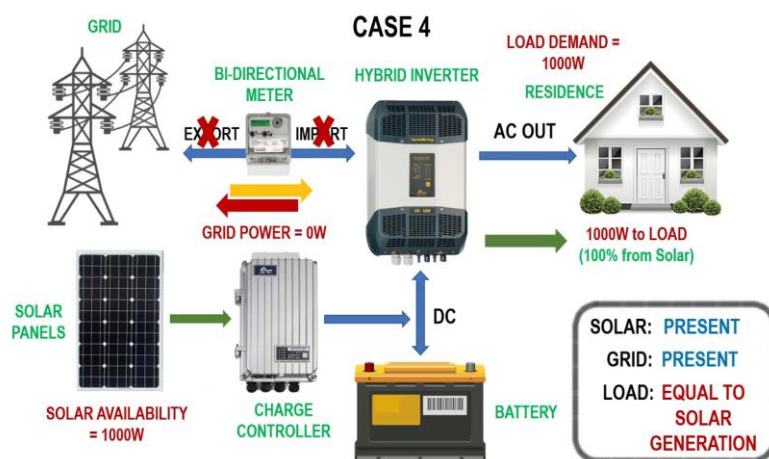


Figure 5. Case #4.

Case #4 (Figure 5) shows a case where the PV modules generate 1000W, and the consumers demand the same amount of energy, 1000W, thus that whole demand energy is completely satisfied with the generated energy from the PV modules. No excess of generated energy exists.

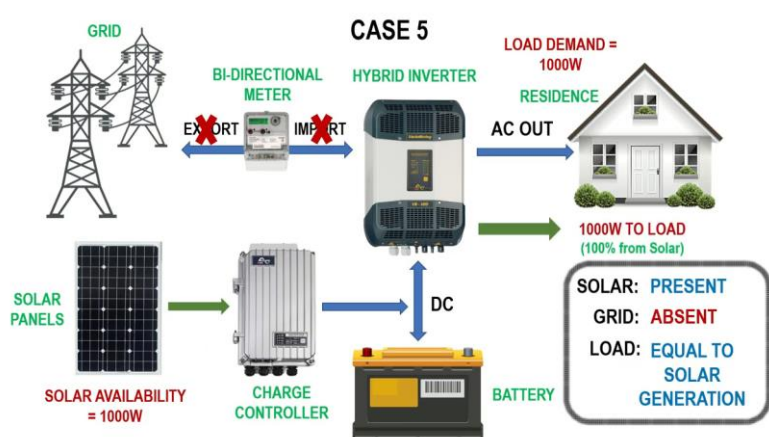


Figure 6. Case #5.

In case #5 (Figure 6), the power supply from the electrical grid due to some technical problems in the grid is fully interrupted, thus the grid in such case is absent. The PV modules generate 1000W, and the consumers' demand hopefully is the same as the PV generation (1000W), thus the existing demand is fully met by the energy from the PV modules.

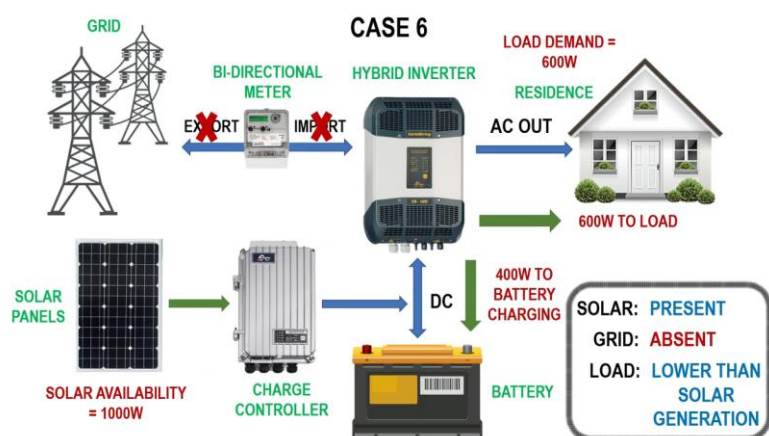


Figure 7. Case #6.

In case #6 (Figure 7) again the power supply from the electrical grid is interrupted due to certain technical reasons, thus the grid is absent. The energy generated by the PV modules (1000W) is partially delivered to meet the needs of consumers which now amounts to 600W and the rest is used to charge the batteries of the battery storage system with the remaining 400W.



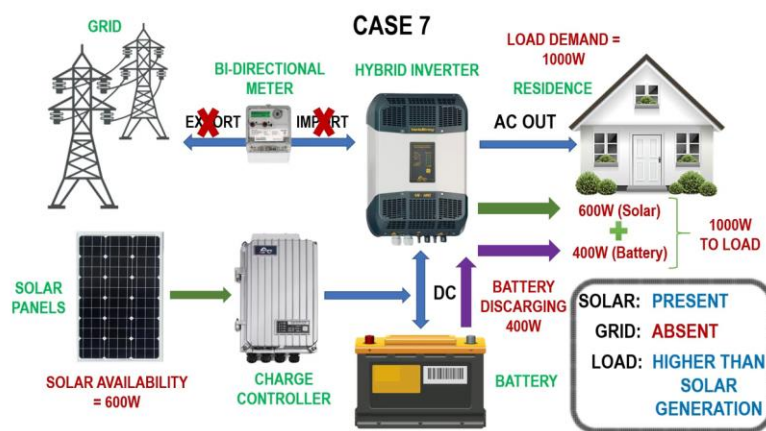


Figure 8. Case #7.

Even in this case #7 (Figure 8), the power supply from the electrical grid is absent, i.e. interrupted due to certain technical reasons. In this case, we have reduced energy production from PV modules (600W), and increased energy demand by the consumers (1000W). The difference in power for consumers will be provided by the battery system (400W).



Figure 9. Case #8.

Finally, in case #8 (Figure 9), the power supply from the electrical grid is interrupted due to some technical problems in it and the PV modules do not generate energy (non-sunny hours or nighttime). In this case, the overall energy demand of the consumers will be covered only and if possible by the energy from the battery system (600W).

These eight cases or topologies of the HPV-battery system gave us a simplified pictorial illustration of how the energy could flow in the HPV system made of „Power Grid – PV modules – Battery – Consumers“ could be pre-programmed to enable reliable and stable power supply under various network and weather conditions [5]. This system also provides bi-directional power measurements between the generation facilities (PV modules), power grid, and the consumers, which from a financial viewpoint could be highly beneficial in case this kind of subsidy is enabled.

## Conclusions

Properly sized and controlled photovoltaic systems significantly can increase the quality of energy supply to the consumers who use the energy from those photovoltaic systems. Such a system is the grid-connected hybrid photovoltaic system with battery storage.

This system compared to the stand-alone and on-grid system provides maximum autonomy in terms of power supply and continuous and quality energy supply to the consumers who use the energy generated by its photovoltaic modules. This system at the same time uses solar energy and allows storage of excess generated energy in the battery energy storage system. In cases when batteries are already fully charged, this excess of generated energy is delivered to the electrical grid for other customers. The hybrid system could be pre-programmed to optimize

the three energy sources, the PV modules, batteries, and power grid network, enabling continuous and reliable delivery of electric power to connected consumers.

During the process of design and sizing of the PV systems, the performance of the system can be predicted through appropriate simulation software. The most important point during this process is to determine the exact geographical location of the location where the photovoltaic modules would be placed.

The computer program HOMER (Hybrid Optimization Model for Electric Renewables) is used to analyze and simulate several variants and select the optimal solution for designing and operating a hybrid power generation system that uses renewable energy sources. Our next planned activity is the simulation of the operation of a hybrid photovoltaic system in real conditions in the HOMER program package.

## References:

- [1] Neel Kamal Saini and Vineet Shekher (2011). Grid Connected Hybrid PV / Battery Distributed System, VSRD International Journal of Electrical, Electronics & Comm. Eng. Vol. 1 (7), 420-428
- [2] Vlatko Cingoski, "Basics of renewable energy sources", lectures, Faculty of Electrical Engineering, University "Goce Delchev", Shtip, 2018.
- [3] <https://www.solarreviews.com/blog>
- [4] <https://www.cleanenergyreviews.info/blog/>
- [5] Topologies of Hybrid Solar PV System, <https://www.youtube.com/watch?v=iWnSV5FCyrg>



## INVESTIGATION ON STABILITY OF PANCAKE COILS WOUND WITH BUNDLED MULTIPLE REBCO CONDUCTORS

**Kazuma Kodaka<sup>1</sup>, So Noguchi<sup>1</sup>**

<sup>1</sup>Graduate School of Information Science and Technology, Hokkaido University, email: [kodaka@em.hokudai.ac.jp](mailto:kodaka@em.hokudai.ac.jp)

### Abstract

REBCO (Rare-Earth Barium Copper Oxide) pancake coils without turn-to-turn insulation, called no-insulation (NI) winding technique, have shown a high thermal stability against normal state transition. REBCO is the 2nd-generation high-temperature superconductor (HTS) with great properties. In recent years, NI REBCO coils have been desired for practical ultra-high magnetic field applications. It has been reported, as an experimental result, that the excitation delay, which is a problem of the conventional NI REBCO pancake coils, is improved by coils wound with multi-bundled REBCO conductor (MB NI REBCO coils). As an operating current may not be evenly distributed in each bundled tape due to the different inductances, the current distribution in MB NI coils is complicated. Therefore, we must clarify the excitation characteristics and the current and thermal stability of MB NI REBCO pancake coils using numerical simulation. We also compared the cases with and without insulation between turns. For a current simulation, an MB NI REBCO coil is modeled using a Partial Element Equivalent Circuit (PEEC) method. From the simulation results, it was confirmed that the excitation delay was improved by a multi-bundled REBCO conductor. Furthermore, we found that the MB NI REBCO coil without turn-to-turn insulation was the most stable because the current could be distributed widely, not concentrated.

### Key words

HTS magnets, No-insulation, thermal-stability, ultra-high field.

### Introduction

2nd-generation (2G) high-temperature superconducting (HTS) magnets can generate very high magnetic fields, because they can carry large currents with small cross-sectional area at extremely low temperatures [1]. 2G HTS magnets are expected to be applied to high field applications; magnetic resonance imaging (MRI), nuclear magnetic resonance (NMR), and particle accelerators. These applications need high magnetic fields for high performances. REBCO (Rare-Earth Barium Copper Oxide) which is 2G HTS has a high critical field and excellent electrical properties. However, conventional REBCO pancake coils have a serious problem against quench protection [2].

To solve this problem, a no-insulation (NI) winding method was proposed by Hahn, *et al.* [3],[4]. It enables to drastically enhance the thermal stability of HTS magnets due to eliminating turn-to-turn insulation and allowing currents to radially bypass a local normal-state region through the turn-to-turn contacts. Also, the NI winding method makes HTS magnets more compact with the higher engineering current density than ever. In these recent years, because of these advantages, NI REBCO pancake coils have been strongly desired for practical ultra-high magnetic field (>30 T) applications.

Although NI REBCO coils have these above-mentioned merits, no turn-to-turn insulation causes a charging delay. This is a major issue for a long time [5],[6]. To overcome this issue, a few different methods have been proposed [7],[8],[9]. One of them is a multi-bundled



REBCO tape winding method, where a pancake coil is wound with multi-bundled REBCO conductors without insulation between bundled tapes. It was reported, as an experimental result, a charging delay was improved because the inductance per one tape of the NI pancake coils wound with multi-bundled REBCO conductors (MB NI REBCO pancake coils) is smaller than that of a conventional NI pancake coils wound with a single REBCO conductor [10]. In addition, the high current density of the MB NI coil is expected. However, as the current behavior of MB NI coil is complicated, the stability has not yet been investigated in detail. For example, an operating current may not be evenly distributed in each bundled tape due to their different inductances. The purpose of this study is to clarify the charging characteristics and the stability of MB NI REBCO pancake coils based on the current and thermal distributions obtained by numerical simulation. We will also compare the cases with and without insulation between turn-to-turn.

## 1. Simulation method

To obtain the detailed current distribution, an MB NI REBCO pancake coil is modeled using a Partial Element Equivalent Circuit (PEEC) method [5]. Since, in the PEEC model, the equivalent circuit is built by dividing the MB NI REBCO coil in the circumferential and radial directions, it is possible to observe the local phenomena inside the coil. The electrical resistance of the REBCO layer is approximated by an  $n$ -index model [11], and the critical current density required for the  $n$ -index model is calculated using approximate equations obtained from experiments. Since the  $n$ -index model involves a strong nonlinearity, the Newton-Raphson method is introduced as a nonlinear solver. The heat generation in each resistance component is computed from the obtained current distribution, and the thermal distribution is obtained using a Finite Element Method (FEM).

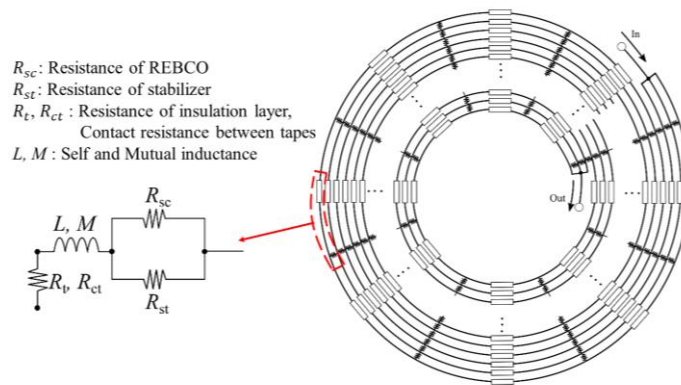


**Fig. 1 PEEC model of MB NI coil (3 tapes bundled).**

## 2. Analysis models

The coil models and the specifications of REBCO tape and coils used in this study are shown in Fig. 2 and Table 1. It is supposed that all the coils are wound with SuperPower 2G-HTS tape wires and the contact resistivity between bundled tapes is  $70 \mu\Omega \cdot \text{cm}^2$  based on experimental results [12]. To investigate the effect of turn-to-turn resistance on the stability of MB NI REBCO coils, 3 coils with different values of turn-to-turn resistance are compared. All the 3 coils are wound with 3-bundled REBCO conductors. The turn-to-turn resistivity of each coil is equal to the no-insulation (1 times), 10 times ( $10 \times 70 \mu\Omega \cdot \text{cm}^2$ ), and infinity (insulated). These 3 coils are called A, B, and C, respectively, also the bundled tapes are called Tapes 1, 2 and 3 from the outside of the coils in this paper.

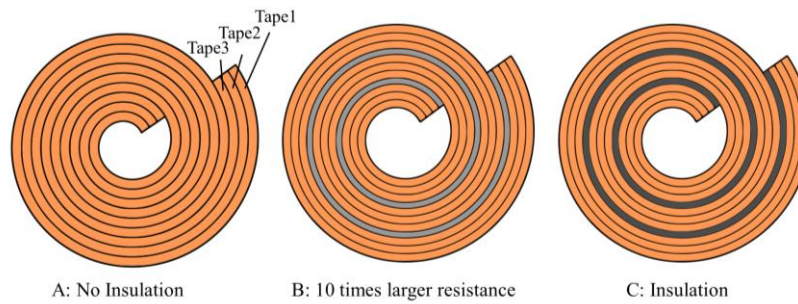


Fig. 2 3 MB NI coil models with different turn-to-turn resistance.

Table 1 Specifications of REBCO tape and coils

Parameters	Value		
Coil model	A	B	C
<b>REBCO tape</b>			
Tape width [mm]		4.0	
Tape thickness [mm]		0.1	
Insulation layer thickness [mm]		0.03	
REBCO layer thickness [ $\mu\text{m}$ ]		2.0	
Copper stabilizer thickness [ $\mu\text{m}$ ]		20.0	
Critical current at 77K, self-field [A]		120.0	
<b>Pancake coil</b>			
Coil i.d., o.d. [mm]	120.0, 144.0	120.0, 146.4	120.0, 146.4
Number of bundle tapes		3	
Number of turns		40	
Azimuthal division		8	
Contact resistivity (Tape-to-Tape) [ $\mu\Omega \cdot \text{cm}^2$ ]		70.0	
Contact resistivity (Turn-to- Turn) [ $\mu\Omega \cdot \text{cm}^2$ ]	70.0	700.0	Insulation
Inductance [mH]	3.524	3.485	3.485

### 3. Charging simulations

Experimental results showed that MB NI REBCO coils could reduce the charging delay compared to a conventional NI coil [10]. However, there is a possibility that the operating current is not evenly distributed in bundled tapes during charging due to the variety of tape inductances. The detailed current phenomenon has not yet been known. Therefore, we simulated the current and temperature distributions inside the MB NI REBCO coils during charging, and then investigated the stability of the charging.

The simulation conditions for the charging test are shown in Table 2. The operating current is increased for all three coils at 1 A/s per tapes and stays for 50 s after reaching 450 A. Here, the operating current is indicated as the sum of the currents flowing in all three bundled conductors.

Table 2 Simulation condition of charging test

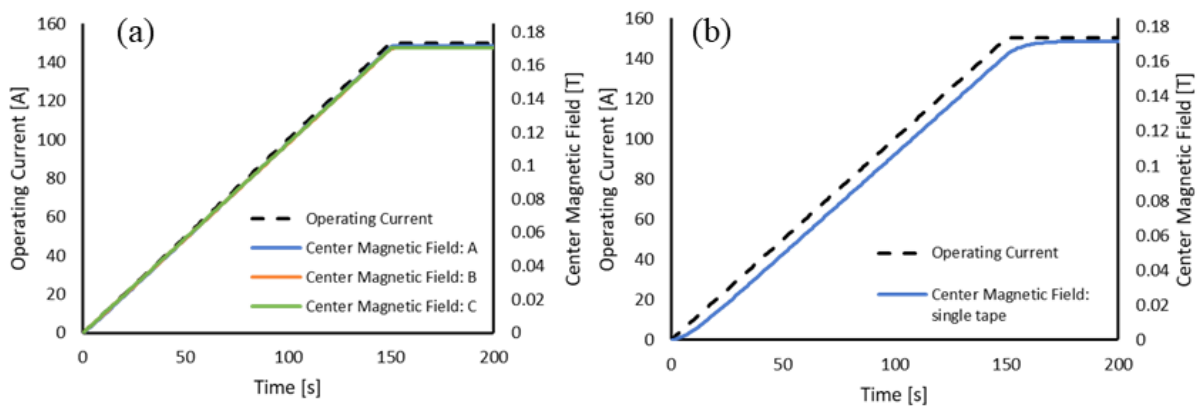
Simulation Condition	
Time step [s]	0.1
Simulation time [s]	200.0
Operating temperature [K]	20.0
Operating current [A]	0 to 450
Charging speed [A/s]	1.0

Fig. 3 shows the time variation of the operating current and the axial magnetic field for the MB NI coil and the conventional NI coil. From the results, multi-bundled coils are confirmed to improve the excitation delay caused by the NI winding technique. Fig. 4 shows the azimuthal

current distribution during the coil excitation. We found that there were some current differences between the tapes. However, these differences are not expected to have a significant impact on the operating conditions or the magnet stability. In addition, no current differences are observed immediately after the end of excitation. Thus, the MB NI coil is effective against the charging delay, and has the high stability during charging.

#### 4. Quench simulations

The sudden normal-state transition in NI pancake coils is called “quench.” When a quench occurs in a conventional NI coil (single tape), the current is diverted via the turn-to-turn low resistance path, thereby preventing a pessimistic temperature rise. At a quench event of an NI coil, currents are induced in the adjacent tape wires to compensate the magnetic field, which results in unbalance currents between tapes. In the MB NI coil, the current distribution would be complicated in each bundled tape during quench.



**Fig. 3** Time variation of the operating current and the coil center magnetic field, (a) MB NI coil, (b) single tape NI coil.

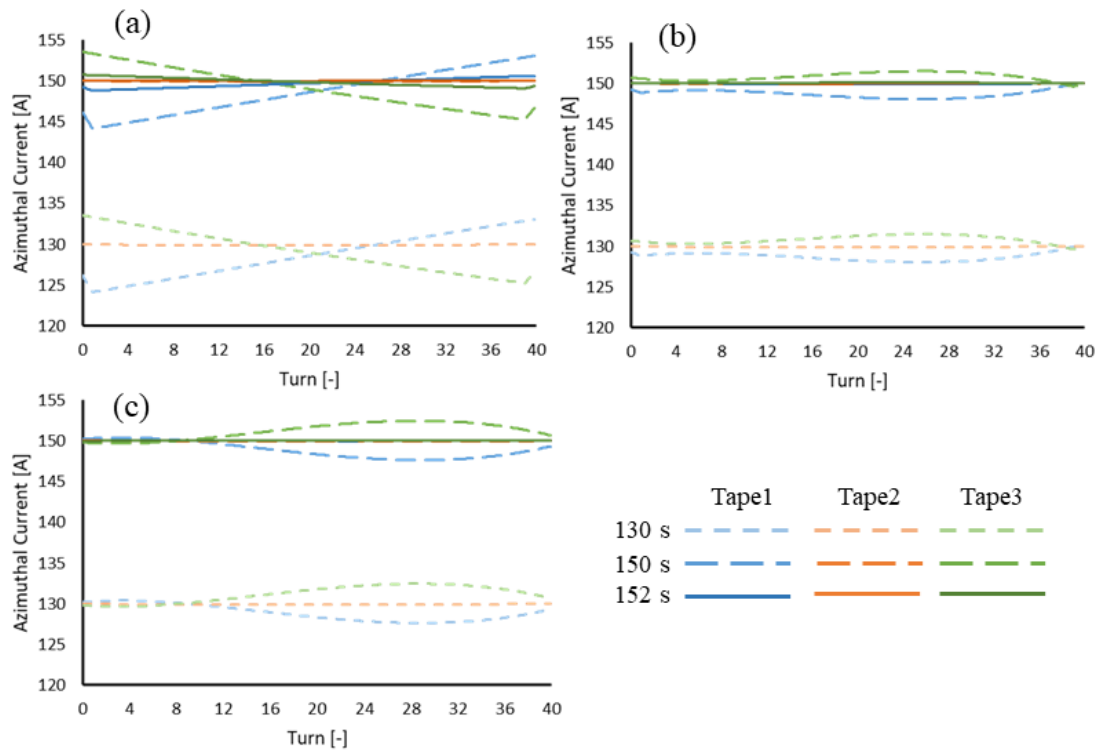


**Fig. 4** Time variation of the current distribution during exciting, (a) coil A, (b) coil B, (c) coil C.

The quench simulations were conducted to verify the stability of the MB NI REBCO coil against quench. For MB NI coils A, B, and C, with a steady state current of 450 A, the one turn (mid-turn) of the outer tape (Tape 1) is quenched at 0 s. The operating current remained constant after quench. The simulation conditions for the quench simulations are listed in Table 3.

Fig. 5 shows the results of the quench simulations. In all the coils, it can be seen that when the quench occurs, the current at the quench region in Tape1 is transferred to the other tapes. The current of Tape 2 reaches to the maximum value near the normal-state element, with the smallest value in coil A, which has no insulation, and the largest value in coil C, which has turn-to-turn insulation. This is because the insulation layer between the turns prevents the current from passing from Tape 1 to 3, and the current concentrates on Tape 2. Furthermore, in coils B and C, the current in Tape 3 is also transferred to Tape 2 at 0.01 s after the quench. It is considered that this is due to the strong influence of the inductances.

From these results, it is considered that the MB NI coil has a high thermal stability against the normal-state transition, but there is a possibility that the current may concentrate on one tape and reach the critical current depending on the operating current. However, no temperature rise is observed in all the coils, as shown in Fig. 6.

Table 3 Simulation condition of quench test	
Simulation Condition	
Time step [s]	0.001
Simulation time [s]	1.0
Operating temperature [K]	20.0
Operating current [A]	450

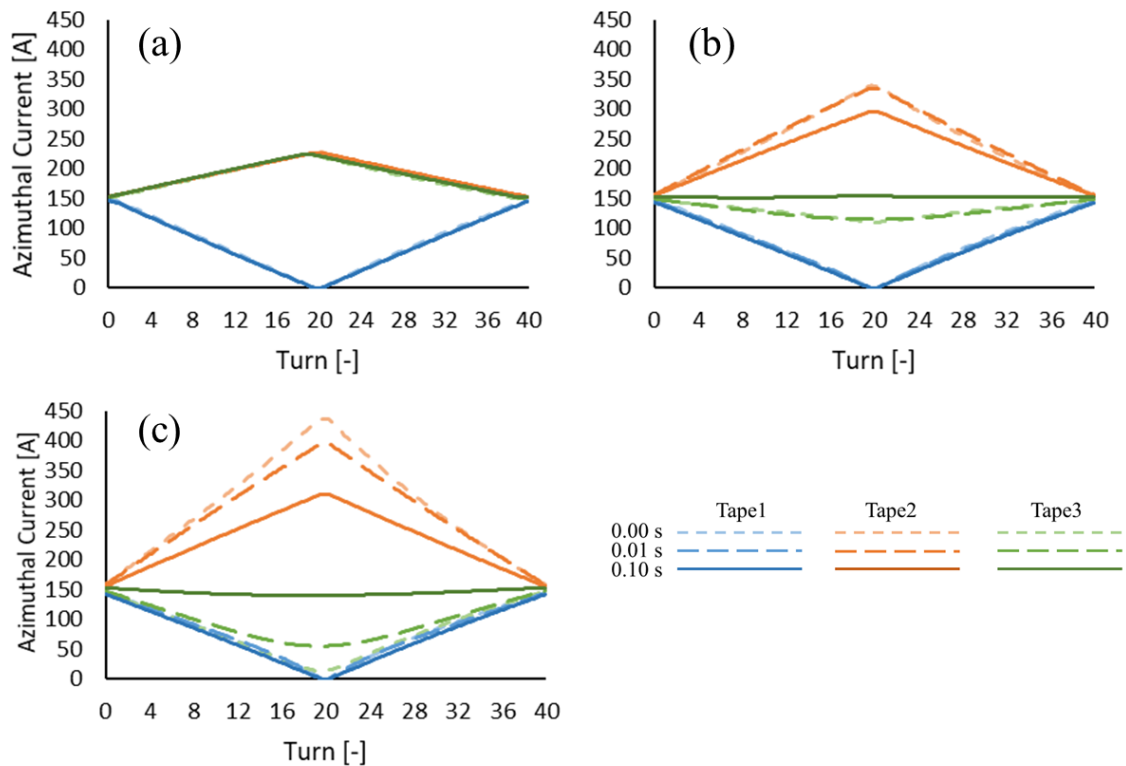
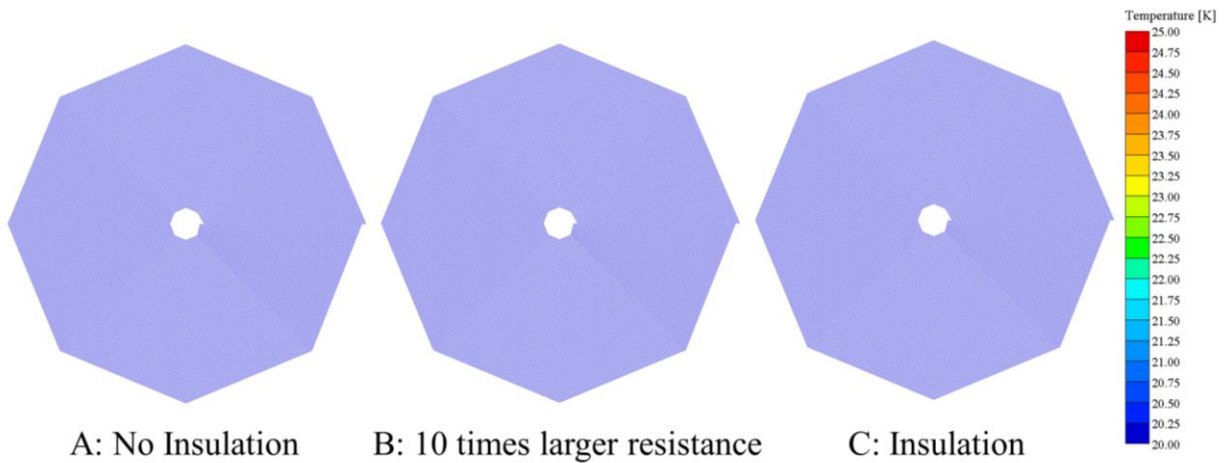


Fig. 5 Time variation of current distribution in quench test, (a) coil A, (b) coil B, (c) coil C.



**Fig. 6 Temperature distribution at 0.1 s after the quench.**

## Conclusions

For the practical use of REBCO magnets, NI coils are expected to have both the high current density and the high thermal stability, but an excitation delay is an issue to be solved. The proposed MB NI coil was reported to be able to improve the charging delay. Nevertheless, the distribution of the current flowing in the coil has not been clarified, and the stability against the normal-state transition has not been confirmed. In this study, we investigated the current and temperature distributions of the MB NI coil by numerical simulation using the PEEC method and the thermal finite element method.

From the excitation test results, it was confirmed that the MB NI coils could improve the charging delay. During the excitation of the MB NI coils, there is no large current difference between the tapes, and a stable excitation is expected to be possible.

From the quench simulation results, the MB NI coil is thermally stable with no pessimistic temperature rise even when a quench occurs. However, we found that current differences occur between bundled tapes, and if the turn-to-turn are insulated, there is a threat that almost all of the operating current would flow to one tape. Therefore, no-insulation between turn-to-turn of MB NI coils seems to be desirable.

## References

- [1] Hahn, Seungyong. et al.: “45.5-tesla direct-current magnetic field generated with a high-temperature superconducting magnet”. *Nature* 570, pp. 496-499, Jun. 2019.
- [2] Ishiyama, Atsushi. et al.: “A criterion for determining stabilizer thickness of YABCO coated conductors based on coil protection”. *IEEE Trans. Appl. Supercond.*, 17(2), 2007, pp. 2430-2433.
- [3] Hahn, Seungyong. et al.: “HTS pancake coils without turn-to-turn insulation”. *IEEE Trans. Appl. Supercond.*, 21(3), 2011, pp. 1592-1595.
- [4] Choi, Sukjin. et al.: “A study on the no insulation winding method of the HTS coil”. *IEEE Trans. Appl. Supercond.*, 22(3), 2012, Art. no. 4904004.
- [5] Wang, Tao. et al.: “Analysis of transient behaviors of no-insulation REBCO pancake coils during sudden discharging and overcurrent”. *IEEE Trans. Appl. Supercond.*, 25(3), 2015, Art. no. 4603409.
- [6] Wang, Yawei. et al.: “An equivalent circuit model for no-insulation HTS pancake coils”. *Supercond. Sci. Technol.*, 28(4), 2015, Art. no. 045017.
- [7] Choi, Y. H. et al.: “Partial insulation of GdBCO single pancake coils for protection-free HTS power applications”. *Supercond. Sci. Technol.*, 24, 2011, Art. no. 125013.
- [8] Kim, Seong Geyom. et al.: “Study on thermal-quench behaviors of GdBCO coils wound with silicon grease as an insulation material”. *IEEE Trans. Appl. Supercond.*, 27(4), 2017, Art. no. 4700905.
- [9] Yang, Dong Gyu. et al.: “A study on electrical characteristics of multilayered metallic-insulation coils”. *IEEE Trans. Appl. Supercond.*, 27(4), 2017, Art. no. 7700206.
- [10] Geng, Jianzhao. Zhang, Min: “A parallel co-wound no-insulation REBCO pancake coil for improving charging delays”. *Supercond. Sci. Technol.*, 32, 2019, Art. no. 084002.
- [11] Selvamanickam, V. et al.: “The low-temperature, high-magnetic-field critical current characteristics of Zr-added (Gd, Y)Ba<sub>2</sub>Cu<sub>3</sub>O<sub>x</sub> superconducting tapes”. *Supercond. Sci. Technol.*, 25, 2012, Art. no. 125013.
- [12] Wang, Xudong. et al.: “Turn-to-turn contact characteristics for an equivalent circuit model of no-insulation REBCO pancake coil”. *Supercond. Sci. Technol.*, 26, 2013, Art. no. 035012.





## ON-LINE МУЛТИМЕДИСКИ ОБРАЗОВНИ КАРТИЧКИ

м-р Зорица Каевик, ООУ „Александар Македонски“ – Скопје  
zoricakaevikhristova@hotmail.com

проф. д-р Сашо Гелев, УГД, saso.gelev@gmail.com

Ана Дионисиева, ООУ „Аврам Писевски“ – Скопје, an.dionisieva@gmail.com

Александар Рајковчевски, ЕУРМ – Скопје, aleksandarlek@gmail.com

### Абстракт

Најновите информатички и комуникациски технологии овозможуваат создавање, употреба и дистрибуција на информации преку компактни дигитални преносни уреди. Мобилните уреди овозможуваат создавање и дистрибуција на дигитални податоци и нивно складирање независно од медиумот, т.е. без оглед на платформата. Мобилните информатички и комуникациски технологии не ги заобиколија ниту образовните процеси. Основата на оваа апликација е база на знаење (домен на знаење), која се состои од таканаречени основни концепти, како основни градежни блокови. Со цел да им се покаже на студентите, содржината на концептите се трансформира во хиперпросторот, користејќи мултимедијални рамки. Презентацијата на содржината на концептите е групирана во курсеви. Курсевите се во суштина аналогни на предметите. Курсевите се состојат од единици за учење. Тие се аналогни на наставните единици. Содржината на единицата за учење е збир на мултимедијални описи на содржината на доменските концепти на знаење т.е. збир на мултимедијални рамки. Основните концепти на базата на знаење се хиерархиски поврзани, што значи дека нивните мултимедијални рамки во хиперпросторот се исто така хиерархиски поврзани во доменот на курсот. Хиерархиската структура се регулира во зависност од наставната програма што ја дефинира Министерството за образование и наука на Република Северна Македонија. Наставникот, во зависност од целите на учењето и профилот на учениците, создава сценарио за учење со избирање на соодветен концепт од доменот на знаењето, соодветна единица за учење, т.е. група на On-line мултимедиски образовни картички. На овој начин, наставникот создава предавање во реално време, според реалните тековни потреби.

### Вовед

Е-учењето е несомнено главната „критична мисија“ во образовните системи низ целиот свет и најверојатно ќе остане така во догледна иднина.

Со учење со помош на технологија, учениците можат да учат според распоредот и достапноста, помагајќи им да го искористат своето време подобро.

Покрај тоа, иновативните методологии како симулации и сериозни игри можат да го поттикнат интересот на учениците, обезбедувајќи можност да учат и да учат преку знаење базирано на апликација.

Можноста за вежбање и усовршување или усовршување на вештините не само што обезбедува поголема продуктивност и квалитет на работа, туку влева чувство на доверба кај учениците што им помага да постигнат целокупна извонредност.

Со повеќе и повеќе индустрии кои го прифаќаат учењето со помош на технологија како избран начин на обука и испорака на учење, јасно е дека е-учењето ќе продолжи да дава неговото постојано влијание и радикално го менува начинот на кој учиме.

Збирот од мултимедијални ресурси ќе овозможи учениците интерактивност, достапност во секое време.

## **1. Образовен систем**

### **1.1 Образовен процес**

**Образование** е процес на промена на личноста во посакуваната насока со усвојување на различни содржини во зависност од возраста и потребите на поединци.

**Учење** претставува збир на активности на поединецот кои резултираат со стекнување на знаења, вештини и навики, како и стекнување на одредени ставови и вредности.

**Е-учењето** може да се дефинира како процес на трансфер на знаење и вештини по електронски пат со употреба на соодветни компјутерски апликации, т.е. посветени програми и средини во процесот на учење[2]. Овие апликации и процеси вклучуваат учење преку интернет, компјутери, дигитални училници, а содржината сепренесува преку интернет, интра-мрежа / екстранет, аудио и видеоленти, сателитска телевизија ... [3] [4]. Преминувањето кон е-учење не значи отфрлање на постоечката содржина за предавање / учење, туку само подобрување на постојниот образовен материјал, односно негова модернизација.

Денешните форми на е-учење вклучуваат различни аспекти на употребата на информатичката и комуникациската технологија во образованието, а во зависност од интензитетот и начинот на употреба, се разликуваат неколку форми на е-учење: [1]

- Класична настава – настава во училница (f2f или лице в лице);
- Настава со помош на информатичка и комуникациска технологија – технологија во функција на подобрување на класичното предавање (подржано учење од страна на ИКТ);
- Хибридна или мешана настава – комбинација на настава во училница и настава со помош на технологии (хибриден, мешан режим или мешано учење);
- Онлајн настава - наставата е целосно организирана со помош на информатичка и комуникациска технологија (целосно онлајн).

## **2. Дигитални образовни картички**

Апликацијата “Дигитална образовна картичка” претставува софтверска веб апликација која на наставниците/учениците им овозможува презентација, учење, утврдување и тестирање/самотестирање на даден образовен материјал во реално време (online) преку било кој компјутер или мобилен уред. Времето и местото не се важен фактор кога станува збор за користење на оваа апликација. Главната цел е да се овозможи брз и лесен пристап на сите наставници/ученици до наставните содржини кои сакаат да презентираат, учат, утврдуваат и да го проверат стекнатото знаење за даден дел од наставната програма. Истовремено и наставниците имаат можност да ги следат сите активности на учениците, да го тестираат нивното стекнато знаење, предлагаат со кои картички да го продолжат процесот на учење/самоучење.

На овој начин учениците имаат можност класичните наставни ливчиња, кои што се користат во традиционалната настава во образованието, да ги работат на поинтересен и позабавен начин преку технологиските уреди од кои се зависни и во време кога тие сакаат.

Целта на оваа апликација е да се дигитализираат сите наставни предмети и наставни единици со содржина која ќе биде прилагодена на возраста и нивото на знаење на учениците. Во главно, оваа апликација има за цел да овозможи на наставниците/учениците:

- Привлечна и забавна презентација на наставните содржини, преку користење на мултимедијата, хипермедијата и интерактивноста.
- Ефикасно и квалитетно разбирање, стекнување на нови знаења и нивно подолгопамтење.
- Продлабочување на знаења на учениците за сите наставни содржини и единици кои ги имаат поминато во даден период на тековната наставна програма.
- Можност за тестирање и самотестирање на стекнатите знаења преку контролни тестови, преглед на постигнатите резултати после секој тест и преглед на одговорите кои учениците ги дале, како и преглед на точните одговори.
- Насочување на текот на процесот на учење врз основа на постигнатите тестирања поединечно или групно.
- Достапност до апликацијата во секое време и од секој компјутер или мобилен уред.

Според истражувањата комбинацијата од класичниот начин на следење на настава и користење на е-образовни содржини е видливо поефективна од класичната настава. Некои истражувања покажуваат дека учениците кои користат on-line едукативни апликации се повеќе исполнителни од учениците кои го практикуваат традиционалниот начин на следење на настава.

## 2.1 *Опис на структура*

Компјутерски поддржаните модуларни системи имаат таканаречена модуларна структура. Тие се изградени од модули, кои заедно функционираат во една целина како систем. Основата на модуларната структура „**Дигитална образовна картичка**“ се состои од: Модул за најава, Модул за знаење, Модул на учење и подучување, Модул на корисник (учител/ученик), Модул за тестирање и оценување, База „Е-наставна картичка“, Комуникациски модул.

### 2.1.1 *Модул за најава (login модул)*

Овој модул служи за најава, односно регистрација на наставникот/ученикот. Во овој дел наставникот/ученикот се регистрира со сопствено корисничко име и лозинка преку кои се логира. Во рамките на овој модул, при првата најава, корисникот ги внесува своите матични податоци (шифра, презиме, име, наставник/ученик, училиште, одделение). Врз основа на внесените матични податоци апликацијата му придружува кои се неговите права за користење на апликацијата, односно му се дефинира неговиот профил. Надвор од доделените права корисникот не може да дејствува[1].

### 2.1.2 *Модулна знаење*

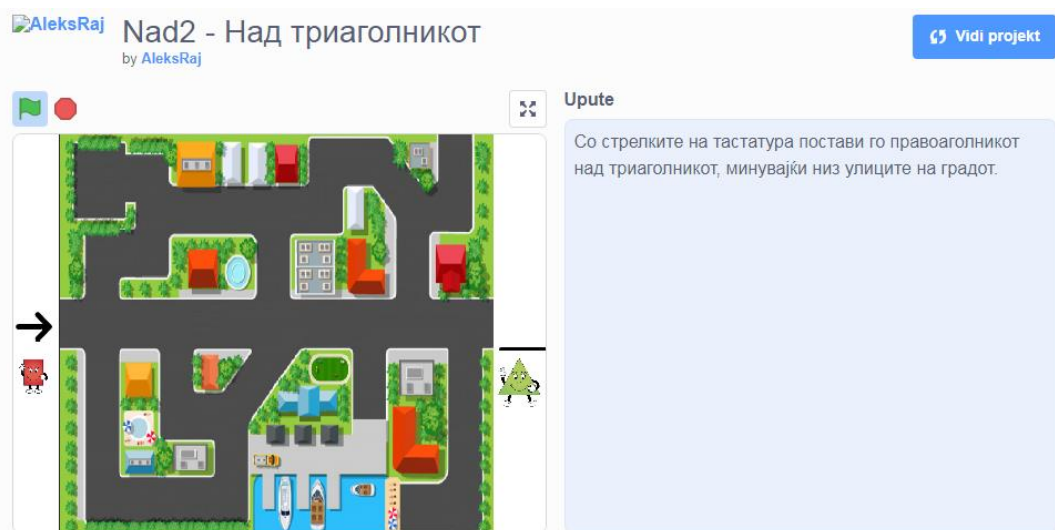
Главниот модул или ‘рбетот на образовниот систем е модулот на знаење (домен на знаење). Знаењето кое се користи во процесот на учење и подучување е структурирано во овој модул. Во текот на своето функционирање, останатите модули мора да комуницираат со него.

Основа на овој модул претставува базата на знаење, во која се запишани сите информации за наставната содржина која треба да се совлада во текот на процесот на учење и подучување. Базата на знаењето претставува множество на основни концепти. Основен концепт, наречен доменски концепт, претставува елементарна честичка на

знаење која понатаму не може да се дели на помали делови. Основниот концепт во овој труд претставува „Дигитална мултимедиска образовна картичка“.

Преку образовната картичка мултимедијално се презентираат основните наставни поими на сликовит и забавен начин со употреба на текст, графика, фотографии, анимации, аудио и видеозаписи. При нивното креирање се користат софтверските алатки: Paint, PowerPoint, Word и Scratch.

На Слика 1 е прикажана образовна картичка **Dvgore** во која, со помош на анимација изработена во Scratch, се објаснува математичкиот поим „Над“.



Слика1: Образовна картичка [Nad2](#)

Основните концепти се меѓусебно условно поврзани, односно учењето на еден концепт зависи од познавање на содржината на друг концепт. Концептите меѓусебно се поврзани во мрежа која има облик на мрежа на графови.

### 2.1.3 Модул на учење и подучување

Модулот за учење и подучување служи како алатка за изведување на процесот на учење/подучување од страна на наставникот или ученикот.

Овој модул мора добро да ги анализира и одговори на одредени прашања за да може успешно да ја извршува својата основна функција - управување со процесот на стекнување на знаења и вештини.

Прашањата што најчесто треба да се анализираат се од типот:

- Кое е нивото на способност на ученикот?
- Како ученикот се однесува во текот на учењето?
- Кои методи на претставување на наставниот материјал ги преферира ученикот?
- Во колкава мера ученикот го владее материјалот?
- За кои подрачја кои се надвор од наставниот материјал се интересира ученикот?

Со помош на соодветни тестирања се добиваат и одговорите на овие прашања, врз чија основа се избира автоматско сценарио на учење, кое модулот за учење и подучување го препорачува, или пак наставникот го одбира врз основа на резултатите од тестирањето, своето искуство и познавањето на ученикот. Овој модул треба да го насочува секој ученик посебно/група на ученици, во зависност од неговите резултати. Тоа е всушност и главната цел на овој модул, да ги насочува активностите врз основа на знаењето структурирано во модулот на знаење.

Сценариото претставува множество од пакети на инструкции (наставни картички). Ваквите сценарија треба да бидат така дефинирани и осмислени, да се користат само од групата на ученици/ученик со одредено ниво на знаење, кое одговара на резултатите при тестирањето. За секоја група/поединец постојат пакети на инструкции/картички преку кои наставникот може да ја интерпретира само содржината која дадената група на ученици не ја познава добро. Како расте тежинскиот фактор на групата, така се намалува бројот на инструкции во соодветниот пакет или пак се намалува начинот на приказ на истата наставна содржина.

Пакетите на инструкции/картички се поделени во три групи:

- Прва или почетна група, во која се повторува претходно стекнатиот материјал. Ако при тестирањето се утврди дека ученикот или групата од ученици не го познаваат претходниот материјал во доволна мера, тогаш следува повторување на материјалот.
- Втората или тековна група, е група која содржи инструкции кои го упатуваат ученикот на новиот (тековниот) материјал. Пакетите од оваа група се поделени по теми и наставни единици. После одреден број на поминати области следува тестирање. Од резултатите на тестирањето се определува дали ќе се изврши повторување на тековниот материјал или ќе се продолжи понатаму.
- Трета или крајна група, во суштина е иста како тековната група, со разлика што ученикот ги следи инструкциите што системот ги дефинира во зависност од резултатите на сите наставни единици предвидени по тој предмет, за таа учебна година.

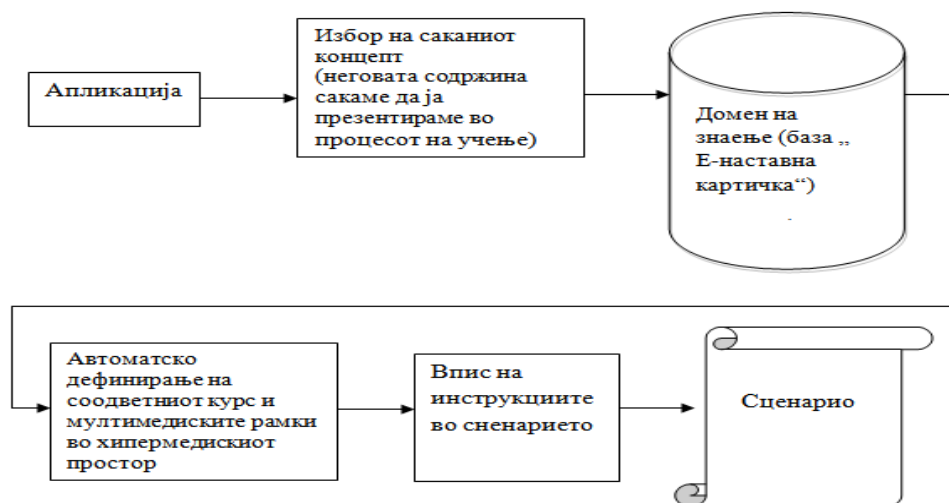
Наставните картички опфатени со сценарието не се статични, односно предавачот/наставникот може да ги менува по потреба.

Сценариото за мултимедијална презентација на наставна содржина во процесот на учење / настава (домен на сценарио) се креира на два начина: автоматски или по избор на наставникот (Слика 2 и 3).

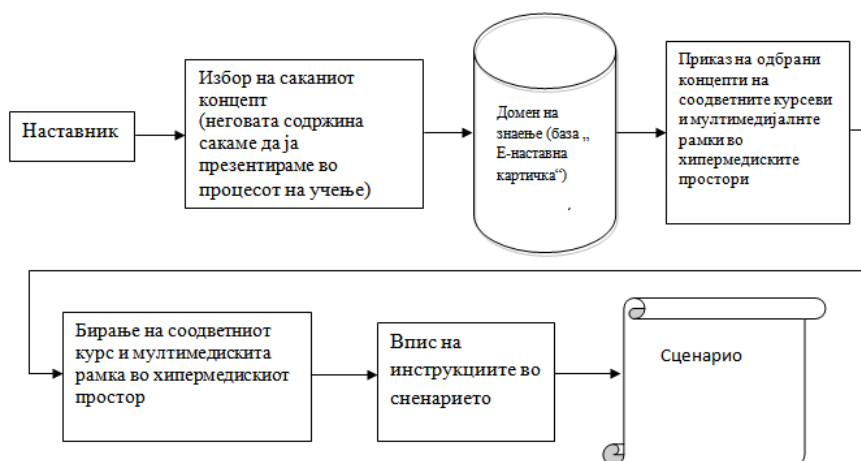
Сценариото е збир на пакети со инструкции за учење. Пакетите се групирани по курсеви (предмети). Курсевите се состојат од теми, темите од единици за учење (наставни единици), а единиците се состојат од таканаречени мултимедиски образовни картички кои користат мултимедија за презентирање на наставната содржина во процесот на учење / настава. Секоја картичка активира одредена мултимедијална рамка.

Бројот и видот на упатствата во пакетот зависи од групата ученици за кои е наменето предавањето, т.е. од нивото на просечно знаење на учениците. Ако знаењето е поголемо, бројот на упатства се намалува. Се толкуваат само содржините што учениците не ги знаат. Факторот на тежина на знаење се оценува од 1 до 5. Кога има вредност од 1, сите упатства се изведуваат. Кога има вредност 5, пакетот е празен, студентите ја научиле наставната содржина.

Создавањето сценарио се врши автоматски кое го дефинира концептот, во зависност од избраниот курс и единица, влегува во мултимедијалните рамки за скрипти и нивни адреси, од каде што можат да активираат и да презентираат соодветна наставна содржина (Слика 2), или наставникот лично креира скрипта во зависност од нивното знаење за карактеристиките на ученикот (Слика 3).



Слика2: Автоматско креирање на сценарио за учење



Слика3: Креирање на сценарио од страна на наставникот

Ред. број	Опис на мултимедиската рамка	Адреса
1	Pred1 – Постави го кругот пред триаголникот	<a href="https://scratch.mit.edu/studios/25457774/projects/">https://scratch.mit.edu/studios/25457774/projects/</a>
2	Zad1 – Постави го триаголникот зад кругот	<a href="https://scratch.mit.edu/studios/25457774/projects/">https://scratch.mit.edu/studios/25457774/projects/</a>
3	Nad1 – Над правоаголникот	<a href="https://scratch.mit.edu/studios/25457774/projects/">https://scratch.mit.edu/studios/25457774/projects/</a>
4	Nad2 – Над триаголникот	<a href="https://scratch.mit.edu/studios/25457774/projects/">https://scratch.mit.edu/studios/25457774/projects/</a>
5	Pod2 – Под кругот	<a href="https://scratch.mit.edu/studios/25457774/projects/">https://scratch.mit.edu/studios/25457774/projects/</a>
6	Pod3 – Под линијата	<a href="https://scratch.mit.edu/studios/25457774/projects/">https://scratch.mit.edu/studios/25457774/projects/</a>
7	Do1 – До училиштето	<a href="https://scratch.mit.edu/studios/25457774/projects/">https://scratch.mit.edu/studios/25457774/projects/</a>
8	DVgore1 – Искачи го триаголникот	<a href="https://scratch.mit.edu/studios/25457774/projects/">https://scratch.mit.edu/studios/25457774/projects/</a>
9	Vnatre 1 – Внатре во кругот	<a href="https://scratch.mit.edu/studios/25457774/projects/">https://scratch.mit.edu/studios/25457774/projects/</a>

Слика4: Сценарио за наставна единица „Местоположба, движење и насока“

При реализацијата на сценариото, наставникот влегува во базата на сценарија, го бира сценариото кое е автоматско креирано или го креира сам и презентира мултимедијалните рамки за одбраните картички.





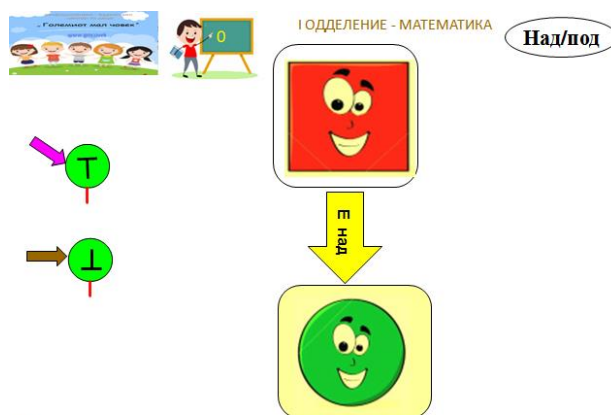
Слика5: Активирање на сценарио од страна на наставник/ученик

#### 2.1.4 Модул корисник (учител/ученик)

Корисничкиот модул е основа на секој систем за адаптација на корисникот, бидејќи ги содржи сите информации за него. Без информации за корисникот, системот не може да соработува со секој корисник лично, туку се однесува кон сите корисници на ист начин. Корисничкиот модул мора да ги содржи сите карактеристики на корисникот, неговото однесување и неговото знаење, т.е. мора да ги содржи сите фактори кои влијаат на процесот на учење и ефективната потрошувачка на знаење од страна на корисникот. Во зависност од информациите за корисникот и апликацијата „Технологија и информатика во образованието“ се утврдуваат дали сценариото за наставна содржина ќе се креира автоматски од апликацијата или рачно од наставник. Корисничките податоци се статични: матичен број, презиме, име, функција за кориснички права (наставник, студент или администратор) или динамично: датум и време на влегување или излез од апликацијата.

#### 2.1.5 Модул за тестирање и оценување

Секој наставник/ученик, во рамките на својот профил, има можност да одбере каков вид на тестирање сака да изврши, од која наставна содржина и со која тежина. Полињата кои што имаат можност да се одберат се следните опции: избирање на одделение, наставен предмет, наставна единица, тежина на тест.



Квадратот е над кругот! Кликни на стрелката која го означува точното тврдење.

Слика8: Прва слика од мултимедиска образовна тест картичка T-nad-pod

#### 2.1.6 База „Е-наставна картичка“

##### 2.1.6.1 Вовед

Главниот модул или ‘рбетот на образовниот систем е модулот на знаење. Знаењето кое се користи во процесот на учење и подучување е структурирано во овој модул. Во текот на своето функционирање, останатите модули мора да комуницираат со него. Основа на овој модул претставува базата на знаење, во која се запишани сите информации за

наставната содржина која треба да се совлада во текот на процесот на учење и подучување. Постојат два вида на бази: општи и експертски. Општите бази содржат податоци од сите наставни области, а експертските бази се оние во кои се запишани податоци за наставните содржини само од одредено подрачје на знаење.

#### 2.1.6.2 Структура

База на знаење „Е-наставна картичка“ е релативна база на податоци. Нејзината структурата е сегментирана, односно се состои од следните релации: **obraz\_karticka, korisnik, predmet, test\_karticka, test\_rezultat, učenje\_plan, nastavnaedinica.**

#### 2.1.7 Комуникациски модул

Наставникот/ученикот мора да му пристапи на концептот (наставната картичка) и да ја проучи неговата содржина со цел да ја разбере. Во таа насока, содржината на концептот треба да се претстави во соодветна форма во просторот за хипермедија. Ова се постигнува на тој начин што доменскиот концепт се опишува со една или повеќе мултимедијални страници. Како што доменската мрежа е претставена со јазли (концепти) и врски помеѓу нив, така и мрежата на хиперпросторот е претставена со јазли (хипермедиски страници) и со врските помеѓу нив. Хипермедијалните страници и нивните врски формираат мрежа на хиперпросторот. Ако мрежата на домени е структурирана според наставни теми, цели за учење, наставни програми, со групните или индивидуалните карактеристики на учениците, тогаш структурата на мрежата на домени претставува педагошка структура на доменот на знаење. Мрежата на домени и мрежата на хиперпростор се аналогни. Хиперпросторската мрежа се користи за прикажување на содржината во доменот на знаење пред наставниците/учениците.



Слика 10. Релација концепт – мултимедиска рамка

#### Заклучок

Употребата на информатичката технологија во образованието не само што помага во процесот на учење, туку и ја подобрува креативноста на учениците и помага во решавањето на проблеми.

Учењето со помош на компјутер или мобилен уред е иднината во современиот образовен систем. Технологијата расте и рапидно се развива, со што информатичката технологија станува неизоставен дел од нашето секојдневие. Компјутерите и мобилните уреди се имплементираат во сите сфери на развој, од технолошките и производни процеси, до современата медицина. Поради тоа, потребно е да се внесат и во примарните области како што е образованието.

Користењето на овој вид на учење и подучување е од голема корист и помош за наставниците и учениците во наставниот процес, придонесува во реформирање на образованието и со користење на нови методи на учење дури и промена на улогата на наставникот.

Методите кои денес се нудат во образованието, и покрај големиот број реформи, сè уште се само на почеток на воведување на концептот за електронско учење. Ова особено се однесува на реформите во основното образование, на возраст на која на учениците им е најпогодно да создадат и развијат информатичка култура. Поради тоа, наставната програма треба да се развива со помош на информатиката како основна образовна гранка и со помош на техничките уреди. На тој начин, ученикот интерактивно ќе биде поврзан со целата програма и посвесно и самостојно ќе го тестира знаењето кое го има и ќе може да си ги провери сите информации за било кои наставни предмети на многу лесен и едноставен начин. Апликацијата “Е-наставни ливчиња” е апликација која нуди самостојност, интерактивност и пред се забава на сите ученици. Таа несвесно нуди брз и лесен начин на проверка на сопственото знаење. Таа дава едно поинакво гледиште на компјутерската-информатичка наука која се користи во образовните системи. Технологијата е нашата иднина, иднината на младите ученици, тоа е фактот со кој се соочуваме и поради кој мора да размислуваме и да создаваме апликации кои се во ист чекор со нејзиниот развој

### Литература

- [1] Risto Hristov, “*Obrazoven Softver*”, 2010 godina
- [2] van Dam, N., Cerda, V., Williams, M. et al., Global Headquarters, E-learning for kids, web portal (<http://www.e-learningforkids.org>).
- [3] Robinson, Rhonda; Molenda, Michael; Rezabek, Landra. „*Facilitating Learning*” (PDF). Association for Educational Communications and Technology.
- [4] Woo, Stu (30. 1. 2017). „*What's Better in the Classroom—Teacher or Machine?*”. *Wall Street Journal*.



## АЛГОРИТАМОТ „ВЕШТАЧКА КОЛОНИЈА НА ПЧЕЛИ“

м-р Билјана Раичевиќ Велковска, СУГС Гимназија „Орце Николов“ – Скопје

проф. Д-р Сашо Гелев, УГД

проф. д-р Анис Сефиданоски, ЕУРМ

м-р Зорица Каевиќ, ООУ „Александар Македонски“ - Скопје

### Абстракт

Алгоритмот Вештачка колонија на пчели - (Artificial bee colony) ABC е од неодамна воведен алгоритам за глобална оптимизација. Припаѓа во групата на пчелни алгоритми, односно во групата на интелигенција на ројот (Swarmintelligence). Тој симулира интелигентно однесување на ројот пчели во пронаоѓање на храна – мед. Овој алгоритам е едноставен и доста флексибилен, како и со тенденција на постојано усовршување.

Токму интелигентното однесувањето на ројот пчели (Swarm Intelligence) е главната идеја за содавањето на овој алгоритам. Тој, врз основа на интелигентното однесување на пчелите во ројот, го организира функционирањето на компјутерскиот систем и неговите комуникации со опкружувањето. Со други зборови ги организира поделбата на улогите, начинот на комуникација и пренесувањето на поволните информации.

ABC алгоритмот, кој ги користи принципите на функционирањето на таканаречената вештачка колонија на пчели и вештачки невронски мрежи, во овој труд се користи за решавање на проблемот препознавање на банкноти.

### Клучни зборови

Алгоритмот „Вештачка колонија на пчели“, интелигенција на ројот, ABC алгоритмот, препознавање на банкноти.

### Вовед

Пчелите се инсекти кои живеат во роеви. Животот во пчелините роеви е строго организиран, речиси на ниво на организиран на човечкото општество. Секоја пчела има своја функција и живее и работи спрема правилата кои владеат во нивното општество. Целта на ваквата организираност е што побрзо и поефикасно пронаоѓање извори за храна и производство на мед, односно чување на безбедноста на ројот.

Интелигентното однесување на пчелите и општествената организираност на роевите пчели е погодна за имитирање и усовршување на логичката структура на алгоритмите кои се користат при дефинирање на функционирањето на компјутерскиот систем.

## 1. Вештачка колонија на пчели

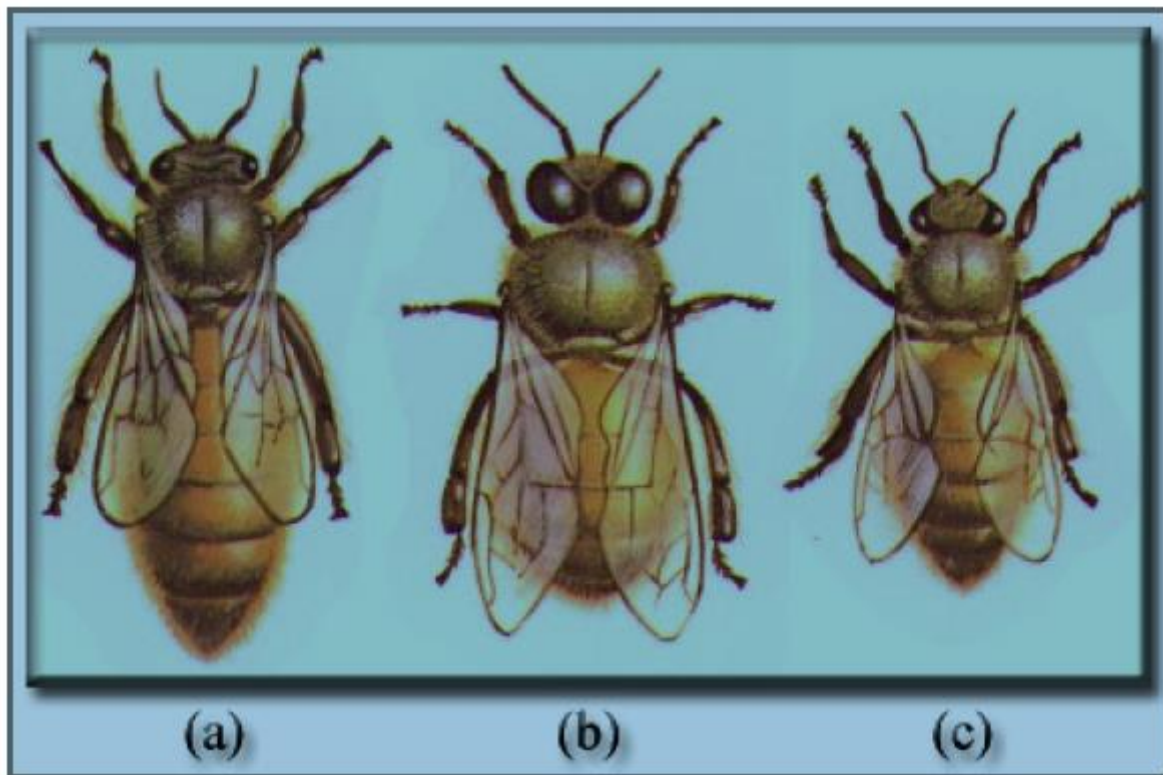
**Алгоритмот Вештачка колонија на пчели** - ABC е од неодамна воведен алгоритам за глобална оптимизација. Припаѓа во групата на пчелни алгоритми, односно во групата на интелигенција на ројот (*Swarmintelligence*). Тој симулира интелигентно однесување на ројот пчели во пронаоѓање на храна – мед. Овој алгоритам е едноставен и доста флексибилен, како и со тенденција на постојано усовршување.

Токму интелигентното однесувањето на ројот пчели (*Swarm Intelligence*) е главната идеја за содавањето на овој алгоритам. Тој, врз основа на интелигентното однесување на пчелите во ројот, го организира функционирањето на компјутерскиот систем и неговите комуникации со опкружувањето. Со други зборови ги организира поделбата на улогите, начинот на комуникација и пренесувањето на поволните информации [1].

### 1.1 Поделба на улогите

Системот рој на пчелите беспрекорно функционира во своите активности, благодарейќи на специјализацијата на неговите единки, поделбата на работата, симултаноста и самоорганизацијата. Негова главна задача е прибирање на храна (мед). За успешно да се изведува оваа задача, семејството на пчели е поделено на: **матица**, **трут** и **пчели работнички** (Слика 1).

Матиците се задолжени да лежат на јајцата, а трутовите за оплодување на матицата. Бидејќи создавањето и уништувањето на единките во алгоритмот не е потребно, акцент се става на третиот вид на пчели – **работнички**. Постојат два вида на пчели работнички **извидници** (*scout bees*) и **собирачи** (*forager bees*). Собирачите се делат на запослени и незапослени (наблудувачи кои чекаат информации за изворите во експлоатација и за потенцијалните извори).



Слика 1: Илустрација на видови пчели: матица (a), трут (b), работничка (c)

Извидниците се движат по случаен избор во потрага по нови извори. Откако ќе го пронајдат изворот, тие се враќаат во кошницата и со пчелин танц го промовираат посетениот извор со информации за неговиот квалитет. Вообичаено е кај пчелните колонии бројот на собирачи значително да го надмине бројот на извидници. По танцот, извидниците се враќаат во својот извор во придружба на пчели собирачи. Нивниот број зависи од квалитетот на пораката што ја пренесуваат извидувачите.

Собирачите се однесуваат реактивно кон извидниците, односно зависно од добиените информации. Пчелите во колонијата ги гледаат извидниците во просторот предвиден за танцување. Во зависност од промовираниот квалитет на изворот, тие одлучуваат дали се заинтересирани за новиот извор и ги запомнуваат упатствата. Исто така го запомнуваат мирисот на изворот (бидејќи извидникот бил таму) за да знаат кога ќе ја достигнат целта. Бидејќи сонцето постојано се движи, пчелите имаат внатрешно чувство за време, па затоа ги прилагодуваат информациите за состојба на изворот, да одговараат на моментот кога ги примиле. Собирачите, кога ќе се вратат, можат да продолжат да го посетуваат истиот извор или да одат во потрага по нов извор, прегледувајќи ги новите информации на „подиумот за танц“. Системот според кој пчелите донесуваат одлуки не е целосно познат, но може да се претпостави дали ќе останат на стариот извор или ќе тргнат да работат на нов извор, во зависност од споредбата на добиените информации за квалитетот на новиот извор и информациите за стариот.

### 1.1 Пчелин танц

Пчелите комуницираат со **танц** (*waggle dance*) чие значење го дешифрирал Karl von Frisch [2]. Танцот на пчелите се одвива во две фази: мафтање и кружно враќање. Кружното враќање се одвива наизменично - прво на едната страна, а потоа на другата, што вкупно формира движење во вид на осмица. Фазата на мафтање е клучна за пренесување информации на други пчели.

Пчелите со помош на својот танц кодираат три клучни податоци:

- насока на изворот;
- оддалеченост на изворот;
- квалитет на изворот.

На тој начин секоја пчела може да го осознае надворешниот свет дури и ако никогаш не ја напушти кошницата. Пчелите со тоа ги комбинираат своите сознанија со туѓите, па донесуваат одлуки за следниот потег.

Насока на изворот претставува најсложено дизајниран податок. Имено, пчелите ја користат гравитацијата и положбата на сонцето. Со танцот по вертикалната површина на кошницата (горе-долу) пренесуваат информации за насоката на изворот на храна во однос на гравитацијата, а со танц по хоризонталната површина пренесуваат информации за насоката на храната во однос на насоката на сонцето. Постојат следните правила на танцот:

- Кога пчелите се движат по вертикалната рамнина на пчелината кошница према горе, ја означуваат насоката спротивна од насоката на гравитацијата.
- Кога пчелите се движат по вертикалната рамнина на пчелината кошница према долу, ја означуваат насоката на гравитацијата.
- Кога пчелите се движат по хоризонталната рамнина ја означуваат насоката од кошницата кон сонцето.

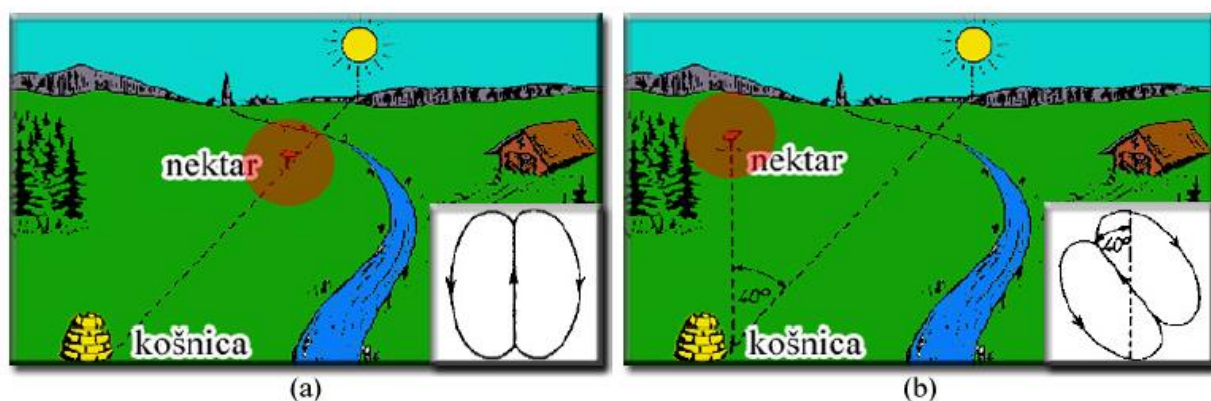
Двете насоки се пресекуваат под некој агол, во насока на движење стрелките на часовникот или спротивно. Овој агол означува дали изворот на храна е десно или лево од сонцето, односно аголот кој го сочинуваат правата на насоката кошница – сонце и



правата на насоката кошница – извор. Двете прави почнуваат од иста точка, точката во која се наоѓа кошницата (Слика 2).

Со движењето за време на танцот извидниците прават фигури во вид на осмица.

На Слика 2 пчелата извидник и дава информации на пчелата работник дека изворот се наоѓа во насока кошница – сонце (a), но изворот се наоѓа поместен за агол од  $40^\circ$  во насока спротивно од насоката на движење на стрелките на часовникот (b).



Слика 2 Пчелин танц за упатство спрема сонцето (a) и спротивно од насоката на стрелките на часовникот во однос на сонцето (b)

Информација за оддалеченоста на изворот од кошницата во која се изведува танцот се добива од брзината на танцот (опишување на фигурите осмици). Поголема брзина, значи дека изворот е поблиску и обратно помала брзина означува дека е подалеку.

По добиените информации, пчелата доаѓа до изворот на храна (цветот) и собира мед. Таа собира и информации за квалитетот на храната и количината со која располага изворот. Кога ќе се врати во кошницата овие информации им ги пренесува на другите преку брзината на кружната фаза и времетраењето на танцот. Другите пчели можат да добијат индикација за квалитетот на изворот и од бројот на пчели кои го промовираат истиот извор. Изворот со повисок квалитет го посетиле поголем број пчели.

## 2. Алгоритам

Принципите на вештачката колонија на пчели се искористени за креирање на таканаречениот ABC алгоритам (*пчелин алгоритам*). Алгоритамот се користи за тренирање на невронска мрежа (*artificial neural network*) која има задача да препознава книжни банкноти, односно да ги класифицира во одредени групи.

Клучниот механизам на пчелиниот алгоритам се истражување (*research*) и експлоатација (*exploitation*). Пчелите извидници се задолжени за фазата извидување, а пчелите собирачи за фазата експлоатација.

Клучниот механизам на алгоритмите на пчелите лежи во добриот сооднос на истражување (*exploration*) и експлоатација (*exploitation*). Пчели извидници се задолжени за фазата истражување, а пчелите собирачи за фазата експлоатација. Покрај тоа, алгоритмот е исто така многу флексибилен. Лесно се прилагодува на динамички променливите проблеми и успешно се справува со надминување на локалните крајности во потрага по глобалните.

Вештачка пчелина колонија е поделена на три групи: вработени пчели (*employed bees*), наблудувачи (*onlookers*) и извидници (*scouts*). Пчелата работник ја истражува околината на изворот што претходно го посетила. Пчелите наблудувачи во фигуративна смисла ги набљудуваат пчелите на подиумот што изведуваат пчелин танц и носат одлука која пчела ќе ја следат. Извидниците спроведуваат случајно пребарување каде би можело да има храна.

Пчелната колонијата се состои претежно од пчели работнички и пчели извидници, во приближно ист процент. Активностите на извидниците се јавуваат или кога почнуваат со барање на нов извор или кога експлоатацијата на постоечките извори завршила.

Структурата на алгоритмот се состои од јамка со повторување на три основни чекори. Секој чекор е задолжен за одреден вид на пчели. Прво пчелите работнички го мерат квалитетот на нивните решенија. Потоа информациите за квалитетот се споделуваат со набљудувачите. Набљудувачите понатаму ја посетуваат околината на изворот за кој се одлучиле. Итерацијата се затвора со фаза на извинување, која се случува само ако се напуштат постоечките решениа.

Гледано од аспект на ABC алгоритмот, локацијата на изворот на нектар преставува можно решение на проблемот кој го оптимизираме, а количината на нектарот е еквивалентна на квалитетот на набљудуваното решението на проблемот.

Адекватно на пчелите од природата одговараат виртуелни пчели во алгоритмот.

Ознаката  $N$  се воведува како променлива на популацијата на пчелите во кошницата. Секој тип на пчели генерира свое решение  $x_i$  ( $i = 1, 2, \dots, N$ ) каде  $x_i$  е  $D$ -димензионален вектор. Вредноста на димензијата  $D$  е еднаква на бројот на параметрите кои треба да се оптимизираат. Дополнително, во алгоритмот, се воведува ознака за итерација  $C = 1, 2, \dots, \text{Stax}$ .

### 2.1 Пчели работнички

Пчелите работнички, собирајќи нектар од изворот, истовремено ја набљудуваат неговата околина во насока на пронаоѓање на поквалитетен извор од постоечкиот. Ако најдат поповолен извор, носат решение да се напушти стариот извор, се враќаат во кошницата и ги информираат останатите пчели набљудувачи за новото решение. Набљудувачи се дел од пчелите работнички кои моментално не се запослени, кои чекаат запослените работнички да ги информираат за експлоатираните или потенцијаните извори.

Исто се случува и со вештачките пчели во алгоритмот. Вештачката пчела набљудувач го анализира новото решение и ако е поквалитетно од старото го памти и го користи. Во спротивно останува поврзана со старото.

Во продолжение е дадена основната формула на пчелиниот алгоритам која, освен пчелите работнички, го користат и пчелите набљудувачи. Со таа формула, врз основа на старото решение (векторот  $x_i$ ), алгоритмот генерира ново решение (вектор  $v_i$ ) за сите пчели:

$$v_{ij} = x_{ij} + rand(-1,1) * (x_{ij} - x_{kj})$$

Каде  $k \in \{1, 2, \dots, N\}$  и  $j \in \{1, 2, \dots, D\}$  се случајно избрани индекси. Со алчна метода се памети само подобриот вектор помеѓу  $x_i$  и  $v_i$ .

### 2.2 Пчели набљудувачи

Извештајот на пчелите работнички кои се запослени го набљудуваат невработените пчели (пчели набљудувачи). Пчелите даваат информации за изворот кој го користеле или за нов извор за кои мислат дека е подобар. Тие ги анализираат и споредуваат предложените решенија (предложените извори). Логично е пчелите што носат информации за подобри решенија да привлечат поголем број „следбеници“. Овој принцип се реализира со методот на едноставна селекција наречена тркало за рулет селекција (*roulette wheel selection*).

Веројатноста да прифатат одредено решение се пресметува со релацијата:

$$P_i = \frac{fit_i}{\sum_{i=1}^N fit_i} \quad \text{-----} 2$$

каде  $P_i$  преставува веројатноста дека пчелата посматрач ќе го прифати решението "i" како свое. Посматрачите по донесената одлука кое решение ќе го прифатат, ги спроведуваат истите постапки како пчелите запослени работнички.

### 2.3 Пчели извидници

Извидниците (освен при иницијализација) преставуваат малцинство во колонијата, во споредба со другите две групи. Потребата за извидување се јавува само кога решението е одбиено, затоа е потребно да се најде ново, независно од претходните решенија. Тогаш се воведува нов извидник кој наоѓа ново решение внатре во зададените граници. Долната граница е одредена со вектор  $d$ , а горната граница со вектор  $g$ . Координатите на новиот извор се пресметуваат со релацијата:

$$x_{ij} = d_j + rand(0,1) * (g_j - d_j) \quad \text{-----} 3$$

Истата формула се користи во текот на иницијализацијата на алгоритмот, кога се генерира почетната состојба на базата со податоците на познатите извори, односно со решенијата за нивно користење.

### 2.4 Псевдокод

Со комбинирање на претходно опишаните однесувања на пчелите се добива ABC алгоритам кој ги обединува сите четири селекциски процеси: локална селекција (формула 1), глобална селекција (формула 5.2), селекција по случаен избор (формула 3) и алчна селекција која се отчитува со алчно бирање и измена на старото и новото решение. Со претходно опишаните постапки можат да се реализира следниот псевдокод:

*Inicijalizacija:*

**ZA**  $i = 1$  **DO**  $N$

Inicijaliziraj go vektorot  $x_i$  sprema formula 5.3

**KRAJ ZA**

iteracija = 1

**POVTORUVAJ**

*Faza na zaposleni pčeli:*

**ZA SEKOJA** zaposlena pčela ( $i$ )

Presmetaj  $v_i$  vrz osnova na  $x_i$  sprema formula 1

**AKO**  $kvalitet(v_i) > kvalitet(x_i)$  **TOGAS**  $x_i = v_i$

**KRAJ ZA SEKOJA**

*Faza na nabluduvач:*

**ZA**  $i = 1$  **DO**  $N$

Presmetaj ja verojatnosta  $P_i$  od  $x_i$  sprema formula 2

**KRAJ ZA**

**ZA SEKOJA** pčela-nabluduvач (i)

Izberi  $x_i = x_j$  (so verovatnost  $P_j$ )

Presmetaj  $v_i$  vrz osnova na  $x_i$  sprema formula 1

**AKO** kvalitet( $v_i$ ) > kvalitet( $x_i$ ) **TOGAŠ**  $x_i = v_i$

**KRAJ ZA SEKOJA**

*Faza izvidnici:*

**ZA SEKOE** otfrleno rešenje ( $x_i$ )

Generiraj novo slučajno rješenje  $x_i$  sprema formula 3

**KRAJ ZA SVAKO**

**AKO** MaxRešenje(iteracija) > MaxRešenje **TOGAŠ**

MaxRješenje = MaxRješenje(iteracija)

iteracija = iteracija + 1

**AKO** (iteracija == Cmax) **TOGAŠ PREKINI**

**KRAJ POVTORUVAJ**

Слика 3 Псевдокод на алгоритмот „Вештачка колонија на пчели“

## Заклучок

„Вештачка колонија на пчели“ (англ. artificial bee colony- ABC) претставува алгоритам за оптимизација кој спаѓа во групата на пчелини алгоритми, односно на интелигенцијата (анг. swarm intelligence) на колонијата на пчели. Развиен е во повеќе верзии, но сите тие го користат основниот принцип, спој помеѓу истражување (извидување) (*research*) и експлоатација (*exploitation*). Пчелите извидници се задолжени за фазата извидување, а пчелите собирачи за фазата експлоатација.

Со неговото дефинирање, овој алгоритам прогресивно почна да се применува за решавање на голем број комплексни проблеми за оптимизација во математиката, дизајнот и оптиматизацијата на компјутерските системи, инжењерството, управувањето со производните процеси во индустријата, роботиката, биоинжењерингот итн.

## Литература

[1] д-р Анис Сефиданоски, м-р Зорица Каевиќ, м-р Билјана Раичевиќ Велковска, Препознавање на облици, Скопје, 2020

[2] K. V. Frisch (1973). "Nobel Lecture: Decoding the Language of the Bee". University of Munich, Federal Republic of Germany.

*Додатна литература наменета за проширување на знаењето на читателот*

[3] "Detailed Pseudocode of the ABC Algorithm" (2008).  
<http://mf.erciyes.edu.tr/abc/index.htm>, 7.5.2010.

[4] "Detailed Pseudocode of the ABC Algorithm" (2008).  
<http://mf.erciyes.edu.tr/abc/index.htm>, 7.5.2010.